Halladale-1 DW2
Well Completion Report
Interpretive Data

Photo: Damian White

VIC/P37(v)
Offshore Otway Basin
Victoria

A.Constantine, M.Lonergan & J.Parvar
Origin Energy Resources Ltd
339 Coronation Drive
MILTON QLD 4064
Australia
December 2007

origin

Halladale-1 DW2 Document Information

PREPARED BY	POSITION	DATE	SIGNATURE
Andrew Constantine	Staff Geologist	19/12/07	

APPROVED BY	POSITION	DATE	SIGNATURE
Jenny Bauer	Manager E&P Geoscience	19/12/07	
Deidre Brooks	Geoscience Leader Southern Australia	19/12/07	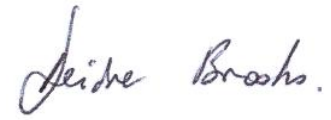
Randall Taylor	Chief Geophysicist	19/12/07	
Richard Suttill	Chief Geologist	19/12/07	

Contents

1. WELL INDEX SHEET 4
2. WELL SUMMARY 5
3. INTRODUCTION 7
   - 3.1 Exploration History 7
   - 3.2 Tectonic History of the Otway Basin 7
   - 3.3 Geological Setting 11
   - 3.4 Local Stratigraphy 11
4. SEISMIC EVALUATION 15
   - 4.1 Seismic Data Acquisition 15
   - 4.2 Seismic Markers 15
   - 4.3 Depth Conversion 17
   - 4.4 Actual vs Predicted Depths 17
   - 4.5 Well Tie 19
   - 4.6 Structure 19
5. WELL STRATIGRAPHY 28
6. HYDROCARBON SHOWS 37
7. RESERVOIR EVALUATION 38
   - 7.1 Petrophysical Analysis 38
   - 7.2 Core Analysis 38
   - 7.3 Core Description 39
   - 7.4 STAR Interpretation 40
8. FORMATION TESTING 42
   - 8.1 Formation Pressure Testing 42
   - 8.2 Fluid Sampling 43
   - 8.3 Production Testing 43
9. GEOCHEMICAL STUDIES 44
   - 9.1 Gas Composition 44
   - 9.2 Condensate GC-MS 45
   - 9.3 Compound Specific Isotope Analysis 45
   - 9.4 CO_2 Carbon Isotope Analysis 46
   - 9.5 Mud Gas Isotope Analysis 46
   - 9.6 Fluid Inclusion Screening 47
10. CONTRIBUTIONS TO GEOLOGICAL KNOWLEDGE 48
11. REFERENCES 49

FIGURES

1. VIC/P37(v) permit location map
2. Antares 3D MSS bathymetry
3. Generalised stratigraphy of the Port Campbell Embayment - Northern Shipwreck Trough
4. Late Cretaceous structural elements map for the eastern Otway Basin
5. Antares 3D MSS Inline 1852 across Black Watch and Halladale showing key seismic markers
6. Halladale-1 DW2 predicted versus actual stratigraphy
7. Halladale-1 DW2 synthetic
8. Top Waarre C depth structure map
9. Top Waarre A depth structure map
10. Top Upper Nullawarre depth structure map
11. Top Lower Nullawarre depth structure map
12. Antares 3D MSS seismic traverse along Halladale-1 DW1 and DW2 well paths

TABLES

1. 2D seismic previously acquired within VIC/P37(v)
2. Halladale-1 DW2 actual vs predicted formation tops
3. Paaratte Formation micropalaeontological results
4. Skull Creek Mudstone micropalaeontological results
5. Belfast Formation micropalaeontological results
6. Flaxman Formation micropalaeontological results
7. Waarre C palynology micropalaeontological results
8. Waarre B palynology micropalaeontological results
9. Waarre A palynology micropalaeontological results
10. Eumeralla Formation micropalaeontological results
11. Halladale-1 DW2 petrophysical summary
12. Halladale-1 DW2 pressure survey summary
13. Composition of Waarre C gas samples from Halladale-1 DW1 and DW2
14. CSIA of Waarre C gases in Halladale-1 DW1 and DW2

ENCLOSURES

1. Halladale-1 DW2 Composite Well Log

APPENDICES

1. Biostratigraphy Report
2. Petrology Report
3. Petrophysics Report
4. Special Core Analysis Report
5. Core Interpretation Report
6. STAR Interpretation Report
7. RCI Interpretation Report
8. PVT Report
9. Condensate Geochemistry Report
10. Mud Gas Isotope and CSIA Report
11. FIS Report

1. WELL INDEX SHEET

Well Name:	Halladale-1 DW2
Basin:	Offshore Otway
Permit:	VIC/P37(v)
Type:	Deviated Exploration Well
Operator:	Origin
Water Depth:	44.8m (LAT)
Rotary Table:	21.5m
Latitude:	38° 34' 45.54"S (GDA 94)
Longitude:	142° 43' 50.95"E
Easting:	650 763.2 metres (MGA Grid Zone 54)
Northing:	5 728 485.2 metres

Rig Name:	Ocean Patriot
Rig on Location:	17:30 hrs 21/03/2005
Spud:	07:30 hrs 10/04/2005
Reached TD:	17:30 hrs 17/04/2005
Total Depth:	1941m MDRT (Driller)
DW2 Abandoned:	15:00 hrs 21/04/2005
Rig Released:	05:30 hrs 02/05/2005
Total Time on Location	44.5 days (Halladale-1 DW1, 2 & 3 combined)
Seismic Reference:	Antares 3D MSS Inline 1938 Crossline 1115
Well Cost:	A$ 23,329,727 (Halladale-1 DW1, 2 & 3 combined)
Well Status:	Plugged & Abandoned

FORMATION TOPS

FORMATION	TOPS (m)			REMARKS/SHOWS
	mMDRT	mTVDSS	THICKNESS (mTVD)	
Port Campbell Limestone				
Gellibrand Marl				
Clifton Fm				
Narrawaturk Marl				
Mepunga Fm				
Dilwyn Fm				
Pember Mudstone				Kicked off at 853.0 mMD; silty claystone and sandstone
Pebble Point Fm	870.9	848.9	67.8	Sandstone with minor silty claystone
Massacre Shale	938.7	916.7	9.2	Claystone
Paaratte Fm	948.0	925.9	416.4	Interbedded sandstone, silty claystone and sandy claystone
Skull Creek Mudstone	1386.3	1342.3	140.0	Silty claystone with sandstone and claystone
Nullawarre Fm	1537.8	1482.3	47.5	Silty claystone and sandstone
Belfast Fm (hanging wall)	1588.8	1529.8	17.9	Claystone
FAULT	1608.1	1547.7		
Belfast Fm (foot wall)	1608.1	1547.7	122.7	Claystone with occassional interbedded silty claystone, glauconitic claystone and sandstone
Flaxman Fm	1740.2	1670.4	59.1	Interbedded silty claystone and sandstone with minor glauconitic claystone
Waarre Fm Unit C	1803.7	1729.5	21.9	*Gas-bearing sandstone with minor silty claystone*
Waarre Fm Unit B	1827.2	1751.4	26.1	Interbedded silty claystone and argillaceous siltstone
Waarre Fm Unit A	1855.1	1777.5	40.0	Interbedded sandstone and silty claystone
Eumeralla Fm	1897.6	1817.5	41.0	Interbedded sandstone and silty claystone
TOTAL DEPTH	1941.0	1858.5		

FORMATION EVALUATION WHILE DRILLING

Hole Size (mm)	Interval (mMD)	Logs Acquired
216	853.0 – 1514.0	DGR-EWRP4-PWD-SLD-CTN-BATSonic-DM-ABI
216	1514.0 – 1808.0	DGR-EWRP4-PWD-SLD-CTN-BATSonic-DM-ABI
216	1808.0 – 1941.0	DGR-EWRP4-PWD-SLD-CTN-BATSonic-DM

WIRELINE LOGS

Suite #	Run #	Interval (mMD)	Logs Acquired
1	1	730.0 – 1936.0	XMAC-ORIT-STAR-DSL
1	2	1542.0 – 1856.5	RCI-DSL (pressures)
1	3	1804.6 – 1902.4	RCI-DSL (samples)

CORE- CONVENTIONAL

Core #	Interval (mMD)	Cut (m)	Recovered (m)	Formation
1	1808.0 – 1835.0 (drillers depth)	27.0	25.4 (94.1%)	Waarre C & Waarre B

CORE – SIDEWALL

Suite#	Run#	Type	Interval (mMD)	Bullets	Mud	Empty	Low Rec	Recovered
None Taken								

PRESSURE TESTING AND FLUID SAMPLING

Suite#	Run#	Type	Interval (mMD)	Total Tests	Valid Tests	Supercharged	Tight Tests	Retests	Lost Seal	Samples Collected
1	2	RCI	1542.0 – 1856.5	26	11	0	15	0	0	0
1	3	RCI	1858.3 – 1902.4	6	4	0	2	0	0	3

HOLE & CASING DETAILS

Hole Size (inch)	Interval (mMD)	Casing Size (inch)	Shoe Setting Depth (mMD)
8 ½	853.0 – 1941.0 (TD)		

2. WELL SUMMARY

Halladale-1 DW2 was the second well in a three well programme targeting two adjacent fault-dependent closures with AVO anomalies at the Late Cretaceous Waarre and Nullawarre levels in offshore exploration permit VIC/P37(v) at the eastern end of the Otway Basin (see Figure 1). The three wells were drilled in succession using the Ocean Bounty semi-submersible drilling rig located in 44.8 m of water approximately 4 km from shore. The wells were drilled using the same top-hole section and then directionally steered toward their respective targets, with the first well, Halladale-1 DW1 (Location Black Watch), targeting the southern prospect (Black Watch), and the second and third wells, Halladale-1 DW2 and Halladale-1 DW3, targeting the northern prospect (Halladale).

Halladale-1 DW2 was drilled as a side-track off the Halladale-1 DW1 borehole targeting anomalous amplitudes at the Waarre C level on the eastern flank of the Halladale Prospect. The underlying Waarre A at this location was expected to be water wet, while the Upper Nullawarre and Lower Nullawarre in the well were both expected to be gas-bearing. Halladale-1 DW2 side-track operations commenced 10th April 2005 with the well reaching TD (1941 mMD / 1858.5 mTVDSS) on the 17th April 2005. The well was kicked-off at a depth of 853.0 mMD in Pember Mudstone just below the $9^3/_8$" casing shoe (833.5 mMD) and then directionally steered along an azimuth of 343° and inclination of 20° toward the Waarre C target, bottoming in Eumeralla Formation approximately 330 m north-northwest of the top hole location and 606 m north of the Halladale-1 DW1 bottom hole location.

The top of the Nullawarre Formation in the well was intersected 22 m low to prognosis at a depth of 1537.8 mMD (1482.3 mTVDSS). Two sands were again encountered, but no gas shows were observed. The top of the Waarre C in the well was intersected 21 m high to prognosis at a depth of 1803.7 mMD (1729.5 mTVDSS). Immediately upon penetrating the top of the unit, strong gas shows were observed, so a 27 m long core was cut (94.1% recovery). After the core had been retrieved, the well was drilled to TD with no further gas shows observed. The well was then logged, and formation pressure measurements and fluid samples acquired from the Waarre C. The well was then plugged back to the $9^3/_8$" casing shoe in order to prepare for the commencement of Halladale-1 DW3 side track operations.

Petrophysical analysis of logs from Halladale-1 DW2 indicate the well encountered 18.6 mMD of net gas pay in the Waarre C (79.1% N:G) with an average effective porosity of 22.3% and water saturation of 18.5%. The GWC for the Waarre C was not intersected in the well, but gas pressure measurements from the unit indicate it has gas gradient approximately 10 psi lower than the Waarre C gas gradient at Black Watch, indicating the two pools are not in pressure communication. No net pay was calculated for underlying Waarre A which was

water wet on logs. The Upper Nullawarre and Lower Nullawarre, which were both expected to be gas-bearing in the well, proved water wet instead.

Geochemical analysis of gas recovered from the Waarre C indicates it is fairly dry (90.67% C_1) with a C5+ ratio (11.3 bbls/MMscf) and an inerts content of 1.81 %.

3. INTRODUCTION

3.1 Exploration History

VIC/P37(v) is a shallow-water "three-mile zone" permit located in Victorian state territorial waters at the eastern end of the Otway Basin between the coastal townships of Port Fairy and Peterborough (see Figure 1). The permit was awarded to the VIC/P37(v) JV on 17 April 2003 and covers an area of about 493 km^2. It is approximately 78 km in length and extends seaward three nautical miles out from the high water mark. Water depth across the block ranges from zero to 60 m (see Figure 2).

The exploration history of VIC/P37(v) is remarkably sparse in comparison to the activity that has taken place over the last forty years in adjacent permits to the north and south. Prior to 2003, no wells had been drilled in VIC/P37(v) and only 427 line kms of 2D seismic had been acquired (see Table 1), 80% of which had been recorded between 1963 and 1966.

Table 1. 2D seismic previously acquired within VIC/P37(v)

Survey	Operator	Year	# Lines inside VIC/P37(v)	Line KM
OH94	BHP PETROLEUM	1994	10	41.1
OH91	BHP PETROLEUM	1991	17	26.7
OE81A	ESSO	1981	1	0.1
OE80A	ESSO	1980	1	3.0
H04	HEMATITIE	1974	2	9.7
OS66A	SHELL	1966	14	131.3
OS66C	SHELL	1966	18	59.3
OFBH63D	FROME BROKEN HILL	1963	14	155.6
TOTAL			**77**	**426.8**

The Black Watch and Halladale fields are located near the eastern end of VIC/P37(v) approximately 13 km west of the coastal township of Peterborough midway between the offshore Martha gas field and the onshore Croft gas field (see Figure 2). The closest offshore well is Martha-1 drilled by SANTOS in 2004. The closest onshore well is Flaxmans-1 drilled by Frome Broken Hill in 1961.

3.2 Tectonic History of the Otway Basin

The Otway Basin is a NW-SE striking passive margin rift basin approximately 500 km long that extends from Cape Jaffa in South Australia to the northwest tip of Tasmania. It is one of a series of basins that formed along the southern margin of mainland Australia during the Late Jurassic - Cenozoic as Australia began to separate from Antarctica. The sedimentary section in the basin is up to 10,000 m thick and ranges from Late Jurassic to Recent in age

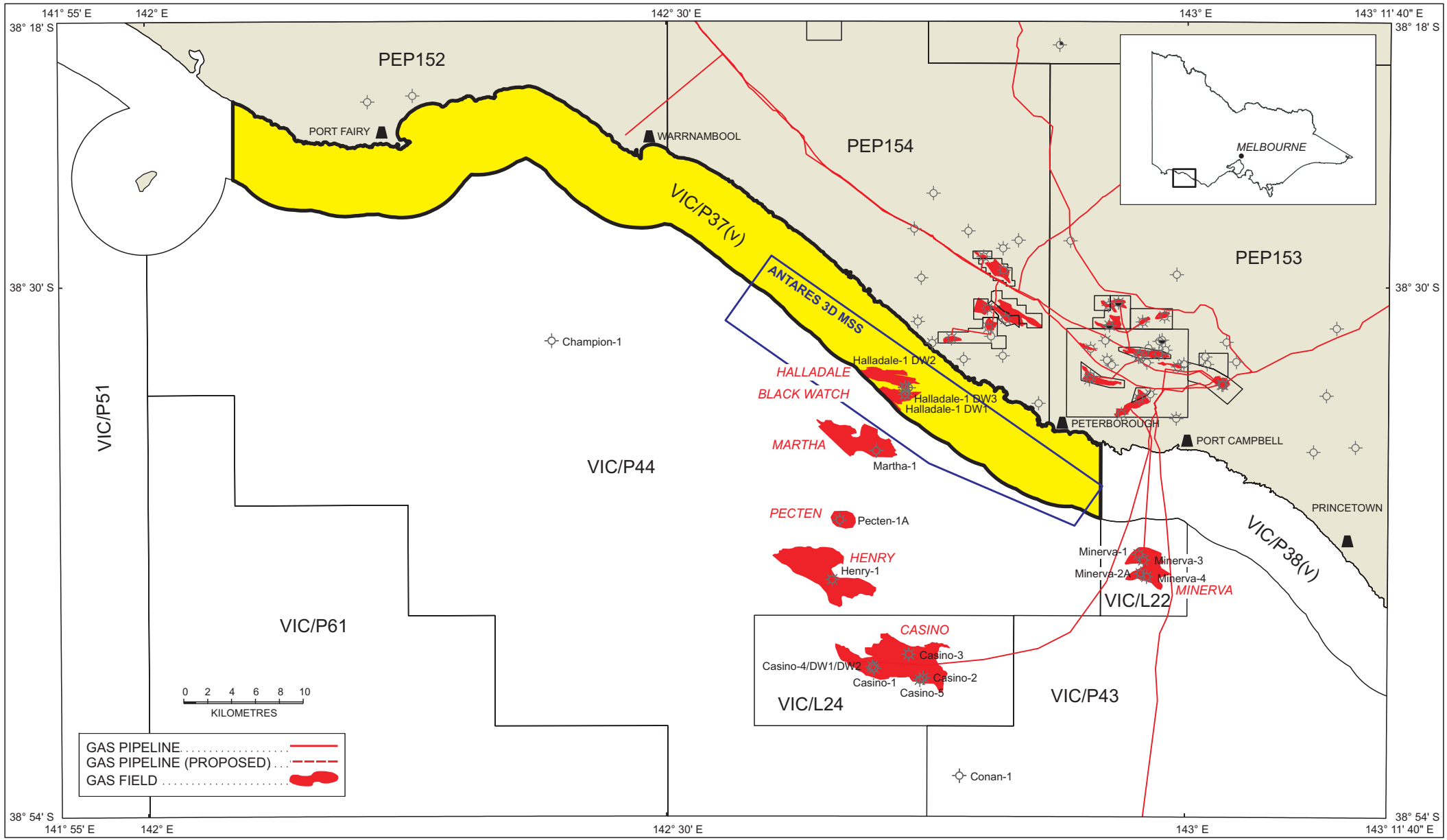

Figure 1. Permit location map.

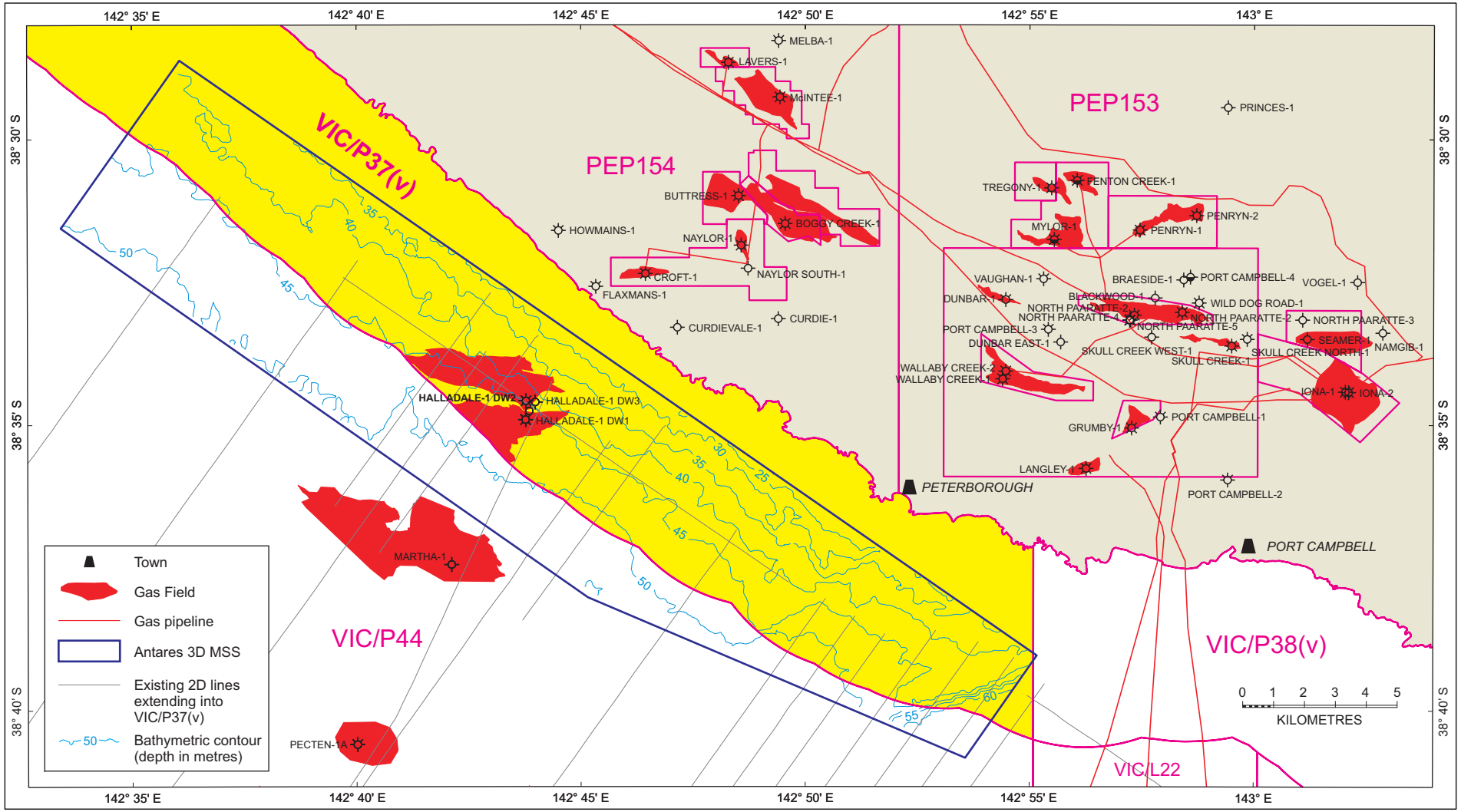

Figure 2. Antares 3D MSS bathymetry.

and covers an area of approximately 155,000 km^2, approximately 80% of which is located offshore.

The Otway Basin has a complex tectonstratigraphic history involving two periods of NE-SW extension punctuated by several episodes of compression, uplift and erosion, thermal subsidence, and inversion. The first period of rifting resulted in the formation of a series of small NW-SE and E-W striking half-grabens onshore that were filled with up to 5000 m of non-marine sediments and volcanics known as the Crayfish Group. This event was then followed by a period of tectonic quiescence and thermal subsidence that spanned the Aptian – Albian during which up to 3000 m of fluvial – lacustrine sediments known as the Eumeralla Formation were deposited.

During the Cenomanian, the basin experienced a short period of NW-SE compression, uplift and erosion, resulting in the development of a major regional unconformity known as the Cenomanian Unconformity. At the end of the Cenomanian, the basin began to undergo extension again, with the locus of extension shifting offshore. This extension continued all the way through the rest of the Late Cretaceous resulting in the deposition of up to 5000 m of fluvial to offshore marine clastic sediments known as the Sherbrook Group in the Voluta Trough.

Toward the end of the Maastrichtian, mainland Australia began to separate from Antarctica and the two continents started to drift slowly apart, with Tasmania still attached to both. This event in the basin is marked by a prominent unconformity at the top of the Sherbrook Group known as the Base Tertiary Unconformity. This slow period of spreading lasted until the middle Eocene during which up to 300 m of deltaic to shallow marine clastic sediments known as the Wangerrip Group were deposited on the shelf.

The end of the middle Eocene saw a significant increase in the spreading rate in the Southern Ocean when Antarctica finally separated from mainland Australia and Tasmania. This event caused the Otway margin to subside, resulting in a marine transgression and the deposition of up to 100 m of Middle Eocene to Early Oligocene nearshore to offshore marine clastic and carbonate sediments known as the Nirranda Group. This event was then followed by the deposition of up to 1600 m of marl and limestone belonging to the Late Oligocene – Late Miocene Heytesbury Group as the shelf edge began to prograde back out into the basin.

At the end of the Late Miocene, the Otway Basin experienced another period of NW-SE directed compression causing significant folding, uplift and erosion of the sedimentary fill, mostly at the eastern end of the basin, resulting in the development of a series of broad low-relief NE-SW striking anticlines and synclines across the eastern Otway Basin.

3.3 Geological Setting

The key structural elements in the eastern Otway Basin are the Shipwreck Trough and Port Campbell Embayment (see Figure 3). Over the past thirty years, twenty-four gas fields have been discovered in these two areas, five of them offshore in the Shipwreck Trough and nineteen onshore in the Port Campbell Embayment, with the bulk of the gas found occurring in the non-marine to marginal-marine Waarre Formation at the base of the Late Cretaceous Sherbrook Group.

The Shipwreck Trough is a N-S striking zone of Late Cretaceous transtension, wrenching and down-warping approximately 25 km wide and 100 km long bounded to the west and east by two broad Late Cretaceous highs called the Mussel and Prawn platforms respectively. The trough is believed to have formed in response to sinistral shear on a pre-existing basement weakness when the basin was undergoing NE-SW extension during the breakup of mainland Australia and Antarctica. The western edge of the trough is delineated by the western limit of Unit C of the Waarre Formation ("Waarre C") and its eastern edge by the Sorell Fault Zone.

The Port Campbell Embayment, the onshore extension of the Shipwreck Trough, is a broad semi-circular shaped Late Cretaceous depression up to 50 km wide that extends up to 20 km inland from the coast. Its western, northern and eastern limits are defined by the subcrop extent of the Waarre C.

VIC/P37(v) is located at the northern end of the Shipwreck Trough directly opposite the Port Campbell Embayment. Approximately two-thirds of the permit lies on the Mussel Platform with the eastern third extending about halfway across the Shipwreck Trough. The Black Watch and Halladale fields are located near the eastern end of the permit on the nose of a prominent NE-SW striking Late Cretaceous anticline called Pecten High.

3.4 Local Stratigraphy

The stratigraphy of the Port Campbell Embayment and northern Shipwreck Trough is illustrated in Figure 4. The late Early Cretaceous – Tertiary sequence in the area is divided into five groups comprising over twenty formations. For a detailed description of the lithology, thickness, distribution and depositional environments of these formations see Tickell et al (1992), GSV (1995) and Partridge (2001).

The Sherbrook Group, which contains the primary and secondary objectives, is divided into seven lithostratigraphic units called, from base to top, the Waarre Formation, Flaxman

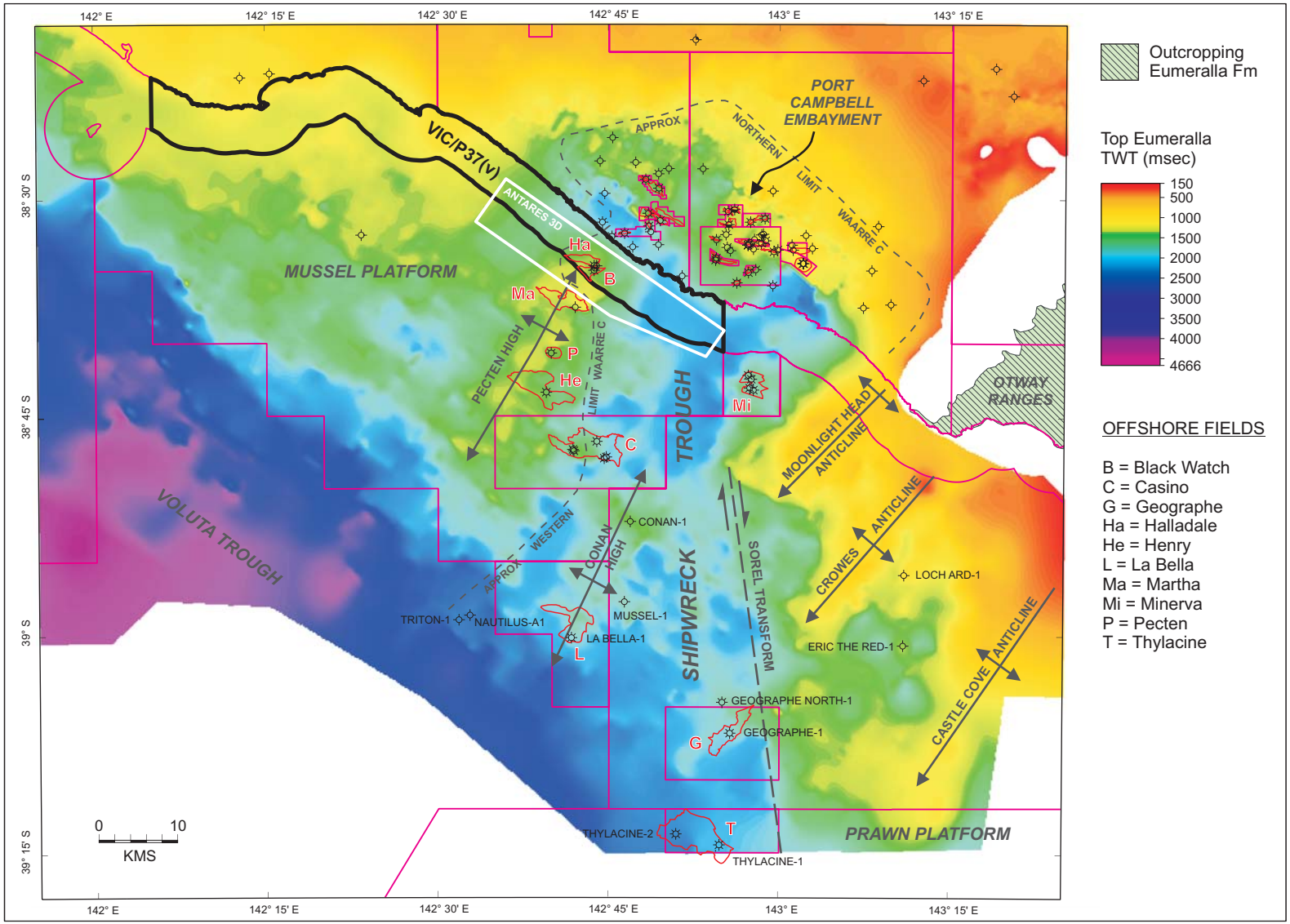

Figure 3. Late Cretaceous structural elements of the Eastern Otway Basin.

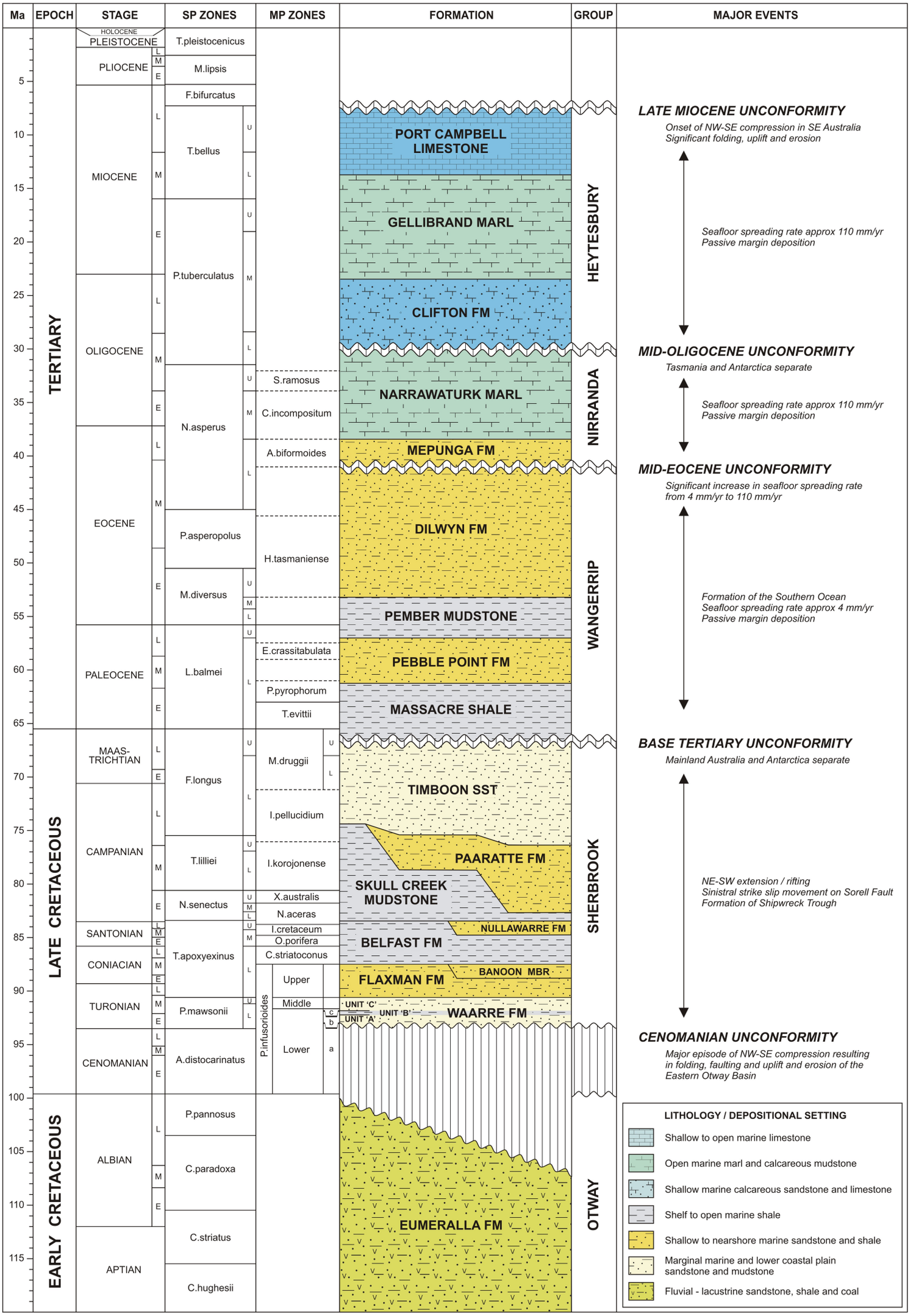

Figure 4. Generalised stratigraphy of the Port Campbell Embayment - Northern Shipreck Trough.

Formation, Belfast Formation, Nullawarre Formation, Skull Creek Mudstone, Paaratte Formation and Timboon Sandstone.

In the Port Campbell Embayment, the Waarre Formation, the primary objective at Black Watch and Halladale, is divided into three units called (in ascending stratigraphic order) A, B and C. Unit A is sequence of interbedded estuarine to marginal marine shale and sandstone up to 43 m thick with a highly variable net to gross and moderate porosity and permeability. It is overlain by a very nearshore to offshore marine argillaceous shale up to 37 m thick (Unit B) which is in turn overlain by a fluvial to tidally-influenced marginal-marine medium- to coarse-grained quartz-rich sandstone up to 41 m thick with a high net to gross and excellent porosity and permeability (Unit C). The bulk of the gas discovered onshore occurs within Unit C, with Unit A at Boggy Creek, Wallaby Creek and Skull Creek also containing small volumes of gas. The sealing units for the Waarre C onshore are the Flaxman Formation (top seal) and Belfast Formation (cross-fault seal).

The Nullawarre Formation, the secondary objective in Halladale-1 DW1, is a shallow marine glauconitic sandstone. The formation is up to 100 m thick in the northern part of the Port Campbell Embayment and thins toward the south, pinching out just south of the present day coastline.

4. SEISMIC EVALUATION

4.1 Seismic Data Acquisition

The Antares 3D MSS was acquired by PGS on behalf of the VIC/P37(v) JV between 25 October and 11 November 2003. It was recorded over the eastern half of VIC/P37(v), with some ingress into adjacent permits VIC/P44, VIC/P38(v) and VIC/L22 to the south and east. The survey totalled 211 km^2 in area, with 134 km^2 of full-fold data acquired within VIC/P37(v).

4.2 Seismic Markers

Figure 5 is an Inline from the Antares 3D across the Black Watch and Halladale fields showing key seismic markers. Sixteen horizons were mapped in total from the Narrawaturk Marl down to the Eumeralla Formation, with strong amplitudes observed at the Upper Nullawarre, Lower Nullawarre, Waarre C and Waarre A levels.

The four parallel high amplitude seismic reflections at approximately 1.4 seconds in Figure 5 were interpreted to represent the tops of the Waarre C, Waarre B, Waarre A and Eumeralla Formation based on character ties into key onshore wells (ie. Croft-1, Naylor-1, Naylor South-1, Wallaby Creek-1, Grumby-1 and Langley-1) as it was not possible to get a direct seismic tie into the onshore 2D / 3D seismic due to the data gap along the coastal zone. An attempt was made to tie these events at Black Watch and Halladale directly into Minerva-1, Minerva-2A, Casino-1, Casino-2 and Pecten-1A offshore, but this proved difficult due to the distances between the wells and the high degree of faulting.

The four parallel high amplitude seismic reflections approximately 200 milliseconds above the Top Waarre C seismic event were interpreted to represent the top and base of two sandstone beds based on the seismic character of the Nullawarre Formation onshore in the vicinity of Curdie-1, 8.5 km to the ENE of Halladale-1 DW1, where the formation is represented by two sands, each approximately 14 m thick, separated by a 26 m thick shale. Again, an attempt was made to tie these events at Black Watch and Halladale directly into Minerva-1, Minerva-2A, Casino-1, Casino-2 and Pecten-1A offshore, but this too proved difficult.

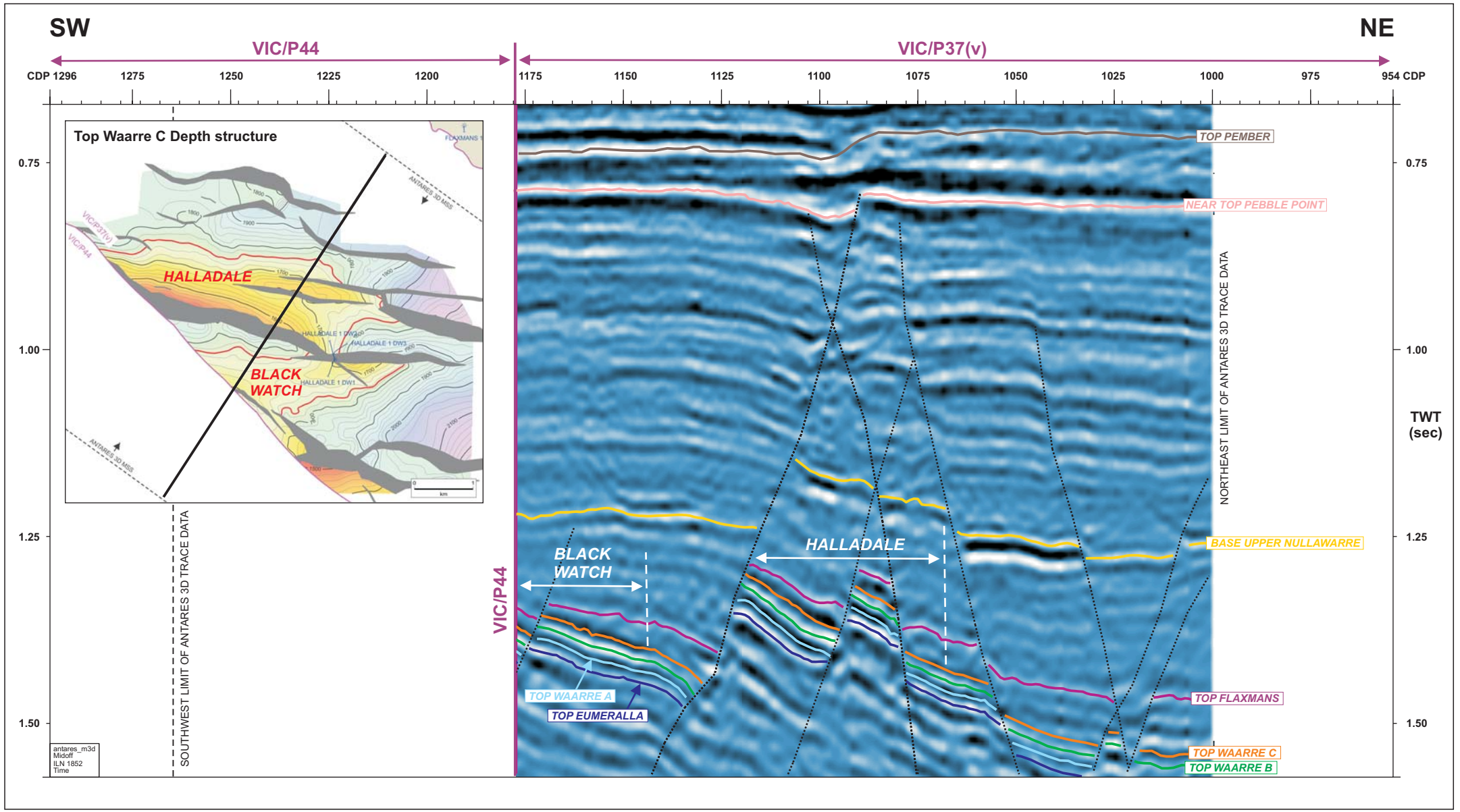

Figure 5. Antares 3D Inline 1852 across Black Watch and Halladale showing key seismic markers.

4.3 Depth Conversion

The seismic markers were converted to depth using a composite regional time-depth function based on check shot data and seismic times from nearby onshore wells. The upper part of the function down to approximately 1400 mSS was derived by fitting a best-fit line of regression through check shot data from Curdie-1, Grumby-1, Wallaby Creek-1, Langley-1, Port Campbell-2, Howmains-1 and Flaxmans-1, while the deeper part of the function was derived by passing a line of best fit through a cross-plot of well depths and seismic times for the tops of the Waarre C, Waarre B, Waarre A and Eumeralla in Boggy Creek-1, Croft-1, Dunbar-1, Dunbar East-1, Grumby-1, Naylor-1, Naylor South-1, Vaughan-1, Wallaby Creek-1, Wallaby Creek-2 and Langley-1.

4.4 Actual vs Predicted Depths

The pre- and post-drill stratigraphy of Halladale-1 DW1 is illustrated in Figure 6. Seven tops came in high to prognosis by between 1.5 and 21.1 m, and four low to prognosis by between 11.5 and 30.3 m (see Table 2). The tops of the Waarre C, Waarre B, and Waarre A all came in high to prognosis by between 16.2 and 21.1 mTVD, and the top of the Eumeralla low to prognosis by 11.5 mTVD. The top and base of the Nullawarre Formation, the secondary objective, came in 22.1 m and 12.4 m low to prognosis respectively.

Table 2. Halladale-1 DW2 actual vs predicted formation tops

FORMATION	PREDICTED DEPTH (mTVDSS)	ACTUAL DEPTH (mTVDSS)	Δ (m)	HIGH/LOW
Port Campbell Limestone				
Gellibrand Marl				
Clifton Formation				
Narrawaturk Marl				
Mepunga Formation				
Dilwyn Formation				
Pember Mudstone				
Pebble Point Formation	850.4	848.9	1.5	HIGH
Massacre Shale	not prognosed	916.7		
Paaratte Formation	927.7	925.9	1.8	HIGH
Skull Creek Mudstone	1347.5	1342.3	5.2	HIGH
Nullawarre Formation	1460.2	1482.3	22.1	LOW
Belfast Formation (HW)	not prognosed	1529.8	12.4	LOW
FAULT	1517.4	1547.7	30.3	LOW
Belfast Formation (FW)	1517.4	1547.7	30.3	LOW
Flaxman Formation	1686.6	1670.4	16.2	HIGH
Waarre C	1750.0	1729.5	21.5	HIGH
Waarre B	1769.4	1751.4	18.0	HIGH
Waarre A	Not prognosed	1777.5	16.6	HIGH
Eumeralla Formation	1806.0	1817.5	11.5	LOW

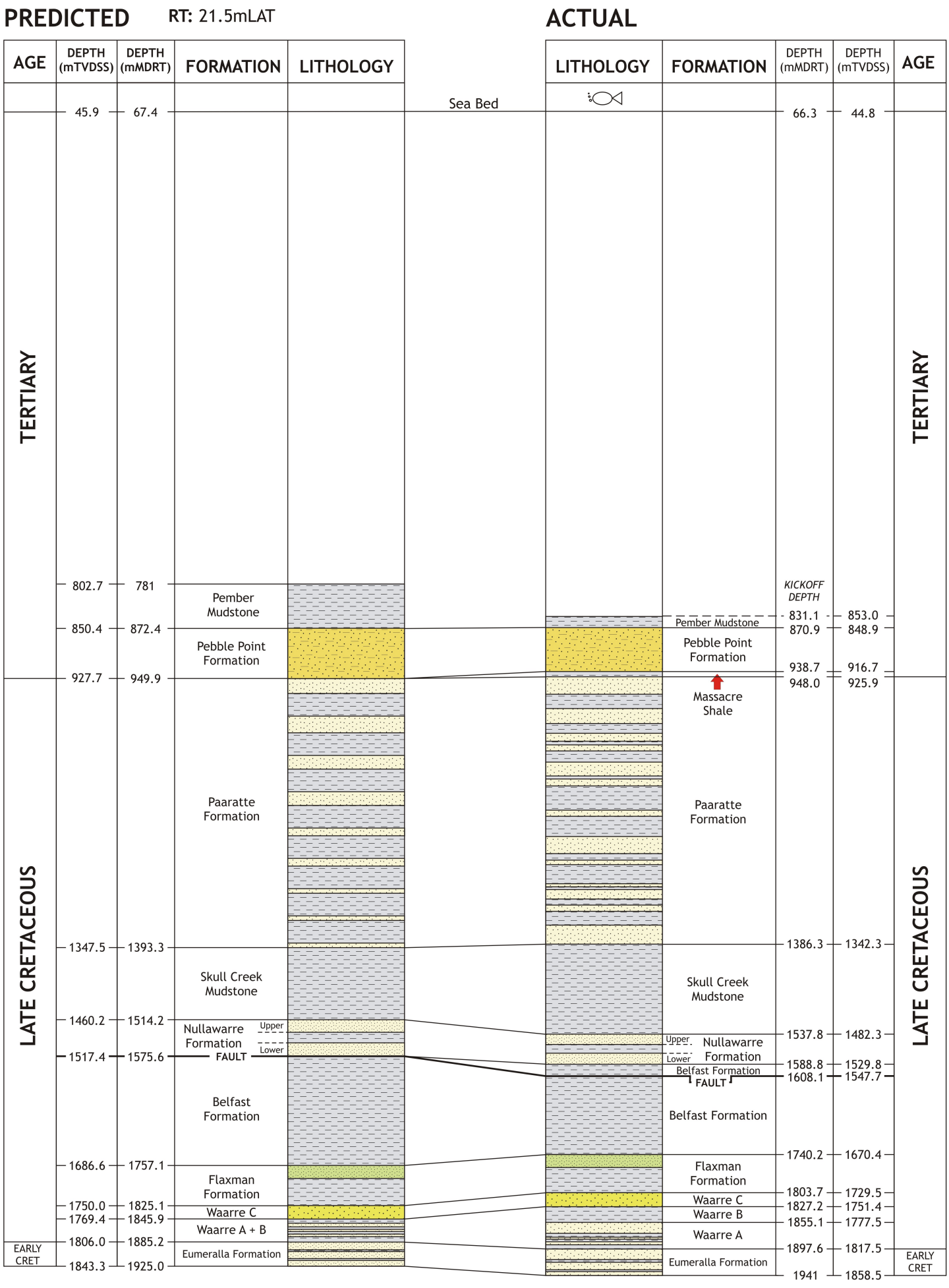

Figure 6. Halladale-1 DW2 predicted vs actual stratigraphy.

4.5 Well Tie

Figure 7 is a synthetic seismogram for Halladale-1 DW1 from the Skull Creek Formation down to the Eumeralla Formation generated using a wavelet extracted from the Antares 3D. A VSP was not run in Halladale-1 DW2 due to the proximity of the well to Halladale-1 DW1, in which a VSP was recorded.

4.6 Structure

The structure of Black Watch and Halladale at the Top Waarre C and Top Waarre A levels inside VIC/P37(v) is illustrated in Figures 8 and 9 respectively. The interpreted GWCs for the two units, as determined from formation pressure data (see Section 8.1), are also shown along with the well paths for Halladale-1 DW1, DW2 and DW3. The Top Waarre C depth map is based on the post-drill corrected time interpretation converted to depth using the pre-drill time-depth function and then depth-shifted to tie with the top of the Waarre C in Halladale-1 DW1, DW2 and DW3. The Top Waarre A depth map is based on the pre-drill time interpretation.

The Black Watch Field at the Top Waarre C level is an ENE-WSW striking fault-dependent closure with up to 170 m of vertical relief relative to the interpreted GWC (1770 mSS). The closure straddles the VIC/P37(v) / VIC/P44 permit boundary and consists of two opposing tilted fault blocks that dip toward each other connected by a saddle located approximately 35 m above the GWC about 1 km east of the VIC/P37(v) / VIC/P44 permit boundary. The VIC/P37(v) portion of Black Watch is 2.3 sq km in area and widens to the west from approximately 500 m at the eastern end of the field to 2 km along the VIC/P37(v) / VIC/P44 permit boundary. The southern side of the field is down-faulted against Eumeralla Formation by an E-W striking normal fault with approximately 160 m of throw, while the northern side of the field at its eastern end is delineated by an ENE-WSW striking normal fault with up to 100 m of throw to the north.

The Halladale Field is a WNW-ESE striking fault-dependent three-way dip closure bounded to the south-southwest by a down-to-south normal fault. The closure, as defined by the interpreted GWC (1760 mSS), which is 10 m shallower than the Black Watch Waarre C GWC (1770 mSS), is approximately 5 km long and 1 km wide with a vertical relief of 240 m and area of 4 sq km.

The structure of Black Watch and Halladale at the Top Waarre A level inside VIC/P37(v) is almost identical in form to that of the Top Waarre C. The gas pool intersected in Halladale-1 DW1 at the top of the Waarre A is restricted to the small tilted fault block at the eastern end of Black Watch. The closure defined by the GWC (1766 mSS), as determined from

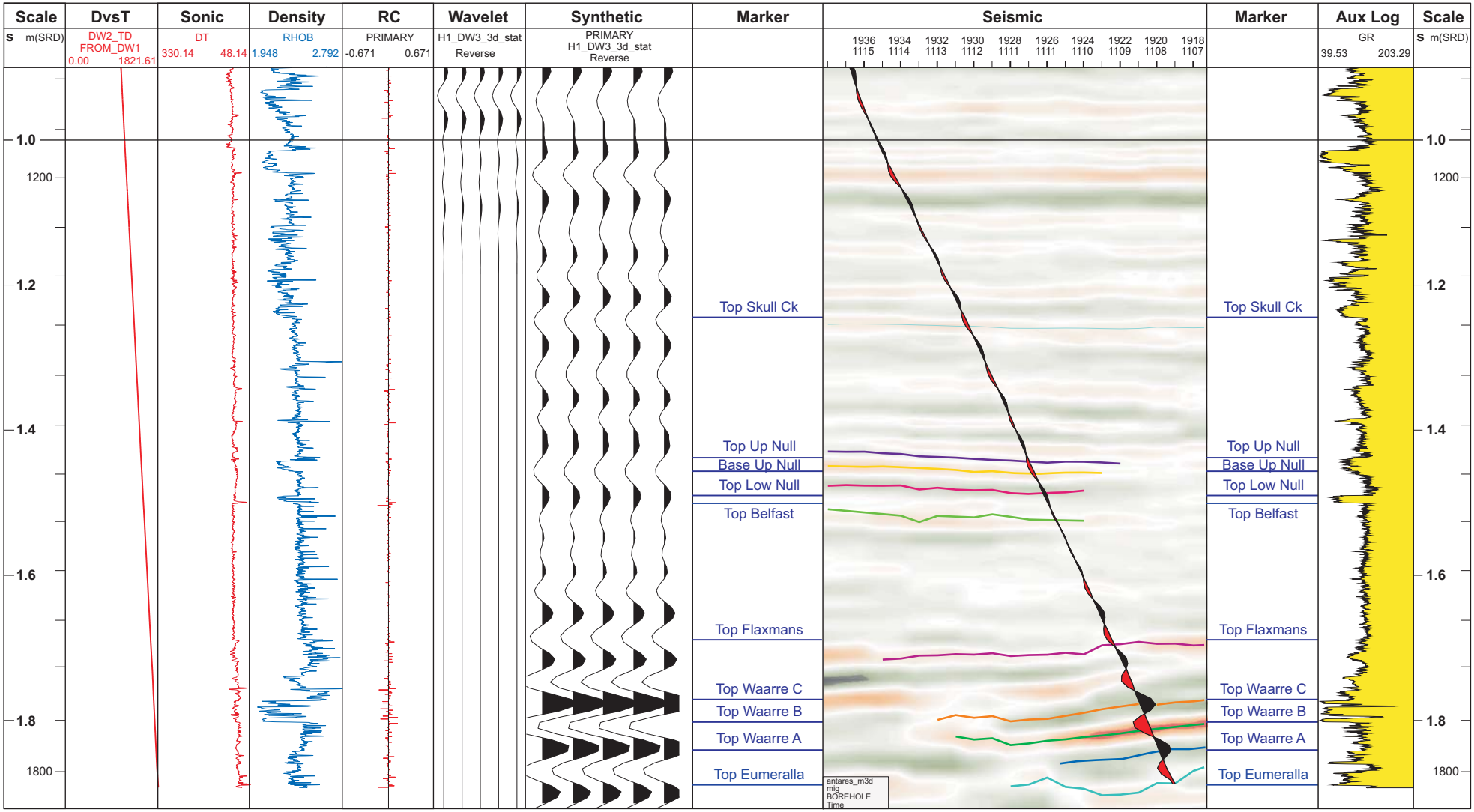

Figure 7. Halladale-1 DW2 synthetic seismogram (black wiggle trace) tied to seismic using VSP checkshot data from Halladale-1 Dw1.

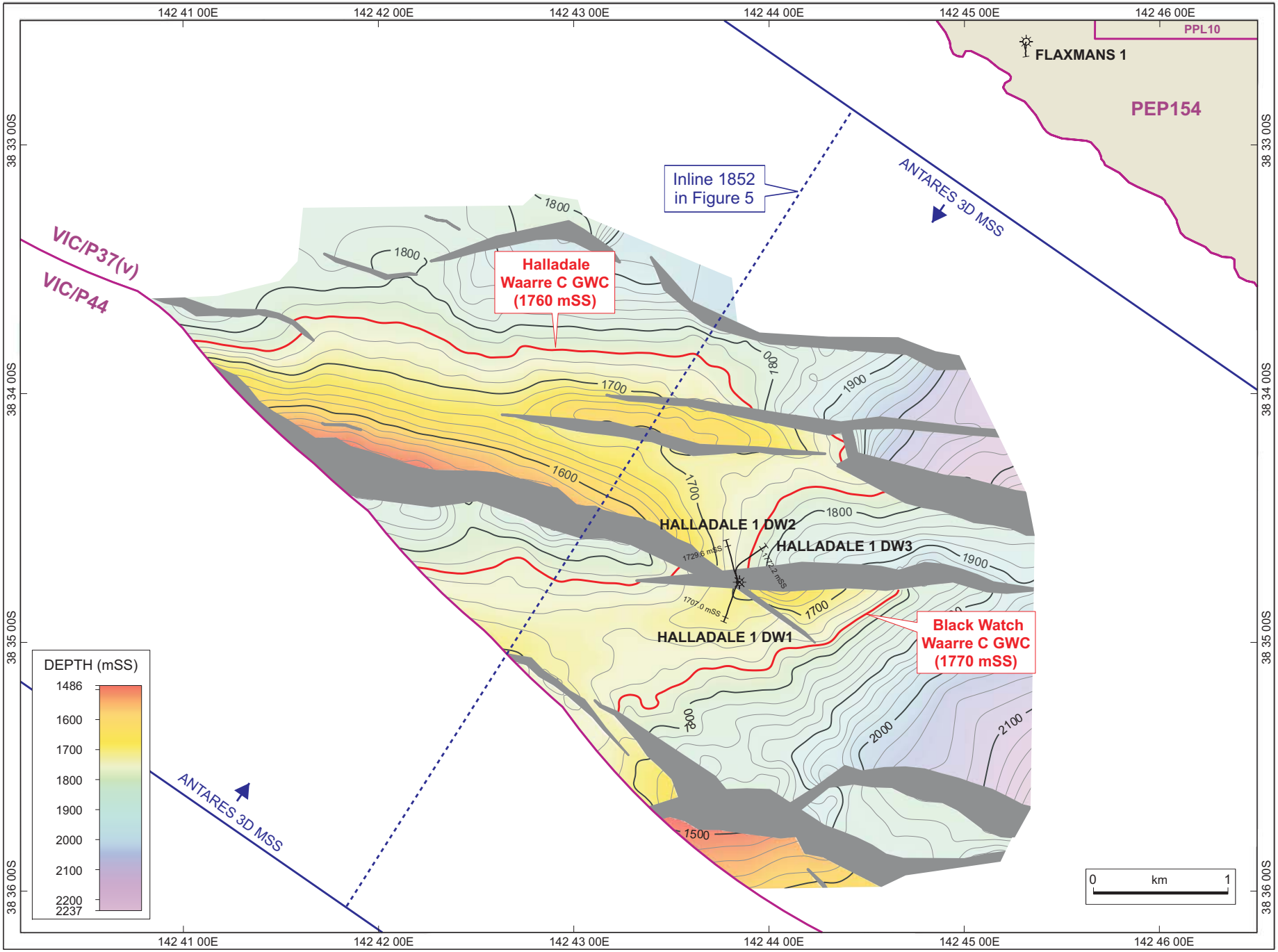

Figure 8. Top Waarre C depth structure map. Black Watch Waarre C GWC (1770 mSS) and Halladale Waarre C GWC (1760 mSS) shown in red.

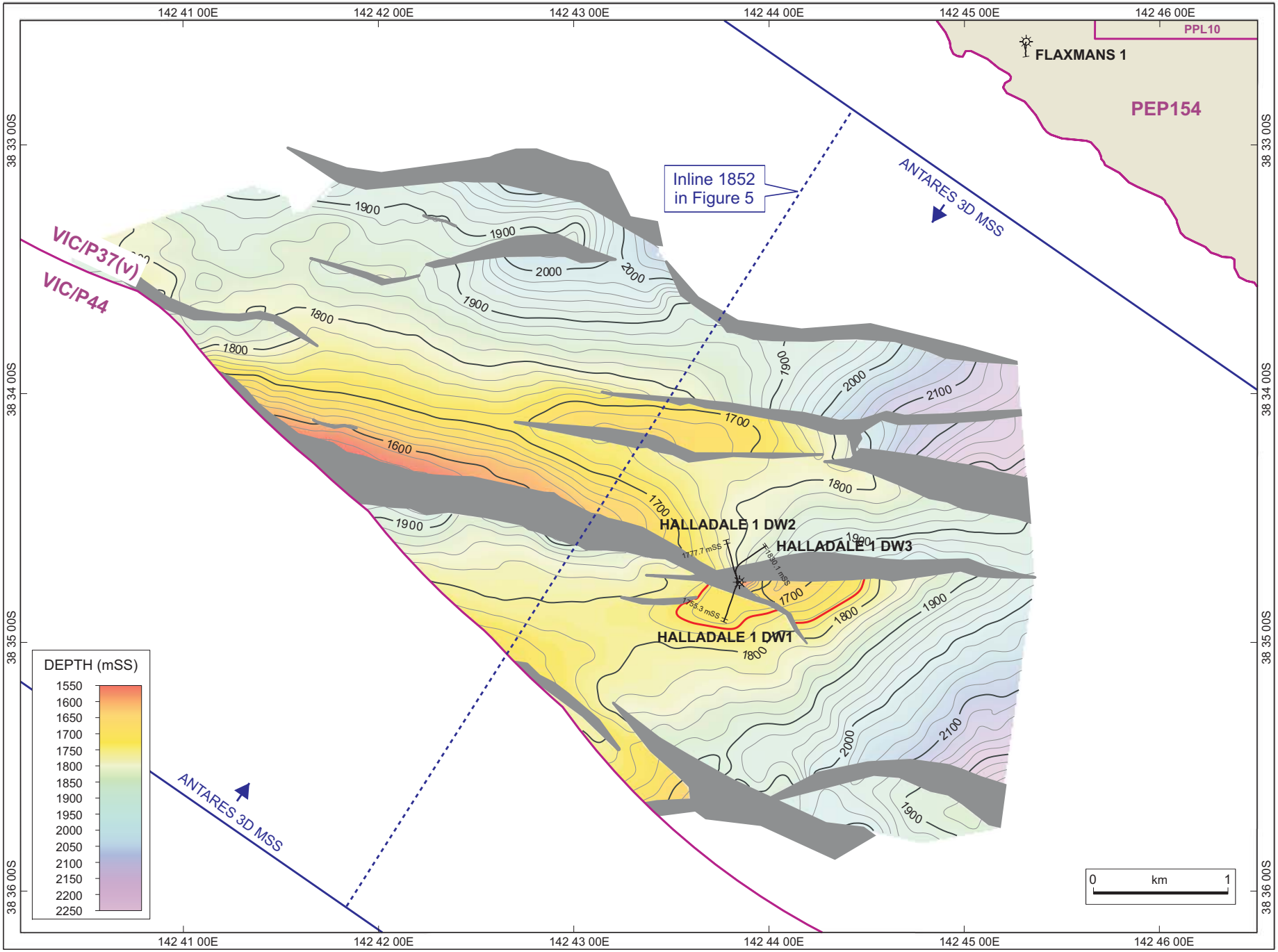

Figure 9. Top Waarre A depth structure map with Black Watch GWC (1766 mSS) shown in red.

pressure and log data, is very small (< 1 sq km) and has a vertical relief of about 90 m. The Waarre A in the adjacent Halladale fault block to the north was water wet in both in Halladale-1 DW2 and Halladale-1 DW3.

The structure of the Nullawarre Formation upstairs of Black Watch and Halladale at the Top Upper Nullawarre and Top Lower Nullawarre levels is illustrated in Figures 10 and 11 respectively. The two depth structure maps are based on the pre-drill time interpretation converted to depth using the pre-drill time-depth function and then depth-shifted to tie with the tops of the Upper Nullawarre and Lower Nullawarre in Halladale-1 DW1, DW2 and DW3. The interpreted GWCs for the two sands, 1481 mSS (Upper Nullawarre) and 1515 mSS (Lower Nullawarre), which are based on pressure data (see Section 8.1), are also shown in Figures 10 and 11 along with the well paths for Halladale-1 DW1, DW2 and DW3 and the outline of the Black Watch and Halladale fields at the Top Waarre C level (Figure 10 only). The two Nullawarre closures have an area of approximately 7 sq km and consist of small broad ENE-WSW striking faulted anticline approximately 3.2 km long and 1.2 km wide with 50 m of relief downthrown to the north against a prominent WNW-ESE striking horst-like feature approximately 4 km long, 1 km wide and 130 m in relief.

Figure 12 is a seismic traverse along the Halladale-1 DW1 and Halladale-1 DW2 well paths. The top hole section is located in a small downthrown keystone block where the tips of the two opposing normal faults bounding the north side of Black Watch and the south side of Halladale crossover. Halladale-1 DW2 was kicked-off at a depth of approximately 860 mMD in Pember Mudstone just below the Halladale-1 DW1 $9^3/_8$" casing shoe (833.5 mMD) and then directionally steered toward the north-northwest at an inclination of 21^o. The well was designed to intersect the Upper Nullawarre and Lower Nullawarre on the hanging wall side of the fault bounding the south side of Halladale before penetrating the fault and intersecting the Waarre C on the footwall side on the eastern flank of the structure approximately 220 m down-dip of the crest and 30 m up-dip of the seismic amplitude shutoff which was interpreted to represent a GWC.

As with Halladale-1 DW1, the primary aim of Halladale-1 DW2 was to determine if the anomalous amplitudes observed on seismic in the Waarre C on the Halladale fault block represented gas fill. The eastern flank of Halladale was chosen as the target location for the well so that the third well on the Halladale fault block, Halladale-1 DW3, would be able to reach far enough down-dip of the Waarre C seismic amplitude shutoff to ensure it obtained a water gradient from the Waarre C. The Upper Nullawarre and Lower Nullawarre in Halladale-1 DW2 were not a pre-drill objective as they had already been successfully tested in Halladale-1 DW1 which intersected the two sands about 350 m to the south in the same keystone block. Both sands were expected to be gas-bearing in Halladale-1 DW2 based on the presence of amplitudes at the planned penetration point, but this did not prove to

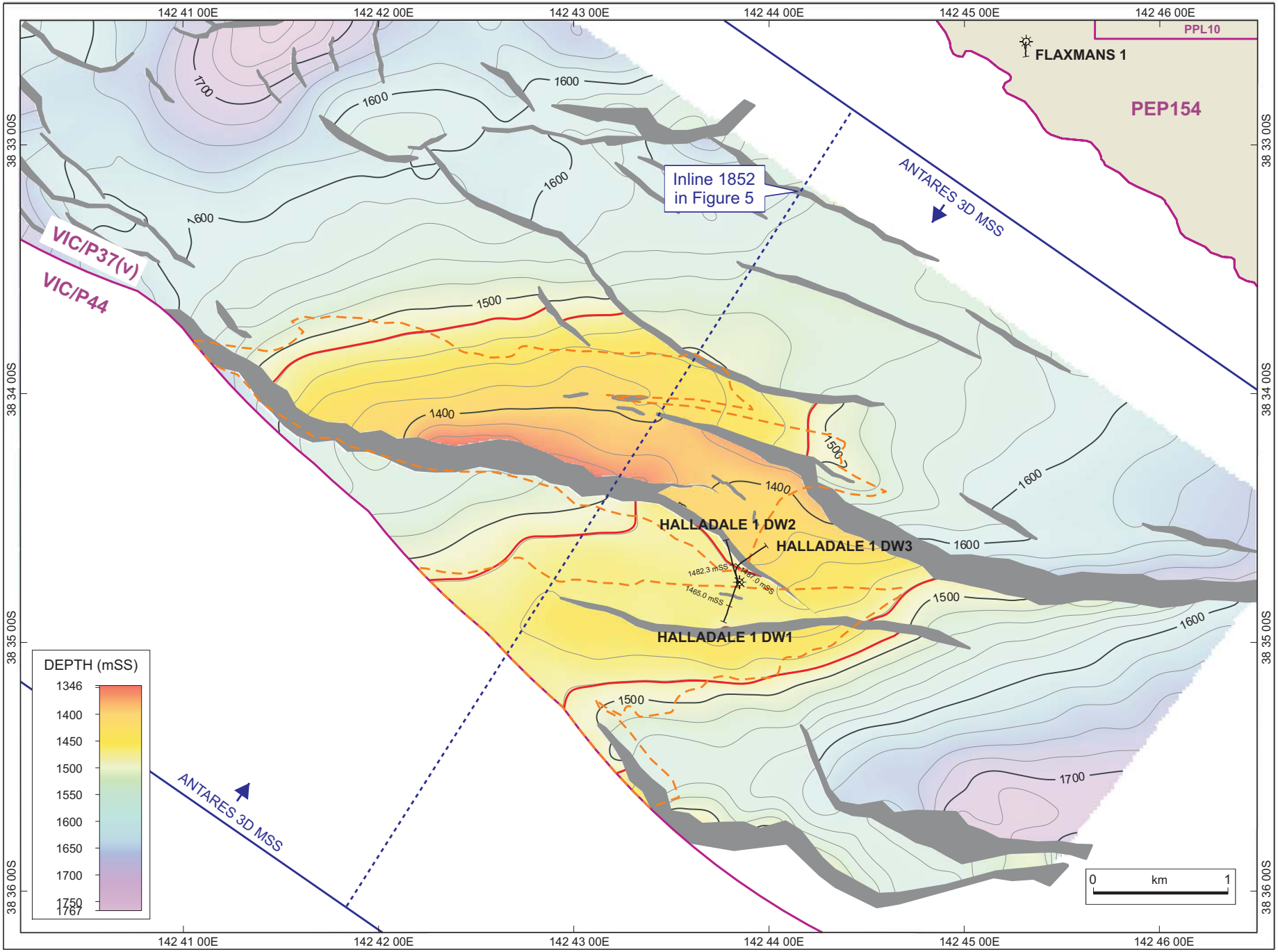

Figure 10. Top Upper Nullawaarre depth structure map with GWC (1481 mSS) shown in red. Outline of Black Watch and Halladale fields at Top Waarre C level shown in orange (dash).

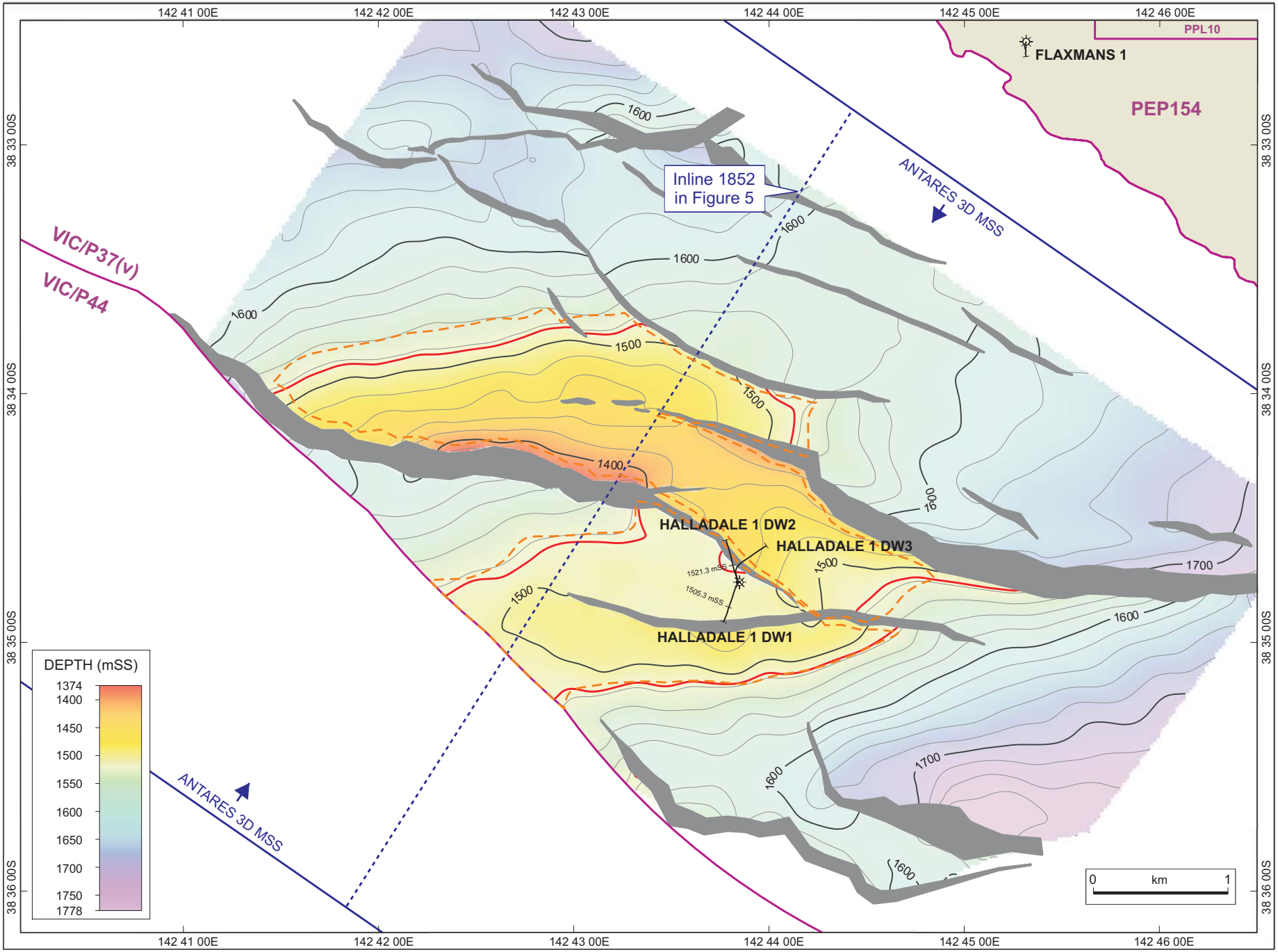

Figure 11. Top Lower Nullawaarre depth structure map. Lower Nullawarre GWC (1515 mSS) shown in red. Upper Nullawarre closure is shown in orange (dash). Note: Lower Nullawarre was not intersected in Halladale-1 DW3.

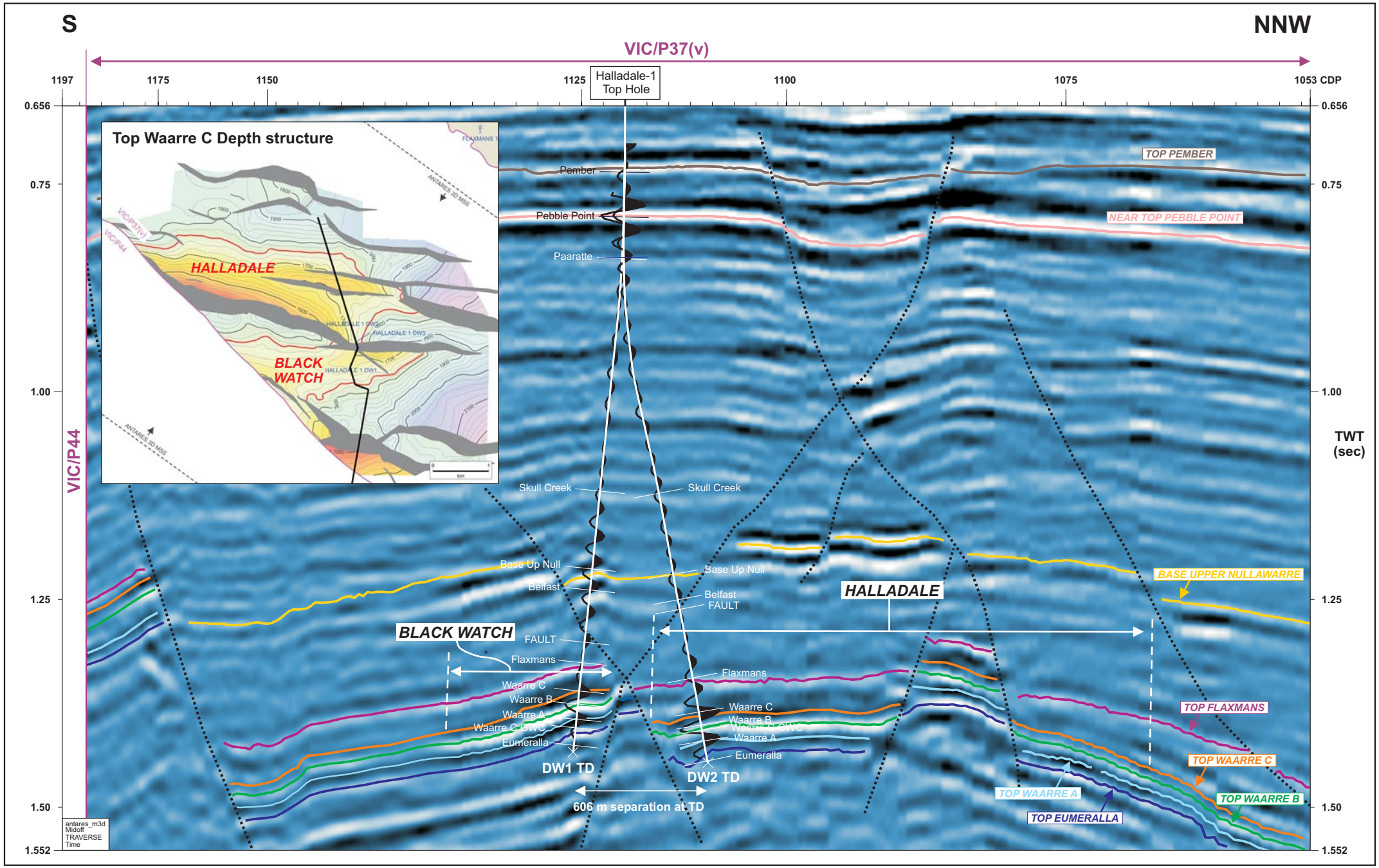

Figure 12. Seismic traverse along Halladale-1 DW1 and Halladale-1 DW2 well paths.

be the case, with the top of the Upper Nullawarre coming in 22 mTVD deeper than predicted and water-wet. The Waarre A in Halladale-1 DW2 also proved water-wet, but this was not unexpected, and it is possible there could be gas in the unit further up-dip on the structure.

5. WELL STRATIGRAPHY

The stratigraphic section intersected in Halladale-1 DW2 is illustrated in the Composite Well Log (Enclosure 1). Formation tops were picked based primarily on electric logs supported by cuttings lithologies and ROP breaks.

Cuttings in Halladale-1 DW2 were collected, washed and described at ten metre intervals from 855 mMD down to 1770 mMD, then at five metre intervals down to TD (1941 mMD) except over the cored interval (1808.0 – 1835.0 mMD) where they were collected at intervals of between one and eight metres. The lithology and composition of the cuttings is summarised in Appendix 6 of the Halladale-1 DW2 Basic Data Report.

To date the Cretaceous interval intersected in the well, thirty cuttings samples were collected for palynological analysis, plus three samples from Core 1. No samples were collected from the Tertiary section. The samples were processed by Core Laboratories in Perth and examined by Dr Roger Morgan of Morgan Palaeo Associates. A copy of the species lists for these samples is included in Appendix 11 of the Halladale-1 DW2 Basic Data Report, and a copy of the interpretive report in Appendix 1 of this volume.

Five sandstone samples were also collected for petrographic examination; one from the Flaxman Formation and four from the Waarre C. The samples were prepared by Petrographic Technical Services in Queensland and described by Dr Sally Phillips of Phillips-Gerrard Petrology Consultants. A copy of the petrology report is included in Appendix 2 of this volume.

WANGERRIP GROUP

Pember Mudstone
(– 870.9 mMD)

The Pember Mudstone in Halladale-1 DW2 is represented by 72.9 mTVD of silty claystone with minor interbedded sandstone and siltstone. The silty claystone ranges from light grey to greenish-grey, pale brown and yellowish grey in colour, and is soft, amorphous to dispersive, with trace to 5% pyrite and trace glauconite. The siltstones are dark grey to brownish grey in colour and sub-blocky with trace mica. The sandstones are colourless to frosted white in colour, translucent to transparent, loose, and either very fine or fine- to medium-grained, with subangular to subrounded, poorly-sorted, slightly spherical to spherical grains and 10 to 15% visual porosity.

Pebble Point Formation
(870.9 – 938.7 mMD)

The Pebble Point Formation in Halladale-1 DW2 is represented by 67.8 mTVD of sandstone with minor interbedded silty claystone and claystone. The sandstone is pale orange-brown to light brown and greyish-orange in colour, translucent to clear, loose, and predominantly fine- to medium-grained, with angular to sub-rounded (occasionally rounded), poorly to occasionally moderately sorted, sub-spherical grains and 20% visible porosity. The silty claystone varies from medium grey to medium dark-grey and greyish orange in colour, and is generally soft, amorphous and dispersive. The claystone is medium dark grey to dark grey in colour, soft to firm, amorphous, and dispersive.

Massacre Shale
(938.7 – 948.0 mMD)

The Massacre Shale in Halladale-1 DW2 is represented by 9.2 mTVD of silty claystone with a distinctive high GR response that grades up into a fine-grained argillaceous sandstone.

SHERBROOK GROUP

Paaratte Formation
(948.0 – 1386.3 mMD)

The Paaratte Formation in Halladale-1 DW2, which here includes the Timboon Sandstone, is represented by 416.4 mTVD of interbedded sandstone, sandy claystone, silty claystone and claystone. The sandstones range in colour from very light grey to yellowish-grey and very pale orange near the top of the unit (948.0 – 980.0 mMD), to yellowish-grey to very light grey and white in the middle (980.0 – 1280.0 mMD), and light-grey toward the base (1280.0 – 1386.3 mMD). They are predominantly very fine- to fine-grained, occasionally medium-grained, loose to friable, with angular to rounded, poorly to moderately sorted, slightly elongate to slightly spherical framework grains with 15 to 20% visual porosity. Calcite cement is present in trace amounts below 1220 m and pyrite is a common trace accessory below 1120 mMD.

The sandy claystones in the upper half of the formation down to 1180 mMD range in colour down-hole from medium dark-grey to light olive grey and medium grey (960 – 1010 mMD), to medium light grey and medium grey (1040 – 1110 mMD), occasionally dark grey (1120 – 1140 mMD), then light grey to medium grey (1160 – 1180 mMD). The sandy claystones are

described as being very soft to soft, amorphous to dispersive, with coal, pyrite, mica and glauconite present in trace amounts.

The silty claystones primarily occur in the lower half of the formation between 1190 and 1330 mMD, but also near the top of the formation between 1000 and 1020 mMD. They are predominantly light to medium grey in colour, occasionally dark grey, brownish grey or light olive grey, and very soft to soft (occasionally soft to firm), amorphous to dispersive. Carbonaceous matter is common, with pyrite, lithic fragments and mica present in trace.

The claystones occur at the base of the formation below 1340 mMD. They are mainly medium light grey to light grey in colour, occasionally light olive grey and brownish grey, very soft to soft, amorphous and dispersive, with trace amounts of carbonaceous matter and pyrite.

Biostratigraphic dating (Table 3) indicates the formation in the well ranges from Lower A *X.australis* Zone to *M.druggi* Zone (Middle Campanian to Late Maastrichtian) in age and was deposited in a shelfal marine environment at the base trending to nearshore marine, possibly very nearshore marine, toward the top.

Table 3. Paaratte Formation micropalaeontological results

SAMPLE DEPTH (mMD)	TYPE	DINOFLAGELLATE ZONE	AGE	ENVIRONMENT
960 - 970	CUTTS	*M.druggii*	Middle to Late Maastrichtian	very nearshore marine
1000 – 1010	CUTTS	*I.pellucidum*	Late Campanian – early Maastrichtian	nearshore marine
1050 - 1060	CUTTS	*I.pellucidum*	Late Campanian – early Maastrichtian	marginal marine
1100 - 1110	CUTTS	*I.korojonense*	Late Campanian	nearshore marine
1180 - 1190	CUTTS	*X.australis* Upper	Middle Campanian	marine
1240 - 1250	CUTTS	*X.australis* Lower C	Middle Campanian	shelfal marine
1310 - 1320	CUTTS	*X.australis* Lower A	Middle Campanian	shelfal marine

Skull Creek Mudstone
(1386.3 – 1537.8 mMD)

The Skull Creek Mudstone in Halladale-1 DW2 is represented by 140.0 mTVD of silty claystone with minor interbedded sandstone.

The silty claystone is predominantly light grey to medium grey and brownish-grey in colour, occasionally light brownish-grey to dark grey and light olive grey, largely very soft to soft (occasionally soft to firm), with an amorphous to dispersive fracture (occasionally blocky), and trace carbonaceous matter, pyrite, glauconite and mica.

The sandstones are light grey to white in colour, transparent to translucent, loose, very fine to medium-grained, with subangular to subrounded, moderate to well-sorted, slightly elongate to slightly spherical framework grains. Visual porosity is very good (20%) with mica and/or pyrite present in trace amounts.

Biostratigraphic dating (Table 4) indicates the formation is *N.aceras* Zone (Early Campanian) in age and was deposited in a nearshore to very nearshore marine environment.

Table 4. Skull Creek Mudstone micropalaeontological results

SAMPLE DEPTH (mMD)	TYPE	DINOFLAGELLATE ZONE	AGE	ENVIRONMENT
1400 - 1410	CUTTS	*N.aceras*	Early Campanian	very nearshore marine
1450 - 1460	CUTTS	*N.aceras*	Early Campanian	very nearshore marine
1510 - 1520	CUTTS	*N.aceras*	Early Campanian	nearshore marine

Nullawarre Formation
(1537.8 – 1588.8 mMD)

The Nullawarre Formation in Halladale-1 DW2 is 47.5 mTVD thick and consists of two sandstones 14.7 and 8.5 m thick separated by a 24.3 m thick silty claystone. The upper sandstone (1537.8 – 1553.6 mMD) is light grey in colour, transparent, loose, predominantly very fine-grained and moderate to well-sorted, with subrounded to rounded, slightly spherical to spherical framework grains and 15% visual porosity. Glauconite and mica are present in trace amounts. The lower sandstone (1579.7 – 1588.8 mMD) is very light grey in colour, transparent, loose to friable, largely very-fine grained, with subangular to rounded, moderate to well-sorted, slightly spherical to spherical framework grains and a visual porosity of 15%. Trace amounts of glauconite were also observed along with trace amounts of calcite and dolomite cement.

The silty claystone that separates the two sandstones is 24.3 mTVD thick and is light grey, light olive-grey to brownish-grey in colour, very soft to soft (occasionally firm), amorphous to dispersive or sub-blocky, with up to 2% carbonaceous matter and trace glauconite.

Belfast Formation
(1588.8 – 1740.2 mMD)

The Belfast Formation in Halladale-1 DW2 is represented by 140.6 mTVD of silty claystone and claystone. The silty claystone primarily occurs in the lower half of the formation from 1670 mMD down. It is generally medium light grey to olive grey in colour, occasionally brownish-grey or speckled greenish-grey, soft to firm, amorphous to blocky or massive, with

up to 20% glauconite and trace pyrite. The claystone in the upper half of the formation is light grey to light olive grey in colour, occasionally brownish-grey or mottled green, soft to firm, amorphous to sticky, with up to 5% glauconite and trace pyrite, carbonaceous matter and calcite cement.

Halladale-1 DW2 is interpreted to have intersected the bounding fault on the south side of the Halladale Prospect approximately 20 mMD below the top of the Belfast Formation at a depth of 1608.8 mMD.

Biostratigraphic dating (Table 5) indicates the formation in the well ranges from Upper *C.striatoconus* Zone to *I.cretaceum* Zone (Coniacian to Santonian) in age and was deposited in a largely very nearshore to nearshore marine environment deepening to offshore marine toward the top.

Table 5. Belfast Formation micropalaeontological results

SAMPLE DEPTH (mMD)	TYPE	DINOFLAGELLATE ZONE	AGE	ENVIRONMENT
1590 - 1600	CUTTS	*I.cretaceum*	Santonian	offshore marine
1620 - 1630	CUTTS	*I.cretaceum*	Santonian	offshore marine
1650 - 1660	CUTTS	*I.cretaceum*	Santonian	nearshore marine
1680 - 1690	CUTTS	*I.cretaceum*	Santonian	nearshore marine
1690 - 1700	CUTTS	*O.porifera* Upper	Early Santonian	very nearshore marine
1710 – 1720	CUTTS	*O.porifera* Upper	Early Santonian	very nearshore marine
1730 - 1740	CUTTS	*C.striatoconus* Upper	Coniacian	nearshore marine

Flaxman Formation
(1740.2 - 1803.7 mMD)

The Flaxman Formation in Halladale-1 DW2 is represented by 59.1 mTVD of predominantly silty claystone with lesser claystone and minor argillaceous siltstone and sandstone.

The silty claystones are found in the upper half of the formation and vary markedly in colour from light olive grey to medium grey, dark grey, purplish-grey, olive grey, green, speckled green, greenish-grey, pale yellow and pale yellowish-brown. Those between 1760 and 1775 mMD are described as soft to firm and amorphous to sub-blocky in appearance, whereas those higher up in the formation between 1740 and 1760 mMD are described as firm to moderately hard and blocky to massive in appearance. Glauconite is common (up to 10%) with mica and pyrite present in trace amounts. The claystones occur in the lower half of the formation below 1775 mMD and are predominantly light grey in colour, occasionally medium light grey, and very soft to soft, amorphous to sticky, with trace glauconite and carbonaceous matter.

The argillaceous siltstones occur toward the top of the formation and are medium to dark grey in colour, occasionally brownish grey to yellowish brown, mottled in parts. It is soft to firm and amorphous to blocky in appearance, and slightly calcareous with trace glauconite.

The sandstones in the upper part of the formation are described as light grey to white in colour, occasionally pale green to pale yellow, loose, predominantly medium- to coarse-grained, with subrounded to rounded, poor to well-sorted, slightly elliptical to slightly spherical framework grains, and 20% visual porosity. Petrographic analysis of cuttings from the interval where this sandstone is described yielded three types of rock fragments: 1) silty to sandy mudstone, 2) carbonate cemented sandy ironstone, and 3) glauconitic mudstone (see Appendix 2). The carbonate cemented sandy ironstone consists of fine to medium sand-size iron-rich ooids with cores of hematite and quartz surrounded by concentric laminae of goethite and/or siderite. Authigenic minerals present include rounded medium sand size bright green grains of glaucony with a wormy texture typical of glauconite. The glauconite, ooids and quartz grains are all rimmed by chlorite, but the rims are absent at grain contacts suggesting the chlorite precipitated after the onset of compaction. The remaining pore spaces are filled by clear carbonate spar which also partially replaces detrital quartz grains in places.

The sandstones near the base of the formation are very light grey to light grey and white in colour, occasionally pale green to pale yellow, loose to friable and very fine-grained, with subrounded to rounded, well to very well sorted, slightly spherical to spherical framework grains and 10% visual porosity.

The age of the Flaxman Formation in Halladale-1 DW2 is poorly constrained due to the absence of key taxa and low microfossil yields. No age determination could be assigned to the four deepest samples (see Table 6), while the two shallowest samples could only be tentatively assigned to the Lower *C.striatoconus* Zone which would make the top of the unit possibly early Coniacian in age. Environment of deposition is interpreted to largely nearshore marine.

Table 6. Flaxman Formation micropalaeontological results

SAMPLE DEPTH (mMD)	TYPE	DINOFLAGELLATE ZONE	AGE	ENVIRONMENT
1740 - 1750	CUTTS	*C.striatoconus* Lower ?	early Coniacian ?	nearshore marine
1750 - 1760	CUTTS	*C.striatoconus* Lower ?	early Coniacian ?	shelfal marine
1765 - 1770	CUTTS	indeterminate	unknown	nearshore marine
1775 - 1780	CUTTS	indeterminate	unknown	nearshore marine
1785 - 1790	CUTTS	indeterminate	unknown	marine (undiff)
1795 - 1800	CUTTS	indeterminate	unknown	marine (undiff)

Waarre Formation
(1803.7 – 1897.6 mMD)

Waarre C
(1803.7 – 1827.2 mMD)

The Waarre C in Halladale-1 DW2 is 21.9 mTVD thick and consists largely of sandstone with two beds of interbedded silty claystone, siltstone and claystone approximately 1.3 and 1.6 mTVD thick near the top and base of the unit respectively.

The sandstone is predominantly very light-grey in colour, occasionally pale yellow to light-grey and off-white, translucent to transparent, loose, medium- to coarse-grained, with angular to subrounded, poorly to moderately sorted, slightly elongated to slightly spherical framework grains and 20% visual porosity. Carbonaceous matter is present in trace amounts. Petrographic analysis of four core plug offcuts from Core 1, including two from the carbonate-cemented band at 1818.6 mMD, indicates the sandstones are quartz-rich with an average Q:F:R ratio of 91:4:5.

The siltstones are predominantly brownish-grey in colour, occasionally olive grey to greyish-brown, firm to moderately hard, sub-blocky to massive, with 5% glauconite and trace mica, carboaneous matter and pyrite. The silty claystones range from greenish-grey, light grey, medium grey to brownish-grey in colour (occasionally light greenish-grey or pale brown), and are very soft to soft, amorphous to sticky, with trace glauconite, carbonaceous matter and pyrite. The claystones are yellowish-grey to pale brown and very light brown in colour, very soft to soft and amorphous to dispersive.

Two samples were collected from the Waarre C in Core 1 for biostratigraphic dating, one from the shale near the top of the core and the other from the shale near the base. Both samples yielded *P.infusorioides* middle 'a' Zone (Turonian) dinoflagellates. Environment of deposition is interpreted to be marginal marine.

Table 7. Waarre C micropalaeontological results

SAMPLE DEPTH (mMD)	TYPE	DINOFLAGELLATE ZONE	AGE	ENVIRONMENT
1801.67	CORE	*P.infusorioides* Middle 'a'	Turonian	marginal marine
1821.53	CORE	*P.infusorioides* Middle 'a'	Turonian	marginal marine

Waarre B

(1827.2 – 1855.1 mMD)

The Waarre B in Halladale-1 DW2 is represented by 26.1 mTVD of silty claystone with minor interbedded claystone, argillaceous siltstone and sandstone. The silty claystone is largely light to medium grey in colour, occasionally dark grey or brownish-grey to greenish-grey, very soft to soft, amorphous to dispersive, blocky, with trace glauconite, carbonaceous matter and mica. The claystone is also largely light to medium grey in colour, occasionally very light grey, brownish-grey to dark grey, and very soft to firm, amorphous to sticky, with trace glauconite, carbonaceous matter, mica and pyrite. The argillaceous siltstones are primarily medium grey in colour, occasionally dark grey or brownish-grey, soft to firm, amorphous to blocky, with trace glauconite and carbonaceous matter. The sandstones are white, off-white to very light grey in colour, occasionally pale yellow, loose, medium to coarse-grained, with angular to subrounded, poor to moderately well-sorted, slightly elongate to slightly spherical framework grains and 20% visual porosity.

Three samples were collected from the Waarre B for biostratigraphic dating, one from the top of the unit at the base of the Core 1 and two cuttings from the middle and base of the unit (see Table 8). The samples indicate the unit spans the *P.infusorioides* Lower 'b' and *P.infusorioides* Middle 'a' Zones and is Turonian in age. The environment of deposition is interpreted to be nearshore to very nearshore marine, possibly shelfal marine at the base.

Table 8. Waarre B micropalaeontological results

SAMPLE DEPTH (mMD)	TYPE	DINOFLAGELLATE ZONE	AGE	ENVIRONMENT
1831.23	CORE	*P.infusorioides* Middle 'a'	Turonian	nearshore marine
1835 - 40	CUTTS	*P.infusorioides* Lower 'c'	Turonian	very nearshore marine
1850 - 55	CUTTS	*P.infusorioides* Lower 'b'	Turonian	shelfal marine ?

Waarre A

(1855.1 – 1897.6 mMD)

The Waarre A in Halladale-1 DW2 is represented by 40.0 mTVD of interbedded silty claystone and sandstone. The silty claystones vary from light grey, medium grey, brownish grey, light brown, light greenish grey, light green to white in colour, and are typically very soft to soft, amorphous to dispersive, with trace carbonaceous matter and glauconite. The sandstones are light grey to white in colour, translucent, loose, typically fine- to medium grained (occasionally very fine-grained), with subangular to subrounded , poorly to well-sorted, slightly elongate to slightly spherical framework grains and 20% visual porosity with trace pyrite and glauconite.

Biostratigraphic analysis of three samples from the top, middle and base of the unit (see Table 9) indicates it is *P.infusorioides* lower 'b' Zone (Turonian) in age and was deposited in a nearshore marine environment.

Table 9. Waarre A micropalaeontological results

SAMPLE DEPTH (mMD)	TYPE	DINOFLAGELLATE ZONE	AGE	ENVIRONMENT
1865 - 1870	CUTTS	*P.infusorioides* Lower 'b'	Turonian	nearshore marine
1870 - 1875	CUTTS	*P.infusorioides* Lower 'b'	Turonian	nearshore marine
1875 - 1880	CUTTS	*P.infusorioides* Lower 'b'	Turonian	nearshore marine

OTWAY GROUP

Eumeralla Formation
(1897.6 – 1941.0 mMD TD)

The Eumeralla Formation is represented by 41.0 mTVD of interbedded sandstone and silty claystone.

The sandstones are predominantly light grey to white in colour (occasionally light yellow or light green), translucent, loose, and fine- to medium-grained, with subangular to subrounded, moderate to well-sorted, slightly elongate to slightly spherical grains, 15% visual porosity, trace calcite cement, and trace accessory chlorite and carbonaceous matter.

The silty claystones are predominantly light brownish grey, brownish grey, light greenish grey to light green in colour, soft to firm, and amorphous to blocky in appearance, with trace chlorite and carbonaceous matter.

Only one sample was collected from the Eumeralla Formation in Halladale-1 DW2 for biostratigraphic dating (see Table 10). The sample yielded *P.infusorioides* Lower 'b' Zone dinoflagellates, but Morgan (see Appendix 1) believes this age determination is questionable as the sample yield was extremely low and the majority of identified key taxa were probably cavings from higher up in the well.

Table 10. Eumeralla Formation micropalaeontological results

SAMPLE DEPTH (mMD)	TYPE	DINOFLAGELLATE ZONE	AGE	ENVIRONMENT
1900 - 1905	CUTTS	*P.infusorioides* Lower 'b'	Turonian	nearshore marine

6. HYDROCARBON SHOWS

The recording of mud log gas data in Halladale-1 DW2 commenced at a depth of 835 mMD in the middle of the Pember Mudstone. From this point down to the middle of the Flaxman Formation, the total gas reading in the well rarely exceeded 1.0% except for several small peaks at 1256 mMD (1.94 %), 1443.5 mMD (3.18%), 1547.5 mMD (1.47 %) and 1585.5 mMD (2.55 %) associated with thin sands in the Paaratte, Skull Creek and Nullawarre formations. No fluorescence was observed in any of these sands.

At 1783 mMD, in the middle of the Flaxman Formation, the total gas reading in the well rose slightly, peaking several times in the lower half of the formation at 1784.0 mMD (5.02 %), 1794.0 mMD (2.52 %) and 1797.0 mMD (2.49 %). Soon after penetrating the top of the Waarre C (1803.7 mMD), the total gas reading in the well started to climb rapidly, peaking at 13.54 % at 1807.5 mMD. At 1808.0 mMD, a 27 m long conventional core (Core 1: 1808.0 – 1835.0 mMD) was acquired through the Waarre C (1803.7 – 1827.2 mMD) and upper part of the Waarre B (1827.2 – 1855.1 mMD). The total gas reading during this operation ranged between 0.19 and 26.90% over the Waarre C interval (average 7.52 %), and 0.10 to 1.52 % over the Waarre B interval (average 0.46 %). No fluorescence was observed during coring operations.

After Core 1 had been retrieved, drilling continued down through the rest of the Waarre B, the Waarre A, and into the Eumeralla Formation until TD was reached (1941.0 mMD). During this period, the total gas reading over this interval ranged between 0.11 to 0.57 % (average 0.34 %). No gas peaks or fluorescence observed.

7. RESERVOIR EVALUATION

7.1 Petrophysical Analysis

A detailed petrophysical review of the Late Cretaceous section intersected in Halladale-1 DW2 was conducted to assess the reservoir quality and hydrocarbon saturation of all zones that displayed good hydrocarbon shows while drilling. A copy of the petrophysical report is included in Appendix 3 of this volume, with a summary of the net sand and net pay in the well provided below in Table 11.

Table 11: Halladale-1 DW2 petrophysical summary

FORMATION	GROSS THICKNESS			NET SAND				NET PAY				
	TOP (mMD)	BASE (mMD)	THICK (mMD)	THICK (mMD)	N:G (%)	PHIT (%)	K (mD)	THICK (mMD)	N:G (%)	PHIT (%)	K (mD)	Sw (%)
Nullawarre	1538.5	1589.3	50.8	18.4	36.2	25.2	1.3	0	0			
Belfast	1589.3	1749.2	159.9	0	0							
Flaxman	1749.2	1803.7	54.5	3.2	0.6	22.2	2224	0	0			
Waarre C	1803.7	1827.2	23.5	18.6	79.1	22.3	1628	18.6	79.1	22.3	1628	18.5
Waarre B	1827.2	1855.1	27.9	0	0							
Waarre A	1855.1	1897.9	42.8	17.6	41.1	20.4	11.1	0	0			
Eumeralla	1897.9	1941.0	43.1	1.0	2.3	19.6	8.6	0	0			

Net Sand cut-offs: Vshale < 40%, K > 0.2 mD
Net Pay cut-offs: Net Sand = 1, Sw < 60%

Log analysis indicates the Upper and Lower Nullawarre Sandstones in Halladale-1 DW2 are both water wet. The two sands have a combined gross thickness of 24.9 mMD with a net sand thickness of 18.4 mMD (73.9% N:G) and average porosity of 25.2%.

The Waarre C is 23.5 mMD thick with 18.6 mMD of net sand (79.1% N:G). The calculated net pay is 18.6 mMD with an average porosity of 22.3% and water saturation of 18.5%. The GWC for this unit was not intersected in the well.

The Waarre A in the well is 42.8 mMD thick with 17.6 mMD of net sand (41.1% N:G). No net pay was calculated for this unit.

7.2 Core Analysis

To calibrate the petrophysical work done on Halladale-1 DW2, Core 1 (1808.0 – 1835.0 mMD) was sent to Core Laboratories Australia Pty Ltd in Perth for Routine Core Analysis (RCA) and Special Core Analysis (SCAL).

For the RCA study, eighty-four horizontal plugs were collected from Core 1 at intervals of between 20 and 40 cm, fifty-three from the Waarre C and twenty-one from the Waarre B, plus sixteen additional vertical plugs at intervals of approximately 1 metre. The average

overburden porosity and permeability of the Waarre C plugs is 20.7 % (range: 2.6 – 28.0%) and 2492 mD (range: 0.033 - >10,000 mD), with thirteen (24.5%) of the plugs having permeabilities greater than 5000 mD, including six with permeabilities greater than 10000 mD. The Waarre B plugs, in contrast, have an average overburden porosity and permeability of 8.6% (range: 4.5 – 10.9 %) and 0.012 mD (range: 0.003 – 0.046 mD) respectively. A copy of the RCA report is included in Appendix 13 of the Halladale-1 DW2 Basic Report.

For the SCAL study, twenty-eight plugs from the Waarre C were selected for analysis. The results of this study are contained in the SCAL report located in Appendix 4 of this volume.

7.3 Core Description

To understand the depositional setting of the Waarre C and Waarre B at Halladale, a detailed sedimentological and ichnological study of Core 1 (1808.0 – 1835.0 mMD) was undertaken. A copy of the Core Description report, including core photographs and graphical core log representations, is included in Appendix 5 of this volume.

The Waarre B portion of the core consists of 7.0 m of interbedded bioturbated muddy siltstone and laminated sandstone, interlaminated bioturbated muddy siltstone and laminated silty sandstone, intensely bioturbated muddy sandstone with rare weakly bioturbated mudstone laminations, and intensely bioturbated muddy siltstone. The sediments are interpreted to have been deposited in a restricted marginal marine environment ranging from distal lower shoreface, offshore transition, transgressive shoreface to upper offshore based on the types of primary sedimentary structures present in each and trace fossil assemblages.

The Waarre C portion of the core consists of 19.0 m of cross-bedded medium-grained sandstone to granule conglomerate, massive mudstone with interbedded sandstone and sandy siltstone to sandstone with common mudstone laminations. The sediments are interpreted to have been deposited in a fluvial environment comprising low sinuosity fluvial channels, ponded abandoned channels infilled by crevasse splays, and tidally-influenced fluvial channels.

Analysis of the RCA data from Core 1 indicates reservoir quality is strongly facies dependent, with the fluvial channel and tidally-influenced fluvial channel deposits in the Waarre C having the highest permeability and porosity, closely followed by the amalgamated crevasse splay sediments, whilst the restricted marine sediments have the lowest permeability and porosity.

7.4 STAR Interpretation

A high-resolution resistivity formation image was run in Halladale-1 DW2 over the interval 1680 – 1900 mMD from the middle of the Belfast Formation down to just below the top of the Eumeralla Formation using the Baker Atlas STAR tool. The aim of the survey was to provide additional information on the palaeoenvironmental setting of the Waarre A and Waarre C in the well, including sediment palaeotransport directions and data on the orientation and density of natural and induced fractures in the borehole. A copy of the STAR Interpretation report is included in Appendix 6 of this volume.

Structural dip analysis indicates the stratigraphic interval covered by STAR image can be divided into three structural zones whose boundaries correspond with the base of the glauconitic argillaceous sandstone near the top of the Flaxman Formation, and top of the Waarre B. The analysis indicates the Waarre A, B and C and lower half of the Flaxman Formation dip toward to east-northeast at between 16 and 19^{o}, while the overlying upper Flaxman Formation and lower half of the Belfast Formation dip toward the southeast at about 16^{o} (see Table 3 in Appendix 6)

The sedimentological component of the study was carried out using wireline logs and cuttings to help interpret the fabrics observed in the STAR images. Six lithofacies were identified and five lithofacies associations. The Waarre A in the well (1855.1 – 1897.6 mMD) is interpreted to consist predominantly of tidal flat / tidal channel deposits, with possible lower shoreface and offshore shelf deposits in the middle of the unit between 1869 and 1880 mMD, while the Waarre C is interpreted to consist predominantly of low sinuosity fluvial channel deposits (71.7% of unit) interbedded with fine-grained abandoned channel fills (15.2%) and lesser crevasse-splay (6.5%) and tidally-influenced channel (6.5%) deposits.

Palaeotransport analysis of sandstones within the Waarre A indicates they are characterised by internal stratification fabrics with low azimuthal variation. The relationship between intra-set lamination (cross bedding) and coset boundaries suggest that sediment transport occurred normal to the depositional dip. The cross beds show a low azimuthal spread with a predominant east to southeast direction, while the flat lying intraset surfaces show a 270° azimuthal spread, indicative of deposition within channel and crevasse splay environments. Sedimentary dips within sandstones within the Waarre A display 180º azimuthal spread, with an overall westerly orientation that reflects the predominant current direction. These sediments are mainly interpreted to have been deposited in a tidal flat/shoreface environment.

Borehole breakout analysis indicates fractures in the borehole produced by compressional failure are oriented NE-SW, with an average strike orientation of 048^{o} - 228^{o}. The

orientation of the breakouts indicates Shmax is oriented NW – SE (138^{o} – 318^{o}), which is inline with Shmax orientations obtained in other offshore wells in the eastern Otway such as Minerva-1 (142^{o} – 322^{o}), Minerva-2A (144^{o} – 324^{o}) and Eric The Red-1 (137^{o} – 317^{o}) (http://www.asprg.adelaide.edu.au/asm/).

8. FORMATION TESTING

8.1 Formation Pressure Testing

Two runs were made with the Baker Atlas Reservoir Characterisation Instrument (RCI) in Halladale-1 DW2. The first run (Suite 1 Run 2) acquired formation pressure data from the Upper Nullawarre Sandstone, Lower Nullawarre Sandstone, Flaxman Formation, Waarre C and Waarre A over the interval 1542.0 to 1856.5 mMD. At 1858 mMD, the RCI tool became stuck. After it had been worked free, the tool was removed from the hole and then run back in on pipe (Suite 1 Run 3) to collect additional formation pressure data from the Waarre A over the interval 1858.3 mMD to 1902.4 mMD, plus fluid samples from the Waarre C (see Section 8.3). The stratigraphic position of the pretest points in Halladale-1 DW2 is shown on the Composite Well Log (Enclosure 1).

A total of thirty-two pretests were performed over the two RCI runs, resulting in fifteen valid pressures - one from the Upper Nullawarre Sandstone, ten from the Waarre C, and four from the Waarre A (see Table 12). The basic data from these surveys is tabled in Appendix 8 of the Halladale-1 DW2 Basic Data Report, and a copy the interpretive report included in Appendix 7 of this volume.

Table 12. Halladale-1 DW2 pressure survey summary

FORMATION	# of PRETESTS	VALID	FLUID
Upper Nullawarre Sst	3	1	WATER
Lower Nullawarre Sst	4	0	WATER
Flaxman Formation	3	0	WATER
Waarre C	10	10	GAS
Waarre B	4	0	WATER
Waarre A	7	4	WATER
Eumeralla Formation	1	0	WATER

Figure 3 in Appendix 7 is a pressure versus depth plot for the Waarre C and Waarre A in Halladale-1 DW1, DW2 and DW3. Analysis of the pressure data from the Waarre A in Halladale-1 DW2 indicate the water points fall on the same water line as the water points from the Waarre A in Halladale-1 DW1, which indicates the Waarre A aquifers at Black Watch and Halladale are in pressure communication. The pressure data from the Waarre C in Halladale-1 DW2 yielded a gas line approximately 11 psi lower than the gas line from the Waarre C in Halladale-1 DW1, indicating the Waarre C gas columns at Black Watch and Halladale are not in pressure communication. The interpreted GWC for the Waarre C at Halladale is 1760 mSS using the Waarre C water line from Halladale-1 DW3.

A single valid pressure point was also obtained from water-wet Upper Nullawarre Sandstone in Halladale-1 DW2. If the pressure point is reliable, then the water gradient in the sand is approximately 26 psi higher than the water gradient onshore in the Nullawarre Sandstone in McIntee-1, 13 km to the northeast of Halladale-1 DW2.

8.2 Fluid Sampling

Three 840 cc gas samples were collected from the top of the Waarre C at 1804.7 mMD during the second RCI run (Suite 1 Run 3). The results of the gas analysis are summarised in Section 9.1. No other fluid samples were collected from the well.

8.3 Production Testing

No production tests were run in Halladale-1 DW2.

9. GEOCHEMICAL STUDIES

9.1 Gas Composition

The reservoir fluid recovered from the Waarre C in Halladale-1 DW2 was sent to Petrolab Laboratory in Adelaide for compositional, PVT, condensate physical properties, gas contamination (H_2S, Hg) and BTX analysis. A detailed report on the results of these tests is included in Appendix 8 of this volume. Compositional analysis of the gas in the Waarre C at Halladale indicates it is very similar in composition to the gas in the Waarre C at Black Watch but is slightly drier (90.67% C_1 v 87.8% C_1), has a slightly lower C5+ ratio (11.3 bbls/MMscf v 12.6 bbls/MMscf), and contains slightly less nitrogen (1.36 % v 2.00%) but about the same amount of carbon dioxide (0.45 % v 0.48 %) (see Table 13). The slight difference in the composition of the two gases suggests the pools are not in communication with each other, which is supported by the 10 psi difference in the two gas lines (see Section 8.1).

Table 13. Composition of Waarre C gas samples from Halladale-1 DW1 and DW2

Well	DW1	DW1	DW2	DW2	DW2
Formation	Waarre C	Waarre C	Waarre C	Waarre C	Waarre C
Cylinder	L-128	L-007	L-332	L-188	L-076
Depth (mRT)	1772.6	1772.6	1804.6	1804.6	1804.6
	MOLE %	MOLE %	MOLE %	MOLE %	MOLE %
H2S	0	0	0	0	0
CO2	0.46	0.49	0.47	0.39	0.50
N2	1.88	2.11	1.36	1.36	1.38
C1	87.85	87.49	90.65	90.47	90.89
C2	5.30	5.24	4.17	4.26	4.20
C3	2.19	2.17	1.62	1.59	1.61
iC4	0.56	0.52	0.30	0.38	0.32
nC4	0.56	0.62	0.38	0.42	0.35
iC5	0.19	0.21	0.12	0.13	0.11
nC5	0.15	0.17	0.10	0.11	0.09
C6	0.26	0.30	0.18	0.20	0.15
C7	0.34	0.38	0.28	0.30	0.21
C8	0.12	0.14	0.11	0.1	0.07
C9	0.09	0.10	0.11	0.13	0.05
C10	0.04	0.05	0.08	0.08	0.03
C11	0.01	0.01	0.04	0.01	0.03
C12+	0.00	0.00	0.03	0.01	0.01
Molecular Weight C12+	275.0	275.0	186.4	188.4	173.4
Density C12+(gm/cc @-60°F)	0.862	0.862	0.808	0.821	0.810
C5+ Ratio (STB/MMSCF)	11.8	13.3	11.0	11.5	7.5
LPG Ratio (Tonnes/MMSCF)	1.93	1.93	1.32	1.39	1.31
Wetness (C2-C4/C1-C4)*100	8.9%	8.9	6.7	6.8	6.7

Wet chemistry analysis indicates the Waarre C gas at Halladale has virtually no H2S (< 0.2 ppm) but has a relatively high mercury content of between 200 to 270 PPB. However, the RCI containers used for sampling were not specifically prepared for this sort of test and could have been contaminated beforehand. BTX analysis indicates low level of benzene, toluene and xylene are also present.

9.2 Condensate GC-MS

A sample of the condensate recovered from the Waarre C in Halladale-1 DW2 was sent to Geotechnical Services in Perth for whole oil, saturate, aromatic and branched/cyclic GC-MS analysis. A copy of the results of this study is included in Appendix 9 of this volume. As with the Black Watch Waarre C condensate (see Halladale-1 DW1 Interpretive WCR), the Halladale Waarre C condensate has an n-alkane profile indicative of high thermal maturity but it also has a relatively high concentration of 1,2,5-trimethylnaphthalene suggesting it has been partially contaminated by organic matter of lower thermal maturity, either indigenous to sediments along the migration pathway or in the reservoir itself, which is consistent with its Methyl Phenanthrene Index (0.37). Biomarker data also suggests the organic matter in the condensate is largely marine algal in origin, with some contribution from a terrestrial higher plant source. The isosterane distribution and high pristane - phytane ratio (7.78) suggest the source rocks accumulated in a near shore marine environment, probably in an estuarine or bay type setting, under oxic conditions. The abundance of marine-derived organic matter in the condensate with a concomitant contribution of terrigenous derived material is consistent with deposition in such a setting. The overall similarity in the composition of the Halladale and Black Watch condensate samples suggests they are genetically related and probably came from the same, or very similar, source facies.

9.3 Compound Specific Isotope Analysis

To help determine the maturity and source of the gas recovered by the RCI tool from the Waarre C in Halladale-1 DW2, a sample of the gas was sent to Isolab in Neerijnen, Holland, for compound specific isotope analysis (CSIA).

Table 14. CSIA of Waarre C gases from Halladale-1 DW1 and Halladale-1 DW2

SAMPLE ID	$\delta^{13}C$ C_1	$\delta^{13}C$ C_2	$\delta^{13}C$ C_3	$\delta^{13}C$ i-C_4	$\delta^{13}C$ n-C_4	$\delta^{13}C$ i-C_5	$\delta^{13}C$ n-C_5	δD C_1	$\delta^{13}C$ CO_2	$\delta^{15}N$ N_2
DW1 1772.6 mMD	-32.8	-23.3	-22.5	-22.0	-21.6	-22.5	-22.2	-166.0	-12.9	-4.3
DW2 1804.6 mMD	-31.7	-23.2	-22.6	-22.1	-21.9	-22.9	-22.8	-163.0	-12.2	+4.1

The isotope data (Table 14) indicates the gas samples from the Waarre C at Black Watch and Halladale have similar but slightly different isotopic compositions consistent with them being separate pools. As with the Black Watch Waarre C gas sample, the CSIA profile of the Halladale Waarre C gas sample matches the CSIA profiles for the gas onshore in the Boggy Creek, Fenton Creek, Lavers and Mylor fields, but not the gas offshore in the Minerva, La Bella, Geographe or Thylacine fields, suggesting the gas in the Waarre C at Halladale probably came from the same source facies that charged the onshore fields.

9.4 CO_2 Carbon Isotope Analysis

Carbon dioxide comprises 0.45% of the gas at Halladale. Stable carbon isotope analysis indicates the CO_2 has a $\delta^{13}C$ value of -12.2 ‰, which suggests it was probably generated during the diagenesis of Type III organic matter as magmatic CO_2 has isotopically heavier $\delta^{13}C$ values of between -8 and -4‰ as observed onshore at Boggy Creek where the CO_2, which comprises 88.7% of the gas in the field, has a $\delta^{13}C$ value of -6.4 ‰ (Mehin and Link, 1994).

9.5 Mud Gas Isotope Analysis

To assess the vertical and lateral connectivity of the Upper Nullawarre, Lower Nullawarre, Waarre C and Waarre A at Black Watch and Halladale, and whether the gas at these levels is from the same source, 78 mud gas samples were collected from Halladale-1 DW1, DW2 and DW3 for compositional and carbon isotope analysis. The twenty-two samples from Halladale-1 DW2 were collected at regular intervals of approximately 50 mMD from the Pember Mudstone down to TD, with additional samples collected at every significant gas peak. The basic data from this study is tabled in Appendix 16 of the Halladale-1 DW1 Basic Data Report. A copy of the interpretive report is included in Appendix 9 of this volume.

Figure 2 in Appendix 9 illustrates how the carbon isotope composition of methane, ethane and propane varies with depth in Halladale-1 DW1, DW2 and DW3. The stable isotope data indicates there is little difference in the $\delta^{13}C$ value of methane both down and between the three boreholes, suggesting a high degree of vertical connectivity between formations. The methane isotope data also indicates the gas is also very mature with $\delta^{13}C$ values ranging between -34.9‰ and -32.4 ‰. The narrow spread in the methane carbon isotope values, and the carbon isotope values for ethane (-24.0 to -22.9 ‰) and propane (-23.5 to -22.3 ‰), also suggest the gas is from the same source.

9.6 Fluid Inclusion Screening

To understand the migration of hydrocarbons into Black Watch and Halladale, 174 cuttings samples were collected from Halladale-1 DW1, DW2 and DW3 for Fluid Inclusion Screening (FIS). In Halladale-1 DW2, the cuttings (n = 62) were collected at intervals of 20 mMD from the Pember Mudstone down to the middle Flaxman Formation, then at 5 mMD intervals down to the base of the Flaxman Formation, then at intervals of between 5 and 27 mMD down to TD. A copy of the interpretive report is included in Appendix 10 of this volume.

No significant hydrocarbon indicator anomalies were identified in Halladale-1 DW2 except for a very minor gas / liquids signal at 1795 m near the base of the Flaxman Formation. No proximity-to-pay (PTP) anomalies were detected either. The absence of a FIS response over the Waarre C gas column could be because the formation in the well has not reached temperatures high enough for the formation of substantial quartz overgrowths (ie. > 80^{o}C), but this is considered unlikely because wireline readings from the well indicate the current formation temperature at the Waarre C level is approximately 85^{o}C and quartz overgrowths were observed in all four sandstone thin-sections from the Waarre C portion of Core 1 (see Appendix 2). One possible explanation is the Waarre C interval in the well (1803.7 – 1827.2 mMD) may have not been sampled heavily enough to see a FIS response, as only one sample was actually collected from the Waarre C itself (1808 mMD), with the next closest samples coming from the base of the Flaxman Formation (1800 mMD) and top of the Waarre B (1835 mMD).

10. CONTRIBUTIONS TO GEOLOGICAL KNOWLEDGE

Halladale-1 DW2 reached TD in Eumeralla Formation having met all of its technical objectives and demonstrated the anomalous amplitudes observed on seismic do represent gas-fill.

Geochemical analysis of the gas recovered from the Waarre C at Halladale indicates it is slightly drier than the gas at Black Watch (90.67% C1 v 87.8% C1). It also contains slightly less liquids (11.3 bbls/MMscf v 12.6 bbls/MMscf) and has a lower inerts content (1.81 % v 2.48%). Carbon isotope analysis indicates the gas was expelled during the early to peak gas window from a humic or lacustrine source, while CSIA indicates the gas probably came from the same source facies as the gas onshore in the Boggy Creek, Fenton Creek, Lavers and Mylor gas fields.

The slight difference in composition of the gas in the Waarre C at Black Watch and Halladale suggests the two pools are not in communication with each other, which is supported by pressure data which demonstrates there is a 10 psi difference in the Waarre C gas gradients at Black Watch and Halladale. Water pressure data from the Waarre A in Halladale-1 DW2 also yielded a water gradient matching the Waarre A water gradient in Halladale-1 DW1, confirming a common aquifer exists between the two fault blocks.

11. REFERENCES

GEOLOGICAL SURVEY OF VICTORIA 1995. The stratigraphy, structure geophysics and hydrocarbon potential of the Eastern Otway Basin. *Geological Survey of Victoria 103*. Department of Energy and Minerals.

MEHIN, K. AND LINK, A.G., 1994. Source, migration and entrapment of hydrocarbons and carbon dioxide in the Otway Basin, Victoria. *Australian Petroleum Exploration Association Journal, 34(1), pp. 439-459.*

PARTRIDGE, A., 2001. Revisied Stratigraphy of the Sherbrook Group, Otway Basin. Eastern Australasian Basins Symposium 2001, Hill, K.C. & Bernecker, T (eds.), p.455 – 464.

TICKELL, S.J., EDWARDS, J. & ABELE, C., 1992. Port Campbell Embayment 1:100,000 Map Geological Report. *Geological Survey of Victoria Report 95*. Department of Energy and Minerals.

APPENDIX 1:
BIOSTRATIGRAPHY REPORT

PALYNOLOGY OF

HALLADALE-1 DW1 AND DW2

OFFSHORE OTWAY BASIN, VICTORIA

BY

ROGER MORGAN

for **Origin Energy** **October 2005**

REF: OTW.HALLDALE-1 DW1&DW2

PALYNOLOGY OF

HALLADALE-1 DW1 AND DW2

OFFSHORE OTWAY BASIN, VICTORIA

CONTENTS **PAGE**

1	SUMMARY	3
2	INTRODUCTION	6
3	PALYNOSTRATIGRAPHY	11
4	REFERENCES	28

Table 1	Individual Sample Summary – Halladale-1 DW1	
Table 2	Individual Sample Summary – Halladale-1 DW2	
Figure 1	Cretaceous Zonation used herein (adapted from Morgan, 2001)	
Figure 2	Comparison of Zonations of Morgan (1992, 2001, herein) and Partridge (1998). Lithostratigraphy from Partridge (1998)	
Appendix 1	Palynological Data Charts	Halladale-1 DW1
		Halladale-1 DW2

1 SUMMARY

Halladale-1 DW1

960/70 m (cuatts) : *M. druggii* Zone (and *F. longus* Zone, upper subzone) : Maastrichtian : very nearshore marine

1050/60 m (cutts) : *I. pellucidum* Zone (and *F. longus*, lower subzone) : Maastrichtian : nearshore marine

1100/10 m (cutts) : *I. pellucidum* Zone : Maastrichtian : very nearshore marine

1190/1200 m (cutts) : *X. australis* Zone, upper subzone/*N. senectus* Zone : Campanian : very nearshore marine

1250/60 m (cutts) : *X. australis* Zone, lower c subzone/*N. senectus* Zone : Campanian : shelfal marine

1310/20 m (cutts) : *X. australis* Zone, lower a subzone : Campanian : marine

1390/1400 m, 1440/50 m, 1500/10 m (all cutts) : *N. aceras* Zone : Campanian : nearshore marine

1540/50 m, 1570/80 m, 1600/10 m, 1630/40 m, 1660/70 m (all cutts) : *I. cretaceum* Zone, subzones not clear : Santonian : nearshore to shelfal marine

1670/80 m, 1680/90 m, 1695/1700 m (all cutts) : *O. porifera* Zone, upper subzone : Santonian : nearshore marine

1705/10 m (cutts) : *C. striatoconus* Zone, upper subzone : Coniacian : nearshore marine

1710/15 m (cutts) : ?*C. striatoconus* Zone, ?lower subzone : ?Coniacian : nearshore marine

1725/30 m, 1735.409 m, 1745/50 m, 1755.60 m, 1765/70 m (all cutts) : ?*P. infusorioides* Zone, ?upper subzone : ?Turonian : nearshore marine

1791.56 m (core) : *P. infusorioides* Zone, middle a subzone : Turonian : very nearshore marine

1796.2 m core, 1800/05 m (cutts) : *P. infusorioides* Zone, lower c subzone : Turonian : offshore to nearshore marine

1805/10 m, 1815/20 m, 1825/30 m (all cutts) : *P. infusorioides* Zone, lower b subzone : Turonian : nearshore marine

1840/45 m, 1855/60 m (cutts) : *P. infusorioides* Zone, lower a subzone : Turonian : marginal marine

1875/80 m, 1900/05 m (cutts) : near barren and indeterminate :

Halladale-1 DW2

960/70 m (cutts) : *M. druggii* Zone (and *F. longus* Zone, upper subzone) : Maastrichtian : very nearshore marine

1000/10 m (cutts) : *I. pellucidum* Zone (and *F. longus* Zone, lower subzone) : Maastrichtian : nearshore marine

1050/60 m (cutts) : *I. pellucidum* Zone : Maastrichtian : very nearshore marine

1100/10 m (cutts) : *I. korojonense* Zone : Campanian : very nearshore marine

1180/90 m (cutts) : *X. australis* Zone, upper subzone/*N. senectus* Zone : Campanian : very nearshore marine

1240/50 m (cutts) : *X. australis* Zone, lower c subzone/*N. senectus* Zone : Campanian : shelfal marine

1310/20 m (cutts) : *X. australis* Zone, lower a subzone : Campanian : amrine

1400/10 m, 1450/60 m, 1510/20 m (all cutts) : *N. aceras* Zone : Campanian : nearshore marine

1560/70 m (cutts) : Indeterminate : nearshore marine

1590/1600 m, 1620/30 m 1650/60 m, 1680/90 m (all cutts) : *I. cretaceum* Zone, subzones not clear : Santonian : nearshore to shelfal marine

1690/1700 m, 1710/20 m (cutts) : *O. porifera* Zone, upper subzone : Santonian : very nearshore marine

1730/40 m (cutts) : *C. striatoconus* Zone, upper subzone : Coniacian : nearshore marine

1740/50 m 1750/60 m (cutts) : ?*C. striatoconus* Zone, ?lower subzone : ?Coniacian : nearshore marine

1765/70 m, 1775/80 m, 1785/90 m, 1795.1800 m (all cutts) : lean and indeterminate : nearshore marine

1810.67 m, 1821.53 m, 1831.23 m (all cores) : *P. infusorioides* Zone, middle a subzone : Turonian : nearshore to marginal marine

1835/40 m (cutts) : *P. infusorioides* Zone, lower c subzone : Turonian : very nearshore marine

1850/55 m 1865/70 m, 1870/75 m, 1875/80 m, 1900/05 m (all cutts) : *P. infusorioides* Zone, lower b subzone or older : Turonian or older : ?nearshore marine

2 INTRODUCTION

The extensive sample suites studied in the Thylacine-Geographe wells plus new study of older wells, has produced a much improved palynology zonation, as summarised in Figure 1 within the framework of Helby, Morgan and Partridge (1987). Figure 2 compares the new zonation with that of Partridge (1998) and the lithostratigraphy of Partridge (1998, 2001). Table 1 and 2 summarises the palynological details of the samples.

A total of 67 samples have been studied from the two Halladale-1 sections (34 from DW1, 33 from DW2). Processing by Corelabs has yielded variable and poor yields of fossils, with the DW2 section yielding less microfossils than DW1.

All informal species names are shown in quotation marks and many are those of Marshall (1984) or my unpublished names. Names are given in full when first mentioned in the text, but only the genus initial and full species name is given when subsequently mentioned.

Raw palynological data are included in Appendix 1. The data are based on a 100 specimen count from which an indication of marine microplankton to terrestrial palynomorph proportions can be derived. The microplankton percentages are listed in Table 1, which also summarizes other palynological details. Environmental assessments are derived from the palynomorph counts using content and diversity of saline taxa (dinoflagellates and spiny acritarchs), other microplankton (mostly freshwater algae), and terrestrial spores and pollen. The criteria for these assessments are defined in Table 1. However, dinoflagellate content and diversity in the Otway Basin are lower than might be expected from other data sources, especially sedimentology in the offshore marine shales. It may be that dinoflagellate productivity is suppressed by lowered salinity or restricted oceanic circulation caused by the enclosed nature of a long narrow marine gulf. Environments interpreted here may therefore underestimate marine influence in this section with environments really being more marine than interpreted here. In running text, frequency of taxa is discussed in the following intervals: Very rare = <1%, Rare = 1-3%, Frequent = 4-10%, Common = 11-29%, Abundant = 30-49%, Super-abundant = 50-100%.

TABLE 1

SUMMARY OF PALYNOLOGICAL DATA : HALLADALE-1 DW1

LOG DEPTH (m)	SAMPLE TYPE	MICROFOSSIL YIELD	PERCENTAGE				DIVERSITY *1		SPORE-POLLEN SUBZONE	DINOFLAGELLATE ZONE/ACME	ENVIRONMENT*2
			MICROPLANKTON			SPORE-POLLEN-	SALINE MICROPLANKTON	SPORE-POLLEN			
			SALINE DINOFLAG	SPINY AC.	FRESH ALGAE						
960/70	CUTTS	HIGH	6	0	1	93	LOW	HIGH	F. LONGUS, UPPER	M. DRUGGII	NEARSHORE MARINE
1050/60	CUTTS	MODERATE	31	0	2	67	LOW	HIGH	F. LONGUS, LOWER	I. PELLUCIDUM	NEARSHORE MARINE
1100/10	CUTTS	MODERATE	4	0	6	90	LOW	HIGH		I. PELLUCIDUM	VERY NEARSHORE MARINE
1190/1200	CUTTS	MODERATE	<1	0	0	99+	LOW	HIGH	N. SENECTUS	X. AUSTRALIS, UPPER	VERY NEARSHORE MARINE
1250/60	CUTTS	LOW	58	0	2	40	LOW	MODERATE	N. SENECTUS	X. AUSTRALIS, LOWER c	SHELFAL MARINE
1310/20	CUTTS	NEAR BARREN	-	-	-	-	EX LOW	EX LOW		X. AUSTRALIS, LOWER a	MARINE
1390/1400	CUTTS	EX LEAN	25	0	0	75	LOW	MODERATE		N. ACERAS	NEARSHORE MARINE
1440/50	CUTTS	NEAR BARREN	18	0	0	82	EX LOW	LOW		N. ACERAS	NEARSHORE MARINE
1500/10	CUTTS	MODERATE	13	1	2	84	MODERATE	HIGH		N. ACERAS	NEARSHORE MARINE
1540/50	CUTTS	MODERATE	23	1	2	74	LOW	HIGH		I. CRETACEUM	NEARSHORE MARINE
1570/80	CUTTS	MODERATE	30	0	3	67	MODERATE	HIGH		I. CRETACEUM	NEARSHORE MARINE
1600/10	CUTTS	MODERATE	45	0	2	52	MODERATE	HIGH		I. CRETACEUM	SHELFAL MARINE
1630/40	CUTTS	MODERATE	62	0	9	38	MODERATE	MODERATE		I. CRETACEUM	NEARSHORE MARINE
1660/70	CUTTS	MODERATE	20	1	1	78	HIGH	HIGH		I. CRETACEUM	VERY NEARSHORE MARINE
1670/80	CUTTS	MODERATE	6	1	0	93	MODERATE	HIGH		O. PORFIERA, UPPER	NEARSHORE MARINE
1680/90	CUTTS	MODERATE	18	0	0	82	HIGH	HIGH		O. PORFIERA, UPPER	NEARSHORE MARINE
1695/1700	CUTTS	MODEATE	21	3	4	72	MODERATE	HIGH		O. PORIFERA, UPPER	NEARSHORE MARINE
1705/10	CUTTS	MODERATE	20	4	1	75	HIGH	HIGH		C. STRIATOCONUS, UPPER	NEARSHORE MARINE
1710/15	CUTTS	LOW	14	3	1	82	HIGH	HIGH		?C. STRIATOCONUS, ?LOWER	NEARSHORE MARINE
1725/30	CUTTS	LOW	17	1	0	82	MODERATE	HIGH		?P. INFUSORIOIDES, ?UPPER	NEARSHORE MARINE
1735/40	CUTTS	LOW	10	2	2	86	HIGH	HIGH		?P. INFUSORIOIDES, ?UPPER	NEARSHORE MARINE
1745/50	CUTTS	LOW	7	2	3	88	MODERATE	HIGH		?P. INFUSORIOIDES, ?UPPER	VERY NEARSHORE MARINE
1755/60	CUTTS	EX LOW	6	2	6	86	MODERATE	HIGH		?P. INFUSORIOIDES, ?UPPER	VERY NEARSHORE MARINE
1765/70	CUTTS	EX LOW	15	3	10	72	MODERATE	HIGH		?P. INFUSORIOIDES, ?UPPER	NEARSHORE MARINE
1791.56	CORE	HIGH	9	<1	0	91	LOW	MODERATE		P. INFUSORIOIDES, MIDDLE a	VERY NEARSHORE MARINE
1796.62	CORE	HIGH	74	0	3	26	LOW	MODERATE		P. INFUSORIOIDES, LOWER c	OFFSHORE MARINE
1800/05	CUTTS	MODERATE	4	2	12	82	LOW	HIGH		P. INFUSORIOIDES, LOWER c	VERY NEARSHORE MARINE
1805/10	CUTTS	LOW	9	8	0	82	EX LOW	MODERATE		P. INFUSORIOIDES, LOWER b	VERY NEARSHORE MARINE
1815/20	CUTTS	MODERATE	16	0	2	82	LOW	HIGH		P. INFUSORIOIDES, LOWER b	NEARSHORE MARINE
1825/30	CUTTS	EX LOW	25	0	0	75	LOW	MODERATE		P. INFUSORIOIDES, LOWER b	NEARSHORE MARINE
1840/45	CUTTS	EX LOW	10	0	6	84	EX LOW	MODERATE		P. INFUSORIOIDES, LOWER a	NEARSHORE MARINE
1855/60	CUTTS	EX LOW	14	0	0	86	EX LOW	MODERATE		P. INFUSORIOIDES, LOWER a	NEARSHORE MARINE
1875/80	CUTTS	NEAR BARREN	-	-	-	-	-	-		INDETERMINATE	
1900/05	CUTTS	NEAR BARREN	-	-	-	-	-	-		INDETERMINATE	

*1 DIVERSITY	
V HIGH	30+ SPECIES
HIGH	20-29 SPECIES
MOD	10-19 SPECIES
LOW	5-9 SPECIES
EX LOW	1-4 SPECIES

*2 ENVIRONMENTS	DINOFLAGELLATE CONTENT%	DINOFLAGELLATE DIVERSITY	FRESHWATER ALGAE CONTENT %
OFFSHORE MARINE	67 to 100	VERY HIGH	LOW
SHELFAL MARINE	34 to 66	HIGH	"
NEARSHORE MARINE	11 to 33	MODERATE	"
VERY NEARSHORE MARINE	5 to 10	MODERATE-LOW	"
MARGINAL MARINE	<1 to 4	LOW-VERY LOW	"
BRACKISH	0, SPINY ACRITARCHS ONLY	EXTREMELY LOW	"
NON-MARINE (UNDIFF)	0, NO SPINY ACRITARCHS	NIL	LOW
NON-MARINE (LACUSTRINE)	0, NO SPINY ACRITARCHS	NIL	MODERATE 10%+

TABLE 2

SUMMARY OF PALYNOLOGICAL DATA : HALLADALE-1 DW2

LOG DEPTH (m)	SAMPLE TYPE	MICROFOSSIL YIELD	PERCENTAGE				DIVERSITY *1		SPORE-POLLEN SUBZONE	DINOFLAGELLATE ZONE/ACME	ENVIRONMENT*2
			MICROPLANKTON			SPORE-POLLEN-	SALINE MICROPLANKTON	SPORE-POLLEN			
			SALINE DINOFLAG	SPINY AC.	FRESH ALGAE						
960/70	CUTTS	MODERATE	2	0	2	96	EX LOW	VERY HGIH	F. LONGUS, UPPER	M. DRUGGII	VERY NEARSHORE MARINE
1000/10	CUTTS	MODERATE	16	0	2	82	MODERATE	HIGH	F. LONGUS, LOWER	I. PELLUCIDUM	NEARSHORE MARINE
1050/60	CUTTS	MODERATE	2	0	5	93	LOW	HIGH		I. PELLUCIDUM	MARGINAL MARINE
1100/10	CUTTS	MODERATE	7	0	8	85	LOW	HIGH		I. KOROJONENSE	NEARSHORE MARINE
1180/90	CUTTS	NEAR BARREN	-	-	-	-	EX LOW	LOW	N. SENECTUS	X. AUSTRALIS, UPPER	MARINE
1240/50	CUTTS	EX LOW	65	0	0	35	EX LOW	MODERATE	N. SENECTUS	X. AUSTRALIS, LOWER c	SHELFAL MARINE
1310/20	CUTTS	EX LOW	55	0	0	45	EX LOW	MODERATE		X. AUSTRALIS, LOWER a	SHELFAL MARINE
1400/10	CUTTS	MODERATE	7	0	0	93	LOW	HIGH		N. ACERAS	VERY NEARSHORE MARINE
1450/60	CUTTS	MODERATE	9	0	0	91	EX LOW	HIGH		N. ACERAS	VERY NEARSHORE MARINE
1510/20	CUTTS	MODERATE	26	0	0	74	LOW	HIGH		N. ACERAS	NEARSHORE MARINE
1560/70	CUTTS	EX LOW	24	0	0	76	EX LOW	LOW		INDETERMINATE	NEARSHORE MARINE
1590/600	CUTTS	MODERATE	66	0	0	34	MODERATE	MODERATE		I. CRETACEUM	OFFSHORE MARINE
1620/30	CUTTS	EX LOW	70	0	0	30	MODERATE	LOW		I. CRETACEUM	OFFSHORE MARINE
1650/60	CUTTS	MODERATE	15	<1	0	85	HIGH	HIGH		I. CRETACEUM	NEARSHORE MARINE
1680/90	CUTTS	MODERATE	17	2	1	80	MODERATE	MODERATE		I. CRETACEUM	NEARSHORE MARINE
1690/1700	CUTTS	LOW	7	1	0	92	MODERATE	HIGH		O. PORIFERA, UPPER	VERY NEARSHORE MARINE
1710/20	CUTTS	MODERATE	5	1	0	96	MODERATE	HIGH		O. PORIFERA, UPPER	VERY NEARSHORE MARINE
1730/40	CUTTS	MODERATE	28	0	0	72	MODERATE	HIGH		C. STRIATOCONUS, UPPER	NEARSHORE MARINE
1740/50	CUTTS	EX LOW	28	0	0	72	LOW	MODERATE		?C. STRIATOCONUS, ?LOWER	NEARSHORE MARINE
1750/60	CUTTS	EX LOW	40	1	1	58	MODERATE	MODERATE		?C, STRIATOCONUS, ?LOWER	SHELFAL MARINE
1765/70	CUTTS	EX LOW	21	0	0	79	LOW	MODERATE		INDETERMINATE	NEARSHORE MARINE
1775/80	CUTTS	NEAR BARREN	26	0	0	74	EX LOW	LOW		INDETERMINATE	NEARSHORE MARINE
1785/90	CUTTS	EX LOW	50	0	0	50	LOW	MODERATE		INDETERMINATE	MARINE
1795/1800	CUTTS	NEAR BARREN	-	-	-	-	EX LOW	LOW		INDETERMINATE	MARINE
1810.67	CORE	MODERATE	1	1	2	96	EX LOW	MODERATE		P. INFUSORIOIDES, MIDDLE a	MARGINAL MARINE
1821.53	CORE	HIGH	1	<1	0	99	EX LOW	MODERATE		P. INFUSORIOIDES, MIDDLE a	MARGINAL MARINE
1831.23	CORE	HIGH	11	0	2	87	LOW	HIGH		P. INFUSORIOIDES, MIDDLE a	NEARSHORE MARINE
1835/40	CUTTS	MODERATE	6	0	0	94	LOW	HIGH		P. INFUSORIOIDES, LOWER c	VERY NEARSHORE MARINE
1850/55	CUTTS	MODERATE	(40)	1	0	59	(MODERATE)	MODERATE		P. INFUSORIOIDES, LOWER b	?SHELFAL MARINE
1865/70	CUTTS	EX LEAN	16	0	1	83	EX LOW	MODERATE		P. INFUSORIOIDES, LOWER b	NEARSHORE MARINE
1870/75	CUTTS	EX LEAN	13	0	6	81	EX LOW	MODERATE		P. INFUSORIOIDES, LOWER b	NEARSHORE MARINE
1875/80	CUTTS	LOW	(12)	0	0	88	EX LOW	MODERATE		P. INFUSORIOIDES, LOWER b	NEARSHORE MARINE
1900/05	CUTTS	EX LOW	(25)	0	2	73	(LOW)	MODERATE		(P. INFUSORIOIDES, LOWER b)	(NEARSHORE MARINE)

*1 DIVERSITY	
V HIGH	30+ SPECIES
HIGH	20-29 SPECIES
MOD	10-19 SPECIES
LOW	5-9 SPECIES
EX LOW	1-4 SPECIES

*2 ENVIRONMENTS	DINOFLAGELLATE CONTENT%	DINOFLAGELLATE DIVERSITY	FRESHWATER ALGAE CONTENT %
OFFSHORE MARINE	67 to 100	VERY HIGH	LOW
SHELFAL MARINE	34 to 66	HIGH	"
NEARSHORE MARINE	11 to 33	MODERATE	"
VERY NEARSHORE MARINE	5 to 10	MODERATE-LOW	"
MARGINAL MARINE	<1 to 4	LOW-VERY LOW	"
BRACKISH	0, SPINY ACRITARCHS ONLY	EXTREMELY LOW	"
NON-MARINE (UNDIFF)	0, NO SPINY ACRITARCHS	NIL	LOW
NON-MARINE (LACUSTRINE)	0, NO SPINY ACRITARCHS	NIL	MODERATE 10%+

BRACKETS ( ) IN CUTTINGS INDICATES LIKELY CAVING

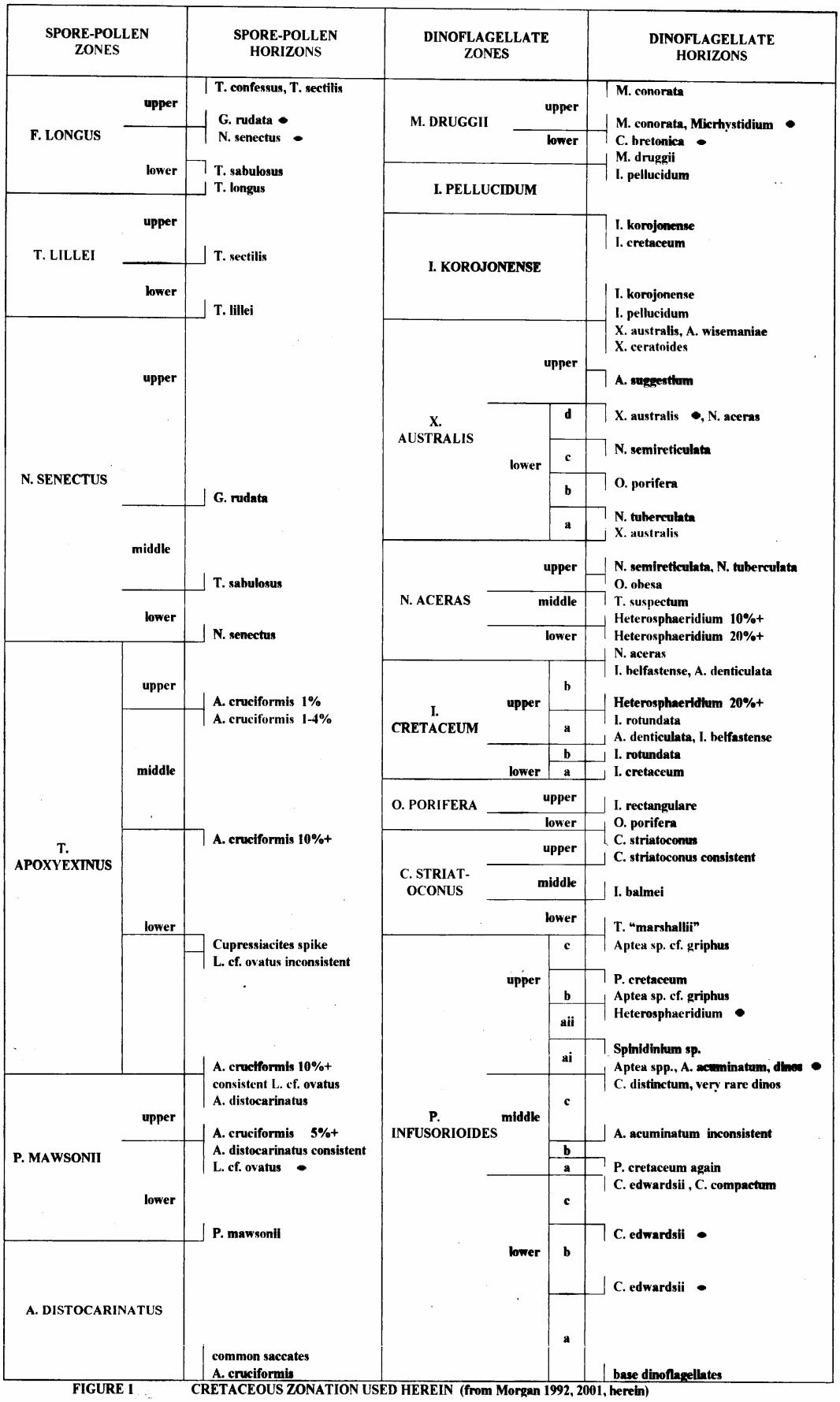

FIGURE 1 CRETACEOUS ZONATION USED HEREIN (from Morgan 1992, 2001, herein)

● = frequent (4-10%) ● = common (11-30%)

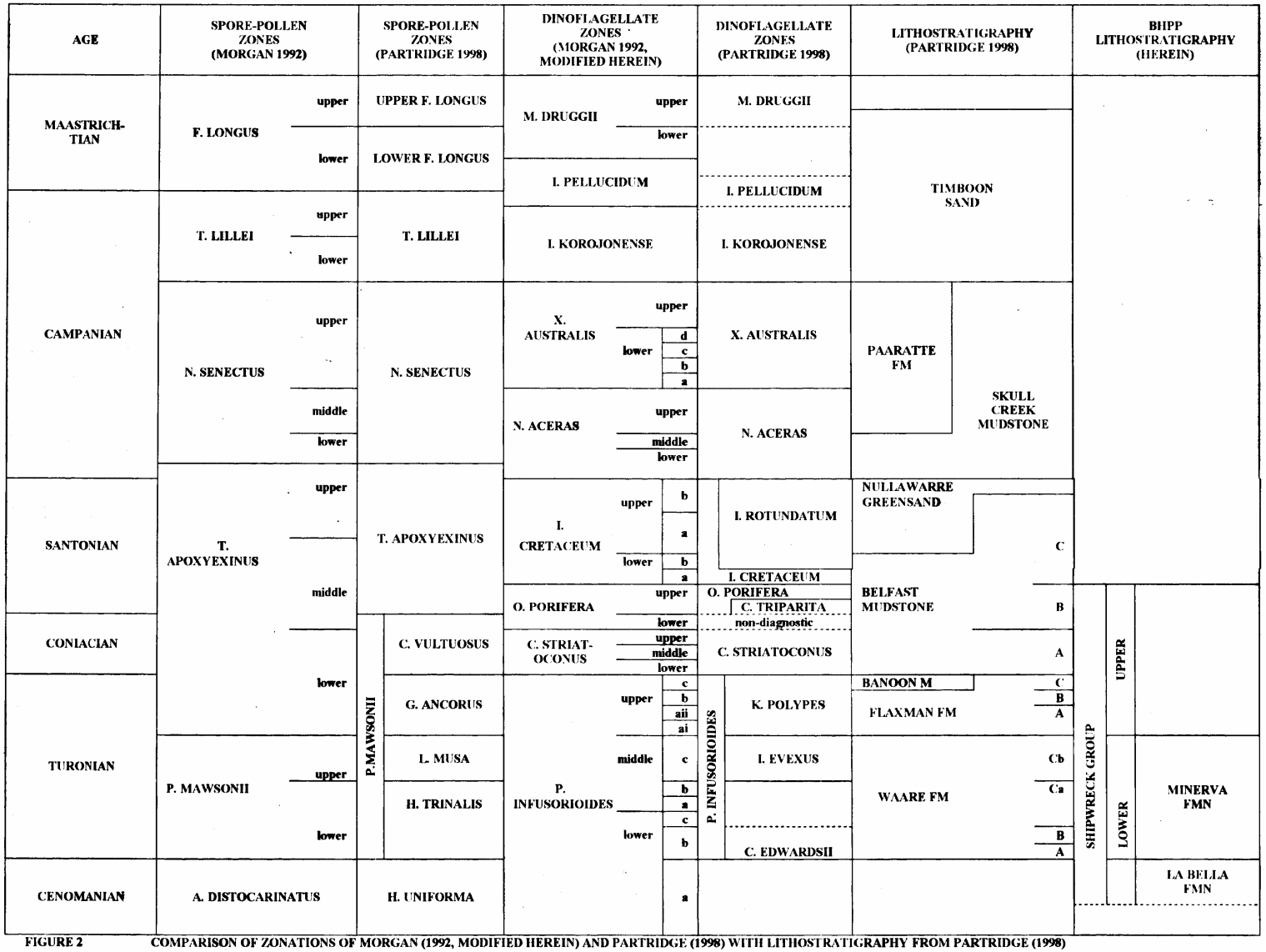

FIGURE 2 COMPARISON OF ZONATIONS OF MORGAN (1992, MODIFIED HEREIN) AND PARTRIDGE (1998) WITH LITHOSTRATIGRAPHY FROM PARTRIDGE (1998)

3 PALYNOSTRATIGRAPHY

3.1 Halladale-1 DW1

3.1.1 960/70 m (cutts) : *M. druggii* Zone (and *F. longus* Zone, upper subzone)

Assignment to the *M. druggii* Zone is indicated by the presence of *Manumiella druggii* and *Manumiella conorata* without older markers. Dinoflagellates are rare with *Manumiella* the most frequent taxon. Rare elements include *Alterbia acutula* and *Areoligera coronata*.

Spores and pollen are totally dominant and zonal assignment is indicated by youngest *Forcipites longus, Battenipollis sectilis* and *Tubulifloridites lilliei* with oldest common *Gambierina rudata*. Common are *Proteacidites* spp. and *G. rudata* with frequent *Ceratosporites equalis, Cyathidites australis, Falcisporites similis, Laevigatosporites ovatus, Phyllocladidites mawsonii* and *Stereisporites antiquasporites.*

Very nearshore marine environments are indicated by the totally dominant and highly diverse spores and pollen and the minor low diversity dinoflagellates.

This assemblage is seen in DW2 at 960/70 m (cutts).

3.1.2 1050/60 m (cutts) : *I. pellucidum* Zone (and *F. longus* Zone, lower subzone)

Assignment to the *I. pellucidum* Zone is indicated by youngest *Isabelidinium pellucidum* without older markers. *M. conorata* is present but may be caved. Frequent are *Canninginopsis bretonica, Heterosphaeridium heteracanthum, I. pellucidum* and *M. conorata* with rare *A. acutula*.

Spores and pollen are dominant and zonal assignment is indicated by youngest *Battenipollis "megasectilis"* and oldest *Tetracolporites verrucosus*. Common are *F. similis* and *Proteacidites* spp., with frequent *C. equalis, C. australis* and *Dictyophyllidites* spp.

Nearshore marine environments are indicated by the dominant and diverse spores and pollen and subordinate low diversity dinoflagellates.

This assemblage is seen in DW2 at 1000/10 m (cutts).

3.1.3 1100/10 m (cutts) : *I. pellucidum* Zone

Assignment is indicated by *I. pellucidum* above older markers, and confirmed by youngest *Cribroperidinium "mayii"* seen in DW2 at 1050/60 m. Dinoflagellates are very rare with the algal *Nummus* frequent.

Spores and pollen are dominant with common *Cyathidites minor, F. similis* and *Proteacidites* spp. and frequent *Dictyophyllidites* spp., *L. ovatus, Retitriletes austroclavatidites* and *Vitreisporites pallidus*. However, key taxa are very rare and the probably *T. lilliei* zonal assignment cannot be confirmed.

Very nearshore marine environments are indicated by the totally dominant and highly diverse spores and pollen, and minor low diversity dinoflagellates.

This assemblage is seen at 1050/60 m in DW2.

3.1.4 1190/1200 m (cutts) : *X. australis* Zone, upper subzone/*N. senectus* Zone

Assignment is indicated by youngest *Xenikoon australis* above *Nelsoniella aceras*. Dinoflagellates are rare and include *Anthosphaeridium "wisemaniae", C. "mayii", Odontochitina porifera* (considered reworked), *Xenascus ceratoides* and *X. australis.*

Spores and pollen are dominant with common *C. minor, F. similis* and *Proteacidites* spp. and frequent *Dictyophyllidites* spp., *Dilwynites granulatus, Nothofagidites endurus* and *Vitreisporites pallidus*. Permian reworking is prominent. The presence of *Forcipites sabulosus* and *N. endurus* indicate the *N. senectus* spore-pollen zone.

Very nearshore marine environments are indicated by the totally dominant and highly diverse spores and pollen, and minor low diversity dinoflagellates.

This assemblage is seen at 1050/60 m in DW2.

3.1.5 1250/60- m (cutts) : *X. australis* Zone, lower c subzone/*N. senectus* Zone

Assignment is indicated by youngest *Nelsoniella semireticulata* without older markers. The assemblage is very distinctive with common *N. semireticulata*, *N. aceras* and *X. australis*. Rare elements include *Odontochitina* spp. and *Trithyrodinium* spp.

Spores and pollen are subordinate with frequent *C. minor, F. similis* and *Proteacidites* spp. Rare *F. sabulosus* indicates the *N. senectus* spore-pollen zone.

Shelfal marine environments are indicated by the subequal proportions of moderately diverse spores and pollen and low diversity dinoflagellates.

This very distinctive assemblage is seen at 1240/50 m in DW2.

3.1.6 1310/20 m (cutts) : *X. australis* Zone, lower a subzone

Assignment is indicated by youngest *Nelsoniella tuberculata* amongst an assemblage totally dominated by large fragments of inertinite and cuticle, with very few identifiable palynomorphs. Amongst the dinoflagellates is *N. aceras*.

Only a single pollen specimen was seen and zonal assignment is not possible.

Marine environments are indicated by the presence of dinoflagellates, but too few identifiable taxa have been seen for a reliable estimate of distance from shore.

An equivalent assemblage was seen at 1310/20 m in DW2.

3.1.7 1390/1400 , 1440/50, 1500/10 m (all cutts) : *N. aceras* Zone

Assignment is indicated by continued *N. aceras* without younger markers considered in place and without older markers. Rare dinoflagellates with minor *Heterosphaeridium* at 1390/1400 m and 1440/50 m suggest the upper subzone. Youngest *Odontochitina "obesa"* and frequent *Heterosphaeridium* at 1500/10 m suggests the middle subzone. The absence of the lower subzone suggests condensation or loss of this interval.

Spores and pollen are dominant but in poor palynomorphs yields at 1390/1400 m and 1440/50 m and lack zone diagnostic taxa. Common is *F. similis* with frequent *C. australis, C. minor, P. mawsonii, Proteacidites* spp. and *V. pallidus.*

Nearshore marine environments are indicated by the dominant and diverse spores and pollen and the subordinant low diversity dinoflagellates.

These assemblages are seen in DW2 at 1400/10 m, 1450/60 m and 1510/20 m.

3.1.8 1540/50, 1570/80, 1600/10, 1630/40, 1660/70 m (all cutts) : *I. cretaceum* Zone, subzones not clear

Zonal assignment is indicated at the top by youngest *Eucladinium kaikourense* (1540/50), *Amphidiadema denticulata* and *Isabelidinium belfastense "belfastense"* (both at 1570/80 m). At the base, the absence of older markers is indicative. Within the zone, identifiable taxa are not frequent, with inertinite totally dominant and the usual subzones cannot be crisply identified especially in cuttings. The interval may be mostly the upper subzone, with the lower subzone condensed or absent. However, the following events may be locally useful.

1540/50 m : top *E. kaikourense*, top frequent *T. "thick retic"*
1570/80 m : top *A. denticulata, I. belfastense "belfastense"*
1600/10 m : top *Odontochitina "no horns", Odontochinia "stubby"*, frequent *O. operculata,* frequent *T. glabrum*
1630/40 m : major acme *Trithyrodinium glabrum* (26%)
1660/70 m : top *Isabelidinium belfastense "rotundata"*

Dinoflagellates are subordinate in most samples with common *Heterosphaeridium conjunctum* and frequent *T. "thick retic"* (1540/50 m, 1570/80 m) and *T. "glabrum"* (1600/10, 1630/40, 1660/70 m). Rare elements include *A. denticulata, Chatangiella victoriensis, K. kaikourense, I. belfastense "belfastense", Odontochitina porifera* and *Trithyrodinium "marshallii*."

Spores and pollen are dominant but not zone diagnostic. Common is *F. similis* with frequent *C. minor, Proteacidites* spp. and *V. pallidus.*

Nearshore to shelfal marine environments are indicated by the dominant and diverse spores and pollen and the subordinate but diverse dinoflagellates.

These assemblages are seen at 1590/1600, 1620/30, 1650/60 and 1680/90 m in DW2.

3.1.9 1670/80 m, 1680/90 m, 1695/1700 m (all cutts) : *O. porifera* Zone, upper subzone

Assignment is indicated at the top by the youngest *Isabelidinium rectangulare* and the absence of *Isabelidinium cretaceum*. At the base, assignment is indicated by oldest *I. rectangulare,* consistent *O. porifera* (which is caved below) and the absence of older markers (especially *Conosphaeridium abbreviatum* seen at 1705/10 m below). Common is *Heterosphaeridium conjunctum* with other dinoflagellates rare including *I. rectangulare, Odontochitina cribropoda, O. porifera, T. glabrum, T. "marshallii"* and the obviously caved *E. kaikourense* and *N. aceras.* A single *Aptea* cf. *griphus* (= *V. griphus* of Patridge) occurs at 1670/80m, but is not considered diagnostic of the older *K. polypea* subzone. The lower *O. porifera* subzone appears to be condensed or absent.

Spores and pollen are totally dominant and moderately diverse, but lack zone diagnostic taxa. The base of frequent *Proteacidites* at 1670/80 m suggests the base of upper *T. apoxyexinus* Zone. Common are *F. similis* and *C. minor* with frequent *C. australis, Dictyophyllidites* spp., *Gleicheniidites* spp. and *V. pallidus*.

Nearshore marine environments are indicated by the low content of moderately diverse dinoflagellates with the dominant and diverse spores and pollen.

These assemblages are seen at 1690/1700 m and 1710/20 m in DW2.

3.1.10 1705/10 m (cutts) : *C. striatoconus* Zone, upper subzone

Assignment is indicated by frequent *C. abbreviatum* and rare *C. striatoconus*. Their inconsistent occurrence below is considered to be caving. Frequent are *Amosopollis cruciformis, C. abbreviatum, O. operculata* and *T. "marshallii"*. Rare elements include *Apteodinium* sp. and *Isabelidinium glabrum*. Rare *O. porifera* and *N. tuberculata* are considered caved.

Spores and pollen are dominant but lack zone diagnostic taxa. Frequent *A. cruciformis* suggest the middle *T. apoxyexinus* Zone. Common is *F. similis* with frequent *C. australis, C. minor, Dictyphyllidites* spp., *Microcachryidites antarcticus, Phyllocladidites mawsonii* and *V. pallidus*.

Nearshore marine environments are indicated by the low content of moderately diverse dinoflagellates with the dominant and diverse spores and pollen.

This assemblage occurs at 1730/40 m in DW2, although the original preparation was mislabelled as 1330/40 m.

3.1.11 1710/15 m (cutts) : ?*C. striatoconus* Zone, ?lower subzone

Assignment is tentative, based on *T. "marshallii"* without older markers and without younger markers considered in place. *Isabelidinium balmei* was not seen, suggesting the absence of the middle subzone. Several specimens of *C. abbreviatum* suggest the upper subzone, but are considered caved. Other obvious caving includes *E. kaikourense, I. rectangulare, N. aceras* and *O. porifera*. Very rare *Cribroperidinium edwardsii* is considered reworked. All taxa are rare but include *Batiacasphaera rugulata, Gillinia hymenophora* and *T. "marshallii"*.

Spores and pollen are dominant but lack zone diagnostic taxa. Common are *F. similis* and *C. minor* with frequent *Araucariacites australis, M. antarcticus, P. mawsonii* and *V. pallidus*.

Nearshore marine environments are indicated by the low content of moderately diverse dinoflagellates with the dominant and diverse spores and pollen.

This assemblage is seen at 1740/50 m and 1750/60 m in DW2.

3.1.12 1725/30 m, 1735.40 m, 1745/50 m, 1755/60 m, 1765/70 m (all cutts) : ?*P. infusorioides* Zone, ?upper subzone

Assignment is tentative. Inertinite is totally dominant with identifiable fossils rare, especially in the bottom two samples. Rare *A.* cf. *griphus* occurs in the top 3 samples, but without *Kiokansium polypes, Chlamydophorella nyei* or *Palaeoperidinium cretaceum*, its usual associates in the subzone (= *K. polypes* subzone of Partridge). In addition, *T. "marshallii"* occurs consistently (suggesting the *C. striatoconus*, lower subzone) but could be caved in these cuttings. Very rare *C. edwardsii* occurs in the top 2 samples and is considered reworked from the Waare B Formation seen below. This interval could therefore be either *C. striatoconus* lower subzone (Belfast equivalent) or *P. infusorioides*, upper subzone (Flaxmans

equivalent), but on balance I favour the older assignment with low confidence. Rare elements considered in place include *Aptea* cf. *griphus, Apteodinium* sp., *H. heteracanthum* and *O. operculata*. Rare elements certainly caved include *N. aceras* and *X. australis*. Rare elements possibly caved include *C. abbreviatum, Odontochitina "stubby", T. glabrum* and *T. "thick retic"*.

Spores and pollen are dominant and diverse, with common *F. similis, C. minor, M. antarcticus* and *P. mawsonii* and frequent *C. australis, Dilwynites granulatus, O. wellmanii* and *V. pallidus*. Rare Permian reworking was seen. Rare taxa considered caved include *Nothofagidites endurus* and *F. sabulosus*.

Nearshore marine environments are indicated by the low content of moderately diverse dinoflagellates with the dominant and diverse spores and pollen.

This assemblage may be equivalent to the very lean indeterminate samples at 1765/70, 1775/80, 1785/90 and 1795/1800 m in DW2.

3.1.13 1791.56 m (core) : *P. infusorioides* Zone, middle a subzone

Assignment is indicated by youngest *P. cretaceum* above older markers. Dinoflagellates are minor with very low diversity and comprise frequent *H. heteracanthum* with rare *Cyclonephelium compactum, Oligosphaeridium complex* and *P. cretaceum*. This equates to the *Heterosphaeridium* subzone of Partridge.

Spores and pollen are totally dominant with abundant *Dilwynites pusillum*, common *M. antarcticus* and frequent *C. minor* and *F. similis*. Youngest *Appendicisporites tricornitatus* with *P. mawsonii* indicates the *P. mawsonii* Zone, but subzone markers (such as *Hoegisporis "trinalis"*) were not seen.

Very nearshore marine environments are indicated by the low content of very low diversity dinoflagellates with the dominant and diverse spores and pollen.

This assemblage is seen at 1810.67 m core – 1831.23 m in DW2.

3.1.14 1796.2 m core, 1800/05 m (cutts) : *P. infusorioides* Zone, lower c subzone

Assignment is indicated by youngest rare *C. edwardsii* above youngest frequent/common *C. edwardsii*. At 1796.2 m, *H. heteracanthum* is super-abundant

with consistent *Botryococcus, K. polypes* and *O. complex* and rare *C. edwardsii*. At 1800/05 m, frequent are diaphanous leiospheres and *Botryococcus* with rare *C. edwardsii* and *H. heteracanthum* and caved *Chantangiella victoriensis. I. cretaceum* and *O. "no horns"*.

Spores and pollen are subordinate (1796.62 m) to dominant (1800/05 m) with common *C. minor* and *F. similis* and frequent *A. australis* and *C. australis*. Rare elements include *Cicatricosisporites australiensis, A. tricornitatus* and *Trilobosporites trioreticulosus*. Subzone markers were not seen.

Offshore (1796.2 m) to nearshore (1800/05 m) marine environments are indicated by the relative proportions of marine dinoflagellates to terrestrial spores and pollen.

This assemblage is seen at 1835.40 m in DW2.

3.1.15 1805/10 m, 1815/20 m, 1825/30 m (all cutts) : *P. infusorioides* Zone, lower b subzone

Assignment is indicated by youngest frequent to common *C. edwardsii* above rare *C. edwardsii*. Frequent is *C. edwardsii* with consistent *H. heteracanthum*. At 1815/20 m, a richer assemblage includes *C. nyei, K. polypes* and *Oligosphaeridium pulcherrimum*. Considered caved are *Odontochitina "stubby", Trithyrodinium* spp. and *X. australis*.

Spores and pollen are dominant and include common *C. australis, C. minor* and *F. similis*. Rare elements include *Appendicisporites distocarinatus, Balmeisporites holodictyus* and *Trilobosporites trioreticulosus*. Very rare are *Laevigatosporites "musa"* and *Pilosisporites parvispinosus*.

Nearshore marine environments are indicated by the low content of low to very low diversity dinoflagellates amongst the dominant and diverse spores and pollen.

This assemblage is seen at 1835.40 m – 1900/05 m in DW2 but at least the lower part of this interval is probably older, but masked by caving.

3.1.16 1840/45 m, 1855/60 m (cutts) : *P. infusorioides* Zone, lower a subzone

These samples are very lean of recognisable palynomorphs and those seen may be entirely caved. Tentative assignment is on a rare *C. edwardsii* below the acme. Of the dinoflagellates, *C. edwardsii* may be in place, but the *Trithyrodinium* spp. and *Chatangiella* spp. seen are considered caved.

Spores and pollen are dominant with common *F. similis* and *C. australis* and frequent *M. antarcticus*. Rare elements include *L. "musa"* and *T. trioreticulosus* but are not zone diagnostic.

Marginal marine environments are indicated by the very rare very low diversity dinoflagellates amongst the dominant and diverse spores and pollen.

This interval is not clearly seen in DW2 but it may be masked by caving.

3.1.17 1875/80 m, 1900/05 m (cutts) : near barren and indeterminate

These samples are totally dominated by inertinite with very few recognizable palynomorphs, mostly caved. All of the dinoflagellates (including *H. conjunctum, T. glabrum* and *X. australis*) are certainly caved.

Spores and pollen are very rare and not age diagnostic.

Environments are indeterminate as too few palynomorphs were seen and all the dinoflagellates are probably caved.

These samples may be equivalent to the basal samples in DW2 which are masked by caving.

3.2 Halladale-1 DW2

3.2.1 960/70 m (cutts) : *M. druggii* Zone (and *F. longus* Zone, upper subzone)

Assignment to the dinoflagellate zone is indicated by the presence of *M. druggii* and *M. conorata* without older markers. Dinoflagellates are rare with *M. drugii* the most frequent taxon.

Spores and pollen are totally dominant and sub zonal assignment is indicated by youngest *B. sectilis, F. longus* and frequent *G. rudata* at the top, and oldest frequent *G. rudata* at the base. Common are *F. similis, Proteacidites* spp. and *V. pallidus* with frequent *C. australis, C. minor, G. rudata, M. antarcticus, P. mawsonii* and *Stereisporites antiquasporites.*

Very nearshore marine environments are indicated by the totally dominant and highly diverse spores and pollen and the minor low diversity dinoflagellates.

3.2.2 1000/10 m (cutts) : *I. pellucidum* Zone (and *F. longus* Zone, lower subzone)

Assignment to the dinoflagellate zone is indicated by youngest *I. pellucidum* without older markers. Present are *M. conorata* and frequent *M. druggii* but these may be caved. Frequent are *C. bretonica* and *M. druggii* with consistent *Areoligera senonensis, H. heteracanthum* and *M. conorata.* Rare are *Odontochitina* spp.

Spores and pollen are dominant and subzonal assignment is indicated by oldest *T. verrucosus* without younger markers. Rare elements include *Lygistepollenites balmei, N. endurus* and *T. verrucosus.* Permian reworking is consistent.

Nearshore marine environments are indicated by the dominant and diverse spores and pollen and subordinate low diversity dinoflagellates.

3.2.3 1050/60 m (cutts) : *I. pellucidum* Zone

Assignment is indicated by *I. pellucidum* above older markers, and confirmed by youngest *Cribroperidinium "mayii".* Dinoflagellates are very rare with the algal *Nummus* consistent, with rare *C. bretonica, C. "mayii", H. heteracanthum, I. pellucidum* and *T. "marshallii".*

Spores and pollen are dominant with common *Cyathidites minor, F. similis* and *Proteacidites* spp. and frequent *Dictyophyllidites* spp., *L. ovatus* and *Vitreisporites pallidus.* However, key taxa are very rare and the probable *T. lilliei* zonal assignment cannot be confirmed. Rare are N. *endurus, F. sabulosus* and *Tricolpites confessus.*

Very nearshore marine environments are indicated by the totally dominant and highly diverse spores and pollen, and minor low diversity dinoflagellates.

3.2.4 1100/10 m (cutts) : *I. korojonense* Zone

Assignment is indicated by youngest *Isabelidinium korojonense* without older markers. Frequent are *Nummus* spp. and *H. heteracanthum* with consistent *Trichodinium* sp. and rare *C. bretonica, C. "mayii", I. pellucidum, Odontochitina "indistincta"* and *T. "marshallii"*.

Spores and pollen are dominant and diverse with common *F. similis* and *Proteacidites* and frequent *C. minor, Dictyophyllidites, P. mawsonii* and *V. pallidus*. Rare elements include *Aequitriradites spinulosus, Australopollis obscuris, F. sabulosus, G. rudata, L. balmei* and *N. endurus.*

Very nearshore marine environments are indicated by the totally dominant and highly diverse spores and pollen, and minor low diversity dinoflagellates.

This dinoflagellate zone is not seen in DW1 and is probably unsampled at this horizon.

3.2.5 1180/90 m (cutts) : *X. australis* Zone, upper subzone/*N. senectus* Zone

This sample is extremely lean of recognisable fossils but assignment is indicated by youngest *Xenikoon australis* above *Nelsoniella aceras*. Dinoflagellates are extremely rare and include only *X. australis*.

Spores and pollen are dominant with frequent *C. minor* and *Proteacidites* spp. The presence of rare *N. endurus* indicates the *N. senectus* spore-pollen zone.

Very nearshore marine environments are indicated by the totally dominant and highly diverse spores and pollen, and minor low diversity dinoflagellates.

3.2.6 1240/50 m (cutts) : *X. australis* Zone, lower c subzone/*N. senectus* Zone

Assignment is indicated by youngest *Nelsoniella semireticulata* without older markers. Although the yield is very poor, the assemblage is very distinctive with common *N. semireticulata, N. aceras* and *X. australis*.

Spores and pollen are subordinate with frequent *C. australis, F. similis* and *Proteacidites* spp.

Shelfal marine environments are indicated by the subequal proportions of moderately diverse spores and pollen and low diversity dinoflagellates.

3.2.7 1310/20 m (cutts) : *X. australis* Zone, lower a subzone

Despite a very poor yield, assignment is indicated by youngest *Nelsoniella tuberculata* amongst an assemblage totally dominated by large fragments of inertinite and cuticle, with very few identifiable palynomorphs. Amongst the dinoflagellates are *Heterosphaeridium* spp. and frequent *X. australis*.

Only very rare spores and pollen are seen and zonal assignment is not possible.

Marine environments are indicated by the presence of dinoflagellates but too few identifiable taxa have been seen for a reliable estimate of distance from shore.

3.2.8 1400/10 m, 14450/60 m, 1510/20 m (all cutts) : *N. aceras* Zone

Assignment is indicated by continued *N. aceras* without younger markers considered in place and without older markers. Rare dinoflagellates with minor *Heterosphaeridium* at 1400/10 m and 1450/60 m suggest the upper subzone and oldest *N. tuberculata* at 1400/10 m supports the subzone assignment. Youngest *Odontochitina "obesa"* and frequent *Heterosphaeridium* at 1510/20 m suggests the middle subzone. The apparent absence of the lower subzone suggests condensation or loss of this interval. Rare throughout are *O. porifera* and *T. "marshallii"*.

Spores and pollen are dominant but lack may zone diagnostic taxa. *F. sabulosus* at 1400/10 m suggest the middle *N. senectus* spore pollen subzone. Common is *F. similis* with frequent *C. australis, C. minor, P. mawsonii, Proteacidites* spp. and *V. pallidus.*

Nearshore marine environments are indicated by the dominant and diverse spores and pollen and the subordinant low diversity dinoflagellates.

3.2.9 1560/70 m (cutts) : Indeterminate

This sample contains abundant inertinite but very few identifiable fossils. The rare dinoflagellates are either non-descript (*Heterosphaeridium* spp.) or clearly caved (*N. aceras*).

Spores and pollen are very rare but numerically dominant over the dinoflagellates. They are longranging and not zone diagnostic.

Nearshore environments are suggested by the dominant spores and pollen and rare mostly caved dinoflagellates.

3.2.10 1590/1600 m, 1620/30 m, 1650/60 m 1680/90 m (all cutts) : *I. cretaceum* Zone, subzones not clear

Zonal assignment is indicated at the top by youngest *Eucladinium kaikourense* and at the base by consistent *I. cretaceum* and the absence of older markers. Within the zone, identifiable taxa are not frequent, with inertinite totally dominant, and the usual subzones cannot be crisply identified especially in cuttings. The interval may be mostly the upper subzone, with the lower subzone condensed or absent. However, the following events may be locally useful.

1590/600 m : top *E. kaikourense*, top frequent *T. "thick retic"*, *Odontochitina "stubby"*, frequent *O. operculata*
1620/30 m : top *Odontochitina "no horns"*, frequent *T. glabrum*
1650/60 m : top *I. belfastense "rotundata"*
1680/90 m : single *Aptea* cf. *griphus*

Dinoflagellates are subordinate in most samples with common *Batiacasphaera rugulata* (1620/30 m), *Heterosphaeridium conjunctum* and frequent *T. "thick retic"* (1590/1600 m) and *Heterosphaeridium* spp. (1650/60 m, 1680/90 m). Rare elements include *Chatangiella victoriensis, E. kaikourense, Odontochitina porifera* and *Trithyrodinium "marshallii"*.

Spores and pollen are dominant but not zone diagnostic. Common is *F. similis* with frequent *C. minor, Dictyophyllidites* spp., *M. antarcticus, Proteacidites* spp. and *V. pallidus.*

Nearshore to shelfal marine environments are indicated by the dominant and diverse spores and pollen and the subordinate but diverse dinoflagellates.

3.2.11 1690/1700 m, 1710/20 m (all cutts) : *O. porifera* Zone, upper subzone

Assignment is indicated at the top by the youngest *Isabelidinium rectangulare* with *Isabelidinium cretaceum* presumed caved. At the base, assignment is indicated by oldest *I. rectangulare* in place, consistent *O. porifera* (which is caved below) and the absence of older markers (especially *Conosphaeridium abbreviatum* seen at 1730/40 m below). Dinoflagellates are rare including *I. rectangulare, Odontochitina cribropoda, O. porifera, T. glabrum, T. "marshallii"* and the abviously caved *X. australis* and *N. aceras*. A single *Aptea* cf. *griphus* (=*V. griphus* of Partridge) occurs at 1710/20 m but is not diagnostic of the *K. polypes* subzone. The lower subzone appears to be condensed or absent.

Spores and pollen are totally dominant and moderately diverse but lack zone diagnostic taxa. Common are *F. similis* and *Dictyophyllidites* spp. with frequent *C. australis, C. minor, Gleicheniidites* spp. and *V. pallidus.*

Very nearshore marine environments are indicated by the low content of moderately diverse dinoflagellates with the dominant and diverse spores and pollen.

3.2.12 1730/40 m (cutts) : *C. striatoconus* Zone, upper subzone

Assignment is indicated by the presence of *C. abbreviatum*. Common are *Heterosphaeridium* spp. Rare elements include *O. operculata* and *T. "marshallii"*. Rare *O. cribropoda* and *N. aceras* are considered caved.

Spores and pollen are dominant but lack zone diagnostic taxa. Rare *C. ohaiensis* suggest the middle *T. apoxyexinus* Zone. Common is *F. similis* with frequent *C. australis, C. minor, Dictyophyllidites* spp. and *Microcachryidites antarcticus.*

Nearshore to shelfal marine environments are indicated by the dominant and diverse spores and pollen and the subordinate but diverse dinoflagellates.

3.2.13 1740/50 m, 1750/60 m (cutts) : ?*C. striatoconus* Zone, ?lower subzone

Assignment is tentative, based on *T. "marshallii"* without older markers and without younger markers considered in place. *Isabelidinium balmei* was not seen, suggesting the absence of the middle subzone. Obvious caving includes *I. rectangulare, N. aceras* and *X. australis*. Very rare *Cribroperidinium edwardsii* is considered reworked.

Common are *Heterosphaeridium* spp. with frequent *Apteodinium* spp. and rare *T. "marshallii"*.

Spores and pollen are dominant but lack zone diagnostic taxa. Common is *F. similis* with frequent *C. minor, C. australis* and *M. antarcticus*.

Nearshore to shelfal marine environments are indicated by the dominant and diverse spores and pollen and the subordinate but diverse dinoflagellates.

3.2.14 1765/70 m, 1775/80 m, 1785/90, 1795/1800 m (all cutts) : lean and indeterminate

Although containing abundant inertinite, these samples contain very few recognisable fossils. A single *A.* cf. *griphus* at 1765/70 m suggests that it may belong to the *P. infusorioides* Zone, upper subzone, but the absence of more specimens or the other taxa usually associated, results in very low confidence. Some younger markers (*I. belfastense, N. aceras, O. porifera, T. glabrum*) are considered caved. Most numerous in very low specimen counts are *Heterosphaeridium* spp.

Spores and pollen are dominant with common *F. similis* and frequent *C. minor* and *Proteacidites* spp. Rare elements include *Coptospora "pileosa"* and *P. notensis*. Permian reworking is persistent.

Nearshore to shelfal marine environments are indicated by the dominant and diverse spores and pollen and the subordinate but diverse dinoflagellates.

3.2.15 1810.67 m, 1821.53 m, 1831.23 m (all core) : *P. infusoriodes* Zone, middle a subzone

Assignment is indicated by youngest *P. cretaceum* above older markers. Dinoflagellates are minor with very low diversity. At 1831.23 m, frequent is *H. heteracanthum* with rare *O. operculata, Oligosphaeridium complex* and *P. cretaceum.* This equates to the *Heterosphaeridium* subzone of Partridge. At 1810.67 m and 1821.53 m, dinoflagellates are extremely rare.

Spores and pollen are totally dominant with common *C. minor, Dilwynites* spp, *F. similis* and *M. antarcticus* and frequent *A. australis, C. australis* and *V. pallidus*. Youngest *Appendicisporites distocarinatus* with *P. mawsonii* at 1821.23 m indicates the *P. mawsonii* Zone, but subzone markers were not seen.

Nearshore (1831.23 m) to marginal marine environments are indicated by the low content of very low diversity dinoflagellates with the dominant and diverse spores and pollen.

This assemblage is seen at 1810.67 m core – 1831.23 m in DW1.

3.2.16 1835/40 m (cutts) : *P. infusorioides* Zone, lower c subzone

Assignment is indicated by youngest rare *C. edwardsii* above youngest frequent/common *C. edwardsii*. Dinoflagellates are rare with only *C. edwardsii* and *H. heteracanthum* considered in place with *N. aceras, T. glabrum* and *T. "marshallii"* considered caved.

Spores and pollen are with common *C. australis, C. minor* and *F. similis* and frequent *M. antarcticus* and *O. wellmanii*. Rare elements include *Cicatricosisporites australiensis, A. distocarinatus* and *Trilobosporites trioreticulosus*. Subzone markers were not seen.

Very nearshore marine environments are indicated by the low proportions of marine dinoflagellates to terrestrial spores and pollen.

3.2.17 1850/55 m, 1865/70 m, 1870/75 m, 1875/80 m, 1900/05 m (all cutts) : *P. infusorioides* Zone, lower b subzone

Assignment is indicated by youngest frequent to common *C. edwardsii* above rare *C. edwardsii*. Frequent is *C. edwardsii* with consistent *H. heteracanthum*, but this assemblage may be caved in the lower samples and masking something older. Fossils yields are extremely poor in the bottom 3 samples with inertinite abundant. Common to frequent is *C. edwardsii* with common *H. heteracanthum* at 1850/55 m only. Considered caved are E. *kaikourense*, *N. aceras*, *Trithyrodinium* spp. and *X. australis*.

Spores and pollen are dominant and include common *C. australis*, *C. minor* and *F. similis*. Rare elements include *Appendicisporites distocarinatus, Balmeisporites holodictyus* and *Trilobosporites tribotrys*. Very rare are *P. mawsonii* (down to 1870/75 m) and *Pilosisporites parvispinosus*.

Nearshore marine environments are indicated by the low content of low to very low diversity in place dinoflagellates amongst the dominant and diverse spores and pollen.

4 REFERENCES

Helby, R., Morgan, R., & Partridge, A.D., (1987) A palynological zonation of the Australian Mesozoic. Mem. Assoc. Aust. Palaeontol. 4, 1-94.

Marshall, N.G., (1984) Late Cretaceous dinoflagellates from the Perth Basin, Western Australia. Unpubl. Ph.D. thesis, U.W.A.

Morgan, R.P., (1992) Overview of new cuttings based Late Cretaceous correlations, Otway Basin, Australia. Unpubl. rept. for BHPP

Morgan, R.P., (2001) Palynology of Thylacine-1, offshore Otway Basin, Australia, Unpubl. rept. for Woodside Energy Ltd.

Morgan, R.P., (2002) New palynology of LaBella-1, offshore Otway Basin, Victoria, Unpubl. rept. for Woodside Energy Ltd

Partridge, A.D., (1997) New Upper Cretaceous palynology of the Sherbrook Group, Otway Basin. In Victoria Supplement PESA News April/May p. 9

Partridge, A.D., (1998) Biostratigraphy and interpreted stratigraphy of Champion-1 and Conan-1 from open file basic data. Unpubl. rept. Biostrata 1998/02

Partridge, A.D., (2001) Revised stratigraphy of the Sherbrook Group, Otway Basin In Hill, K.C. and Bernecker, T. (Eds) Eastern Australian Basins Symposium, a refocused energy perspective for the future PESA spec. Publ. 455-464

Well Name : HALLADALE-1 DW2

Operator : ORIGIN
Interval : 950m - 1925m
Scale : 1:5000
Chart date: 13 October 2005

Palynological Data Chart : INTERPRETIVE DATA
% Abundance histogram : Highest occurrence
Roger Morgan

HALLADALE-1 DW2

Morgan Palaeo Associates
Maitland, South Australia

Enclosure 1

Sampling
Cutting
Core
Sidewall core

Text Keys
*1 % within discipline (40mm=100%)
*2 In-Situ occurrences
*3 ALBO

Depth | Samples (Samples in Discretes) | Pay | Chronostratigraphy: Age | HMP DINOCYST ZONES: Zone | Sub Zone | HMP MIOSPORE ZONES: Zone | Sub Zone

Dinoflagellate Cysts — % within discipline (40mm=100%) *1 / In-Situ occurrences *2

Marumiella spocata
Marumiella druggii
Areoligera senonensis
Canningnopsis bretonica "spiny"
Heterosphaeridium heteroclianthum
Isabelidinium pellucidum
Kokaniasun polypes
Odontochitina "hollow body"
Odontochitina spinosa
Paracalanniella indentata
Trithyrodinium glabra
Xenikoon australis
Acanthaulax wilsonii
Cerodinium diebelii
Cribroperidinium "tmayi"
Trichodinium sp.
Trithyrodinium "marshallii"
Heterosphaeridium conjunctum
Isabelidinium korojonense
Odontochitina "operculata"
Spiniferites ramosus
Nelsoniella aceras
Nelsoniella semireticulata
Nelsoniella tuberculata
Isabelidinium belfastense "rotundatum"
Odontochitina porifera
Nelsoniella "psilata"
Odontochitina "obesa"
Trithyrodinium "evittii"
Batiacasphaera inpulata
Chatangiella tripartita
Eucladinium kaikourense
Heterosphaeridium cf. labrocrachus
Isabelidinium "korojonense"
Odontochitina cribropoda
Odontochitina operculata
Trithyrodinium suspectum
Trithyrodinium vermiculum
Apteodinium granulatum
Ecochosphaeridium phragmites
Odontochitina "no horn"
Trithyrodinium "puncate"
Chatangiella victoriensis
Cribroperidinium delicatum
Isabelidinium cretaceum "cretaceum"
Isabelidinium sp.
Maduradinium pentagonum
Odontochitina costata
Apiea sp. cf. giphus
Escharisphaeridia spp.
Trithyrodinium "granulatum"
Isabelidinium cooksoniae "constrictum"
Isabelidinium rectangulare "rectangulare"
Isabelidinium rectangulare "diversum"
Odontochitina "no horn"
Dinogymnium euclaense
Isabelidinium rectangulare "diversum"
Odontochitina sp.
Conosphaeridium abbrevidum
Cribroperidinium edwardsii
Eucladinium madurense
Eucladinium "solida"
Hystrichodinium pulchrum
Palaeohystrichophora infusorioides
Isabelidinium "evexa"
Oligosphaeridium complex
Isabelidinium belfastense "belfastense"
Isabelidinium cretaceum "cretaceum"
Nummus inaequalis
Nummus spp.
Amosopolis cruciformis
Microdictyon spp.
Diaphanous leiosphere
Schizosporis psilatus
Botryococcus spp.
Reworking - Cretaceous
Reworking - Permian

Spores And Pollen — % within discipline (40mm=100%) / In-Situ occurrences

Acaantiopollis obscuris
Batteronella aerolus
Camerozonosporites ohaiensis
Ceratosporites equalis
Cicatricosisporites australiensis
Cyathidites australis
Cyathidites minor
Dictyophyllidites spp.
Divisyrites granulatus
Falcisporites similis
Forcipites longis
Gambierina rudata
Gleicheniidites spp.
Helorogacidites harrisii
Herkosporites elliottii
Laevigatosporites ovatus
Laevigatosporites vulsinites
Lygistepollenites balmei
Microachrysidites antarcticus
Nothofagidites endurus
Ornamentifera sentosa
Penninsulapollis gillii
Phyllocladidites mawsonii
Protoclavatites spp.
Retitriletes austroclavatidites
Stereisporites antiquasporites
Vitreisporites pallidus
Aequitriradites spinulosus
Cicatricosisporites australiensis
Clavifera triplex
Foveotriletes margaritae
Lycopodiacidites rugulatus
Murospora florida
Paxillitriletes phyllicus
Rugulatisporites mallatus
Staplinisporites caminus
Triporoletes reticulatus
Appendicisporites jansonii
Appendicisporites tricornitatus
Cicatricosisporites hughesi
Clavifera crassa
Crybelosporites stylosus
Dictyotosporites speciosus
Lycopodiumsporites austroclavatidites
Murospora florida
Phimopollenites pannosus
Reticulatisporites magnidictyus
Retitriletes austroclavatidites
Rugulatisporites mallatus
Staplinisporites caminus
Triporoletes reticulatus
Appendicisporites jansonii
Appendicisporites tricornitatus
Cicatricosisporites hughesi
Clavifera crassa
Crybelosporites stylosus
Dictyotosporites speciosus
Lycopodiumsporites austroclavatidites
Murospora florida
Phimopollenites pannosus
Reticulatisporites magnidictyus
Retitriletes austroclavatidites
Rugulatisporites mallatus
Staplinisporites caminus
Triporoletes reticulatus
Appendicisporites jansonii
Appendicisporites tricornitatus
Cicatricosisporites hughesi
Clavifera crassa
Crybelosporites stylosus
Dictyotosporites speciosus
Lycopodiumsporites austroclavatidites
Murospora florida
Phimopollenites pannosus
Reticulatisporites magnidictyus
Retitriletes austroclavatidites
Rugulatisporites mallatus
Staplinisporites caminus
Triporoletes reticulatus
Appendicisporites jansonii
Appendicisporites tricornitatus
Cicatricosisporites hughesi
Clavifera crassa
Crybelosporites stylosus
Dictyotosporites speciosus
Lycopodiumsporites austroclavatidites
Murospora florida
Phimopollenites pannosus
Reticulatisporites magnidictyus
Retitriletes austroclavatidites
Rugulatisporites mallatus
Staplinisporites caminus
Triporoletes reticulatus

AC | FT | AL | ?? | MP

Samples | Total Count — Total count: Total Count / In-Situ occurrences | % Category — Category %: % Category / In-Situ occurrences

FU | FT | AL | AC | MP | SP | DC | ALBO

Depth	Age	Zone	Sub Zone	Zone	Sub Zone
970.00m CU				970	Upper
1010.00m CU	Maastrichtian	1010 M.druggii		1010 F. longus	Lower
1060.00m CU		1060 I. pellucidum		1060	
1110.00m CU		I.korojonense		1110	
1190.00m CU		1190	1190 Upper	1190 N.senectus	
1250.00m CU		X.australis	lower c	1250	
1320.00m CU	Campanian	1320	lower a		
1410.00m CU		1410 N.aceras			
1460.00m CU					
1520.00m CU		1520			
1570.00m CU		Indeterminant			
1600.00m CU		1600			
1630.00m CU	Santonian	I.cretaceum			
1660.00m CU		1680			
1690.00m CU					
1700.00m CU		1720 O.porifera	Upper		
1720.00m CU	Coniacian	C.striatoconus	Upper		
1740.00m CU	?Coniacian	?C.striatoconus	?Lower		
1750.00m CU					
1760.00m CU	Indeterminate	Indeterminant			
1780.00m CU					
1790.00m CU					
1800.00m CU	Turonian	P.infusorioides	middle a		
1810.67m CO					
1821.53m CO					
1831.23m CO					
1840.00m CO			lower c		
1855.00m CU		1855	1855 lower b - or older		
1870.00m CU	Turonian - or older	P.infusoroides - or older			
1875.00m CU		1905	1905		
1880.00m CU					
1905.00m CU					

APPENDIX 2:
PETROLOGY REPORT

Report prepared for:

ORIGIN ENERGY RESOURCES LTD
339 Coronation Drive
Milton
QLD 4064

PETROLOGY REPORT

HALLADALE-1

OTWAY BASIN

Report prepared by:

Dr S E PHILLIPS
PGPC
1c Short Crescent
Beaumont SA 5066

October 2005

In requesting the services of Phillips-Gerrard Petrology Consultants (PGPC) the client agrees that PGPC is acting in an advisory capacity and shall not be liable or responsible for any loss, damages or expenses incurred by the client, or any other person or company, resulting from any data or interpretation presented in this report.

Mobile: 0414 712 728 Fax/phone: (61) 08 8379 8281 Email:pgpc@bigpond.com.au

CONTENTS

PAGE

1. SUMMARY..... 2

2. INTRODUCTION..... 3
Table 1 Summary of samples & services

3. METHODS..... 3

4. PETROLOGY..... 4
Table 2 Point count data for the Waarre Unit C..... 4
4.1 Halladale-1 DW1, cuttings, depth 1520-30mMD..... 5
4.2 Halladale-1 DW1, cuttings, depth 1550-60mMD..... 8
4.3 Halladale-1 DW1, cuttings, depth 1730-35mMD..... 11
4.4 Halladale-1 DW2, cuttings, depth 1760-65mMD..... 14
4.5 Halladale-1 DW1, core plug, depth 1792.7mMD..... 16
4.6 Halladale-1 DW2, core plug, depth 1812.9mMD..... 18
4.7 Halladale-1 DW2, core plug, depth 1818.3mMD..... 20
4.8 Halladale-1 DW2, core plug, depth 1818.58mMD..... 22
4.9 Halladale-1 DW2, core plug, depth 1825.15mMD..... 24

5. GRAIN SIZE ANALYSIS..... 26

6. DISCUSSION..... 28
6.1 Lithology..... 28
6.2 Detrital mineralogy & sediment provenance..... 29
6.3 Depositional environments..... 30
6.4 Authigenic mineralogy & diagenetic alteration..... 30
6.5 Reservoir quality..... 32

7. CONCLUSIONS..... 34

8. GLOSSARY..... 35

9. REFERENCES..... 36

Front cover:
Thin section photomicrograph, Halladale-1 DW2, core plug, depth 1825.15mMD. Plane light. Horizontal field of view 1.30mm.

1. SUMMARY

Origin Energy Resources Ltd sent thin sections of nine samples to PGPC from the well Halladale-1 in the Otway Basin for petrological description. Basic descriptions were requested of four cuttings from the Nullawarre Sandstone and Flaxman Formation. The study of five core plug offcuts from Unit C of the Waarre Formation was designed to provide interpretation of the sediment provenance, depositional environments, diagenetic alteration and factors controlling reservoir quality. All samples were described in thin section and photographed, but only those from the Waarre Formation were point counted and had grain size analysis.

Nullawarre Sandstone cuttings from 1520-30m are comprised of silty mudstone, sandy mudstone, fine grained carbonate cemented sandstone and crushed fine grained sandstone. At 1550-60m there are chips of fine to medium grained carbonate cemented sandstone, silty to sandy mudstone and fine grained sandstone. In cuttings from the Flaxman Formation at 1730-35m and 1760-65m there are chips of silty to sandy mudstone, glauconitic mudstone, sandy ironstone and carbonate cemented sandy ironstone. A high percentage of cuttings at 1760-65m are mudstones, including significant contamination from the drilling mud.

Unit C of the Waarre Formation at Halladale-1 is comprised of fine to coarse grained, poor to moderately well sorted, subarkoses. There are almost equal proportions of K-feldspars and lithics in the sandstones. Detrital mineralogy at the time of deposition would have been more feldspar rich but these grains are now altered to kaolin and illite. Typically detrital grains are subangular to subrounded with low to moderate sphericity and range from clay to granules in size. Grain size distributions are commonly unimodal with slight negative skewness and at 1818.58m the distribution is bimodal with peaks of very coarse and medium grain sizes.

The detrital mineralogy suggests sediment was derived from both metamorphic and igneous (plutonic) terranes which might have been exposed by uplift of Palaeozoic basement in the Lachlan Fold Belt. The abundance of polycrystalline quartz in coarse grained subarkoses at 1818.3m and 1818.58m may indicate a period dominated by an igneous source with relatively short distances of sediment transport. Rare brecciated quartz could reflect minor derivation from a faulted zone. After this phase the metamorphic terrane was probably more important as a source of K-feldspars, lithics of quartzite and micaceous schist, and biotite flakes.

Petrological evidence is consistent with a marginal marine depositional environment that was influenced by rivers. Sorting and grain shape are consistent with fluvial sands, but the grain size distributions suggest reworking by wave action to remove the fines. Trace amounts of glauconite and framboidal pyrite probably reflect the marine conditions, whilst ?siderite may have precipitated during flushing by meteoric waters.

Early diagenetic alteration of the subarkoses was related to the depositional environments. After burial feldspars and micas were altered to kaolin and minor illite, and quartz overgrowths precipitated. There is minimal evidence of mechanical compaction and only minor dissolution of labile grains. The final phase of pore filling and grain replacing carbonate spar is pervasive in the coarse grained subarkoses from 1818.3m and 1818.58m. The composition of the carbonate should be ascertained to help determine if it formed due an increase in CO_2 either associated with Pleistocene/Recent igneous activity or due to hydrocarbon maturation.

Reservoir quality is probably excellent where primary intergranular pores are dominant (13-14%). These pores were probably preserved due to minor development of early quartz overgrowths. Later carbonate spar has significantly limited reservoir quality in selected samples. Dissolution pores (3-5%) are grain sized, intragranular and honeycomb in nature and occur in all samples. Micropores are associated with grain replacing and pore filling kaolin but may not contribute to effective porosity.

2. INTRODUCTION

Origin Energy Resources Ltd submitted four cuttings and five core plug offcuts to PGPC from the well Halladale-1 in the Otway Basin. Samples were selected from the Santonian Nullawarre Sandstone, Turonian Flaxman Formation and Unit C of the Waarre Formation for petrological description. The study was design to provide basic descriptions of the Nullawarre and Flaxman cuttings. For the Waarre Formation descriptions and interpretation of the lithology, mineralogy, sediment provenance, depositional environments, diagenetic alteration and factors controlling reservoir quality were requested.

Services listed below (Table 1) were provided by PGPC. The client supplied the thin sections.

TABLE 1 SUMMARY OF SAMPLES & SERVICES

DW	Depth (mMD)	Unit	TS description	Grain size analysis	Point count
1	1520-30	Nullawarre	*	-	-
1	1550-60	Nullawarre	*	-	-
1	1730-35	Flaxman	*	-	-
2	1760-65	Flaxman	*	-	-
1	1792.7	Waarre C	*	*	*
2	1812.9	Waarre C	*	*	*
2	1818.3	Waarre C	*	*	*
2	1818.58	Waarre C	*	*	*
2	1825.15	Waarre C	*	*	*

3. METHODS

Thin section

Thin sections were systematically scanned to determine lithology, composition, porosity and textural relationships. Siliciclastics have been classified according to guidelines by Folk (1974) and carbonates using the nomenclature of Tucker (2001). Grain morphology (both sphericity and roundness) was estimated by comparison with charts in Pettijohn *et al* (1987), grain fabric (packing and texture) from the diagram in Tucker (2001) and sorting from diagrams by Harrell (1984). All percentages of composition given in Table 2 are counts of 500 points following the method of Stanton & Wilson (1994).

The basic data for grain size analyses was collected by measuring the long axis of 100 representative grains in thin section. The graphic mean, mode and inclusive graphic standard deviation (Folk, 1974) were then calculated.

4. PETROLOGY

TABLE 2 POINT COUNT DATA FOR THE WAARRE UNIT C

DW	1	2	2	2	2
Depth (mMD)	1792.7	1812.9	1818.3	1818.58	1825.15
Framework grains					
Quartz - mono	53.8	56.4	48.6	40.4	57.4
- poly	5.0	6.0	16.2	17.6	8.4
K-Feldspar	1.8	4.8	2.2	2.6	2.6
Lithics - chert	0.2	0.0	0.0	0.0	0.0
- quartzite	1.0	2.4	0.6	1.2	1.6
- micaceous schist	0.4	1.4	0.4	0.0	0.6
- ?granite	0.2	0.4	1.0	1.4	1.0
- others	0.0	0.6	0.0	0.0	0.0
Mica - muscovite	0.4	0.8	0.2	0.0	0.2
- biotite	0.0	0.8	0.0	0.0	0.0
Accessory - zircon	0.8	0.0	0.2	0.0	0.0
- tourmaline	0.6	0.4	0.0	0.0	0.4
- rutile	0.6	0.0	0.0	0.0	0.2
- monazite	0.4	0.0	0.0	0.2	0.0
Matrix					
Clay	0.8	0.0	0.0	0.0	0.0
Organic matter	0.8	0.4	0.0	0.0	0.4
Authigenic minerals					
Glaucony - glauconite	0.6	0.0	0.0	0.0	0.2
- chlorite	0.6	0.0	0.0	0.0	0.0
Fe carbonate - replace	0.8	0.8	0.0	0.2	0.0
- fill pores	0.0	0.0	0.0	0.0	0.0
Clear carbonate - replace	0.0	0.0	8.4	11.0	0.4
- fill pores	0.0	0.0	10.6	16.0	0.2
Quartz	6.2	3.4	2.2	1.4	2.8
Illite - replace	0.0	0.8	0.0	0.2	0.6
Kaolin - replace	3.0	0.6	0.8	0.6	1.4
- fill pores	1.8	0.6	0.4	0.0	1.2
Pyrite - replace	0.4	0.4	0.4	0.6	0.0
- fill pores	1.0	0.2	1.8	1.0	0.4
Porosity					
Intergranular	13.2	14.2	2.6	1.0	14.8
Dissolution	5.0	4.4	3.2	3.4	4.8
Fracture	0.0	0.0	0.0	1.2	0.0
Micropores	0.6	0.2	0.2	0.0	0.4
TOTAL	100.0	100.0	100.0	100.0	100.0

4.1 Halladale-1 DW1, cuttings, depth 1520-30mMD, Nullawarre Sandstone

Rock types present in the cuttings:

1. Silty mudstone (Fig. 1a)
Grain alignment & numerous discontinuous stringers of opaque organic matter indicate the orientation of bedding in the silty mudstone. Texturally the mudstone is matrix supported with silt to fine sand size detrital grains floating in the detrital clay. Typically detrital grains are angular to subrounded with low sphericity and consist of monocrystalline quartz, feldspars, lithics of chert & ?micaceous schist, muscovite & biotite flakes, calcareous ?foram tests (rare examples are globular & planktonic) filled with either pyrite or chert, & larger siliceous tests (?agglutinated forams) filled with pyrite. Matrix is comprised of anhedral brown clay & organic matter. Authigenic minerals of grain replacing glaucony (?chlorite & glauconite) & framboidal pyrite are apparent.

2. Sandy mudstone (Fig. 1b)
Silt to medium sand size angular to subrounded detrital grains float in anhedral mudstone. No sedimentary structures are apparent. Shell fragments derived from either brachiopods or bivalves are apparent. Other detrital grains consist of monocrystalline quartz, polycrystalline quartz, muscovite, ?chloritic volcanic lithics & other highly altered grains. Authigenic minerals include minor replacement of matrix by anhedral micritic siderite, grain replacing chlorite & pyrite framboids.

3. Fine grained carbonate cemented sandstone (Fig. 1c)
The sandstone is fine grained, moderately well sorted, and mineralogically mature. Grain size ranges from silt to medium sand. Angular detrital grains with low sphericity float in dusty anhedral carbonate spar. The dusty appearance could be due to partial crushing. There are no sedimentary structures preserved in the chips. Porosity is restricted to rare intragranular pores within lithics. Detrital grains are comprised of monocrystalline quartz, polycrystalline quartz, rare ?metamorphic lithics, straight muscovite flakes, rare glaucony & accessory opaques. Scattered throughout the grain replacing & pore filling carbonate spar there are pyrite framboids.

Rare chips of Fe rich anhedral microspar also contain fine sand & framboidal pyrite.

4. Crushed sandstone (Fig. 1d)
Fine grained, poorly sorted, mineralogically mature sandstone. Crenulated stingers of detrital clay (?stylolites) and blocky opaque organic matter indicate the presence of bedding. Grain size ranges from silt to medium sand and typically grains are subangular to subrounded with low sphericity. Texturally the sandstone is grain supported with tangential & concavo-convex grain contacts dominant. Porosity is restricted to honeycomb pores within corroded K-feldspars. Detrital grains consist of monocrystalline quartz, rare polycrystalline quartz, K-feldspars, bent biotite flakes, traces of glaucony & accessory zircon. Dark brown anhedral clay matrix with minor illitic laths. Authigenic minerals of chlorite replacing elongate grains (?biotite), and blocky & framboidal pyrite concentrating in the detrital clay & organic matter.

5. Contaminants & single grains
Crushed grains and drilling mud. Single grains of chert, fish bone, monocrystalline quartz, polycrystalline quartz, K-feldspar, twinned clear carbonate spar, medium sand size grains of bright green glauconite, tourmaline & zircon.

Figure 1a
General field of view illustrating the laminated nature of silty mudstone. Note the green gains which appear to be composed of both grain replacing chlorite and glauconite, and a foram test partially filled with pyrite (arrow). Halladale-1 DW1, cuttings, depth 1520-30mMD. Plane light. Horizontal field of view 1.30mm.

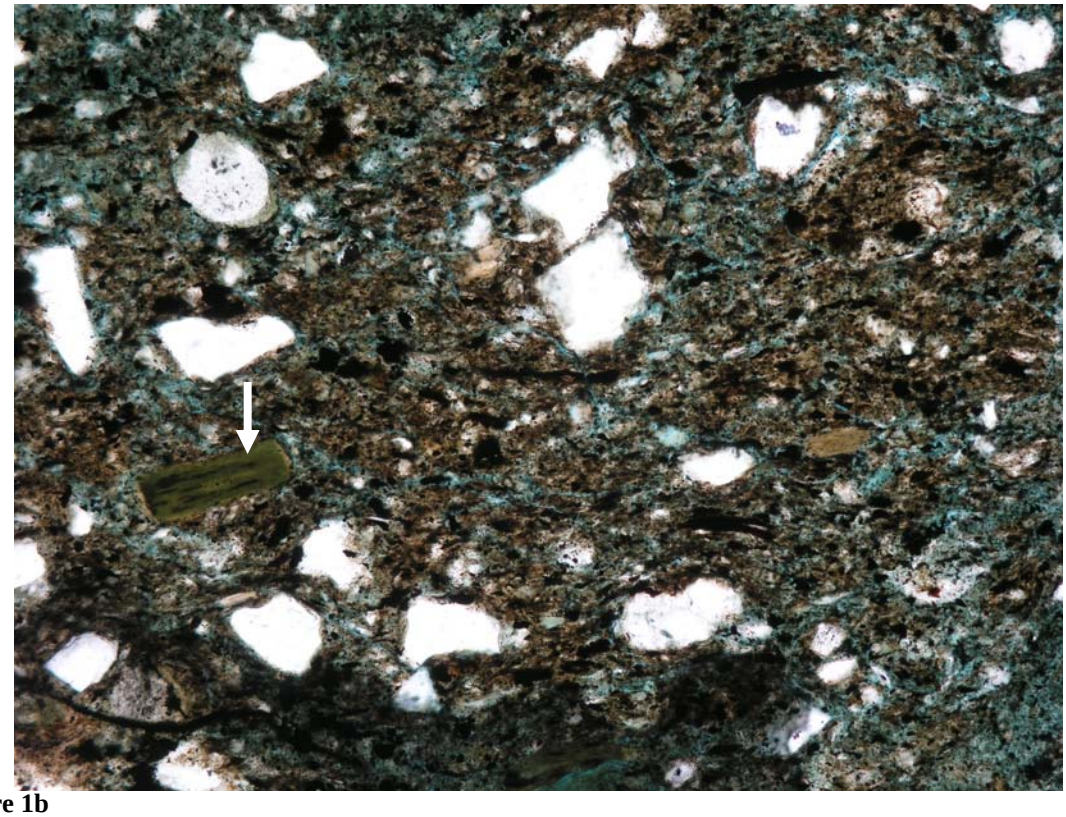

Figure 1b

Although the central chip of sandy mudstone has been crushed, it has still retained weak grain alignment. Note the angular nature of detrital grains and a rectangular grain (?biotite) replaced by chlorite (arrow). Halladale-1 DW1, cuttings, depth 1520-30mMD. Plane light. Horizontal field of view 1.30mm.

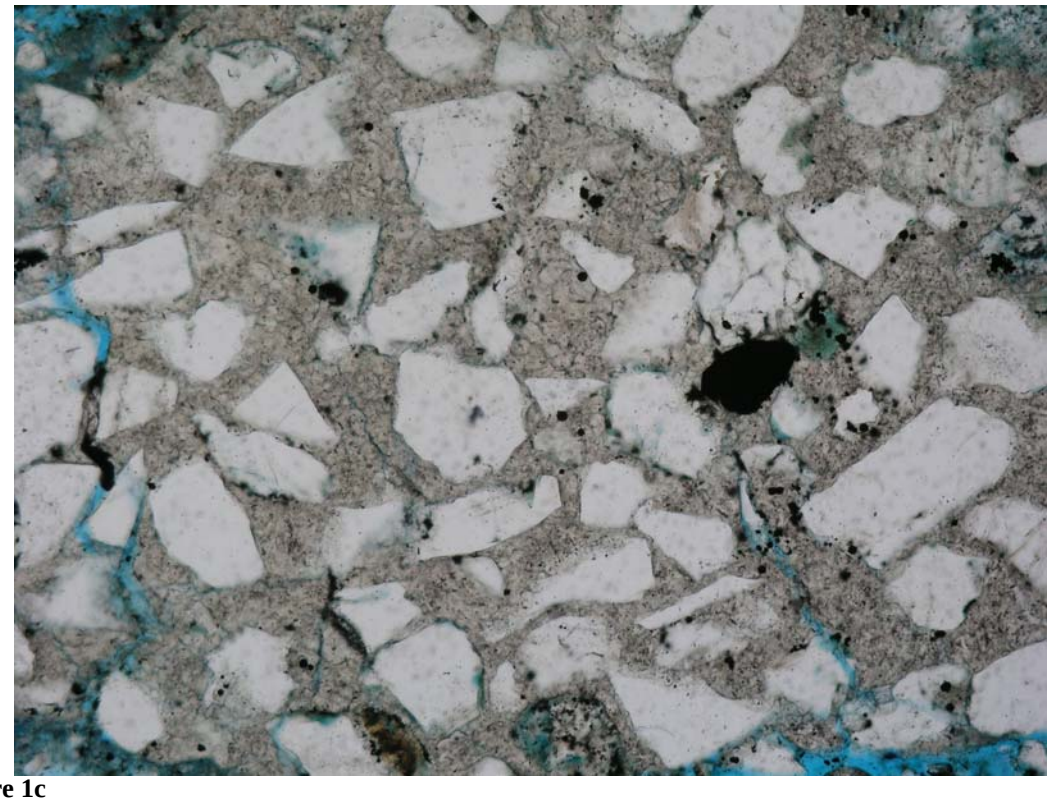

Figure 1c

This carbonate cemented sandstone would probably be a quartzarenite in composition. Detrital grains are angular and appear to float within the slightly dusty carbonate spar. Pyrite framboids (opaque) are scattered throughout the spar. Halladale-1 DW1, cuttings, depth 1520-30mMD. Plane light. Horizontal field of view 1.30mm.

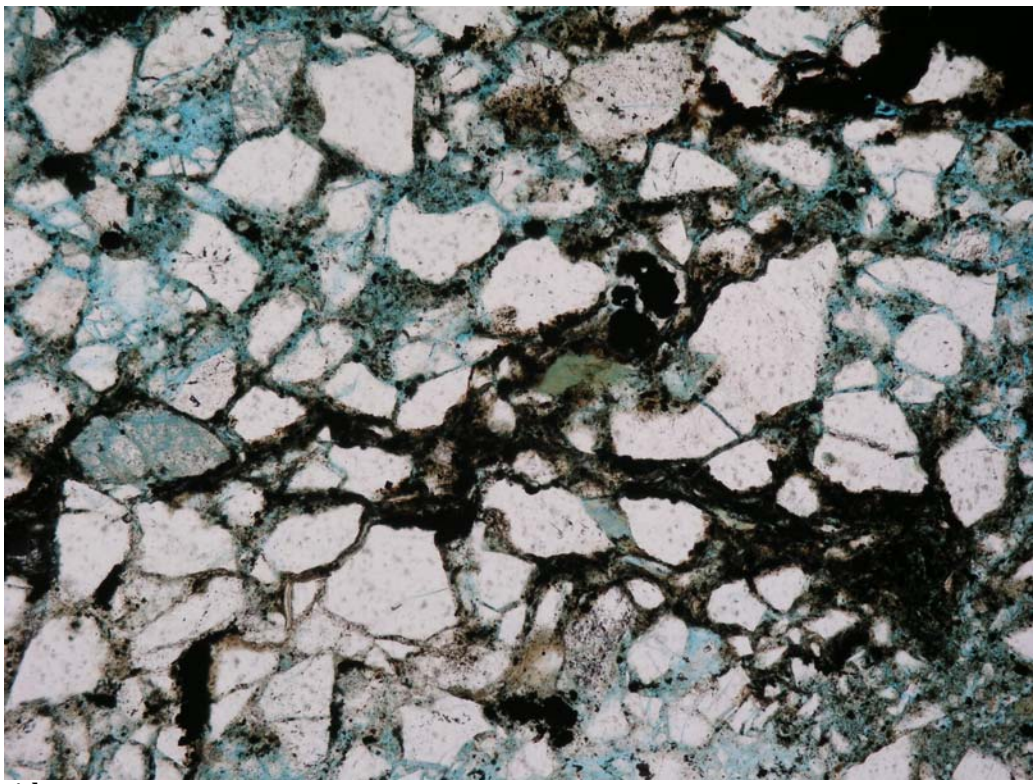

Figure 1d

Crenulated stringers of detrital dark brown clay & organic matter are evident in this disrupted chip of fine grained sandstone. Halladale-1 DW1, cuttings, depth 1520-30mMD. Plane light. Horizontal field of view 1.30mm.

4.2 Halladale-1 DW1, cuttings, depth 1550-60mMD, Nullawarre Sandstone

Rock types present in the cuttings:

1. Fine to medium grained carbonate cemented sandstone (Fig. 2a)

Rare minute chips of carbonate cemented sandstone could represent downhole contaminants from cuttings at 1520-30m. Cements vary from clear carbonate spar to anhedral Fe rich microspar. One chip has a pore filling cement of clear spar but there are scalenohedra of Fe rich microspar to spar aligned near grain margins. Angular to subrounded detrital grains of monocrystalline quartz float in the carbonate.

2. Silty to sandy mudstone (Fig. 2b)

Silty to sandy mudstone is the dominant lithology present but it might represent a downhole contaminant since there is no significant difference from the mudstone described from 1520-30m. Laminae within the mudstone are outlined by variations in the percentage of detrital grains & organic matter. Silt to medium sand size grains of monocrystalline & polycrystalline quartz, feldspars, lithics of quartzite & ?micaceous schist, straight muscovite flakes & bent biotite. Matrix of dark to light brown anhedral clay with minor opaque to reddish organic matter. Authigenic blocky & framboidal pyrite, bright green rounded and highly deformed grains of glaucony (?chlorite & glauconite) & grain replacing chlorite. Rarely chips have irregular patches of Fe rich micrite up to fine sand in size. These patches could be replacing detrital grains.

3. Fine grained sandstone (Fig. 2c)

One partially crushed chip of fine grained, moderately well sorted, mineralogically mature sandstone. Where grain contacts have not been disrupted by sampling there are tangential contacts evident. Texturally the sandstone was grain supported with moderately close packing. Typically grains are subangular with low sphericity. No porosity or sedimentary structures are apparent. Framework grains consist of monocrystalline quartz, polycrystalline quartz, hornblende & tourmaline. Authigenic grain replacing chlorite & rare ?chlorite rims approximately 5 microns thick filling intergranular pores are evident. Isolated grains have been replaced by minute (less than 5 microns diameter) booklets of ?kaolin. There could be micropores associated with this ?kaolin. Rare straight grain contacts might indicate the presence of quartz overgrowths.

4. Contaminants & single grains

Crushed grains and drilling mud. Single grains of monocrystalline quartz up to coarse sand in size, clear carbonate spar, glauconite, forams replaced by ?siderite & filled with chert, glauconite & tourmaline.

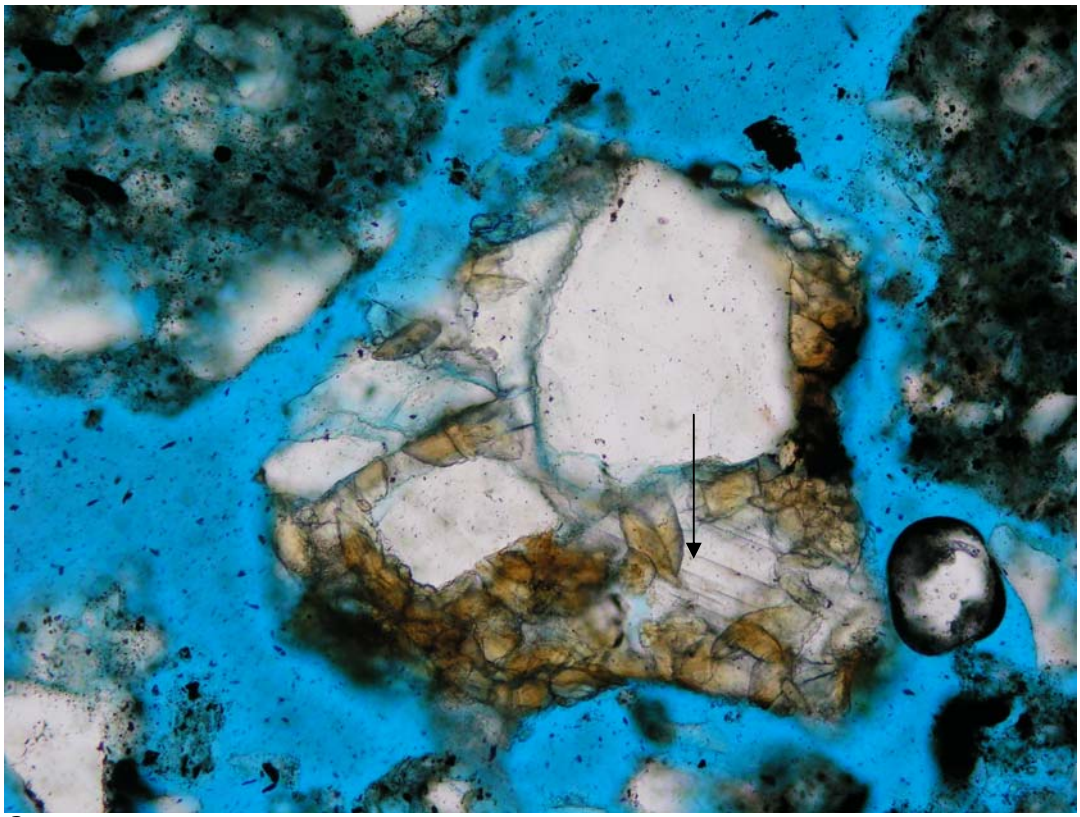

Figure 2a
These quartz grains are cemented by clear twinned carbonate spar (arrow) and a Fe rich phase of carbonate which was probably early diagenetic siderite (reddish-brown). Halladale-1 DW1, cuttings, depth 1550-60mMD. Plane light. Horizontal field of view 0.65mm.

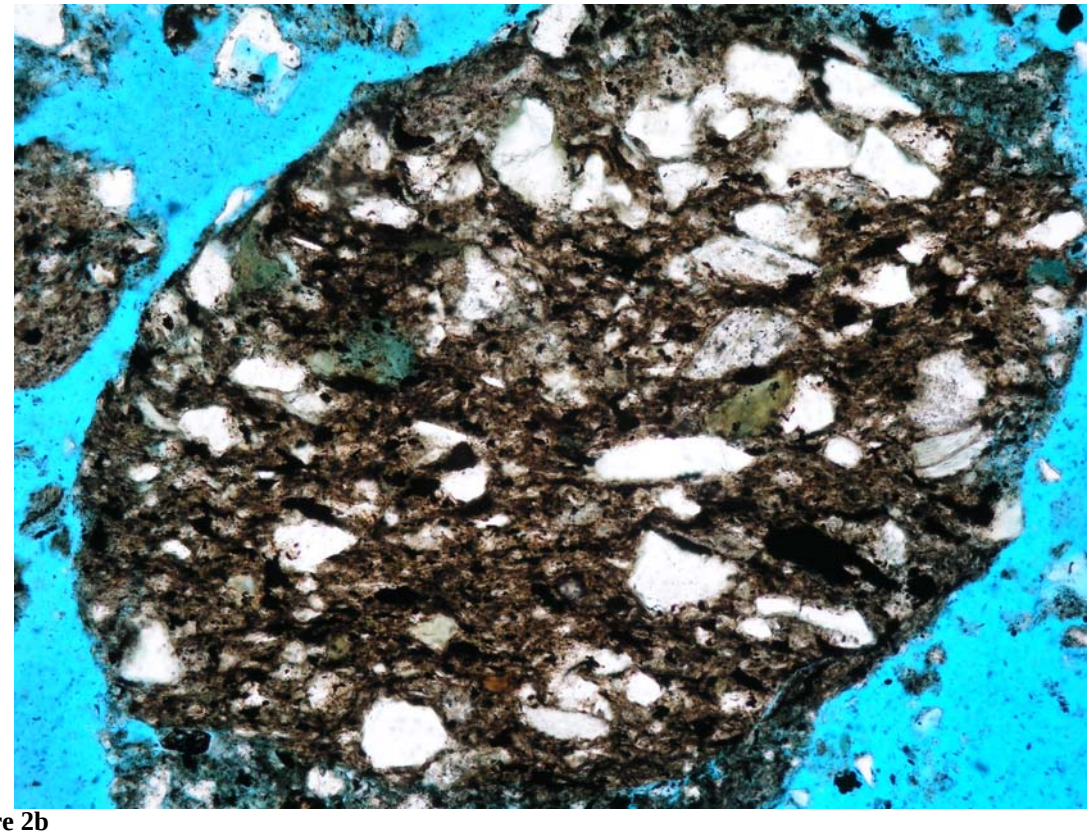

Figure 2b
Typical field of view of sandy mudstone which is matrix supported. The percentage of detrital grains and their grain size is highly variable. Halladale-1 DW1, cuttings, depth 1550-60mMD. Plane light. Horizontal field of view 1.30mm.

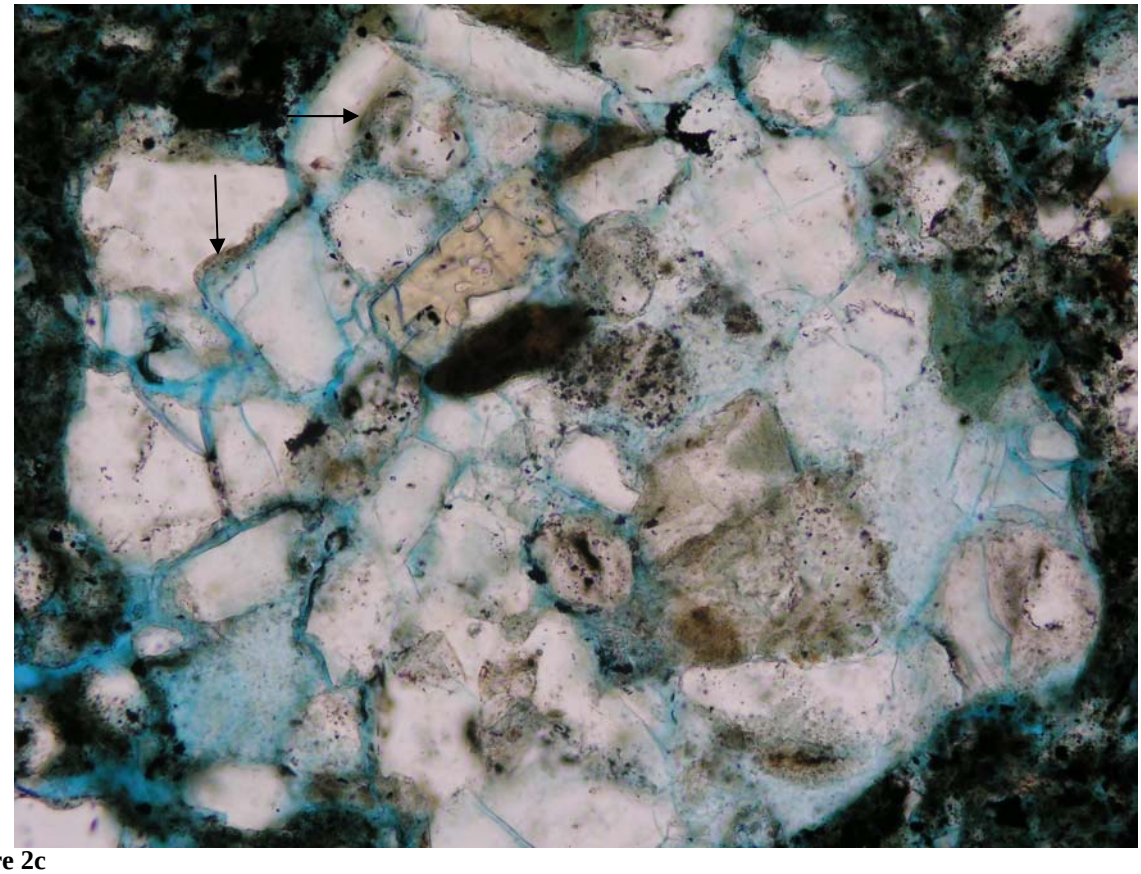

Figure 2c
This is the only chip of fine grained sandstone. Note the slightly oxidised ?chlorite rims (arrows) that fill an intergranular pore near a grain of yellowish tourmaline. Other grains are partially replaced by chlorite. Halladale-1 DW1, cuttings, depth 1550-60mMD. Plane light. Horizontal field of view 0.65mm.

4.3 Halladale-1 DW1, cuttings, depth 1730-35mMD, Flaxman Formation

Rock types present in the cuttings:

1. Silty to sandy mudstone
This lithology is probably a downhole contaminant since there is no significant compositional variation from descriptions at 1550-60m.

2. Glauconitic mudstone (Fig 3a)
Poorly sorted detrital and authigenic grains are supported by dark brown anhedral clay. Silt to medium sand size detrital grains of angular to subrounded monocrystalline quartz, polycrystalline quartz, K-feldspar, ?volcanic lithics, rare curved fragments of polycrystalline quartz in one chip could represent segments of agglutinated forams and there are grains of chert present. Bright green medium to coarse sand size rounded grains of glauconite are rarely partially oxidised and there are similar sized grains of unknown origin that are completely oxidised. Where the percentage of glauconite is high these grains are deformed and the mudstones could be described as greensands. Opaque organic matter and framboidal pyrite occur within the matrix and framboids have partially replaced the glauconite. Chlorite has partially replaced polycrystalline quartz & ?volcanic lithics. Matrix is partially replaced by anhedral single crystals of carbonate spar up to 30 microns in diameter in isolated chips.

3. Sandy Ironstone to carbonate cemented sandy ironstone (Figs 3b & c)
The sandy ironstone is moderately well sorted and mineralogically very mature. Average grain size is medium sand, with a range from fine sand to granules. Typically grains are subangular to subrounded with moderate sphericity. Texturally the ironstone is cement supported. Moderately open packing is indicated by the point and tangential grain contacts. The only evidence of porosity is cracking around grains which are probably an artifact of sampling. Detrital grains are dominated by monocrystalline quartz. Iron rich ooids have cores of hematite & quartz, & partial to complete concentric laminae of goethite &/or siderite. These ooids are rounded with moderate sphericity and range in diameter from fine to medium sand. Authigenic minerals include rounded medium sand size bright green grains of glaucony with wormy texture typical of glauconite. Grains of glauconite, ooids and quartz are all rimmed by chlorite but these rims are absent at rare grain contacts suggesting formation after minor compaction. Typically the rims appear to be up to 10 microns in thickness. Chlorite has also replaced grains of unknown origin. Clear carbonate spar has filled the remaining pore space and partially replaced the detrital quartz grains.

Several chips are comprised of hematite and chlorite rich ooids, and fine to medium sand size oxidised (hematite) grains & angular quartz grains floating in a matrix of chlorite. The ooids are typically 0.50mm in diameter (range from fine to coarse sand) with a core of either hematite or quartz and multiple concentric laminae of chlorite. Clear carbonate spar has partially replaced the ooids and there are single crystals of anhedral spar in the chloritic matrix.

4. Contaminants & single grains
Drilling mud and crushed grains. Single grains of silt to coarse sand size monocrystalline & polycrystalline quartz, muscovite flakes, Fe rich ooids up to 0.35mm diameter with multiple concentric laminae, anhedral Fe rich carbonate & clear carbonate spar.

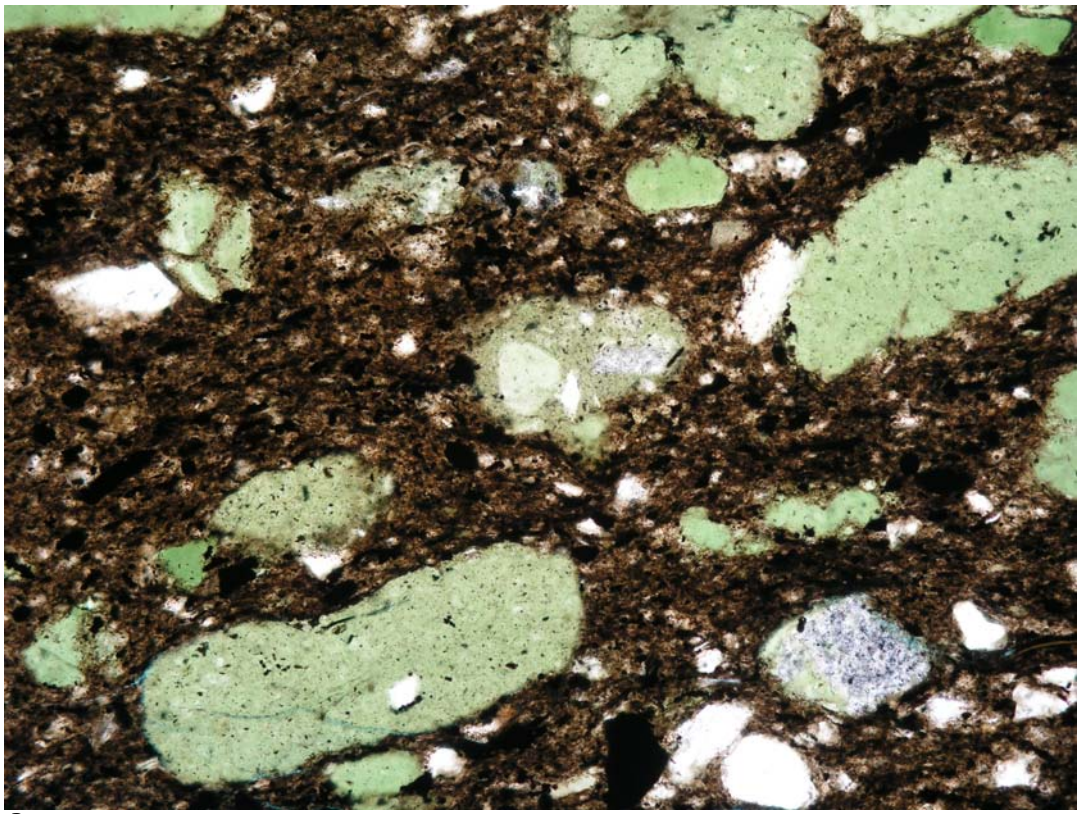

Figure 3a

Typical chip of glauconitic mudstone with bright green grains of glaucony surrounded by detrital dark brown clay and traces of pyrite and organic matter (opaque). Halladale-1 DW1, cuttings, depth 1730-35mMD. Plane light. Horizontal field of view 1.30mm.

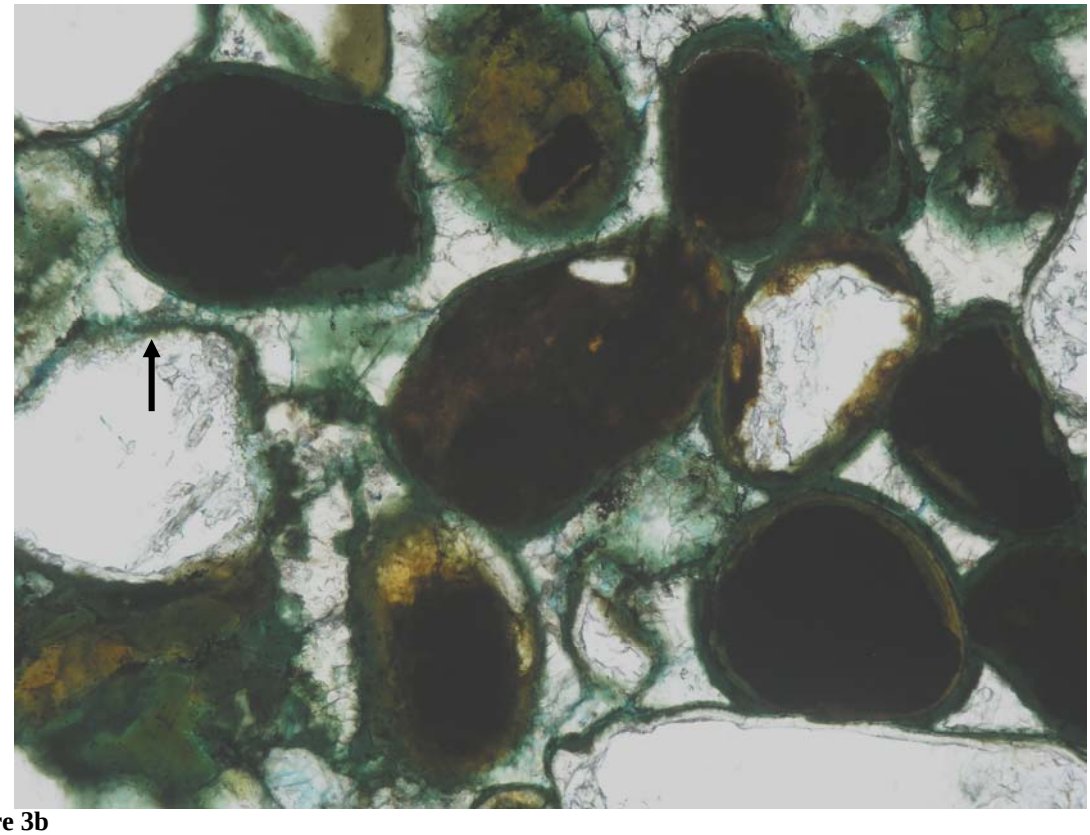

Figure 3b

Ooids and detrital grains of quartz are rimmed by chlorite (arrow) and then the remaining pores filled with blocky carbonate spar. Halladale-1 DW1, cuttings, depth 1730-35mMD. Plane light. Horizontal field of view 1.30mm.

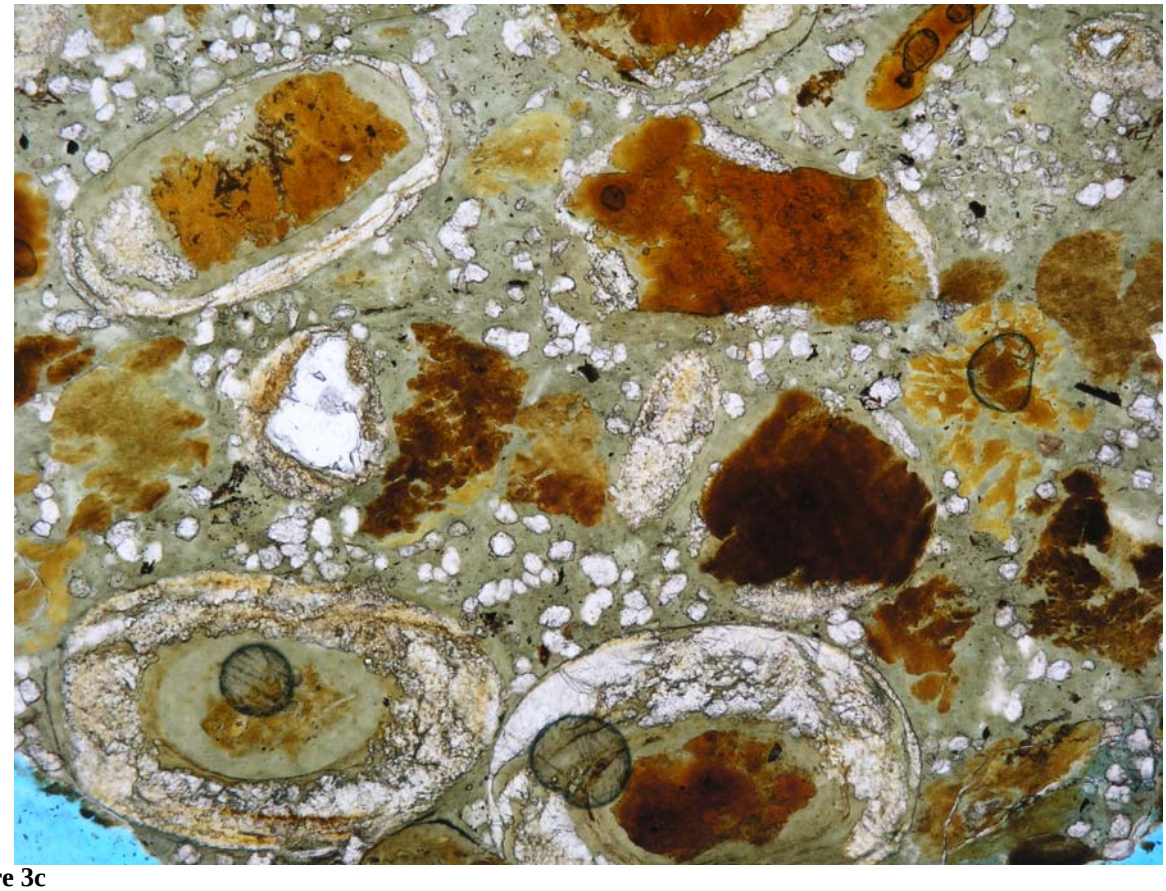

Figure 3c

In this chip the matrix is chloritic and ooids have cores of reddish hematite and rims of chlorite. Carbonate (white) has partially replaced the ooids and the matrix. Spheres with black rims are bubbles in the glue used for thin section preparation. Halladale-1 DW1, cuttings, depth 1730-35mMD. Plane light. Horizontal field of view 1.30mm.

4.4 Halladale-1 DW2, cuttings, depth 1760-65mMD, Flaxman Formation

Rock types present in the cuttings:

1. Silty to sandy mudstone

As per descriptions from 1520-30m and 1550-60m. The relative abundance of this lithology suggests it could be repeated at this depth. There might be interbedding of silty mudstone with sandy mudstone. Detrital grains in both lithologies consist of monocrystalline & polycrystalline quartz, ?corroded K-feldspars, chert, muscovite & biotite flakes, & accessory tourmaline. Matrix is anhedral brown clay with minor opaque organic matter. Authigenic minerals of pyrite, silt size bright green glauconite & unidentified oxidised grains.

2. Carbonate cemented ironstone

As per the description from 1730-35m.

3. Glauconitic mudstone

As per the description from 1730-35m.

4. Contaminant & single grains

The bulk of this sample is mudstone of various types mixed with drilling mud & single grains. Single grains include numerous chips of angular clear twinned carbonate spar, silt to coarse sand size monocrystalline & polycrystalline quartz, rare feldspars, possible metamorphic lithics, chert, Fe rich ooids, rare silicified foram tests filled with pyrite, anhedral Fe rich carbonate spar, fine sand size bright green glauconite, pyrite & rare grains replaced by chlorite. It is possible that carbonate cemented sandstone composed of these single grains has been disaggregated.

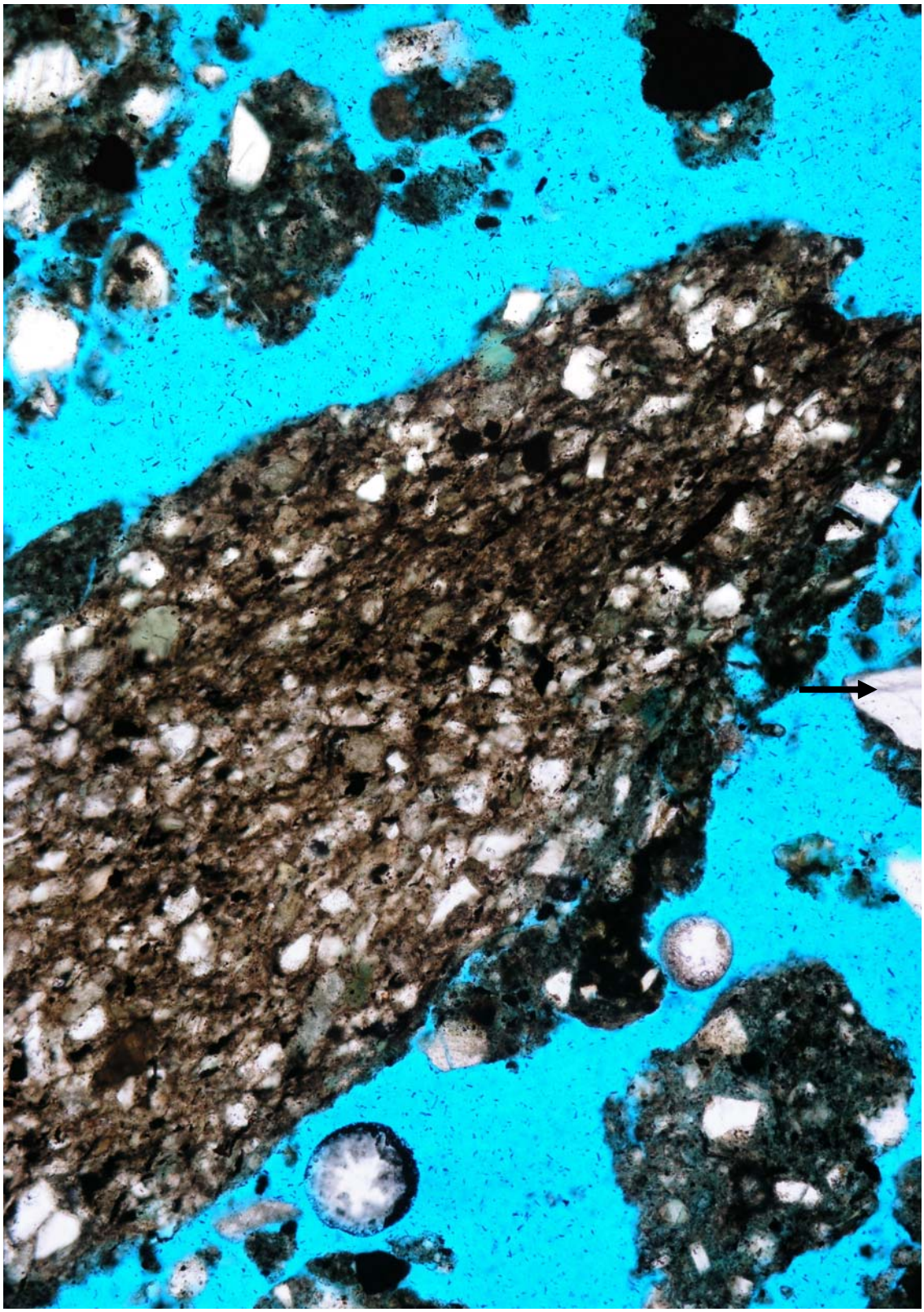

Figure 4
General field of view illustrating a large chip of silty mudstone and other single grains cemented by drilling mud. Angular chips of carbonate spar (arrow) are evident in the drilling mud. Halladale-1 DW2, cuttings, depth 1760-65mMD. Plane light. Horizontal field of view 1.30mm.

4.5 Halladale-1 DW1, core plug offcut, depth 1792.7mMD, Waarre C

Rock classification: **Subarkose**

Texture:

Sedimentary structures:	crenulated discontinuous stringers of accessory minerals, detrital clay & organic matter outline cross laminae
Average grain size:	fine sand
Range in grain size:	clay to coarse sand
Roundness / sphericity:	prior to silicification grains were subangular to subrounded with low to moderate sphericity
Sorting:	poor
Texture:	grain supported
Packing / grain contacts:	moderately open / typically point & tangential grain contacts, rare suturing adjacent to laminae
Pore types:	primary intergranular pores are dominant, honeycomb pores have developed where feldspars are corroded, rare grain size dissolution pores, intragranular pores within polycrystalline quartz, micropores where grains replaced by kaolin

Composition:

Framework grains:	monocrystalline quartz with rare mineral inclusions of biotite & rutile needles, polycrystalline quartz with either sutured or straight crystal boundaries, fresh, sericitised & corroded K-feldspars with minor tartan twinning, lithics of chert, quartzite, micaceous schist & possible granite (quartz + K-feldspar), bent & splayed muscovite flakes up to 0.60mm in length, accessory silt to fine sand size tourmaline, zircon, monazite & rutile
Matrix:	anhedral dark brown clay, silt & blocky opaque organic matter
Authigenic minerals:	fine to coarse sand size green grains of deformed glaucony have a slightly fibrous habit typical of chlorite & rarely display wormy texture characteristic of glauconite, prismatic & rhombohedral syntaxial quartz overgrowths outlined by euhedral terminations on pores, straight grain contacts & rare dust rims, grain replacing kaolin occurs as booklets & rare verms from 20 to 50 microns in diameter, booklets also fill adjacent intergranular pores & have a jagged contact with quartz overgrowths, where micas have been partially replaced by vermiform kaolin the booklet diameters are large, blocky pore filling & grain replacing pyrite is scattered throughout the section, pyrite also forms reaction rims on accessory ?rutile & is concentrated where replacing grains of glaucony, dusty anhedral Fe rich micrite partially replacing micas & lithics & forming patches within the matrix

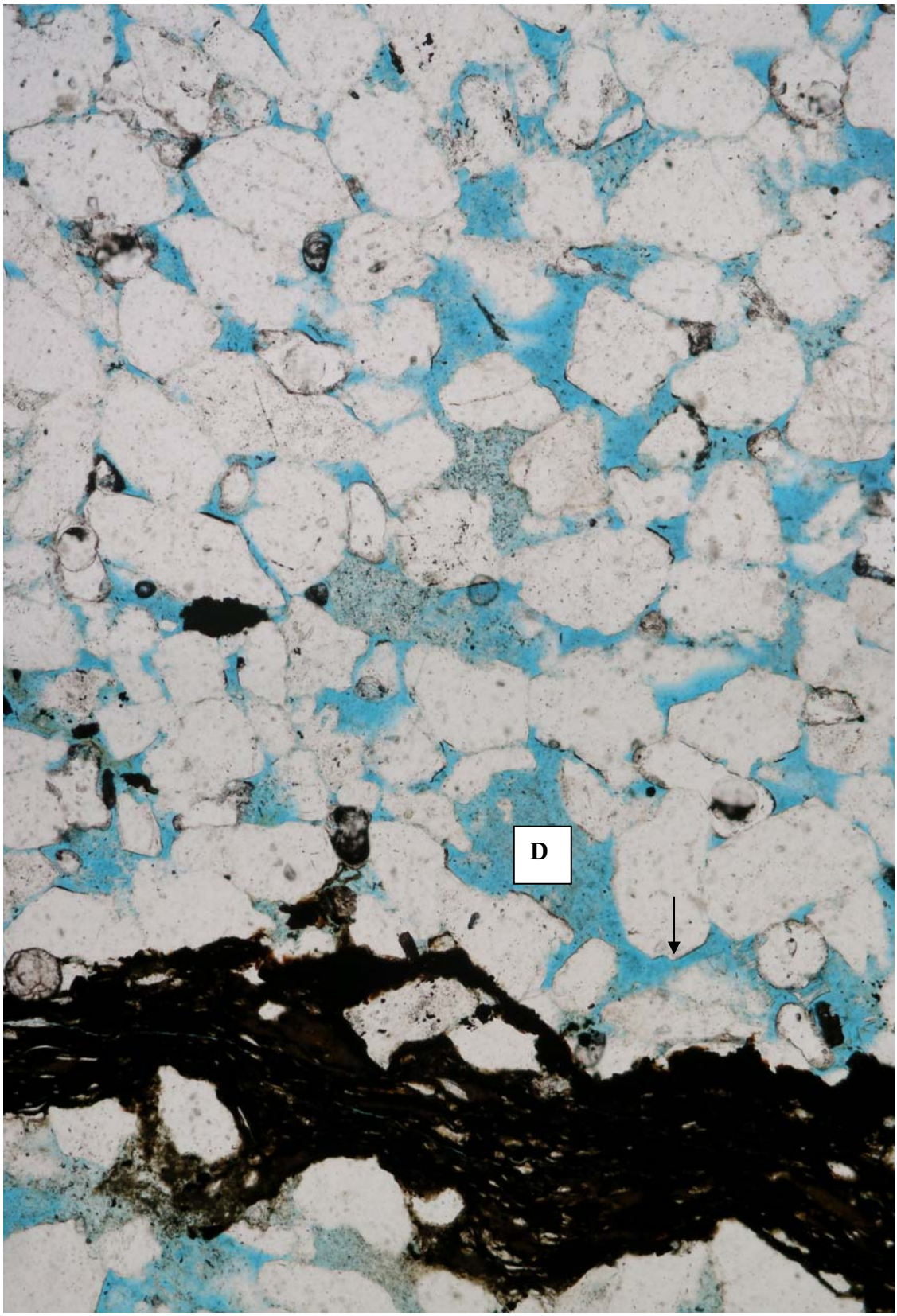

Figure 5

Laminae (dark brown) are discontinuous and therefore unlikely to represent permeability barriers within this sandstone. Packing is moderately open and there are euhedral terminations (arrow) where quartz overgrowths are apparent. Note the dominance of primary intergranular pores (blue) with minor grain size dissolution pores (D). Halladale-1 DW1, core plug offcut, depth 1792.7mMD. Plane light. Horizontal field of view 1.30mm.

4.6 Halladale-1 DW2, core plug offcut, depth 1812.9mMD, Waarre C

Rock classification: **Subarkose**

Texture:

Sedimentary structures:	grain alignment & changes in grain size indicate the presence of planar laminae
Average grain size:	medium sand
Range in grain size:	very fine to very coarse sand
Roundness / sphericity:	subangular to subrounded with low to moderate sphericity
Sorting:	moderately well sorted
Texture:	grain supported
Packing / grain contacts:	moderately open / point & tangential
Pore types:	primary intergranular pores, grain size dissolution pores, honeycomb pores where feldspars are corroded, intragranular pores within lithics & where inclusions in quartz have been dissolved, micropores associated with kaolin, the abundance of bubbles in the thin section glue may have been caused by the presence of hydrocarbons

Composition:

Framework grains:	monocrystalline quartz with rare mineral inclusions of apatite, zircon & tourmaline, polycrystalline quartz with either straight or sutured crystal boundaries, corroded K-feldspars lack twinning & partially corroded grains have remnants of tartan twinning, lithics of quartzite, micaceous schist, ?granite & other highly altered possibly metamorphic lithics, bent & splayed highly altered muscovite & biotite up to 0.70mm in length, accessory very fine to fine sand size tourmaline
Matrix:	traces of blocky opaque organic matter
Authigenic minerals:	prismatic & rhombohedral quartz overgrowths outlined by euhedral terminations on pore margins, single crystals of euhedral rhombic Fe rich microspar to spar have partially replaced biotite & clusters of anhedral Fe rich microspar has completely replaced other unidentified grains, deformed illitic grains of unknown origin are rarely partially replaced by Fe rich carbonate, other grains replaced by a mixture of kaolin booklets & illite or only kaolin, kaolin booklets are typically 5-20 microns in diameter, where kaolin is associated with polycrystalline quartz it has probably replaced the feldspar in an igneous lithic, kaolin has been squeezed into primary intergranular pores adjacent to grain replacing kaolin, rare blocky grain replacing (biotite) & pore filling pyrite

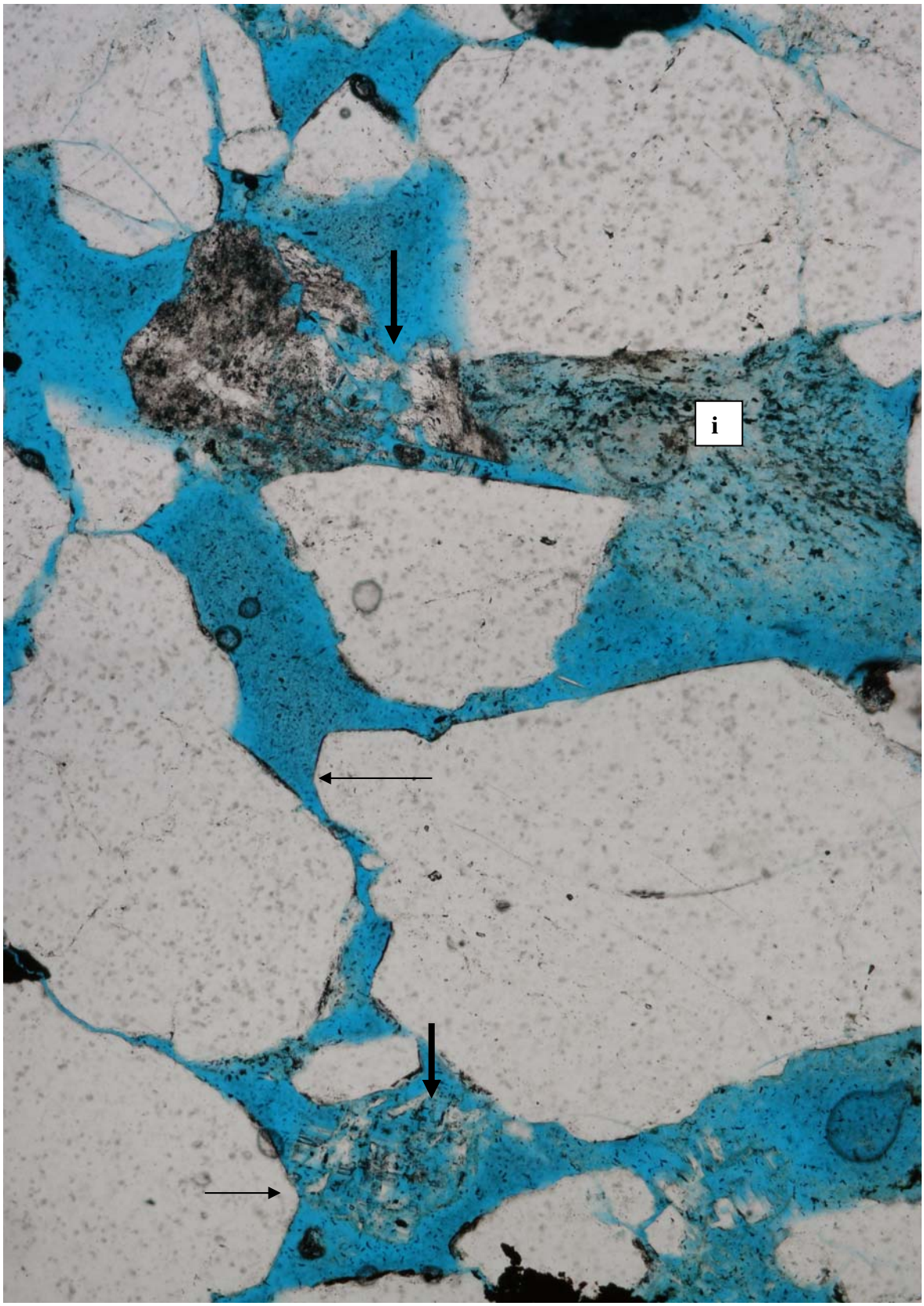

Figure 6

Corroded feldspars (large arrows), deformed grains replaced by illite (i) & quartz overgrowths (small arrows) are evident within this coarser grained laminae. Elongate primary intergranular pores (blue) indicate good permeability. Halladale-1 DW2, core plug offcut, depth 1812.9mMD. Plane light. Horizontal field of view 1.30mm.

4.7 Halladale-1 DW2, core plug offcut, depth 1818.3mMD, Waarre C

Rock classification: **Carbonate cemented subarkose**

Texture:

Sedimentary structures:	none apparent
Average grain size:	coarse sand
Range in grain size:	fine sand to granules
Roundness / sphericity:	subangular to subrounded with low to moderate sphericity
Sorting:	moderately sorted
Texture:	grain supported
Packing / grain contacts:	open packing / point & tangential grain contacts
Pore types:	intergranular pores tend to concentrate in zones of finer grain size that are better sorted, elsewhere there are grain size dissolution pores, honeycomb pores where feldspars are corroded, rare intragranular pores in lithics & micropores associated with kaolin

Composition:

Framework grains:	monocrystalline quartz with rare mineral inclusions of muscovite, zircon & tourmaline, polycrystalline quartz with either straight or sutured crystal boundaries, corroded K-feldspars either lack twinning or have remnants of tartan twinning, lithics of micaceous schist, quartzite & ?granite (polycrystalline quartz + K-feldspar), muscovite flakes up to 0.4mm in length, accessory very fine sand size zircon
Matrix:	none apparent
Authigenic minerals:	vermiform kaolin booklets up to 50 microns in diameter have filled pores, replaced grains & been replaced by clear carbonate spar, prismatic quartz overgrowths prior to pore filling spar, pervasive poikilotopic clear carbonate spar has filled pores & replaced grains, on pore margins the spar has either euhedral terminations or is corroded, corroded feldspars are partially replaced by carbonate spar, framboidal & blocky pyrite concentrates along grain margins, blocks pore throats & partially replaces grains

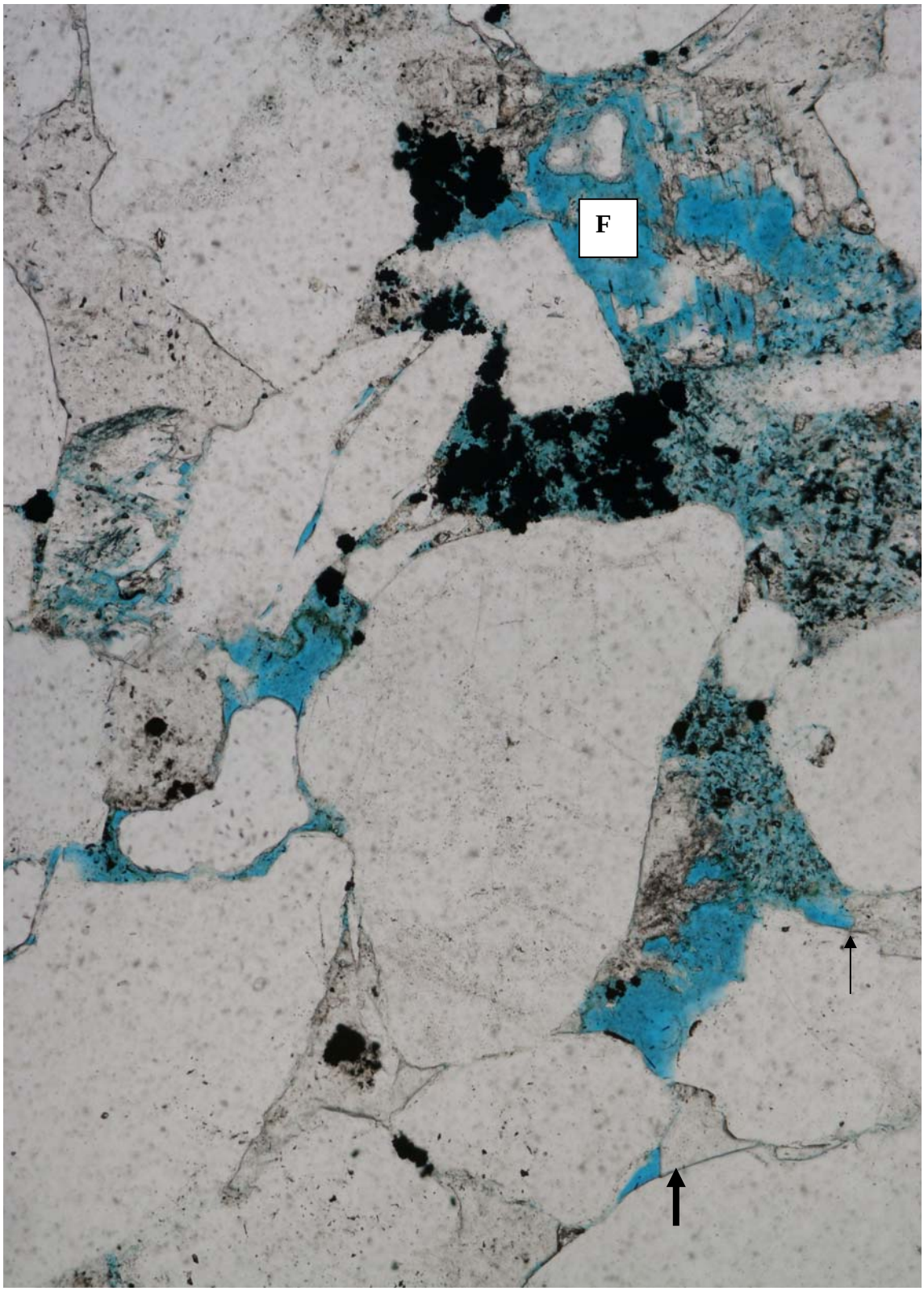

Figure 7

In this field of view there is evidence of pyrite (opaque) filling pores & replacing grains, honeycomb pores where feldspars are corroded (F), grain replacing kaolin (speckled), and pore filling clear carbonate spar. The latter has both euhedral terminations in intergranular pores (large arrow) and corroded margins adjacent secondary pores (small arrow). Halladale-1 DW2, core plug offcut, depth 1818.3mMD. Plane light. Horizontal field of view 1.30mm.

4.8 Halladale-1 DW2, core plug offcut, depth 1818.58mMD, Waarre C

Rock classification: **Carbonate cemented subarkose**

Texture:

Sedimentary structures:	none apparent
Average grain size:	coarse sand
Range in grain size:	very fine to granules
Roundness / sphericity:	subangular to subrounded with low to moderate sphericity
Sorting:	moderately sorted
Texture:	grain supported
Packing / grain contacts:	open packing / point & tangential grain contacts
Pore types:	intergranular pores, honeycomb pores due to corrosion of feldspars, intragranular pores where inclusions in quartz have been dissolved, open fractures through grains & the complete thin section are possibly an artifact of sampling

Composition:

Framework grains:	monocrystalline quartz with rare mineral inclusions of muscovite, polycrystalline quartz with either straight or sutured crystal boundaries, rare polycrystalline quartz appears to be brecciated, corroded K-feldspars either lack twinning or have remnants of simple & tartan twinning, lithics of quartzite & ?granite (monocrystalline quartz + fresh microcline), accessory very fine sand size ?monazite
Matrix:	none apparent
Authigenic minerals:	grain replacing kaolin booklets up to 35 microns diameter are replaced by carbonate spar, where kaolin occurs within corroded feldspars it has not been replaced by spar, prismatic quartz overgrowths outlined by euhedral terminations & dust rims formed prior to the spar, pervasive pore filling & grain replacing clear twinned poikilotopic carbonate spar has euhedral terminations, spar has partially replaced corroded feldspars, trace amounts of anhedral Fe rich micrite associated with altered lithics, blocky & framboidal pyrite concentrates on pore margins, within pore throats & partially replacing grains, rare grains of unknown origin replaced by illite

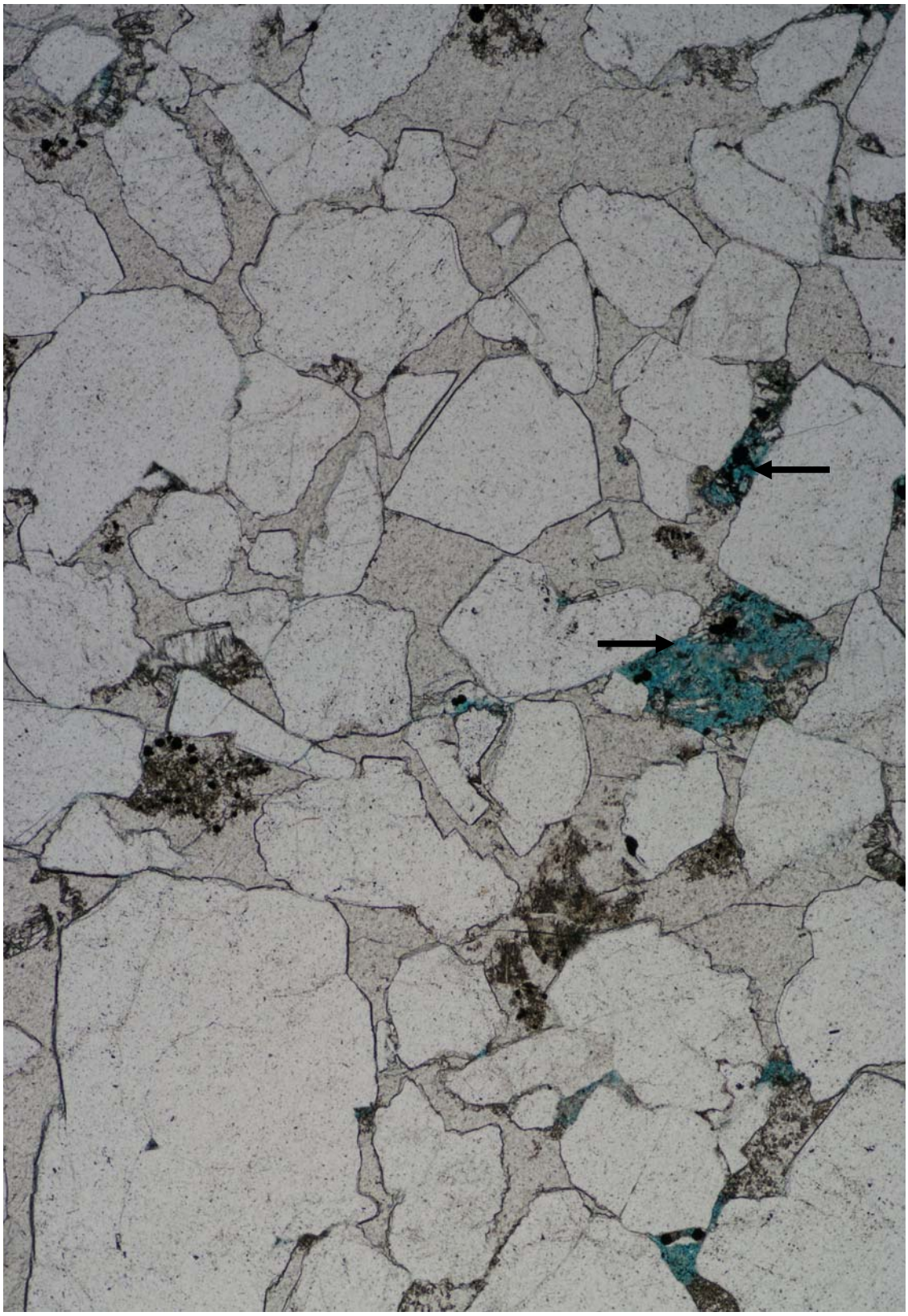

Figure 8

Lack of interconnection between secondary pores (arrows) indicates that permeability may be limited in this sample. Note the pervasive pore filling carbonate spar and dusty inclusions where grains have been replaced. Halladale-1 DW2, core plug offcut, depth 1818.58mMD. Plane light. Horizontal field of view 3.25mm.

4.9 Halladale-1 DW2, core plug offcut, depth 1825.15mMD, Waarre C

Rock classification: **Subarkose**

Texture:

Sedimentary structures:	none apparent
Average grain size:	coarse sand
Range in grain size:	fine to very coarse sand
Roundness / sphericity:	subangular to subrounded with low to moderate sphericity
Sorting:	moderately sorted
Texture:	grain supported
Packing / grain contacts:	open packing/ point & tangential grain contacts
Pore types:	primary intergranular pores, minor grain size, intragranular (where labile components in quartz grains dissolved) & honeycomb dissolution pores, micropores associated with kaolin, drilling mud has accumulated as a partial rim on pores

Composition:

Framework grains:	monocrystalline quartz with rare mineral inclusions of muscovite, monazite, tourmaline, biotite & rutile, polycrystalline quartz with dominantly straight crystal boundaries, rare examples of polycrystalline quartz with sutured crystal boundaries & one example that might have been derived from a breccia, corroded & fresh K-feldspars with examples that have tartan & simple twinning, lithics of quartzite, micaceous schist & ?granite, splayed & highly altered muscovite flakes up to 0.65mm in length, accessory fine sand size rutile & medium sand size tourmaline
Matrix:	fragmented blocky opaque material is probably organic matter
Authigenic minerals:	silt size bright green glaucony, prismatic quartz overgrowths have euhedral terminations, grain replacing kaolin booklets & verms are up to 0.35mm in diameter, where grains have been replaced the adjacent intergranular pores are also filled with kaolin, trace amounts of pore filling & grain replacing blocky twinned clear carbonate spar, framboidal pyrite up to 10 microns in diameter & blocky pyrite are concentrated in pore throats, rare grains of unknown origin replaced by illite

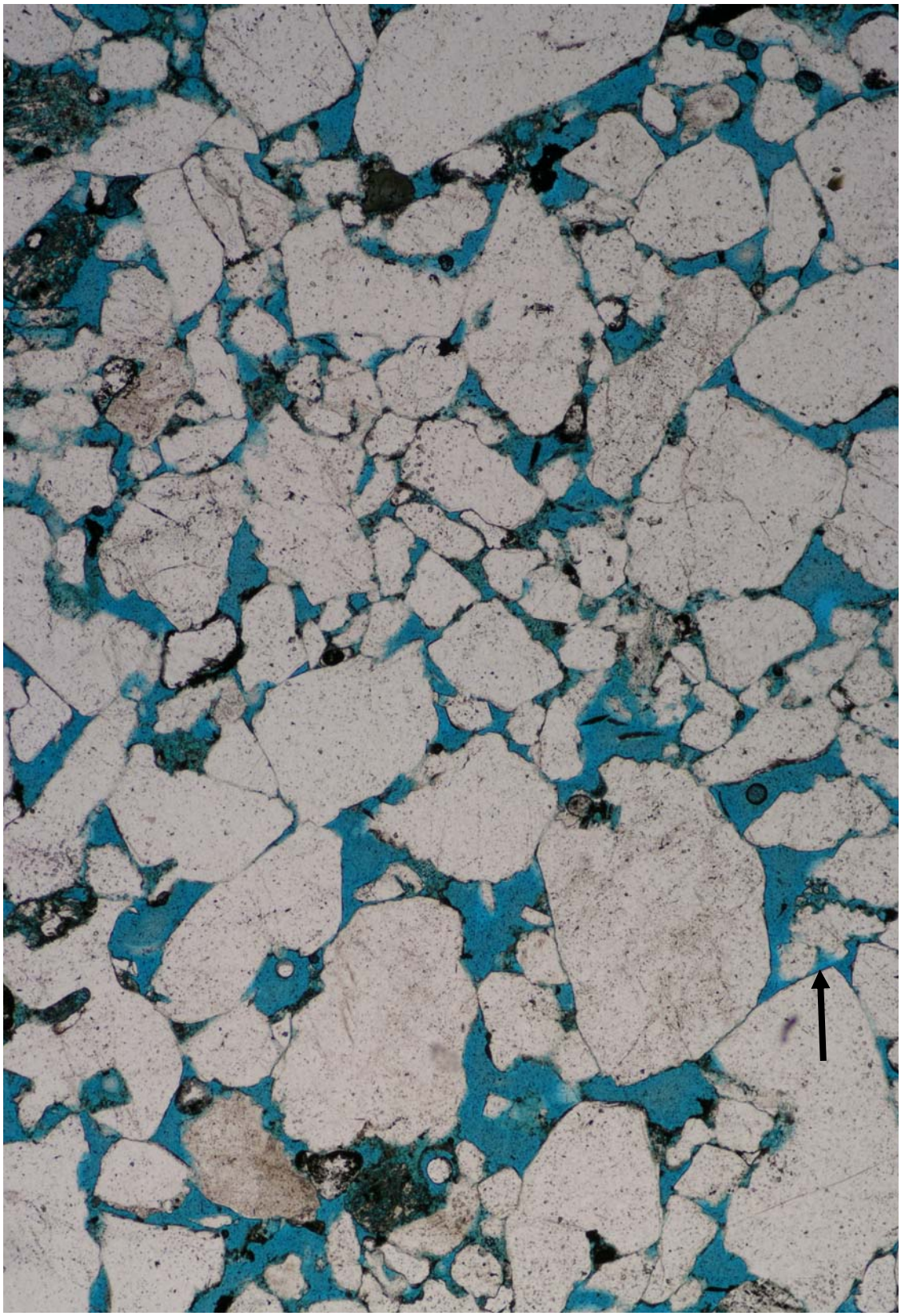

Figure 9

General field of view illustrating the dominance of intergranular pores in this quartzarenite. Note the euhedral terminations on quartz grains (arrow) that indicate the presence of quartz overgrowths. Rare highly corroded feldspars appear grey at this magnification. Halladale-1 DW2, core plug offcut, depth 1825.15mMD. Plane light. Horizontal field of view 3.25mm.

5. GRAIN SIZE ANALYSIS

Thin Section Statistics				Frequency Distribution
DW:		**1**		
Depth (mMD)		**1792.70**		
Parameter		mm	φ	
Mean		0.21 fine sand	2.50	
Mode		0.20 fine sand	2.30	
Range:	min	0.002	8.97	
	max	0.56	0.84	
Standard Deviation		0.09 poorly sorted	1.12	
DW:		**2**		
Depth (mMD)		**1812.90**		
Parameter		mm	φ	
Mean		0.41 medium sand	1.45	
Mode		0.34 medium sand	1.56	
Range:	min	0.10	3.32	
	max	1.07	-0.10	
Standard Deviation		0.20 moderately well sorted	0.71	
DW:		**2**		
Depth (mMD)		**1818.30**		
Parameter		mm	φ	
Mean		0.84 coarse sand	0.59	
Mode		0.54 coarse sand	0.89	
Range:	min	0.20	2.32	
	max	3.60	-1.85	
Standard Deviation		0.69 moderately sorted	0.92	
DW:		**2**		
Depth (mMD)		**1818.58**		
Parameter		mm	φ	
Mean		0.79 coarse sand	0.62	
Mode		0.48 medium sand	1.04	
Range:	min	0.08	3.64	
	max	3.25	-1.70	
Standard Deviation		0.54 moderately sorted	0.89	

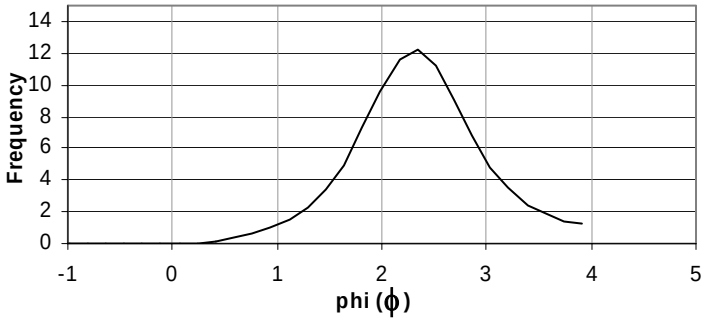

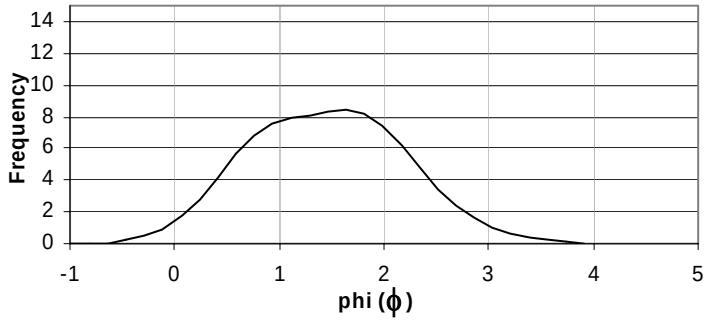

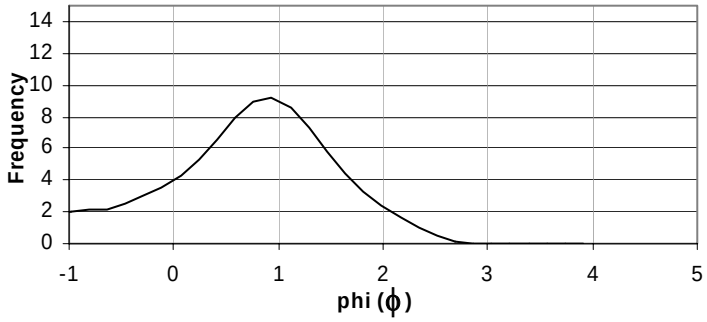

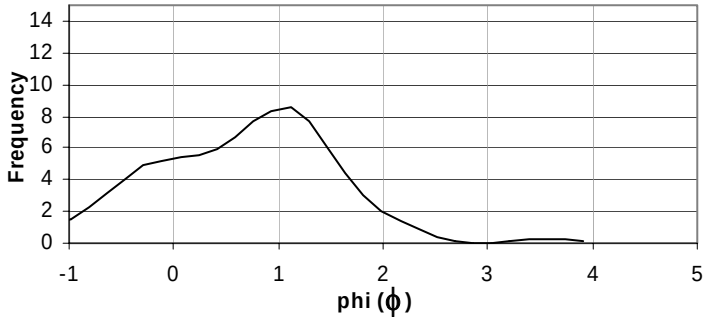

DW:	**2**	
Depth (mMD)	**1825.15**	
Parameter	mm	φ
Mean	0.55	1.10
	coarse sand	
Mode	0.48	1.05
	medium sand	
Range: min	0.13	2.94
max	1.57	-0.65
Standard Deviation	0.31	0.82
	moderately sorted	

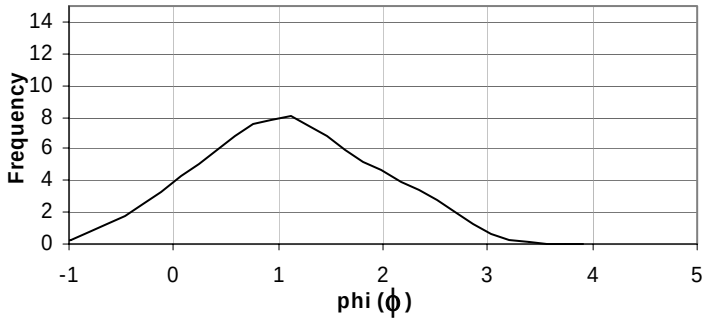

6. DISCUSSION

This discussion is confined to the five core samples from Unit C in the Late Cretaceous Waarre Formation at Halladale-1.

6.1 Lithology & texture

Core plug offcuts from Halladale-1 are comprised of fine to coarse grained, poor to moderately well sorted, mineralogically mature subarkose. Grain size ranges from clay to granules and grains are typically subangular to subrounded with low to moderate sphericity. Grain size distributions are unimodal with a tendency towards negative skewness in the coarser grained sands. Slight bimodal grain size is evident at 1818.58mMD. All the subarkoses have a grain supported texture with open to moderately open packing characterised by point and tangential grain contacts. Rare planar laminae are outlined by detrital clay, the concentration of accessory minerals and changes in grain size. Laminae of accessory minerals at 1792.7m might influence the wireline logs.

Lithologically all the sandstones have been classified as subarkoses. This classification strictly follows the recommendations of Folk (1974) that requires granite lithics to be counted with the feldspar fraction. If the granite lithics are included with other rock fragments (Fig. 10) then it is clear that most of the sandstones actually have almost equal proportions of feldspars and lithics. When these sandstones were deposited there were probably more feldspars present (~1 to 4%) but these have now been converted to kaolin. Based on this alteration there is no doubt that the sandstones were originally subarkosic in composition.

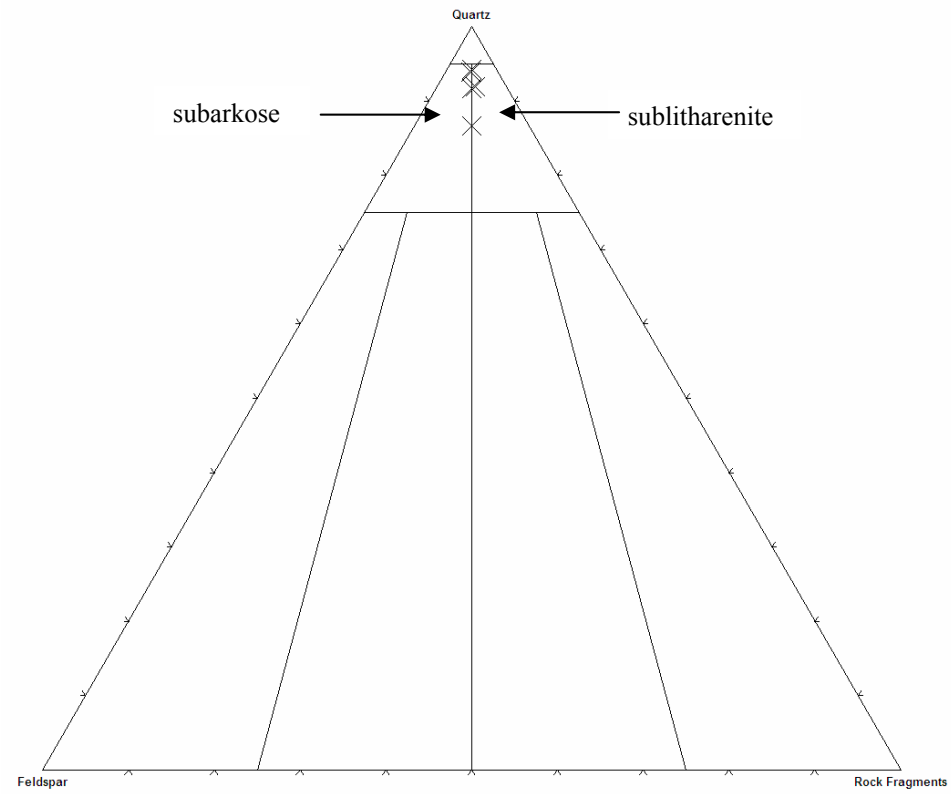

Figure 10. Relative percentages of quartz, feldspar and rock fragments in sandstones from Unit C Waarre Formation at Halladale-1.

Previously the Waarre Formation Unit C in the Port Campbell Embayment was described by Buffin (1989) as a quartz rich medium to coarse grained, well sorted sandstone with intervals of interlaminated claystone and very fine sandstone. More recent workers (Partridge, 2001; Cliff *et al* 2004; Sharp & Wood, 2004) have subdivided Unit C into a lower (Ca) and upper (Cb) unit based on palynological evidence. Typically the lower unit is considered finer grained and the upper unit is medium to coarse grained, texturally mature subarkoses and quartzarenites in the Casino Field. At Thylacine-1 (Cliff *et al*, 2004) the upper unit is fine to coarse grained, moderately well sorted quartz rich sandstone interbedded with siltstone and minor claystone. Sandstones from Halladale-1 are lithologically similar to the mineralogically mature upper unit C (Cb) based on these earlier descriptions.

6.2 Detrital mineralogy & sediment provenance

Detrital grains in the subarkoses from Halladale-1 indicate that sediment was derived from both metamorphic and igneous terranes. A metamorphic source is suggested by grains of polycrystalline quartz with sutured crystal boundaries, lithics of quartzite and micaceous schist, and accessory rutile, but may also have contributed mica flakes and accessory zircon. The igneous source was plutonic and is apparent from grains of polycrystalline quartz with straight crystal boundaries, ?granitic lithics of quartz and K-feldspar, and accessory tourmaline and monazite. Geary *et al* (2001) indicated that sediment for the Waarre Formation in the eastern Otway Basin was derived from erosion and uplift of both Palaeozoic basement (Lachlan fold belt) and older Otway Group sediments. The absence at Halladale-1 of volcanic lithics which would have been derived from the Eumeralla Formation and other Otway Group sediments is consistent with the interpretation that Palaeozoic basement was the major sediment provenance. Furthermore, it confirms that this is Unit C of the Waarre Formation in Halladale-1. Volcanic lithics are also absent from Unit C in the Casino Field (Sharp & Wood, 2004) but are present in Unit A.

There might be evidence of a sedimentation break or change in sediment provenance between 1818.3m and 1812.9m. In the basal coarse grained sands (depths 1825.15m, 1818.58m & 1818.3m) there are indications that an igneous source was dominant but above that depth it would appear that a metamorphic source was more important. Rare brecciated polycrystalline quartz at 1818.58m and 1825.15m might also reflect the erosion of a faulted zoned at this time. These same samples contain K-feldspars with simple twinning that are not evident in the shallower subarkose. The igneous source shed significant percentages of polycrystalline quartz (8-17%) with straight crystal boundaries and possible granitic lithics (1-1.4%). Transport distances must have been relatively short for the coarse grained polycrystalline quartz to be preserved. Normally these grains are disaggregated during transport. At 1812.9m there is an increase in the percentage of metamorphic lithics (3.8%), K-feldspars (4.8%), biotite and altered metamorphic lithics but there is less polycrystalline quartz (6%). These components would be consistent with the dominance of a metamorphic provenance.

It is also plausible that the apparent change or break in sedimentation might be a function of the hydraulic regime. Polycrystalline quartz and granitic lithics might have concentrated where mean flow velocity was high enough to deposit the coarse grained sediments. Bimodal grain size at 1818.58mD could indicate either two sources of sediment, or two different mechanisms of transport. The peaks occur in the very coarse sand size and medium sand size. The latter is also the mode (0.48mm) of this sample which is identical to the mode in the underlying sample at 1825.15m. A marked difference in the proportion of polycrystalline quartz between these samples is consistent with two sources of sediment. Medium grain sizes were probably associated with the metamorphic provenance and very coarse sand may have been locally derived from a plutonic source.

6.3 Depositional environments

Previous interpretations of depositional environments for Unit C of the Waarre Formation have included a tidal beach-barrier complex (Buffin, 1989) and fluvio-deltaic systems (Geary *et al*, 2001). More detailed work has indicated a lower delta plain to marginal marine setting for the lower unit (Ca) and fluvial dominated upper delta plain (?braidplain) with distributary channels for the upper (Cb) unit (Cliff *et al*, 2004; Sharp & Wood, 2004). At the top of unit Cb in the Casino Field and at Minerva-1 and -2A there is a return to shallow marginal marine conditions thought to characterise a mid to upper delta plain (Sharp & Wood, 2004).

Petrology samples from Halladale-1 contain evidence to support the interpretation of a marginal marine and possibly fluvial influenced depositional setting for Unit C. Trace amounts of coarse grained bright green glauconite at 1792.7m and silt size grains at 1825.15m are thought to characterise the marine influence. A green colour indicates the glauconite is mature and has not been oxidised during transport. Glauconite is thought to form at the sediment –water interface in marine settings during low rates of sedimentation when pH is near 8 and Eh is slightly reducing. Framboidal pyrite was also identified in the coarser subarkoses from 1825.15m, 1818.58m and 1818.3m and could further support the hypothesised marginal marine setting. Pyrite commonly forms due to bacterial reduction in association with organic matter and sea water. The latter is the source of sulphate.

Slight negative skewness of the grain size distributions might be indicative of wave influenced sands (Tucker, 2001) where the fine component has been removed. However, the moderate sorting and subangular to subrounded grain shapes are more typical of fluvial sands. Perhaps riverine sands have been reworked by wave action to produce these apparently contradictory granulometric characteristics. The fine grained sand at 1792.70m where there are laminae containing accessory heavy minerals could have been transported via saltation. All the other sands are coarser grained and were probably transported via bedload. Blocky organic matter noted at 1792.7m, 1812.9m and 1825.15m might have had a terrestrial origin. Trace amounts of Fe rich carbonate (probably siderite) at 1792.7m, 1812.9m and 1818.58m could also suggest a meteoric influence during deposition since siderite can only form when sulphate activity is low. Flushing of marine sequences by meteoric waters can result in the precipitation of siderite if carbonate activity is high.

Any further interpretation of depositional environments for Unit C at Halladale-1 should be based on the integration of information from the core, palynology and wireline logs.

6.4 Authigenic mineralogy & diagenetic alteration

Early diagenetic phases of glauconite, framboidal pyrite and ?siderite in Waarre Unit C at Halladale-1 were probably related to the depositional environment(s) and will not be further discussed in this section. There is another phase of pyrite which is blocky that has replaced grains and partially filled pores. The timing of this authigenic mineral is difficult to determine but it could either have formed at the same time as the framboidal pyrite, or later in the sequence when bacterial decomposition of organic matter produced reducing conditions. Where glaucony has a slightly fibrous habit at 1792.7m it has been described as chlorite. These grains are rare (0.6%) and could be micas and/or lithics that were altered prior to deposition. Other phases of diagenetic alteration all appear to follow the same paragenetic sequence (Fig. 11) for Unit C at Halladale-1.

Replacement of feldspars and micas by kaolin booklets and verms that range in diameter from 5 to 50 microns probably occurred due to flushing by acidic meteoric waters soon after burial. Kaolin forms when pH (4-7) is acid and there is low K^+ activity. Grain replacing kaolin represents 0.6 to 3.0 % of the total rock composition, with additional amounts of up to 1.8% where it has been squeezed into adjacent intergranular pores during mechanical compaction. Kaolin is associated with grain replacing illite, it has a jagged contact with quartz overgrowths

and has been replaced by carbonate spar. Flushing by meteoric waters could also have produced grain size dissolution pores, intragranular pores and honeycomb pores in feldspars. Rare grains (0-0.8%) replaced by illite may have formed when K^+ activity increased and pH became slightly less acid (5.5-7) after kaolin had precipitated. There is no evidence that illite is replacing kaolin, a process which is reported from more deeply buried sedimentary sequences.

Prismatic and rhombohedral syntaxial quartz overgrowths could have precipitated after the kaolin due to either an excess of silica remaining from the replacement of feldspars, or dissolution at clay/mica - quartz contacts. The fact that these sediments have moderately open to open packing could indicate that compaction was not the source of silica. This observation also suggests that quartz overgrowths formed relatively early in the paragenetic sequence thus providing a rigid framework that minimised compaction. Quartz overgrowths are most abundant (6.2%) in the fine grained subarkose at 1792.7m where there are the least number of lithics and polycrystalline quartz. Where lithics are more abundant the number of sites for silica precipitation was limited.

Clear carbonate spar is concentrated in the coarse grained subarkoses from 1818.3m and 1818.58m where it represents 19 to 27% of the total rock composition. The spar is twinned and poikilotopic which indicates it formed relatively slowly after burial and is therefore not early diagenetic. Spar has filled intergranular pores and replaced grains including feldspars and kaolin. On pore margins the spar typically has euhedral terminations which suggests there has been minimal subsequent dissolution. However, at 1818.3m there are instances where the spar appears corroded but this might reflect an underlying corroded grain that was replaced. There are slightly less dissolution pores in the coarse grained subarkoses than other samples and this might suggest dissolution occurred before the introduction of carbonate cement. The composition of this carbonate spar should be determined by X-ray diffraction and/or elemental analysis in a scanning electron microscope or electron microprobe. It would then be possible to compare this data from Halladale-1 with results from Watson *et al* (2004) which might explain the source of CO_2 for this carbonate. Watson *et al* (2004) suggested that late stage carbonates formed after CO_2 entered the reservoirs as a result of Pleistocene to Recent igneous activity in the Otway Basin. Alternatively the carbonate might have formed when CO_2 was released by decarboxylation prior to hydrocarbon migration. Since this carbonate cement has such a significant impact on reservoir quality it is important to understand its spatial distribution from logs and core.

Event	Diagenetic Stage Early Middle Late
	Late Cretaceous Pleistocene/Recent
glauconite	---
pyrite	--- ?----
?siderite	---
dissolution	-------
kaolin	------
illite	---
mechanical compaction	----------
quartz	-----
?CO_2 from igneous activity	------
clear carbonate spar	-----
?hydrocarbon migration	-----

Figure 11. Possible paragenetic sequence for Waarre Formation Unit C at Halladale-1.

6.5 Reservoir quality

The relative proportions of different pore types in the subarkoses of Unit C at Halladale-1 are illustrated in Figure 12. Primary intergranular pores are dominant in three of the samples and these sandstones probably have good reservoir quality because the pores are interconnected. Invasion by drilling mud in the subarkose at 1825.15m demonstrates that this sandstone has excellent permeability. The other samples have limited preservation of primary intergranular pores due to pervasive carbonate cement. Relative percentages of dissolution pores are similar in all samples (3.2 to 5%) and are the result of corrosion of labile grains to produce grain size pores, honeycomb pores in feldspars and intragranular pores in lithics and quartz grains where inclusions have been dissolved. Fracturing is restricted to one sample and is probably an artifact of sampling. Micropores associated with grain replacing and pore filling authigenic kaolin are most abundant at 1792.7m. Although these pores contribute to total porosity and would be effective for gas, they may not represent effective porosity for the migration of oil.

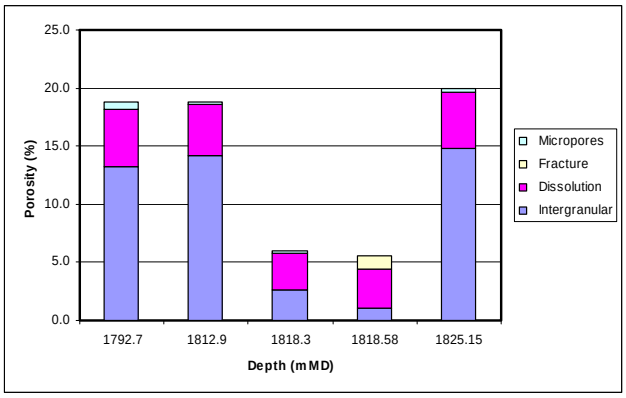

Figure 12 Pore types in Waarre Unit C at Halladale-1

Statistical assessment of the factors controlling reservoir quality is of limited validity when only considering five samples. However, some very generalised conclusions can be drawn about what has controlled the abundance of primary intergranular pores at Halladale-1. Porosity can be influenced by depth of burial (temperature and time) and rock characteristics (grain size, sorting, packing, detrital and authigenic minerals). Permeability is controlled by porosity and rock characteristics. Since petrological descriptions can only very vaguely estimate permeability it is assumed for the purposes of this discussion that the percentage of intergranular pores reflects permeability. Reservoir quality is unlikely to be influenced by depth of burial in this data set because differences in depth between samples are minimal. Although the primary control of porosity and permeability at the time of deposition was probably sorting and grain size (Fig. 13) the importance of these factors is no longer apparent. The reason for this decline in importance is the combined influence of authigenic minerals (carbonate, quartz, kaolin and pyrite) filling the pores.

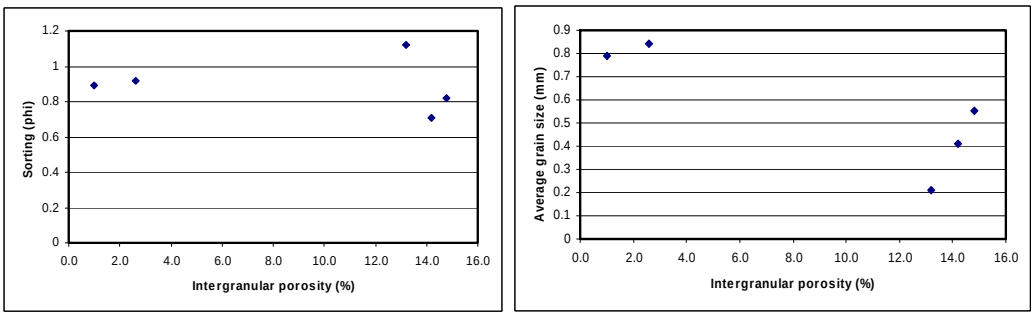

Figure 13. Comparison of sorting and grain size as controls of intergranular porosity at Halladale-1. In both graphs there are two points on the LHS which represent the carbonate cemented subarkoses.

Quartz overgrowths commonly provide a rigid framework to unconsolidated sand and therefore initially aid in the preservation of intergranular pores. When the abundance of quartz overgrowths is high then pores become filled with silica and reservoir quality declines. Based on these facts it is normal to find a correlation between the percentage of quartz overgrowths and intergranular porosity. Initially there is an increase in porosity preservation as the proportion of overgrowths increases and then there is a decline in the number of pores. The cut-off for the change in this trend is commonly approximately 6% authigenic quartz. Results from Halladale-1 (Fig. 14) appear to be consistent with this general trend.

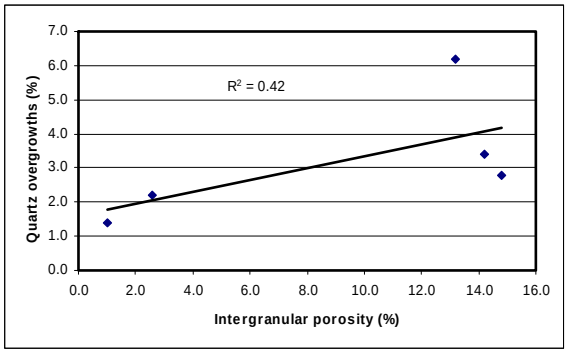

Figure 14. Correlation between the percentages of quartz overgrowths and intergranular pores in subarkoses from Halladale-1.

The correlation between all authigenic minerals (kaolin, pyrite, clear carbonate spar and pyrite framboids) filling pores and the preservation of intergranular pores appears to be very strong (Fig. 15) for the subarkoses from Unit C at Halladale-1. The two data points with high percentages of cement are the coarse grained carbonate cemented subarkoses. The actual correlation with only clear carbonate spar can not be assessed because there are insufficient data points.

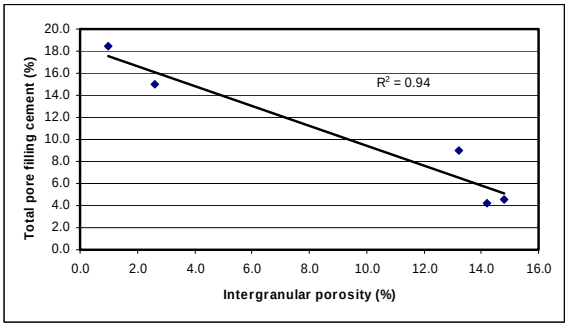

Figure 15. Combined influence of all authigenic minerals filling pores.

7. CONCLUSIONS

1. Unit C of the Waarre Formation at Halladale-1 is comprised of fine to coarse grained, poor to moderately well sorted, subarkoses. Detrital mineralogy at the time of deposition would have been more feldspar rich.

2. Sediment was derived from both metamorphic and igneous terranes. The abundance of polycrystalline quartz in coarse grained subarkoses might indicate a period dominated by an igneous source with relatively short distances of transport.

3. Petrological evidence is consistent with a marginal marine depositional environment that was influenced by rivers.

4. Early diagenetic alteration was related to the depositional environments with precipitation of glauconite and framboidal pyrite when there was a marine influence and ?siderite where meteoric waters prevailed. After burial feldspars and micas were altered to kaolin and minor illite, and quartz overgrowths precipitated. There is minimal evidence of mechanical compaction and dissolution. The final phase of pore filling and grain replacing carbonate spar could have formed due an increase in CO_2 either associated with Pleistocene/Recent igneous activity or hydrocarbon maturation.

5. Reservoir quality is probably excellent where primary intergranular pores are dominant. These pores were preserved due to minor development of quartz overgrowths. Later carbonate spar has significantly limited reservoir quality in selected samples.

8. GLOSSARY OF TERMS

Framboid
A cluster of pyrite crystals with a spheroidal outline.

Glaucony
A term used to describe green minerals without any genetic connotations. If the green minerals can be identified, a specific mineral name is given.

Glauconite
An Fe-rich dioctahedral illite. The term is also used to refer to a family of Fe-rich dioctahedral clays with varying ratios of expanded (smectite) and non-expanded layers.

Honeycomb Porosity
Secondary porosity produced by the corrosion (etching) of detrital grains.

Hydrocarbon envelope
Solid bitumen surrounding a mineral containing radioactive elements. Radiation causes polymerisation of hydrocarbon chains within oil that rims grains.

Microporosity
Porosity directly associated with clay minerals.

Neomorphism
All transformations between a mineral and the same mineral, or another of the same general composition.

Poikilotopic
A sedimentary textural term denoting a single crystal of carbonate enclosing more than one framework grain.

Vacuole
Gas or liquid filled inclusion.

9. REFERENCES

ADAMS, A.E., W.S. MACKENZIE & C. GUILFORD (1984) *Atlas of sedimentary rocks under the microscope*. Longman Scientific & Technical, 104p.

BUFFIN, A.J. (1989) Waarre sandstone development within the Port Campbell Embayment. *The APEA Journal*, 29, 1, pp. 299-311.

CLIFF, D.C.B., S.C. TYE & R. TAYLOR (2004) The Thylacine and Geographe gas discoveries, offshore eastern Otway Basin. *The APPEA Journal*, 44, 1, pp. 441-461.

FOLK, R.L. (1974) *Petrology of sedimentary rocks*. Hemphill, 182p.

GEARY, G.C., A.E. CONSTANTINE & I.S.A. REID (2001) New perspectives on structural style and petroleum prospectivity, offshore eastern Otway Basin. In HILL, K.C. & T. BERNECKER (Eds) *Eastern Australasian Basin Symposium, A Refocused Energy Perspective for the Future,* Petroleum Exploration Society of Australia, Special Publication, pp. 507-517.

HARRELL, J. (1984) A visual comparator for degree of sorting in thin and plane sections. *Journal of Sedimentary Petrology*. 54, pp. 646-650.

PARTRIDGE, A.D. (2001) Revisited stratigraphy of the Sherbrook Group, Otway Basin. In HILL, K.C. & T. BERNECKER (Eds) *Eastern Australasian Basin Symposium, A Refocused Energy Perspective for the Future,* Petroleum Exploration Society of Australia, Special Publication, pp. 455-464.

PETTIJOHN, F.J., P.E. POTTER & R. SIEVER (1987) *Sand and sandstone*. Springer-Verlag, New York, 553p.

SHARP, N.C. & G.R. WOOD (2004) Casino gas field, offshore Otway Basin – the appraisal story and some stratigraphic enlightenment. In BOULT, P.J., D.R. JOHNS & S.C. LANG (Eds) *Eastern Australasian Basin Symposium II,* Petroleum Exploration Society of Australia, Special Publication, pp. 1-11.

STANTON, P.T. & M.D. WILSON (1994) Measurement of independent variables - composition. In M.D. WILSON (Ed) Reservoir quality assessment and prediction in clastic rocks. *SEPM Short Course* 30, 432p.

TERRY R.D. & G.V. CHILINGAR (1955) Summary of "Concerning some additional aids in studying sedimentary formations" by M.S. Shrestor. *Journal of Sedimentary Petrology*, 25, pp. 229-234.

TUCKER, M.E. (2001) *Sedimentary petrology, an introduction to the origin of sedimentary rocks*. (3rd Ed) Blackwell Scientific, 262p.

WATSON, M.N., C.J. BOREHAM & P.R. TINGATE (2004) Carbon dioxide and carbonate cements in the Otway Basin: implications for geological storage of carbon dioxide. *The APPEA Journal*, 44,1, pp. 703-720.

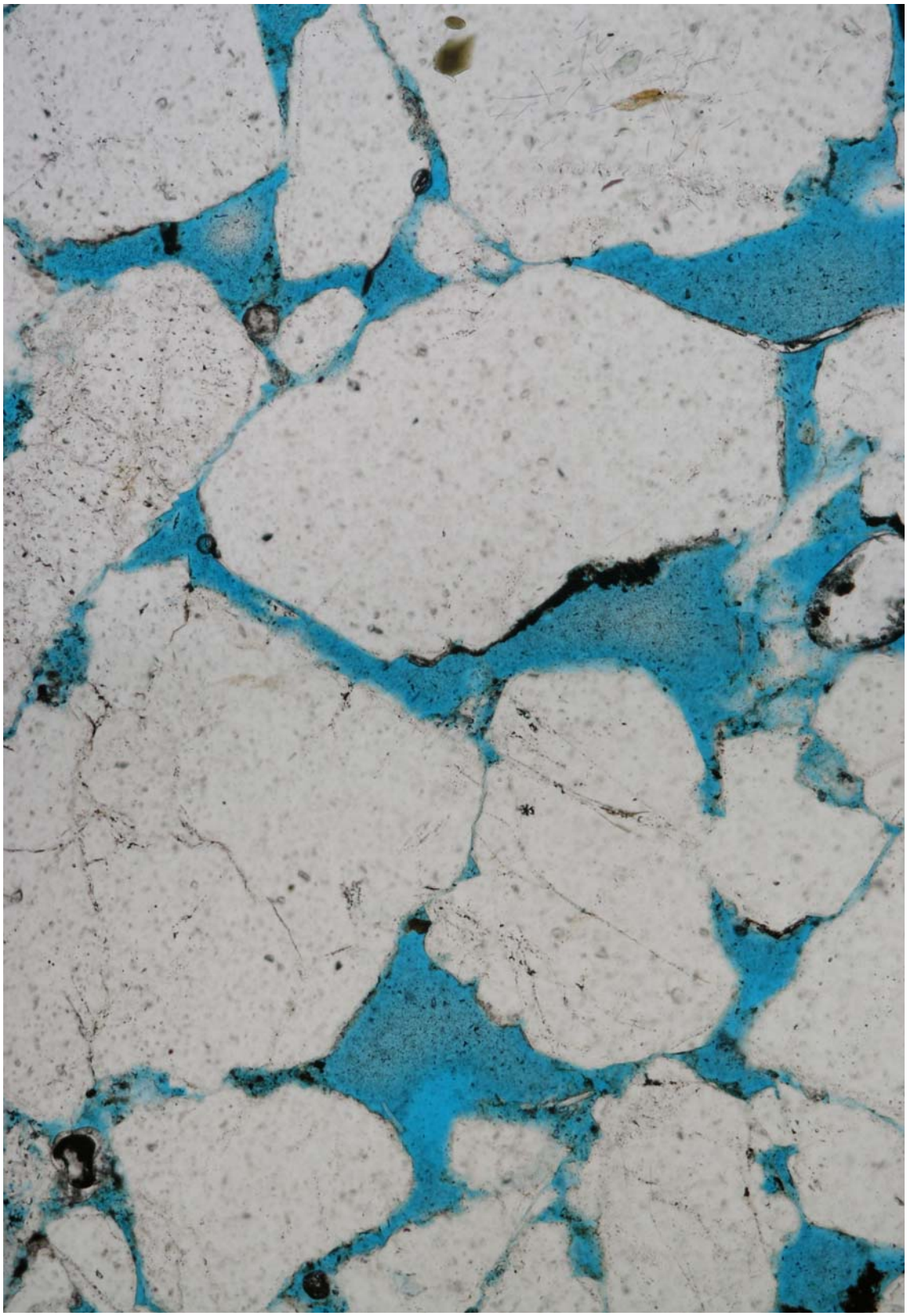

APPENDIX 3:
PETROPHYSICS REPORT

VIC/P37(v), OTWAY BASIN, VICTORIA

HALLADALE DW1, DW2 & DW3

PETROPHYSICAL INTERPRETATION

Origin Energy Resources Limited
Second Floor, South Tower, John Oxley Centre
339 Coronation Drive
MILTON QLD 4064

Andy Hall, September 2005

EXECUTIVE SUMMARY

The Halladale-1 DW1 and DW2 wells were drilled in Permit VIC/P37(v) as exploration wells targeting gas in the Waarre C and Waarre A Formations in the Black Watch and Halladale structures respectively. Halladale-1 DW3 was drilled as an appraisal well targeting the water column in the Waarre C sandstone beneath the Halladale gas column to obtain water gradient data to allow the GWC to be determined from pressure data.

These wells were drilled consecutively between 22nd March and 24th April 2005.

The wells were logged with LWD gamma – sonic – neutron- density – resistivity. Pressure measurements were also taken in the Waarre C Formation in all wells and in the Nullawarre and Waarre A in DW1 and DW2 to estimate fluid contacts.

The Waarre C Formation was cored in DW1, where only Sand II was cored, and DW2, where most of the Waarre C interval was cored. Routine and special core analysis has been carried out on these cores and is incorporated into the interpretations in this report.

No production tests were conducted in any of the Halladale-1 wells.

When DW1 was drilled, gas columns were encountered in the Nullawarre, the Waarre C and the Waarre A Formations. DW2 encountered a gas column only in the Waarre C Formation. DW3 was drilled below the GWC determined for all formations to allow the measurement of the pressure gradient in the water leg for the Waarre C Formation.

Petrophysical analysis, integrating the core and log data, has been conducted for each well from the Nullawarre to the Eumeralla Formation and applying consistent input parameters across the wells for each Formation. The results of this interpretation are presented in Tables 1 to 3.

Sandstones were encountered at the top and base of the Nullawarre Formation in each well with a shale section separating them. In DW1, these sands were both found to be gas bearing, but pressure data proved the columns were not in communication and only had a limited extent beneath the well penetration. The highest sand thickness was encountered in DW2, where the shallower Nullawarre sand is best developed. This well has 18 mMD of net sand with an average porosity of 25%, but the sands have only low gas saturation throughout. The sandstones are thinner and water bearing in DW3.

The Waarre C varied in thickness from 22.4 mMD in DW1 to 36.8 mMD in DW3. A stratigraphy for the Waarre C has been applied in this work based upon lithostratigraphy (Figure 1).

Average properties for the entire Formation are also presented. Gas columns were encountered in DW1 and DW2 with no contact encountered in the wells. Pressure data shows that these columns have GWC contacts at 1769 mTVDSS and 1760 mTVDSS respectively using the water gradient data from DW3. In all wells, the sandstones have excellent reservoir quality, with average porosity in excess of 20% and geometric average permeability greater than 900 mD.

The Waarre A was encountered at the GWC in DW1. Consequently the gas saturation is quite low and little net pay is calculated. The formation was encountered below the GWC in both DW2 and DW3, where the TD was within the Waarre A interval. Net sand thickness ranges up to 17.6 metres. The porosity is interpreted in DW1 and DW2 to be 20 – 21%. The porosity in DW3 is interpreted to be significantly higher (25%), but this is derived mainly from the resistivity log as no conventional porosity logs were acquired and should be considered less well constrained. Permeability was derived from the MDT mobility function and is low relative to the Waarre C.

In summary:

- Halladale-1 DW1 has a net pay thickness of 21.6 mMD, with an average porosity of 23% and permeability of 980 mD. The average water saturation is 25%. 18.4 mMD of this net pay is in the Waarre C Formation.
- Halladale-1 DW2 has a net pay thickness of 19.9 mMD, with an average porosity of 22% and permeability of 1522 mD. The average water saturation is 20%. 18.6 mMD of this net pay is in the Waarre C Formation.
- Halladale-1 DW3 has a no net pay thickness as it was drilled below the GWC at Waarre C and Waarre A level to measure the formation water gradient.

Figure 1: Waarre C Stratigraphy Used in this Report

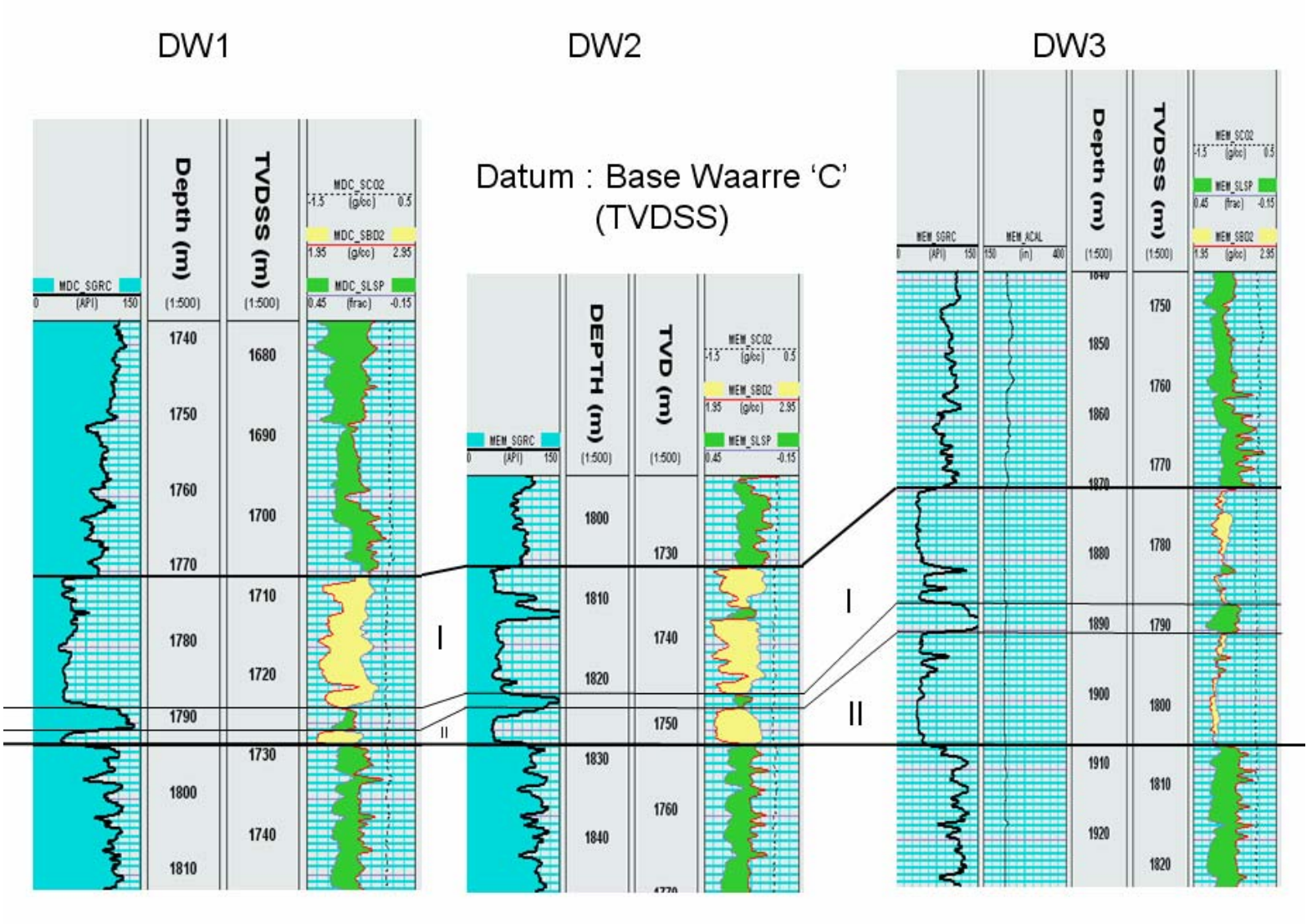

Table 1: Results of the Petrophysical Interpretation for Halladale-1 DW1

Halladale-1 DW-1														
	Gross Thickness			Net Sand					Net Pay					
	Top	Base	Thickness	Thickness	NTG	PHIT	PHIE	Perm	Thickness	NTG	PHIT	PHIE	Perm	Sw
Formation	(mRT)	(mRT)	(mMD)	(mMD)	(Fraction)	(Fraction)	(Fraction)	(mD)	(mMD)	(Fraction)	(Fraction)	(Fraction)	(mD)	(Fraction)
Nullawarre	1515.5	1565.1	49.6	8.5	0.171	0.231	0.177		1.9	0.038	0.260	0.214	1.51	0.529
Belfast	1565.1	1723.1	158.0	0	0.000					0.000				
Flaxman	1723.1	1770.7	47.6	0	0.000					0.000				
Waarre C	1770.7	1793.1	22.4	18.4	0.821	0.228	0.207	1147	18.4	0.821	0.228	0.207	1147	0.196
WC I	*1770.7*	*1788.1*	*17.4*	*16.6*	*0.954*	*0.226*	*0.205*	*1185*	*16.6*	*0.954*	*0.226*	*0.205*	*1185*	*0.182*
IWCS	*1788.1*	*1791.0*	*2.9*	*0*	*0.000*				*0*	*0.000*				
WC II	*1791.0*	*1793.1*	*2.1*	*1.8*	*0.857*	*0.247*	*0.230*	*793*	*1.8*	*0.857*	*0.247*	*0.230*	*793*	*0.311*
Waarre B	1793.1	1821.6	28.5	0	0.000					0.000				
Waarre A	1821.6	1873.6	52.0	13.0	0.250	0.212	0.164	14.9	1.3	0.025	0.247	0.198	46.6	0.514
Eumeralla	1873.6	1918.0	> 44.4	6.1	0.137	0.186	0.135	5.8	0	0.000				
			402.5	**46**	**0.114**	**0.218**	**0.180**	**464**	**21.6**	**0.054**	**0.232**	**0.207**	**980**	**0.249**

Net Sand	Net Pay
Shale Volume < 40%	Net Sand = 1
Permeabiity > 0.20 mD	Water Saturation < 50%

Figure 2: Waarre C to Waarre A Sandstones in Halladale-1 DW1

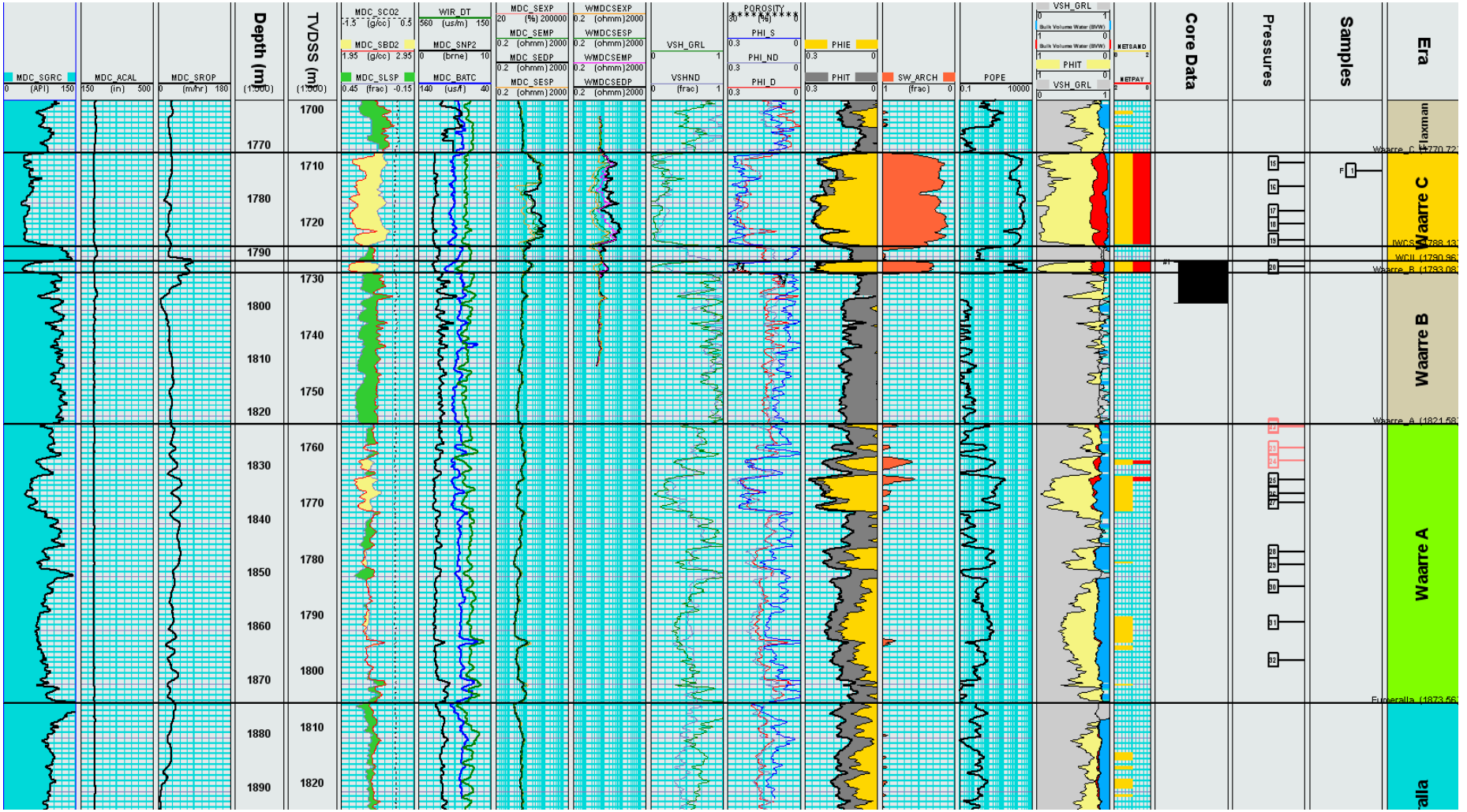

Table 2: Results of the Petrophysical Interpretation for Halladale-1 DW2

Halladale-1 DW-2														
	Gross Thickness			Net Sand					Net Pay					
	Top	Base	Thickness	Thickness	NTG	PHIT	PHIE	Perm	Thickness	NTG	PHIT	PHIE	Perm	Sw
Formation	(mRT)	(mRT)	(mMD)	(mMD)	(Fraction)	(Fraction)	(Fraction)	(mD)	(mMD)	(Fraction)	(Fraction)	(Fraction)	(mD)	(Fraction)
Nullawarre	1538.5	1589.3	50.8	18.4	0.362	0.252	0.23	1.29	0	0.000				
Belfast	1589.3	1749.2	159.9	0	0.000				0	0.000				
Flaxman	1749.2	1803.7	54.5	3.2	0.059	0.222	0.180	2224	0	0.000				
Waarre C	1803.7	1827.2	23.5	18.6	0.791	0.223	0.208	1628	18.6	0.791	0.223	0.208	1628	0.185
WC I	*1803.7*	*1820.2*	*16.5*	*14.3*	*0.867*	*0.223*	*0.206*	*1181*	*14.3*	*0.867*	*0.223*	*0.206*	*1181*	*0.195*
/WCS	*1820.2*	*1821.9*	*1.7*	*0*	*0.000*				*0*	*0.000*				
WC II	*1821.9*	*1827.2*	*5.3*	*4.3*	*0.811*	*0.224*	*0.213*	*3115*	*4.3*	*0.811*	*0.224*	*0.213*	*3115*	*0.154*
Waarre B	1827.2	1855.1	27.9	0	0.000				0	0.000				
Waarre A	1855.1	1897.9	42.8	17.6	0.411	0.204	0.168	11.1	0	0.000				
Eumeralla	1897.9	1941.0	> 43.1	1.0	0.023	0.196	0.155	8.6	0	0.000				
			402.5	**58.8**	**0.146**	**0.226**	**0.200**	**640**	**18.6**	**0.046**	**0.223**	**0.208**	**1628**	**0.185**

Net Sand	Net Pay
Shale Volume < 40%	Net Sand = 1
Permeabiity > 0.20 mD	Water Saturation < 50%

Figure 3: Waarre C to Waarre A Sandstones in Halladale-1 DW2

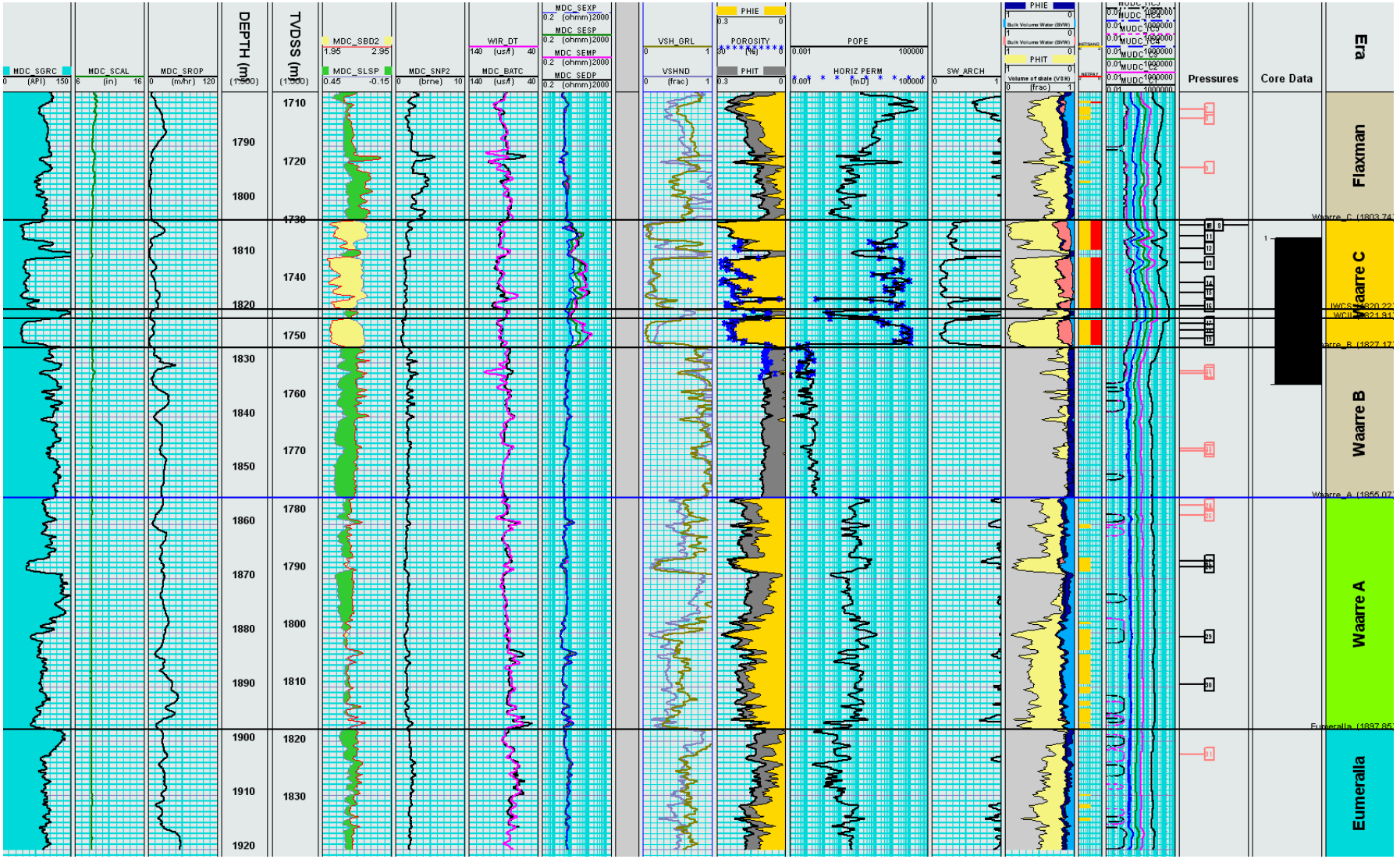

Table 3: Results of the Petrophysical Interpretation for Halladale-1 DW3

Halladale-1 DW-3														
	Gross Thickness			Net Sand					Net Pay					
	Top	Base	Thickness	Thickness	NTG	PHIT	PHIE	Perm	Thickness	NTG	PHIT	PHIE	Perm	Sw
Formation	(mRT)	(mRT)	(mMD)	(mMD)	(Fraction)	(Fraction)	(Fraction)	(mD)	(mMD)	(Fraction)	(Fraction)	(Fraction)	(mD)	(Fraction)
Nullawarre	1497.6	1547.8	50.2	2.4	0.048	0.233	0.117		0	0.000				
Belfast	1547.8	1798.1	250.3	0	0.000				0	0.000				
Flaxman	1798.1	1869.7	71.6	0.6	0.008	0.092	0.033		0	0.000				
Waarre C	1869.7	1906.5	36.8	30.3	0.823	0.259	0.245	2702	0	0.000				
WC I	*1869.7*	*1886.2*	*16.5*	*14.9*	*0.903*	*0.240*	*0.228*	*1650*	0	*0.000*				
IWCS	*1886.2*	*1890.3*	*4.1*	*0*	*0.000*				0	*0.000*				
WC II	*1890.3*	*1906.5*	*16.2*	*15.4*	*0.951*	*0.277*	*0.261*	*3720*	0	*0.000*				
Waarre B	1906.5	1935.7	29.2	0	0.000				0	0.000				
Waarre A	1935.7	1969.0	> 33.3	5.2	0.156	0.249	0.204	44.2	0	0.000				
Eumeralla	Not penetrated													
			471.4	**38.5**	**0.082**	**0.253**	**0.228**	**2133**	**0.0**	**0.000**				

Net Sand	Net Pay
Shale Volume < 40%	Net Sand = 1
Permeabiity > 0.20 mD	Water Saturation < 50%

Figure 4: Waarre C to Waarre A Sandstones in Halladale-1 DW3

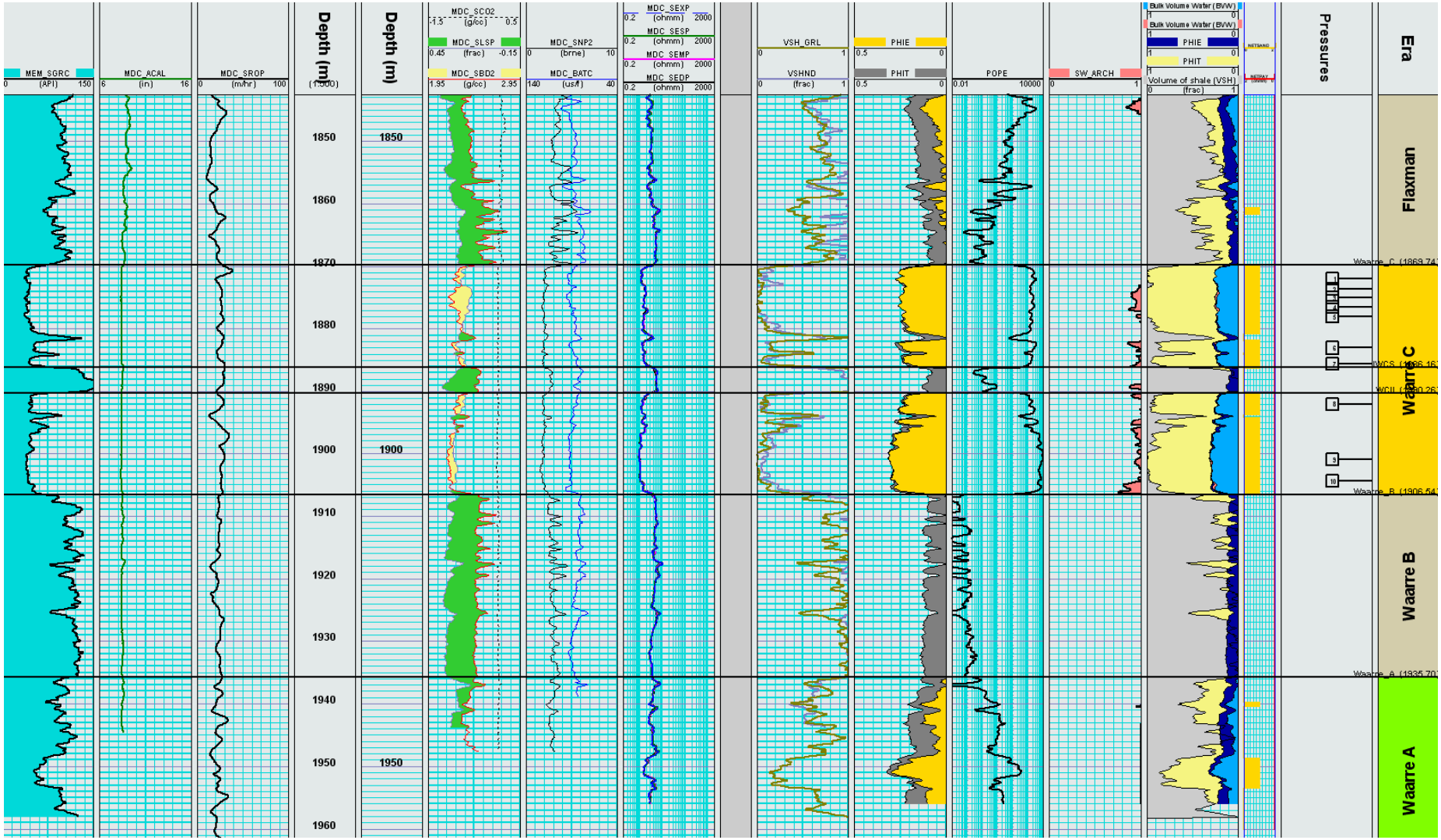

TABLE OF CONTENTS

EXECUTIVE SUMMARY 2

WELL DETAILS 14
Borehole Deviation 14
Log Data 15
Core Data 16
Formation Water Salinity 18
Formation Fluid Density 19

INTERPRETATION METHODOLOGY 30
Shale Volume 30
Porosity 30
Permeability 30
Water Saturation 31
Net Sand / Net Pay 31
Estimation of GWC 31

INTERPRETATION BY FORMATION 39
Nullawarre Formation 39
Belfast Formation 39
Flaxman Formation 40
Waarre C 40
Waarre B 41
Waarre A 42
Eumeralla Formation 42

LIST OF FIGURES

Figure 1: Waarre C Stratigraphy Used in this Report 4
Figure 2: Waarre C to Waarre A Sandstones in Halladale-1 DW1 6
Figure 3: Waarre C to Waarre A Sandstones in Halladale-1 DW2 8
Figure 4: Waarre C to Waarre A Sandstones in Halladale-1 DW3 10
Figure 5: Well Bore Deviation for the Halladale-1 wells 20
Figure 6: Grain Density Measurements from the Core Data 21
Figure 7: Porosity / Permeability Trends from the Core Data 22
Figure 8: Formation Resistivity Factor for the Waarre C Reservoir 23
Figure 9: Saturation Exponent for the Waarre C Reservoirs 24
Figure 10: Relationship between Porosity and CEC from the SCAL Data 25
Figure 11: Saturation vs. J Function Relationships for the Waarre C Reservoirs 26
Figure 12: Formation Water Salinity for the Waarre C & Waarre A Formations 27
Figure 13: Formation Water Salinity for the Nullawarre Formation 28
Figure 14: Fluid density Determination for the Cored Intervals 29
Figure 15 : Fluid Mobility vs. Log Porosity for the Nullawarre Formation 34
Figure 16 : Fluid Mobility vs. Log Porosity for the Waarre A and Eumeralla Formations 35
Figure 17: Nullawarre Fluid Pressure Gradient in DW1 and DW2 36
Figure 18: Waarre C and Waarre A Fluid Pressure Gradients 37
Figure 19: Waarre C Section in DW1 Showing the Agreement Between Capillary Pressure and Resistivity Calculated Water Saturation with a GWC at 1769 mTVDSS 38
Figure 20: Waarre C Section in DW2 Showing the Agreement Between Capillary Pressure and Resistivity Calculated Water Saturation With a GWC at 1760.5 mTVDSS 38

LIST OF TABLES

Table 1: Results of the Petrophysical Interpretation for Halladale-1 DW1 5
Table 2: Results of the Petrophysical Interpretation for Halladale-1 DW2 7
Table 3: Results of the Petrophysical Interpretation for Halladale-1 DW3 9
Table 4: Wireline Logging Runs Conducted in Wells Halladale-1 DW1, DW2 and DW3 16
Table 5: Grain Density by Reservoir from the Halladale-1 DW1 & DW2 Core Data 17
Table 6: Summary of the Cation Exchange Capacity Results.....18

ENCLOSURES

Enclosure 1: Interpreted Log and Core Section Over the Nullawarre to Eumeralla Formations for Halladale-1 DW1

Enclosure 2: Interpreted Log and Core Section Over the Nullawarre to Eumeralla Formations for Halladale-1 DW2

Enclosure 3: Interpreted Log and Core Section Over the Nullawarre to Eumeralla Formations for Halladale-1 DW3

WELL DETAILS

The Halladale-1 DW1 and DW2 wells were drilled in Permit VIC/P37(v) as exploration wells targeting gas in the Waarre C and Waarre A Formations in the Black Watch and Halladale structures respectively. Halladale-1 DW3 was drilled as an appraisal well targeting the water column in the Waarre C sandstone beneath the Halladale gas column to obtain water gradient data to allow the GWC to be determined from pressure data.

Latitude		**Longitude**	**Easting**		**Northing**
38° 34' 45.54" S		142° 43' 50.95" E	650,763		5,728,485
Drill Floor		21.5 m			
Water Depth		44.8 metres	**Rig**		Ocean Patriot
Borehole Record			**Casing Record**		
Inches	**mm**	**Base (mRT)**	**Inches**	**mm**	**Shoe Depth (mRT)**
36	914	101	30	762	99.5
17 ½	445	427	13 3/8	340	421
12 ¼	311	839	9 5/8	244	834
8 ½	216	See below			
Halladale-1 DW1					
Spud date		22 March 2005	**TD (mRT)**		1918
End Date		10 April 2005	**TD (mTVDRT)**		1869
Halladale-1 DW2					
Spud date		10 April 2005	**TD (mRT)**		1941
End Date		21 April 2005	**TD (mTVDRT)**		1875
Halladale-1 DW3					
Spud date		21 April 2005	**TD (mRT)**		1969
TD Date		24 April 2005	**TD (mTVDRT)**		1881

Borehole Deviation

All wells were drilled from the same surface location targeting different parts of the Halladale / Black Watch structure. The deviation and inclination plots for the wells are presented in Figure 5.

DW1 targeted the crest of the Black Watch structure to the southwest of the fault dividing the prospects. The well was drilled at an azimuth of approximately 200^{o} and with a maximum inclination of 18.7^{o} to a target 317 metres from the surface location.

DW2 targeted the gas column within the Halladale structure. The well kicked off from the DW1 borehole at approximately 800 metres and was drilled at an azimuth of 340^{o} and with a maximum inclination of 23.7^{o} to a target 328 metres from the surface location.

DW3 targeted the water column also within the Halladale structure to obtain pressure data for comparison with reservoir gas column pressures. The well kicked off from the DW2 borehole at approximately 1150 metres and was drilled at an azimuth of 55^{o} and with a maximum inclination of 30.3^{o} to a target 323 metres from the surface location.

Log Data

All wells were logged with the Sperry Sun FEWD (Formation Evaluation While Drilling) tools. Through the Nullawarre, Waarre C and Waarre A reservoir sections, the LWD logs[i] acquired were:

- GR-ACAL-SC02-SBD2-SLSP-SNP2-BATC-SEXP-SESP-SEMP-SEDP

Four additional wireline logging runs were conducted in Halladale-1 DW1 (Table 4). During Run 3, the RCI got stuck and had to be fished.

Three wireline logging runs were conducted in DW2 (Table 4). As the RCI became stuck in DW1, the sample acquisition RCI run was pipe conveyed.

The LWD neutron-density curves in DW3 did not reach the base of the Waarre A formation. This was, however, covered by the LWD gamma and resistivity logs. One wireline logging run (Table 4) was undertaken in DW3, with ten RCI pressure points being acquired in the Waarre C reservoir.

Four wireline logging runs were conducted in DW1. The temperatures from the logging runs had were at different depths and may be less reliable than other suites. These gave a corrected temperature at 1839 mTVDSS of 87.5^{o}C, equivalent to a geothermal gradient of 43.2^{o}Ckm^{-1}.

Three wireline logging runs were conducted in DW2. These gave a corrected temperature at 1849 mTVDSS of 90.7^{o}C, equivalent to a geothermal gradient of 44.7^{o}Ckm^{-1}.

Only one wireline logging run was conducted in DW3 and so no corrected temperature can be derived. The measured temperature (which will be an under-estimate) was 82.7^{o}C at 1938 mRT (1832.2 mTVDSS). This corresponds to a geothermal gradient of 40.7^{o}Ckm^{-1}.

The temperature gradient for DW2 appears to be the most reliable and this temperature data was used for all wells in the interpretation.

The depth datum for all wells was taken to be Run 1 of the wireline log data in each well. All LWD and mud logs were adjusted to fit this datum.

Table 4: Wireline Logging Runs Conducted in Wells Halladale-1 DW1, DW2 and DW3

Well	Run Number	Tools[ii]
Halladale-1 DW1	1	ORIT-STAR-XMAC-DSL
Halladale-1 DW1	2	GR-RCI (Pressures only)
Halladale-1 DW1	3	GR-RCI (Samples only)
Halladale-1 DW1	4	VSP
Halladale-1 DW2	1	ORIT-STAR-XMAC-DSL
Halladale-1 DW2	2	GR-RCI (Pressures only)
Halladale-1 DW2	3	PCL GR-RCI (Pressures and Samples)
Halladale-1 DW3	1	GR-RCI (Pressures only)

Core Data

Full diameter core was acquired in DW1 and DW2.

Core gamma logs were recorded in both wells and used to correct the logs to the wireline depth datum. In DW1, the core was 1.1 metres deep of the wireline depth datum. In DW2, the core was 0.4 metres deep of the wireline datum.

Core porosity and permeability were measured at 800 psi net overburden pressure (NOBP) and reservoir conditions, assumed to be 3100 psi NOBP. The data measured at reservoir conditions was used in the interpretation.

In DW1, the core was acquired through the Waarre C Sandstone II and upper interval of the Waarre B only. Porosity and permeability was measured on 25 plugs, with 21 plugs yielding valid data. The core in DW2 was acquired through the Waarre C Sand I, the IWC shale, Waarre C Sand II and into the Waarre B.

Grain Density was measured on 38 samples from the Waarre C Sand I, 10 samples from the IWC Shale, 24 samples from the Waarre C Sand II and 31 samples form the Waarre B (Figure 6). The average grain density applied to each reservoir is presented in Table 5.

The overburden corrected porosity / permeability relationships from the core data, along with the correlation line used in the interpretation is presented in Figure 7. The relationship between porosity and permeability is similar for all reservoirs except the Waarre C Sand II, where the trends are different, presumably due to facies variation. The trends presented were applied for the wells / intervals specified, whilst the average function was applied to Halladale-1 DW3.

Table 5: Grain Density by Reservoir from the Halladale-1 DW1 & DW2 Core Data

Reservoir	Grain Density (gcm^{-3})	Comments
Nullawarre	2.655	Not cored. Average property from Waarre C used
Waarre C Sand I	2.658	Cored only in Halladale-1 DW2
IWC Shale	2.644	Significant variation between DW1 and DW2, but all non-net
Waarre C Sand II	2.652	Average of DW1 and DW2 core data
Waarre B	2.670	Mode of distribution from DW1 and DW2 used
Waarre A	2.655	Not cored. Average property from Waarre C used

Eight plugs (four from each of the Waarre C Sand I and Sand II) from DW2 and one plug from the Waarre C Sand II in DW1 were submitted for electrical SCAL.

The cementation exponent ('m') was measured on the SCAL plugs (Figure 8). When plotted, assuming that 'a' = 1, m was determined to be 1.81. This was applied to all reservoirs in the Archie and Indonesia water saturation determinations. The shaly sand equivalent (m* = 1.88) was applied to the Waxman Smits derivation of water saturation.

The saturation exponent ('n') was also determined on the SCAL plugs (Figure 9). When plotted, 'n' can be seen to be different for the Waarre C I and II sandstones. In the Archie and Indonesia water saturation interpretations, n = 1.84 (n* = 2.04) was used in the Waarre C Sand I and n = 2.00 (n* = 2.19) in the Waarre C Sand II. n = 1.90 was applied to the Waarre A and Nullawarre reservoirs. The shaly sand equivalent was applied to the Waxman Smits derivation of water saturation.

The Cation Exchange Capacity (CEC) was measured on the SCAL plugs. Five measurements were available for the Waarre C Sand I (average 1.51 meq/100g, range 0.47 – 2.88 meq/100g) and four for Sand II (average 1.47 meq/100g, range 1.21 – 1.84 meq/100g) (Table 6). A comparison against various log properties (for instance, shale volume) was made without finding a significant trend. The effective concentration of exchange cations per unit volume of pore fluid (Qv) applied in the interpretation was a relationship to core porosity (Figure 10).

Capillary pressure measurements were made on five plugs in DW2 from the from the Waarre C Sand I, one plug in DW2 from the Intra-Waarre C Shale and one plug in DW1 and three plugs in DW2 from the from the Waarre C Sand II. Plots have been produced of the saturation plotted against calculated J Function (Figure 11) and the equations quoted on these plots were used to determine the capillary pressure derived water saturation in the Waarre C reservoir in all wells. No capillary pressure water saturation was derived for the Nullawarre or Waarre A reservoirs.

Table 6: Summary of the Cation Exchange Capacity Results

Summary of the cation exchange capacity (CEC) analysis results.								
Well	Reservoir	Sample no.	Core Depth (m)	Permeability to air (mD)	Porosity (Fraction)	Grain Density (g/cc)	CEC (meq/100gm)	QV (meq/cc pv)
DW-2	WC I	29	1809.05	649	0.223	2.67	2.88	0.27
DW-2	WC I	44	1813.50	3150	0.211	2.63	1.26	0.12
DW-2	WC I	57A	1817.50	3178	0.192	2.66	0.47	0.05
DW-2	WC I	62B	1818.84	392	0.127	2.68	2.06	0.38
DW-2	WC I	64	1819.50	3680	0.258	2.64	0.86	0.07
							1.51	**0.18**
DW-1	WC II	7	1793.00	899	0.260	2.65	1.33	0.10
DW-2	WC II	72	1821.90	51.1	0.180	2.67	1.84	0.22
DW-2	WC II	77A	1823.36	366	0.243	2.65	1.50	0.12
DW-2	WC II	84	1825.50	8230	0.224	2.65	1.21	0.11
							1.47	**0.14**

Formation Water Salinity

The formation water salinities for the Waarre C and Waarre A Formations were derived from the Pickett plots for the DW3 and DW2 wells respectively. The water resistivity for the Waarre A in DW3 could not be derived as the porosity logs do not extend across the interval, so the resistivity was been used (with an assumed water saturation of 100% and salinity) to derive porosity.

The formation water salinity (Figure 12) is derived to be 0.294 ohm.m at 25^{o}C (19,725 ppm NaCl equiv.) for the Waarre C and 0.517 ohm.m at 25^{o}C (10,710 ppm NaCl equiv.) for the Waarre A.

The formation water salinity for the Nullawarre was examined from the three wells (Figure 13). Only Halladale-1 DW1 shows any significant hydrocarbon signal. The formation water salinity was set to 0.403 ohm.m at 25^{o}C (13,990 ppm NaCl equiv) in each well.

Formation Fluid Density

Formation fluid density can be estimated by cross-plotting overburden corrected core porosity against log density and be used to derive a log porosity that, on average through the interval, honours the core data. The fluid density plots are presented in Figure 14.

In the WC II sandstone in DW1, the average grain density through the cored interval is 2.637 gcm^{-3}, which when cross-plotted against log density, yields a fluid density (to match the log to the core data) of 0.366 gcm^{-3}.

Figure 5: Well Bore Deviation for the Halladale-1 wells

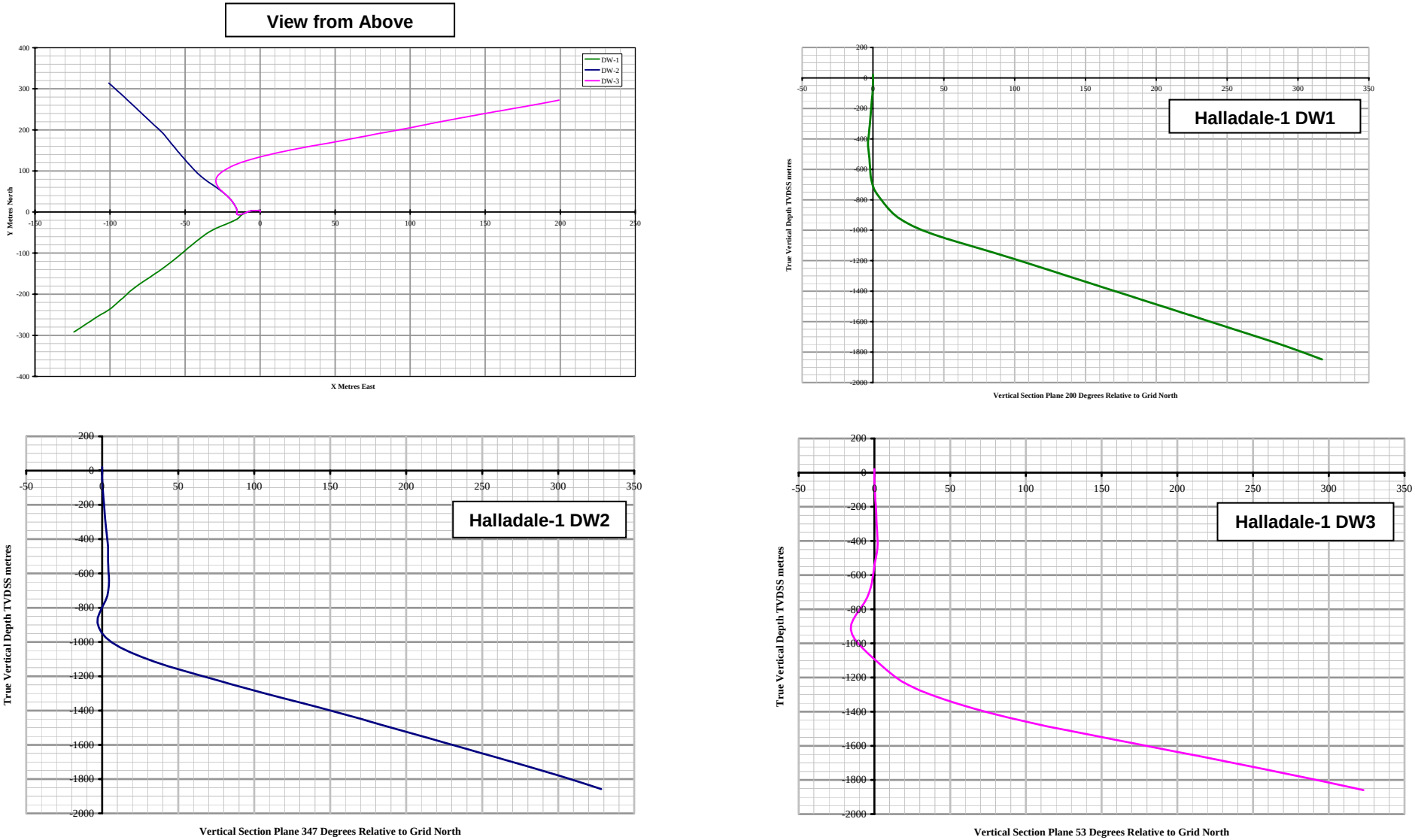

Figure 6: Grain Density Measurements from the Core Data

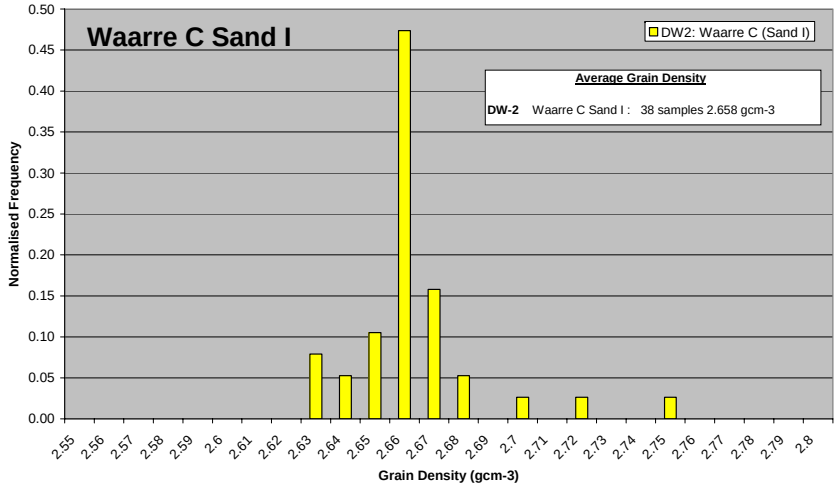

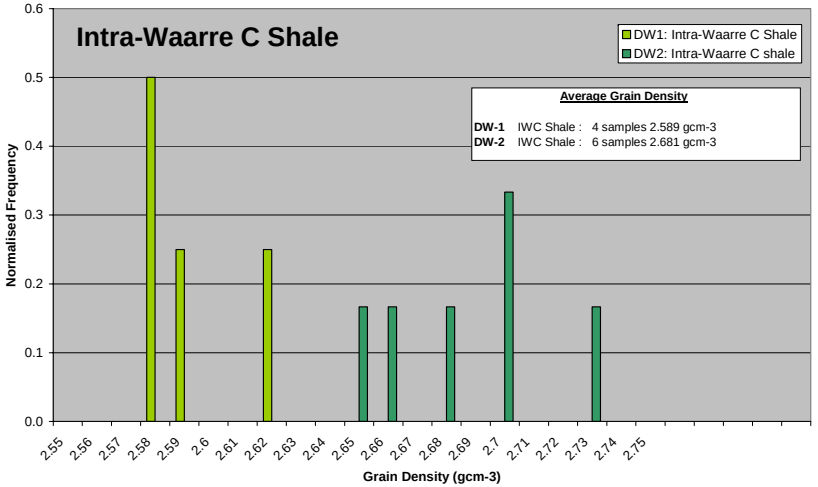

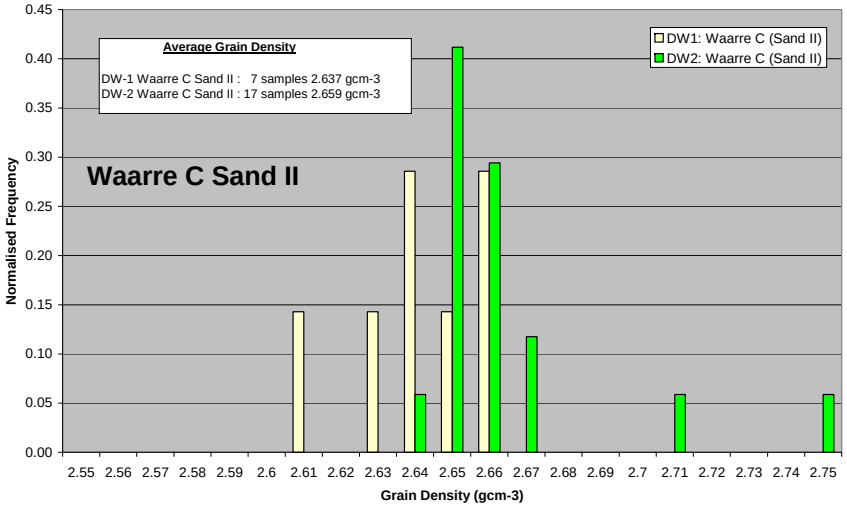

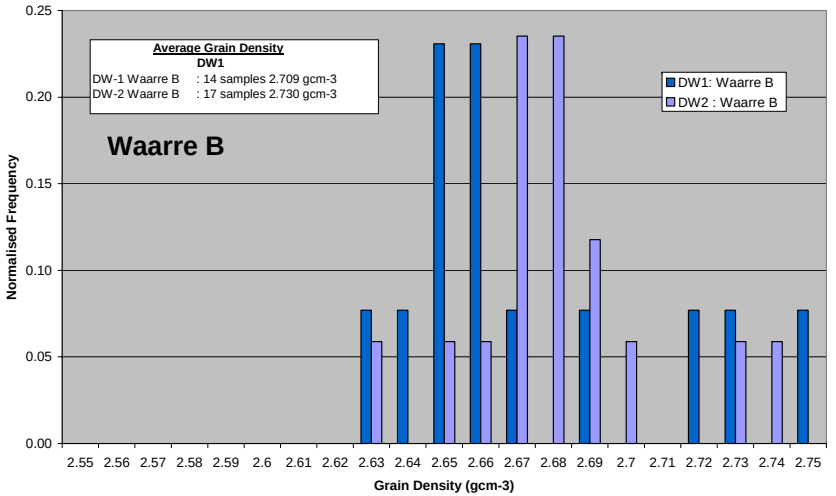

Figure 7: Porosity / Permeability Trends from the Core Data

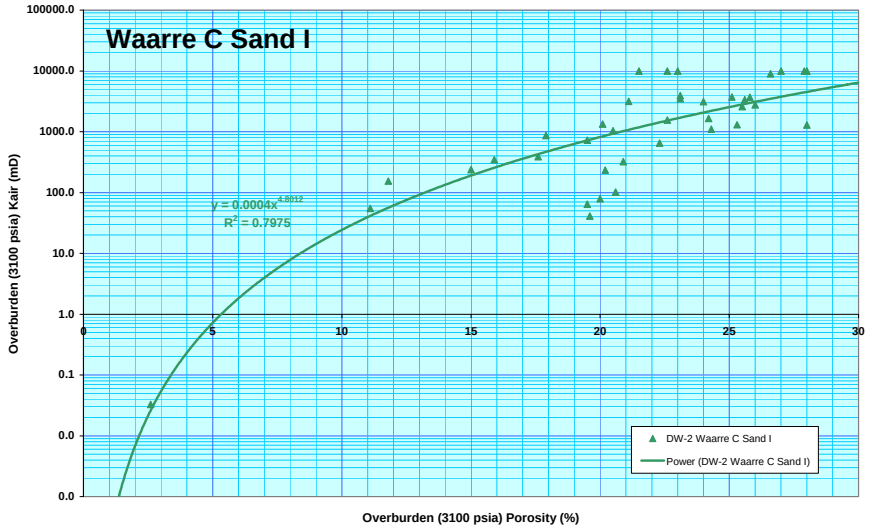

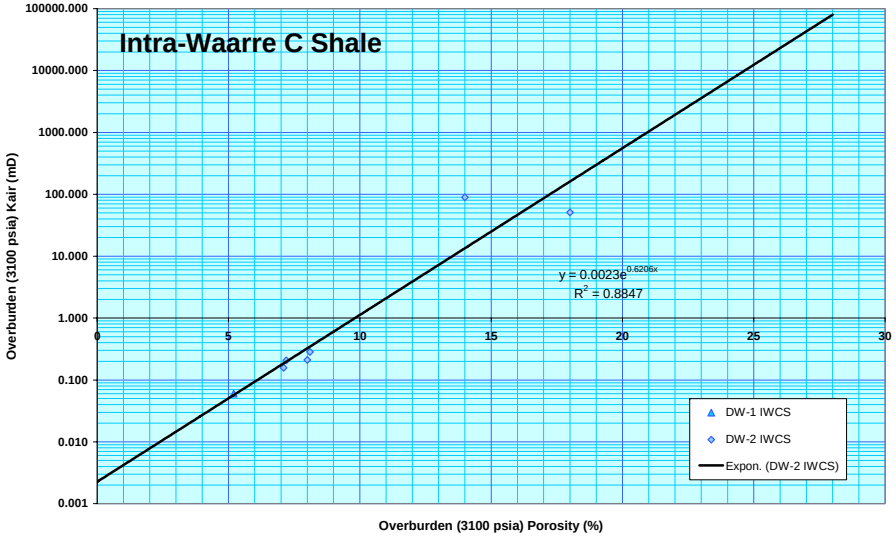

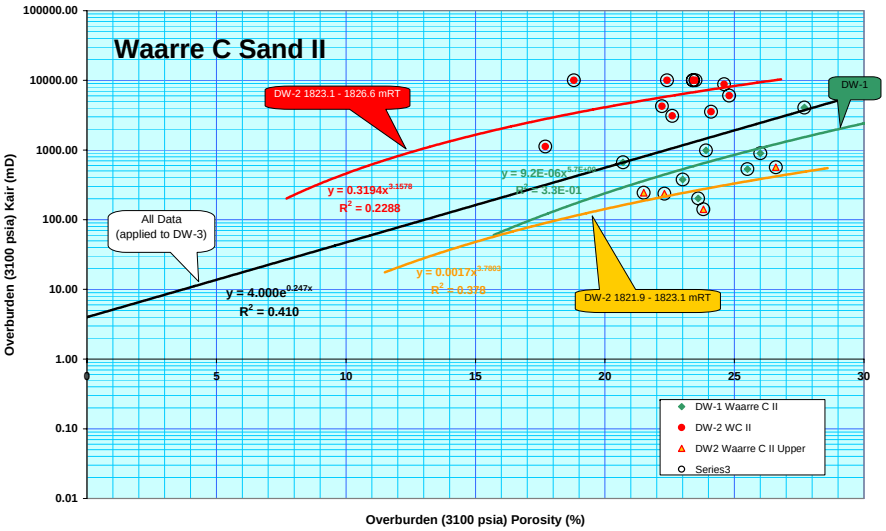

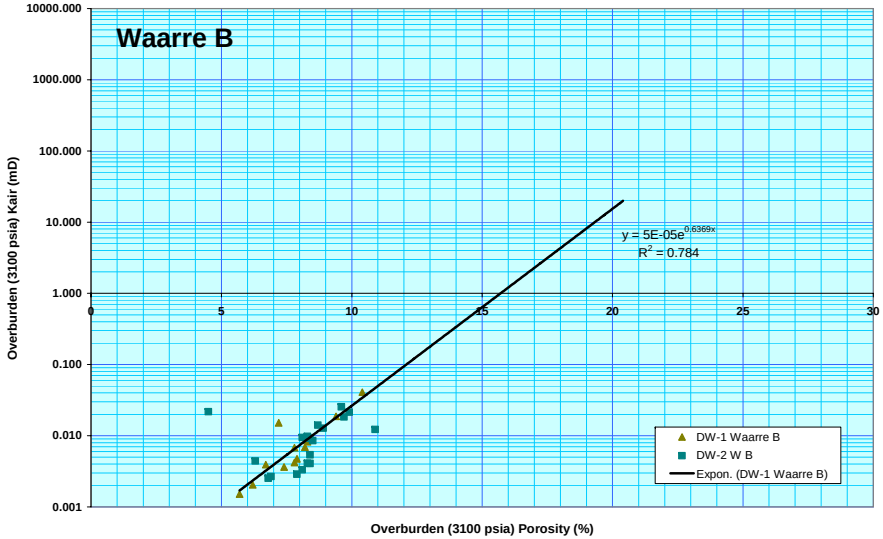

Figure 8: Formation Resistivity Factor for the Waarre C Reservoir

Cementation Exponent at a NOBP of 3100 psi

WELL	RESERVOIR	Sample no.	Core Depth (m)	K air at NOBP (md)	Porosity (%)	FRF (Clean)	FRF* (Shaly)	Cementation exponent m	Cementation exponent m*
DW-1	WC II	7	1793.00	899	26.0	11.5	12.7	1.82	1.88
DW-2	WC I	29	1809.05	649	22.3	14.2	17.9	1.77	1.92
DW-2	WC I	44	1813.50	3150	21.1	16.9	18.9	1.82	1.89
DW-2	WC I	57A	1817.50	2750	19.2	21.2	22.3	1.85	1.88
DW-2	WC I	62B	1818.84	392	12.7	30.1	41.3	1.65	1.80
DW-2	WC I	64	1819.50	3680	25.8	10.9	11.6	1.76	1.81
DW-2	WC II	72	1821.90	51.1	18.0	21.6	26.4	1.79	1.91
DW-2	WC II	77A	1823.36	366	24.3	14.0	15.7	1.87	1.95
DW-2	WC II	84	1825.50	8230	22.4	15.0	16.6	1.81	1.88
					Average m (forced regression with a = 1) =			1.81	1.88

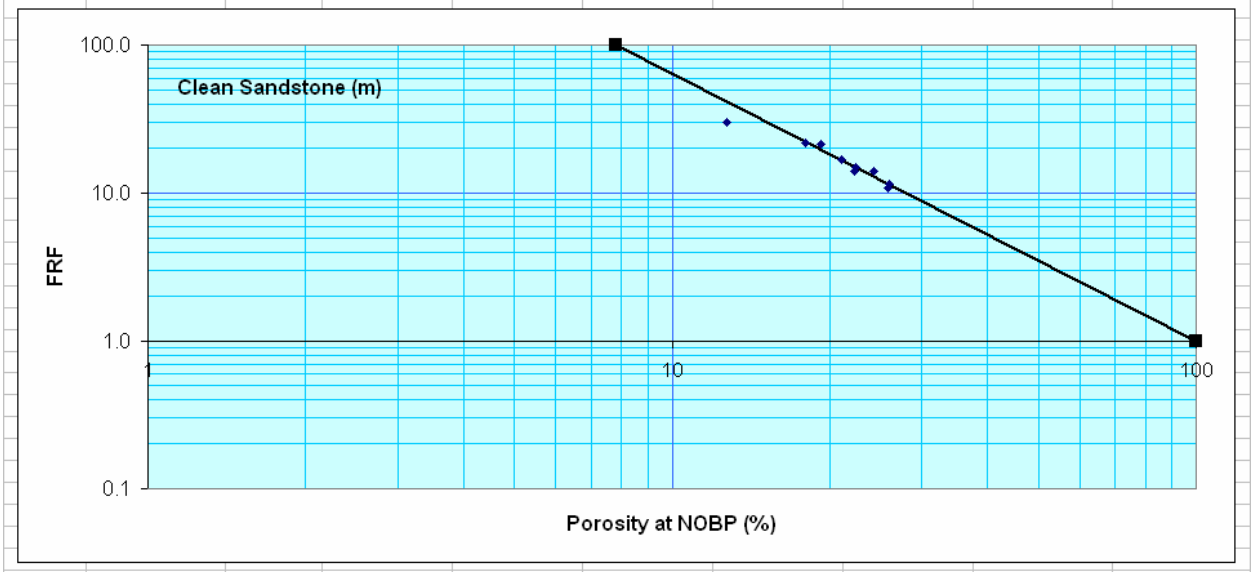

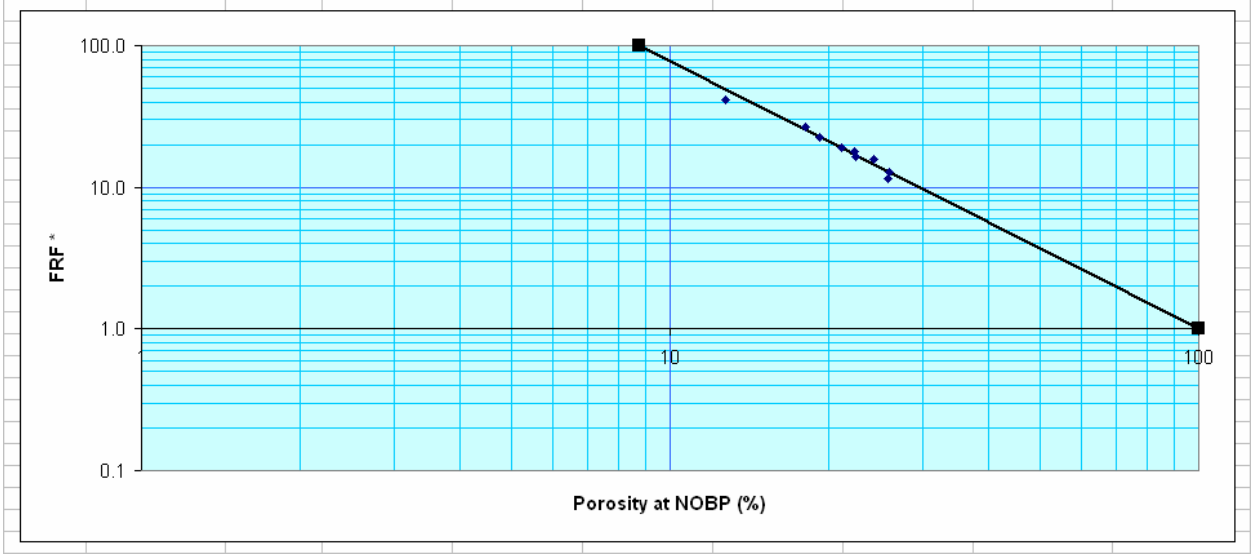

Figure 9: Saturation Exponent for the Waarre C Reservoirs

Saturation Exponent at a NOBP of 3100 psi

WELL	RESERVOIR	Sample no.	Core Depth (m)	K air at NOBP (md)	Porosity (%)	Saturation exponent "m"
DW-2	WC I	29	1809.05	649	22.3	2.03
DW-2	WC I	44	1813.50	3150	21.1	1.68
DW-2	WC I	57A	1817.50	2750	19.2	1.86
DW-2	WC I	62B	1818.84	392	12.7	1.66
DW-2	WC I	64	1819.50	3680	25.8	1.95
						1.84
DW-2	WC II	72	1821.90	51.1	18.0	2.06
DW-2	WC II	77A	1823.36	366	24.3	2.06
DW-2	WC II	84	1825.50	8230	22.4	1.84
DW-1	WC II	7	1793.00	899	26.0	2.05
						2.00

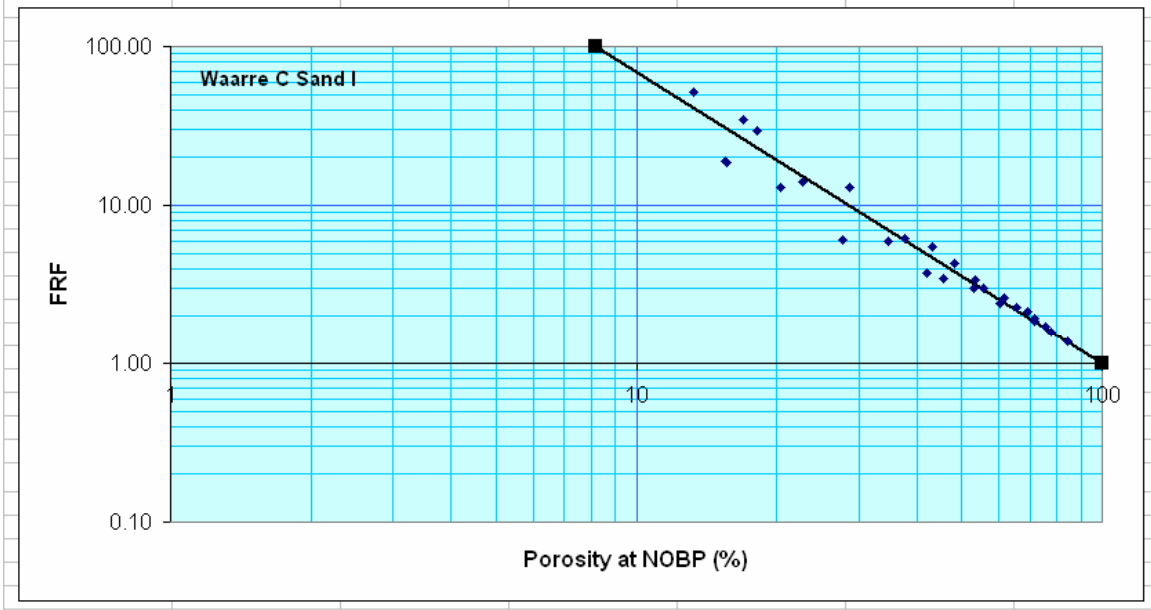

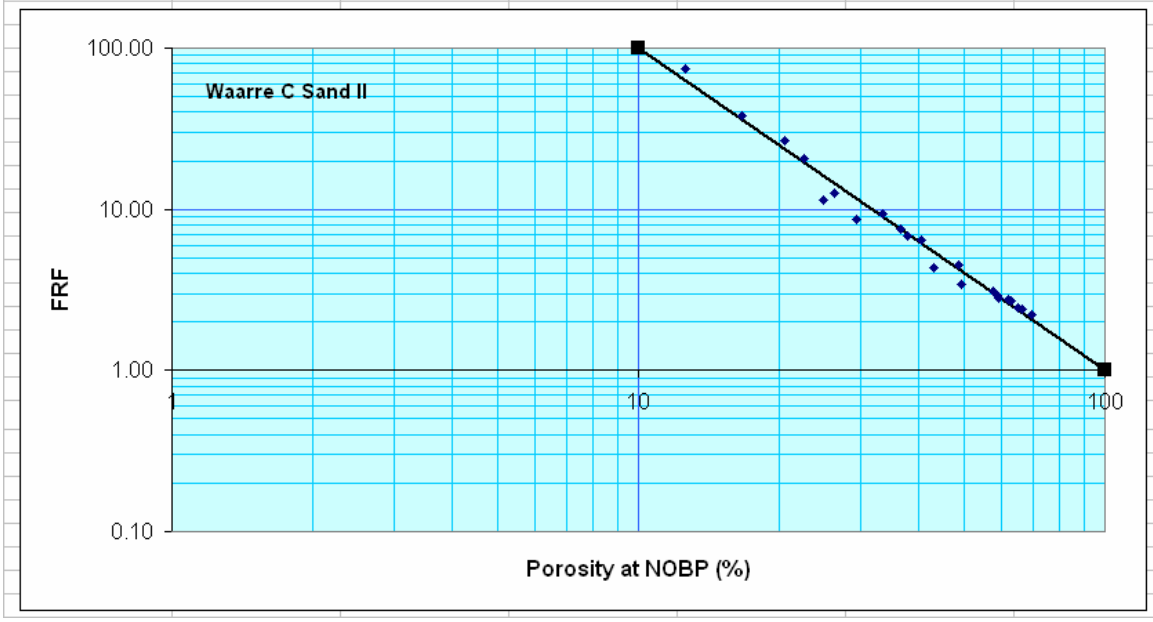

Figure 10: Relationship between Porosity and CEC from the SCAL Data

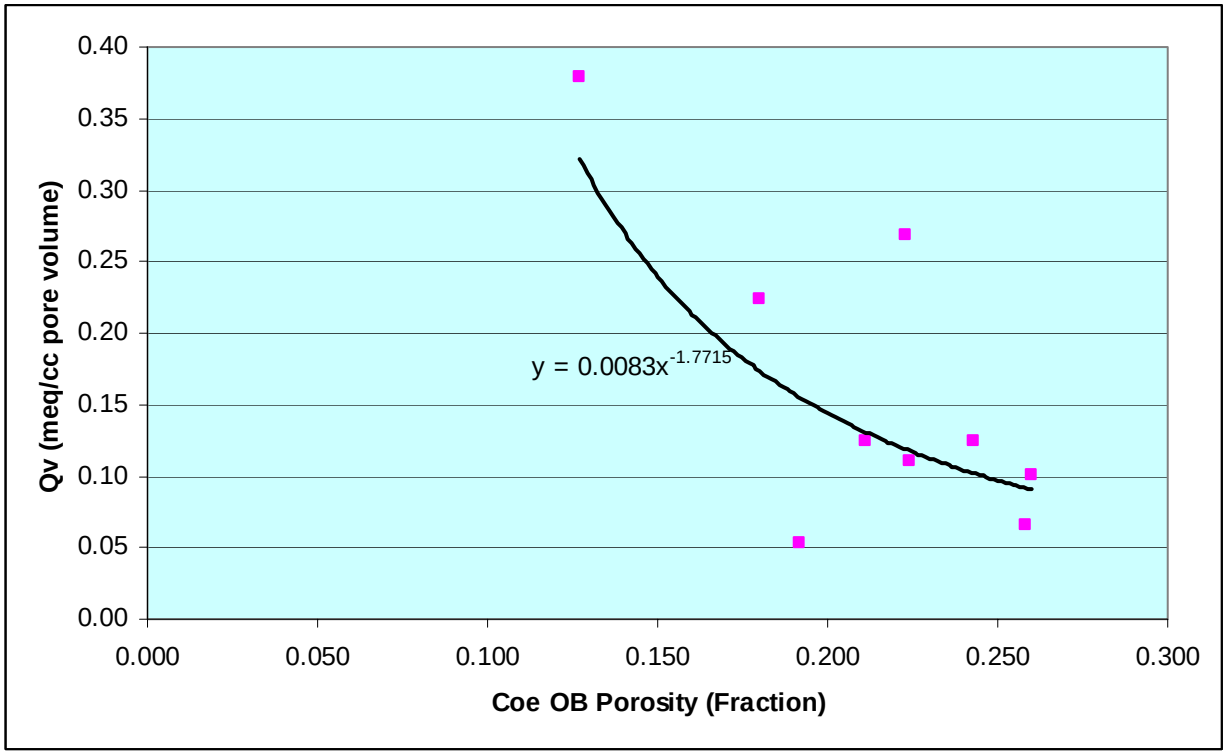

Figure 11: Saturation vs. J Function Relationships for the Waarre C Reservoirs

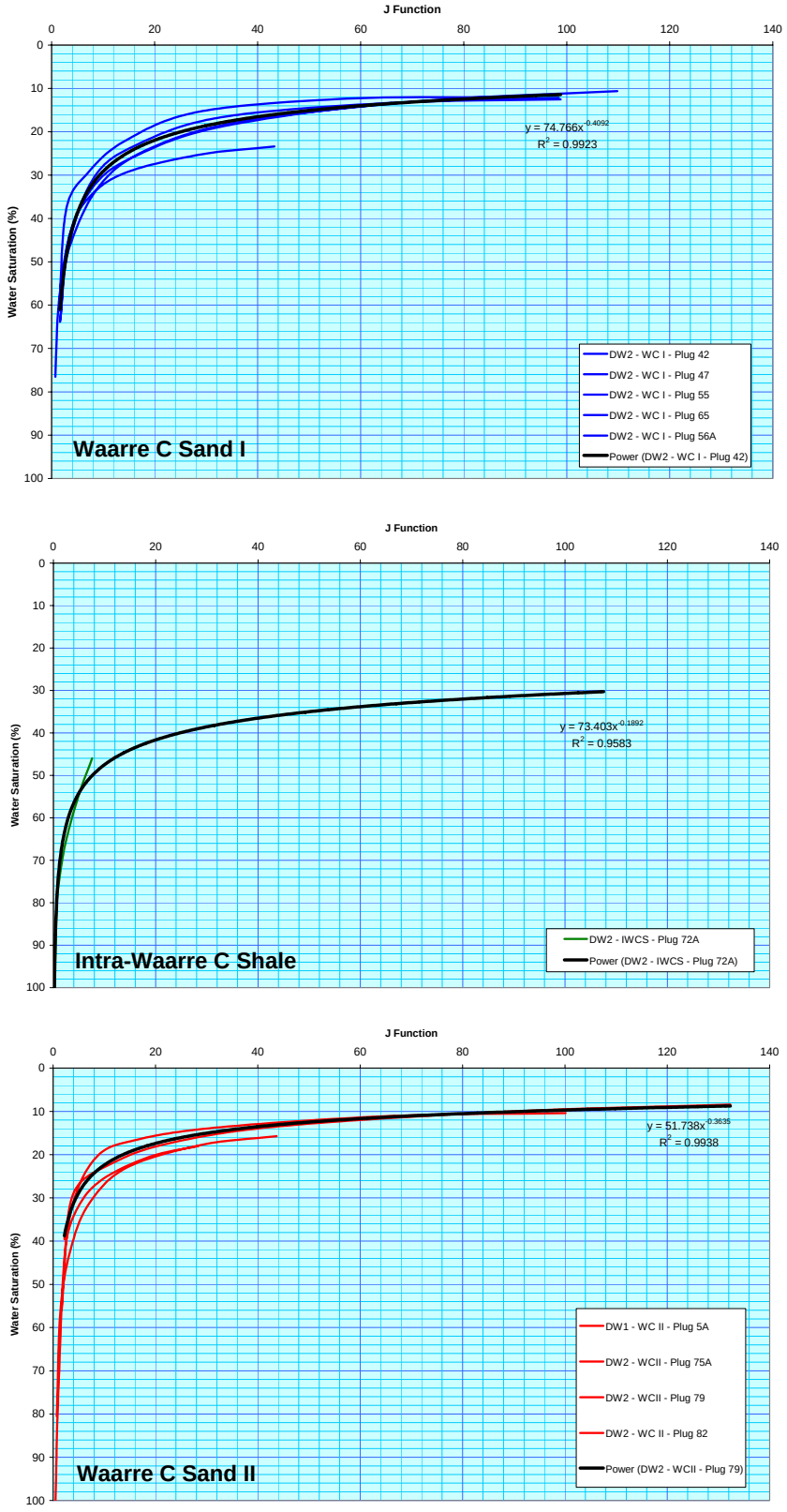

Figure 12: Formation Water Salinity for the Waarre C & Waarre A Formations

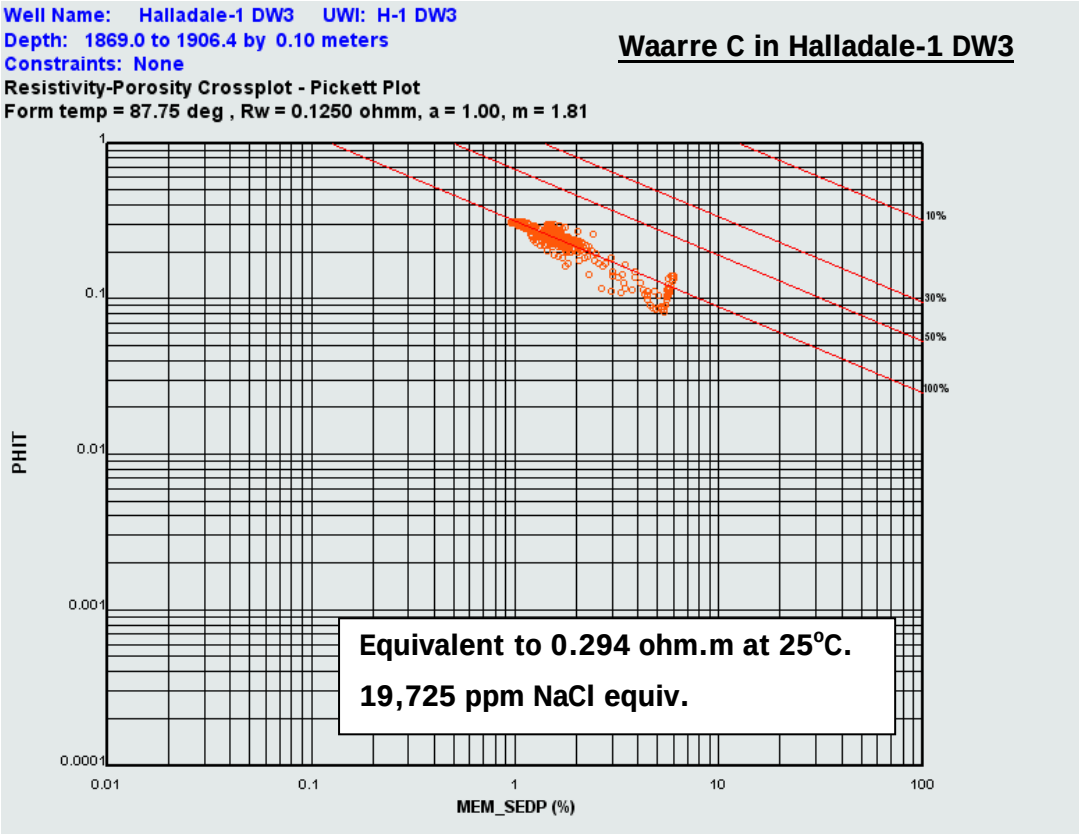

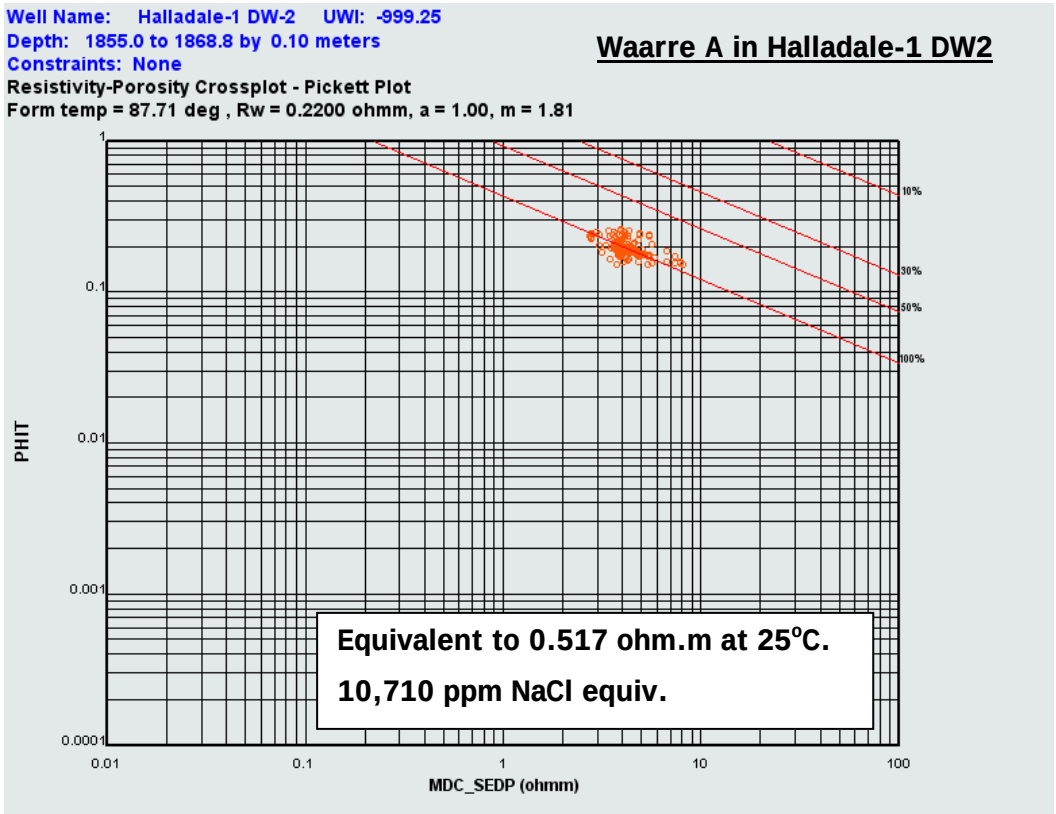

Figure 13: Formation Water Salinity for the Nullawarre Formation

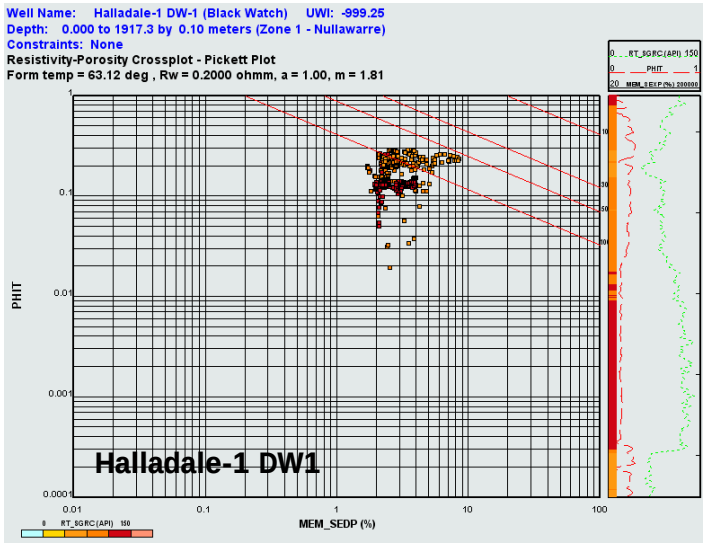

0.364 ohm.m at 25°C

15,600 ppm NaCl equiv

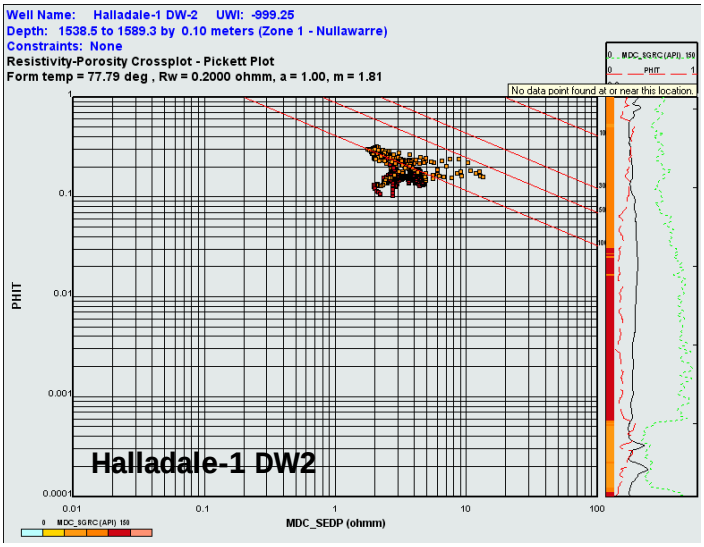

0.427 ohm.m at 25°C

13,140 ppm NaCl equiv

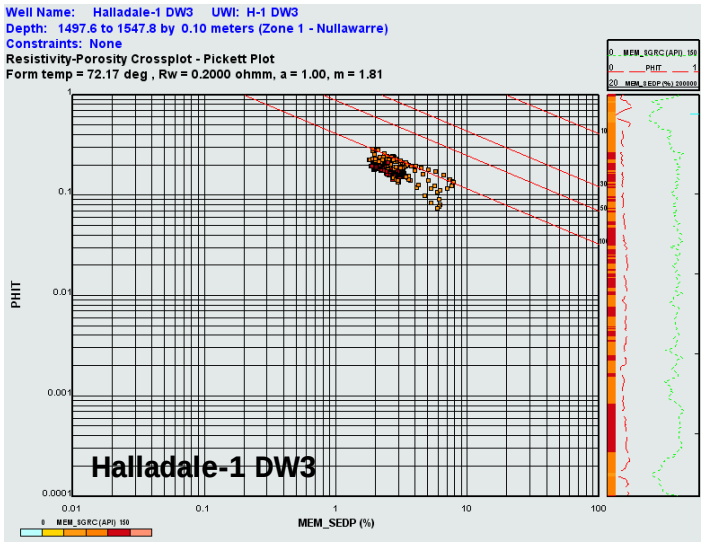

0.403 ohm.m at 25°C

13,990 ppm NaCl equiv

Figure 14: Fluid density Determination for the Cored Intervals

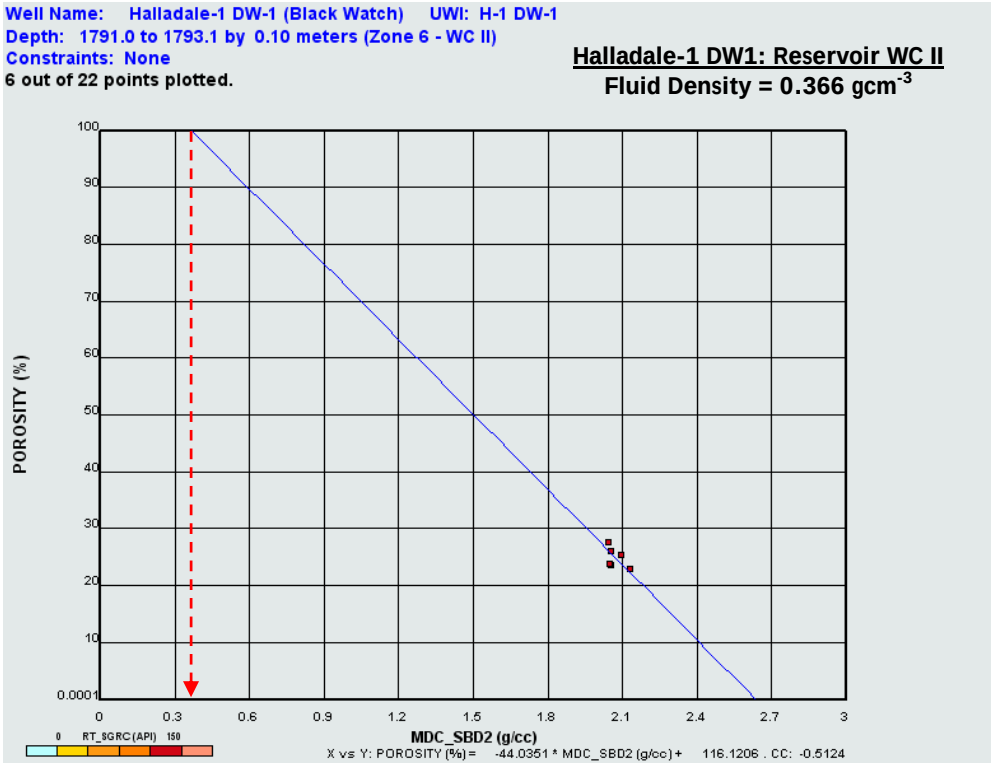

INTERPRETATION METHODOLOGY

Shale Volume

Shale volume was calculated from the neutron-density cross-plot and the gamma ray logs. The fluid density and neutron response in the gas zones (DW1: Nullawarre, Waarre C and Waarre A and DW2: Waarre C) was adjusted so that the calculated shale volume from gamma and density / neutron was similar. The minimum calculated shale volume from the two methods was used in the ongoing interpretation.

Porosity

In the cored intervals (DW1 WCII and DW2 lower WC I, IWCS & WC II), total porosity was derived directly from the interpolated core data. In other zones in DW1 and DW2, the porosity was calculated from the neutron-density cross-plot.

In DW3, the porosity was derived from the neutron-density cross-plot for most of the section. At the base of the Waarre A, below 1930 mRT, porosity was calculated from the resistivity log using the Archie equation as no other porosity logs were acquired.

Permeability

In the cored intervals, the permeability was derived directly from the interpolated core data.

Elsewhere in the wells, permeability was calculated from the log derived porosity using the appropriate core-derived porosity / permeability transform.

Transform Derived in …	**Applied to …**		
Nullawarre (MDT mobility)	Nullawarre		
Waarre C Sand I	Waarre C Sand I		
Intra-Waarre C shale	Intra-Waarre C shale	Flaxman	
Waarre C Sand II	Waarre C Sand II	Waarre A	Nullawarre
Waarre B	Waarre B	Eumeralla	Belfast

The porosity / permeability transform for the Nullawarre Formation was derived by cross-plotting the MDT fluid mobility against the log derived porosity at the same depth (Figure 15). The scatter in the data probably represents differences in the fluid viscosity being tested.

Since no correction has been applied for this, the average curve on Figure 15 was used to determine permeability.

In a similar fashion, the permeability for the Waarre A and Eumeralla was determined from the MDT mobilities acquired in that interval (Figure 16).

Water Saturation

Water saturation was calculated in the Waarre C Sandstone using the Waxman Smits equation using the formation water and electric parameters determined from the core data.

The water saturation for all other intervals was calculated from the Indonesia equation, using surrounding shales as a guide to the clay conductivity in the formation. Whilst this is not ideal, the laminated shales may have different properties to the disseminated clays in the sandstones, it is considered better than simply applying electric properties from the Waarre C sandstone throughout the interpretation interval.

Water saturation was also calculated for the Waarre C from the capillary pressure data from the cores in DW1 and DW2 and used to estimate the Gas-Water-Contact (see Estimation of GWC below).

Water saturation in DW3 was simple calculated using the Archie equation as a screening exercise as the well was drilled below the GWC at all levels. No significant hydrocarbon saturation was calculated to be present.

Net Sand / Net Pay

Net sand was calculated to be present where the shale volume is less than 40% and the permeability is greater than 0.2 mD. No porosity cut-off was explicitly applied, although the determination of the permeability from the porosity / permeability core relationship implies one (that will vary by reservoir). Net Pay was calculated to be where Net Sand = 1 and water saturation is less than 50%.

Estimation of GWC

The gas-water contact can be estimated from pressure data provided that the pressure gradient for the hydrocarbon and water are known. Additionally, if capillary pressure is

available, the GWC can be estimated by comparing the calculated water saturation from the capillary pressure data to the water saturation calculated from the resistivity data.

Black Watch

The pressure data for the hydrocarbon legs in the Nullawarre Formation can be compared to one valid water pressure acquired in DW2 (Figure 17). Hence, there is some uncertainty in the water gradient that is applicable to the Nullawarre in Black Watch. The pressure data from DW1 does, however, confirm that the two gas columns are discrete and have fairly short (10 – 12 metres below the well) hydrocarbon columns.

The lowest known gas in the Waarre C in Black Watch is at 1728 mTVDSS (1793 mRT) in DW1. The pressure gradient data (Figure 18) gives a gas gradient that intersects the water gradient from the Waarre C Formation in DW3 at 1769 mTVDSS (1836 mRT in DW1). Coincidentally (or maybe not), the Waarre A gas pressures are on the same gradient as the Waarre C points. Should the Waarre A water gradient be applicable to the Waarre C Formation in Black Watch, therefore, the GWC would be coincident with the Waarre A GWC (at 1766 mTVDSS, 1832.8 mRT). When the capillary pressure water saturation is calculated with this contact, the values are equivalent to the resistivity derived water saturation in the better sands in the Waarre C Sand I (Figure 19). The derived capillary pressure water saturation is too high in the shalier intervals suggesting either that the capillary pressure plugs are not relevant in this facies. The capillary pressure derived water saturation is also too high in the thin Waarre C Sand II interval. As the porosity and permeability are derived from core and the capillary pressure relationship applied was derived from a core plug in the interval, the agreements should have been better. The discrepancy is probably due to the shoulder effects on the resistivity log in the thin bed. The effect could be a reduction is gas saturation in a transition zone, but this is considered unlikely as the Waarre C Sand I interval above would have lower gas saturation and the pressure gradient required to have a significantly shallower GWC in DW1 would be significantly outside the pressure gradient range from the other wells.

The Waarre A GWC in DW1 is defined by pressure data (Figure 18) to be at about 1766 mTVDSS (1833 mRT in DW1). This corresponds well with the gas-down-to (GDT) observed in the well. No capillary pressure data is available for comparison as no core was acquired in the Waarre A.

Halladale

DW2 has a gas accumulation in the Waarre C reservoir. An examination of the hydrocarbon gradient (Figure 16), along with the water gradient obtained in the same fault block from DW3, suggests a GWC at about 1760.5 mTVDSS (1837 mRT in DW2). The deepest known gas in

DW2 is at the base of the Waarre C formation at 1827 mRT (1751.3 mTVDSS). When the capillary pressure water saturation was calculated, the agreement with the resistivity data was very good across the cored interval (Figure 20). The agreement above the cored interval in the Waarre C is not so good suggesting either that the log derived porosity or, more likely, permeability is pessimistic or that the capillary pressure function has changed.

The Waarre A in DW2 is below the Waarre A GWC seen in Black Watch. Gas is assumed to be present up-dip of the well location in Halladale, but has not yet been proven. DW3 was intentionally drilled below the expected GWC at all levels to obtain aquifer pressures.

Figure 15 : Fluid Mobility vs. Log Porosity for the Nullawarre Formation

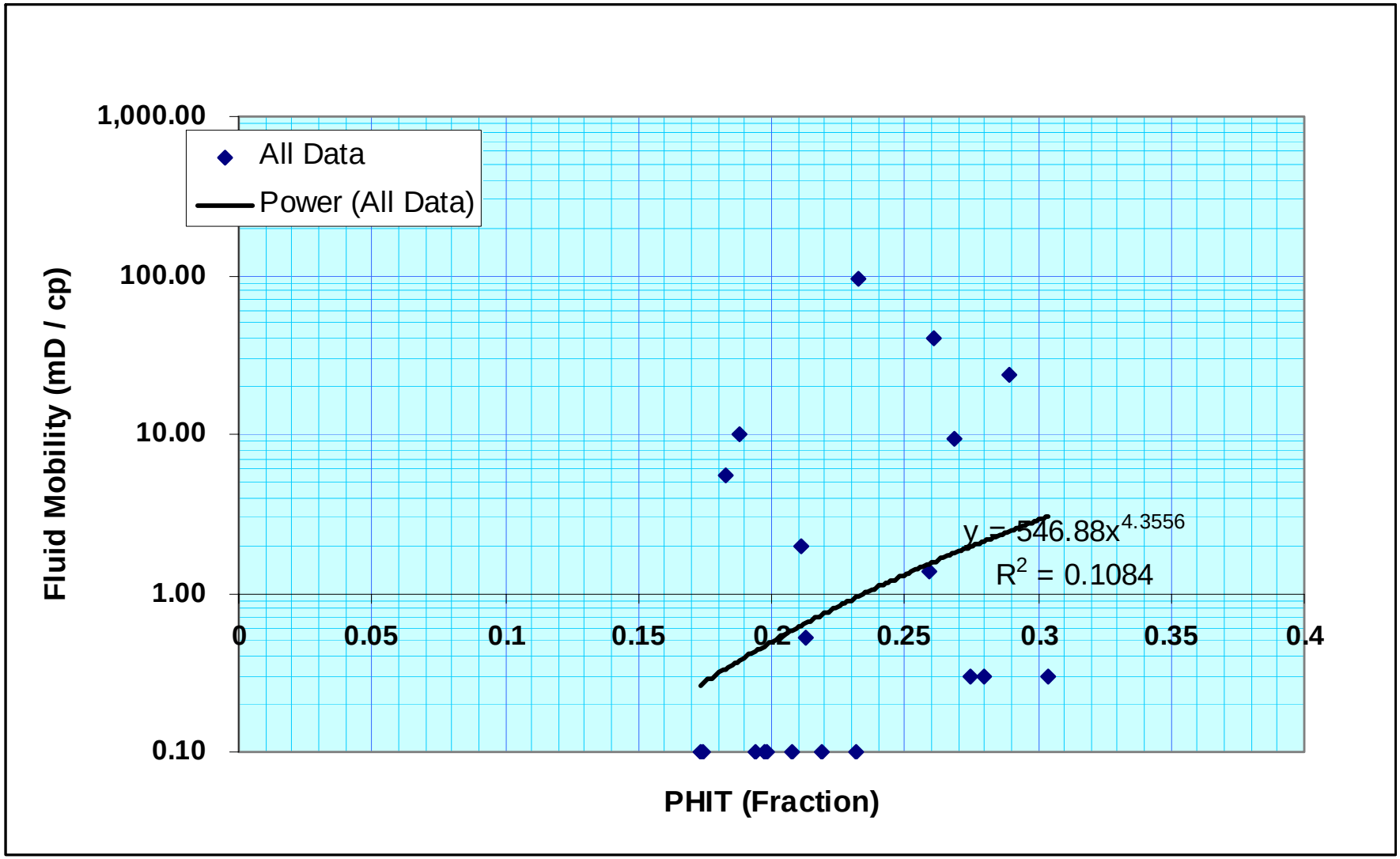

Figure 16 : Fluid Mobility vs. Log Porosity for the Waarre A and Eumeralla Formations

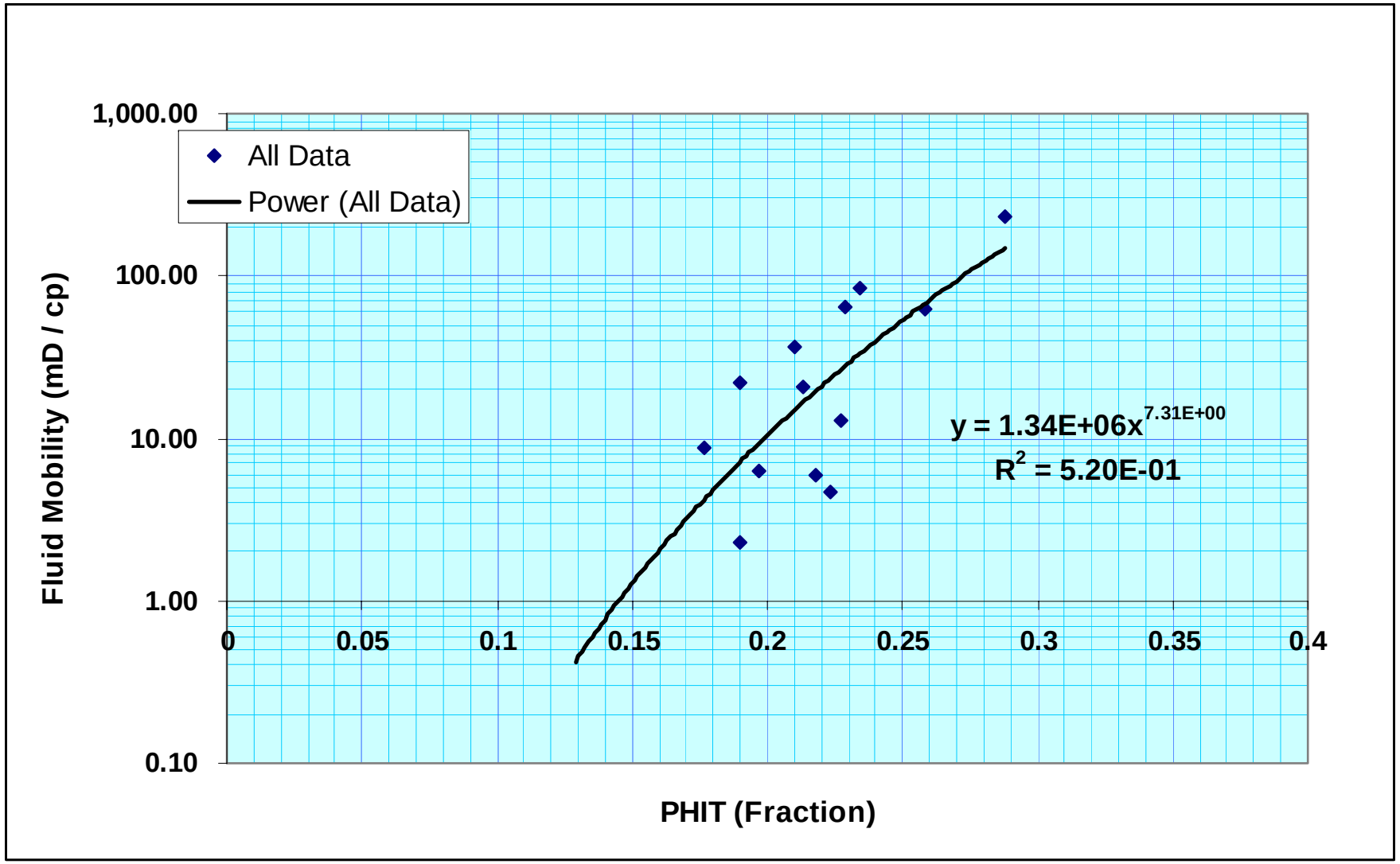

Figure 17: Nullawarre Fluid Pressure Gradient in DW1 and DW2

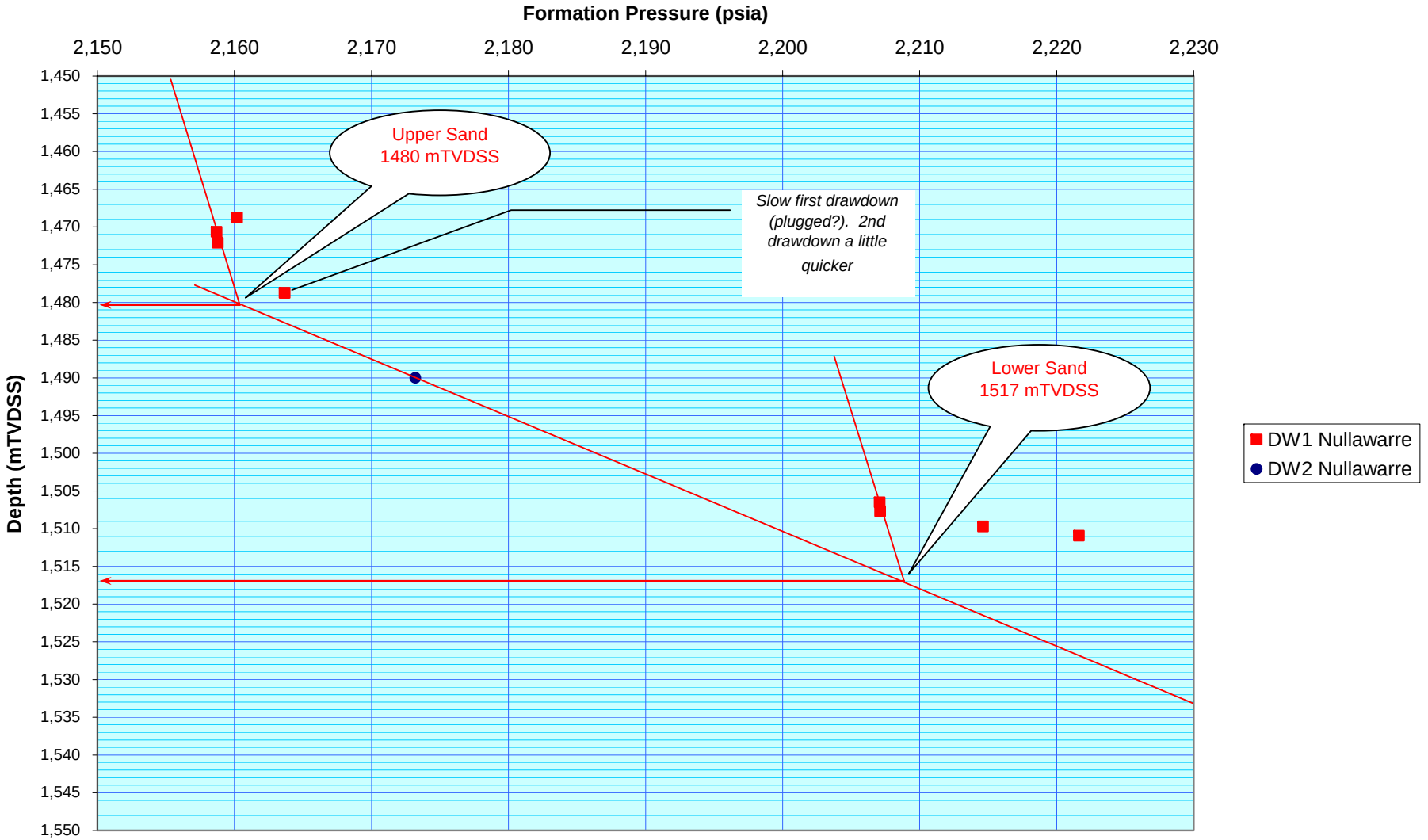

Figure 18: Waarre C and Waarre A Fluid Pressure Gradients

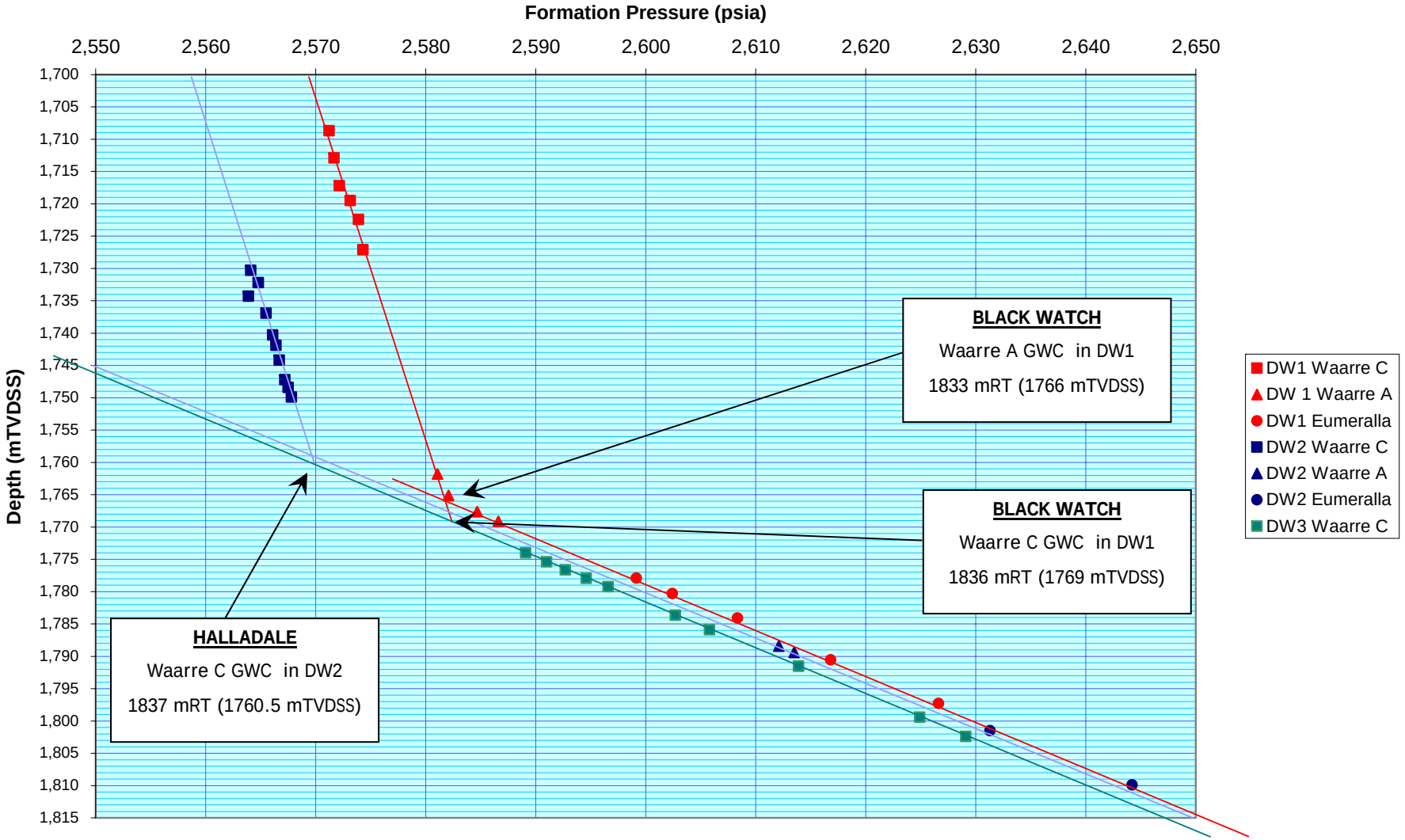

Figure 19: Waarre C Section in DW1 Showing the Agreement Between Capillary Pressure and Resistivity Calculated Water Saturation with a GWC at 1769 mTVDSS

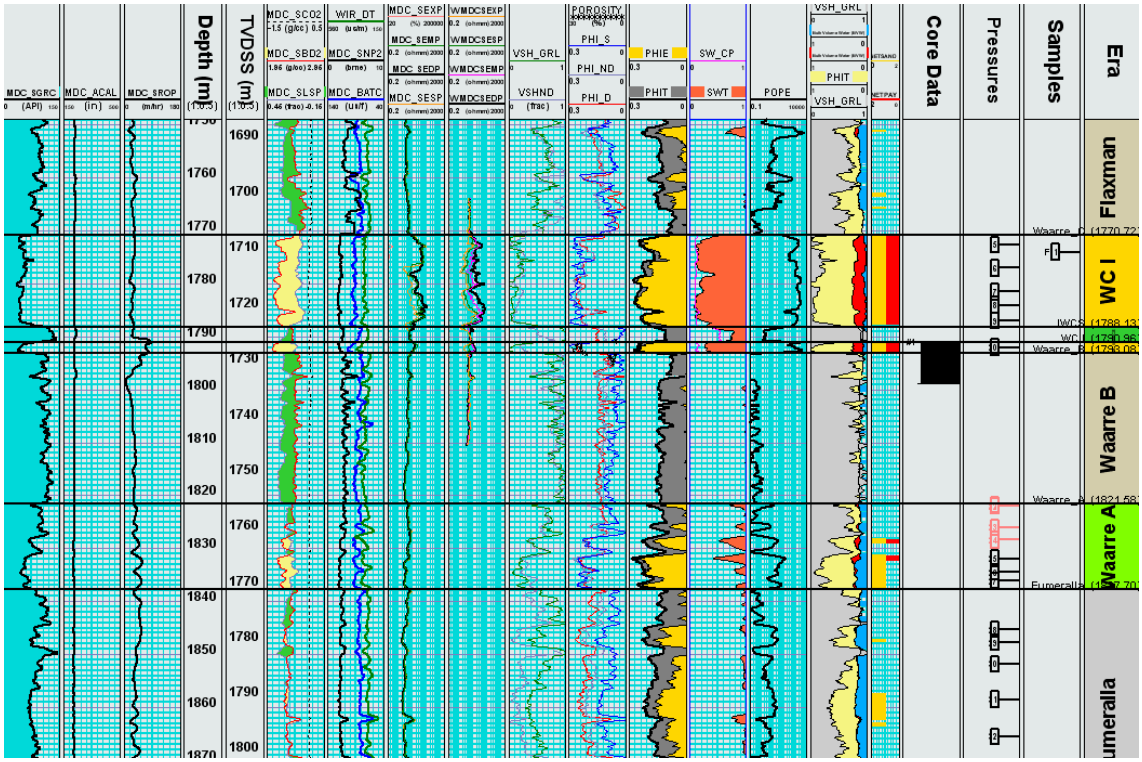

Figure 20: Waarre C Section in DW2 Showing the Agreement Between Capillary Pressure and Resistivity Calculated Water Saturation With a GWC at 1760.5 mTVDSS

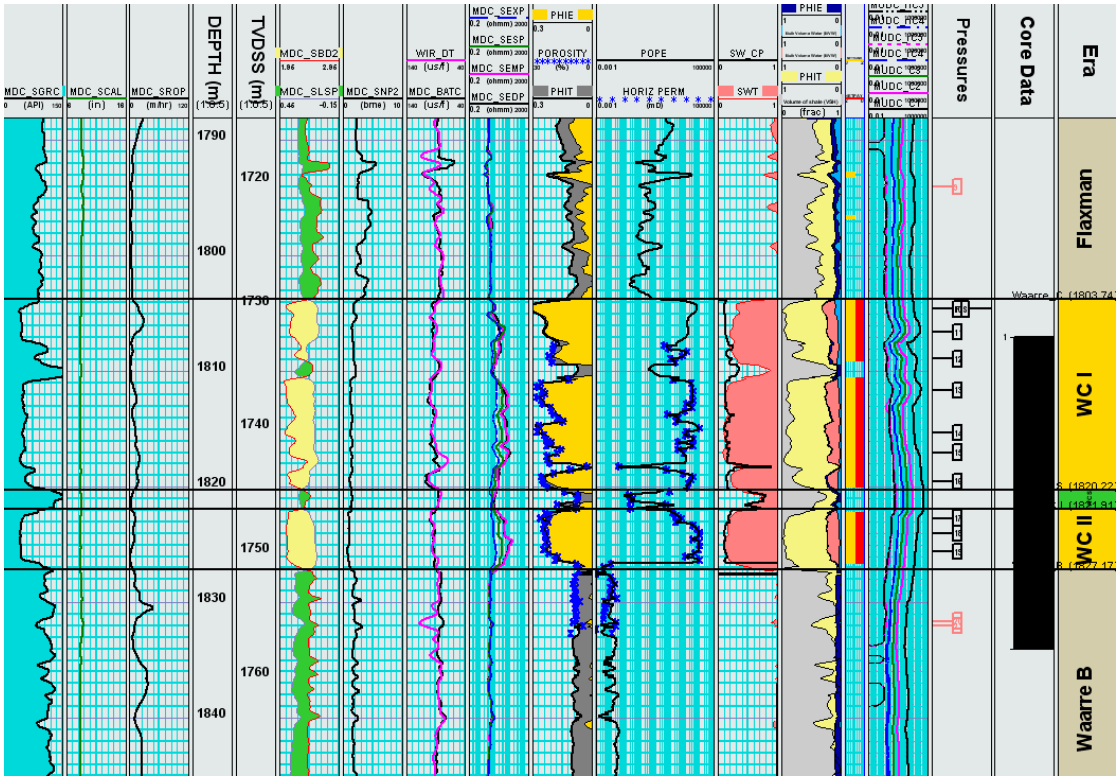

INTERPRETATION BY FORMATION

Interpretation was conducted for the Nullawarre, Belfast, Flaxman, Waarre C, Waarre B, Waarre A and Eumeralla formations using the parameters described previously in this report.

Nullawarre Formation

Well	Top (mRT)	Base (mRT)	Gross Thickness (mMD)	Inclination Through Formation	Gross Thickness (m AVT[1])
Halladale-1 DW1	1515.1	1565.1	49.6	18.6	47.0
Halladale-1 DW2	1538.5	1589.3	50.8	21.9	47.1
Halladale-1 DW3	1497.6	1547.8	50.2	25.0	45.5

m AVT = metres apparent vertical thickness, taking no account of bed dip

The Nullawarre Formation in all wells in this study comprised a two very fine to medium grained sandstones separated by a silty claystone. No cores were taken in this formation, but the MDT mobilities suggest the flow potential is limited. These sandstones were found to be gas bearing in DW1 and water bearing in DW2 and DW3.

Analysis of the DW1 pressure data suggests that the sands have different GWC and that the gas columns do not extend significantly beneath the well. The high calculated water saturation in each sandstone in DW1 also suggests that the sands may be within the transition zone at DW1.

Log analysis suggests some limited pay thickness in DW1 which could be exploited if a significant section above the current well penetration is identified. At the current location, the well would probably cut water fairly quickly.

Belfast Formation

Well	Top (mRT)	Base (mRT)	Gross Thickness (mMD)	Inclination Through Formation	Gross Thickness (m AVT)
Halladale-1 DW1	1565.1	1723.1	158.0	18.5	149.8
Halladale-1 DW2	1589.3	1749.2	159.9	21.5	148.8
Halladale-1 DW3	1547.8	1798.1	250.3	29.0	218.5

The Belfast Formation is described as a massive silty claystone, with some glauconitic intervals.

No net sand or net pay was determined in this formation in any of the wells.

Flaxman Formation

Well	Top (mRT)	Base (mRT)	Gross Thickness (mMD)	Inclination Through Formation	Gross Thickness (m AVT)
Halladale-1 DW1	1723.1	1770.7	47.6	18.5	45.1
Halladale-1 DW2	1749.2	1803.7	54.5	21.3	50.8
Halladale-1 DW3	1798.1	1869.7	71.6	28.5	62.9

At the top of the Flaxman Formation in each well is an interval of dense, high neutron sandstone with a high (5 – 7 b/e) PEF response. In several nearby onshore wells, this interval is described as being an iron rich, goethitic cemented zone. As the neutron and density are both reacting to the unusual mineralogy, the porosity is difficult to determine. As there are, however, no gas shows, the interval is not expected to be net in any of the wells.

The Flaxman Formation is described as mainly a silty claystone interbedded with argillaceous siltstone and argillaceous sandstone. The sandstones are dominantly fine grained, but do have some medium grained intervals.

The net sand thickness ranges between 0 – 3 metres in the wells. No net pay is calculated to be present in any of the wells.

Waarre C

Well	Top (mRT)	Base (mRT)	Gross Thickness (mMD)	Inclination Through Formation	Gross Thickness (m AVT)
Halladale-1 DW1	1770.7	1793.1	22.4	18.4	21.3
Halladale-1 DW2	1803.7	1827.2	23.5	21.0	21.9
Halladale-1 DW3	1869.7	1906.5	36.8	28.7	32.3

The Waarre C was the primary target in the Halladale / Black Watch prospects.

In this study, the Waarre C Sandstone was sub-divided into three intervals, Waarre C Sand I (WC I), Intra-Waarre C Shale (IWCS) and the Waarre C Sand II (WC II), based upon correlation of the Halladale-1 DW1, DW2 and DW3 wells (Figure 1).

The Waarre C is described as generally medium grained sandstone; with some coarse grains and approximately 30% silt or fine sandstone. Some minor silica cement is noted.

The Waarre C was cored in two wells, DW1 and DW2. In DW1, only the Waarre C Sand II was cored. A thicker section, encompassing the WC I, IWCS and WC II was cored in DW2. Core porosity and permeability demonstrated very high quality reservoir porosity and permeability. Electrical and capillary pressure properties were also measured on the core and these are incorporated into this interpretation.

MDT pressure gradients demonstrated that the Waarre C sands in Black Watch and Halladale are not in pressure communication, with a pressure offset of approximately 10 psi. Using the water pressure gradient data from DW3, the gas-water contact was defined as 1760 mTVDSS in Halladale and 1769 mTVDSS in Black Watch. The contact in Halladale was confirmed by an excellent correlation between the capillary pressure and resistivity calculated water saturations. The correlation in DW1 was good in some sands, but poorer in others. The poorest correlation is in DW1 WCII, where the resistivity calculated water saturation is significantly lower than the capillary pressure calculated saturation. This could be due to the sand being within a transition zone, but is more likely to be a thin bed effect on the resistivity logs. More detailed resistivity modelling than conducted in this study should be undertaken to confirm this interpretation.

The net sand thickness varied between 18.4 mMD in DW1 and 30.3 mMD in DW3. The average porosity in DW1 and DW2 is 22 – 23%. In DW3, the average porosity is 26%. All wells are calculated to have a geometric average permeability over 1 Darcy. All the net sand is interpreted to be net pay in DW1 and DW2, with the average water saturation being approximately 20%. No net pay is calculated to be present in DW3 as it is significantly below the gas-water contact for the Halladale discovery.

Waarre B

Well	Top (mRT)	Base (mRT)	Gross Thickness (mMD)	Inclination Through Formation	Gross Thickness (m AVT)
Halladale-1 DW1	1793.1	1821.6	28.5	18.2	27.0
Halladale-1 DW2	1827.2	1855.1	27.9	20.8	26.1
Halladale-1 DW3	1906.5	1935.7	29.2	28.0	25.8

The Waarre B is described as a silty claystone with common carbonaceous specks, trace glauconite, trace pyrite nodules and occasionally grades to a siltstone.

No net sand or net pay is interpreted to be present in this well.

Waarre A

Well	Top (mRT)	Base (mRT)	Gross Thickness (mMD)	Inclination Through Formation	Gross Thickness (m AVT)
Halladale-1 DW1	1821.6	1873.6	52.0	17.3	49.6
Halladale-1 DW2	1855.1	1897.9	42.8	20.5	40.1
Halladale-1 DW3	1935.7	1969.0	> 33.3	27.0	> 29.7

The Waarre A was the secondary target in the Halladale / Black Watch prospects.

The Waarre A in each well has a shaly upper interval with the best, cleanest sandstone being at the base. In DW1 and DW2, the net sand thickness ranges from 13.0 – 17.6 mMD with an average porosity of 20 – 21%. Average porosity in DW3 was calculated to be much higher (25%), but as no porosity logs were acquired across this interval and the porosity is calculated from the resistivity, low confidence should be held in this interpretation. Permeability was calculated from the MDT mobility data and is low confidence, since the scatter on the mobility / log porosity chart is very high.

DW1 intersected the gas-water contact was drilled in the Waarre A, with pressure data and log analysis showing the upper, shaly, sandstones to be gas bearing and the lower, cleaner sands to be water-wet. Consequently, only 1.3 mMD of net pay is calculated to be present in DW1 with an average water saturation of 51%. The gas saturation is likely to increase significantly up-dip and the net pay / net sand ratio is likely to increase significantly.

Eumeralla Formation

Well	Top (mRT)	Base (mRT)	Gross Thickness (mMD)	Inclination Through Formation	Gross Thickness (m AVT)
Halladale-1 DW1	1873.6	1918.0	> 44.4	16.5	> 42.6
Halladale-1 DW2	1897.9	1941.0	> 43.1	19.5	> 40.6
Halladale-1 DW3	Not penetrated				

DW1 and DW2 were still in the Eumeralla Formation at TD and, hence, the quoted thicknesses refer to drilled thickness, rather than formation thickness at this location. DW3 reached TD in the Waarre A, above the Eumeralla Formation.

The Eumeralla Formation is an interbedded sequence of very fine to medium sandstones and silty claystones. The sandstones have some clay matrix, silica or calcite cement.

The net sand thickness is from 1.0 to 6.1 mMD in DW2 and DW1 respectively. The average net sand porosity in DW1 and DW2 is approximately 19% and this is correlated to the MDT mobility to correspond with a permeability of 6 – 9 mD. Although some gas shows were recorded during drilling, especially at DW1, the MDT gradients confirmed poor mobility sandstone throughout. No net pay is interpreted to be present at this location, although these sands may become net pay further up-dip if they have a common GWC with the Waarre A sandstones, as appears likely from the DW1 pressure data.

Appendix A : Terrastation TCL Routine For Halladale-1 DW1

```
 * Mud properties RM (C7), RMF (C9), RMC (C5), MW (C25)
* Temperatures RM (C8), RMF (C10), RMC (C6)
* MW
        C25= 1.26 * 8.34
* Rm
        C7 = 0.1025
        C8 = 21.93
* Rmf
        C9 = 0.0788
        C10 = 20.64
* Rmc
        C5 = 0.1662
        C6 = 21.85
PRINT Mud Properties entered
*-----------------------------------------------------------------
* Temperature Log
*
SET DEPTH INTERVAL 1500 1917
* SET BHT (C13) and Depth (C20), Surface Temp (C14) and Depth (C34)
        C13 = 90.7
        C20 = 1849
        C14 = 10
        C34 = 66.3
C47 = @KEY(TVDSS)
if (C47 > 0)
        C50 = @SETDEPTH (C20)
        C50 = @GETVALUE (TVDSS)
        BEGIN
                VT= C14 + (C13 - C14) * (VTVDSS - C34) / (C50 - C34)
        ENDBEGIN
        PRINT Temperature calculated in mTVDSS
else
        BEGIN
                VT= C14 + (C13 - C14) * (VDEPTH - C34) / (C20 - C34)
        ENDBEGIN
        PRINT Temperature calculated in mMD
endif
PRINT Temperature Log Created
*-----------------------------------------------------------------
* Set depth picks in constant tracks as too slow from mapping file
*
* Nullawarre
        C27 = 1515.55
* Belfast
        C28 = 1565.13
* Flaxman
        C29 = 1723.10
* WC I
        C30 = 1770.72
* IWCS
        C31 = 1788.13
* WC II
        C32 = 1790.96
* Waarre B
        C33 = 1793.08
* Waarre A
        C38 = 1821.58
* Eumeralla
        C21 = 1873.6
*
*****************************************************************
* INTERPRETATION LOOP
*****************************************************************
SET DEPTH INTERVAL 1500 1917
BEGIN
```

```
******************************
* Set Parameters by Reservoir*
******************************
* Matrix GR (C61), Density (C62), Sonic (C63), Neutron (C64)
            C61 = 40
            C62 = 2.637
            C63 = 55
            C64 = -0.05
*
* Shale GR (C65), Density (C66), Sonic (C67), Neutron (C68), CEC (C19)
* Shale compaction factor (C57), Cut-off (C41)
            C65 = 125
            C66 = 2.42
            C67 = 102
            C68 = 0.35
            C19 = 1.49
            C57 = 25
            C59 = 0.24
*
* Fluid GR (C69), Density (C70), Sonic (C71), Neutron (C72)
            C69 = 10
            C70 = 1.0
            C71 = 189
            C72 = 1.0
*
* Net sand and net pay cut-offs
* VSH (< C40), Porosity (> C41), Permeability (> C42), Sw (< C43)
            C40 = 0.40
            C41 = 0.01
            C42 = 0.20
            C43 = 0.60
*-------------------------------------------------------------------
* Grain Density (C62), Fluid density (C70) and Fluid neutron (C72)
* Nullawarre
            if (VDEPTH > C27 & VDEPTH < C28)
                        C62 = 2.655
                        C70 = 0.6
                        C72 = 0.6
            endif
* Belfast
            if (VDEPTH > C28 & VDEPTH < C29)
                        C62 = 2.670
            endif
* Flaxman
            if (VDEPTH > C29 & VDEPTH < C30)
                        C62 = 2.670
            endif
* Waarre C Sand I
            if (VDEPTH > C30 & VDEPTH < C31)
                        C62 = 2.658
                        C70 = 0.4
                        C72 = 0.4
            endif
* IWCS
            if (VDEPTH > C31 & VDEPTH < C32)
                        C62 = 2.644
            endif
* Waarre C Sand II
            if (VDEPTH > C32 & VDEPTH < C33)
                        C62 = 2.637
                        C70 = 0.366
                        C72 = 0.4
            endif
* Waarre B
            if (VDEPTH > C33 & VDEPTH < C38)
                        C62 = 2.670
            endif
```

```
* Waarre A
        if (VDEPTH > C38 & VDEPTH < C21)
                C62 = 2.655
                C70 = 0.5
                C72 = 0.5
        endif
* Eumeralla
        if (VDEPTH > C21 & VDEPTH < C2)
                C62 = 2.670
        endif
*-----------------------------------------------------
* Archie Parameters
* Set a (C16), m (C17), n (C18)
        C16= 1
        C17= 1.81
*
* 'n' in Nullawarre & Waarre A Formations
                C18 = 1.90
* 'n' in WC I
        if (VDEPTH > C30 & VDEPTH < C31)
                C18 = 1.84
        endif
* 'n' in WC II
        if (VDEPTH > C32 & VDEPTH < C33)
                C18 = 2.00
        endif
*-----------------------------------------------------
* Water Resistivity
* Set Rw (C11) and RWT (C12)
*
* Rw in Nullawarre, Belfast & Flaxman
        if (VDEPTH > C27 & VDEPTH < C30)
                C11 = 0.403
                C12 = 25
        endif
* Rw in Waarre C
        if (VDEPTH > C30 & VDEPTH < C33)
                C11 = 0.294
                C12 = 25
        endif
* 'n' in WC II
        if (VDEPTH > C33 & VDEPTH < C2)
                C11 = 0.517
                C12 = 25
        endif
*
        VRW_T = C11 * (C12 + 21.5) / (VT + 21.5)
        VRMF_T = C9 * (C10 + 21.5) / (VT + 21.5)
*******************************************************************************
*******************************************************************************
*
* Shale volume determination
*
        VVSH_GRL = (VMDC_SGRC-C61)/(C65 - C61)
        V1375 = (C62 - C70) * (C72 - VMDC_SLSP) - (VMDC_SBD2 - C70) * (C72 - C64)
        V1376 = (C62 - C70) * (C72 - C68) - (C66 - C70) * (C72 - C64)
        VVSHND=V1375 / V1376
*
                VVSH = VVSH_GRL
                if (VDEPTH > 1869)
                        if (VVSHND < VVSH_GRL)
                                VVSH = VVSHND
                        endif
                endif
*
        if (VVSH < 0)
                VVSH=0
```

```
            endif
            if (VVSH > 1)
                        VVSH=1
            endif
*-------------------------------------------------------------------
*
* Porosity
            VPHI_D = (C62 - VMDC_SBD2) / (C62 - C70)
            VPHI_DW = (C62 - VMDC_SBD2) / (C62 - 1.00)
*
            VNPSC = VSLSP_SS - VVSH * 0.28
            VPHI_ND = @SQT((VPHI_DW^2 + VNPSC^2) / 2)
*
            VDTSC = VMDC_BATC - VVSH * 25
            VPHI_S = (VDTSC - C63) / (C71 - C63)
*
            VPHIT = VPHI_ND
*
* Flaxman Formation
            if (VDEPTH > 1722 & VDEPTH < 1735)
                        VPHIT = VPHI_D
            endif
* Waarre B
            if (VDEPTH > C33 & VDEPTH < C38)
                        VPHIT = VPHI_D
            endif
*
* Waarre C Sand II
            if (VDEPTH > 1791.28 & VDEPTH < 1797.40)
                        VPHIT = VCOREPORO / 100
            endif
            VPHIE = VPHIT - VVSH * 0.17
*
* Lithology Determination ----------------------------------------------
*
            C71 = 189
            C70 = 1.00
            C72 = 1.00
*
            VM= ((C71 - VMDC_BATC) / (VMDC_SBD2 - C70))*0.01
            VN= (C72 - VMDC_SLSP) / (VMDC_SBD2 - C70)
*
            VRHOMAA = (VMDC_SBD2 - VPHIT * C70) / (1 - VPHIT)
            VDTMAA = (VMDC_BATC - VPHIT * C71) / (1 - VPHIT)
            VUMAA = (VMDC_SNP2*((VMDC_SBD2+0.1883)/1.0704)-VPHIT*C73)/(1-VPHIT)
*
*-------------------------------------------------------------------
* Permeability Transforms
* Nullawarre
            if (VDEPTH > C27 & VDEPTH < C28)
                        C55 = 546.88
                        C56 = 4.3556
                        VPOPE = C55*(VPHIT ^ C56)
            endif
* Belfast
            if (VDEPTH > C28 & VDEPTH < C29)
                        C55 = 5 * 10^-5
                        C56 = 0.6369
                        VPOPE = C55*@EXP((VPHIT*100) * C56)
            endif
* Flaxman
            if (VDEPTH > C29 & VDEPTH < C30)
                        C55 = 0.0023
                        C56 = 0.6206
                        VPOPE = C55*@EXP((VPHIT*100) * C56)
            endif
* Waarre C Sand I
```

```
        if (VDEPTH > C30 & VDEPTH < C31)
                C55 = 0.0004
                C56 = 4.8012
                VPOPE = C55*((VPHIT*100) ^ C56)
        endif
* IWCS
        if (VDEPTH > C31 & VDEPTH < C32)
                C55 = 0.0023
                C56 = 0.6206
                VPOPE = C55*@EXP((VPHIT*100) * C56)
        endif
* Waarre C Sand II
        if (VDEPTH > C32 & VDEPTH < C33)
                if (VDEPTH > 1791.28 & VDEPTH < 1797.40)
                        VPOPE = VCOREPERM
                else
                        C55 = 4.0
                        C56 = 0.247
                        VPOPE = C55*@EXP((VPHIT*100) * C56)
                endif
        endif
* Waarre B
        if (VDEPTH > C33 & VDEPTH < C38)
                C55 = 5 * 10^-5
                C56 = 0.6369
                VPOPE = C55*@EXP((VPHIT*100) * C56)
        endif
* Waarre A
        if (VDEPTH > C38 & VDEPTH < C21)
                C55 = 1.34 * 10^6
                C56 = 7.31
                VPOPE = C55*(VPHIT ^ C56)
        endif
* Eumeralla
        if (VDEPTH > C21 & VDEPTH < C2)
                C55 = 1.34 * 10^6
                C56 = 7.31
                VPOPE = C55*(VPHIT ^ C56)
        endif
*******************************************************************************
* WATER SATURATION
*******************************************************************************
*------------------------------------------------------------------------------
* Capillary Pressure Sw calculation
* Gas Gradient (C74), Water Gradient (C75), Oil Gradient (C60)
* J functions related to SW (C44, C45) and GWC (C35)
*
        if (VDEPTH > C30 & VDEPTH < C33)
* Waarre C Sand I
                if (VDEPTH > C30 & VDEPTH < C31)
                        C74 = 0.10
                        C75 = 0.42
                        C60 = 0.295
                        C44 = 74.766
                        C45 = -0.4092
                        C35 = 1769
                endif
* IWCS
                if (VDEPTH > C31 & VDEPTH < C32)
                        C74 = 0.10
                        C75 = 0.42
                        C60 = 0.295
                        C44 = 73.403
                        C45 = -0.1892
                        C35 = 1769
                endif
* Waarre C Sand II
```

```
                        if (VDEPTH > C32 & VDEPTH < C33)
                                C74 = 0.10
                                C75 = 0.42
                                C60 = 0.295
                                C44 = 54.434
                                C45 = -0.3313
                                C35 = 1769
                        endif
*
*
                        VHEIGHT = C35 - VTVDSS
*
                        VLEV_J = (((VHEIGHT * 3.28084 * (C75 - C74))*1.44)/50) * (VPOPE / VPHIT)^0.5
                        VSW_CP = (C44 * VLEV_J^C45) / 100
:END_CP
                endif
*
*-------------------------------------------------------------------------
* Archie Water saturation
                VSW_ARCH = ((C16/VPHIT^C17)*(VRW_T/VMDC_SEDP))^(1/C18)
*
*-------------------------------------------------------------------------
* Indonesia
*
* Shale Resistivity
*               Nullawarre & Belfast
                if (VDEPTH > 1500 & VDEPTH < C29)
                        C19 = 2.0
                endif
*               Flaxman and deeper
                if (VDEPTH > C29 & VDEPTH < C30)
                        C19 = 3.0
                endif
*
                C54 = (C16*VRW_T)/(VPHIE^C17)
                VSW_IND= ((VVSH^(0.5*(2-VVSH)))/(C19/VMDC_SEDP)^0.5+(VMDC_SEDP/C54))^(-2/C18)
                C54 = (C16*VRMF_T)/(VPHIE^C17)
                VSXO_IND=((VVSH^(0.5*(2-VVSH)))/(C19/VMDC_SEXP)^0.5+(VMDC_SEXP/C54))^(-2/C18)
                VSW_IND = ((VSW_IND * VPHIE) + (VPHIT-VPHIE)) / VPHIT
                VSXO_IND = ((VSXO_IND * VPHIE) + (VPHIT-VPHIE)) / VPHIT
*
*---------------------------------------------------------------
* Waxman Smits Water Saturation
* QV = CEC * RHOG * (1 - PORO) / (100 * PORO)
                VQV= 0.0083 * VPHIT ^ -1.7715
*
* B = (0.225 * T  - 1.28 + 0.0004059*T^2) / 1+Rw^1.23*(0.045T-0.27)
                VB=(0.225*VT-1.28+0.0004059*VT^2)/(1+VRW_T^1.23*(0.045*VT-0.27))
*
                VM_STAR = 1.88
                VA_STAR = 1.00
*
                VTERM1=((VA_STAR*VRW_T)/(VMDC_SEDP*VPHIT^VM_STAR))
*
                VSW_TP=VSW_ARCH
                VNWS_T1=1+VRW_T*VB*VQV
                C47=0
:LOOP
                C47=C47+1
                if (C47>20)
                        OUTPUT NUMBER 10 3 VDEPTH
                        OUTPUT TEXT Did not converge
                        PRINT OUTPUT
                        GOTO ENDLOOP
                endif
*
                VN_STAR = 2.2
```

```
            if (VDEPTH > C30 & VDEPTH < C31)
                        VN_STAR = 2.04
            endif
            if (VDEPTH >C32 & VDEPTH < V33)
                        VN_STAR = 2.19
            endif
            VSW_WS = ( VTERM1 * (1/(1+((VRW_T*VB*VQV)/VSW_TP))))^(1/VN_STAR)
            VTEST=@ABS(VSW_WS-VSW_TP)
*
            if (VTEST < 0.01)
                        GOTO ENDLOOP
            else
                        VSW_TP=VSW_WS
                        GOTO LOOP
            endif
:ENDLOOP
*
*-----------------------------------------------------------------
* Calculate SWT
*
            VSWT = VSW_IND
            if (VDEPTH > C30 & VDEPTH < C33)
                        VSWT = VSW_WS
            endif
*
*-----------------------------------------------------------------
* Calculate BVW
            VBVW= VSWT * VPHIT
            if (VBVW > VPHIT)
                        VBVW = VPHIT
            endif
*
*-----------------------------------------------------------------
* Net Sand / Net Pay Flags
            if (VVSH < C40 & VPOPE > C42)
                        VNETSAND = 1
            else
                        VNETSAND = 0
            endif
            if (VNETSAND = 1 & VSWT < C43)
                        VNETPAY = 1
            else
                        VNETPAY = 0
            endif
*******************************************************************************
ENDBEGIN
*******************************************************************************
PRINT STARS
OUTPUT TEXT Well Name:
OUTPUT WELLNAME
PRINT OUTPUT
PRINT SPACES
OUTPUT TEXT RESERVOIR    GROSS INTERVAL        NET SAND            NET PAY
PRINT OUTPUT
OUTPUT TEXT GROSS Top, Base, Thickness
PRINT OUTPUT
OUTPUT TEXT NETSAND Thickness, NTG, PHIT, PHIE, PERMEABILITY
PRINT OUTPUT
OUTPUT TEXT NETPAY Thickness, NTG, PHIT, PHIE, PERMEABILITY, Sw
PRINT OUTPUT
SET CURRENT ZONE INullawarre
C26 = 1
:AVERAGES
IF (C26 = 1)
            OUTPUT TEXT Nullawarre
ENDIF
IF (C26 = 2)
```

```
            OUTPUT TEXT Belfast
ENDIF
IF (C26 = 3)
            OUTPUT TEXT Flaxman
ENDIF
IF (C26 = 4)
            OUTPUT TEXT Waarre C Sand I
ENDIF
IF (C26 = 5)
            OUTPUT TEXT IWCS
ENDIF
IF (C26 = 6)
            OUTPUT TEXT Waarre C Sand II
ENDIF
IF (C26 = 7)
            OUTPUT TEXT Waarre B
ENDIF
IF (C26 = 8)
            OUTPUT TEXT Waarre A
ENDIF
IF (C26 = 9)
            OUTPUT TEXT Eumeralla
ENDIF
C37 = 0
C36 = 0
C54 = 0
C74 = 0
PRINT SPACES
BEGIN
            C36 = C36 + 1
            if (C36 = 1)
                        C75 = VDEPTH
            endif
            if (VNETSAND = 1)
                        C37 = C37 + 1
                        VVSH_NS = VVSH
                        VPHIT_NS = VPHIT
                        VPHIE_NS = VPHIE
                        VPOPE_NS = VPOPE
            endif
            if (VNETPAY = 1)
                        C54 = C54 + 1
                        VVSH_NP = VVSH
                        VPHIT_NP = VPHIT
                        VPHIE_NP = VPHIE
                        VPOPE_NP = VPOPE
                        VSW_NP = VSWT
            endif
            C47 = VDEPTH
ENDBEGIN
                        C48 = C47 - C75
                        C49 = C37 / C36
                        C50 = C49 * C48
                        C51 = C54 / C36
                        C52 = C51 * C48
                        C38 = @AMEAN(VSH_NS)
                        C39 = @AMEAN(PHIT_NS)
                        C40 = @AMEAN(PHIE_NS)
                        C41 = @GMEAN(POPE_NS)
                        C42 = @AMEAN(VSH_NP)
                        C43 = @AMEAN(PHIT_NP)
                        C44 = @AMEAN(PHIE_NP)
                        C45 = @GMEAN(POPE_NP)
                        C46 = @AMEAN(SW_NP)
*
* Gross Interval
OUTPUT NUMBER  7 1 C75
```

```
OUTPUT NUMBER  7 1 C47
OUTPUT NUMBER  6 1 C48
* Net Sand Parameters
OUTPUT NUMBER  6 1 C50
OUTPUT NUMBER  6 3 C49
OUTPUT NUMBER  6 3 C39
OUTPUT NUMBER  6 3 C40
OUTPUT NUMBER  8 2 C41
* Net Pay Parameters
OUTPUT NUMBER 6 1 C52
OUTPUT NUMBER 6 3 C51
OUTPUT NUMBER 6 3 C43
OUTPUT NUMBER 6 3 C44
OUTPUT NUMBER 8 2 C45
OUTPUT NUMBER 6 3 C46
PRINT OUTPUT
SET NEXT ZONE
        if (C26 = 9)
                PRINT STARS
                STOP
        else
                C26 = C26+1
        endif
GOTO AVERAGES
```

Appendix B : Terrastation TCL Routine For Halladale-1 DW2

```
**************************************************
* Mud properties RM (C7), RMF (C9), RMC (C5), MW (C25)
* Temperatures RM (C8), RMF (C10), RMC (C6)
* MW
        C25= 1.26 * 8.34
* Rm
        C7 = 0.078
        C8 = 20.6
* Rmf
        C9 = 0.075
        C10 = 19.9
* Rmc
        C5 = 0.091
        C6 = 21.0
PRINT Mud Properties entered
*-------------------------------------------------------------------
* Temperature Log
*
SET DEPTH INTERVAL 1500 1940
* SET BHT (C13) and Depth (C20), Surface Temp (C14) and Depth (C34)
        C13 = 90.7
        C20 = 1849
        C14 = 10
        C34 = 66.3
C47 = @KEY(TVDSS)
if (C47 > 0)
        C50 = @SETDEPTH (C20)
        C50 = @GETVALUE (TVDSS)
        BEGIN
                VT= C14 + (C13 - C14) * (VTVDSS - C34) / (C50 - C34)
        ENDBEGIN
        PRINT Temperature calculated in mTVDSS
else
        BEGIN
                VT= C14 + (C13 - C14) * (VDEPTH - C34) / (C20 - C34)
        ENDBEGIN
        PRINT Temperature calculated in mMD
endif
PRINT Temperature Log Created
*-------------------------------------------------------------------
* Set depth picks in constant tracks as too slow from mapping file
*
* Nullawarre
        C27 = 1538.48
* Belfast
        C28 = 1589.33
* Flaxman
        C29 = 1749.18
* WC I
        C30 = 1803.74
* IWCS
        C31 = 1820.22
* WC II
        C32 = 1821.91
* Waarre B
        C33 = 1827.17
* Waarre A
        C38 = 1855.07
* Eumeralla
        C21 = 1897.9
*
**********************************************************************
* INTERPRETATION LOOP
**********************************************************************
```

```
SET DEPTH INTERVAL 1500 1920
BEGIN
*******************************
* Set Parameters by Reservoir*
*******************************
* Matrix GR (C61), Density (C62), Sonic (C63), Neutron (C64)
            C61 = 40
            C63 = 55
            C64 = -0.05
*
* Shale GR (C65), Density (C66), Sonic (C67), Neutron (C68), CEC (C19)
* Shale compaction factor (C57), Cut-off (C41)
            C65 = 125
            C66 = 2.42
            C67 = 102
            C68 = 0.35
            C19 = 1.49
            C57 = 25
            C59 = 0.24
*
* Fluid GR (C69), Density (C70), Sonic (C71), Neutron (C72)
            C69 = 10
            C70 = 1.0
            C71 = 189
            C72 = 1.0
*
*-----------------------------------------------------------------
* Net Sand and Net Pay Cut-offs
* VSH (< C40), Porosity (> C41), Permeability (> C42), Sw (< C43)
            C40 = 0.40
            C41 = 0.01
            C42 = 0.20
            C43 = 0.50
*
*-----------------------------------------------------
* Archie Parameters
* Set a (C16), m (C17), n (C18)
            C16= 1
            C17= 1.81
*
* 'n' in Nullawarre & Waarre A Formations
                        C18 = 1.90
* 'n' in WC I
            if (VDEPTH > C30 & VDEPTH < C31)
                        C18 = 1.84
            endif
* 'n' in WC II
            if (VDEPTH > C32 & VDEPTH < C33)
                        C18 = 2.00
            endif
*-----------------------------------------------------
* Water Resistivity
* Set Rw (C11) and RWT (C12)
*
* Rw in Nullawarre, Belfast & Flaxman
            if (VDEPTH > C27 & VDEPTH < C30)
                        C11 = 0.403
                        C12 = 25
            endif
* Rw in Waarre C
            if (VDEPTH > C30 & VDEPTH < C33)
                        C11 = 0.294
                        C12 = 25
            endif
* 'n' in WC II
            if (VDEPTH > C33 & VDEPTH < C2)
                        C11 = 0.517
```

```
                C12 = 25
        endif
*
        VRW_T = C11 * (C12 + 21.5) / (VT + 21.5)
        VRMF_T = C9 * (C10 + 21.5) / (VT + 21.5)
*-------------------------------------------------------------------
* Grain Density (C62), 'n' (C18), Rw (C11)
*
* Nullawarre
        if (VDEPTH > C27 & VDEPTH < C28)
                C62 = 2.655
        endif
* Belfast
        if (VDEPTH > C28 & VDEPTH < C29)
                C62 = 2.670
        endif
* Flaxman
        if (VDEPTH > C29 & VDEPTH < C30)
                C62 = 2.670
        endif
* Waarre C Sand I
        if (VDEPTH > C30 & VDEPTH < C31)
                C62 = 2.658
        endif
* IWCS
        if (VDEPTH > C31 & VDEPTH < C32)
                C62 = 2.644
                C11 = 0.294
        endif
* Waarre C Sand II
        if (VDEPTH > C32 & VDEPTH < C33)
                C62 = 2.652
        endif
* Waarre B
        if (VDEPTH > C33 & VDEPTH < C38)
                C62 = 2.670
        endif
* Waarre A
        if (VDEPTH > C38 & VDEPTH < C21)
                C62 = 2.655
        endif
* Eumeralla
        if (VDEPTH > C21 & VDEPTH < C2)
                C62 = 2.670
        endif
*******************************************************************************
*
* Shale volume determination
*
*       Waarre C Unit Ia
        if (VDEPTH >= 1803 & VDEPTH < 1807.7)
                C62 = 2.659
                C70 = 0.7
                C72 = 0.27
        endif
*       Waarre C Unit Iaa
        if (VDEPTH >= 1807.7 & VDEPTH < 1809)
                C62 = 2.684
                C70 = 0.632
                C72 = 0.6
        endif
*       Waarre C Unit Ib
        if (VDEPTH >= 1809 & VDEPTH < 1810.4)
                C62 = 2.659
                C70 = 0.301
                C72 = 0.8
        endif
```

```
*       Waarre C Unit Ic i
        if (VDEPTH >= 1810.5 & VDEPTH < 1820.4)
                C62 = 2.659
                C70 = 0.301
                C72 = 0.4
        endif
*       Waarre C Unit Ic ii
        if (VDEPTH >= 1810.5 & VDEPTH < 1820.4)
                C62 = 2.659
                C70 = 0.301
                C72 = 0.4
        endif
*       Waarre C Unit Ic iii
        if (VDEPTH >= 1810.5 & VDEPTH < 1820.4)
                C62 = 2.659
                C70 = 0.301
                C72 = 0.4
        endif
*       Waarre C Unit Ic iv
        if (VDEPTH >= 1810.5 & VDEPTH < 1820.4)
                C62 = 2.659
                C70 = 0.301
                C72 = 0.4
        endif
*       Waarre C IWCS
        if (VDEPTH >= 1820.4 & VDEPTH < 1821.9)
                C62 = 2.679
                C70 = 0.056
                C72 = 1.0
        endif
*       Waarre C Unit II Upper
        if (VDEPTH >= 1821.9 & VDEPTH < 1823.2)
                C62 = 2.656
                C70 = 0.219
                C72 = 0.25
        endif
*       Waarre C Unit II Lower A
        if (VDEPTH >= 1823.2 & VDEPTH < 1827.0)
                C62 = 2.648
                C70 = 0.182
                C72 = 0.25
        endif
*       Waarre B PT2
        if (VDEPTH >= 1827.0 & VDEPTH < 1855.0)
                        C62 = 2.730
                        C72 = 1.00
                if (VMDC_SBD2 < 2.55)
                        C70 = -0.367
                else
                        C70 = 0.739
                endif
        endif
*
*
        VVSH_GRL = (VMDC_SGRC-C61)/(C65 - C61)
        V1375 = (C62 - C70) * (C72 - VMDC_SLSP) - (VMDC_SBD2 - C70) * (C72 - C64)
        V1376 = (C62 - C70) * (C72 - C68) - (C66 - C70) * (C72 - C64)
        VVSHND=V1375 / V1376
*
        if (VVSH_GRL <= VVSHND)
                VVSH = VVSH_GRL
        else
                VVSH = VVSHND
        endif
*
:ENDVSHCALC
        if (VVSH < 0)
```

```
                VVSH=0
        endif
        if (VVSH > 1)
                VVSH=1
        endif
*-------------------------------------------------------------------
*
* Porosity
*
        VPHI_D = (C62 - VMDC_SBD2) / (C62 - C70)
        VPHI_DW = (C62 - VMDC_SBD2) / (C62 - 1.00)
        VNPSC = VSLSP_SS - VVSH * 0.25
        VPHI_ND = @SQT((VPHI_DW^2 + VNPSC^2) / 2)
        VDTSC = VMDC_BATC - VVSH * 15
        VPHI_S = (VDTSC - C63) / (C71 - C63)
*
        VPHIT = VPHI_ND
*
        if (VDEPTH > 1749 & VDEPTH < 1766)
                VPHIT = VPHI_D
        endif
*
        if (VDEPTH > 1807.7 & VDEPTH < 1809.3)
                VPHIT = VCOREPORO / 100
                GOTO ENDPHI
        endif
        if (VDEPTH > 1810.5 & VDEPTH < 1832.0)
                VPHIT = VCOREPORO / 100
        endif
* Waarre B
        if (VDEPTH > 1831.9 & VDEPTH < C38)
                VPHIT = VPHI_D
        endif
:ENDPHI
        VPHIE = VPHIT - VVSH * 0.12
*
* Lithology Determination ----------------------------------------------
*
        C71 = 189
        C70 = 1.00
        C72 = 1.00
*
        VM= ((C71 - VMDC_BATC) / (VMDC_SBD2 - C70))*0.01
        VN= (C72 - VMDC_SLSP) / (VMDC_SBD2 - C70)
*
        VRHOMAA = (VMDC_SBD2 - VPHIT * C70) / (1 - VPHIT)
        VDTMAA = (VMDC_BATC - VPHIT * C71) / (1 - VPHIT)
        VUMAA = (VMDC_SNP2*((VMDC_SBD2+0.1883)/1.0704)-VPHIT*C73)/(1-VPHIT)
*
*-------------------------------------------------------------------
* Permeability Transforms
* Above Nullawarre
        if (VDEPTH > 1500 & VDEPTH < C27)
                        C55 = 5 * 10^-5
                        C56 = 0.6369
                        VPOPE = C55*@EXP((VPHIT*100) * C56)
        endif
* Nullawarre
        if (VDEPTH > C27 & VDEPTH < C28)
                C55 = 546.88
                C56 = 4.3556
                VPOPE = C55*(VPHIT ^ C56)
        endif
* Belfast
        if (VDEPTH > C28 & VDEPTH < C29)
                C55 = 5 * 10^-5
                C56 = 0.6369
```

```
                VPOPE = C55*@EXP((VPHIT*100) * C56)
        endif
* Flaxman
        if (VDEPTH > C29 & VDEPTH < C30)
                C55 = 0.0023
                C56 = 0.6206
                VPOPE = C55*@EXP((VPHIT*100) * C56)
        endif
* Waarre C Sand I
        if (VDEPTH > C30 & VDEPTH < C31)
                C55 = 0.0004
                C56 = 4.8012
                VPOPE = C55*((VPHIT*100) ^ C56)
*
                if (VDEPTH > 1807.7 & VDEPTH < 1809.3)
                        VPOPE = VCOREPERM
                endif
                if (VDEPTH > 1810.5 & VDEPTH < 1817.2)
                        VPOPE = VCOREPERM
                endif
                if (VDEPTH > 1818.1)
                        VPOPE = VCOREPERM
                endif
        endif
* IWCS
        if (VDEPTH > C31 & VDEPTH < C32)
                C55 = 0.0023
                C56 = 0.6206
                VPOPE = C55*@EXP((VPHIT*100) * C56)
        endif
* Waarre C Sand II
        if (VDEPTH > C32 & VDEPTH < C33)
                VPOPE = VCOREPERM
        endif
* Waarre B
        if (VDEPTH > C33 & VDEPTH < C38)
                C55 = 5 * 10^-5
                C56 = 0.6369
                VPOPE = C55*@EXP((VPHIT*100) * C56)
        endif
* Waarre A
        if (VDEPTH > C38 & VDEPTH < C21)
                C55 = 1.34 * 10^6
                C56 = 7.31
                VPOPE = C55*(VPHIT ^ C56)
        endif
* Eumeralla
        if (VDEPTH > C21 & VDEPTH < C2)
                C55 = 1.34 * 10^6
                C56 = 7.31
                VPOPE = C55*(VPHIT ^ C56)
        endif
*
*************************************************************************
* WATER SATURATION
*************************************************************************
*------------------------------------------------------------------------
* Capillary Pressure Sw calculation
* Gas Gradient (C74), Water Gradient (C75), Oil Gradient (C60)
* J functions related to SW (C44, C45) and GWC (C35)
*
* Waarre C Sand I
        if (VDEPTH > C30 & VDEPTH < C31)
        C74 = 0.10
        C75 = 0.45
        C60 = 0.295
        C44 = 74.766
```

```
            C45 = -0.4092
            C35 = 1760.5
            endif
* IWCS
            if (VDEPTH > C31 & VDEPTH < C32)
            C74 = 0.10
            C75 = 0.45
            C60 = 0.295
            C44 = 73.403
            C45 = -0.1892
            C35 = 1760.5
            endif
* Waarre C Sand II
            if (VDEPTH > C32 & VDEPTH < C33)
            C74 = 0.10
            C75 = 0.45
            C60 = 0.295
            C44 = 51.738
            C45 = -0.3635
            C35 = 1760.5
            endif
*
*
            VHEIGHT = C35 - VTVDSS
            if (VHEIGHT < 0)
                        VSW_CP = 1
                        GOTO END_CP
            endif
            VLEV_J = (((VHEIGHT * 3.28084 * (C75 - C74))*1.44)/50) * (VPOPE / VPHIT)^0.5
            VSW_CP = (C44 * VLEV_J^C45) / 100
:END_CP
*
*-------------------------------------------------------------------
* Archie Water saturation
            VSW_ARCH = ((C16/VPHIT^C17)*(VRW_T/VMDC_SEDP))^(1/C18)
*
*-------------------------------------------------------------------
* Indonesia
*
* Shale Resistivity
*           Nullawarre & Belfast
            if (VDEPTH > 1500 & VDEPTH < C29)
                        C19 = 2.0
            endif
*           Flaxman and deeper
            if (VDEPTH > C29 & VDEPTH < C30)
                        C19 = 3.0
            endif
*
            C54 = (C16*VRW_T)/(VPHIE^C17)
            VSW_IND= ((VVSH^(0.5*(2-VVSH)))/(C19/VMDC_SEDP)^0.5+(VMDC_SEDP/C54))^(-2/C18)
            C54 = (C16*VRMF_T)/(VPHIE^C17)
            VSXO_IND=((VVSH^(0.5*(2-VVSH)))/(C19/VMDC_SEXP)^0.5+(VMDC_SEXP/C54))^(-2/C18)
            VSW_IND = ((VSW_IND * VPHIE) + (VPHIT-VPHIE)) / VPHIT
            VSXO_IND = ((VSXO_IND * VPHIE) + (VPHIT-VPHIE)) / VPHIT
*
*-------------------------------------------------------------
* Waxman Smits Water Saturation
* QV = CEC * RHOG * (1 - PORO) / (100 * PORO)
            VQV= 0.0083 * VPHIT ^ -1.7715
*
* B = (0.225 * T  - 1.28 + 0.0004059*T^2) / 1+Rw^1.23*(0.045T-0.27)
            VB=(0.225*VT-1.28+0.0004059*VT^2)/(1+VRW_T^1.23*(0.045*VT-0.27))
*
            VM_STAR = 1.88
            VA_STAR = 1.00
*
```

```
            VTERM1=((VA_STAR*VRW_T)/(VMDC_SEDP*VPHIT^VM_STAR))
*
            VSW_TP=VSW_ARCH
            VNWS_T1=1+VRW_T*VB*VQV
            C47=0
:LOOP
            C47=C47+1
            if (C47>20)
                        OUTPUT NUMBER 10 3 VDEPTH
                        OUTPUT TEXT Did not converge
                        PRINT OUTPUT
                        GOTO ENDLOOP
            endif
*
            VN_STAR = 2.2
            if (VDEPTH > C30 & VDEPTH < C31)
                        VN_STAR = 2.04
            endif
            if (VDEPTH >C32 & VDEPTH < V33)
                        VN_STAR = 2.19
            endif
            VSW_WS = ( VTERM1 * (1/(1+((VRW_T*VB*VQV)/VSW_TP))))^(1/VN_STAR)
            VTEST=@ABS(VSW_WS-VSW_TP)
*
            if (VTEST < 0.01)
                        GOTO ENDLOOP
            else
                        VSW_TP=VSW_WS
                        GOTO LOOP
            endif
:ENDLOOP
*
*-------------------------------------------------------------
* Calculate SWT
*
            VSWT = VSW_IND
            if (VDEPTH > C30 & VDEPTH < C33)
                        VSWT = VSW_WS
            endif
*
*-------------------------------------------------------------
* Calculate BVW
            VBVW= VSWT * VPHIT
            if (VBVW > VPHIT)
                        VBVW = VPHIT
            endif
*
*-------------------------------------------------------------
* Net Sand / Net Pay Flags
            if (VVSH < C40 & VPOPE > C42)
                        VNETSAND = 1
            else
                        VNETSAND = 0
            endif
            if (VNETSAND = 1 & VSWT < C43)
                        VNETPAY = 1
            else
                        VNETPAY = 0
            endif
*
            if (VDEPTH > 1920)
                        VNETSAND = 0
                        VNETPAY = 0
            endif
*******************************************************************************
ENDBEGIN
*******************************************************************************
```

```
PRINT STARS
OUTPUT TEXT Well Name:
OUTPUT WELLNAME
PRINT OUTPUT
PRINT SPACES
OUTPUT TEXT RESERVOIR    GROSS INTERVAL        NET SAND            NET PAY
PRINT OUTPUT
OUTPUT TEXT GROSS Top, Base, Thickness
PRINT OUTPUT
OUTPUT TEXT NETSAND Thickness, NTG, PHIT, PHIE, PERMEABILITY
PRINT OUTPUT
OUTPUT TEXT NETPAY Thickness, NTG, PHIT, PHIE, PERMEABILITY, Sw
PRINT OUTPUT
SET CURRENT ZONE INullawarre
C26 = 1
:AVERAGES
IF (C26 = 1)
        OUTPUT TEXT Nullawarre
ENDIF
IF (C26 = 2)
        OUTPUT TEXT Belfast
ENDIF
IF (C26 = 3)
        OUTPUT TEXT Flaxman
ENDIF
IF (C26 = 4)
        OUTPUT TEXT Waarre C Sand I
ENDIF
IF (C26 = 5)
        OUTPUT TEXT IWCS
ENDIF
IF (C26 = 6)
        OUTPUT TEXT Waarre C Sand II
ENDIF
IF (C26 = 7)
        OUTPUT TEXT Waarre B
ENDIF
IF (C26 = 8)
        OUTPUT TEXT Waarre A
ENDIF
IF (C26 = 9)
        OUTPUT TEXT Eumeralla
ENDIF
C37 = 0
C36 = 0
C54 = 0
C74 = 0
PRINT SPACES
BEGIN
        C36 = C36 + 1
        if (C36 = 1)
                C75 = VDEPTH
        endif
        if (VNETSAND = 1)
                C37 = C37 + 1
                VVSH_NS = VVSH
                VPHIT_NS = VPHIT
                VPHIE_NS = VPHIE
                VPOPE_NS = VPOPE
        endif
        if (VNETPAY = 1)
                C54 = C54 + 1
                VVSH_NP = VVSH
                VPHIT_NP = VPHIT
                VPHIE_NP = VPHIE
                VPOPE_NP = VPOPE
                VSW_NP = VSWT
```

```
            endif
            C47 = VDEPTH
ENDBEGIN
                        C48 = C47 - C75
                        C49 = C37 / C36
                        C50 = C49 * C48
                        C51 = C54 / C36
                        C52 = C51 * C48
                        C38 = @AMEAN(VSH_NS)
                        C39 = @AMEAN(PHIT_NS)
                        C40 = @AMEAN(PHIE_NS)
                        C41 = @GMEAN(POPE_NS)
                        C42 = @AMEAN(VSH_NP)
                        C43 = @AMEAN(PHIT_NP)
                        C44 = @AMEAN(PHIE_NP)
                        C45 = @GMEAN(POPE_NP)
                        C46 = @AMEAN(SW_NP)
*
* Gross Interval
OUTPUT NUMBER  7 1 C75
OUTPUT NUMBER  7 1 C47
OUTPUT NUMBER  6 1 C48
* Net Sand Parameters
OUTPUT NUMBER  6 1 C50
OUTPUT NUMBER  6 3 C49
OUTPUT NUMBER  6 3 C39
OUTPUT NUMBER  6 3 C40
OUTPUT NUMBER  8 2 C41
* Net Pay Parameters
OUTPUT NUMBER 6 1 C52
OUTPUT NUMBER 6 3 C51
OUTPUT NUMBER 6 3 C43
OUTPUT NUMBER 6 3 C44
OUTPUT NUMBER 8 2 C45
OUTPUT NUMBER 6 3 C46
PRINT OUTPUT
SET NEXT ZONE
            if (C26 = 9)
                        PRINT STARS
                        STOP
            else
                        C26 = C26+1
            endif
GOTO AVERAGES
```

Appendix C : Terrastation TCL Routine For Halladale-1 DW3

```
**********************************************
* Mud properties RM (C7), RMF (C9), RMC (C5), MW (C25)
* Temperatures RM (C8), RMF (C10), RMC (C6)
* MW
        C25= 1.26 * 8.34
* Rm
        C7 = 0.078
        C8 = 20.6
* Rmf
        C9 = 0.075
        C10 = 19.9
* Rmc
        C5 = 0.091
        C6 = 21.0
PRINT Mud Properties entered
*-------------------------------------------------------------------
* Temperature Log
*
SET DEPTH INTERVAL 1450 1960
* SET BHT (C13) and Depth (C20), Surface Temp (C14) and Depth (C34)
        C13 = 90.7
        C20 = 1849
        C14 = 10
        C34 = 66.3
C47 = @KEY(TVDSS)
if (C47 > 0)
        C50 = @SETDEPTH (C20)
        C50 = @GETVALUE (TVDSS)
        BEGIN
                VT= C14 + (C13 - C14) * (VTVDSS - C34) / (C50 - C34)
        ENDBEGIN
        PRINT Temperature calculated in mTVDSS
else
        BEGIN
                VT= C14 + (C13 - C14) * (VDEPTH - C34) / (C20 - C34)
        ENDBEGIN
        PRINT Temperature calculated in mMD
endif
PRINT Temperature Log Created
**********************************************************************
* INTERPRETATION LOOP ***********************************************
**********************************************************************
* Set depth picks in constant tracks as too slow from mapping file
*
* Nullawarre
        C27 = 1497.62
* Belfast
        C28 = 1547.77
* Flaxman
        C29 = 1798.11
* WC I
        C30 = 1869.74
* IWCS
        C31 = 1886.16
* WC II
        C32 = 1890.26
* Waarre B
        C33 = 1906.54
* Waarre A
        C38 = 1935.70
* Eumeralla
        C21 = 1969.0
*
* Set Parameters by Reservoir*
*****************************
```

```
* Matrix GR (C61), Density (C62), Sonic (C63), Neutron (C64)
        C61 = 40
        C63 = 55
        C64 = -0.05
*
* Shale GR (C65), Density (C66), Sonic (C67), Neutron (C68), Res (C19)
* Shale compaction factor (C57), Cut-off (C41)
        C65 = 125
        C66 = 2.42
        C67 = 102
        C68 = 0.35
        C19 = 1.6
        C57 = 25
        C59 = 0.24
*
* Fluid GR (C69), Density (C70), Sonic (C71), Neutron (C72)
        C69 = 10
        C70 = 1.0
        C71 = 189
        C72 = 1.0
*-------------------------------------------------------------------
* Net sand and net pay cut-offs
* VSH (< C40), Porosity (> C41), Permeability (> C42), Sw (< C43)
        C40 = 0.40
        C41 = 0.01
        C42 = 0.20
        C43 = 0.60
*-------------------------------------------------------------------
BEGIN
* Grain Density
* Nullawarre
        if (VDEPTH > C27 & VDEPTH < C28)
                C62 = 2.655
        endif
* Belfast
        if (VDEPTH > C28 & VDEPTH < C29)
                C62 = 2.670
        endif
* Flaxman
        if (VDEPTH > C29 & VDEPTH < C30)
                C62 = 2.670
        endif
* Waarre C Sand I
        if (VDEPTH > C30 & VDEPTH < C31)
                C62 = 2.658
        endif
* IWCS
        if (VDEPTH > C31 & VDEPTH < C32)
                C62 = 2.644
        endif
* Waarre C Sand II
        if (VDEPTH > C32 & VDEPTH < C33)
                C62 = 2.652
        endif
* Waarre B
        if (VDEPTH > C33 & VDEPTH < C38)
                C62 = 2.670
        endif
* Waarre A
        if (VDEPTH > C38 & VDEPTH < C21)
                C62 = 2.655
        endif
* Eumeralla
        if (VDEPTH > C21 & VDEPTH < C2)
                C62 = 2.670
        endif
*-------------------------------------------------
```

```
* Archie Parameters
* Set a (C16), m (C17), n (C18)
        C16= 1
        C17= 1.81
*
* 'n' in Nullawarre & Waarre A Formations
                C18 = 1.90
* 'n' in WC I
        if (VDEPTH > C30 & VDEPTH < C31)
                C18 = 1.84
        endif
* 'n' in WC II
        if (VDEPTH > C32 & VDEPTH < C33)
                C18 = 2.00
        endif
*-------------------------------------------------
* Water Resistivity
* Set Rw (C11) and RWT (C12)
*
* Rw in Nullawarre, Belfast & Flaxman
        if (VDEPTH > C27 & VDEPTH < C30)
                C11 = 0.403
                C12 = 25
        endif
* Rw in Waarre C
        if (VDEPTH > C30 & VDEPTH < C33)
                C11 = 0.294
                C12 = 25
        endif
* 'n' in WC II
        if (VDEPTH > C33 & VDEPTH < C2)
                C11 = 0.517
                C12 = 25
        endif
*
        VRW_T = C11 * (C12 + 21.5) / (VT + 21.5)
        VRMF_T = C9 * (C10 + 21.5) / (VT + 21.5)
*
*******************************************************************************
*******************************************************************************
*
* Shale volume determination
*
        VVSH_GRL = (VMDC_SGRC-C61)/(C65 - C61)
        V1375 = (C62 - C70)*(C72 - VMDC_SLSP)-(VMDC_SBD2 - C70)*(C72 - C64)
        V1376 = (C62 - C70)*(C72 - C68)-(C66 - C70)*(C72 - C64)
        VVSHND=V1375 / V1376
*
        if (VVSH_GRL < VVSHND)
                VVSH = VVSH_GRL
        else
                VVSH = VVSHND
        endif
        if (VDEPTH > 1943)
                VVSH = VVSH_GRL
        endif
*
        if (VVSH < 0)
                VVSH=0
        endif
        if (VVSH > 1)
                VVSH=1
        endif
*-------------------------------------------------------------------------
*
* Porosity
        VPHI_D = (C62 - VMDC_SBD2) / (C62 - C70)
```

```
            VPHI_DW = (C62 - VMDC_SBD2) / (C62 - 1.00)
*
            VNPSC = VSLSP_SS - VVSH * 0.25
            VPHI_ND = (VPHI_DW + VNPSC) / 2
*
            VDTSC = VMDC_BATC - VVSH * 15
            VPHI_S = (VDTSC - C63) / (C71 - C63)
*
            VPHI_R = ((C16 * VRW_T) / (VMDC_SEDP)) ^ (1 / C17)
*
            VPHIT = VPHI_ND
*
* Waarre B
            if (VDEPTH > C33 & VDEPTH < C38)
                        VPHIT = VPHI_D
            endif
*
            if (VDEPTH > 1943)
                        VPHIT = VPHI_R
            endif
*
            VPHIE = VPHIT - VVSH * 0.17
*
* Lithology Determination ----------------------------------------------
*
            C71 = 189
            C70 = 1.00
            C72 = 1.00
*
            VM= ((C71 - VMDC_BATC) / (VMDC_SBD2 - C70))*0.01
            VN= (C72 - VMDC_SLSP) / (VMDC_SBD2 - C70)
*
            VRHOMAA = (VMDC_SBD2 - VPHIT * C70) / (1 - VPHIT)
            VDTMAA = (VMDC_BATC - VPHIT * C71) / (1 - VPHIT)
            VUMAA = (VMDC_SNP2*((VMDC_SBD2+0.1883)/1.0704)-VPHIT*C73)/(1-VPHIT)
*
*-------------------------------------------------------------------------
* Permeability Transforms
* Nullawarre
            if (VDEPTH > C27 & VDEPTH < C28)
                        C55 = 546.88
                        C56 = 4.3556
                        VPOPE = C55*(VPHIT ^ C56)
            endif
* Belfast
            if (VDEPTH > C28 & VDEPTH < C29)
                        C55 = 5 * 10^-5
                        C56 = 0.6369
                        VPOPE = C55*@EXP((VPHIT*100) * C56)
            endif
* Flaxman
            if (VDEPTH > C29 & VDEPTH < C30)
                        C55 = 0.0023
                        C56 = 0.6206
                        VPOPE = C55*@EXP((VPHIT*100) * C56)
            endif
* Waarre C Sand I
            if (VDEPTH > C30 & VDEPTH < C31)
                        C55 = 0.0004
                        C56 = 4.8012
                        VPOPE = C55*((VPHIT*100) ^ C56)
            endif
* IWCS
            if (VDEPTH > C31 & VDEPTH < C32)
                        C55 = 0.0023
                        C56 = 0.6206
                        VPOPE = C55*@EXP((VPHIT*100) * C56)
```

```
            endif
* Waarre C Sand II
            if (VDEPTH > C32 & VDEPTH < C33)
                        C55 = 4.0
                        C56 = 0.247
                        VPOPE = C55*@EXP((VPHIT*100) * C56)
            endif
* Waarre B
            if (VDEPTH > C33 & VDEPTH < C38)
                        C55 = 5 * 10^-5
                        C56 = 0.6369
                        VPOPE = C55*@EXP((VPHIT*100) * C56)
            endif
* Waarre A
            if (VDEPTH > C38 & VDEPTH < C21)
                        C55 = 1.34 * 10^6
                        C56 = 7.31
                        VPOPE = C55*(VPHIT ^ C56)
            endif
* Eumeralla
            if (VDEPTH > C21 & VDEPTH < C2)
                        C55 = 1.34 * 10^6
                        C56 = 7.31
                        VPOPE = C55*(VPHIT ^ C56)
            endif
*-------------------------------------------------------------------
*
* Archie Water saturation
            VSW_ARCH = ((C16/VPHIT^C17)*(VRW_T/VMDC_SEDP))^(1/C18)
*
*
* Calculate BVW
            VBVW=VSW_ARCH*VPHIT
            if (VBVW > VPHIE)
                        VBVW = VPHIE
            endif
*
* Net Sand / Net Pay Flags
            if (VVSH < C40 & VPOPE > C42)
                        VNETSAND = 1
            else
                        VNETSAND = 0
            endif
            if (VNETSAND = 1 & VSW_ARCH < C43)
                        VNETPAY = 1
            else
                        VNETPAY = 0
            endif
ENDBEGIN
*
*-------------------------------------------------------------------
PRINT STARS
OUTPUT TEXT Well Name:
OUTPUT WELLNAME
PRINT OUTPUT
PRINT SPACES
OUTPUT TEXT RESERVOIR    GROSS INTERVAL        NET SAND            NET PAY
PRINT OUTPUT
OUTPUT TEXT GROSS Top, Base, Thickness
PRINT OUTPUT
OUTPUT TEXT NETSAND Thickness, NTG, PHIT, PHIE, PERMEABILITY
PRINT OUTPUT
OUTPUT TEXT NETPAY Thickness, NTG, PHIT, PHIE, PERMEABILITY, Sw
PRINT OUTPUT
SET CURRENT ZONE INullawarre
C26 = 1
:AVERAGES
```

```
IF (C26 = 1)
        OUTPUT TEXT Nullawarre
ENDIF
IF (C26 = 2)
        OUTPUT TEXT Belfast
ENDIF
IF (C26 = 3)
        OUTPUT TEXT Flaxman
ENDIF
IF (C26 = 4)
        OUTPUT TEXT Waarre C Sand I
ENDIF
IF (C26 = 5)
        OUTPUT TEXT IWCS
ENDIF
IF (C26 = 6)
        OUTPUT TEXT Waarre C Sand II
ENDIF
IF (C26 = 7)
        OUTPUT TEXT Waarre B
ENDIF
IF (C26 = 8)
        OUTPUT TEXT Waarre A
ENDIF
IF (C26 = 9)
        OUTPUT TEXT Eumeralla
ENDIF
*
C37 = 0
C36 = 0
C54 = 0
C74 = 0
PRINT SPACES
BEGIN
        C36 = C36 + 1
        if (C36 = 1)
                C75 = VDEPTH
        endif
        if (VNETSAND = 1)
                C37 = C37 + 1
                VVSH_NS = VVSH
                VPHIT_NS = VPHIT
                VPHIE_NS = VPHIE
                VPOPE_NS = VPOPE
        endif
        if (VNETPAY = 1)
                C54 = C54 + 1
                VVSH_NP = VVSH
                VPHIT_NP = VPHIT
                VPHIE_NP = VPHIE
                VPOPE_NP = VPOPE
                VSW_NP = VSW_ARCH
        endif
        C47 = VDEPTH
ENDBEGIN
                C48 = C47 - C75
                C49 = C37 / C36
                C50 = C49 * C48
                C51 = C54 / C36
                C52 = C51 * C48
                C38 = @AMEAN(VSH_NS)
                C39 = @AMEAN(PHIT_NS)
                C40 = @AMEAN(PHIE_NS)
                C41 = @GMEAN(POPE_NS)
                C42 = @AMEAN(VSH_NP)
                C43 = @AMEAN(PHIT_NP)
                C44 = @AMEAN(PHIE_NP)
```

```
                    C45 = @GMEAN(POPE_NP)
                    C46 = @AMEAN(SW_NP)
*
* Gross Interval
OUTPUT NUMBER  7 1 C75
OUTPUT NUMBER  7 1 C47
OUTPUT NUMBER  6 1 C48
* Net Sand Parameters
OUTPUT NUMBER  6 1 C50
OUTPUT NUMBER  6 3 C49
OUTPUT NUMBER  6 3 C39
OUTPUT NUMBER  6 3 C40
OUTPUT NUMBER  8 2 C41
* Net Pay Parameters
OUTPUT NUMBER 6 1 C52
OUTPUT NUMBER 6 3 C51
OUTPUT NUMBER 6 3 C43
OUTPUT NUMBER 6 3 C44
OUTPUT NUMBER 8 2 C45
OUTPUT NUMBER 6 3 C46
PRINT OUTPUT
SET NEXT ZONE
        if (C26 = 9)
                    PRINT STARS
                    STOP
        else
                    C26 = C26+1
        endif
GOTO AVERAGES
```

[i] Sperry Sun LWD Tool Nomenclature

GR = Gamma Ray,

ACAL = Acoustic caliper,

SCO2 = Density standoff correction,

SBD2 = Density,

SLSP = limestone neutron porosity,

SNP2 = PEF

BATC = acoustic sonic tool

SEXP = micro-resistivity

SESP = shallow resistivity

SEMP = Medium resistivity

SEDP = Deep resistivity

[ii] Baker Hughes Wireline Tool Nomenclature

ORIT = Orientation tool

STAR =

XMAC = Cross Multi-pole Array Acoustilog

DSL =

RCI = Reservoir Characterisation Instrument (similar to the Schlumberger MDT)

PCL = Pipe conveyed logging

Halladale-1 DW-1 (Black Watch)

Permit: Exploration	**RTE:** 21.5 m	**TD (logs):** 1917.3 m
Latitude : 38° 34’ 45.54’ S	**Bit Size:** 216.0 mm	**BHT:** 90.7 degC
Longtitude : 142° 43’ 50.95’ E	**Rm:** 0.102 ohmm at: 21.9 degC	**Vertical Scale** 1:500 m
Easting :	**Rmf:** 0.079 ohmm at: 20.6 degC	**Interpreter :** Andy Hall
Northing :	**Rmc:** 0.166 ohmm at: 21.9 degC	
Datum :	**Plot created on:** 24/Oct/05 at: 15:48: 3	

MDC_SGRC 0 (API) 150 | MDC_ACAL 150 (in) 500 | MDC_SROP 0 (m/hr) 180 | Depth (m) (1:500) | TVDSS (m) (1:500)

MDC_SCO2 -1.5 (g/cc) 0.5 | MDC_SBD2 1.95 (g/cc) 2.95 | MDC_SLSP 0.45 (frac) -0.15 | WIR_DT 560 (us/m) 150 | MDC_SNP2 0 (brne) 10 | MDC_BATC 140 (us/f) 40

MDC_SEXP 20 (%) 200000 | MDC_SEMP 0.2 (ohmm) 2000 | MDC_SEDP 0.2 (ohmm) 2000 | MDC_SESP 0.2 (ohmm) 2000

WMDCSEXP 0.2 (ohmm) 2000 | WMDCSESP 0.2 (ohmm) 2000 | WMDCSEMP 0.2 (ohmm) 2000 | WMDCSEDP 0.2 (ohmm) 2000

VSH_GRL 0 (frac) 1 | VSHND 0 (frac) 1

POROSITY 30 (%) 0 | PHI_S 0.3 0 | PHI_ND 0.3 0 | PHI_D 0.3 0

PHIE 0.3 0 | PHIT 0.3 0

SW_ARCH 1 (frac) 0

POPE 0.1 10000

VSH_GRL 0 1 | Bulk Volume Water (BVW) 1 0 | Bulk Volume Water (BVW) 1 0 | PHIT 1 0 | VSH_GRL 0 1

NETSAND 0 2 | NETPAY 2 0

Core Data

Pressures

Samples

Era

Depth (m) (1:500) / TVDSS (m) (1:500):

Depth (m)	TVDSS (m)
1510	1460
1520	1470
1530	1480
1540	1490
1550	1500
1560	1510
1570	1520
1580	1530
1590	1540
1600	1550
1610	1560
1620	1570
1630	1580
1640	1590
1650	1600
1660	1610
1670	1620
1680	1630
1690	1640
1700	1650
1710	1660
1720	1670
1730	1680
1740	1690
1750	1700
1760	1710
1770	1720
1780	1730
1790	1740
1800	1750
1810	1760
1820	1770
1830	1780
1840	1790
1850	1800
1860	1810
1870	1820
1880	1830
1890	1840
1900	
1910	

Era:

- Skull Creek
- Nullawarre (1515.55)
- Nullawarre
- Belfast (1565.13)
- Belfast
- Flaxman (1723.10)
- Flaxman
- Waarre_C (1770.72)
- Waarre C
- IWCS (1788.13)
- WCH (1790.96)
- Waarre_B (1793.08)
- Waarre B
- Waarre_A (1821.58)
- Waarre A
- Eumeralla (1873.56)
- Eumeralla

Pressures: 1 2 3 7 8 10 11 12 14 15 16 17 18 19 20 21 23 24 25 26 27 28 29 30 31 32

F 1

#1

Halladale-1 DW-2

Permit: Exploration	**RTE:** 21.5 m	**TD (logs):** 1945.1 m
Latitude : 38° 34’ 45.67’ S	**Bit Size:** 216.0 mm	**BHT:** 90.7 degC
Longtitude : 148° 43’ 50.82’ E	**Rm:** 0.078 UNKN at: 20.6 degC	**Vertical Scale** 1:500 m
Easting :	**Rmf:** 0.075 UNKN at: 19.9 degC	**Interpreter :** Andy Hall
Northing :	**Rmc:** 0.091 UNKN at: 21.0 degC	
Datum :	**Plot created on:** 24/Oct/05 at: 15:46:37	

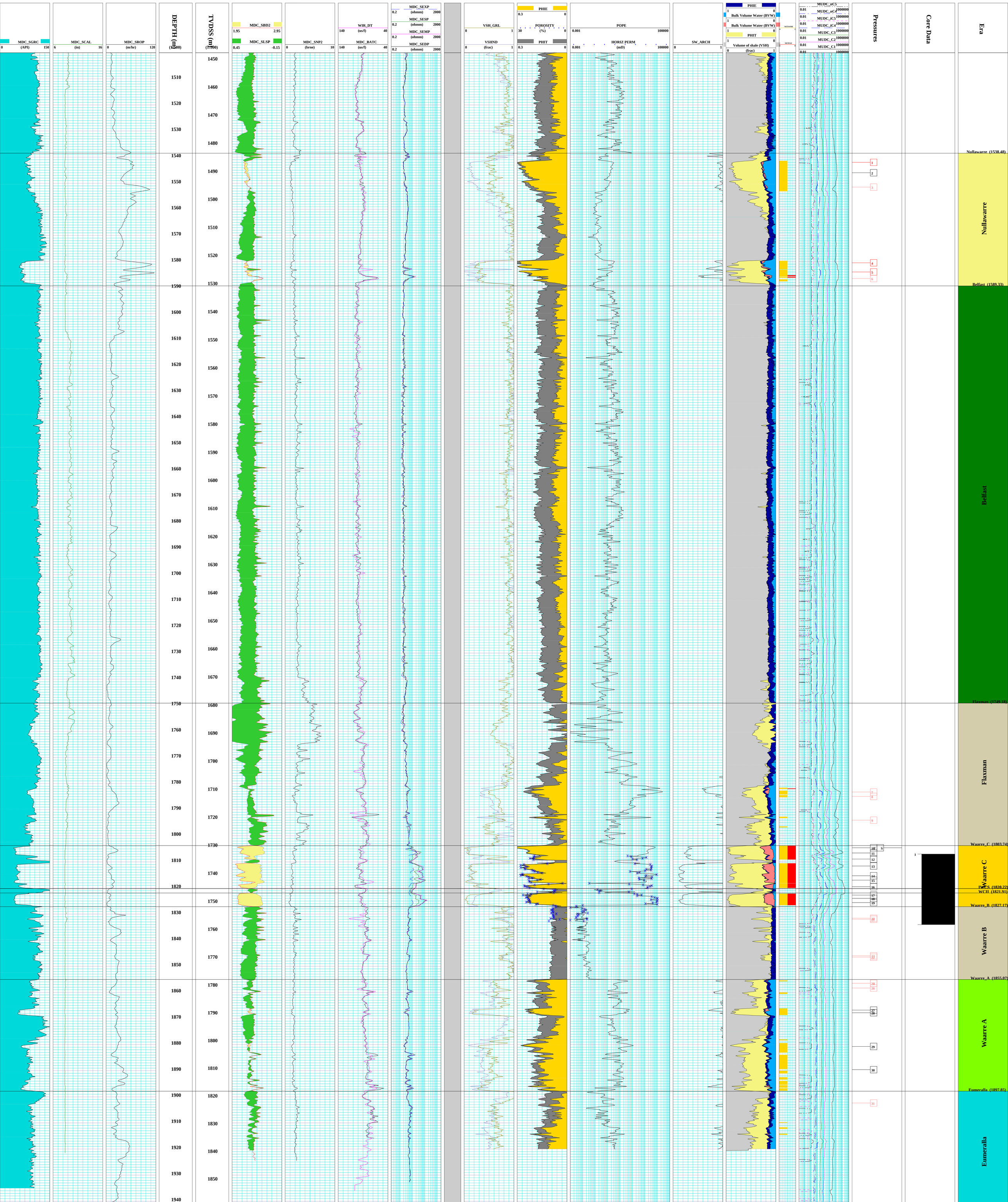

Halladale-1 DW3

Permit: Exploration	**RTE:** 21.5 m	**TD (logs):** 1969.0 m
Latitude : 38° 34' 45.67' S	**Bit Size:** 216.0 mm	**BHT:** 90.7 degC
Longtitude : 148° 43' 50.82' E	**Rm:** 0.078 UNKN at: 20.6 degC	**Vertical Scale** 1:500 m
Easting :	**Rmf:** 0.075 UNKN at: 19.9 degC	**Interpreter :** Andy Hall
Northing :	**Rmc:** 0.091 UNKN at: 21.0 degC	
Datum :	**Plot created on:** 24/Oct/05 at: 15:49: 9	

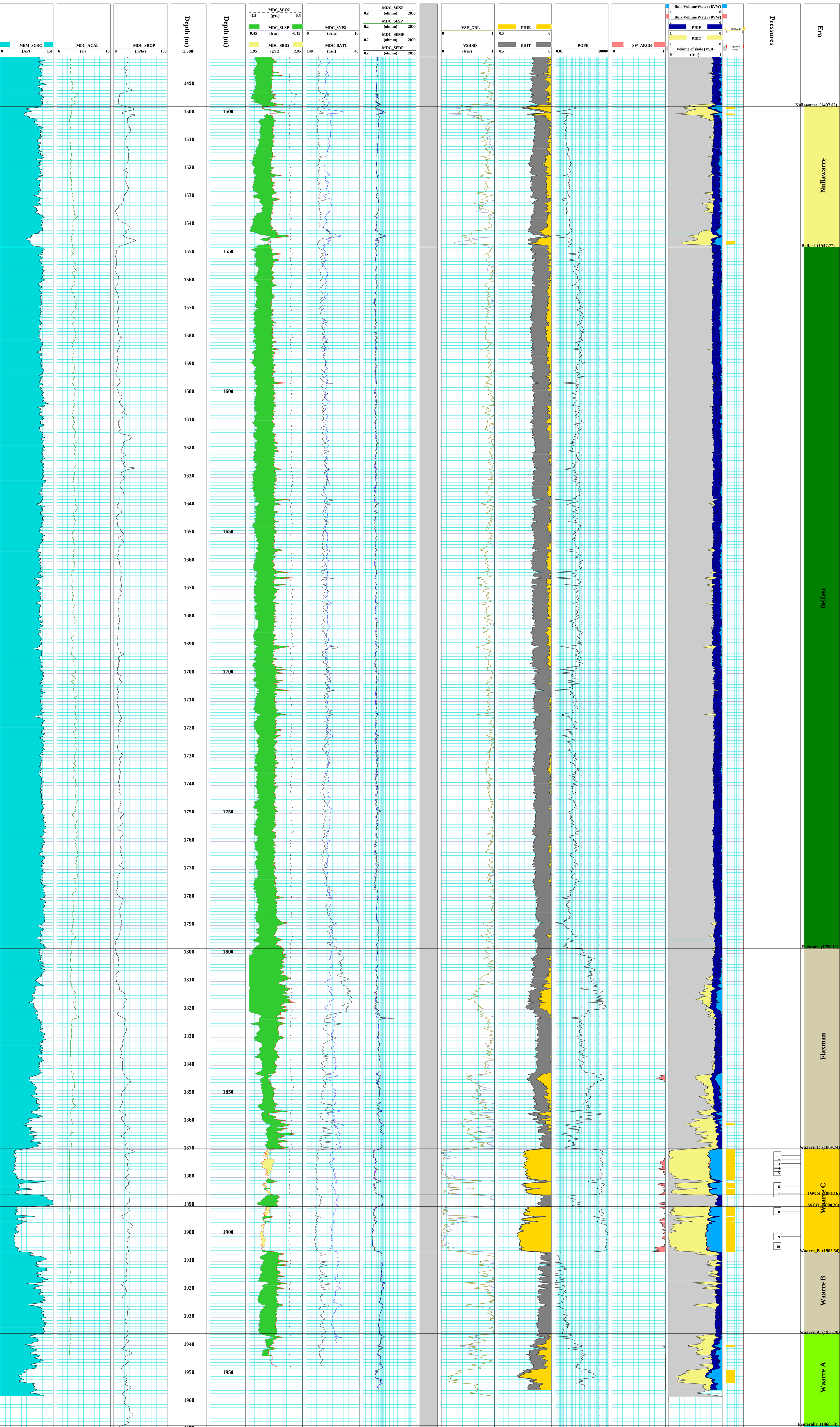

APPENDIX 4:
SPECIAL CORE ANALYSIS REPORT

CORE LABORATORIES AUSTRALIA PTY LTD

447-449 Belmont Ave, Kewdale, Perth WA 6105
Tel : (61 8) 9353 3944 Fax : (61 8) 9353 1369
Email : corelab.australia@corelab.com

A Special Core Analyses Study Of Selected Samples From The Well : Halladale-1 DW-1 and DW-2

Australia

Prepared for
ORIGIN ENERGY LIMITED

SEPTEMBER 2005

File: PRP-05036A

Rock Properties Group
Core Laboratories Australia Pty. Ltd.
Perth
Australia

These analyses, opinions or interpretations are based on observations and materials supplied by the client to whom, and for whose exclusive and confidential use, this report is made. The interpretations or opinions expressed represent the best judgment of Core Laboratories, (all errors and omissions excepted); but Core Laboratories and its officers and employees, assume no responsibility and make no warranty or representations, as to the productivity, proper operations, or profitableness of any oil gas or other mineral well or sand in connection with which such report is used or relied upon.

CORE LABORATORIES AUSTRALIA PTY LTD

9th September 2005

ORIGIN ENERGY LIMITED
Ground Floor, South Tower
John Oxley Centre
339 Coronation Drive
BRISBANE, QLD 4001

Attention : Dr Andrew Constantine

Subject : Special Core Analysis
Well : Halladale-1 DW-1 and DW-2
File : PRP-05036A

Dear Andrew,

Presented herein is the final report of the Special Core Analyses conducted on the selected core plug samples from the well : Halladale-1 DW-1 and DW-2.

Thank you for the opportunity to have been of service to Origin Energy Limited. If you have any questions regarding these results or if we can be of any further assistance please do not hesitate to contact us.

Yours sincerely,
CORE LABORATORIES AUSTRALIA PTY LTD

Ajit Singh
Supervisor - Rock Properties Group Perth

CONTENTS

Page

SECTION 1 : SUMMARY AND INTRODUCTION

- Summary of results 1-1
- Introduction 1-2
- SCAL sample selection and base data 1-3

SECTION 2 : ELECTRICAL PROPERTIES

- Summary of results from the electrical properties measurements 2-1
- Formation resistivity factor at NOBP – tabular and graphical 2-2
- Formation resistivity index at NOBP – graphical 2-3
- Formation resistivity index at NOBP – individual samples 2-4
- Cation exchange capacity (CEC) by wet chemistry method 2-13

SECTION 3 : CAPILLARY PRESSURE

- Summary of the air-brine capillary pressure by centrifuge at ambient 3-1
- Air-brine capillary pressure by centrifuge at ambient 3-2

SECTION 4 : RESIDUAL GAS SATURATION AND RELATIVE PERMEABILITY

- Residual gas saturation by counter-current imbibition 4-1
- Summary of the unsteady-state water-gas relative permeability (end-point) analysis 4-2
- Plot of permeability versus gas recovery (%PV) 4-3
- Plot initial versus residual gas saturation (%PV) 4-4

APPENDICES

- APPENDIX 1 : Summary of the laboratory procedures
- APPENDIX 2 : Samples drilled for mechanical strength tests
- APPENDIX 3 :CT-scan descriptions
- APPENDIX 4 :CT-scan and core plug images

SECTION 1
SUMMARY & INTRODUCTION

Summary of Results

- The samples selected for this SCAL study had permeability (Kair) and porosity values, measured at ambient conditions, ranging from 13.7 to greater than 10000 md and 14.4 to 27.4% respectively. Grain density values ranged from 2.625 to 2.677 g/cc.

- Cementation exponent ("m") values range from 1.76 to 1.87 with an average value of 1.79.

- Saturation exponent ("n") values range from 1.66 to 2.06 (average 1.91).

- Qv values from cation exchange capacity tests (wet chemistry method) range from 0.053 to 0.380 (meq/cm^3).

- Centrifuge air-brine (drainage) capillary pressure tests yielded, at the maximum 60 psi capillary pressure, immobile water saturation (Swi) values between 8.4 and 46.0 percent pore volume. Graphical summary of permeability to air versus Swi indicates the expected relationship of increasing Swi with decreasing permeability.

- Specific permeability to brine (Kw at 100% Sw) values indicated Kw/Kair ratios between 59.1 and 91.8%.

- Gas recoveries from the counter-current imbibition tests (representing "true" imbibition) ranged from 28.9 to 59.0 percent pore volume. Residual gas saturations ranged from 29.1 to 36.1 percent pore volume.

- Gas recoveries from the centrifuge water-gas tests (representing a "forced" imbibition scenario where capillary/gravity forces dominate in the reservoir) ranged from 52.0 to 63.6 percent pore volume. Residual gas saturations ranged from 27.2 to 32.3 percent pore volume.

INTRODUCTION

This report contains the final results of the Special Core Analyses study performed on selected core plug samples from the well : Halladale-1 DW-1 and DW-2. This study was initiated by Andrew Constantine of Origin Energy Limited (Origin).

The test programme involved :

- CT-scanning of selected core plugs
- Core plug photographs
- Porosity and permeability measurements at ambient and overburden pressures
- Formation resistivity factor (FRF) at net overburden pressure (NOBP)
- Formation resistivity index (FRI) at NOBP
- Cation exchange capacity (CEC) by wet chemistry method
- Air-brine drainage capillary pressure by centrifuge
- Specific permeability to brine (100% Sw)
- Residual gas saturation by counter-current imbibition (CCI)
- Centrifuge water-displacing–gas relative permeability (end-point data)

SCAL sample selection was carried out by Tim Conroy and Matthew Waugh of Woodside Energy Limited (as partners in this study). All selected samples were submitted for CT-scanning to ensure their suitability for SCAL testing (e.g contain no micro-fractures, differential cementation etc. which can invalidate SCAL data). Substitute samples, selected for those which failed CT-screening, also underwent CT-scanning. A full list of samples which were selected for this SCAL study and the associated base data (permeability, porosity and grain density values) is given on page 1-3. All selected samples had previously undergone routine core analysis measurements with the exception of twelve samples, as indicated with either an “A” or “B” suffix, which were newly drilled for this study.

At Origin’s request, an additional eighteen samples were drilled for mechanical strength tests (Appendix 2). All samples were CT-scanned prior to forwarding to CSIRO for mechanical strength testing.

The simulated formation brine salinity used for this SCAL study was 25,000 ppm (Origin’s email dated 15th June 2005) comprising 80% sodium chloride and 20% potassium chloride as the dissolved constituents.

Preliminary results from the completed analyses were reported on an on-going basis with all preliminary results forwarded by 21st July 2001.

Images of all core plug CT-scans are presented in Appendix 3. White light images of the samples which underwent SCAL testing are also presented in Appendix 4.

SCAL Sample Selection and Base Data

PLUG	Depth (m)	At Ambient (800 psi)			At 3100 psi NOBP			Grain Density (g/cc)	ANALYSIS										
		Kinf (md)	Kair (md)	Porosity (%)	Kinf (md)	Kair (md)	Porosity (%)		CT-SCAN		Clean/ Dry Kphi	FRF FRI NOBP	Off-Cuts CEC	Cent. Air-Brine Pc	CCl	Kw 100% Sw NOBP	USS KwKg NOBP	PLUG PHOTOS	
									Pass	Fail								CT-SCAN	WHITE LIGHT
5A	1792.55	286	302	26.0	271	286	25.6	2.652	√		√			√				√	√
6A	1792.60	450	470	25.0	428	448	24.5	2.661	√		√					√	√	√	√
7	1793.00	937	958	26.6	877	899	26.0	2.648	√			√	√					√	√
28	1808.70	1750	2110	20.9	1590	1960	20.1	2.662	√							√	√	√	√
29	1809.05	654	699	22.9	606	649	22.3	2.670	√			√	√					√	√
40	1812.30	3500	4060	25.0	3230	3690	24.0	2.653	√							√	√	√	√
42	1812.90	3530	3740	26.6	3140	3360	25.6	2.659	√					√	√			√	√
44*	1813.45	2360	3180	22.1	2410	3150	21.1	2.625	√			√	√					√	√
47*	1814.42	439	501	18.6	341	389	17.6	2.651	√					√				√	√
48*	1814.75	269	415	17.3	160	238	15.0	2.652		√								√	
48A*	1814.81	-	-	-	-	-	-	-		√								√	
51A*	1815.73	**	8890	27.4	**	8750	26.3	2.648	√		√					√	√	√	√
55	1816.80	2960	4220	24.3	2410	3490	23.1	2.656	√					√				√	√
56A*	1817.04	2540	3070	22.0	2360	2780	20.9	2.652	√		√			√	√			√	√
56	1817.10	311	385	16.7	271	347	15.9	2.654		√								√	
57A*	1817.50	**	5470	20.6	**	3180	19.2	2.656	√		√	√	√					√	√
59	1818.05	**	>10000	23.8	**	9040	22.6	2.655	√							√	√	√	√
62B*	1818.84	268	416	13.6	262	392	12.7	2.677	√		√	√	√					√	√
62A	1818.95	-	-	-	-	-	-	-		√								√	
64	1819.50	4110	4140	26.7	3640	3680	25.8	2.642	√			√	√					√	√
65	1819.80	2750	2800	26.3	2530	2590	25.5	2.662	√					√				√	√
67A	1820.49	2220	2260	25.7	2050	2090	24.8	2.672	√		√					√	√	√	√
72	1821.90	50.5	55.4	18.6	46.6	51.1	18.0	2.673	√			√	√					√	√
72A	1821.98	11.8	13.7	16.6	10.3	11.9	16.0	2.656	√		√			√	√			√	√
75A	1822.83	685	706	25.7	635	657	25.0	2.656	√		√			√	√			√	√
76	1823.10	588	606	27.3	547	565	26.6	2.665	√							√	√	√	√
77A	1823.36	369	392	24.9	344	366	24.3	2.652	√		√	√	√					√	√
79	1824.03	5860	6430	25.5	5550	6020	24.8	2.646	√					√	√			√	√
82	1824.90	3050	3380	23.4	2780	3090	22.6	2.640	√					√				√	√
84	1825.50	**	>10000	23.7	6490	8230	22.4	2.650	√			√	√					√	√
86	1826.10	**	8140	22.9	**	7260	22.2	2.648	√							√	√	√	√

Notes

1) 'A' and 'B' suffixed samples are newly drilled. The rest are RCA samples.

2) * Sleeved sample.

3) ** Kinf is not available as the permeability (Kair) measurements were done using the steady-state permeameter.

SECTION 2
ELECTRICAL PROPERTIES

Summary of Results from Electrical Properties Measurements

Brine Concentration : 25,000 ppm

Rw : 0.245 ohm-m at 25°C

Sample Number	Depth (m)	Kinf at NOBP (md)	Kair at NOBP (md)	Porosity at NOBP (%)	Grain Density (g/cc)	Qv from CEC (meq/cm3)	At NOBP		
							Formation Factor FRF	Cementation Exponent m	Saturation Exponent n
7	1793.00	877	899	26.0	2.648	0.100	11.53	1.82	2.05
29	1809.05	606	649	22.3	2.670	0.268	14.15	1.77	2.03
44	1813.45	2410	3150	21.1	2.625	0.124	16.86	1.82	1.68
57A	1817.50	**	3180	19.2	2.656	0.053	21.23	1.85	1.86
62B	1818.84	262	392	12.7	2.677	0.380	30.11	1.65	1.66
64	1819.50	3640	3680	25.8	2.642	0.065	10.91	1.76	1.95
72	1821.90	46.6	51.1	18.0	2.673	0.224	21.62	1.79	2.06
77A	1823.36	344	366	24.3	2.652	0.124	14.03	1.87	2.06
84	1825.50	6490	8230	22.4	2.650	0.111	14.95	1.81	1.84
							Average	1.79	1.91

** Kinf is not available as the permeability (Kair) measurements were done using the steady-state permeameter.

Formation Resistivity Factor at 3100 psi NOBP

Brine Concentration : 25,000 ppm Rw : 0.245 ohm-m at 25°C

Sample Number	Depth (m)	Kinf at NOBP (md)	Kair at NOBP (md)	Porosity at NOBP (%)	Grain Density (g/cc)	At NOBP	
						Formation Factor FRF	Cementation Exponent m
7	1793.00	877	899	26.0	2.648	11.53	1.82
29	1809.05	606	649	22.3	2.670	14.15	1.77
44	1813.45	2410	3150	21.1	2.625	16.86	1.82
57A	1817.50	**	3180	19.2	2.656	21.23	1.85
62B	1818.84	262	392	12.7	2.677	30.11	1.65
64	1819.50	3640	3680	25.8	2.642	10.91	1.76
72	1821.90	46.6	51.1	18.0	2.673	21.62	1.79
77A	1823.36	344	366	24.3	2.652	14.03	1.87
84	1825.50	6490	8230	22.4	2.650	14.95	1.81
						Average	1.79

** Kinf is not available as the permeability (Kair) measurements were done using the steady-state permeameter.

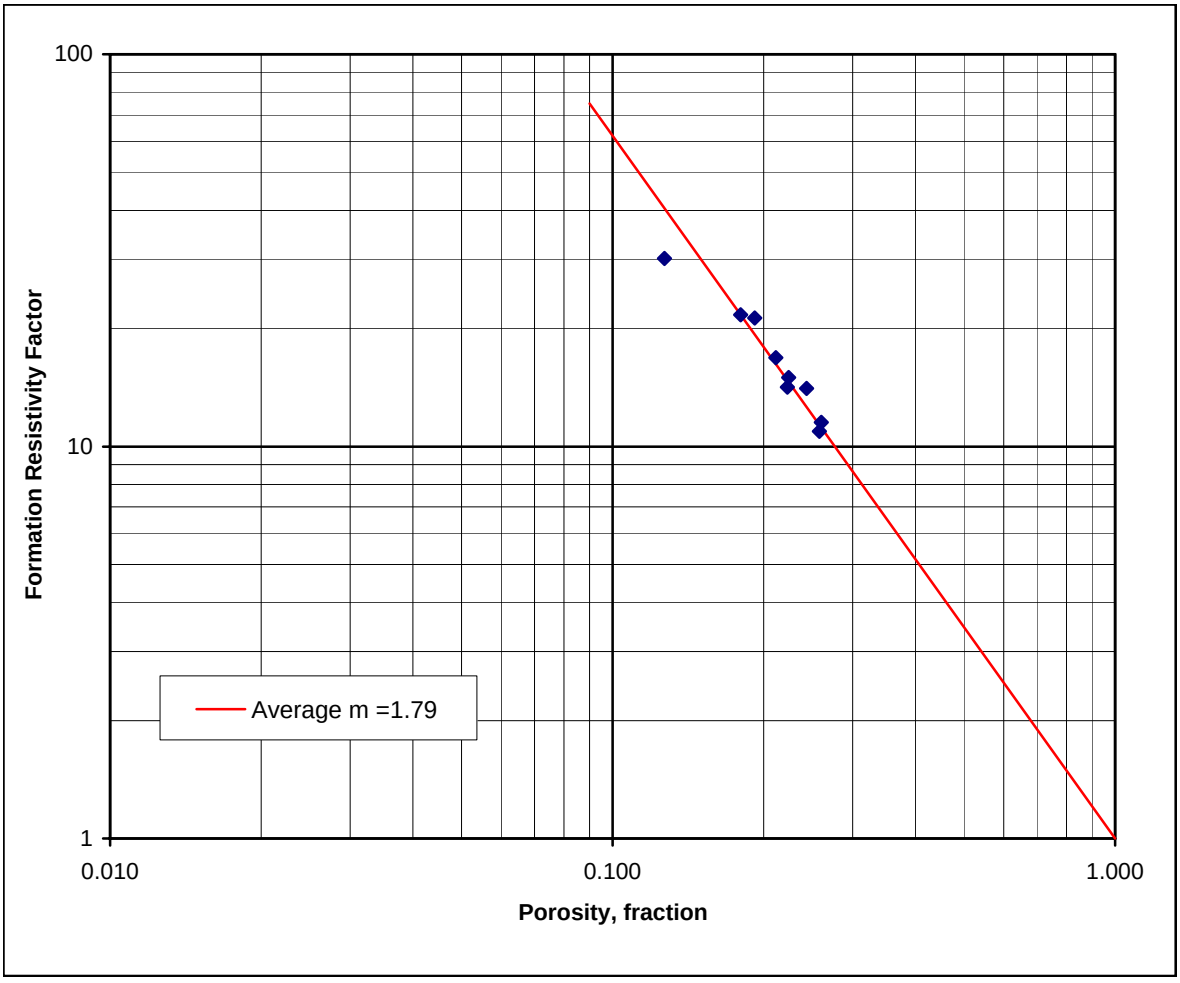

Formation Resistivity Index at 3100 psi NOBP

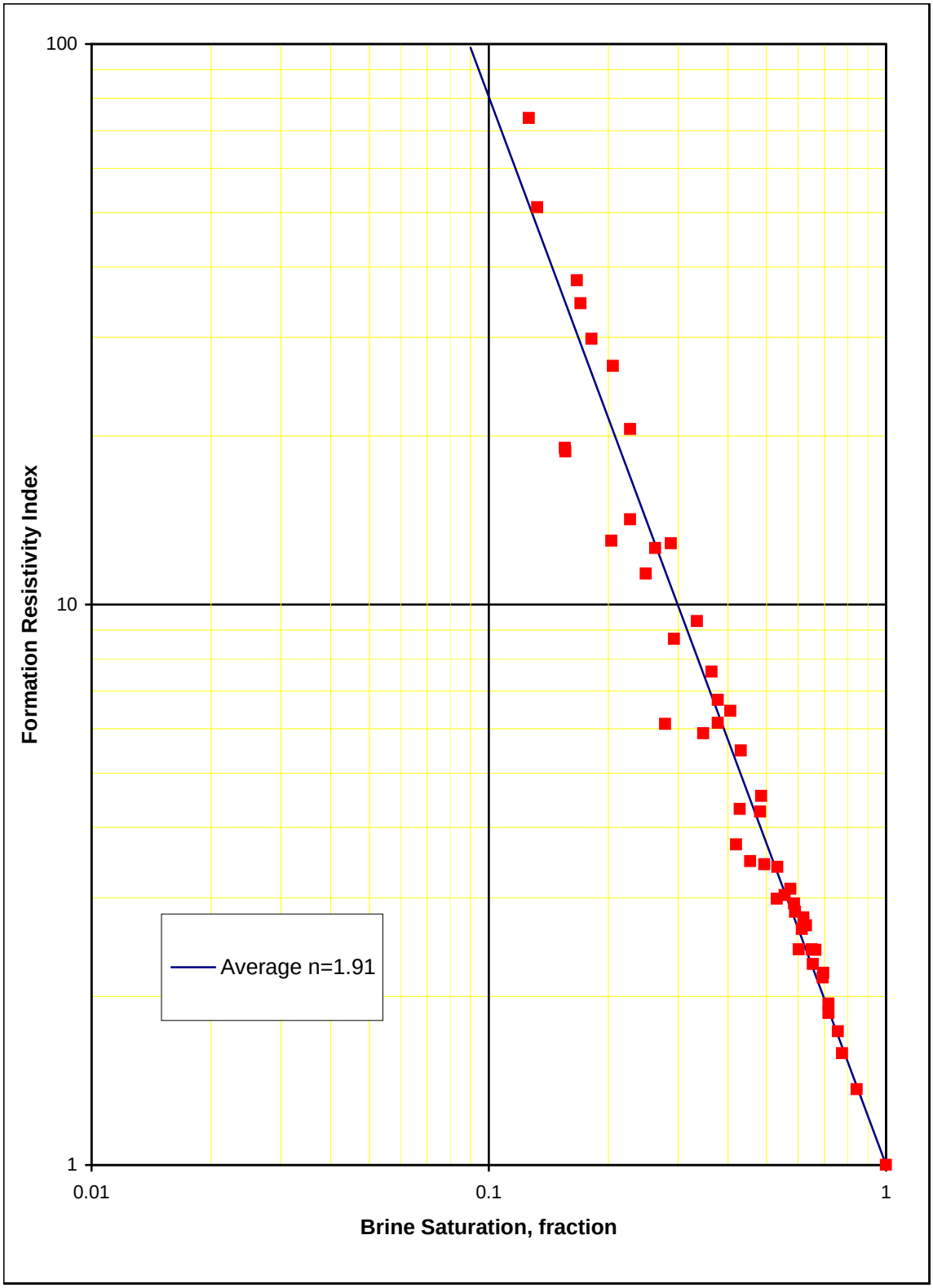

Formation Resistivity Index at 3100 psi NOBP

Sample No.	Depth (metres)	Kair at NOBP (md)	Grain Density (g/cc)	Determined at 3100 psi NOBP			
				Porosity (%)	Brine Saturation (%pv)	Resistivity Index	Sat. Exp. n
7	1793.00	899	2.648	26.0	100.0	1.00	-
					63.0	2.67	2.13
					58.7	2.93	2.02
					37.8	6.76	1.96
					20.5	26.66	2.07
					12.6	73.77	2.08

FRF at NOBP	11.53
Rw at 25°C, ohm-m	0.245

Average Exponent	2.05

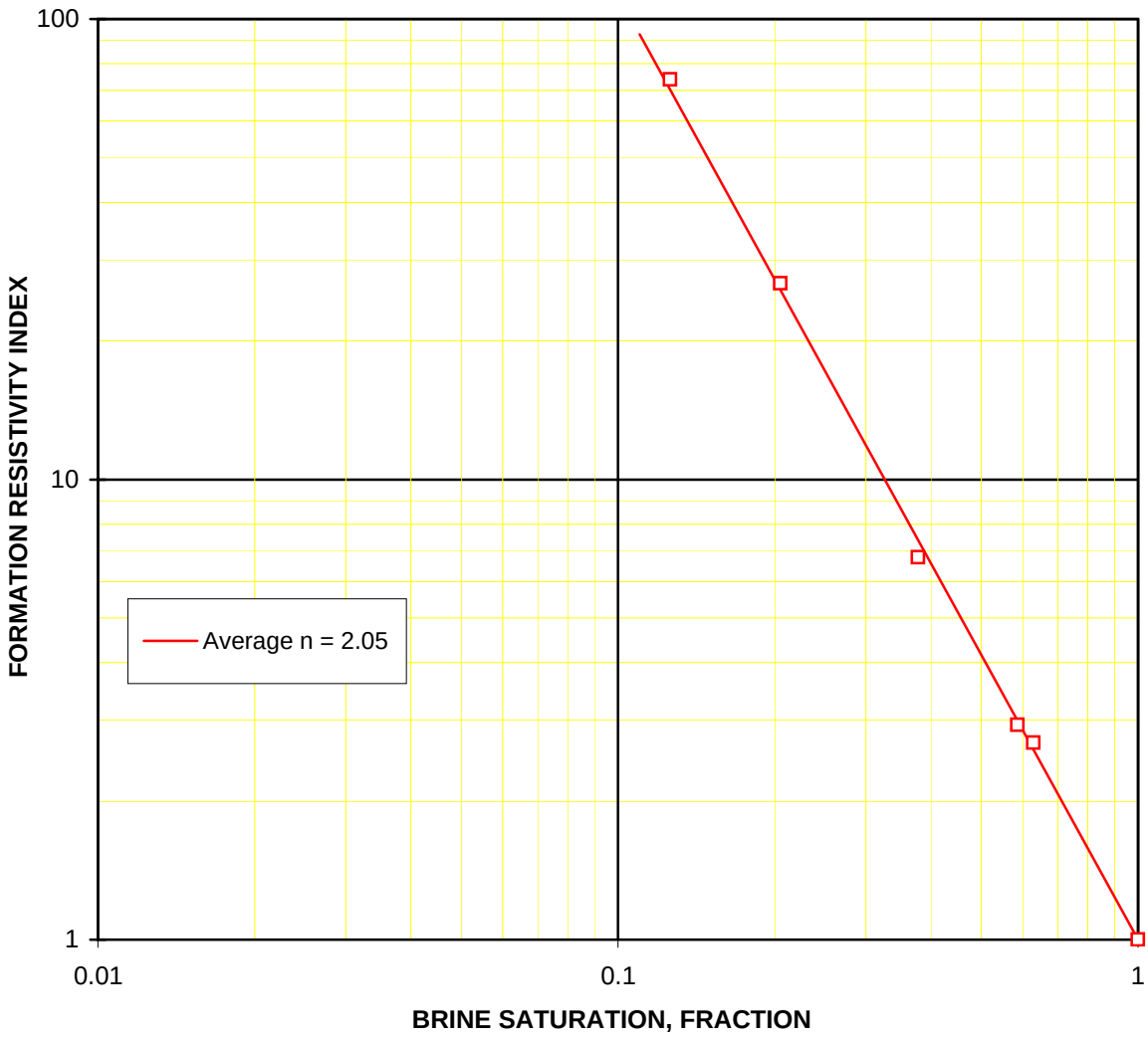

Formation Resistivity Index at 3100 psi NOBP

Sample No.	Depth (metres)	Kair at NOBP (md)	Grain Density (g/cc)	Determined at 3100 psi NOBP			
				Porosity (%)	Brine Saturation (%pv)	Resistivity Index	Sat. Exp. n
29	1809.05	649	2.670	22.3	100.0	1.00	-
					69.4	2.16	2.11
					48.2	4.27	1.99
					43.1	5.49	2.02
					28.7	12.85	2.05
					18.2	29.78	1.99

FRF at NOBP	14.15
Rw at 25°C, ohm-m	0.245

Average Exponent	2.03

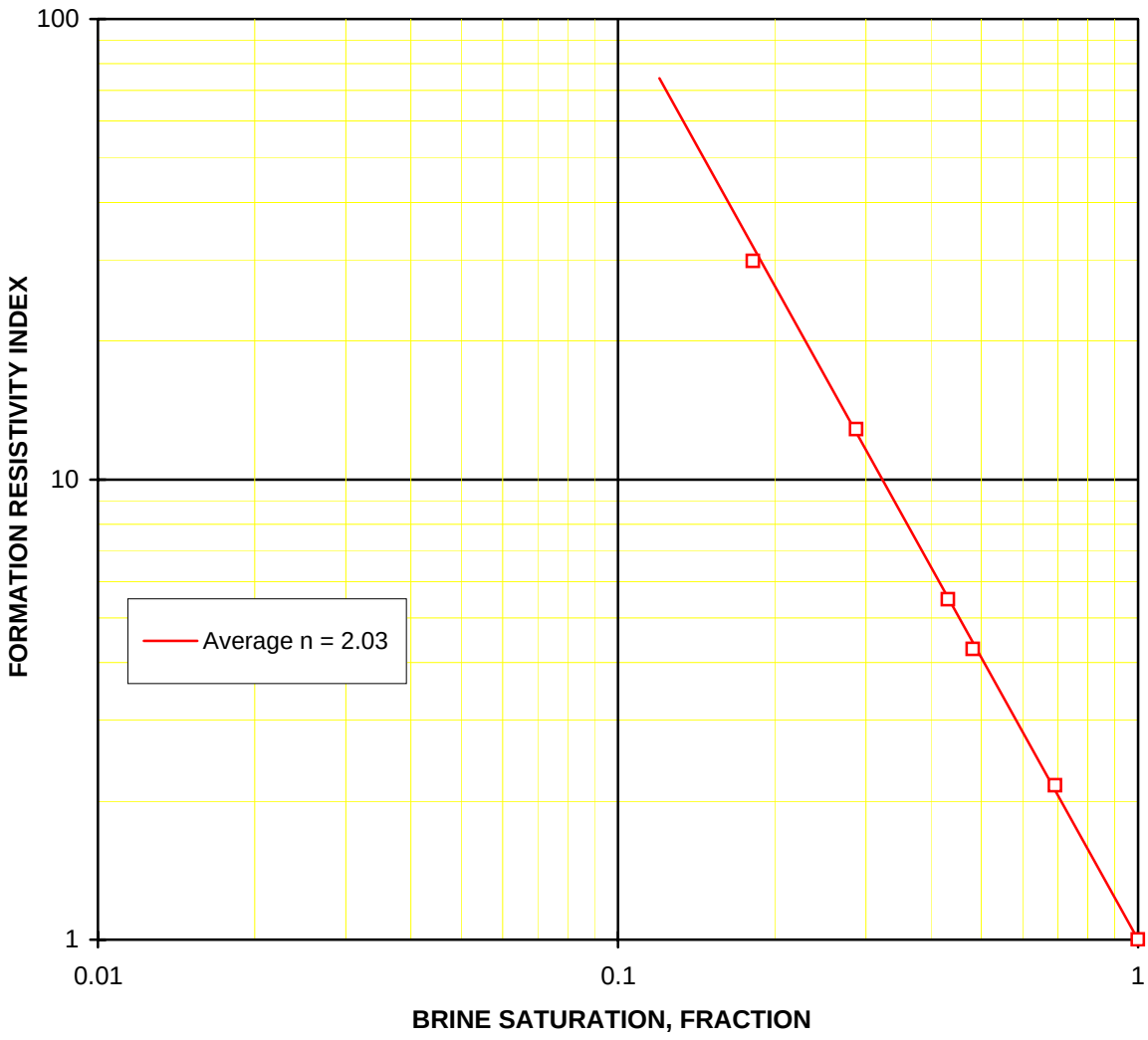

Formation Resistivity Index at 3100 psi NOBP

Sample No.	Depth (metres)	Kair at NOBP (md)	Grain Density (g/cc)	Determined at 3100 psi NOBP			
				Porosity (%)	Brine Saturation (%pv)	Resistivity Index	Sat. Exp. n
44	1813.45	3150	2.625	21.1	100.0	1.00	-
					77.5	1.58	1.80
					53.1	2.98	1.72
					34.7	5.89	1.68
					20.3	12.99	1.61
					15.5	19.02	1.58

FRF at NOBP	16.86
Rw at 25°C, ohm-m	0.245

Average Exponent	1.68

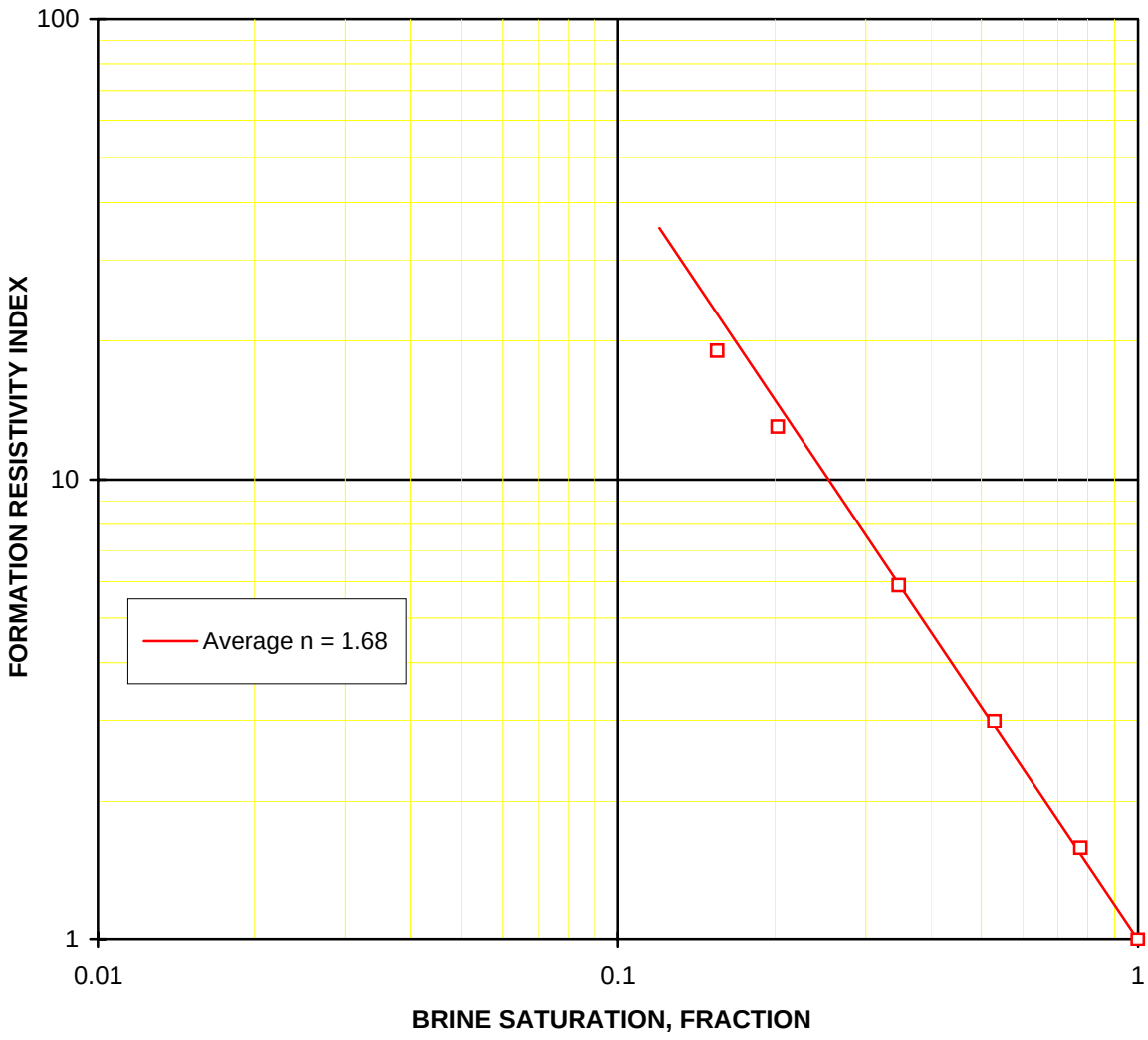

Formation Resistivity Index at 3100 psi NOBP

Sample No.	Depth (metres)	Kair at NOBP (md)	Grain Density (g/cc)	Determined at 3100 psi NOBP			
				Porosity (%)	Brine Saturation (%pv)	Resistivity Index	Sat. Exp. n
57A	1817.50	3180	2.656	19.2	100.0	1.00	-
					75.8	1.73	1.97
					71.6	1.94	1.98
					65.5	2.28	1.95
					55.5	3.03	1.89
					22.7	14.17	1.79
					15.6	18.72	1.58

FRF at NOBP	21.23
Rw at 25°C, ohm-m	0.245

Average Exponent	1.86

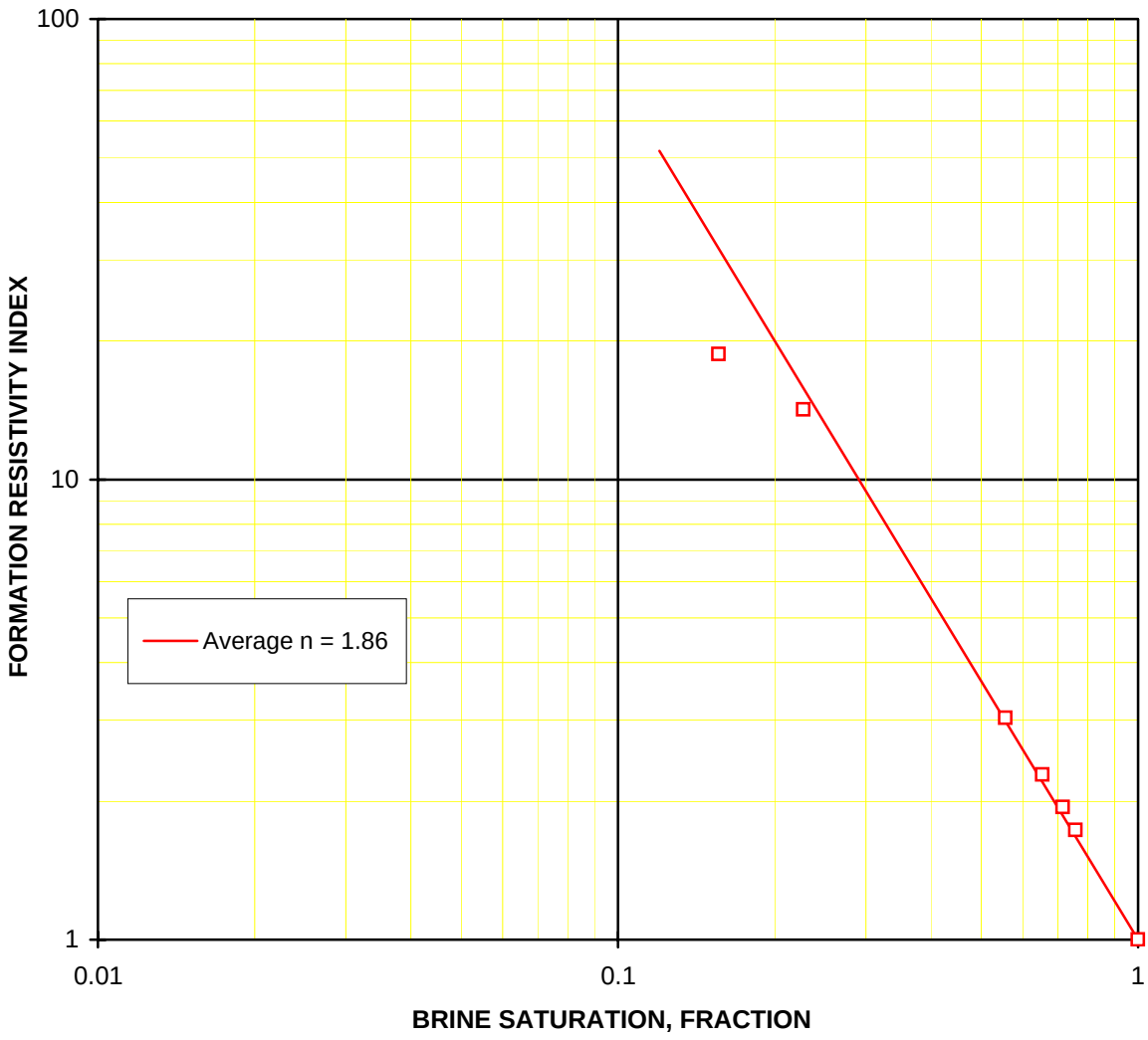

Formation Resistivity Index at 3100 psi NOBP

Sample No.	Depth (metres)	Kair at NOBP (md)	Grain Density (g/cc)	Determined at 3100 psi NOBP			
				Porosity (%)	Brine Saturation (%pv)	Resistivity Index	Sat. Exp. n
62B	1818.84	392	2.677	12.7	100.0	1.00	-
					84.4	1.36	1.83
					71.7	1.87	1.87
					60.4	2.43	1.76
					45.5	3.48	1.58
					41.9	3.73	1.52
					27.8	6.12	1.41

FRF at NOBP	30.11
Rw at 25°C, ohm-m	0.245

Average Exponent	1.66

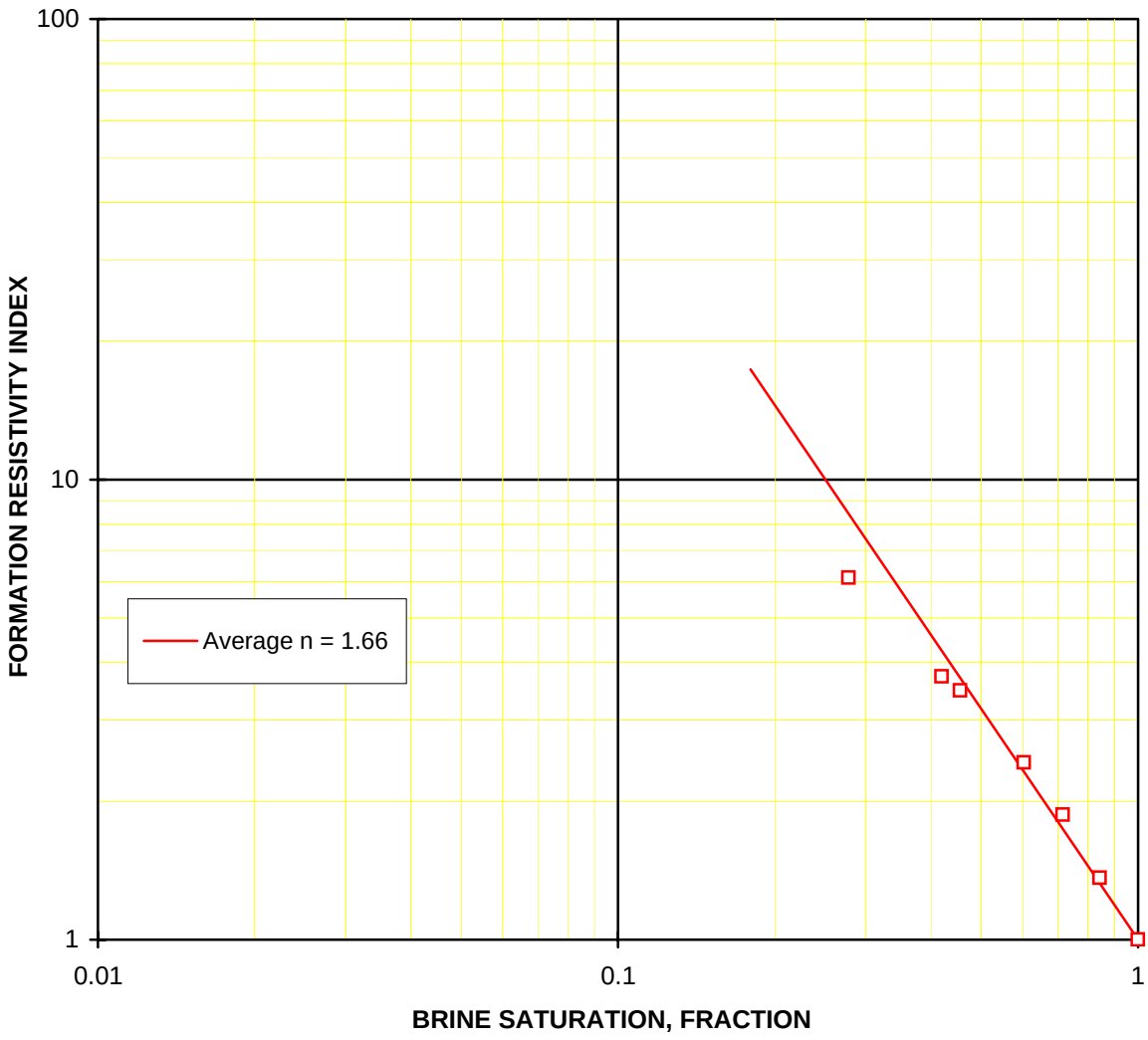

Formation Resistivity Index at 3100 psi NOBP

Sample No.	Depth (metres)	Kair at NOBP (md)	Grain Density (g/cc)	Determined at 3100 psi NOBP			
				Porosity (%)	Brine Saturation (%pv)	Resistivity Index	Sat. Exp. n
64	1819.50	3680	2.642	25.8	100.0	1.00	-
					61.5	2.64	2.00
					53.2	3.40	1.94
					37.8	6.15	1.86
					17.0	34.43	2.00
					13.2	51.16	1.95

FRF at NOBP	10.91
Rw at 25°C, ohm-m	0.245

Average Exponent	1.95

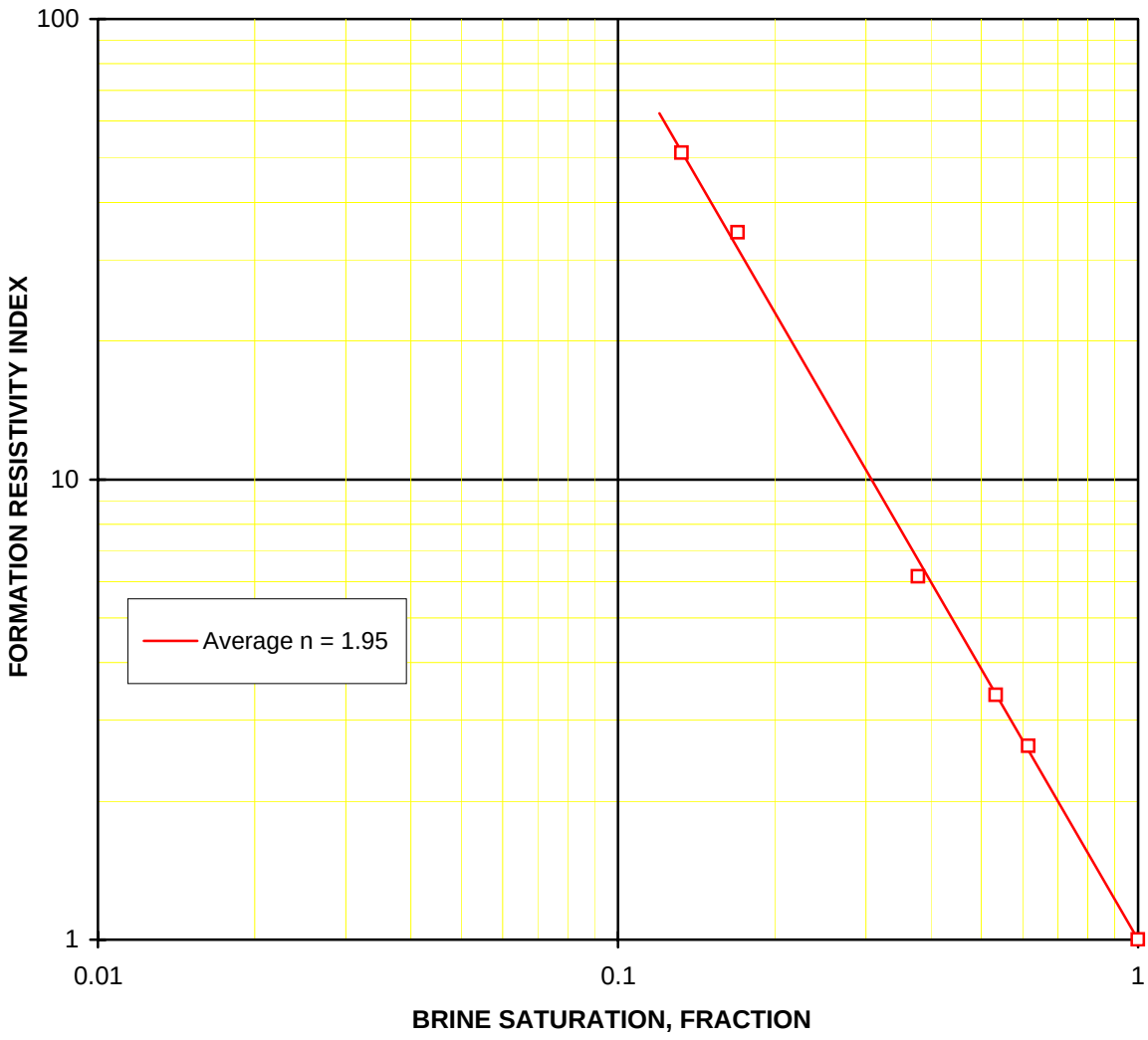

Formation Resistivity Index at 3100 psi NOBP

Sample No.	Depth (metres)	Kair at NOBP (md)	Grain Density (g/cc)	Determined at 3100 psi NOBP			
				Porosity (%)	Brine Saturation (%pv)	Resistivity Index	Sat. Exp. n
72	1821.90	51.1	2.673	18.0	100.0	1.00	-
					66.5	2.42	2.16
					61.9	2.77	2.12
					48.6	4.55	2.10
					40.5	6.46	2.07
					33.4	9.34	2.04
					26.3	12.60	1.90

FRF at NOBP	21.62
Rw at 25°C, ohm-m	0.245

Average Exponent	2.06

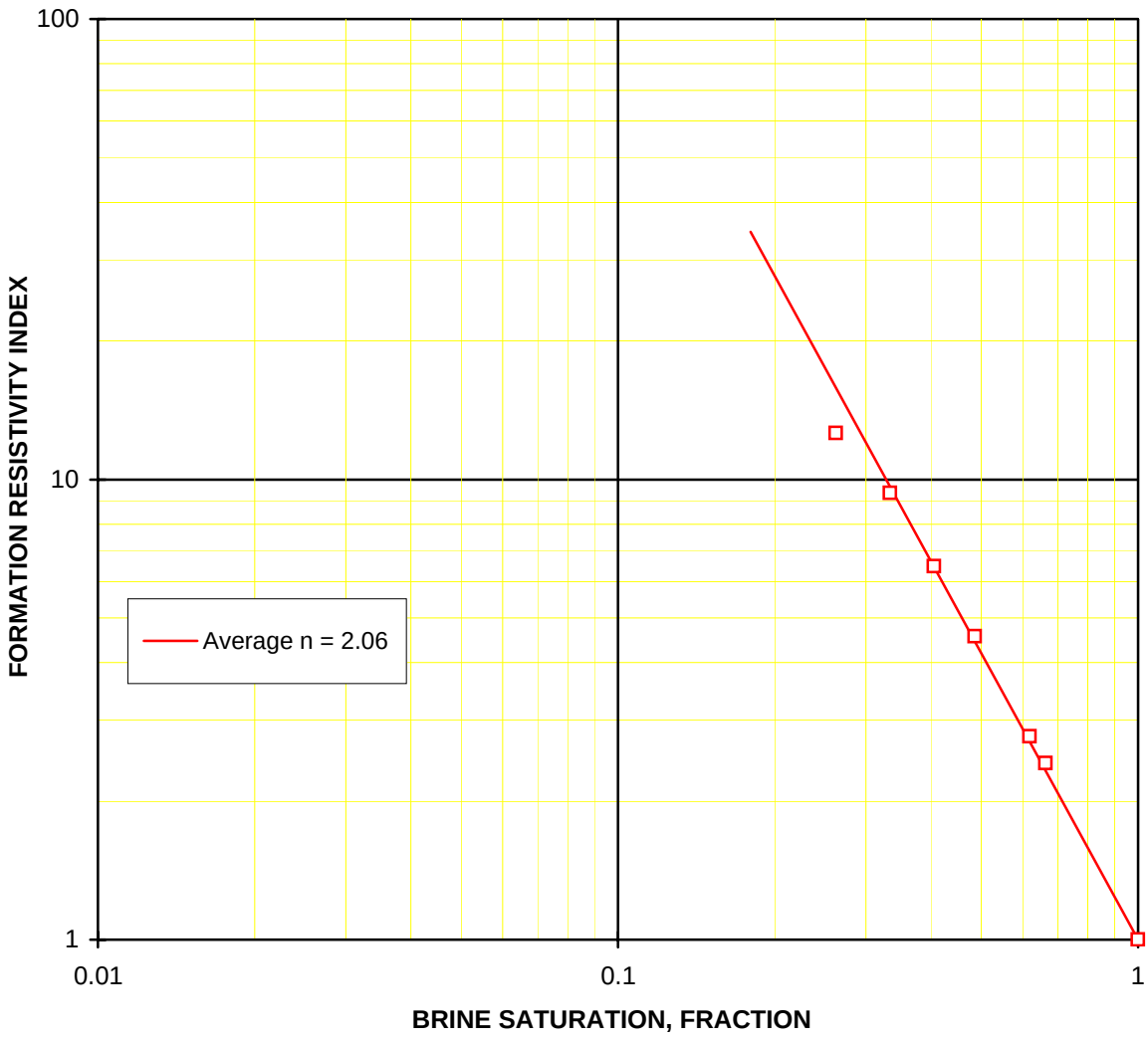

Formation Resistivity Index at 3100 psi NOBP

Sample No.	Depth (metres)	Kair at NOBP (md)	Grain Density (g/cc)	Determined at 3100 psi NOBP			
				Porosity (%)	Brine Saturation (%pv)	Resistivity Index	Sat. Exp. n
77A	1823.36	366	2.652	24.3	100.0	1.00	-
					69.5	2.20	2.17
					57.4	3.11	2.04
					36.4	7.59	2.01
					22.7	20.55	2.04
					16.7	37.84	2.03

FRF at NOBP	14.03
Rw at 25°C, ohm-m	0.245

Average Exponent	2.06

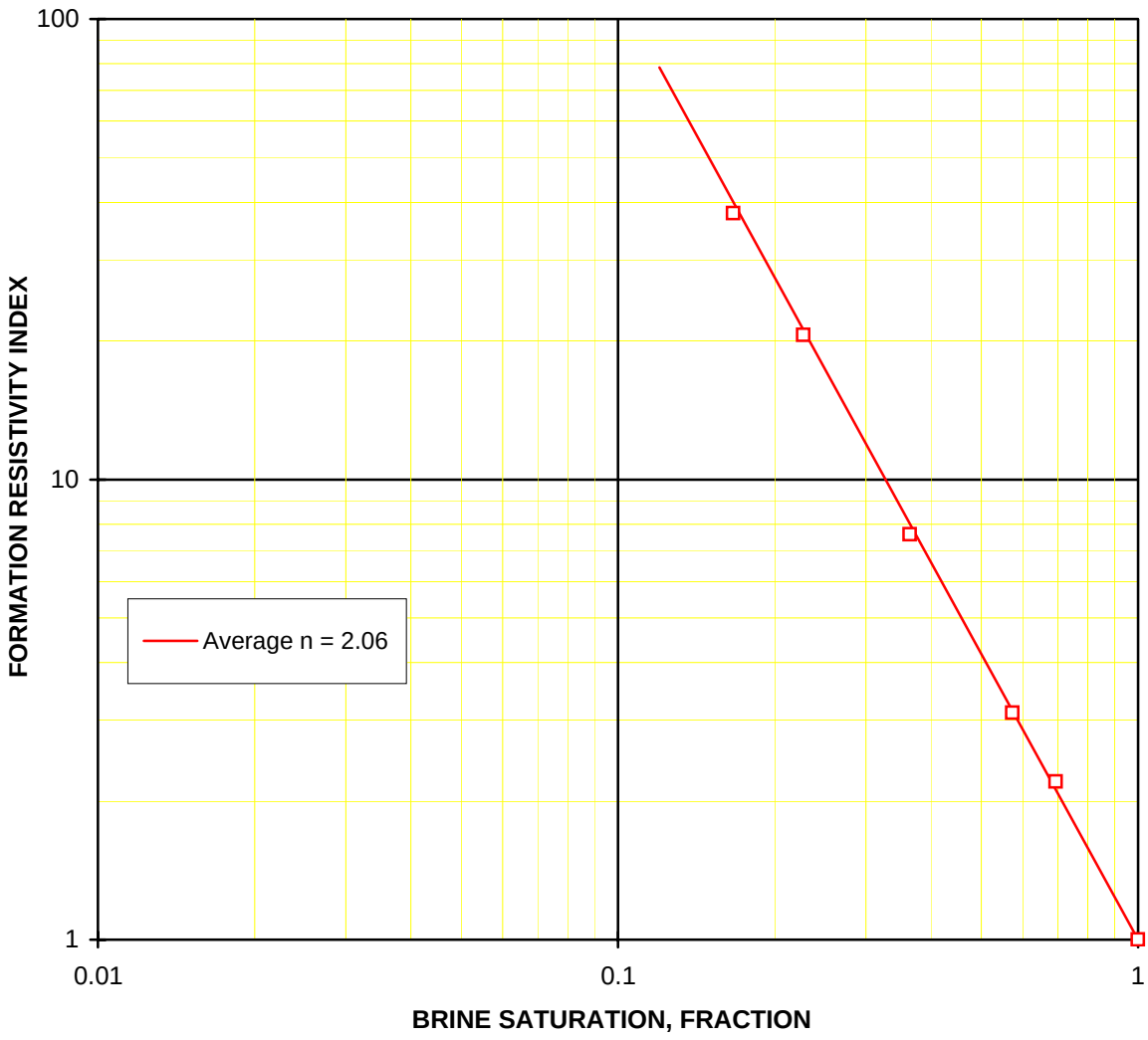

Formation Resistivity Index at 3100 psi NOBP

Sample No.	Depth (metres)	Kair at NOBP (md)	Grain Density (g/cc)	Determined at 3100 psi NOBP			
				Porosity (%)	Brine Saturation (%pv)	Resistivity Index	Sat. Exp. n
84	1825.50	8230	2.650	22.4	100.0	1.00	-
					65.2	2.42	2.07
					59.0	2.83	1.97
					49.4	3.44	1.75
					42.8	4.32	1.72
					29.3	8.68	1.76
					24.9	11.34	1.75

FRF at NOBP	14.95
Rw at 25°C, ohm-m	0.245

Average Exponent	1.84

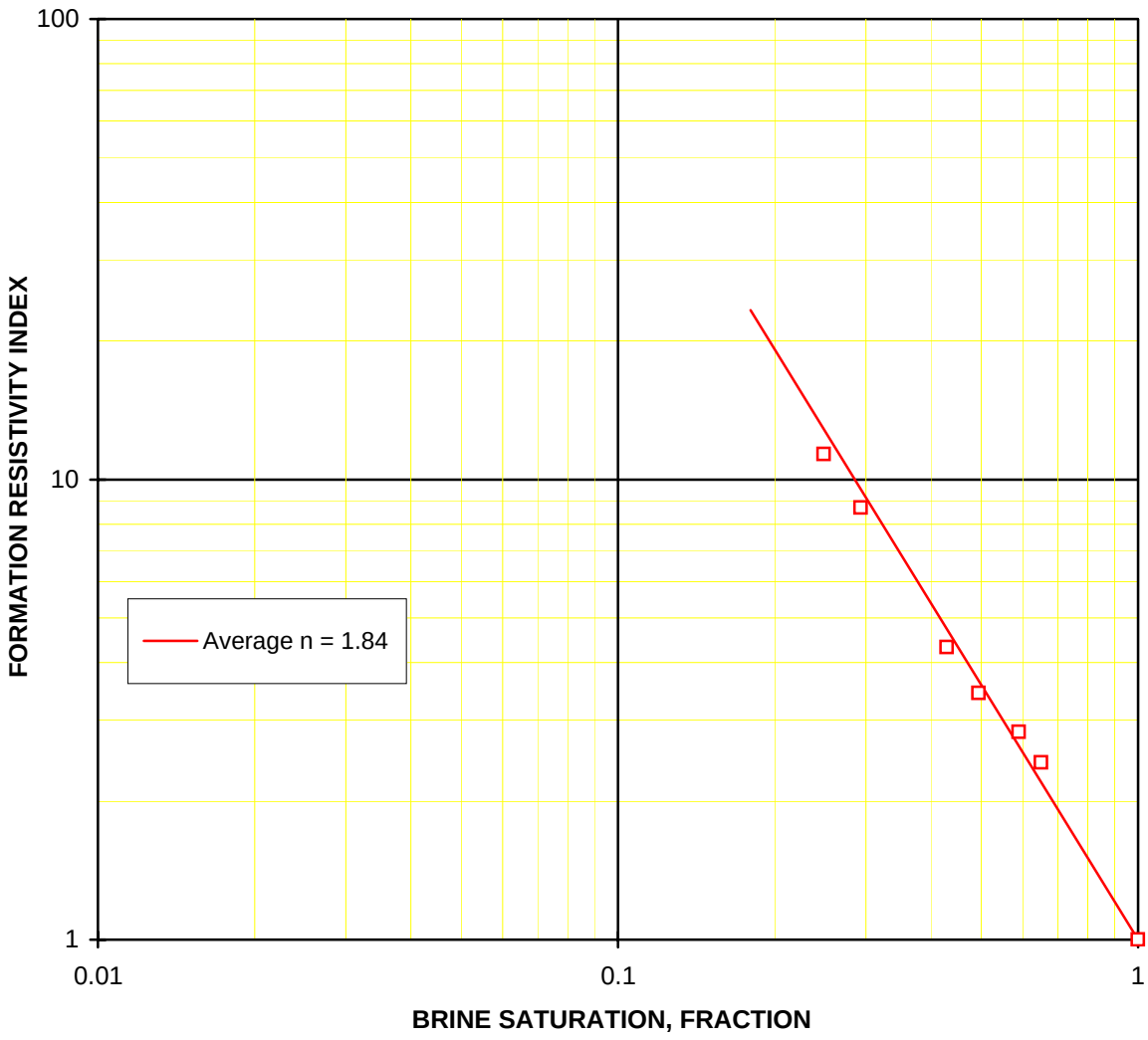

Cation Exchange Capacity by Wet Chemistry Method

Sample no.	Depth (m)	At 3100 psi NOBP		Grain density (g/cc)	CEC (meq/100 g)	Qv from CEC (meq/cm3)
		Kair (md)	Porosity (%)			
7	1793.00	899	26.0	2.648	1.332	0.100
29	1809.05	649	22.3	2.670	2.881	0.268
44	1813.45	3150	21.1	2.625	1.262	0.124
57A	1817.50	3180	19.2	2.656	0.47	0.053
62B	1818.84	392	12.7	2.677	2.063	0.380
64	1819.50	3680	25.8	2.642	0.860	0.065
72	1821.90	51.1	18.0	2.673	1.840	0.224
77A	1823.36	366	24.3	2.652	1.500	0.124
84	1825.50	8230	22.4	2.650	1.21	0.111

CEC analysis conducted on core plug trim-ends.

SECTION 3
CAPILLARY PRESSURE

Summary of the air-brine capillary pressure by centrifuge at ambient

Sample No.	Depth (m)	At Ambient		AIR - BRINE CAPILLARY PRESSURE (psi)							
		Kair (md)	Porosity (%)	0	1	2	5	10	20	40	60
				END-FACE WATER SATURATION Sw (%pv)							
5A	1792.55	302	26.0	100	100	77.4	41.8	32.4	25.9	20.5	18.0
42	1812.90	3740	26.6	100	63.9	46.3	30.5	23.0	16.7	13.3	12.5
47	1814.42	501	18.6	100	76.5	59.1	43.3	35.2	29.4	25.3	23.4
55	1816.80	4220	24.3	100	56.6	45.9	32.7	24.3	17.7	12.8	10.6
56A	1817.04	3070	22.0	100	63.7	45.1	32.4	25.5	18.9	13.5	12.2
65	1819.80	2800	26.3	100	61.3	37.7	29.3	22.0	15.3	12.3	12.0
72A	1821.98	13.7	16.6	100	100	100	80.9	73.6	65.1	54.3	46.0
75A	1822.83	706	25.7	100	80.5	55.7	41.0	30.9	22.9	17.7	15.7
79	1824.03	6430	25.5	100	39.6	27.9	22.3	17.5	13.5	10.1	8.4
82	1824.90	3380	23.4	100	56.0	33.8	20.7	16.5	13.6	11.0	10.4

Water saturation (Swi) vs permeability to air

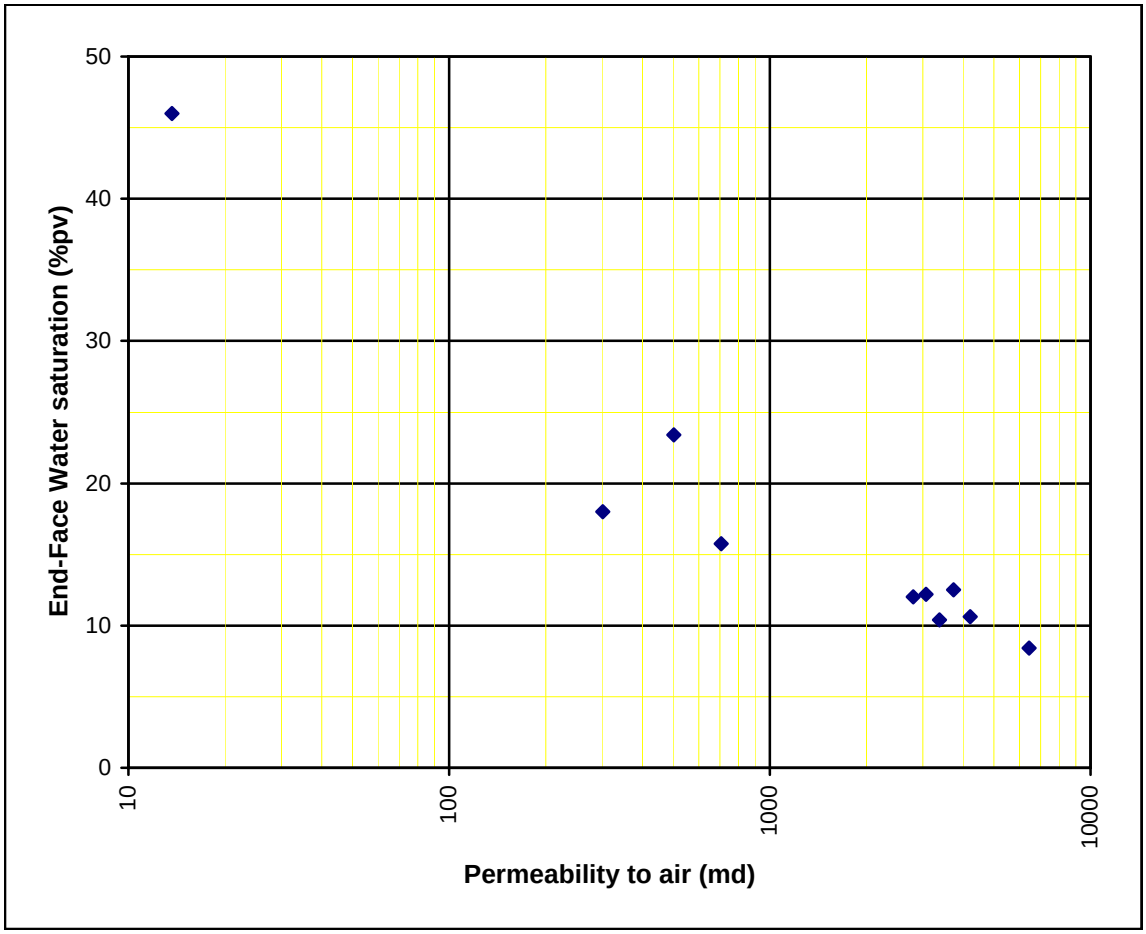

Air-brine Capillary Pressure by Centrifuge at Ambient

Sample no.	Depth (m)	At Ambient		
		Kinf (md)	Kair (md)	Porosity (%)
5A	1792.55	286	302	26.0

Capillary Pressure (psi)	End-Face Water Saturation (%pv)
0	100
1	100
2	77.4
5	41.8
10	32.4
20	25.9
40	20.5
60	18.0

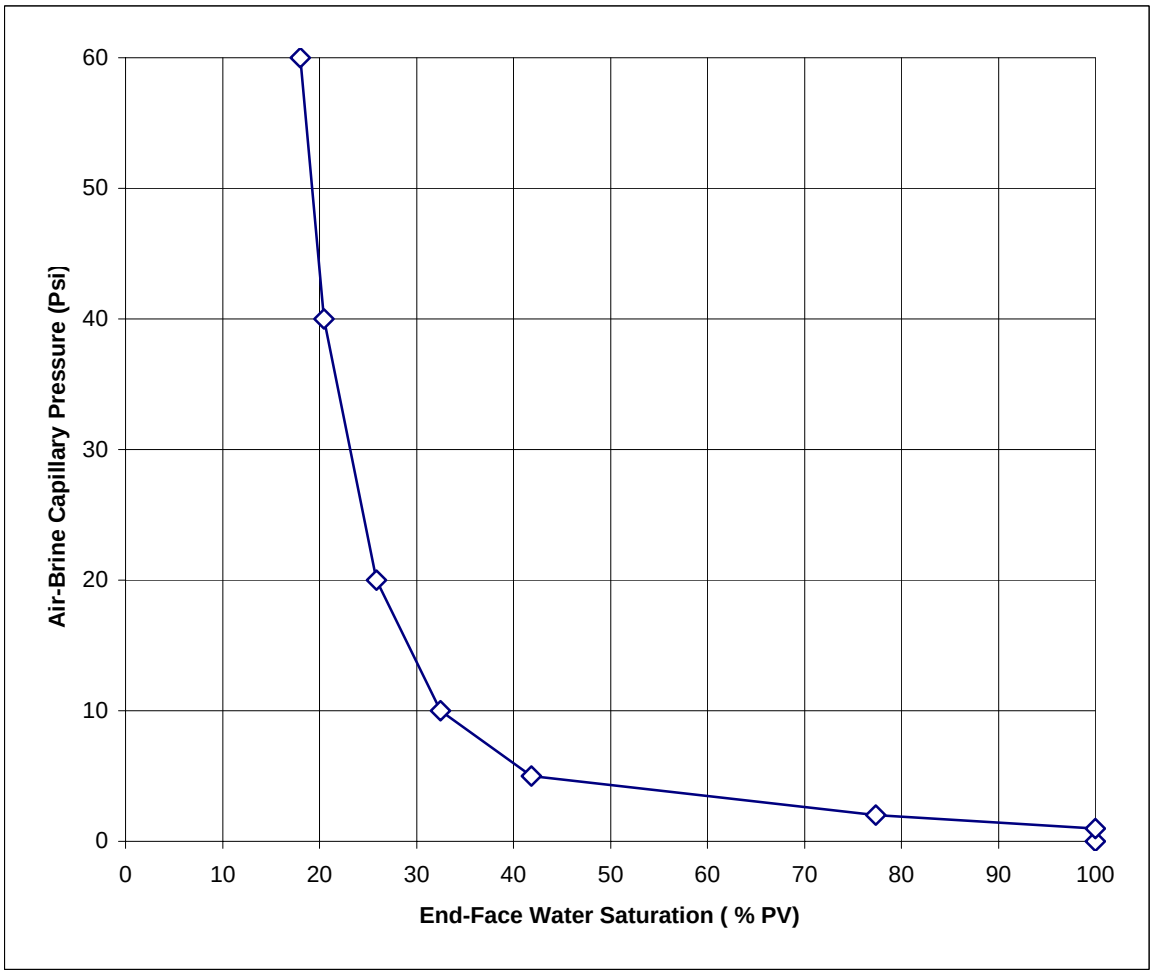

Air-brine Capillary Pressure by Centrifuge at Ambient

Sample no.	Depth (m)	At Ambient		
		Kinf (md)	Kair (md)	Porosity (%)
42	1812.90	3530	3740	26.6

Capillary Pressure (psi)	End-Face Water Saturation (%pv)
0	100
1	63.9
2	46.3
5	30.5
10	23.0
20	16.7
40	13.3
60	12.5

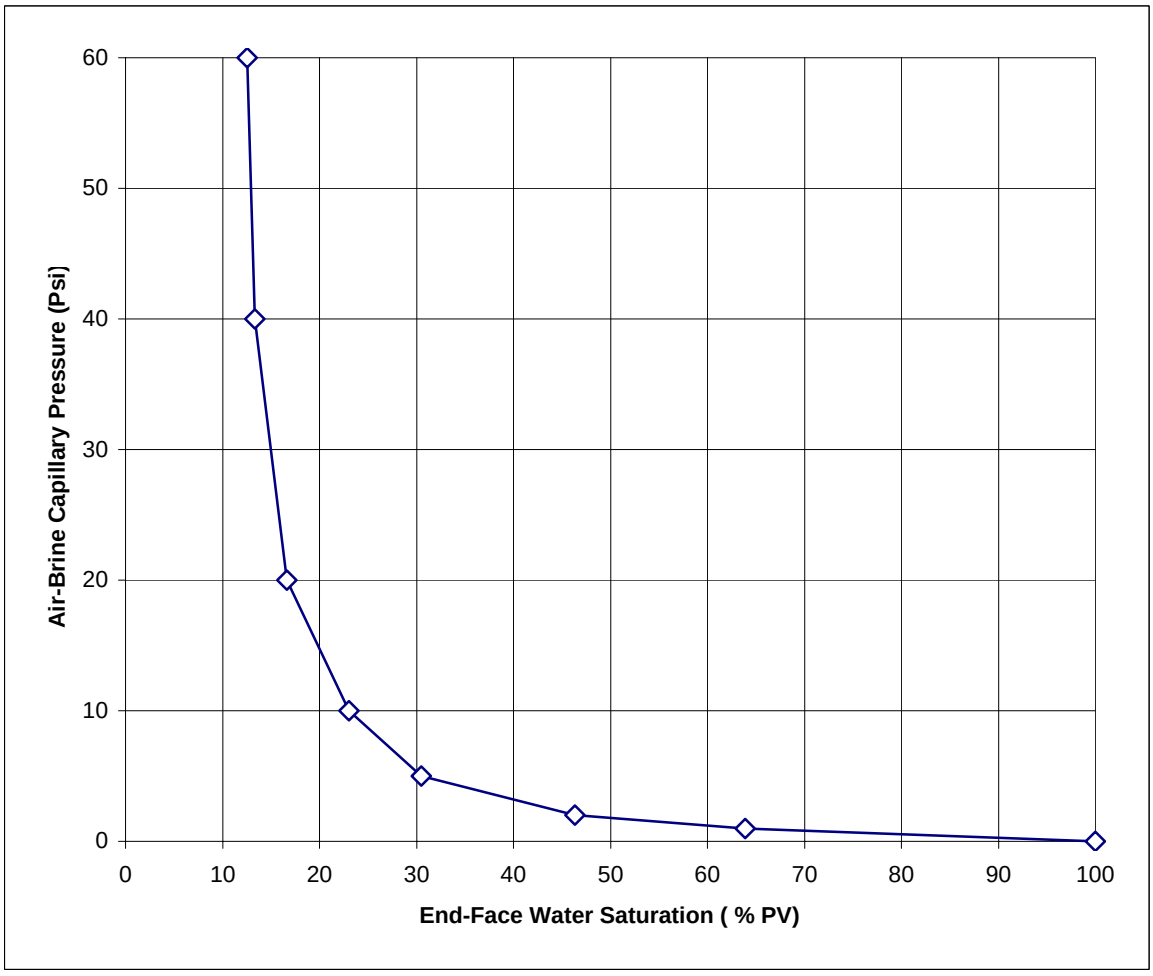

Air-brine Capillary Pressure by Centrifuge at Ambient

Sample no.	Depth (m)	At Ambient		
		Kinf (md)	Kair (md)	Porosity (%)
47	1814.42	439	501	18.6

Capillary Pressure (psi)	End-Face Water Saturation (%pv)
0	100
1	76.5
2	59.1
5	43.3
10	35.2
20	29.4
40	25.3
60	23.4

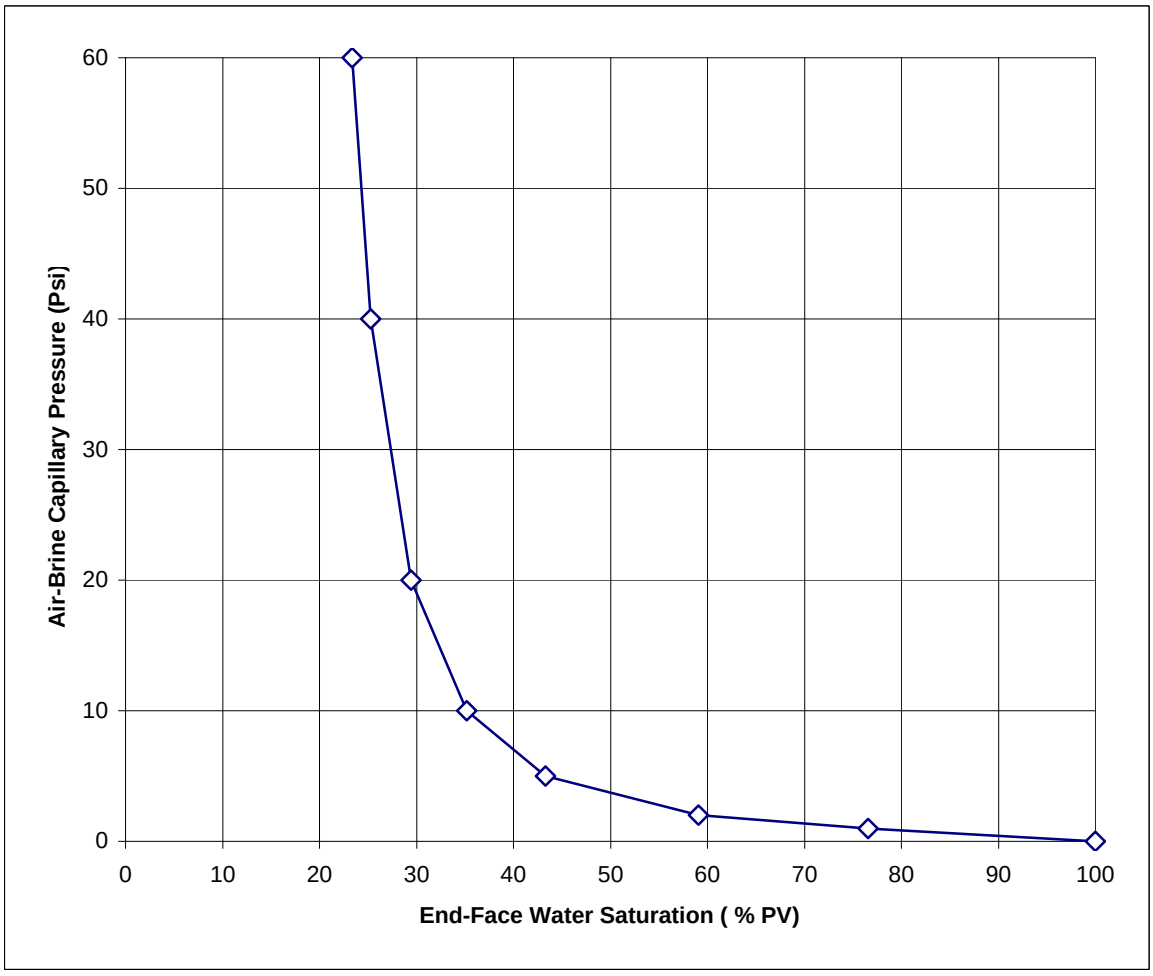

Air-brine Capillary Pressure by Centrifuge at Ambient

Sample no.	Depth (m)	At Ambient		
		Kinf (md)	Kair (md)	Porosity (%)
55	1816.80	2960	4220	24.3

Capillary Pressure (psi)	End-Face Water Saturation (%pv)
0	100
1	56.6
2	45.9
5	32.7
10	24.3
20	17.7
40	12.8
60	10.6

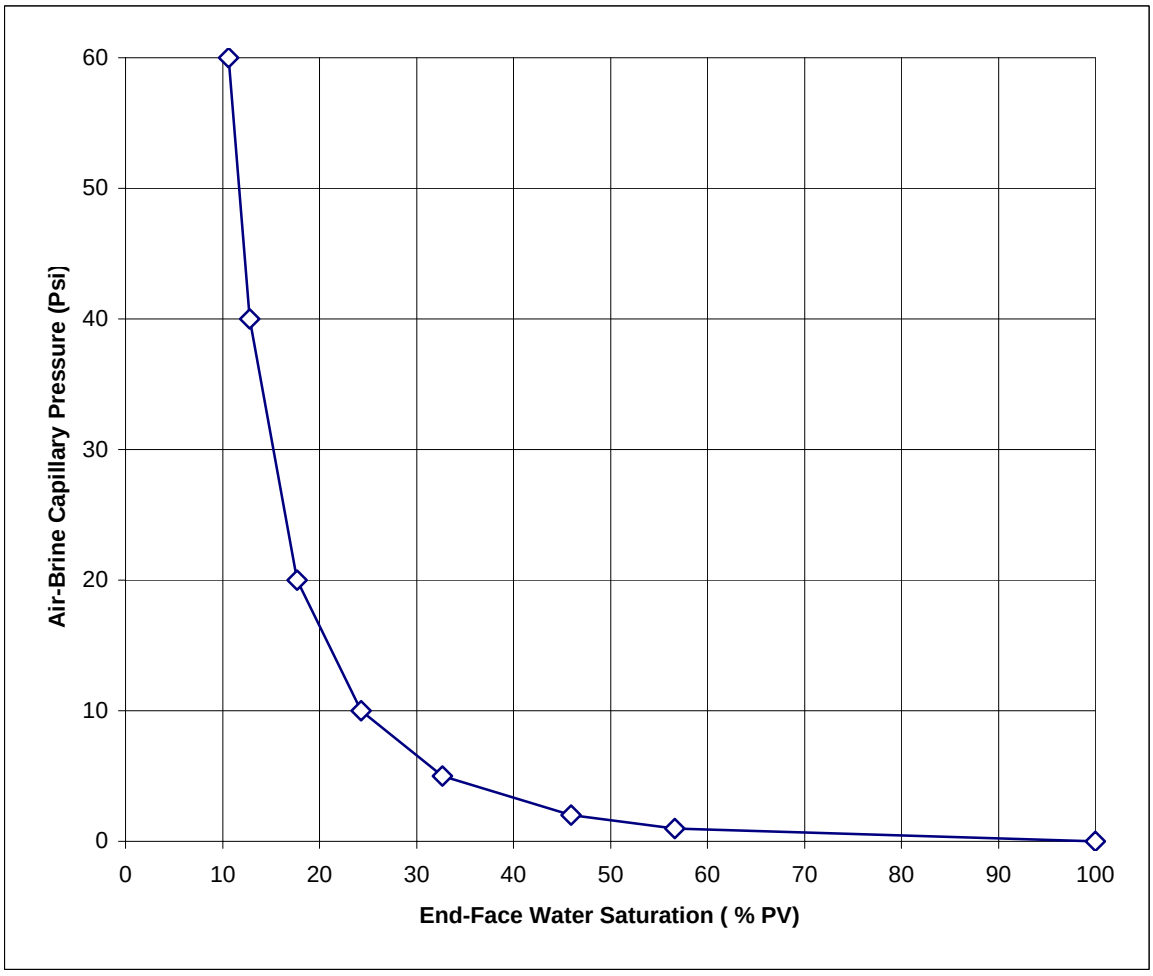

Air-brine Capillary Pressure by Centrifuge at Ambient

Sample no.	Depth (m)	At Ambient		
		Kinf (md)	Kair (md)	Porosity (%)
56A	1817.04	2540	3070	22.0

Capillary Pressure (psi)	End-Face Water Saturation (%pv)
0	100
1	63.7
2	45.1
5	32.4
10	25.5
20	18.9
40	13.5
60	12.2

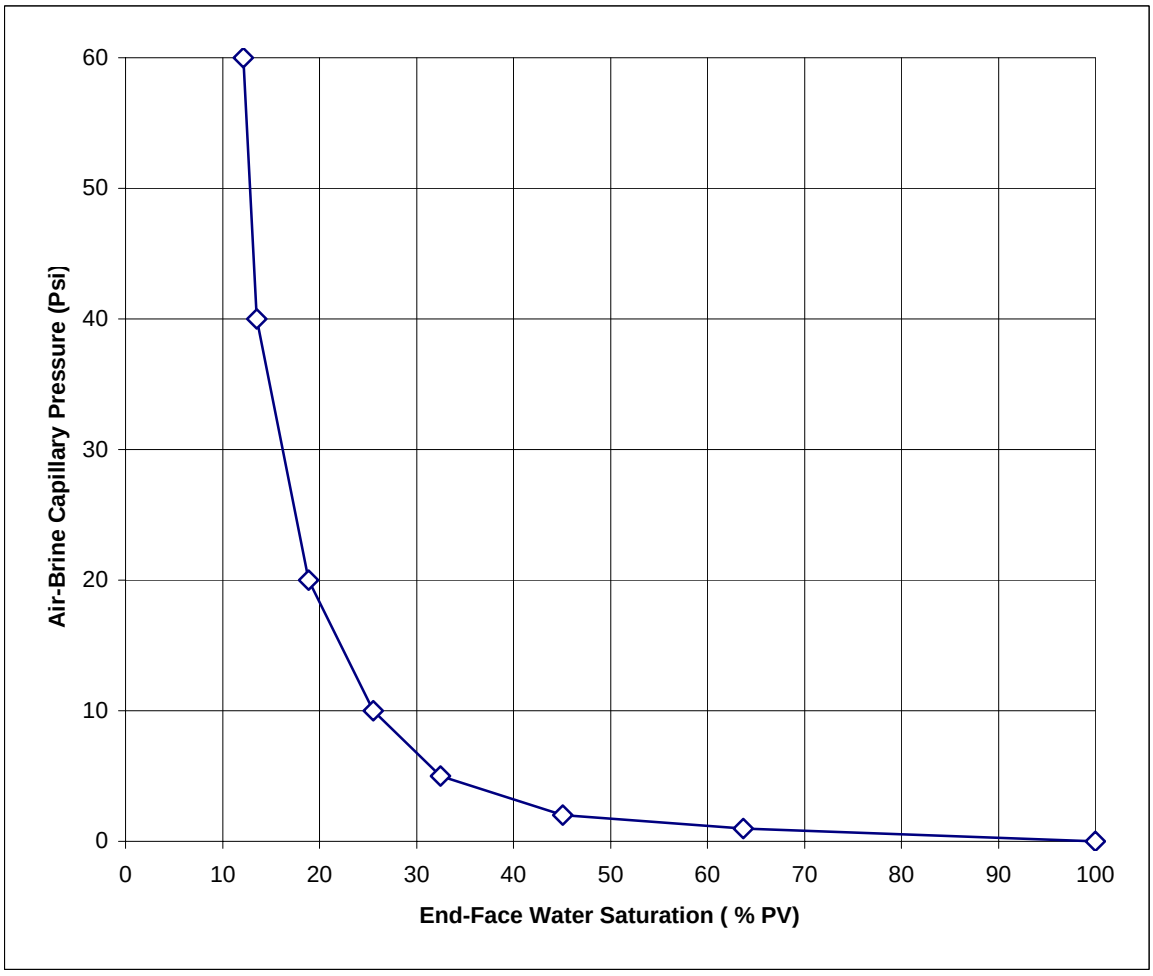

Air-brine Capillary Pressure by Centrifuge at Ambient

Sample no.	Depth (m)	At Ambient		
		Kinf (md)	Kair (md)	Porosity (%)
65	1819.80	2750	2800	26.3

Capillary Pressure (psi)	End-Face Water Saturation (%pv)
0	100
1	61.3
2	37.7
5	29.3
10	22.0
20	15.3
40	12.3
60	12.0

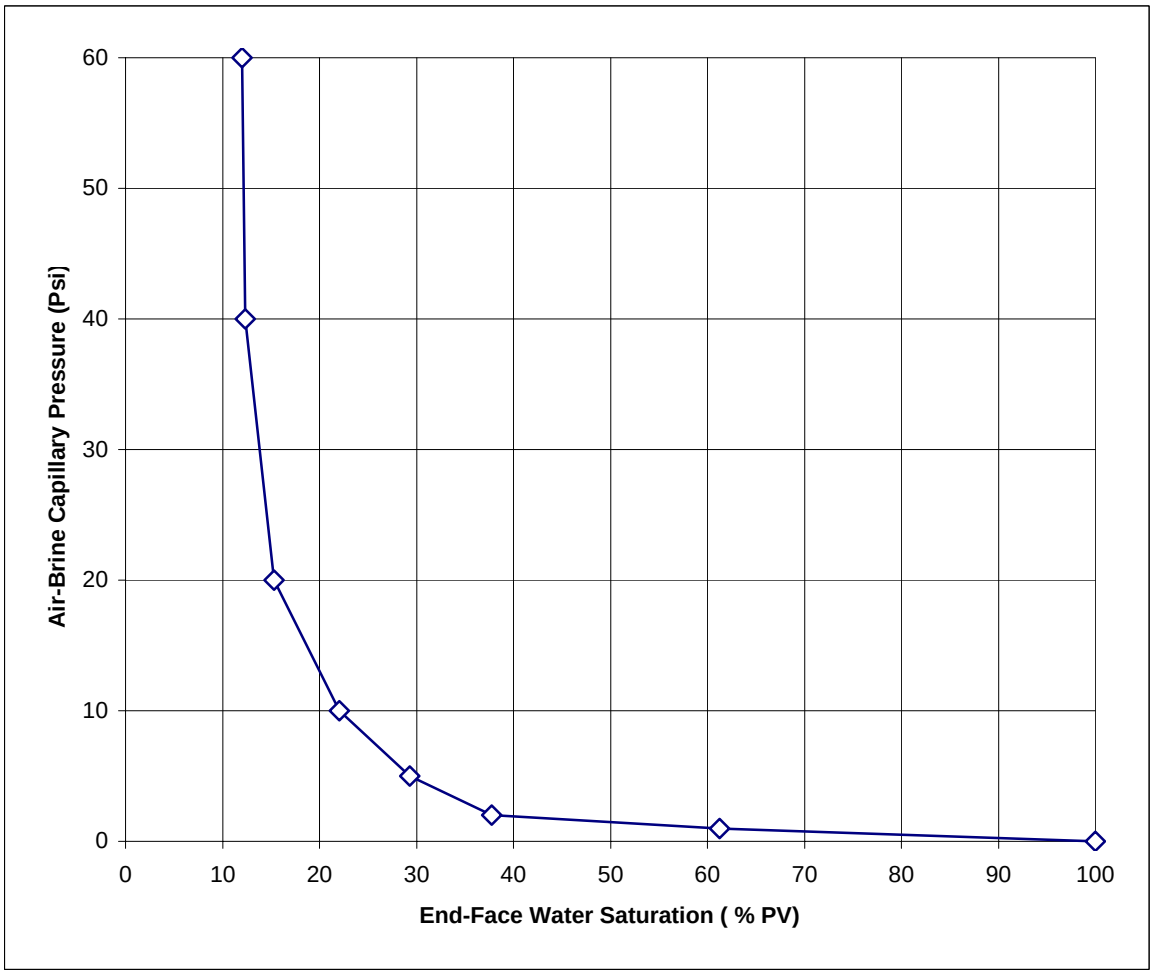

Air-brine Capillary Pressure by Centrifuge at Ambient

Sample no.	Depth (m)	At Ambient		
		Kinf (md)	Kair (md)	Porosity (%)
72A	1821.98	11.8	13.7	16.6

Capillary Pressure (psi)	End-Face Water Saturation (%pv)
0	100
1	100
2	100
5	80.9
10	73.6
20	65.1
40	54.3
60	46.0

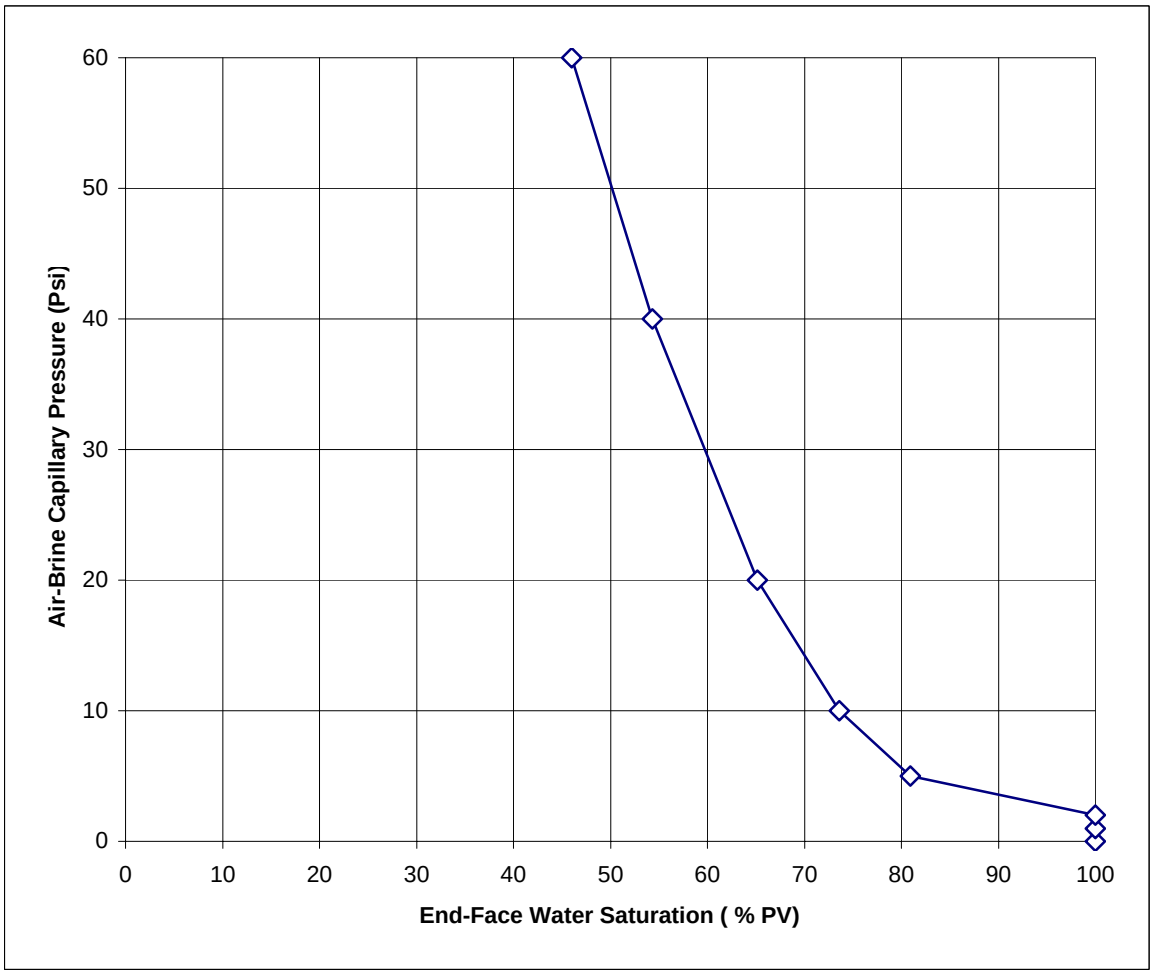

Air-brine Capillary Pressure by Centrifuge at Ambient

Sample no.	Depth (m)	At Ambient		
		Kinf (md)	Kair (md)	Porosity (%)
75A	1822.83	685	706	25.7

Capillary Pressure (psi)	End-Face Water Saturation (%pv)
0	100
1	80.5
2	55.7
5	41.0
10	30.9
20	22.9
40	17.7
60	15.7

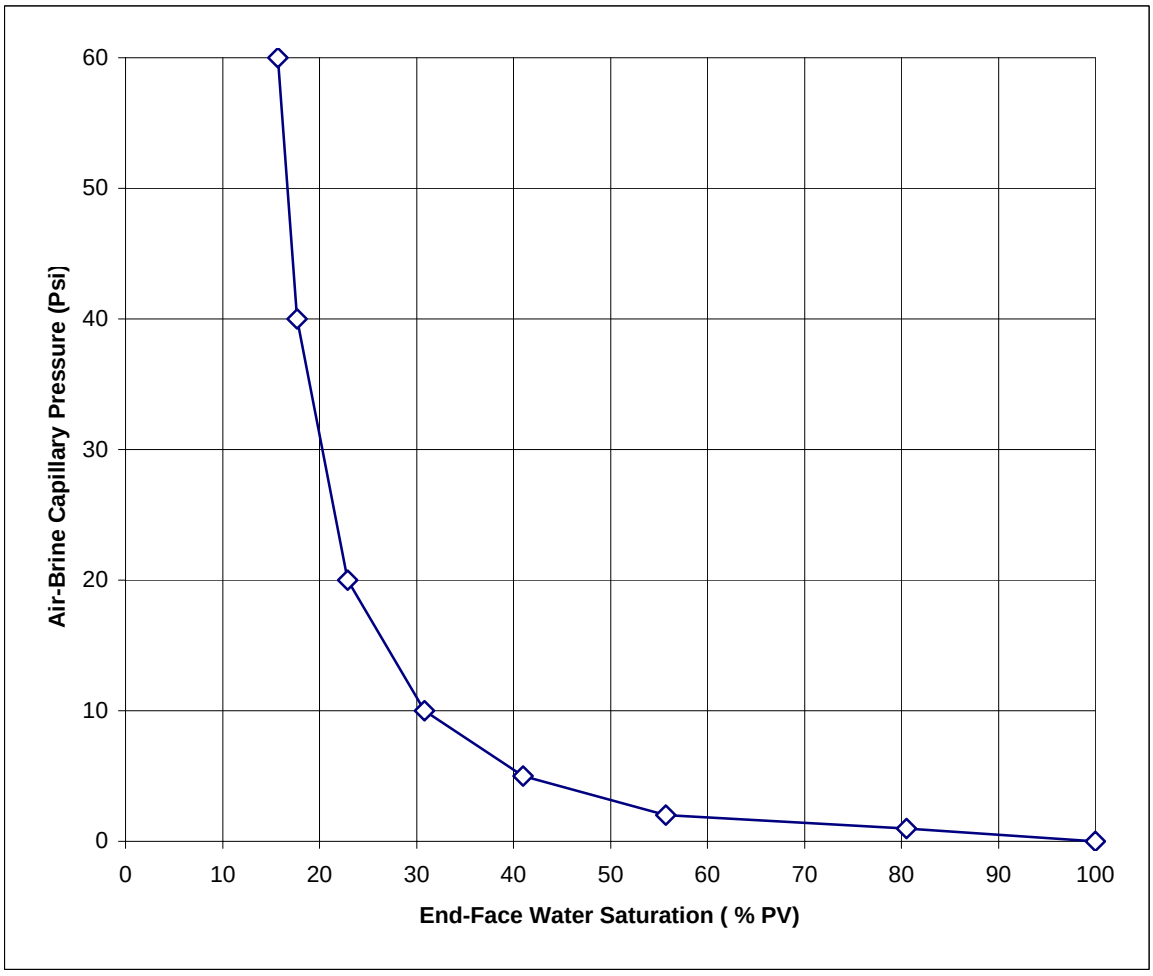

Air-brine Capillary Pressure by Centrifuge at Ambient

Sample no.	Depth (m)	At Ambient		
		Kinf (md)	Kair (md)	Porosity (%)
79	1824.03	5860	6430	25.5

Capillary Pressure (psi)	End-Face Water Saturation (%pv)
0	100
1	39.6
2	27.9
5	22.3
10	17.5
20	13.5
40	10.1
60	8.4

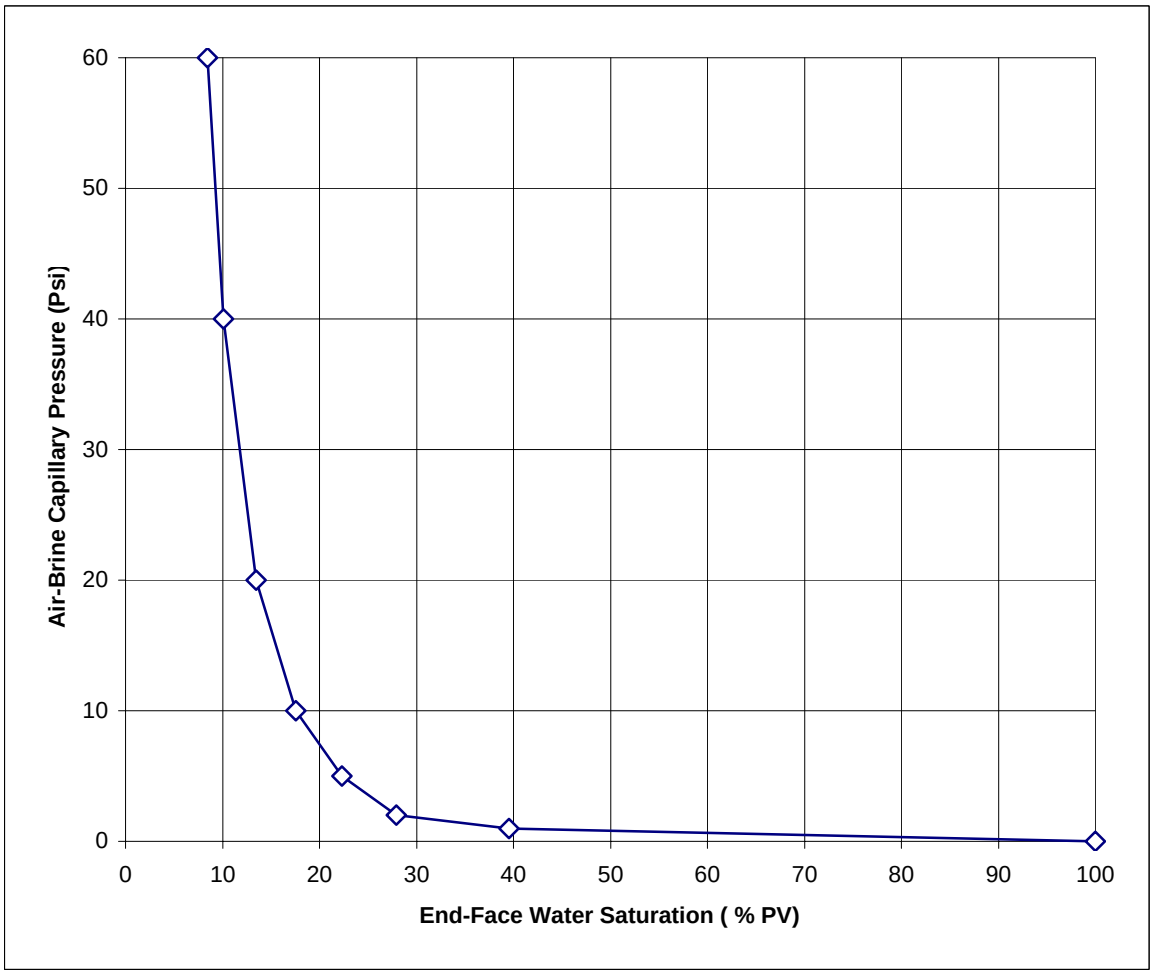

Air-brine Capillary Pressure by Centrifuge at Ambient

Sample no.	Depth (m)	At Ambient		
		Kinf (md)	Kair (md)	Porosity (%)
82	1824.90	3050	3380	23.4

Capillary Pressure (psi)	End-Face Water Saturation (%pv)
0	100
1	56.0
2	33.8
5	20.7
10	16.5
20	13.6
40	11.0
60	10.4

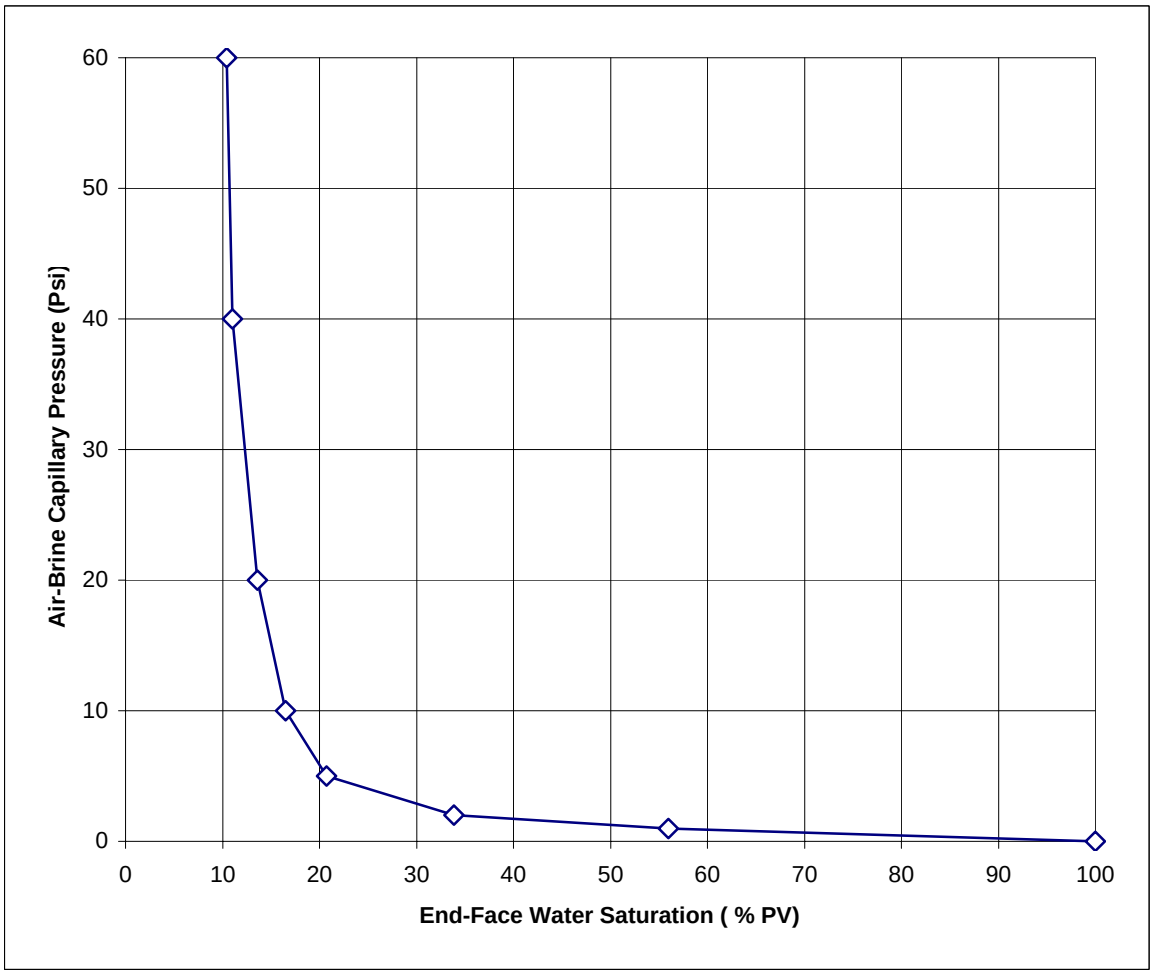

SECTION 4

RESIDUAL GAS SATURATION AND RELATIVE PERMEABILITY

RESIDUAL GAS SATURATION

Counter-Current Imbibition Method

Sample ID	Depth, (m)	Kair (md)	Porosity (%)	Initial Liquid Saturation, % PV	Initial Gas Saturation % PV	Residual Gas Saturation % PV	Gas Displaced	
							% PV	% IGIP
42	1812.90	3740	26.6	15.5	84.5	31.7	52.8	62.5
56A	1817.04	3070	22.0	12.2	87.8	31.5	56.3	64.1
72A	1821.98	13.7	16.6	42.0	58.0	29.1	28.9	49.8
75A	1822.83	706	25.7	19.5	80.5	36.1	44.4	55.2
79	1824.03	6430	25.5	8.7	91.3	32.3	59.0	64.6

Summary of the unsteady-state WATER-GAS relative permeability (end-point) analysis results (determined at 3100 psi NOBP)

Sample No.	Depth (m)	At 3100 psi NOBP				INITIAL CONDITIONS			TERMINAL CONDITIONS			
		Kair (md)	Porosity (%)	Permeability to Brine		Swi (% pv)	Initial gas in place (% pv)	Kgas at Swi (md)	Sgr (% pv)	Gas Recovery		Kw at Sgr (md)
				Kw (md)	Kw/Kair (%)					(% pv)	(% IIGP)	
6A	1792.60	448	24.5	331	73.9	14.9	85.1	421	31.5	53.6	63.0	39.7
28	1808.70	1960	20.1	1530	78.1	16.8	83.2	1739	30.8	52.4	63.0	158
40	1812.30	3690	24.0	2830	76.7	10.3	89.8	3287	31.5	58.2	64.9	251
51A	1815.73	8750	26.3	5170	59.1	9.2	90.8	8500	27.2	63.6	70.1	2429
59	1818.05	9040	22.6	8300	91.8	5.0	95.0	8407	32.3	62.7	66.0	1315
67A	1820.49	2090	24.8	1580	75.6	13.8	86.2	1793	28.8	57.4	66.6	205
76	1823.10	565	26.6	342	60.5	20.6	79.4	470	27.5	52.0	65.4	37.6
86	1826.10	7260	22.2	5200	71.6	11.4	88.6	6405	31.6	56.9	64.3	690

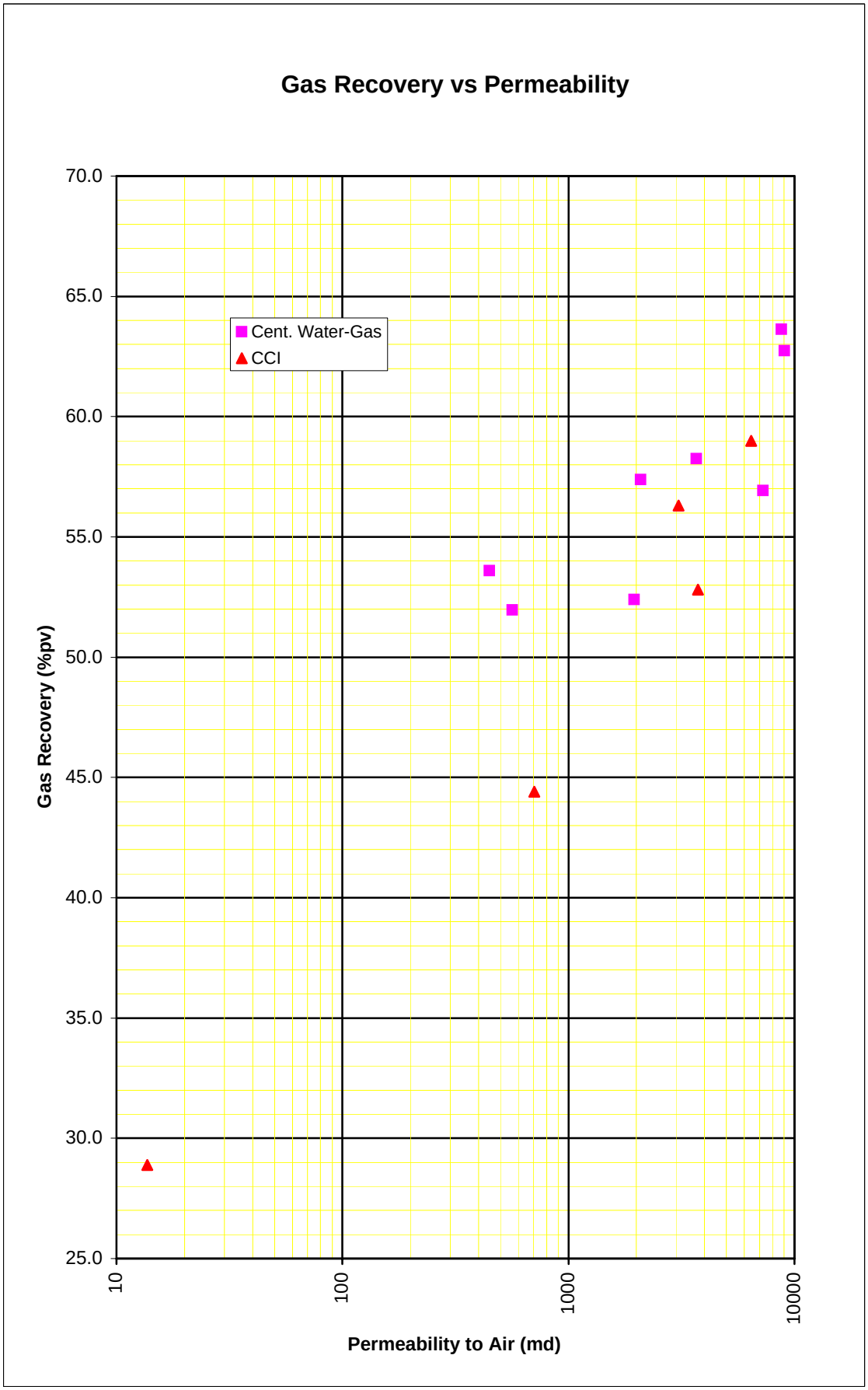
Gas Recovery vs Permeability
70.0
65.0
60.0
55.0
50.0
45.0
40.0
35.0
30.0
25.0
Gas Recovery (%pv)
Cent. Water-Gas
CCI
10
100
1000
10000
Permeability to Air (md)

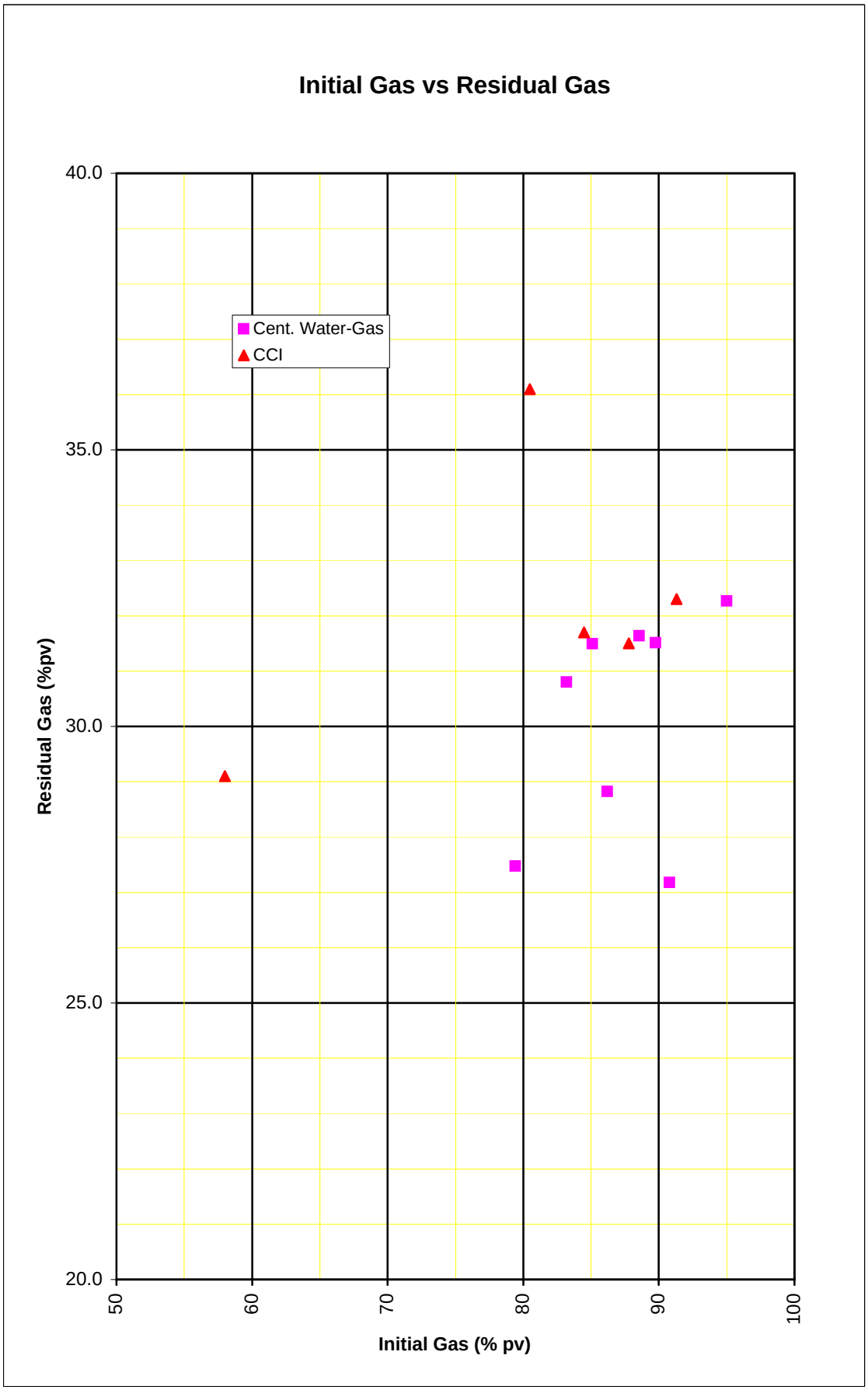
Initial Gas vs Residual Gas
Cent. Water-Gas
CCI
Residual Gas (%pv)
40.0
35.0
30.0
25.0
20.0
50
60
70
80
90
100
Initial Gas (% pv)

APPENDICES

APPENDIX 1
SUMMARY OF LABORATORY PROCEDURES

Summary of Laboratory Procedures

Sample Preparation

The core plugs tested comprised a combination of samples that had either undergone routine core analysis (RCA) or were newly drilled for this SCAL study (samples labelled with “A” or “B” suffices).

All samples selected for the study underwent visual and CT-screening to determine their suitability for SCAL. Samples which failed the screening stage were replaced with substitute samples. All replacement plugs also underwent visual and CT-screening.

The twelve newly drilled samples were cleaned in hot refluxing methanol prior to oven drying (at 90^{o}C) for porosity, permeability and grain density measurements.

Grain Volume and Grain Density

The weight, diameter and length of all samples were measured before they were processed through the Ultrapore^{TM} porosimeter to determine grain volume. As a standard quality control measure, a calibration check plug was run after every ten samples. Grain density data was calculated from grain volume and sample weight data.

Permeability and Porosity

Permeability and pore volume measurements were made on all twelve core plug samples at 800 and 3100 psi confining pressure in the CMS^{TM}300 automated core measurement system. A standard check plug was run with every five plug samples. Klinkenberg permeability (Kinf) values are obtained directly from the CMS-300, since it operates by unsteady-state principles. Porosity data was obtained by combining pore volumes from the CMS-300 with grain volumes from the Ultrapore^{TM} porosimeter.

The complete routine core analysis results are presented on 1-3.

Saturation

All samples undergoing SCAL analyses were evacuated and pressure saturated with a simulated formation brine of 25,000 ppm concentration comprising 80% NaCl and 20% KCl. All samples were weighed after saturation to check measured pore volumes.

Formation Resistivity

Nine samples were selected to undergo electrical properties measurements.

Each fully saturated sample was loaded into a coreholder at the reservoir equivalent NOBP (3100 psi) and the electrical resistivities measured on consecutive days until they were stable, indicating ionic equilibrium in the pore spaces. Formation resistivity factor (FRF) and cementation exponent (“m”) values were then calculated.

Each sample was then desaturated at incrementally increasing pressures using humidified air as the displacing medium. Electrical resistivity of the sample was measured at the incrementally decreasing partial saturations. When the sample had attained electrical equilibrium at each incremental desaturation stage, values of resistivity index (FRI) and saturation exponent (“n”) were calculated.

The trimmed ends of the plugs which underwent FRF and FRI measurements were cleaned in methanol, dried at 60^{o}C in a conventional oven then crushed and subjected to determinations of cation exchange capacity (CEC) using the ammonium acetate wet chemistry technique. These CEC values are used to calculate idealised “m*” and “n*” values using Waxman-Smits-Thomas equations.

Results from the electrical analysis are presented within SECTION 2 of this report.

Air-Brine Capillary Pressure by Centrifuge

The ten selected samples were initially pressure saturated with the simulated formation brine. All samples were weighed after saturation to check measured pore volumes.

The fully saturated samples were each loaded into individual centrifuge cups and loaded into the centrifuge. The samples were then subjected to non-stop centrifugation at rotational rates that were increased incrementally to generate equivalent pressures ranging from 1 to 60 psi in an air-brine system. Effluent brine volumes were monitored as the samples achieved capillary equilibrium at each incremental pressure.

Capillary pressure and end-face saturation data were then calculated from the raw data using data reduction techniques developed by Hassler-Brunner and later modified by other workers (e.g Rajan, Forbes). These results are presented within SECTION 3 of this report.

Residual Gas by Counter-Current-Imbibition (CCI)

On completion of the air-brine capillary pressure tests, a sub-set of five samples was selected to undergo residual gas saturation by CCI method.

The selected samples were re-cleaned, dried and the base data (permeability, porosity and grain density values) re-confirmed. Next the samples were saturated with toluene and their saturated weights checked to confirm helium injection pore volume data.

Each sample was then evaporated to a gravimetrically-determined initial “liquid” saturation with the remaining void pore space being air (“gas”) filled. Initial liquid saturations were estimated from Swi values established during capillary pressure measurements.

The samples were suspended, in turn, in a tared cradle below a weigh balance in a container of toluene. As the toluene imbibed into the samples, gas displacement was recorded by increasing weight versus time. Equilibrium residual gas saturations were then calculated and these data are presented in SECTION 4 of this report.

Specific Permeability to Brine

The eight selected samples were initially pressure saturated with the simulated formation brine. All samples were weighed after saturation to check measured pore volumes.

The brine saturated (100% Sw) samples were loaded into individual hydrostatic core holders and the confining pressure gradually increased to 3100 psi NOBP. Simulated formation brine was flowed through each sample at a slow constant rate. At equilibrium, when constant flow pressure was attained, permeability to brine (Kw at 100% Sw) measurements were recorded.

Unsteady-State Water-Displacing-Gas Relative Permeability (End-Point)

Unsteady-state water-displacing-gas tests were conducted on the same eight samples which underwent specific permeability to brine measurements.

The fully saturated (100% Sw) samples were reduced to immobile water saturation using the centrifuge. The samples were then removed from the centrifuge, weighed, and loaded into individual hydrostatic core holders. The confining stress was gradually increased to 3100 psi. Humidified gas (nitrogen) was then flowed through each sample and Krg at Swi determined.

Next, the sample was flooded at constant rate with simulated formation brine and gas production monitored until residual gas saturation was achieved (based on stable effluent gas volumes and differential pressures). At this stage, an effective permeability to brine at residual gas saturation (Kw at Sgr) was measured.

Utilising data from the unsteady-state water-gas (end-point) analysis, full relative permeability water-displacing-gas curves can be derived using suitable correlations (e.g Corey, MAK and other).

Results from the unsteady-state water-gas relative permeability (end-point) by centrifuge are presented in SECTION 4 of this report.

APPENDIX 2
SAMPLES DRILLED FOR MECHANICAL STRENGTH TESTS

Samples Drilled for Mechanical Strength Tests

Sample ID	Depth (m)

1.5" diameter horizontal plugs drilled with brine

A	1809.45
B	1809.50
C	1812.40
D	1812.45
E	1812.50
F	1817.77
G	1817.83
H	1817.88
I	1819.62
J	1819.67
K	1822.91
L	1822.95
M	1826.27
N	1826.33

1.0" diameter vertical plugs drilled with oil

W	1831.21
X	1831.21
Y	1831.21
Z	1831.21

APPENDIX 3
CT-SCAN DESCRIPTIONS

CT-Scan Descriptions (SCAL Plugs)

Sample 5A : (1792.55 m)

Predominantly fine quartz sandstone containing a few scattered framework grains to medium sand size. Rare greenish grains of possible glauconite are noted and other accessory components include mica and pyrite. Layering of mm-scale is a feature of the attenuation fabric; it trends more or less with the plug axis. Diffuse higher attenuation is related to finer grain size and associated pyrite dust. Rare spots of very high attenuation are almost certainly localised pyrite or possibly pyritised organic matter. The sample is moderately homogeneous and no defects are evident.

Sample 6A : (1792.60 m)

Fine quartz sandstone containing rare greenish grains of possible glauconite. Layering of mm-scale is apparent and this is the main feature of the attenuation fabric. Layers trend lengthwise with the plug axis but crossbedding is noted. Relatively higher attenuation highlighting some layers is attributable to traces of pyrite cement. Pyritised organic matter and glauconite also contributes to localised higher attenuation. More diffuse variations in attenuation relate to pore development; lower attenuation domains are inferred as more porous. The sample is moderately homogeneous and no defects are evident.

Sample 7 : (1793.00 m)

Mainly fine, rarely medium quartz sandstone; it shows layering trending more or less lengthwise with the plug axis. Accessory components include coaly organic matter with associated specks of siderite, greenish grains of possible glauconite and pyrite. The dominant feature of the attenuation fabric is localised very low attenuation (around 50 to 300 HU) inferred as organic matter. Layering of mm-scale is apparent and crossbedding is inferred. Scattered spots of highest attenuation are mainly related to localised pyrite but there also is some contribution from traces of siderite. The sample is moderately homogeneous and no defects are apparent.

CT-Scan Descriptions (SCAL Plugs) … cont'd

Sample 28 : (1808.70 m)

Poorly sorted somewhat bimodal quartz sandstone; it comprises layers that are fine to medium interspersed with coarser layers that are granular to pebbly in places. The layering is mm-scale, somewhat disturbed and trends generally lengthwise with the plug axis. Feldspars are noted amongst the coarser framework grains and accessory components include clays, pyrite and specks of 'coaly' organic matter. The poor layering and localised concentrations of coarser grains are revealed in the attenuation fabric. For the most part these grains float in a finer matrix but in places very low attenuation spots indicate the presence of larger pores. However a few of these are possibly attributable to organic matter. Disseminated spots and specks of very high attenuation are inferred as pyrite cement. The sample is overall moderately homogeneous and no defects are evident.

Sample 29 : (1809.05 m)

Mainly fine to medium, rarely coarse to granular quartz sandstone; it is layered on mm-scale. Accessory components include traces of pyrite, organic matter commonly pyritised, clays and mica. The attenuation fabric shows subplanar layers with a slight lengthwise dip; minor crossbedding is noted. Individual coarsest grains show moderately high attenuation. Several of the laminations also show moderately high attenuation but this is related to finer grain size and in particular the presence of clays. Localised very high attenuation is attributable to pyrite and pyritised organic matter. Lower attenuation speckling and spots point to relatively more porous domains. The sample is moderately homogeneous and no defects are evident.

Sample 40 : (1812.30 m)

Quartz sandstone, it comprises disturbed layers that are alternatively fine to medium and coarse to rarely granular; these are in subequal abundance. Accessory components include traces of organic matter and pyrite. Irregularly disseminated, low attenuation spots and speckles dominate the attenuation fabric. These are open pores. Rare spots of very high attenuation are localised pyrite cement. The disturbed layering is set slightly oblique to the plug axis and trends more or less lengthwise with the plug axis. The sample is moderately homogeneous and no defects are apparent.

CT-Scan Descriptions (SCAL Plugs) … cont'd

Sample 42 : (1812.90 m)

Fine to rarely granular quartz sandstone; it comprises layers that are alternately mainly fine to medium and medium to coarse. Accessory components include traces of pyrite and possible glauconite. The attenuation fabric reveals subplanar mm-scale layers that trend lengthwise with the plug axis. Disseminated very low attenuation spots and speckles and the generally low average attenuation point to a well-developed pore network. Rare very high attenuation is attributable to localised pyrite cement. The sample is moderately homogeneous and no defects are inferred.

Sample 44: (1813.45 m)

The sample is a probable coarse to granular quartz sandstone. The attenuation fabric reveals planar layering set slightly oblique to the plug axis. Disseminated very low attenuation spots and speckles point to a well-developed pore network in some of the layers. A minor streak of very high attenuation is possibly pyritised organic matter and other spots of very high attenuation are almost certainly attributable to traces of localised pyrite. The sample is moderately homogeneous and no defects are inferred.

Sample 47 : (1814.42 m)

The sample is a probable coarse to at least granular quartz sandstone. The fabric is quite chaotic with patchy concentrations of finer and coarser grains. Nevertheless, layering trending more or less lengthwise with the plug axis is apparent. Scattered spots and specks of very low attenuation are mainly attributable larger open pores although traces of organic matter cannot be discounted. Rare spots of very high attenuation are almost certainly localised pyrite cement. The sample is moderately homogeneous and no defects are evident.

CT-Scan Descriptions (SCAL Plugs) … cont'd

Sample 48 : (1814.75 m)

The sample is a probable medium to at least granular quartz sandstone. Disturbed layering trends lengthwise with the plug axis with high attenuation streaks inferred as pyritised organic matter along the layering trend. Other spots of very high attenuation are almost certainly localised pyrite cement. Sporadic very low attenuation spots are open pores, however irregular traces of low attenuation point to an open defect. The homogeneity of the sample is poor to moderate and it is probably defected.

Sample 48A : (1814.81 m)

The sample is a probable fine to medium, rarely coarse quartz sandstone containing minor 'coaly' organic matter and traces of pyrite. Two irregular very low attenuation features dominate the attenuation fabric; one of these is inferred as concentrated organic matter (around 150 to 350 HU) whereas the other is inferred as a possible open defect.

Sample 51A : (1815.73 m)

The sample is a probable coarse to very coarse quartz sandstone. The attenuation fabric reveals poorly defined layering trending more or less lengthwise with the plug axis. Most apparent however are disseminated spots of very low attenuation that point to a well-developed pore network. Overall the sample is essentially homogeneous and no defects are evident.

Sample 55 : (1816.80 m)

Fine to coarse, rarely granular quartz sandstone; it is moderately indurated and shows significant surficial spalling of grains. The attenuation fabric reveals mm-scale planar layers, trending more or less lengthwise with the plug axis. All layers and some more than others show disseminated spots of very low attenuation pointing to a well-developed pore network. The sample is moderately homogeneous and no defects are inferred.

CT-Scan Descriptions (SCAL Plugs) … cont'd

Sample 56 : (1817.00 m)

Fine to granular, rarely pebbly quartz sandstone; it shows disturbed subplanar layering trends at a somewhat oblique angle to the plug axis. Accessory components include traces of 'coaly' organic matter, 'golden' nodular pyrite and clays. The attenuation fabric reveals the layering but also two domains with significantly different average attenuation. The domain showing lower overall attenuation (around 1300 HU) is considered more porous. In contrast, the other domain averages around 1650 HU: it almost certainly contains a greater finer grained component. Several irregular shaped specks of very low attenuation are almost certainly organic matter. Scattered spots of very high attenuation are localised pyrite cement. The sample shows moderately poor homogeneity and no defects are inferred.

Sample 56A : (1817.04 m)

The sample is a probable fine to medium, rarely granular to pebbly quartz sandstone containing accessory traces of 'coaly' organic matter and pyrite. The attenuation fabric shows poorly defined disturbed layering trending lengthwise with the plug axis. Very low attenuation spots are for the most part pores, however larger patches are almost certainly concentrations of organic matter. Rare spots of very high attenuation are almost certainly pyrite cement. The sample is moderately homogeneous and no defects are inferred.

Sample 57A : (1817.50 m)

The sample is a probable medium to at least lower pebbly quartz sandstone. The attenuation fabric reveals mm-scale layering trending more or less lengthwise with the plug axis. Also apparent is cross bedding with layers in this domain set more oblique to the plug axis. Irregularly disseminated spots of very low attenuation are larger open pores although traces of organic matter cannot be discounted. The sample is moderately homogeneous and no defects are inferred.

CT-Scan Descriptions (SCAL Plugs) … cont'd

Sample 59 : (1818.05 m)

Medium to coarse, rarely granular to pebbly quartz sandstone; it is moderately indurated and shows significant surficial spalling of grains. Accessory components include pyrite in the form of 'dust' and 'golden' nodules. The attenuation fabric reveals mm-scale planar layers, trending more or less lengthwise with the plug axis. All layers and some more than others show disseminated spots of very low attenuation pointing to a well-developed pore network. Rare spots of very high attenuation are localised pyrite cement. The sample is moderately homogeneous and no defects are inferred.

Sample 62B : (1818.84 m)

A probable quartz sandstone; it is bimodal with layers that are fine to medium juxtaposed with coarser domains that are dominantly granular to pebbly. The attenuation fabric reveals the layering as well as individual coarser grains. Layering is set somewhat oblique to the plug axis. Irregular very high attenuation streaks and spots are a feature of on finer domain; these are attributable to pyrite, possibly pyritised organic matter. Spots of very low attenuation within the coarser domain are inferred as intergranular pores. The sample shows moderately poor homogeneity and no defects are apparent.

Sample 62A : (1818.95 m)

Mainly very fine, rarely medium silty quartz sandstone; it contains a significant clay component that is in places is associated with pyrite 'dust' as well as traces of 'coaly' organic matter. The speckled somewhat compartmental attenuation fabric is reminiscent of bioturbation. Highest attenuation spots and streaks are attributable to the presence of pyrite. Patchy moderately lower attenuation domains are indicative of cleaner sand. The sample shows poor to moderate homogeneity overall and no defects are inferred.

CT-Scan Descriptions (SCAL Plugs) … cont'd

Sample 64 : (1819.50 m)

Mainly fine to coarse, minor granular quartz sandstone; it is moderately indurated and shows significant surficial spalling of grains. Accessory components include pyrite in the form of 'dust' and 'golden' nodules as well as traces of organic matter. The attenuation fabric reveals poorly defined planar layers, trending more or less lengthwise with the plug axis. Disseminated spots of very low attenuation point to a well-developed pore network. Rare spots of very high attenuation are localised pyrite cement. Several diffuse patches of moderate attenuation are probably finer grained. The sample is moderately homogeneous and no defects are inferred.

Sample 65 : (1819.80 m)

Mainly fine to coarse, minor granular quartz sandstone; it shows layering of mm-scale trending more or less lengthwise with the plug axis. Accessory components include 'coaly' organic matter and pyrite in the form of 'dust' and 'golden' nodules. The attenuation fabric reveals the layering as subplanar; a distinctive lamination showing moderately high attenuation is finer grained with accessory organic matter and clays. Disseminated spots of very low attenuation are indicative of a well-developed pore network. Rare spots of very high attenuation are localised pyrite cement. The sample is moderately homogeneous and no defects are inferred.

Sample 67A : (1820.49 m)

Mainly fine to medium, rarely coarse quartz sandstone with accessory pyrite and traces of organic matter. The attenuation fabric shows evidence of mm-scale planar layering trending lengthwise with the plug axis. Disseminated spots of lower attenuation are predominantly larges pores. Sporadic spots and clumps of very high attenuation are localised pyrite cement. The sample is moderately homogeneous and no defects are inferred.

CT-Scan Descriptions (SCAL Plugs) … cont'd

Sample 72 : (1821.90 m)

Mainly very fine, rarely medium silty quartz sandstone; it contains a significant clay component that is in places is associated with pyrite 'dust' as well as traces of 'coaly' organic matter. Some of the organic matter is pyritised. The attenuation fabric is reminiscent of bioturbation and probable burrows are noted. Highly disturbed layering trends generally lengthwise with the plug axis. Highest attenuation spots and streaks are attributable to relatively finer grainsize and the presence of pyrite cement. Moderately higher attenuation is suggestive of finer grainsize with a somewhat lesser pyrite component. Patchy moderately lower attenuation domains are indicative of cleaner sand. In these domains some relict cross ripples are inferred. The sample shows poor to moderate homogeneity overall and no defects are evident.

Sample 72A : (1821.98 m)

Mainly very fine, rarely medium silty quartz sandstone; it contains a significant clay component, localised pyrite and traces of 'coaly' organic matter. The attenuation fabric is reminiscent of bioturbation and burrow structures are noted. Highest attenuation spots and streaks are attributable to the presence of pyrite. Very low and high attenuation juxtaposed points to pyritised organic matter. Patchy moderately lower attenuation domains are indicative of cleaner sand. The sample shows poor to moderate homogeneity overall and no defects are inferred.

Sample 75A : (1822.83 m)

Mainly fine to medium, rarely pebbly quartz sandstone. Accessory components include traces of pyrite and 'coaly' organic matter. The attenuation fabric shows somewhat disturbed mm-scale layering set at an oblique angle to the plug axis. Minor finer grained laminations are indicated by diffuse slightly higher attenuation. Isolated irregular patches of moderately high attenuation are individual larger grains. Lower attenuation spots are predominantly larger pores although organic matter cannot be discounted. Rare spots of very high attenuation are localised pyrite. The sample is moderately homogeneous and no defects are inferred.

CT-Scan Descriptions (SCAL Plugs) … cont'd

Sample 76 : (1823.10 m)

Mainly fine to medium, rarely granular quartz sandstone; it contains accessory traces of pyrite and 'coaly' organic matter. The attenuation fabric shows possible layering set lengthwise with the plug axis. Lower attenuation spots are predominantly larger pores although organic matter cannot be discounted. A distinctive very high attenuation streak is inferred as a pyritised flake of organic matter. The sample is essentially homogeneous and no defects are inferred.

Sample 77A : (1823.36 m)

Mainly fine to medium quartz sandstone, it contains a minor component of coarser framework grains to at least upper granule-size. The attenuation fabric shows somewhat disturbed mm-scale layering set at an oblique angle to the plug axis. Minor finer grained laminations are indicated by diffuse slightly higher attenuation. Isolated irregular patches of moderately high attenuation are individual larger grains. Lower attenuation spots are predominantly larger pores although organic matter cannot be discounted. Rare spots of very high attenuation are localised pyrite. The sample is moderately homogeneous and no defects are evident.

Sample 79 : (1824.03 m)

Mainly medium, rarely granular quartz sandstone; it contains accessory traces of 'coaly' organic matter and pyrite. A distinctive patch of 'coal' several mm thick is noted at the plug margin. Disseminated very low attenuation spots that for the most part are inferred as larger intergranular pores, dominate the attenuation fabric. More rarely this very low attenuation points to organic matter, as is the case for the largest of these domains. The organic matter noted at the plug margin is not significantly penetrative. The sample is essentially homogeneous and no defects are inferred.

CT-Scan Descriptions (SCAL Plugs) … cont'd

Sample 82 : (1824.90 m)

Mainly medium, rarely granular to pebbly quartz sandstone; it contains accessory traces of pyrite and 'coaly' organic matter. The attenuation fabric reveals mm-scale planar layering set somewhat oblique to the plug axis. However, disseminated very low attenuation spots inferred for the most part as larger intergranular pores dominate the fabric. Largest patches of very low attenuation (around 30 to 300 HU) are inferred as organic matter. Rare spots of very high attenuation are localised pyrite cement. The sample is moderately homogeneous and no defects are evident.

Sample 84 : (1825.50 m)

Mainly medium to coarse, rarely granular to pebbly quartz sandstone; it contains accessory traces of 'coaly' organic matter and pyrite. The attenuation fabric reveals disturbed layering set at an oblique angle to the plug axis. However, dominant disseminated spots of very low attenuation point to a well-developed pore network. The sample is moderately homogeneous and no defects are inferred.

Sample 86 : (1826.10 m)

Mainly fine to coarse, rarely granular quartz sandstone; it contains accessory traces of 'coaly' organic matter and pyrite. The attenuation fabric reveals mm-scale planar layers, these are set oblique to the plug axis. All layers and some more than others show disseminated spots of very low attenuation pointing to a well-developed pore network. The sample is moderately homogeneous and no defects are inferred.

CT-Scan Descriptions (Horizontal Plugs Drilled for Mechanical Strength Tests)

Sample A : (1809.45 m)

Moderately well sorted, fine to coarse, mainly upper fine, quartz sandstone; the minor coarser component (~5%) occurs as rare 'floating' grains as well as in localised patches and as millimetre scale subplanar layers. Accessory components include traces of 'coaly' organic matter, both disseminated and rarely layer-dominant, pyrite, mica and greenish micaceous grains of possible glauconite. The attenuation fabric shows millimetre to centimetre scale subplanar layering set at an oblique angle to the plug axis. Higher attenuation defining some layers is attributable to relatively finer grain size and associated traces of pyrite 'dust'. Lowest attenuation is for the most part attributable to open pore abundance although rare local contribution from organic matter cannot be discounted. The sample shows non-parallel bedding, is moderately homogeneous overall and no defects are evident.

Sample B : (1809.50 m)

Moderately sorted, fine to granular, mainly upper fine, quartz sandstone; the lesser (~10 %) coarser component is predominantly localised in millimetre scale subplanar layers. Accessories include traces of 'coaly' organic matter (~1%), both disseminated and in millimetre scale layers, pyrite as 'dust' and intergranular nodules, and mica. Layering is the dominant feature of the attenuation fabric; it is millimetre scale and set at an oblique angle to the plug axis. Low angle crossbedding is inferred. Higher attenuation defining many of the layers is attributable to relatively finer grain size and the presence of pyrite 'dust'. Streaks of highest attenuation are domains that are pyrite-dominated (possibly pyritised organics). Isolated spots showing highest attenuation are almost certainly attributable to intergranular pyrite. Lowest attenuation is for the most part attributable to open pore abundance although rare local contribution from organic matter cannot be discounted. The sample shows non-parallel bedding, is moderately homogeneous overall and no defects are evident.

CT-Scan Descriptions (Horizontal Plugs Drilled for Mechanical Strength Tests) … cont'd

Sample C : (1812.40 m)

Moderately sorted, very fine to very coarse, mainly medium, quartz sandstone; the minor coarser component (~20%) is localised in millimetre scale subplanar layers. Grain spalling is noted. Accessory components include 'coaly' organic matter, concentrated for the most part in millimetre scale layers, pyrite and mica. The attenuation fabric reveals low angle crossbedding but overall layering is lengthwise with the plug axis. Concentrations of lowest attenuation spots are for the most part attributable to larger pores, and lower attenuation generally is indicative of pore abundance. However, rare spots and specks of low attenuation are due to the presence of organic matter. Highest attenuation specks particularly associated with one layer are probably pyrite concentrations either as pyritised organics or intergranular cement. However, siderite cannot be discounted. The sample is moderately homogeneous overall and no defects are evident.

Sample D : (1812.45 m)

Moderately poorly sorted, fine to pebbly, mainly medium, quartz sandstone; the lesser coarser component (~10%) occurs as localised patches and in millimetre scale subplanar layers. Accessory components include 'coaly' organic matter (~1%), both disseminated and in millimetre scale layers, and traces of pyrite and mica. The attenuation fabric reflects the layering that trends generally lengthwise with the plug axis; low angle crossbedding is apparent. Individual coarsest framework grains are evident and show typical uniform moderately high attenuation. Lower attenuation generally is associated with pore abundance, but in places larger low attenuation specks are almost certainly attributable to organic matter. Rare highest attenuation specks are inferred as pyrite cement. The sample shows poor to moderate homogeneity and no defects are apparent.

Sample E : (1812.50 m)

Moderately well sorted, very fine to granular, predominantly medium, quartz sandstone; the minor coarser component (~10%) is localised in millimetre scale subplanar layers. Grain spalling is noted. Accessory components include 'coaly' organic matter concentrated for the most part in millimetre scale layers, pyrite and mica. The main feature of the attenuation fabric is layering trending generally lengthwise with the plug axis; very low angle crossbedding is apparent. Lower attenuation generally is associated with pore abundance, but in places there is very minor contribution from organic matter. Rare spots of highest attenuation are almost certainly attributable to pyrite cement, however traces of siderite may also contribute in places. The sample is moderately homogeneous and no defects are evident.

CT-Scan Descriptions (Horizontal Plugs Drilled for Mechanical Strength Tests) … cont'd

Sample F : (1817.77 m)

Moderately poorly sorted, medium to lower pebbly, mainly coarse to very coarse, quartz sandstone; significant grain spalling is noted. A trace of pyrite occurs as 'dust' and rare 'golden' nodules. Coarsest individual framework grains and low attenuation macropores are the features most apparent in the fabric; less apparent is layering set parallel to and variably oblique to the plug axis; crossbedding is inferred. Rare specks of highest attenuation (>3000 HU) are almost certainly attributable to localised intergranular pyrite cement. The sample is moderately homogeneous overall and no defects are evident.

Sample G : (1817.83 m)

Moderately poorly sorted, medium to lower pebbly, mainly very coarse to granular, quartz sandstone; significant grain spalling is noted. A trace of pyrite occurs as 'dust' and rare 'golden' nodules. Coarsest individual framework grains and low attenuation macropores are the features most apparent in the fabric. Layering also is evident; it dips at a low angle to the plug axis. Rare specks of highest attenuation (>3000 HU) are almost certainly attributable to localised intergranular pyrite cement. The sample may be more bimodal than is visually apparent but overall it is moderately homogeneous and no defects are evident.

Sample H : (1817.88 m)

Moderately poorly sorted, medium to granular, mainly coarse to very coarse, quartz sandstone; it is a relatively short sample and significant grain spalling is noted. A trace of pyrite occurs as 'dust' and rare 'golden' nodules. Disseminated spots of low attenuation, inferred as open macropores, are the main feature of the attenuation fabric. Poorly developed layering is inferred; it trends more or less lengthwise with the plug axis. Rare spots of very high attenuation are almost certainly attributable to intergranular pyrite cement. The sample is moderately homogeneous and no defects are apparent.

CT-Scan Descriptions (Horizontal Plugs Drilled for Mechanical Strength Tests) … cont'd

Sample I : (1819.62 m)

Moderately well sorted, fine to coarse, mainly medium, quartz sandstone; the minor coarser component (~5%) occurs as rare 'floating' grains as well as concentrated in millimetre scale subplanar layers. Spalling of grains is noted. Accessory components include clay clasts and trails (~1%), traces of 'coaly' organic matter, both disseminated granular and as flecks in millimetre scale layers, pyrite and mica. The attenuation fabric shows disturbed layering trending slightly oblique to the plug axis. Diffuse moderately higher attenuation defining several layers and patches is suggestive of finer grain size, possibly clay concentrations. Rare very high attenuation spots are almost certainly attributable to pyrite cement. Although lower attenuation generally is associated with pore abundance, rarely in places there is a contribution from organic matter; this is the case for several of the larger low attenuation specks. The sample is moderately homogeneous overall and no defects are evident.

Sample J : (1819.67 m)

Moderately sorted, fine to granular, mainly medium quartz sandstone; the minor coarser component (~5%) occurs as rare 'floating' grains as well as concentrated in millimetre scale layers. Accessories include traces of 'coaly' organic matter, both disseminated granular and as flecks in trails associated with clays, pyrite and mica. It is a relatively short sample and grain spalling is noted. The attenuation fabric reveals poorly developed layering set at a low angle to the plug axis; slightly higher attenuation in a marginal layer is attributable to finer grain size, possibly clays. Disseminated low attenuation spots and specks are for the most part attributable to larger pores but there also is a very minor contribution from organic matter. Individual larger framework grains show moderately high attenuation. Rare spots of very high attenuation are almost certainly attributable to pyrite cement. The sample is moderately homogeneous overall and no defects are evident.

CT-Scan Descriptions (Horizontal Plugs Drilled for Mechanical Strength Tests) … cont'd

Sample K : (1822.91 m)

Moderately poorly sorted, fine to very coarse, mainly lower medium silty quartz sandstone. The minor coarser component (~5%) is localised in patches and concentrated in millimetre scale layers. Grain spalling is noted. Accessory components include organic matter in wispy trails (1%), clays (tr-1%) with associated traces of pyrite 'dust', nodular pyrite and mica. The ragged attenuation fabric is reminiscent of bioturbation; disturbed bedding is set at an oblique angle to the plug axis. Moderately higher attenuation in the fabric reflects finer grain size, silt and in particular clays. Highest attenuation (>3000 HU) is almost certainly attributable to pyrite cement. Generally, lower attenuation is associated with pore abundance, however isolated spots of very low attenuation may well be attributable to traces of organic matter. The sample shows poor to moderate homogeneity and no defects are evident.

Sample L : (1822.95 m)

Moderately poorly sorted, fine to granular, mainly lower medium silty quartz sandstone. The minor coarser component (~7%) is localised in patches and concentrated in millimetre scale layers. Grain spalling is noted. Accessory components include traces of organic matter both disseminated and concentrated in millimetre scale layers, clays with associated traces of pyrite 'dust', nodular pyrite, and pale as well as greenish mica. The ragged attenuation fabric is reminiscent of bioturbation; disturbed bedding is set at an oblique angle to the plug axis. Moderately higher attenuation in the fabric reflects finer grain size, silt and in particular clays. Highest attenuation (>3000 HU) is almost certainly attributable to localised pyrite cement. Generally lower attenuation is associated with pore abundance, however isolated spots of very low attenuation may well be attributable to traces of organic matter. The sample shows poor to moderate homogeneity and no defects are apparent.

Sample M : 1826.27 m

Poorly sorted, bimodal quartz sandstone; it is mainly coarse to very coarse with lesser domains (~30%) more of medium sand size. Grain spalling is noted. In places there are rare trails of organic-charged clays, several feldspar grains show evidence of degradation. Irregularly disseminated low attenuation macropores are the most dominant feature of the fabric, layering also is evident; it dips at a low angle to the plug axis and may show very low angle crossbedding. Very rare specks of highest attenuation (>3000 HU) are almost certainly attributable to localised intergranular pyrite cement. The sample is poorly to moderately homogeneous and no defects are evident.

CT-Scan Descriptions (Horizontal Plugs Drilled for Mechanical Strength Tests) … cont'd

Sample N : (1826.33 m)

Poorly sorted, bimodal quartz sandstone; it is mainly medium to coarse with a lesser component (~20%) coarse to very coarse and rarely pebbly. Grain spalling is noted. Accessory components include traces of 'coaly' granular organic matter, localised clays with associated pyrite 'dust', mica and partially degraded feldspars. Low attenuation spots and specks in the fabric are inferred as macropores for the most part but rarely these may also be attributable to organic matter. Layering also is evident; it is subplanar and dips at a low angle to the plug axis. Rare specks of highest attenuation (>3000 HU) are almost certainly attributable to localised intergranular pyrite cement. The sample is poorly to moderately homogeneous and no defects are evident.

CT-Scan Descriptions (Vertical Plugs Drilled for Mechanical Strength Tests)

Sample W : (1831.21 m)

Shale with accessory traces of 'coaly' organic matter in the form of disseminated flecks. Minor patches of silt gradational in part to very fine sand are noted. Minor pyrite cement (~5%) forms elongate intergranular nodules to at least 15 mm; these very high attenuation domains are the most dominant feature of the attenuation fabric. Layering set at a high oblique angle to the plug axis is inferred. No significant fracture defects are apparent but a very minor open defect is inferred; it is partially penetrative lengthwise from one of the plug faces. This defect can be removed by trimming. The sample shows very poor homogeneity.

Sample X: (1831.21 m)

Slightly silty shale with accessory traces of disseminated 'coaly' organic matter; it contains minor nodular pyrite cement (~3%). More diffuse traces of pyrite follow the inferred trend of layering that is set highly oblique to the plug axis. Along this trend is a low attenuation trace inferred as a possible fine open defect. The sample shows poor to moderate homogeneity. The defect can be removed and subsequent homogeneity improved by trimming.

Sample Y : (1831.21 m)

Slightly silty shale with accessory traces of disseminated 'coaly' organic matter; it contains minor nodular pyrite cement (~3%). Apparent layering is set at high oblique angle to the plug axis. No defects are inferred and the sample shows poor to moderate homogeneity.

Sample Z : (1831.21 m)

Slightly silty shale with accessory traces of disseminated 'coaly' organic matter; it contains minor nodular pyrite cement (~3%). Apparent layering is set at high oblique angle to the plug axis. No defects are inferred and the sample shows poor to moderate homogeneity.

APPENDIX 4
CT-SCAN AND CORE PLUG PHOTOGRAPHS

Origin Energy Limited
Halladale - 1
X-ray CT Images and Base Data

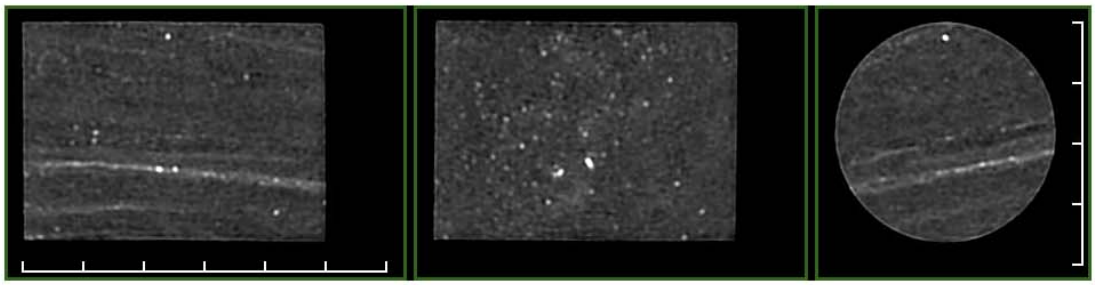

SAMPLE : 5A
DEPTH (m): 1792.55

Ka (mD): 302
Por (%): 26.0
GD (g/cc): 2.652

CT No.(HU): 1292

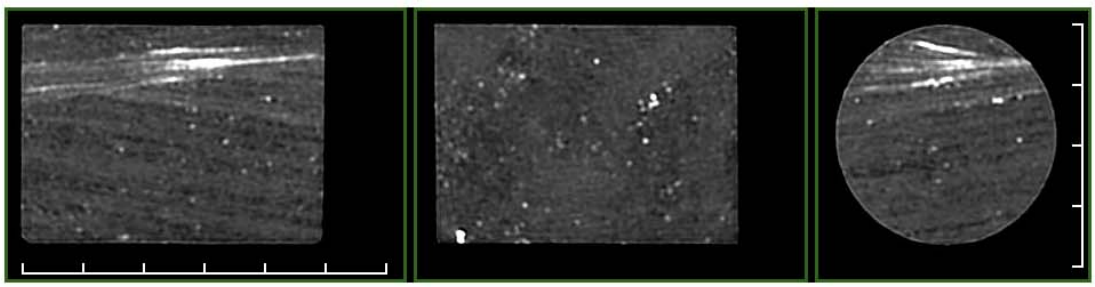

SAMPLE : 6A
DEPTH (m): 1792.60

Ka (mD): 470
Por (%): 25.0
GD (g/cc): 2.661

CT No.(HU): 1379

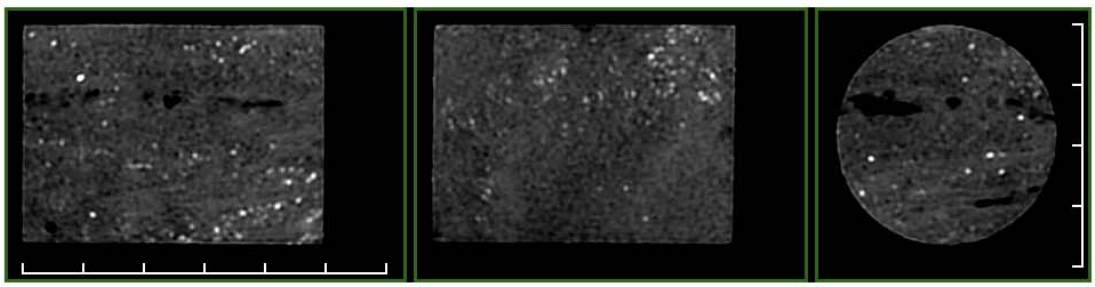

SAMPLE : 7
DEPTH (m): 1793.00

Ka (mD): 958
Por (%): 26.6
GD (g/cc): 2.648

CT No.(HU): 1200

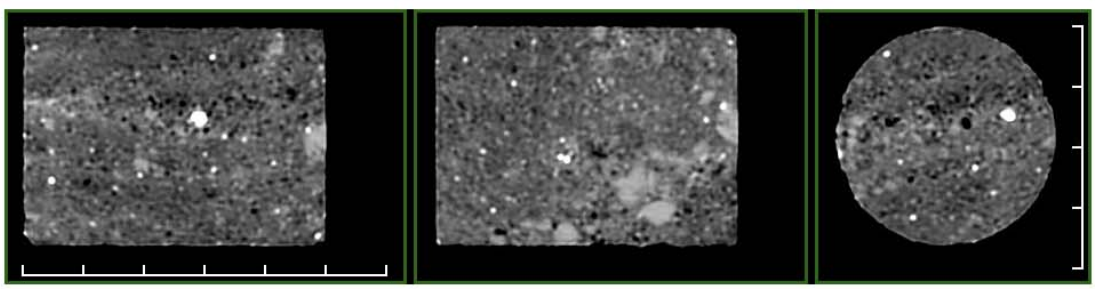

SAMPLE : 28
DEPTH (m): 1808.70

Ka (mD): 2110
Por (%): 20.9
GD (g/cc): 2.662

CT No.(HU): 1445

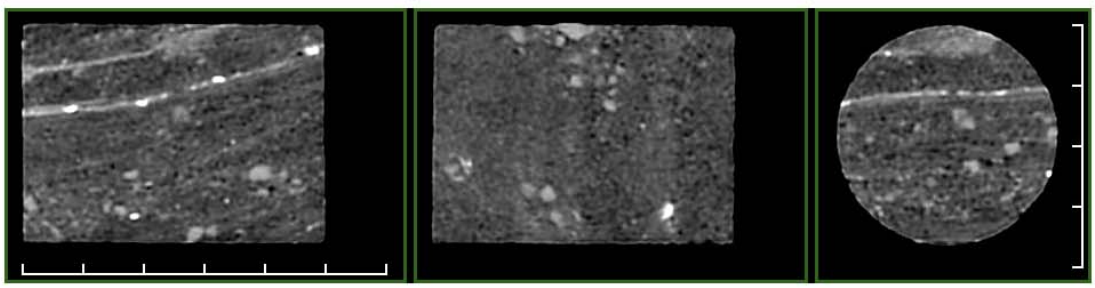

SAMPLE : 29
DEPTH (m): 1809.05

Ka (mD): 699
Por (%): 22.9
GD (g/cc): 2.670

CT No.(HU): 1410

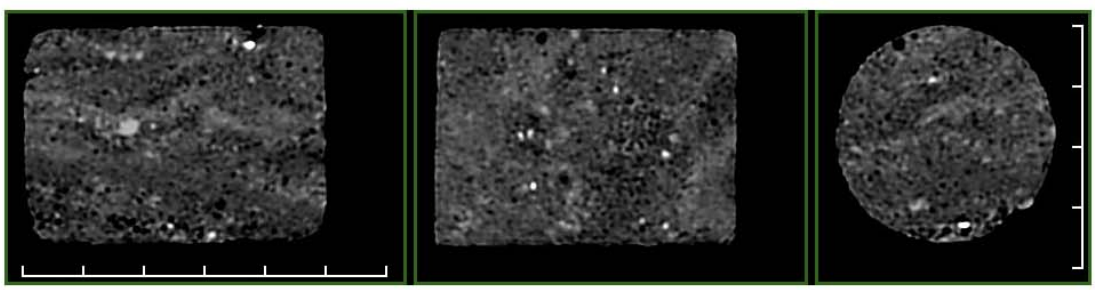

SAMPLE : 40
DEPTH (m): 1812.30

Ka (mD): 4060
Por (%): 25.0
GD (g/cc): 2.653

CT No.(HU): 1289

scale in centimetres

Copyright 2005 All Rights Reserved
Coshell & Associates

Origin Energy Limited
Halladale - 1
X-ray CT Images and Base Data

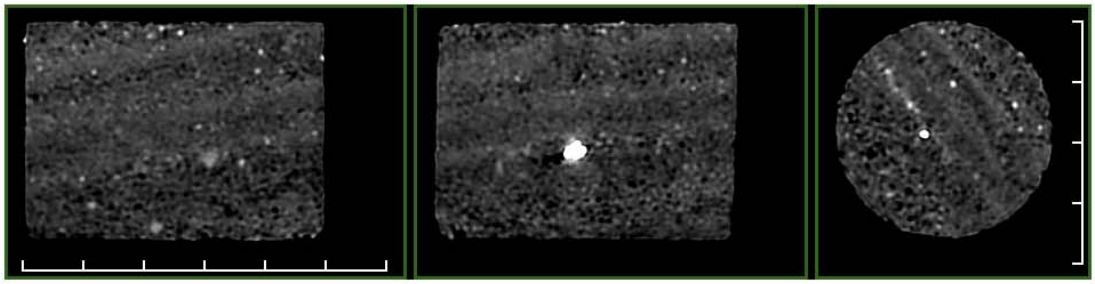

SAMPLE : 42
DEPTH (m): 1812.90

Ka (mD): 3740
Por (%): 26.6
GD (g/cc): 2.659

CT No.(HU): 1264

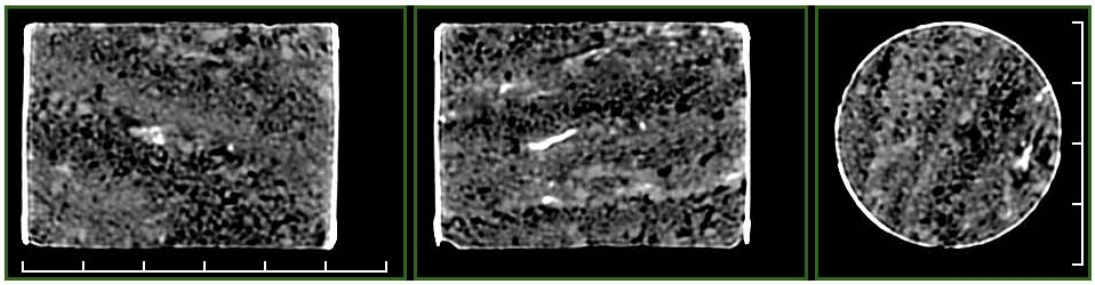

SAMPLE : 44
DEPTH (m): 1813.45

Ka (mD): 3180
Por (%): 22.1
GD (g/cc): 2.625

CT No.(HU): 1377

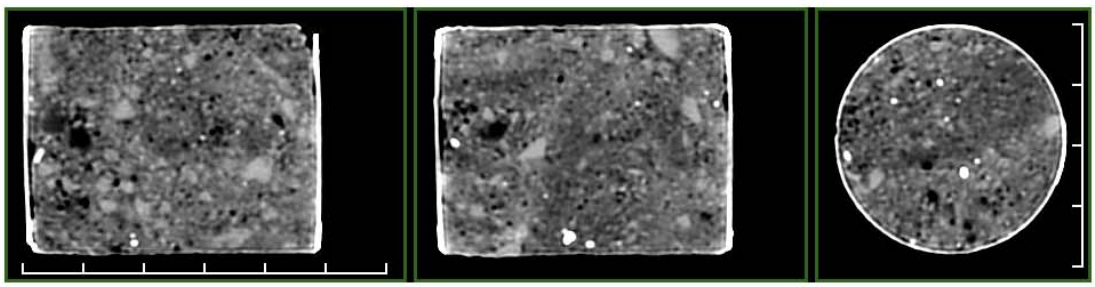

SAMPLE : 47
DEPTH (m): 1814.42

Ka (mD): 501
Por (%): 18.6
GD (g/cc): 2.651

CT No.(HU): 1474

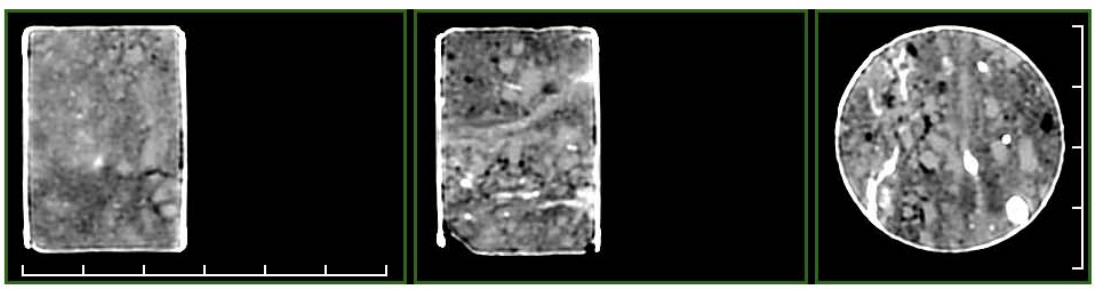

SAMPLE : 48
DEPTH (m): 1814.75

Ka (mD): 415
Por (%): 17.3
GD (g/cc): 2.652

CT No.(HU): 1697

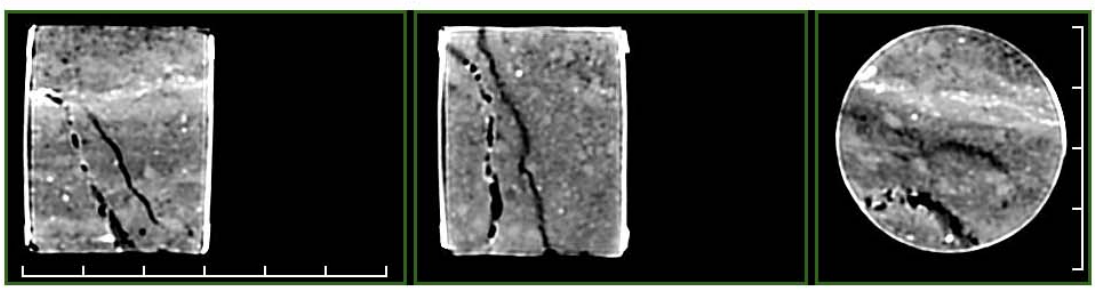

SAMPLE : 48A
DEPTH (m): 1814.81

Ka (mD): -
Por (%): -
GD (g/cc): -

CT No.(HU): 1650

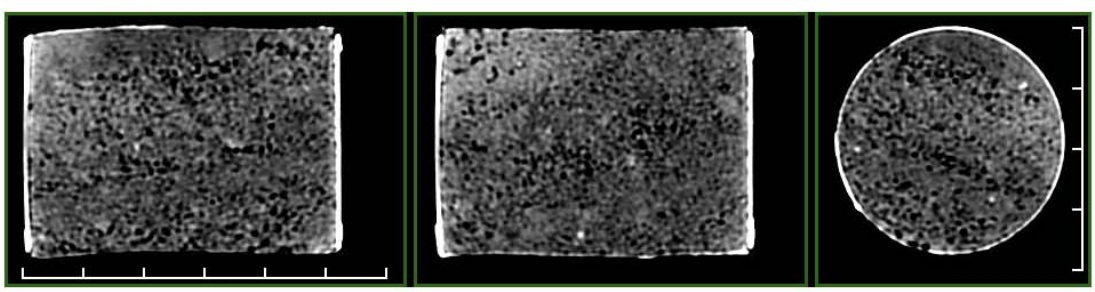

SAMPLE : 51A
DEPTH (m): 1815.73

Ka (mD): 8890
Por (%): 27.4
GD (g/cc): 2.648

CT No.(HU): 1340

scale in centimetres

Copyright 2005 All Rights Reserved
Coshell & Associates

Origin Energy Limited
Halladale - 1
X-ray CT Images and Base Data

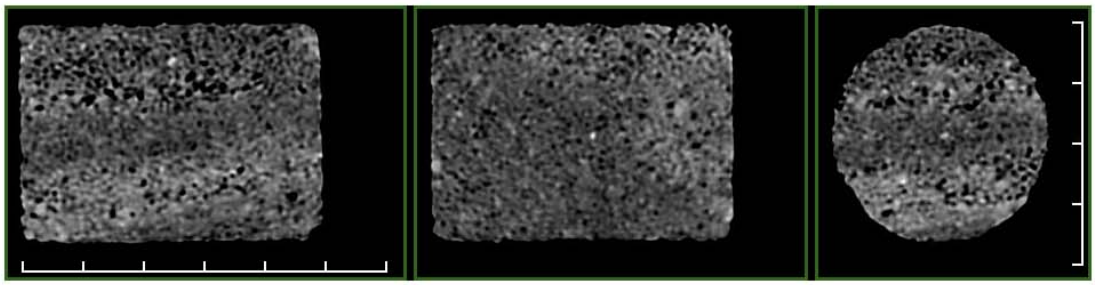

SAMPLE : 55
DEPTH (m): 1816.80

Ka (mD): 4220
Por (%): 24.3
GD (g/cc): 2.656

CT No.(HU): 1395

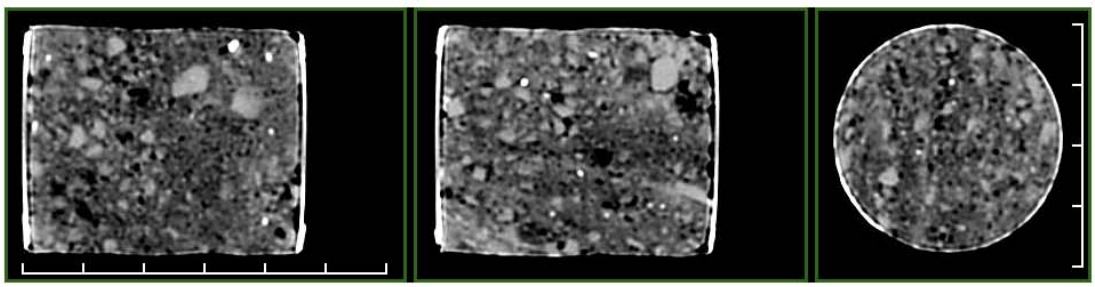

SAMPLE : 56A
DEPTH (m): 1817.04

Ka (mD): 3070
Por (%): 22.0
GD (g/cc): 2.652

CT No.(HU): 1444

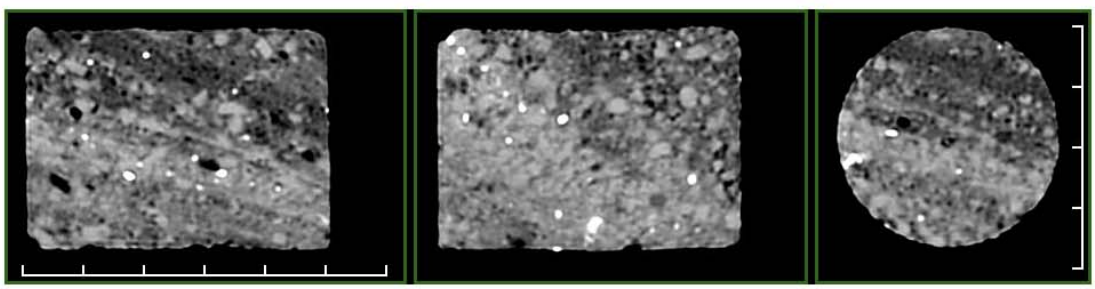

SAMPLE : 56
DEPTH (m): 1817.10

Ka (mD): 385
Por (%): 16.7
GD (g/cc): 2.654

CT No.(HU): 1547

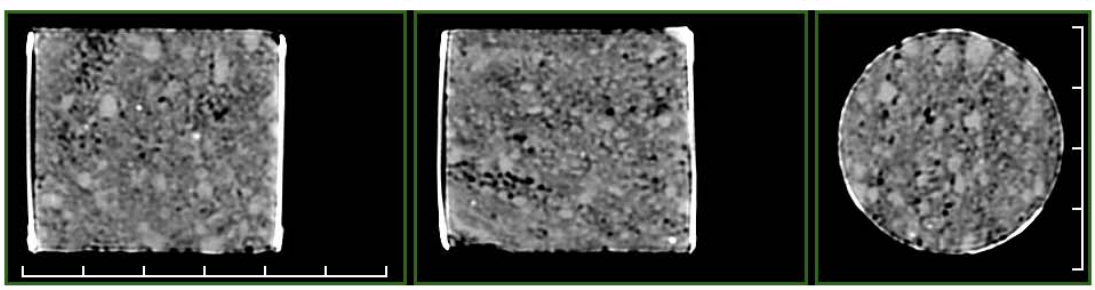

SAMPLE : 57A
DEPTH (m): 1817.50

Ka (mD): 5470
Por (%): 20.6
GD (g/cc): 2.656

CT No.(HU): 1582

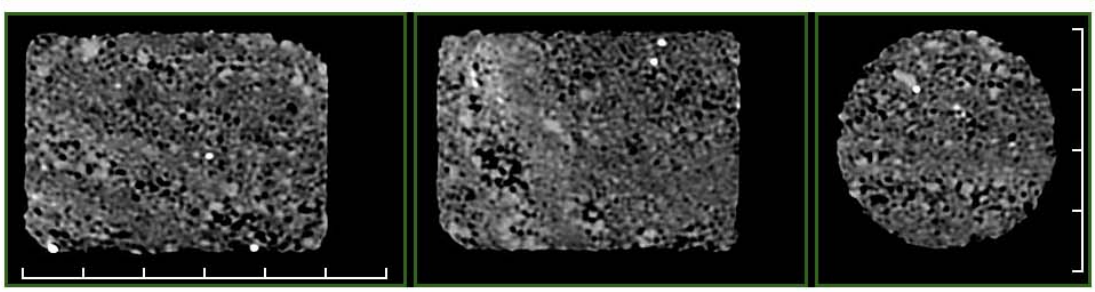

SAMPLE : 59
DEPTH (m): 1818.05

Ka (mD): >10000
Por (%): 23.8
GD (g/cc): 2.655

CT No.(HU): 1368

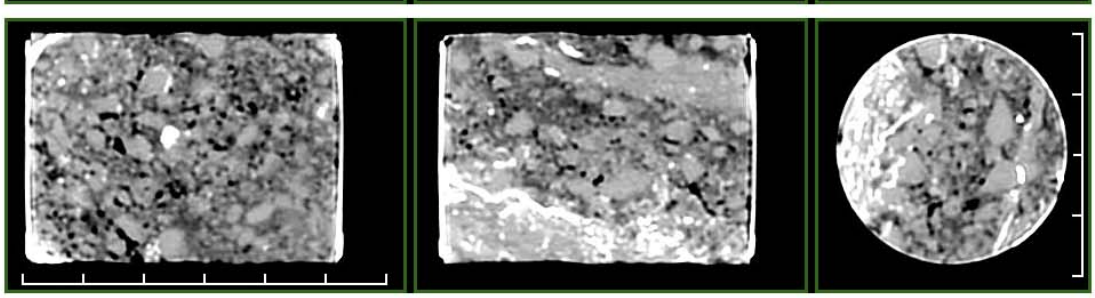

SAMPLE : 62B
DEPTH (m): 1818.84

Ka (mD): 416
Por (%): 13.6
GD (g/cc): 2.677

CT No.(HU): 1830

scale in centimetres

Copyright 2005 All Rights Reserved
Coshell & Associates

Origin Energy Limited
Halladale - 1
X-ray CT Images and Base Data

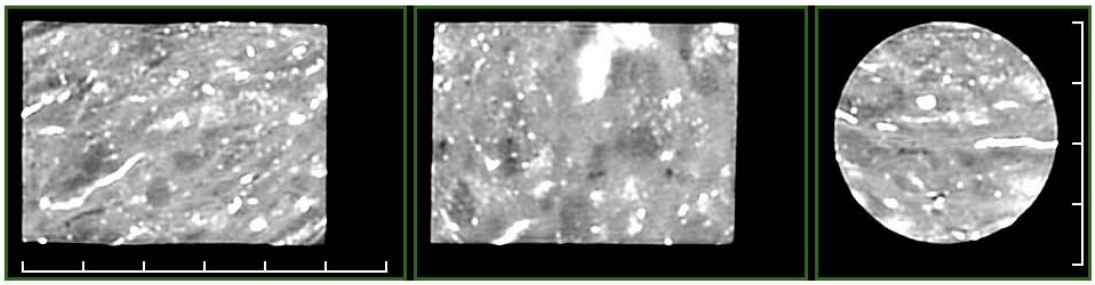

SAMPLE : 62A
DEPTH (m): 1818.95

Ka (mD): -
Por (%): -
GD (g/cc): -

CT No.(HU): 1959

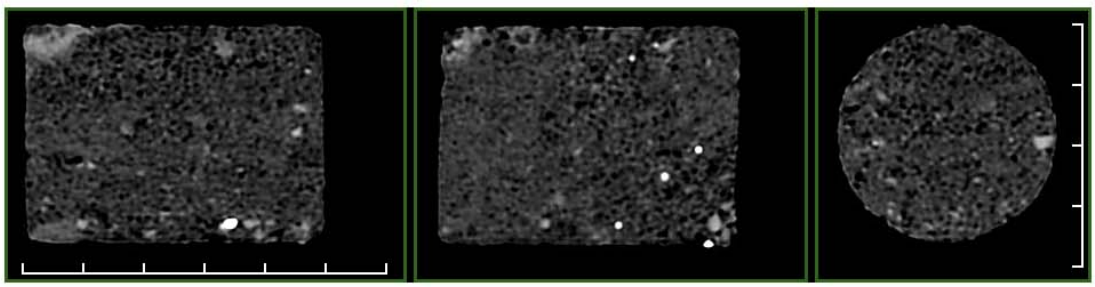

SAMPLE : 64
DEPTH (m): 1819.50

Ka (mD): 4140
Por (%): 26.7
GD (g/cc): 2.642

CT No.(HU): 1215

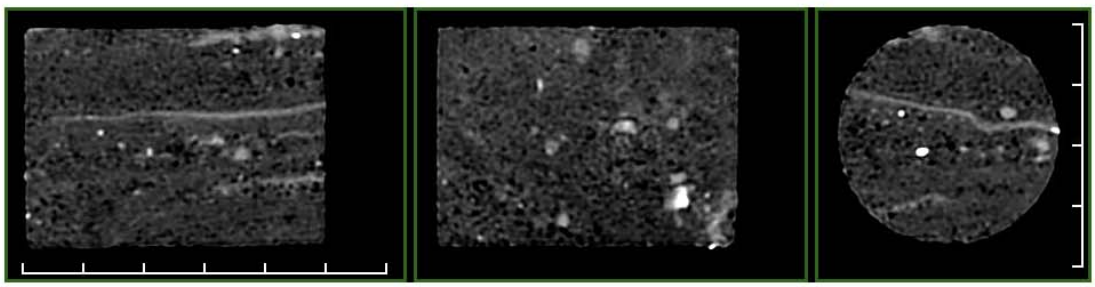

SAMPLE : 65
DEPTH (m): 1819.80

Ka (mD): 2800
Por (%): 26.3
GD (g/cc): 2.662

CT No.(HU): 1243

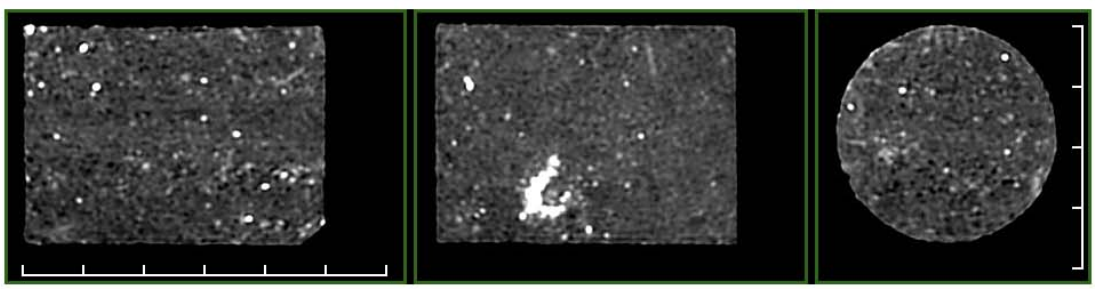

SAMPLE : 67A
DEPTH (m): 1820.49

Ka (mD): 2260
Por (%): 25.7
GD (g/cc): 2.672

CT No.(HU): 1336

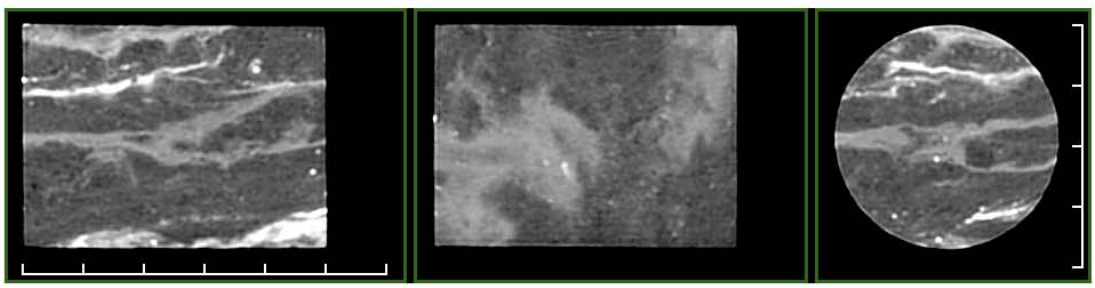

SAMPLE : 72
DEPTH (m): 1821.90

Ka (mD): 55.4
Por (%): 18.6
GD (g/cc): 2.673

CT No.(HU): 1570

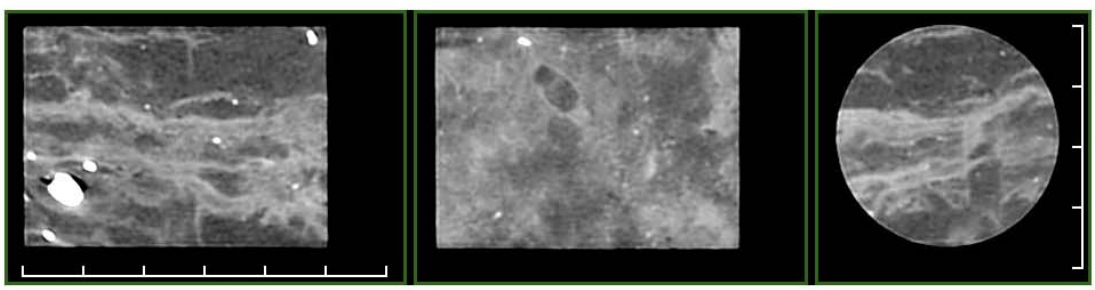

SAMPLE : 72A
DEPTH (m): 1821.98

Ka (mD): 13.7
Por (%): 16.6
GD (g/cc): 2.656

CT No.(HU): 1603

scale in centimetres

Copyright 2005 All Rights Reserved
Coshell & Associates

Origin Energy Limited
Halladale - 1
X-ray CT Images and Base Data

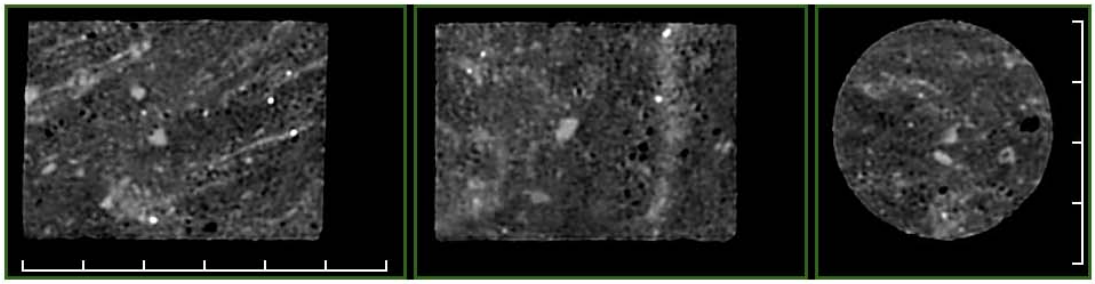

SAMPLE : 75A
DEPTH (m): 1822.83

Ka (mD): 706
Por (%): 25.7
GD (g/cc): 2.656

CT No.(HU): 1290

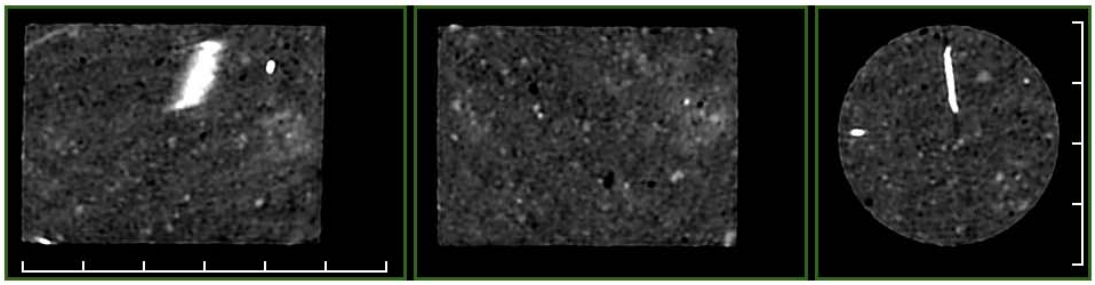

SAMPLE : 76
DEPTH (m): 1823.10

Ka (mD): 606
Por (%): 27.3
GD (g/cc): 2.665

CT No.(HU): 1249

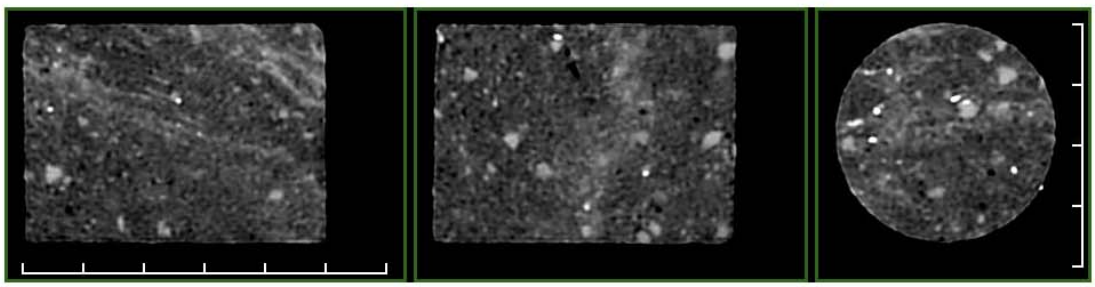

SAMPLE : 77A
DEPTH (m): 1823.36

Ka (mD): 392
Por (%): 24.9
GD (g/cc): 2.652

CT No.(HU): 1356

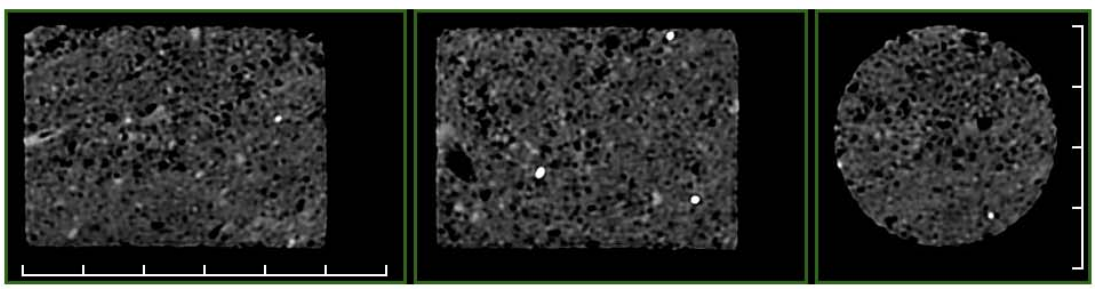

SAMPLE : 79
DEPTH (m): 1824.03

Ka (mD): 6430
Por (%): 25.5
GD (g/cc): 2.646

CT No.(HU): 1240

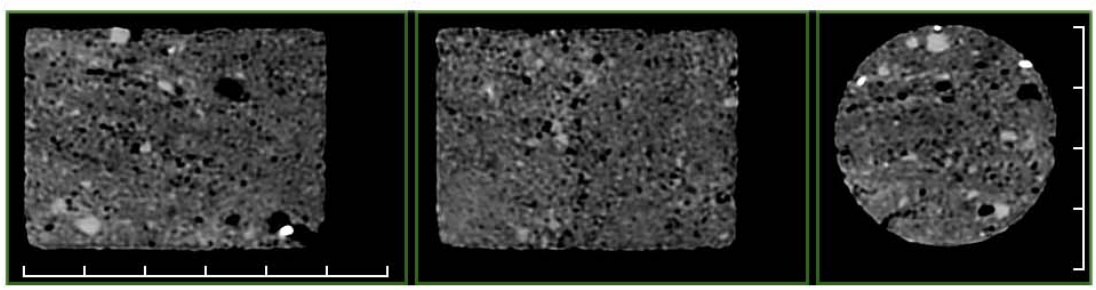

SAMPLE : 82
DEPTH (m): 1824.90

Ka (mD): 3380
Por (%): 23.4
GD (g/cc): 2.640

CT No.(HU): 1384

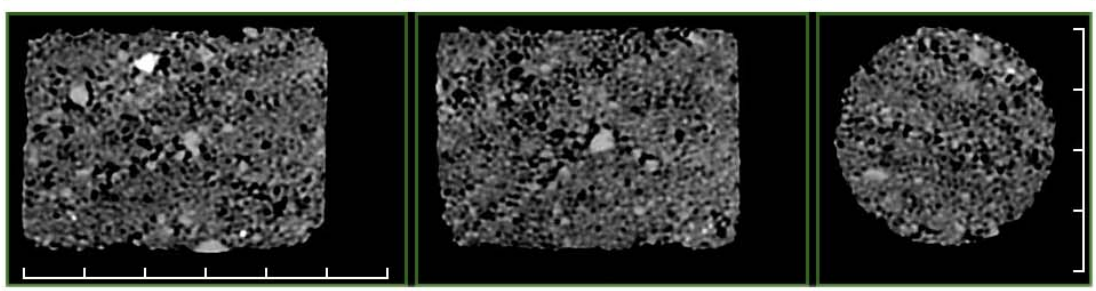

SAMPLE : 84
DEPTH (m): 1825.50

Ka (mD): >10000
Por (%): 23.7
GD (g/cc): 2.650

CT No.(HU): 1349

scale in centimetres

Copyright 2005 All Rights Reserved
Coshell & Associates

Origin Energy Limited
Halladale - 1
X-ray CT Images and Base Data

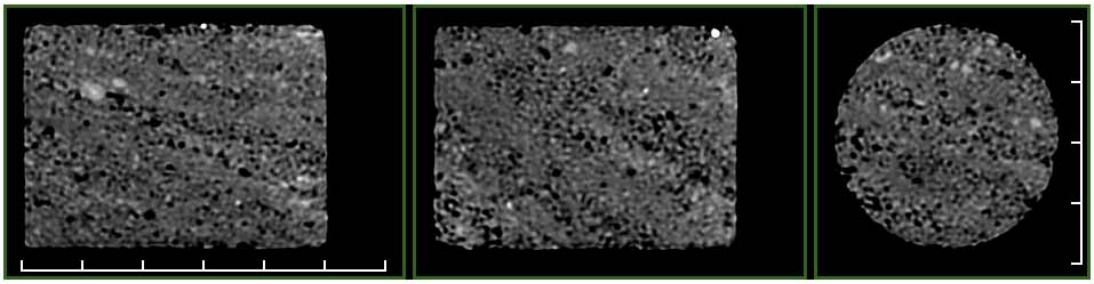

SAMPLE : 86
DEPTH (m): 1826.10

Ka (mD): 8140
Por (%): 22.9
GD (g/cc): 2.648

CT No.(HU): 1358

scale in centimetres

Copyright 2005 All Rights Reserved
Coshell & Associates

Origin Energy Limited
Halladale - 1
X-ray CT Images and Base Data

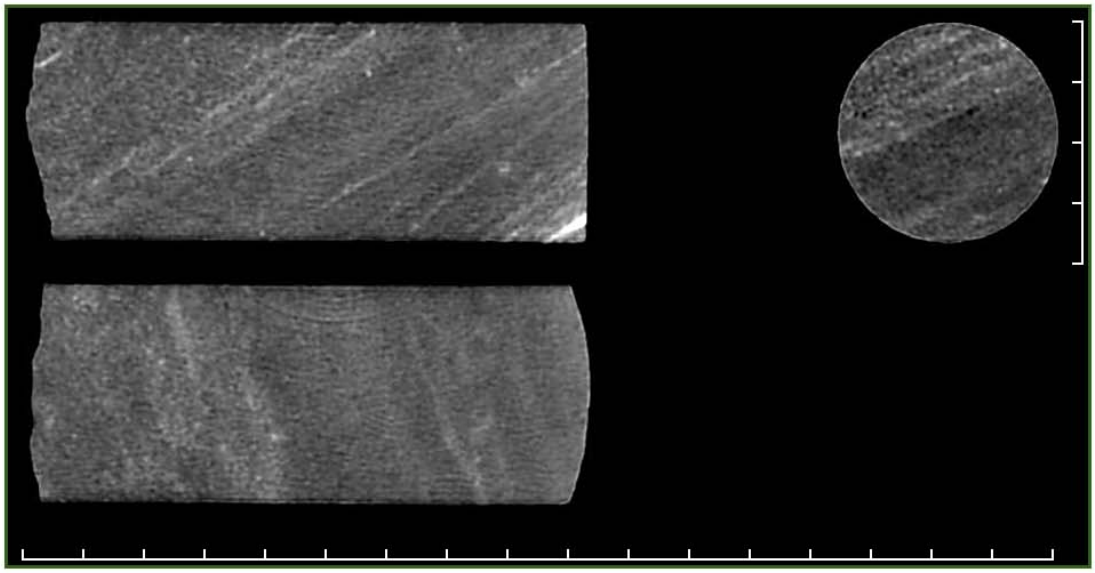

SAMPLE : A
DEPTH (m): 1809.45

CT No.(HU): 1485

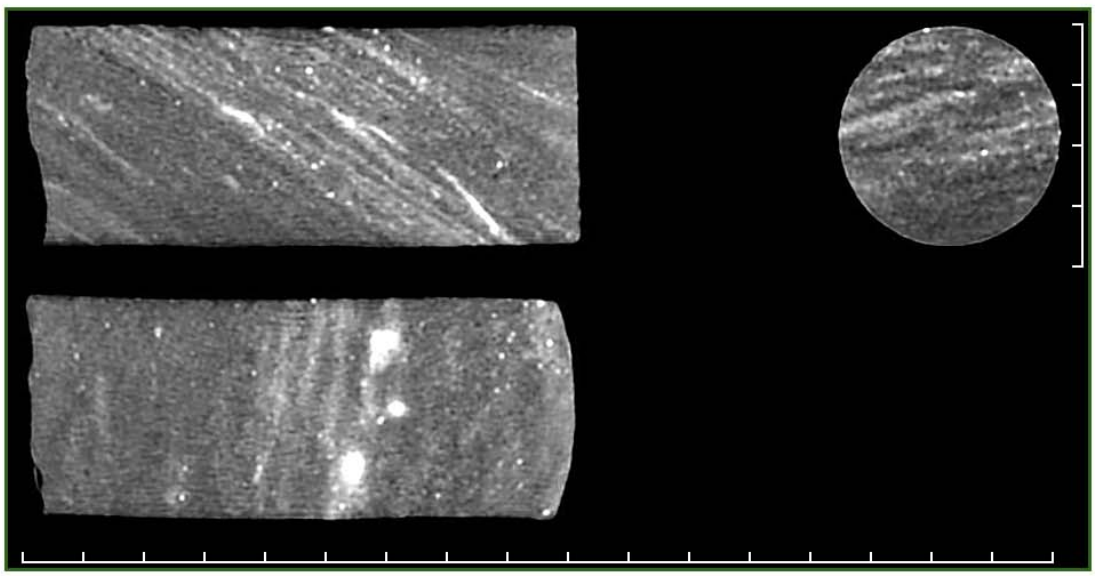

SAMPLE : B
DEPTH (m): 1809.50

CT No.(HU): 1663

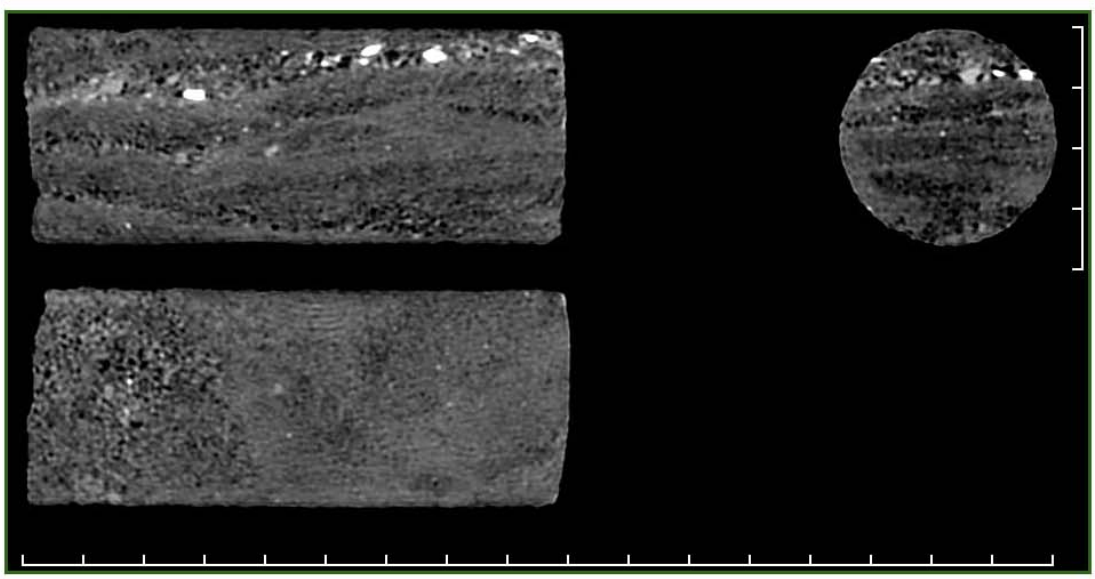

SAMPLE : C
DEPTH (m): 1812.40

CT No.(HU): 1415

scale in centimetres

Copyright 2005 All Rights Reserved
Coshell & Associates

Origin Energy Limited
Halladale - 1
X-ray CT Images and Base Data

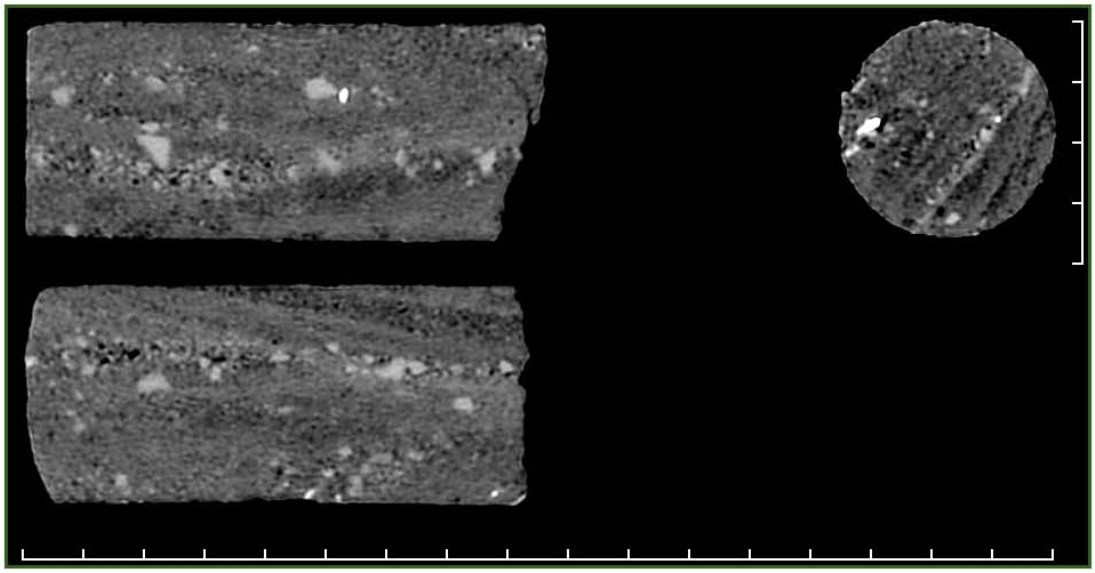

SAMPLE : D
DEPTH (m): 1812.45

CT No.(HU): 1464

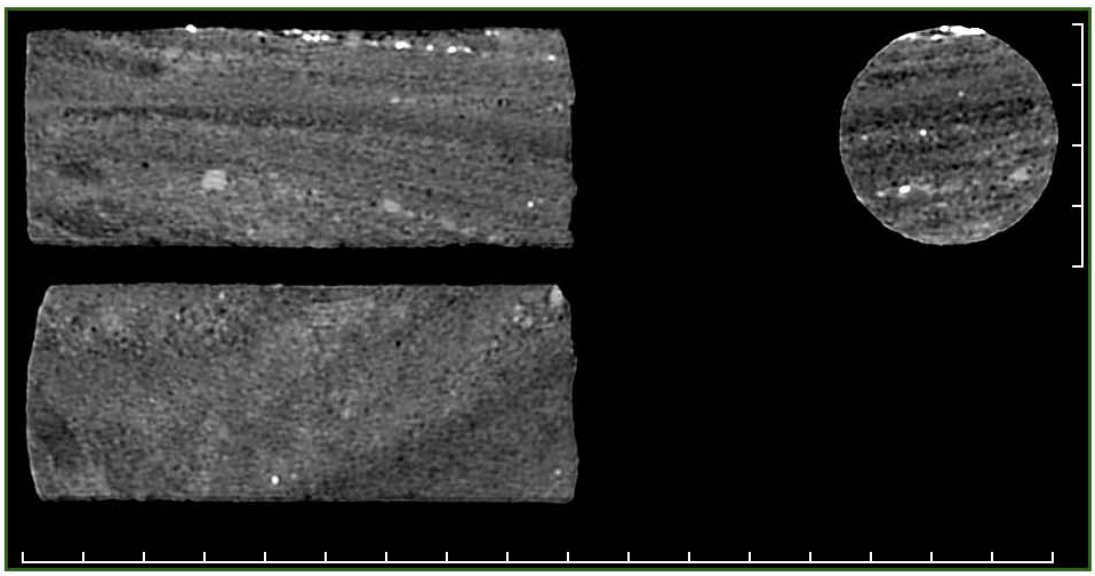

SAMPLE : E
DEPTH (m): 1812.50

CT No.(HU): 1481

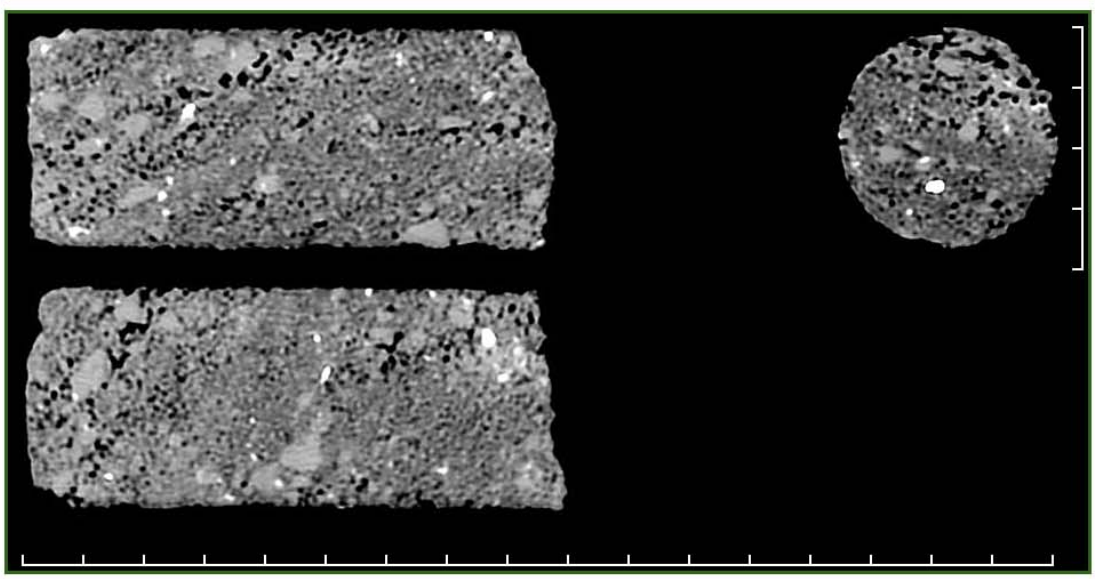

SAMPLE : F
DEPTH (m): 1817.77

CT No.(HU): 1619

scale in centimetres

Copyright 2005 All Rights Reserved
Coshell & Associates

Origin Energy Limited
Halladale - 1
X-ray CT Images and Base Data

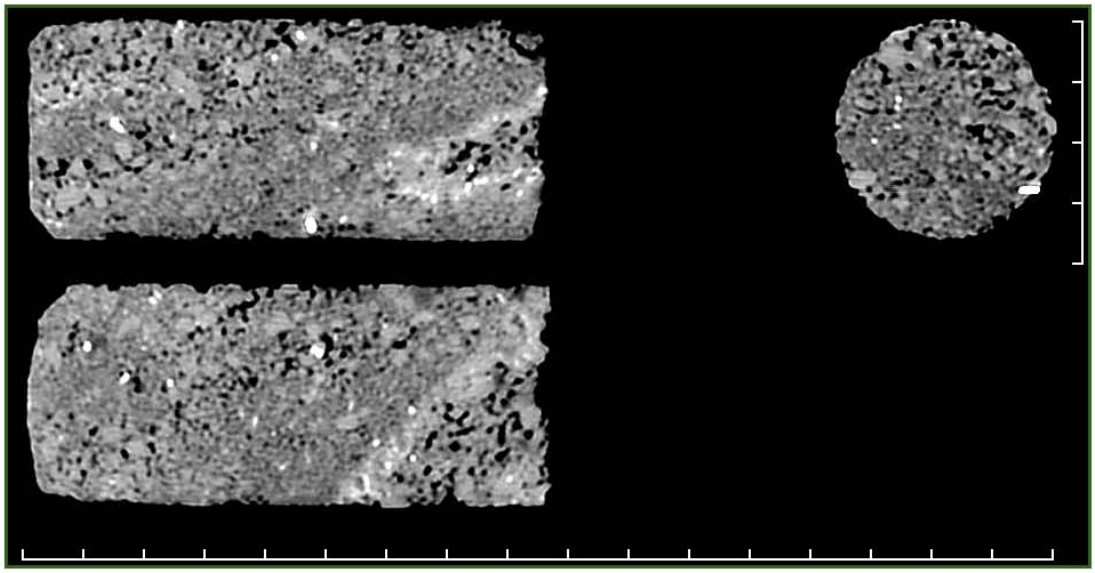

SAMPLE : G
DEPTH (m): 1817.83

CT No.(HU): 1626

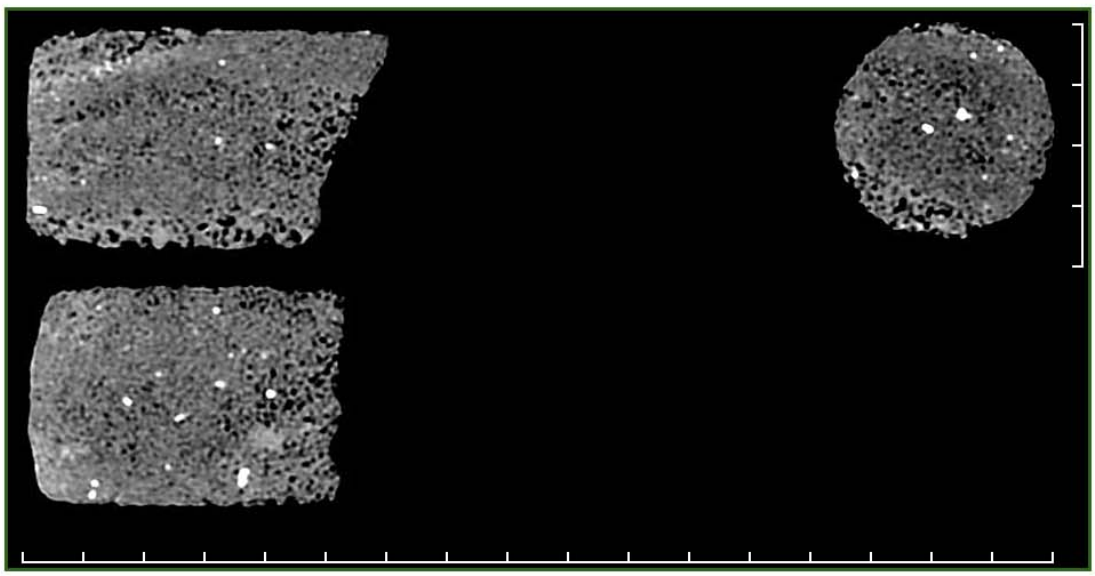

SAMPLE : H
DEPTH (m): 1817.88

CT No.(HU): 1559

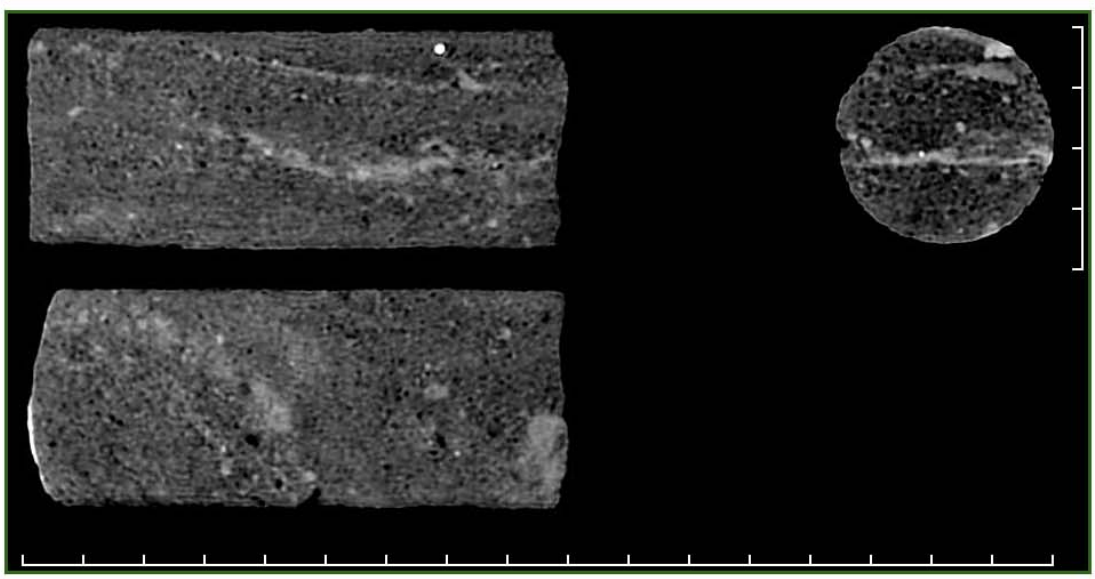

SAMPLE : I
DEPTH (m): 1819.62

CT No.(HU): 1396

scale in centimetres

Copyright 2005 All Rights Reserved
Coshell & Associates

Origin Energy Limited
Halladale - 1
X-ray CT Images and Base Data

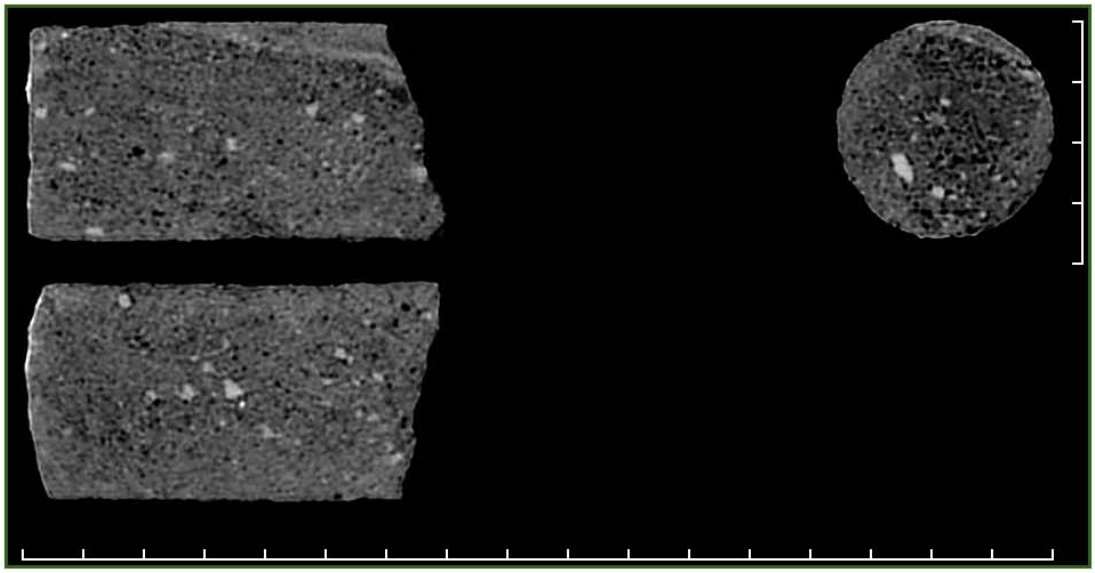

SAMPLE : J
DEPTH (m): 1819.67

CT No.(HU): 1420

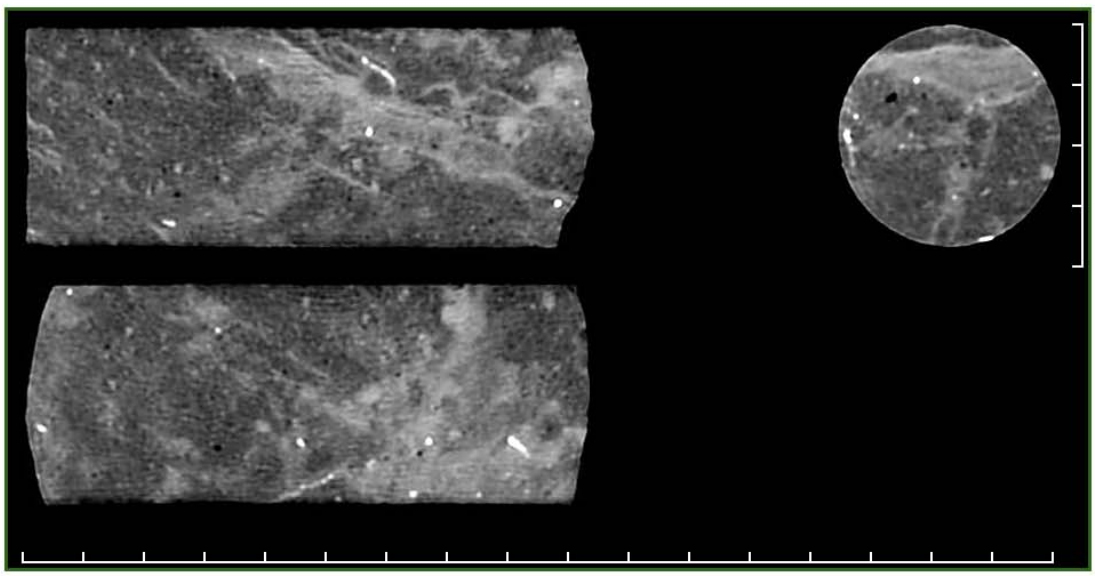

SAMPLE : K
DEPTH (m): 1822.91

CT No.(HU): 1504

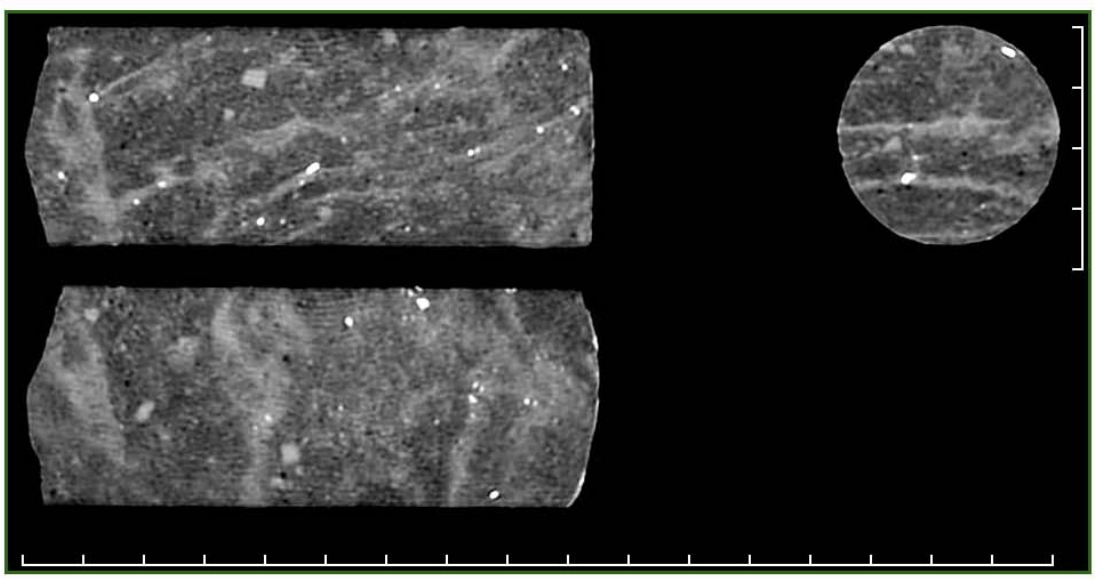

SAMPLE : L
DEPTH (m): 1822.95

CT No.(HU): 1473

scale in centimetres

Copyright 2005 All Rights Reserved
Coshell & Associates

Origin Energy Limited
Halladale - 1
X-ray CT Images and Base Data

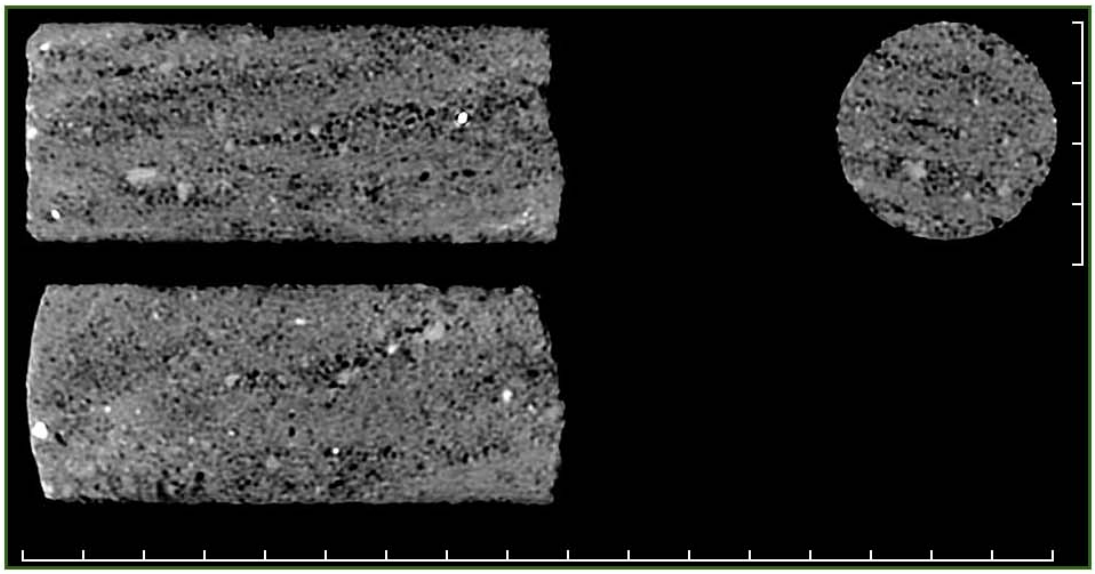

SAMPLE : M
DEPTH (m): 1826.27

CT No.(HU): 1465

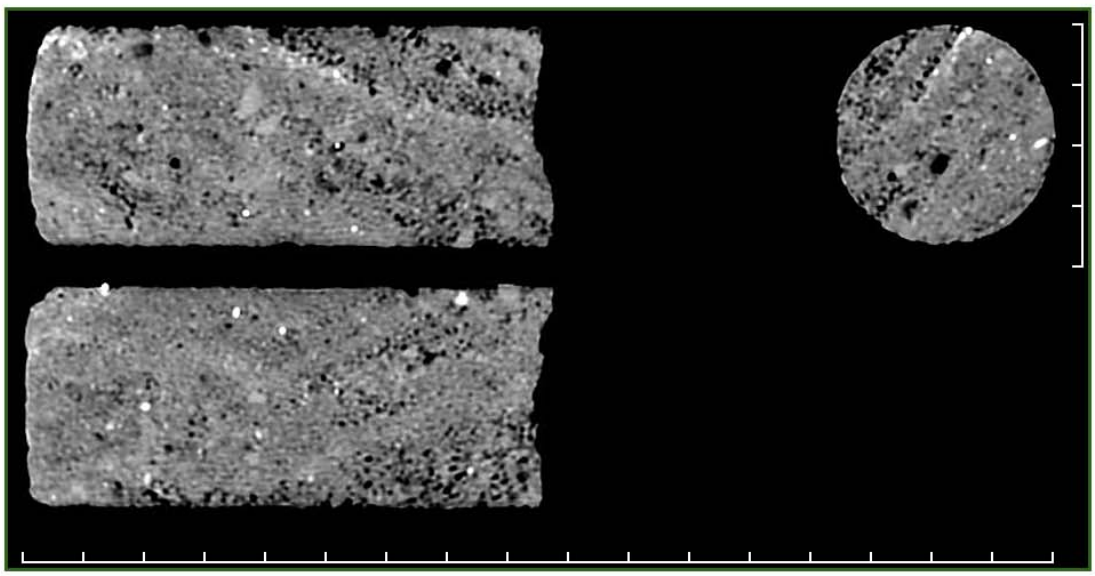

SAMPLE : N
DEPTH (m): 1826.23

CT No.(HU): 1585

scale in centimetres

Copyright 2005 All Rights Reserved
Coshell & Associates

Origin Energy Limited
Halladale - 1
X-ray CT Images and Base Data

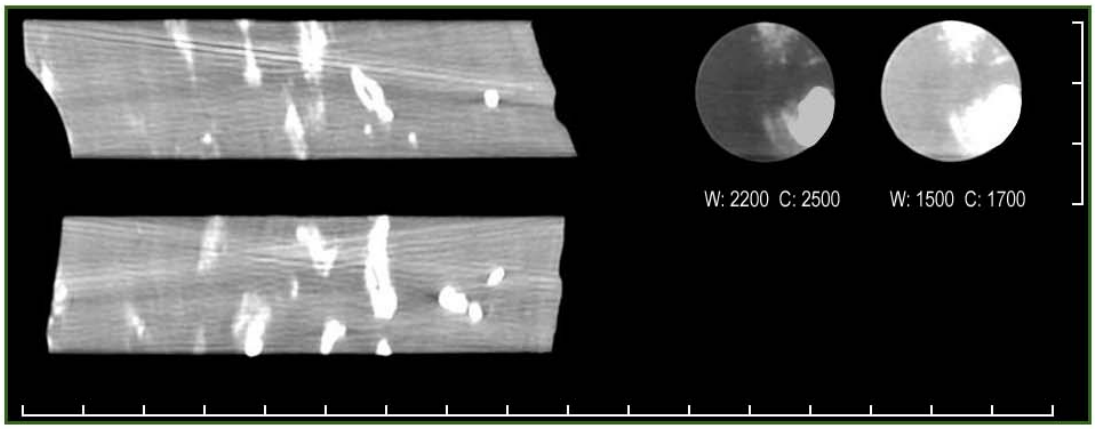

SAMPLE : W
DEPTH (m): 1831.21

CT No.(HU): 2226

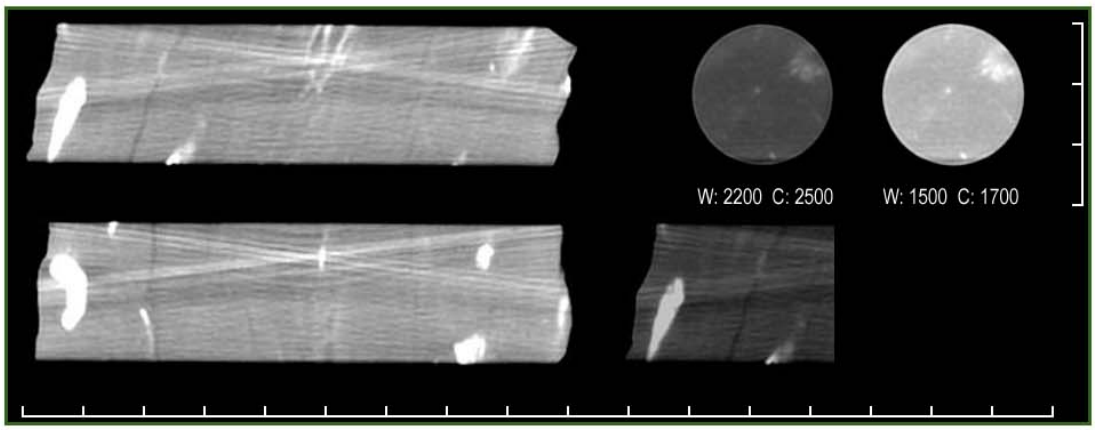

SAMPLE : X
DEPTH (m): 1831.21

CT No.(HU): 2046

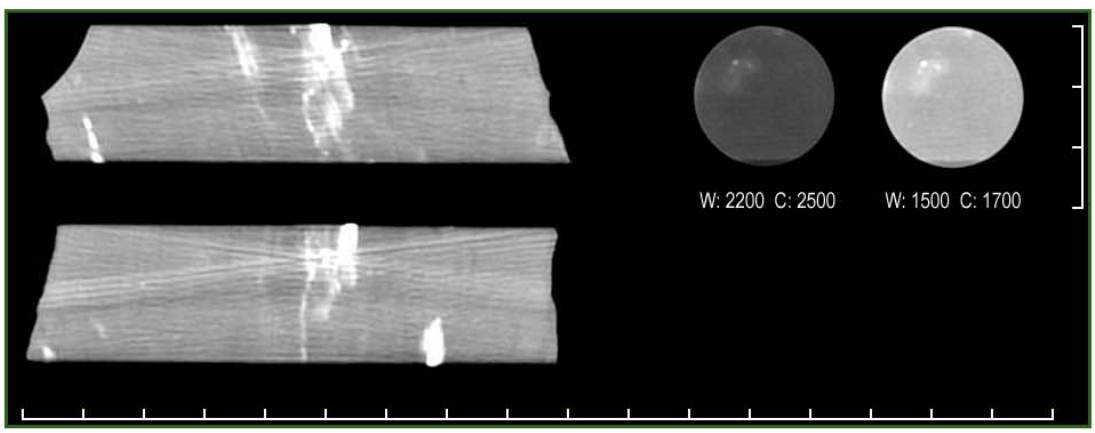

SAMPLE : Y
DEPTH (m): 1831.21

CT No.(HU): 2049

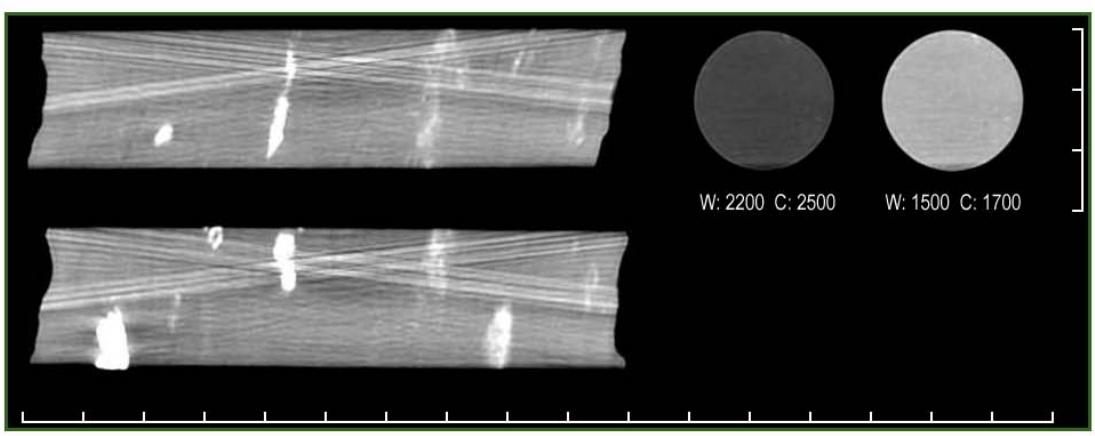

SAMPLE : Z
DEPTH (m): 1831.21

Ka (mD):
Por (%):
GD (g/cc):

CT No.(HU): 1996

scale in centimetres

Copyright 2005 All Rights Reserved
Coshell & Associates

Origin Energy Ltd
HALLADALE-1 DW1 & DW2

Plug Photography

No. 5A
Depth: 1792.55 m
Ka: 302 md
Por: 26.0 %
GD: 2.652 g/cc

No. 6A
Depth: 1792.60 m
Ka: 470 md
Por: 25.0 %
GD: 2.661 g/cc

No. 7
Depth: 1793.00 m
Ka: 958 md
Por: 26.6 %
GD: 2.648 g/cc

No. 28
Depth: 1808.70 m
Ka: 2110 md
Por: 20.9 %
GD: 2.662 g/cc

No. 29
Depth: 1809.05 m
Ka: 699 md
Por: 22.9 %
GD: 2.670 g/cc

No. 40
Depth: 1812.30 m
Ka: 4060 md
Por: 25.0 %
GD: 2.653 g/cc

Origin Energy Ltd
HALLADALE-1 DW1 & DW2

Plug Photography

No. 42
Depth: 1812.90 m
Ka: 3740 md
Por: 26.6 %
GD: 2.659 g/cc

No. 44
Depth: 1813.45 m
Ka: 3180 md
Por: 22.1 %
GD: 2.625 g/cc

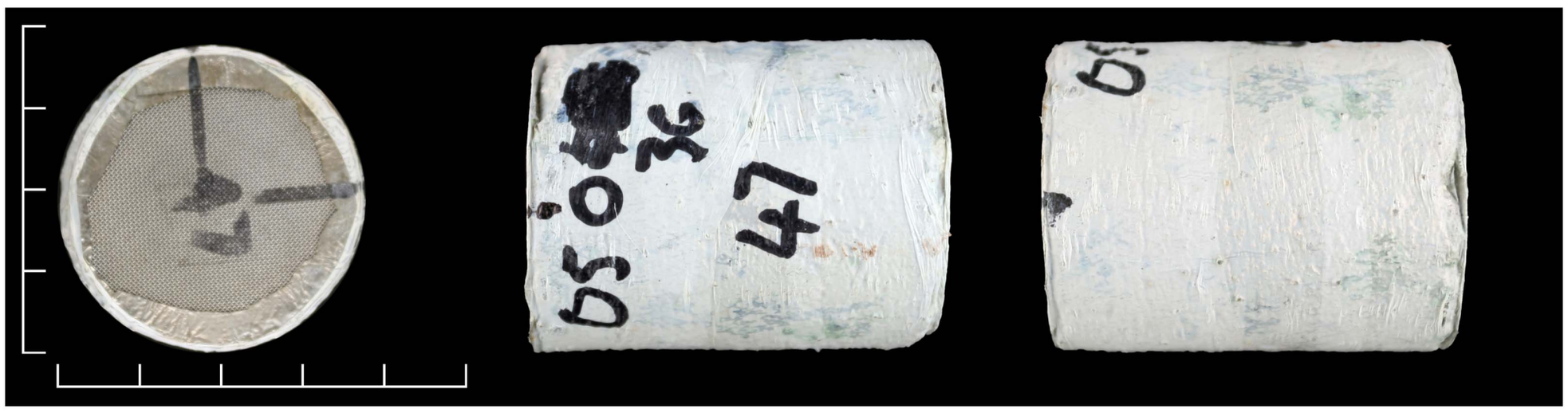

No. 47
Depth: 1814.42 m
Ka: 501 md
Por: 18.6 %
GD: 2.651 g/cc

No. 51A
Depth: 1815.73 m
Ka: 8890 md
Por: 27.4 %
GD: 2.648 g/cc

No. 55
Depth: 1816.80 m
Ka: 4220 md
Por: 24.3 %
GD: 2.656 g/cc

No. 56A
Depth: 1817.04 m
Ka: 3070 md
Por: 22.0 %
GD: 2.652 g/cc

Origin Energy Ltd
HALLADALE-1 DW1 & DW2

Plug Photography

No. 56
Depth: 1817.10 m
Ka: 385 md
Por: 16.7 %
GD: 2.654 g/cc

No. 57A
Depth: 1817.50 m
Ka: 5470 md
Por: 20.6 %
GD: 2.656 g/cc

No. 59
Depth: 1818.05 m
Ka: >10000 md
Por: 23.8 %
GD: 2.655 g/cc

No. 62B
Depth: 1818.84 m
Ka: 416 md
Por: 13.6 %
GD: 2.677 g/cc

No. 64
Depth: 1819.50 m
Ka: 4140 md
Por: 26.7 %
GD: 2.642 g/cc

No. 65
Depth: 1819.80 m
Ka: 2800 md
Por: 26.3 %
GD: 2.662 g/cc

Origin Energy Ltd
HALLADALE-1 DW1 & DW2

Plug Photography

No. 67A
Depth: 1820.49 m
Ka: 2260 md
Por: 25.7 %
GD: 2.672 g/cc

No. 72
Depth: 1821.90 m
Ka: 55.4 md
Por: 18.6 %
GD: 2.673 g/cc

No. 72A
Depth: 1821.98 m
Ka: 13.7 md
Por: 16.6 %
GD: 2.656 g/cc

No. 75A
Depth: 1822.83 m
Ka: 706 md
Por: 25.7 %
GD: 2.656 g/cc

No. 76
Depth: 1823.10 m
Ka: 606 md
Por: 27.3 %
GD: 2.665 g/cc

No. 77A
Depth: 1823.36 m
Ka: 392 md
Por: 24.9 %
GD: 2.652 g/cc

Origin Energy Ltd
HALLADALE-1 DW1 & DW2

Plug Photography

No. 79
Depth: 1824.03 m
Ka: 6430 md
Por: 25.5 %
GD: 2.646 g/cc

No. 82
Depth: 1824.90 m
Ka: 3380 md
Por: 23.4 %
GD: 2.640 g/cc

No. 84
Depth: 1825.50 m
Ka: >10000 md
Por: 23.7 %
GD: 2.650 g/cc

No. 86
Depth: 1826.10 m
Ka: 8140 md
Por: 22.9 %
GD: 2.648 g/cc

APPENDIX 5:
CORE DESCRIPTION REPORT

delivering the goods

Halladale-1 DW2

Core Description Report

VIC P37(V)
OTWAY BASIN

August 2005

EXECUTIVE SUMMARY

A sedimentological study of Core 1 from the Waarre Formation in Halladale-1 DW2 indicates that this interval was deposited in restricted marginal marine and fluvial settings. Interpreted depositional environments within the restricted marine setting include distal lower shoreface, offshore transition, and upper offshore and transgressive shoreface deposits. Within the fluvial setting there is a dominance of lower barform/channel fill deposits with subordinate channel abandonment and tidal-fluvial channel facies.

The degree and low diversity of bioturbation in the marine interval reflect environmental stresses, possibly reduced salinity. Bioturbation within the tidal-fluvial channel facies has a low diversity and is restricted to finer grained intervals at the top of this facies, possibly indicating abandonment of the channel as the majority of this facies is unburrowed. Bioturbation within the abandoned channel facies represents a subaqueous freshwater assemblage of morphologically simple, deposit feeding structures.

High resolution sequence stratigraphy and ichnofacies analysis has been used to subdivide the cored interval into lower-order sequences. A sequence boundary (SB) between the restricted marine and fluvial facies is marked by a characteristic ichnofacies assemblage of robust, sharp walled, passively filled, vertical to sub-vertical domichnia (dwelling burrow), that is excavated into semi-consolidated (firmground) substrates (*Glossifungites* ichnofacies). This surface demarcates discontinuity surfaces that reflect pauses in sedimentation, generally accompanied by erosion.

The fluvial succession is dominated by lower barform/channel fill facies as the upper barforms have been eroded by the overlying channel, implying a high degree of channel amalgamation. The dominance of lower barform/channel fill deposits implies that there was a low rate of increase in the accommodation rate relative to sediment supply. The low accommodation rate indicates that the fluvial system represents a late lowstand to early transgressive systems tract.

Reservoir quality is strongly influenced by facies with the highest permeability occurring in the barform/channel fill facies and the tidal-fluvial channel facies. The restricted marine facies has the lowest reservoir quality and the crevasse splay deposits within the abandoned channel fill facies are intermediate in terms or porosity/permeability.

TABLE OF CONTENTS

EXECUTIVE SUMMARY ..... **i**

INTRODUCTION **1**

Overview **1**

Objectives **1**

Methodology **1**

SEDIMENTOLOGY **2**

Facies A *3*

Facies B *5*

Facies C *6*

Facies D *8*

Facies E *8*

Facies F *10*

Facies G *12*

DEPOSITIONAL MODEL **13**

Restricted marine *13*

Fluvial *13*

SEQUENCE STRATIGRAPHY **13**

Stratal surfaces *14*

Sequence stratigraphic model *14*

RESERVOIR QUALITY **15**

REFERENCES **16**

APPENDIX 1 ..... **19**

INTRODUCTION

Overview

One core, 25.4 m in length, was described in detail from Halladale-1 DW2. The core was cut in the Waarre Formation (1808.0 – 1835.0 m) with a recovery of 94%. All depths refer to drillers depth unless otherwise stated. This core data allows detailed sedimentological and sequence stratigraphic interpretation of the depositional environments.

Objectives

The main objectives of the core description were the following:

1 Provide a detailed description of the cored intervals
2 Determine lithofacies and ichnofacies
3 Interpret depositional environment
4 Describe sedimentary sequences and key stratal surfaces present within the core
5 Describe the reservoir potential

Methodology

Cores were logged at 1:20 scale. Grainsize, colour, composition, physical sedimentary structures, macro palaeontology, ichnology (including Bioturbation index) were recorded. Bioturbation index (BI) records the intensity of bioturbation within a unit on a scale of 1 to 6. Where 1 indicates sparse bioturbation and disturbance of primary physical sedimentary structures and 6 indicates complete reworking of sediment and removal of all evidence of original sedimentary structures. Other ichnology characteristics including community succession resulting from environmental modification as the habitat becomes less suitable; and tiering in which bioturbation is vertically partitioned, resulting from vertical zoning of physical, chemical and biological parameters.

SEDIMENTOLOGY

The cored interval can be subdivided into seven facies on the basis of preserved sedimentary structures and bioturbation that are characteristic of particular depositional environments. The facies, labelled A through G, range from granule conglomerate to mudstone. A summary of the main features of the facies is in Table 1 and the ichnofossils assemblages are in Table 2. Interpreted core photographs are included in Appendix 1.

Table 1. Summary of the main features of the sedimentary facies in Halladale-1 DW2 Core 1

Facies	Lithology	Primary structures	Ichnofacies	Interpretation
A: interbedded bioturbated muddy siltstone and laminated sandstone	Bioturbated muddy siltstone units with common discrete sharp-bounded sandstone beds	Low angle, undulatory parallel lamination (Hummocky cross stratification – HCS) in sandstones; primary structures not preserved in siltstone	Restricted proximal *Cruziana* ichnofacies	Distal lower shoreface
B: interlaminated bioturbated muddy siltstone and laminated silty sandstone	Muddy siltstone and interlaminated sharp-bounded silty sandstone	Linsen, lenticular and wavy bedding	Restricted *Cruziana* ichnofacies	Offshore transition
C: intensely bioturbated muddy sandstone with rare weakly bioturbated mudstone laminations	Muddy sandstone with pebble lags at base, rare mudstone laminations	Primary structures are not preserved in the muddy sandstone; laminations present in mudstone	Mixed restricted *Skolithos*/ *Cruziana* ichnofacies	Transgressive shoreface deposits
D: intensely bioturbated muddy siltstone	Intensely bioturbated siltstone, rare sandy siltstone beds	Local linsen and lenticular bedding	Restricted distal *Cruziana* ichnofacies	Upper offshore
E: cross bedded medium-grained sandstone to granule conglomerate	Medium- to very coarse-grained quartz sandstone with rare granule conglomerate	Cross bedding, lags comprising clastic grains and wood common. Bioturbation absent		Low sinuosity fluvial
F: massive mudstone with interbedded sandstone	Massive mudstone with rare bioturbation interbedded with massive very fine- to medium-grained sandstone	Linsen and lenticular bedding. Sandstone is flat laminated to massive	*Mermia* ichnofacies	Ponded water in abandoned channels, infilled by crevasse splays
G: sandy siltstone to sandstone with common mudstone laminations	Intensely bioturbated sandy siltstone overlying medium- to coarse grained sandstone with mudstone laminations between beds	Cross bedding, mud drapes	Restricted proximal *Cruziana* ichnofacies	Tidal-fluvial channel fill

Facies A

Sedimentology

This facies comprises very fine- to fine-grained sandstone and mudstone interbedded on a variety of scales. The sandstone beds are sharp-based, commonly show weak normal grading and bioturbated tops, and are typically 5 to 10 cm thick. However, erosionally amalgamated sandstone beds up to 20 cm are also present. Preserved primary sedimentary structures are dominated by low angle wavy, undulatory parallel laminae (<10°). Wavy parallel laminae, particularly those that contain upward convex laminations reflect hummocky cross stratification (HCS). Rare angular, elongate mudstone rip-up clasts occur at the base of some sandstone beds. The mudstone is massive, containing linsen and lenticular bedded sandy siltstone.

Ichnology

This facies has a bioturbation index (BI) that ranges between 0 and 4. The sandstone beds are either unbioturbated or weakly bioturbated with fugichnia (escape burrows) the dominant structure present. Softground trace fossils present in the mudstone comprise deposit feeding and dwelling structures with *Planolites* and rare *Thalassinoides*? the only structures present. This suite is characteristic of a stressed *Cruziana* ichnofacies (Bann and Fielding, 2004).

Interpretation

Facies A is interpreted to record deposition in restricted marine, distal lower shoreface conditions, in a moderately storm dominated setting. The sandstone beds reflect deposition by distal storm beds and their waning flow deposits (MacEachern et al, 1992a). Storms, and to a lesser degree, fair-weather waves are the dominant physical processes operating on the lower shoreface. The intensity of burrowing is interpreted to reflect a combination storm intensity, storm frequency and sedimentation rate, coupled with environmental stresses. Fluctuations in sedimentary rates are intimately associated with the episodic nature of storm deposition and this controls the ultimate character of the lower shoreface deposits (MacEachern and Pemberton, 1992). The presence of fugichnia in these units indicates high sedimentation rates and event deposition (Bann and Fielding, 2004).

The low diversity of traces indicates varying levels of stress or restriction on the depositional environment. Marginal marine environments, including the intertidal zone, shallow lagoons, estuaries, bays and delta platforms, characteristically display steep

salinity gradients resulting from variations in 1) amounts of freshwater input from rivers and runoff from land, 2) rainfall, 3) evaporation, 4) tidal range and salinity content in adjacent open ocean coastal waters, 5) morphology of the coastal area, and 6) differences in the wind direction and velocity. Such salinity fluctuations (combined with corresponding changes in temperature, exposure, turbulence, oxygen content, turbidity etc.) result in a physiologically stressful environment for numerous organism groups. In general, the brackish water or stressed marine trace fossil suites are characterised by 1) low diversity, 2) forms typically found in marine environments, 3) simple structures constructed by tropic generalists, 4) suites that are commonly dominated by a single ichnogenus, 5) vertical and horizontal ichnofossils that are common to both the *Skolithos* and *Cruziana* ichnofacies; and 6) some forms may be found in prolific densities (Pemberton and Wightman, 1992).

Table 2. Palaeoenvironmental distribution of trace fossils in the Waarre Formation, Halladale-1 DW2.

Ichnofossils	*Beaconites/ Taenidium*	*Chondrites*	*Cylindrichnus*	*Diplocraterion*	Fugichnia	*Ophiomorpha*	*Palaeophycus*	*Planolites*	*Rhizocorallium*	*Skolithos*	*Teichichnus*	*Thalassinoides*
Tidally influenced fluvial												
Ponded water												
Braided fluvial												
Upper offshore												
Transgressive shoreface												
Offshore transition												
Distal lower shoreface												

Abundant **Moderate** **Rare**

Facies B

Sedimentology

Facies B is gradational with Facies A, C and D, making delineation of boundaries subjective. This facies contains regular interbedding of silty, very fine-grained sandstone, siltstone and muddy siltstones on a millimetre to centimetre scale.

The sandstones and siltstones are sharp-based, show a weak normal grading and range from 0.5 to 5 cm in thickness, but are typically <1 cm. Low angle parallel and undulatory laminations dominate these units. The muddy siltstones contain linsen laminations and rare pyrite.

Ichnology

The Bioturbation Index (BI) is variable, ranging between 0 and 4, but is typically between 3 and 4. The sandstone beds are rarely bioturbated with a low intensity, low diversity ichnofossil association that is characterised by suspension feeding; rare *Cylindrichnus* and *Skolithos*; and escape traces (fugichnia). There is more diverse and intense bioturbation in the muddy siltstone beds with individual burrow types difficult to discern in some intervals, however, these intervals are dominated by a limited number of ichnospecies. The traces present within the siltstone intervals include deposit feeding structures such as *Planolites, Teichichnus, Chondrites* and *Rhizocorallium;* and rare dwelling structures comprising *Palaeophycus*.

Interpretation

An offshore transition facies is interpreted as the depositional environment of Facies B on the basis of the thin, laminated silty sandstone and the dominance of muddy siltstone. This environment represents storm-influenced emplacement with the sandstone beds representing deposition by storm-generated currents as this facies occurs below the fair-weather wave base (Bann and Fielding, 2004). The bioturbation within the silty sandstone beds is characteristic of storm beds – a sharp basal contact; parallel to sub-parallel laminations (HCS); escape structures; burrows inhabited by opportunistic organisms that colonised the storm deposit; lam-scram profiles representing increasing degrees of bioturbation and a fair-weather resident trace fossil suite indicative of a return to quiescent conditions following storm abatement (Pemberton et al, 1992). The trace fossils within the sandstone beds do not constitute a 'doomed pioneer' assemblage. 'Doomed pioneer' assemblages are associated with gravity flow (storm bed deposition etc.) within otherwise unbioturbated sediments and result from entrainment of living organisms in a

turbulent sedimentation event. These organisms then rework the organic-rich sediment in an environment from which they were previously excluded until the reduced oxygen environmental conditions limit the survival time of these transported infaunal dwellers (Pemberton et al, 2001).

The fair-weather resident trace fossil suite is represented by a moderately diverse assemblage representing the burrows of deposit feeding organisms and is characteristic of a restricted *Cruziana* ichnofacies. The persistence of the fair-weather resident assemblage is dependent partly on the conditions imparted by periodic storms as the diversity of the trace fossil assemblage decreases with an increase in storm intensity and/or frequency (Bann and Fielding, 2004). However, the lack of diversity in the fair-weather assemblage could also be attributable to environmental stresses, e.g. reduced salinity. Therefore, this facies is interpreted as representing an offshore transition setting within a restricted marine setting.

Facies C

Sedimentology

Facies C is sharp based, overlies Facies B, and is erosionally based with a matrix supported, poor to moderately sorted, pebble conglomerate that is approximately 10 cm thick. Clasts are predominantly angular to sub-rounded sideritised mudstone rip up clasts that are dominantly elongated in shape. Angular, granule sized quartz grains and elongate sub-angular mudstone rip-up clasts comprise subordinate clast populations. Imbrication is common and grading is not present. The texture and sorting of the matrix is variable and consists of poor to moderately sorted, fine- to medium-grained sandstone at the base but grades upward into poorly–sorted muddy very fine-grained sandstone. Locally, mudstone interbeds are present. The muddy, very fine-grained sandstones and siltstones contain rare, dispersed pebbles, and medium- to very coarse-grained sandstone and granules that are disseminated throughout, producing a speckled or gritty appearance. Primary lamination within the sandstone is very rare, due to the degree of bioturbation, and comprises low angle to undulatory laminations, whereas the interlaminated mudstone is undisturbed.

Ichnology

The base of this facies is delineated by *Diplocraterion* that is excavated into the underlying offshore transition facies and cross cut the background softground trace fossil assemblage

of Facies B. These burrows are filled by coarser-grained sediment than the offshore transition facies.

The conglomerate interval is devoid of trace fossils, however the muddy sandstones shows a BI index of 4 to 5. The high degree of bioturbation commonly obscures the individual biogenic structures, making identification of ichnogenera difficult. The softground suite is dominated by deposit feeding structures, containing abundant *Teichichnus* and common *Planolites.* Softground suspension feeding *Diplocraterion* burrows are present in small numbers as are passive carnivore dwelling structures such as *Palaeophycus*. The assemblage reflects a stressed *Cruziana* ichnofacies.

Interpretation

The presence of the conglomerate at the base of this facies is interpreted as a coarse lag associated with a transgressive surface of erosion (ravinement surface). The degree of sorting indicates waning energy conditions and the presence of intraformational clasts supports a genetic affinity between erosion of the substrate and deposition of the conglomerate. The presence of a firmground trace fossil assemblage (*Glossifungites* ichnofacies) colonising the erosional discontinuity beneath the conglomerate indicates a depositional hiatus between the eroding event and emplacement of the lag, as the tracemakers will only colonise the surface if it is not buried (MacEachaern et al, 1992a).

The well bioturbated muddy sandstones overlying the transgressive lag are interpreted to have been deposited in a restricted marine, offshore transition setting, associated with distal storm events. The low diversity of traces implies environmental stress such as reduced salinity. The intensity of this low diversity assemblage may partly reflect the overall wave climate (MacEachern and Pemberton, 1992) as low wave energy with infrequent storms favours the more thorough biogenic reworking (MacEachern et al, 1992a; Pemberton et al, 2001).

The gradational contact with the transgressive lag supports a genetic (possibly waning energy/distal) association with the transgressive ravinement process. Coarse material is presumedly transported basinward by storms/submarine density flows during erosive shoreface retreat. The dispersed pebbles near the base of the muddy sandstone are consistent with this interpretation. The speckled or gritty appearance, caused by dispersed coarse- to very coarse-grained sandstone, reflects the disturbance of thin stringers of this material. Few deposit feeding organisms are capable of manipulating

these grains, but such material can be disturbed and shifted sideways, downwards and, to a lesser degree, upwards, by virtually all infaunal organisms. The upward decrease in the dispersed grains reflects a continuing, though upward diminishing supply of such material, consistent with a progressively more distal position from the zone of active transgressive ravinement (MacEachern et al, 1992a).

Facies D

Sedimentology

This facies has gradational contacts with Facies B, and comprises a relatively homogeneous mixture of bioturbated mudstone and sandy siltstone. Bed boundaries are usually not distinct due to burrowing, however thin silty sandstone beds are present. These beds are sharp-based, have a weak normal grading and show hints of wavy parallel to undulatory laminations.

Ichnology

This facies has a BI of 5 to 6. This high degree of bioturbation obscures the individual biogenic structures, making identification of ichnogenera difficult. The softground suite is dominated by deposit feeding structures, containing *Teichichnus, Planolites* and *Chondrites*. Small numbers of passive carnivore dwelling structures such as *Palaeophycus* are also present. This assemblage reflects a stressed *Cruziana* ichnofacies.

Interpretation

Facies D is interpreted to have been deposited in an upper offshore setting with very distal storm events. Fluctuations in sedimentary rates are intimately associated with the episodic nature of storm deposition and this controls the ultimate character of the deposits. The intensity of bioturbation and the lack of well defined storm deposits therefore reflect an overall low wave energy climate with infrequent storm events that allows for the more thorough biogenic reworking of the interbedded silty sandstone and muddy siltstone. The low diversity of trace fossils possibly indicates environmental stress, such as reduced salinity, as low wave energy within a fully marine environment would promote high intensity, high diversity bioturbation (MacEachern et al, 1992a).

Facies E

Sedimentology

Facies E is sharp based and overlies the offshore transition deposits of Facies B. The upper contact of this facies is also sharp, and typically overlain by Facies F. The base of Facies E contains a thin matrix supported, moderately sorted granule to pebble conglomerate.

Clasts are predominantly sub-angular to sub-rounded quartz. Granule to cobble sized angular to rounded mudstone clasts and wood fragments are also present. The cobble sized clasts are angular and elongate whereas the granule and small pebble clasts are sub-rounded and more spherical in shape. The larger clasts and wood fragments are aligned with the lamination but imbrication is not present.

The majority of the facies comprises medium- to very coarse-grained sandstone and rare granule conglomerate. The sandstones are poor to moderately sorted with the degree of sorting increasing as the grainsize decreases. The degree of cementation varies from pervasive carbonate cement (1818.45 – 1818.60 m) to very poorly cemented, friable sandstone for the majority of the facies. Very coarse-grained and granule grains commonly form lags at the base of beds; mudstone rip-up clasts are also present at the base of some beds. Wood and plant debris commonly occur either as lags or are present on foreset laminations. The sandstone contains a range of structures including rare flat laminations, common low angle and trough cross beds, and rare planar cross bedding with typical grainsize variations on the foresets. The most commonly preserved structure in this facies is laminations with convex down terminations and inclined to the principal surface of sedimentation, indicating trough cross bedding. Bedding surfaces are commonly scoured with the top of the underlying bedform eroded. The sandstone bodies do not fine upwards and the cross-set thickness varies from 10 to 70 cm but is commonly 20 to 50 cm.

The intervals containing granule conglomerate are moderately sorted and overlie erosional surfaces. Laminations are continuous with the overlying sandstone indicating that the conglomerate forms lags at the base of cross bedded sandstone.

Ichnology

No bioturbation is present within this facies; however, a cross cutting firmground assemblage of trace fossils comprising *Diplocraterion* is present at the base of this facies. These traces are present in Facies B, but are robust suspension feeding structures that have been passively filled by sediment from Facies E. The firmground assemblage constitutes a *Glossifungites* ichnofacies that is genetically related to Facies E.

Interpretation

The dominance of trough cross bedding with conglomeratic lags, the presence of wood and plant debris along laminations, the internal scour surfaces and the lack of bioturbation indicate that this facies was deposited in a fluvial environment (Bann and Fielding, 2004;

Plink-Björklund, 2005). The presence of intraformational clasts and the *Glossifungites* ichnofacies indicate the development of an erosional discontinuity (MacEachern et al, 1992b) and a fall in relative sea level as evident from the juxtaposition of fluvial facies overlying offshore transition facies. The intraformational mudstone clasts at the base of the fluvial facies support a genetic affinity between erosion of the substrate and deposition of the conglomeratic lag. The presence of a firmground trace fossil assemblage (*Glossifungites* ichnofacies) colonising the erosional discontinuity beneath the lag indicates a depositional hiatus between the eroding event and emplacement of the lag, (MacEachern et al, 1992a).

The lack of fining upward trends, the overall coarse grainsize and the multiple erosion surfaces suggest channels with a relatively low sinuosity (Plink-Björklund, 2005). Bedforms within this type of fluvial system comprise channel fills, and lateral and mid channel bars that grow by lateral and downstream accretion (Jo and Chough, 2001; Jones et al, 2001). The trough cross bedded sandstones were deposited as 3D dunes in bars (downstream and lateral accretion macroforms) and channel fill complexes, however without defining the lateral variability in bedding architecture and sand body geometry, it is impossible to determine the exact depositional setting (Jones et al, 2001; Plink-Björklund, 2005). The stratified granule conglomerates represent scour fills and the planar cross bedded sandstones represent 2D dunes that climbed or stacked over the top of the 3D dunes (Jones et al, 2001). The lack of planar cross bedding may be attributable to either current velocity or erosion of the upper barform with only the trough cross bedded lower bar preserved. This would also account for the consistency in the grainsize throughout the facies as the bar tops are eroded by the base of the overlying channel. The depth of channel fills are impossible to determine in this situation and channel widths cannot be determined; however, the degree of channel amalgamation would be high as floodplain and upper bar facies are reduced.

Facies F

Sedimentology

This facies is associated with Facies E and G. The contacts with these facies are sharp and the upper contact is possibly erosional, however there is insufficient evidence in the core for a definitive answer. Facies F predominantly comprises massive mudstone with linsen and lenticular bedded sandstone. Amalgamated sandstone beds up to 20 cm are rare and beds are typically a few millimetres to <5 cm in thickness. The sandstone beds are sharp-based, often with load casts, and may show weak normal grading or no grading at all. The

upper bed boundary is sharp but undulatory to flat. The sandstones are massive to parallel laminated and commonly contain plant debris. Small scale thickening upward cycles of interbedded sandstone and mudstone, approximately 15 to 20 cm thick, are present and are stacked into larger scale coarsening or fining upward intervals 1.0 to 1.3 m thick. Pyrite has nucleated on organic matter in some of the thinner sandstone laminations. Desiccation features and root traces are not present in this facies.

Ichnology

This facies has low levels of bioturbation with the BI typically 0-2. Bioturbation is restricted to the mudstone intervals between the sandstone beds with the exception of rare escape burrows in some sandstone beds. The trace fossils present represent morphologically simple, deposit feeding structures comprising *Planolites* and a large, sub-vertical, meniscate filled burrow attributed to *Beaconites/Taenidium.* This trace fossil assemblage is characterised by low ichnodiversity, simple structures and superficial to very shallow structures and comprise a *Mermia* ichnofacies (Buatois and Mángano, 2002).

Interpretation

The *Mermia* ichnofacies is characterised by a dominance of grazing trails, locomotion trails and dwelling burrows. Due to the section exposed in the core it was not possible to detect the presence of trails in this facies. This ichnofacies represents a permanently subaqueous freshwater environment, as indicated by the lack of exposure features, in a floodplain setting (Buatois and Mángano, 2002).

The dominance of parallel laminations and plant debris in the sandstone beds is interpreted to result from suspension cloud deposits in a marginal to distal bar setting of a crevasse splay. The massive mudstone is interpreted as deposition of mud from suspension in a subaqueous setting (Farrell, 2001). The inferred low aggradation rate that resulted in the truncation of barforms by the overlying channel would not be conducive for the preservation of floodplain sediments and the sharp basal contact of this facies implies rapid abandonment of the underlying channels. Facies F is interpreted to represent abandonment of fluvial channels and formation of ponded water in the abandoned channel. The abandoned channel was progressively infilled with crevasse splay deposits with the proportion of sandstone indicating proximity to the active channel.

Facies G

Sedimentology

Facies G comprises medium- to coarse-grained sandstone that invariably contains cross bedding. The base of this facies is sharp and overlies the abandoned channel facies. Plant debris is common on foreset laminations. Mud drapes are common on bedding surfaces and, more rarely, on foreset laminations. The mud draped bedding surfaces occur at regular intervals (approximately every 15 to 20 cm) throughout the facies whereas the foreset lamination drapes are more random.

Ichnology

Bioturbation within this facies is variable, with a BI of 0-6, and the intensity increases toward the top of the facies where there is a decrease in grainsize. The trace fossils present represent a combination of horizontal deposit feeding structures, comprising *Planolites* and *Rhizocorallium*, and dwelling structures such as *Palaeophycus* and *Ophiomorpha*. The overall diversity is low and this assemblage comprises a mixed, restricted *Skolithos/Cruziana* ichnofacies. The majority of the traces are restricted to silty, very fine-grained sandstones at the top of the facies with the exception of *Ophiomorpha* that is present within coarse-grained sandstone immediately underlying the silty sandstone.

Interpretation

The dominance of cross bedding, the coarse grainsize and the common plant debris indicate deposition within a fluvial channel, however, the mud drapes on bedding surfaces and foreset laminations, and a low diversity trace fossil assemblage indicative of brackish water deposits, implies a tidally influenced setting. This facies is interpreted as a tidally influenced fluvial channel where the fluvial channel changes into a tidal-fluvial channel below the upstream tidal limit (Plink-Björklund, 2005). The mud drapes were deposited during slackwater periods. Individual cross sets in this facies represent tidal bundles, deposited and modified in response to neap-spring-neap tide fluctuations (Dalrymple, 1992). There are no double mud drapes present, inferring that diurnal tides did not influence deposition of this facies (Pemberton et al, 2001).

The almost complete bioturbation of the silty sandstone interval may have resulted from channel abandonment and higher salinity levels permitting more intense bioturbation as freshwater species, not impoverished marine assemblages are present in the upper limits of tidal influence within fluvial channels (Pemberton et al, 2001).

DEPOSITIONAL MODEL

The depositional setting for the succession in the core can be separated into two intervals; the lower interval comprises a restricted marine setting and the upper interval comprises fluvial setting. The significance of the juxtaposition of the depositional settings will be discussed in the Sequence Stratigraphy section.

Restricted marine

This setting comprises distal lower shoreface, offshore transition and upper offshore, and transgressive shoreface facies. The low diversity of bioturbation infers environmental stresses, most likely to be reduced levels of salinity, implying brackish water conditions (Pemberton et al, 2001). The common occurrence of storm beds and the low degree of bioturbation in the fair-weather deposits indicates a combination of moderate intensity and frequency storm events, and environmental conditions.

Fluvial

There is a dominance of barform/channel fill deposits in this setting. Tidally influenced fluvial channel fill and abandoned channel fill form minor components within this setting. The limited grainsize variation in the barform/channel fill deposits is attributable to erosion of the upper bar by the base of the overlying channel, and therefore only the lower barform/channel fill is preserved. The abandonment facies contains subaqueously deposited suspension and crevasse splay sediments deposited in abandoned channels. Tidal-fluvial channels are devoid of bioturbation and the high intensity bioturbation in this facies is most likely associated with channel abandonment and development of brackish water conditions as opposed to the freshwater conditions within active channels.

SEQUENCE STRATIGRAPHY

The stratigraphic record can be subdivided into various scales or orders of cycles, resulting from cyclical variations in sediment supply and relative sea level change, on the basis of the periodicities. These cycles occur at different time scales, forming a hierarchy of sequences at differing frequencies and, therefore, longer period sequences contain several shorter period, higher frequency sequences. In this nested periodicity, the longer period sequences influence the stratal patterns within the higher frequency sequences; this is a function of their position within the longer period sequence. The high resolution sequence stratigraphic approach to the analysis of sedimentary successions focuses attention on key stratal surfaces, facies dislocations and parasequence stacking patterns within the context of relative base level changes.

Stratal surfaces

Key stratal surfaces identified in the core include sequence boundaries (SB), transgressive surfaces of erosion (TSE) and maximum flooding surfaces (MFS). The diagnostic features of these surfaces are described below.

Sequence boundaries (SB)

A low-order sequence boundary occurs between Facies B and Facies E and is characterised by an increase in grainsize, a poorly developed *Glossifungites* ichnofacies, and, most noticeably, by a decrease in the degree of bioturbation across this surface. The SB separates the restricted marine environments from fluvial environments. The facies dislocations indicate a basinward shift in facies associated with a relative sea level fall. A second, higher-order sequence boundary occurs between the tidal-fluvial channels and the overlying fluvial channels.

Transgressive surface of erosion (TSE)

Transgressive surfaces of erosion (ravinement surfaces) are generated in the marine or marginal marine environments by the action of waves and/or tides during rising relative sea level. A high-order TSE associated with a conglomeratic lag occurs in the restricted marine setting between Facies B and Facies C. In the core it is impossible to determine the degree of erosion associated with this surface.

Maximum flooding surface (MFS)

Maximum flooding surfaces record the maximum transgression and are commonly associated with mud dominated intervals predominantly deposited by suspension settling. Two high-order maximum flooding surfaces are present within the restricted marine environment.

Sequence stratigraphic model

The facies within the cored interval were strongly controlled by changes in relative sea level in a marginal marine and fluvial environment. Low amplitude, high-order relative sea level fluctuations produced the variation between distal lower shoreface and upper offshore settings. Erosion associated with rising relative sea level, following a sea level lowstand, produced a combined SB/TSE that separates the two high-order sequences. These high-order sequences comprise transgressive and highstand systems tracts. The shoreface/offshore sediments represent a low-order, early highstand system tract (HST).

A low-order relative sea level fall caused a forced regression in which the fluvial sediments were superimposed onto lower shoreface/offshore environments. The fluvial deposits represent a late lowstand/early transgressive systems tract as incised valley complexes are rarely dominated by lowstand deposits, since the system is largely a zone of sediment bypass and sediments only accumulate when relative sea level is rising (Pemberton et al, 2001). A high-order sequence boundary is present between the tidal-fluvial channel (transgressive systems tract) and fluvial channel deposits.

The dominance of lower barform/channel fill deposits implies that there was a low rate of increase in the accommodation rate relative to sediment supply. The proportion of preserved floodplain deposits and upper bar facies decreases with a decreasing rate of accommodation increase, resulting in a high net to gross section (Posamentier and Allen, 1999).

RESERVOIR QUALITY

Reservoir quality is strongly facies dependent with the fluvial channel fill facies having the highest permeability (Figure 1), with the exception of the carbonate cemented zone. The tidal-fluvial channel has a similar permeability range implying that there is no great variation between these two facies. The amalgamated crevasse splay deposits within the abandoned channels has a lower permeability range than the channel deposits, whereas the thin interbedded splay deposits have an order of magnitude lower permeability. The restricted marine sediments have the lowest permeability.

REFERENCES

Bann, K.L. and Fielding, C.R., 2004. Ichnology & Facies Analysis for Petroleum Exploration. Ichnofacies Pty and University of Nebraska Short Course, April 2004.

Buatois, L.A. and Mángano, M.G., 2002. Trace fossils from Carboniferous floodplain deposits in Western Argentina: implications for ichnofacies models of continental environments. *Palaeogeography, Palaeoclimatology, Palaeoecology,* 183, 71-86.

Dalrymple, R.W., Tidal depositional systems. *In:* Walker, R.G., and James, N.P., eds. *Facies Models: Response to Sea Level Change*. Geological Association of Canada, Newfoundland, 195-218.

Farrell, K.M., 2001. Geomorphology, facies architecture, and high-resolution, non-marine sequence stratigraphy in avulsion deposits, Cumberland Marshes, Saskatchewan. *Sedimentary Geology*, 139, 93-150.

Jo, H.R., and Chough, S.K., 2001. Architectural analysis of fluvial sequences in the northwestern part of the Kyongsang Basin (Early Cretaceous), SE Korea. *Sedimentary Geology*, 144, 307-334.

Jones, S.J., Frostick, L.E. and Astin, T.R., 2001. Braided stream and flod plain architecture: the Rio Vero Formation, Spanish Pyrenees. *Sedimentary Geology*, 139, 229-260.

MacEachern, J.A. and Pemberton, S.G., 1992. Ichnological aspects of Cretaceous shoreface successions and shoreface variability in the Western Interior Seaway of North America. *In:* Pemberton, S.G., ed: *Applications of Ichnology to Petroleum Exploration: A Core Workshop.* Society for Sedimentary Geology, Tulsa, 57-84.

MacEachern, J.A., Bechtel, D.J. and Pemberton, S.G., 1992a. Ichnology and sedimentology of transgressive deposits, transgressive related deposits and transgressive systems tracts in the Viking Formation of Alberta. *In:* Pemberton, S.G., ed: *Applications of Ichnology to Petroleum Exploration: A Core Workshop.* Society for Sedimentary Geology, Tulsa, 251-290.

MacEachern, J.A., Raychaudhuri, I. and Pemberton, S.G., 1992b. Stratigraphic applications of the *Glossifungites* ichnofacies: delineating disconformities in the rock record. *In:* Pemberton, S.G., ed: *Applications of Ichnology to Petroleum Exploration: A Core Workshop.* Society for Sedimentary Geology, Tulsa, 169-198.

Pemberton, S.G. and Wightman, D.M., 1992. Ichnological characteristics of brackish water deposits. *In:* Pemberton, S.G. ed. *Applications of Ichnology to Petroleum Exploration: A Core Workshop*. Society for Sedimentary Geology, Tulsa, pp141-167.

Pemberton S.G., MacEachern, J.A. and Ranger, M.J., 1992. Ichnology and event stratigraphy: the use of trace fossils in recognising tempestites. *In:* Pemberton, S.G., ed: *Applications of Ichnology to Petroleum Exploration: A Core Workshop.* Society for Sedimentary Geology, Tulsa, 85-117.

Plink-Björklund, P., 2005. Stacked fluvial and tide-dominated estuarine deposits in high-frequency (fourth-order) sequences of the Eocene Central Basin, Spitsbergen. *Sedimentology*, 52, 391-428.

Posamentier, H.W. and Allen, G.P. 1999, Siliciclastic Sequence Stratigraphy: Concepts and Applications. Indonesian Sedimentologists Forum, 110p.

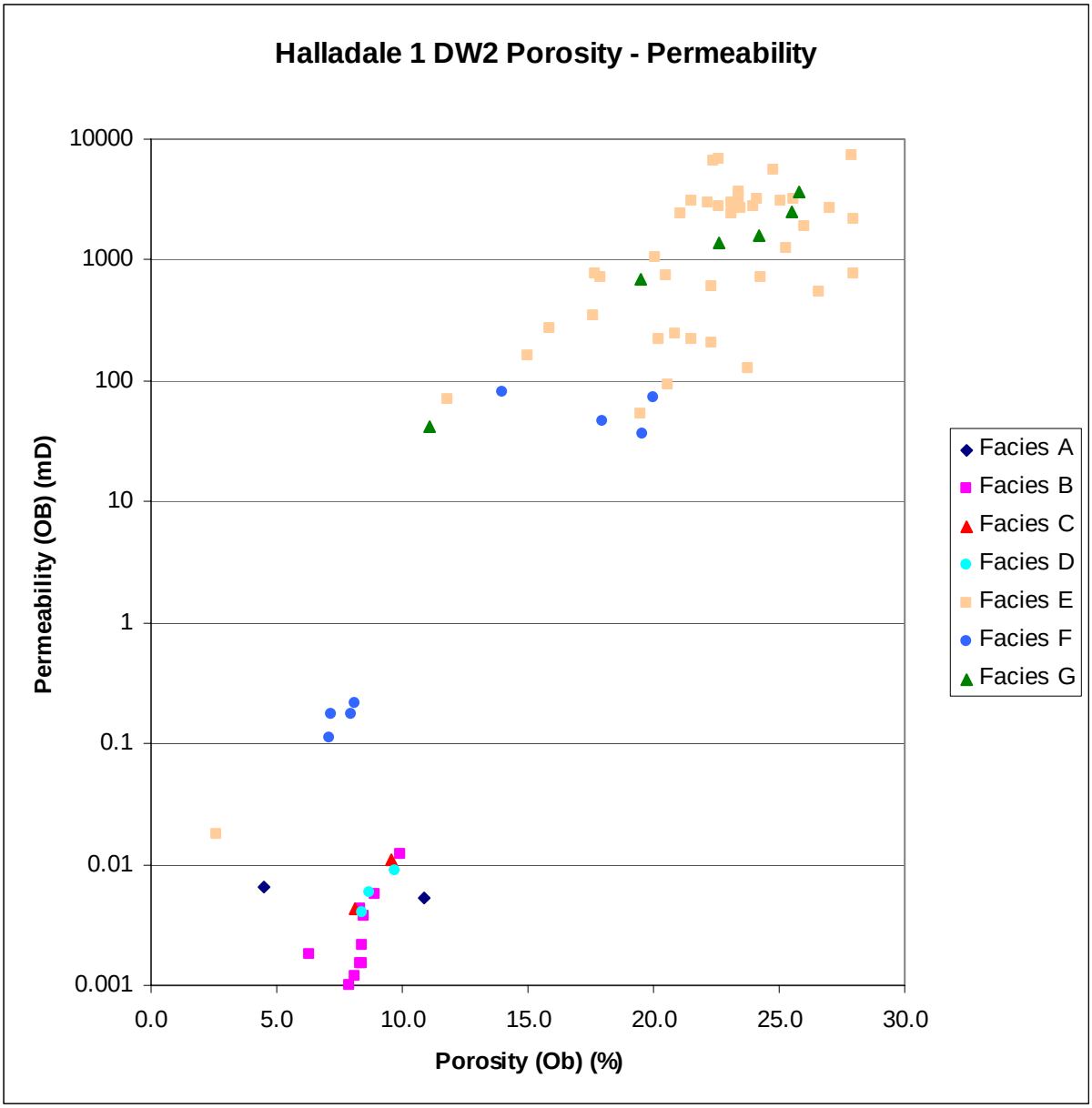

Figure 1. Core porosity and permeability plot for Halladale-1 DW2 showing the relationship between facies and porosity/permeability. The low permeability point in Facies E is a carbonate cemented interval.

APPENDIX 1

HALLADALE-1 DW2
INTERPRETED CORE PHOTOGRAPHS

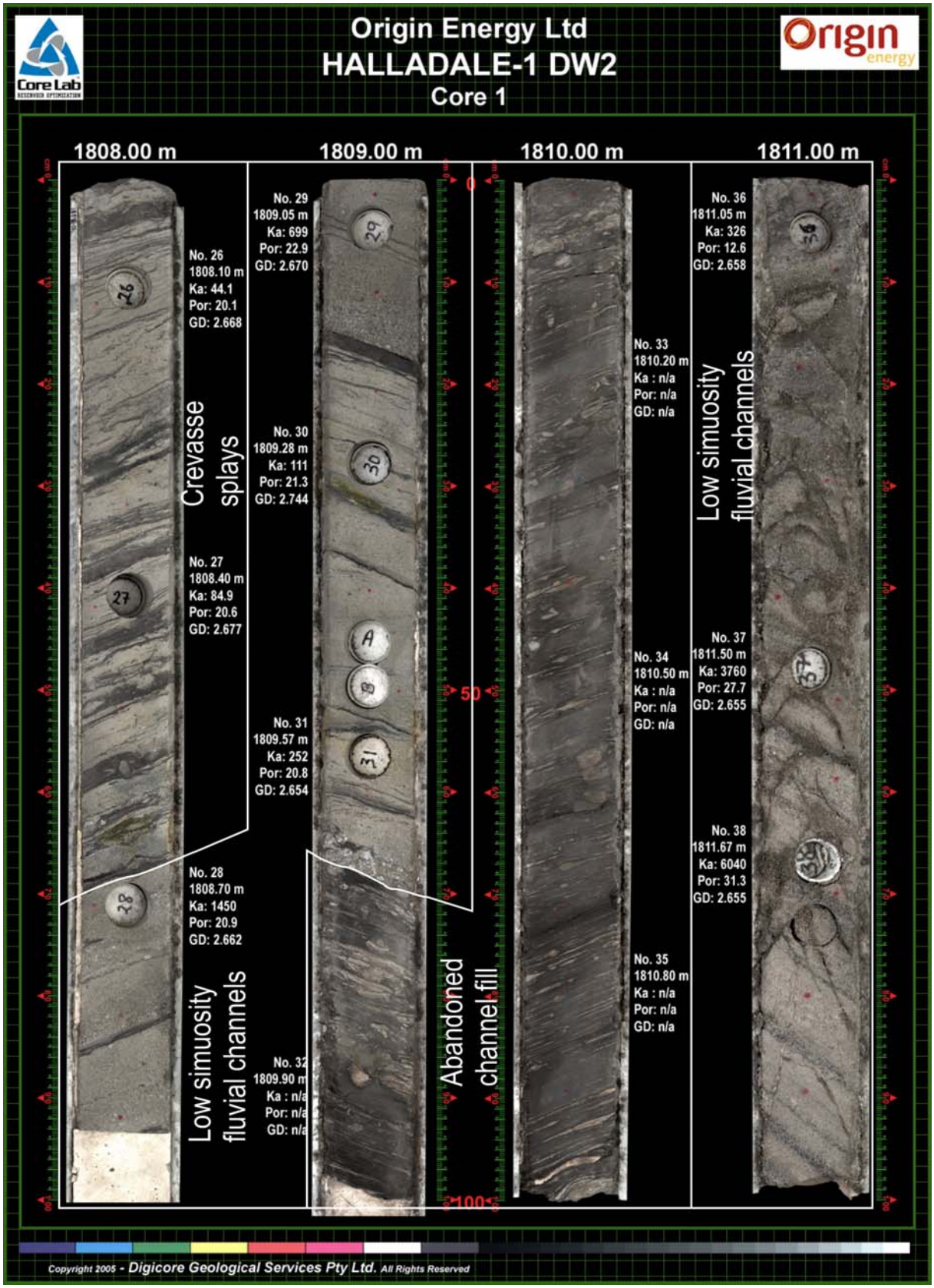
Origin Energy Ltd
HALLADALE-1 DW2
Core 1
1808.00 m
1809.00 m
1810.00 m
1811.00 m
No. 26
1808.10 m
Ka: 44.1
Por: 20.1
GD: 2.668
No. 27
1808.40 m
Ka: 84.9
Por: 20.6
GD: 2.677
No. 28
1808.70 m
Ka: 1450
Por: 20.9
GD: 2.662
No. 29
1809.05 m
Ka: 699
Por: 22.9
GD: 2.670
No. 30
1809.28 m
Ka: 111
Por: 21.3
GD: 2.744
No. 31
1809.57 m
Ka: 252
Por: 20.8
GD: 2.654
No. 32
1809.90 m
Ka : n/a
Por: n/a
GD: n/a
No. 33
1810.20 m
Ka : n/a
Por: n/a
GD: n/a
No. 34
1810.50 m
Ka : n/a
Por: n/a
GD: n/a
No. 35
1810.80 m
Ka : n/a
Por: n/a
GD: n/a
No. 36
1811.05 m
Ka: 326
Por: 12.6
GD: 2.658
No. 37
1811.50 m
Ka: 3760
Por: 27.7
GD: 2.655
No. 38
1811.67 m
Ka: 6040
Por: 31.3
GD: 2.655
Crevasse splays
Low simuosity fluvial channels
Abandoned channel fill
Low simuosity fluvial channels
0
50
100
Copyright 2005 - Digicore Geological Services Pty Ltd. All Rights Reserved

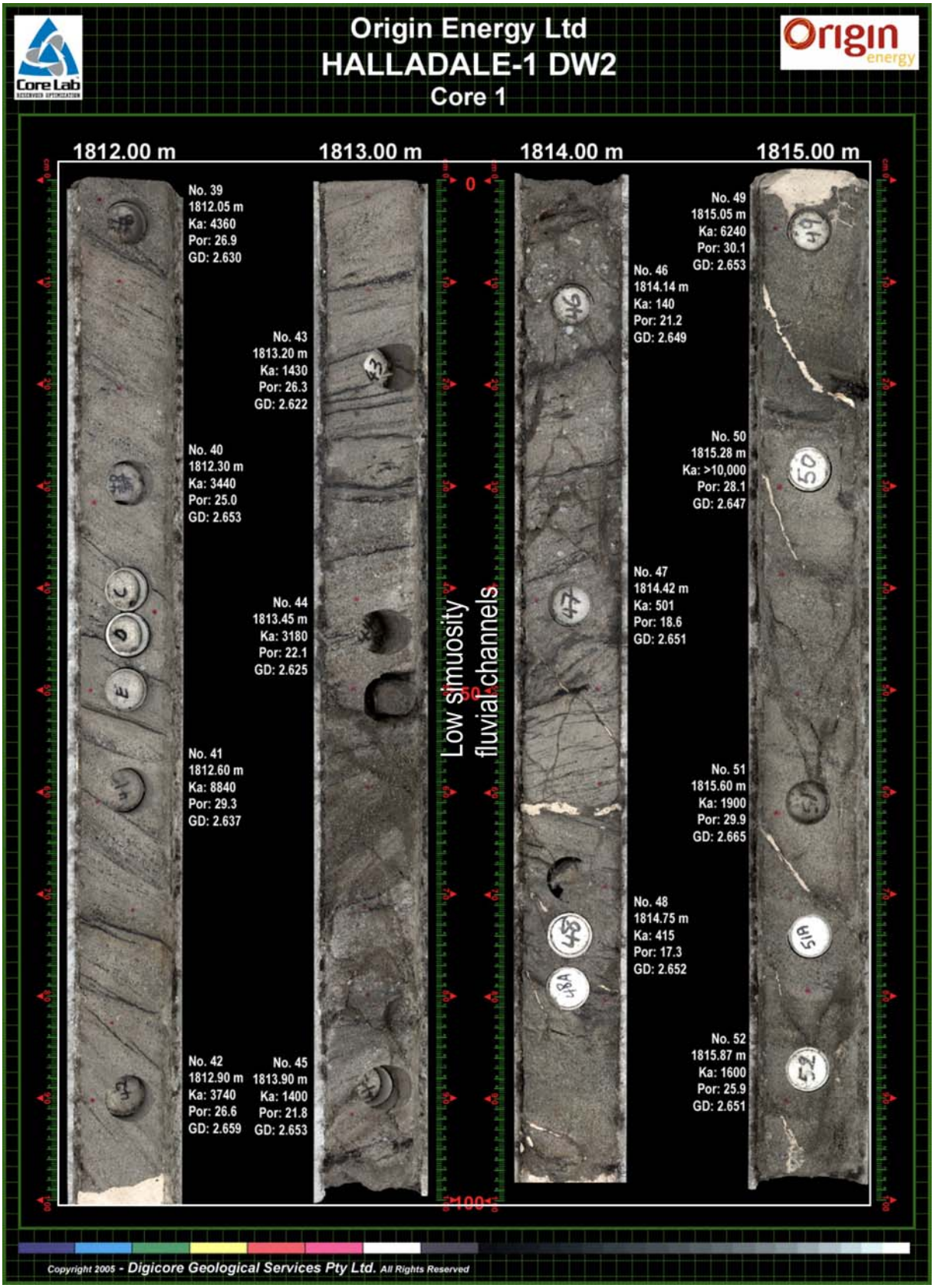
Origin Energy Ltd
HALLADALE-1 DW2
Core 1
1812.00 m
1813.00 m
1814.00 m
1815.00 m
No. 39
1812.05 m
Ka: 4360
Por: 26.9
GD: 2.630
No. 43
1813.20 m
Ka: 1430
Por: 26.3
GD: 2.622
No. 40
1812.30 m
Ka: 3440
Por: 25.0
GD: 2.653
No. 44
1813.45 m
Ka: 3180
Por: 22.1
GD: 2.625
No. 41
1812.60 m
Ka: 8840
Por: 29.3
GD: 2.637
No. 42
1812.90 m
Ka: 3740
Por: 26.6
GD: 2.659
No. 45
1813.90 m
Ka: 1400
Por: 21.8
GD: 2.653
Low simuosity fluvial channels
No. 49
1815.05 m
Ka: 6240
Por: 30.1
GD: 2.653
No. 46
1814.14 m
Ka: 140
Por: 21.2
GD: 2.649
No. 50
1815.28 m
Ka: >10,000
Por: 28.1
GD: 2.647
No. 47
1814.42 m
Ka: 501
Por: 18.6
GD: 2.651
No. 51
1815.60 m
Ka: 1900
Por: 29.9
GD: 2.665
No. 48
1814.75 m
Ka: 415
Por: 17.3
GD: 2.652
No. 52
1815.87 m
Ka: 1600
Por: 25.9
GD: 2.651
Copyright 2005 - Digicore Geological Services Pty Ltd. All Rights Reserved

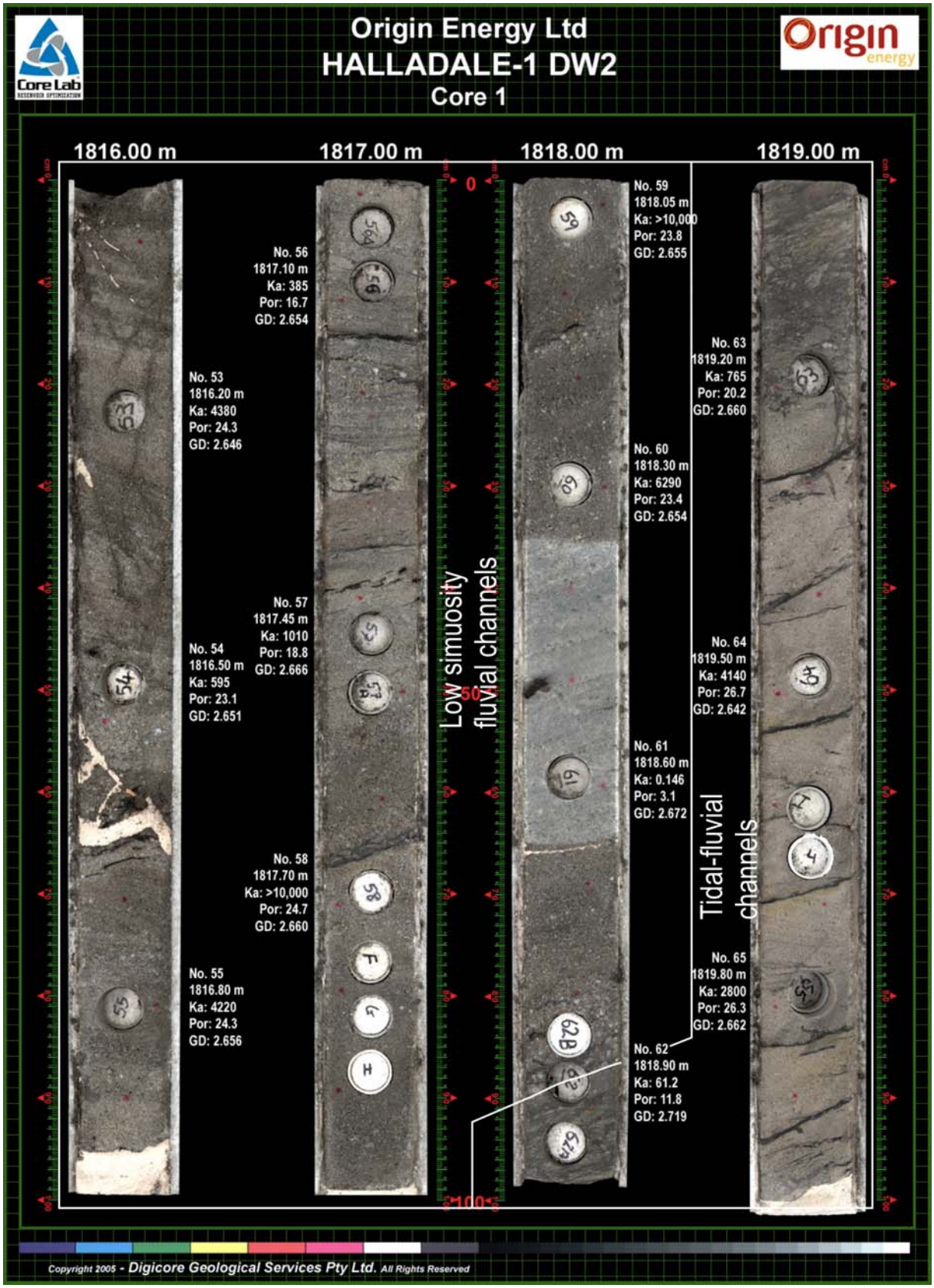
Origin Energy Ltd
HALLADALE-1 DW2
Core 1
1816.00 m
1817.00 m
1818.00 m
1819.00 m
No. 53
1816.20 m
Ka: 4380
Por: 24.3
GD: 2.646
No. 54
1816.50 m
Ka: 595
Por: 23.1
GD: 2.651
No. 55
1816.80 m
Ka: 4220
Por: 24.3
GD: 2.656
No. 56
1817.10 m
Ka: 385
Por: 16.7
GD: 2.654
No. 57
1817.45 m
Ka: 1010
Por: 18.8
GD: 2.666
No. 58
1817.70 m
Ka: >10,000
Por: 24.7
GD: 2.660
No. 59
1818.05 m
Ka: >10,000
Por: 23.8
GD: 2.655
No. 60
1818.30 m
Ka: 6290
Por: 23.4
GD: 2.654
No. 61
1818.60 m
Ka: 0.146
Por: 3.1
GD: 2.672
No. 62
1818.90 m
Ka: 61.2
Por: 11.8
GD: 2.719
No. 63
1819.20 m
Ka: 765
Por: 20.2
GD: 2.660
No. 64
1819.50 m
Ka: 4140
Por: 26.7
GD: 2.642
No. 65
1819.80 m
Ka: 2800
Por: 26.3
GD: 2.662
Low simuosity fluvial channels
Tidal-fluvial channels
Copyright 2005 - Digicore Geological Services Pty Ltd. All Rights Reserved

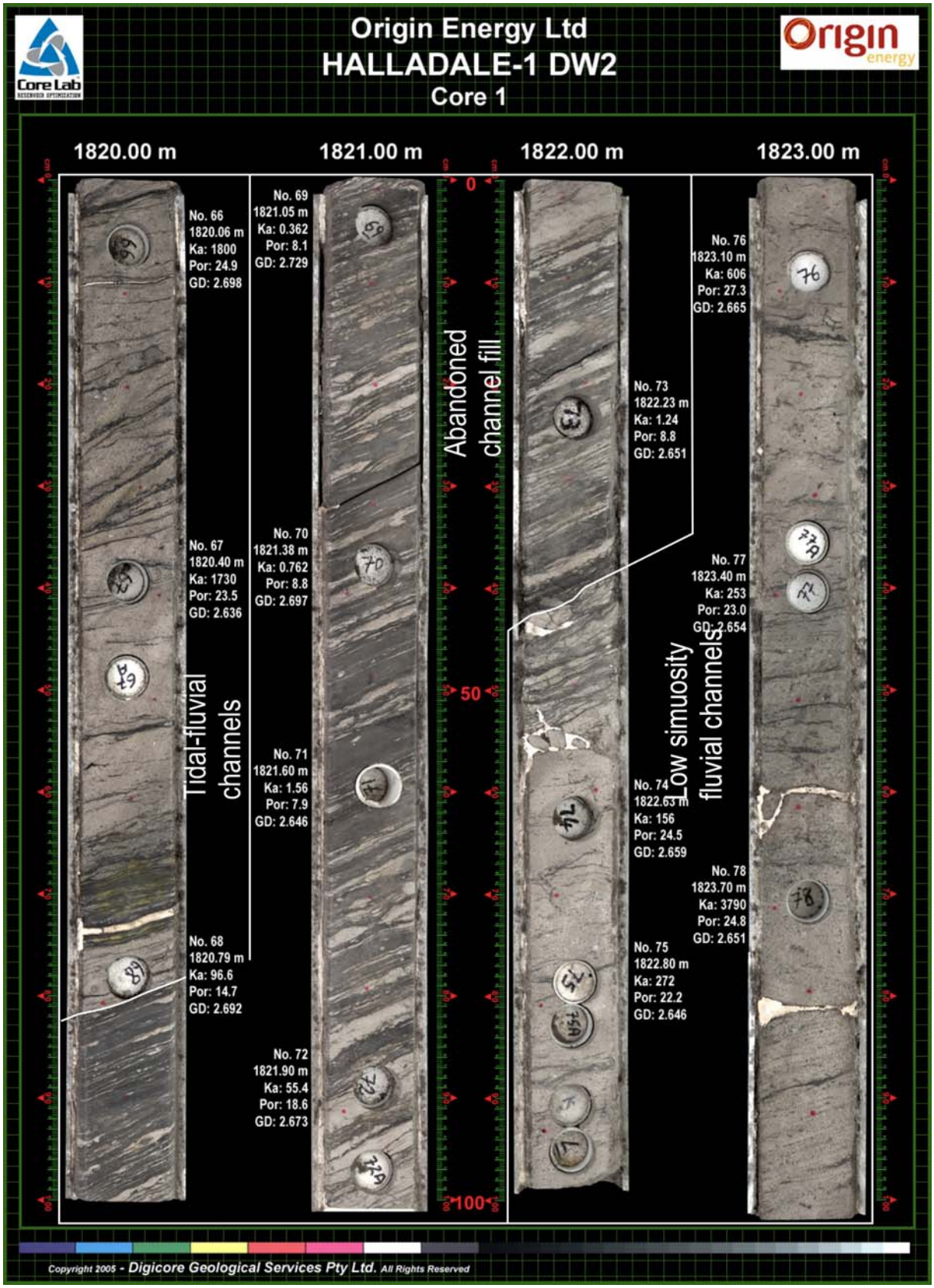
Origin Energy Ltd
HALLADALE-1 DW2
Core 1
1820.00 m
1821.00 m
1822.00 m
1823.00 m
No. 66
1820.06 m
Ka: 1800
Por: 24.9
GD: 2.698
No. 67
1820.40 m
Ka: 1730
Por: 23.5
GD: 2.636
No. 68
1820.79 m
Ka: 96.6
Por: 14.7
GD: 2.692
No. 69
1821.05 m
Ka: 0.362
Por: 8.1
GD: 2.729
No. 70
1821.38 m
Ka: 0.762
Por: 8.8
GD: 2.697
No. 71
1821.60 m
Ka: 1.56
Por: 7.9
GD: 2.646
No. 72
1821.90 m
Ka: 55.4
Por: 18.6
GD: 2.673
Tidal-fluvial channels
Abandoned channel fill
No. 73
1822.23 m
Ka: 1.24
Por: 8.8
GD: 2.651
No. 74
1822.63 m
Ka: 156
Por: 24.5
GD: 2.659
No. 75
1822.80 m
Ka: 272
Por: 22.2
GD: 2.646
Low simuosity fluvial channels
No. 76
1823.10 m
Ka: 606
Por: 27.3
GD: 2.665
No. 77
1823.40 m
Ka: 253
Por: 23.0
GD: 2.654
No. 78
1823.70 m
Ka: 3790
Por: 24.8
GD: 2.651
0
50
100
Copyright 2005 - Digicore Geological Services Pty Ltd. All Rights Reserved

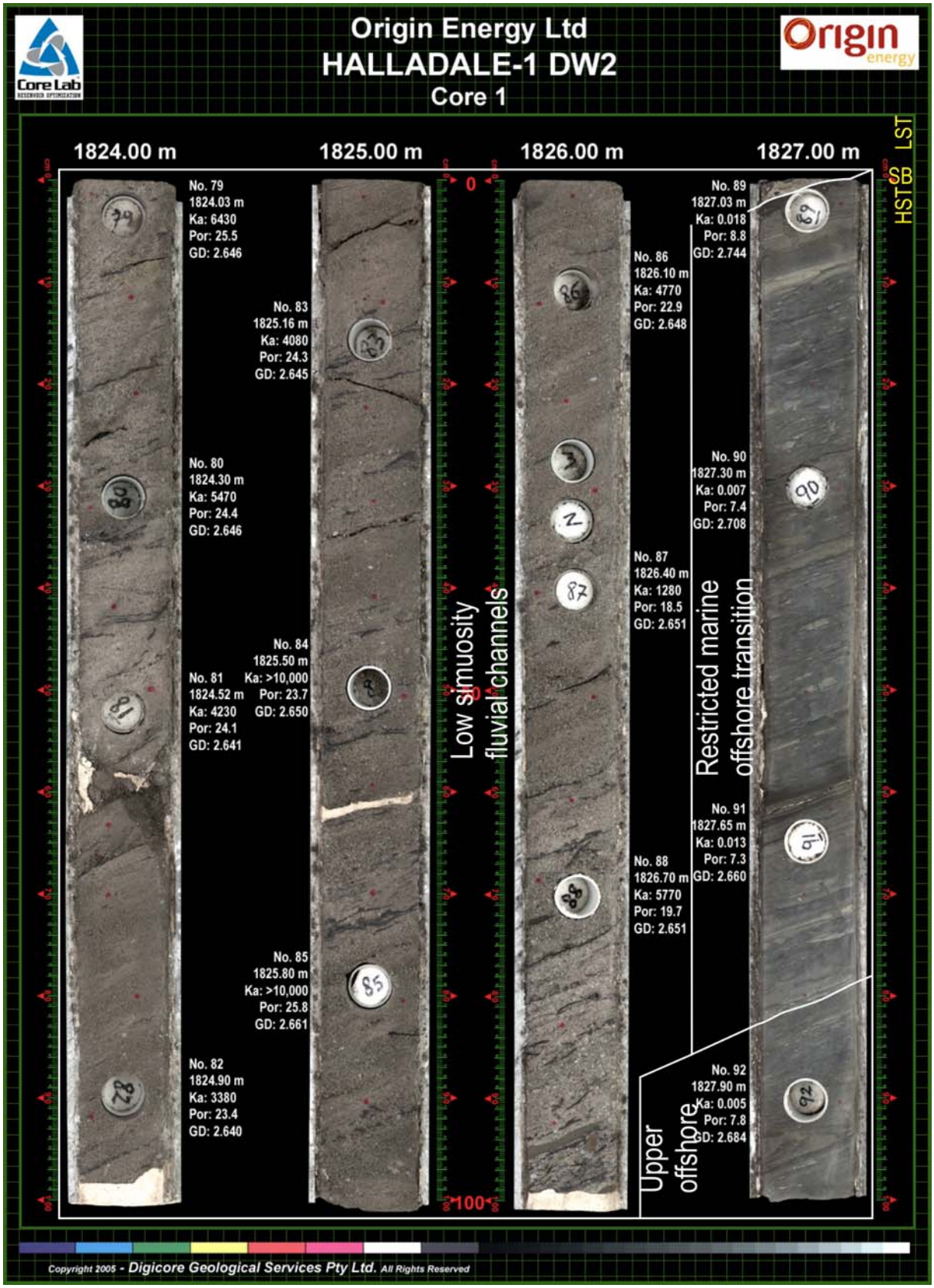
Origin Energy Ltd
HALLADALE-1 DW2
Core 1
1824.00 m
1825.00 m
1826.00 m
1827.00 m
LST
SB
HST
No. 79
1824.03 m
Ka: 6430
Por: 25.5
GD: 2.646
No. 83
1825.16 m
Ka: 4080
Por: 24.3
GD: 2.645
No. 80
1824.30 m
Ka: 5470
Por: 24.4
GD: 2.646
No. 84
1825.50 m
Ka: >10,000
Por: 23.7
GD: 2.650
No. 81
1824.52 m
Ka: 4230
Por: 24.1
GD: 2.641
No. 85
1825.80 m
Ka: >10,000
Por: 25.8
GD: 2.661
No. 82
1824.90 m
Ka: 3380
Por: 23.4
GD: 2.640
No. 86
1826.10 m
Ka: 4770
Por: 22.9
GD: 2.648
No. 87
1826.40 m
Ka: 1280
Por: 18.5
GD: 2.651
No. 88
1826.70 m
Ka: 5770
Por: 19.7
GD: 2.651
No. 89
1827.03 m
Ka: 0.018
Por: 8.8
GD: 2.744
No. 90
1827.30 m
Ka: 0.007
Por: 7.4
GD: 2.708
No. 91
1827.65 m
Ka: 0.013
Por: 7.3
GD: 2.660
No. 92
1827.90 m
Ka: 0.005
Por: 7.8
GD: 2.684
Low simuosity fluvial channels
Restricted marine offshore transition
Upper offshore
0
100
Copyright 2005 - Digicore Geological Services Pty Ltd. All Rights Reserved

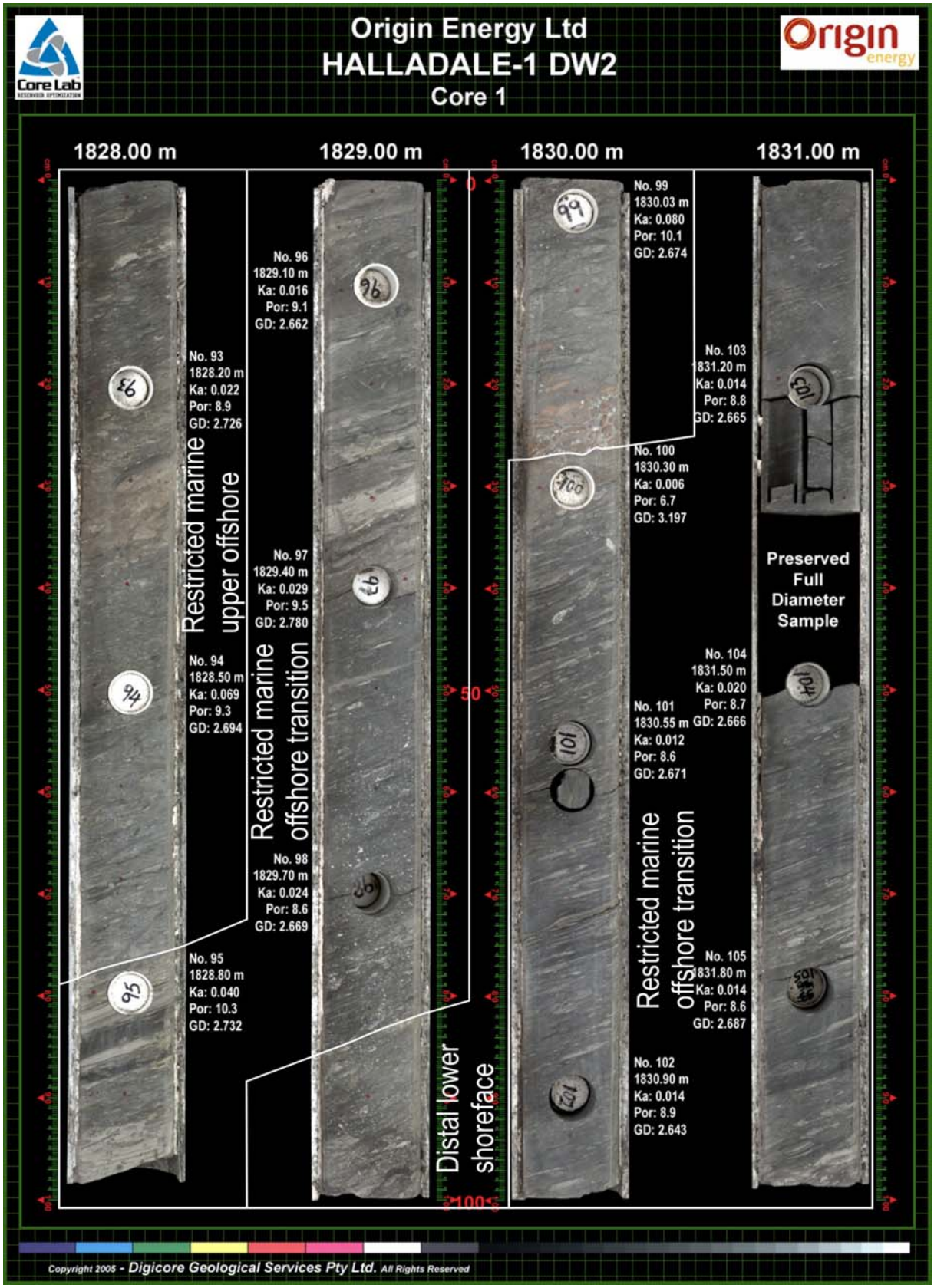
Origin Energy Ltd
HALLADALE-1 DW2
Core 1
1828.00 m
1829.00 m
1830.00 m
1831.00 m
No. 93
1828.20 m
Ka: 0.022
Por: 8.9
GD: 2.726
No. 94
1828.50 m
Ka: 0.069
Por: 9.3
GD: 2.694
No. 95
1828.80 m
Ka: 0.040
Por: 10.3
GD: 2.732
Restricted marine upper offshore
No. 96
1829.10 m
Ka: 0.016
Por: 9.1
GD: 2.662
No. 97
1829.40 m
Ka: 0.029
Por: 9.5
GD: 2.780
No. 98
1829.70 m
Ka: 0.024
Por: 8.6
GD: 2.669
Restricted marine offshore transition
Distal lower shoreface
No. 99
1830.03 m
Ka: 0.080
Por: 10.1
GD: 2.674
No. 100
1830.30 m
Ka: 0.006
Por: 6.7
GD: 3.197
No. 101
1830.55 m
Ka: 0.012
Por: 8.6
GD: 2.671
No. 102
1830.90 m
Ka: 0.014
Por: 8.9
GD: 2.643
No. 103
1831.20 m
Ka: 0.014
Por: 8.8
GD: 2.665
No. 104
1831.50 m
Ka: 0.020
Por: 8.7
GD: 2.666
No. 105
1831.80 m
Ka: 0.014
Por: 8.6
GD: 2.687
Restricted marine offshore transition
Preserved Full Diameter Sample
0
50
100
Copyright 2005 - Digicore Geological Services Pty Ltd. All Rights Reserved

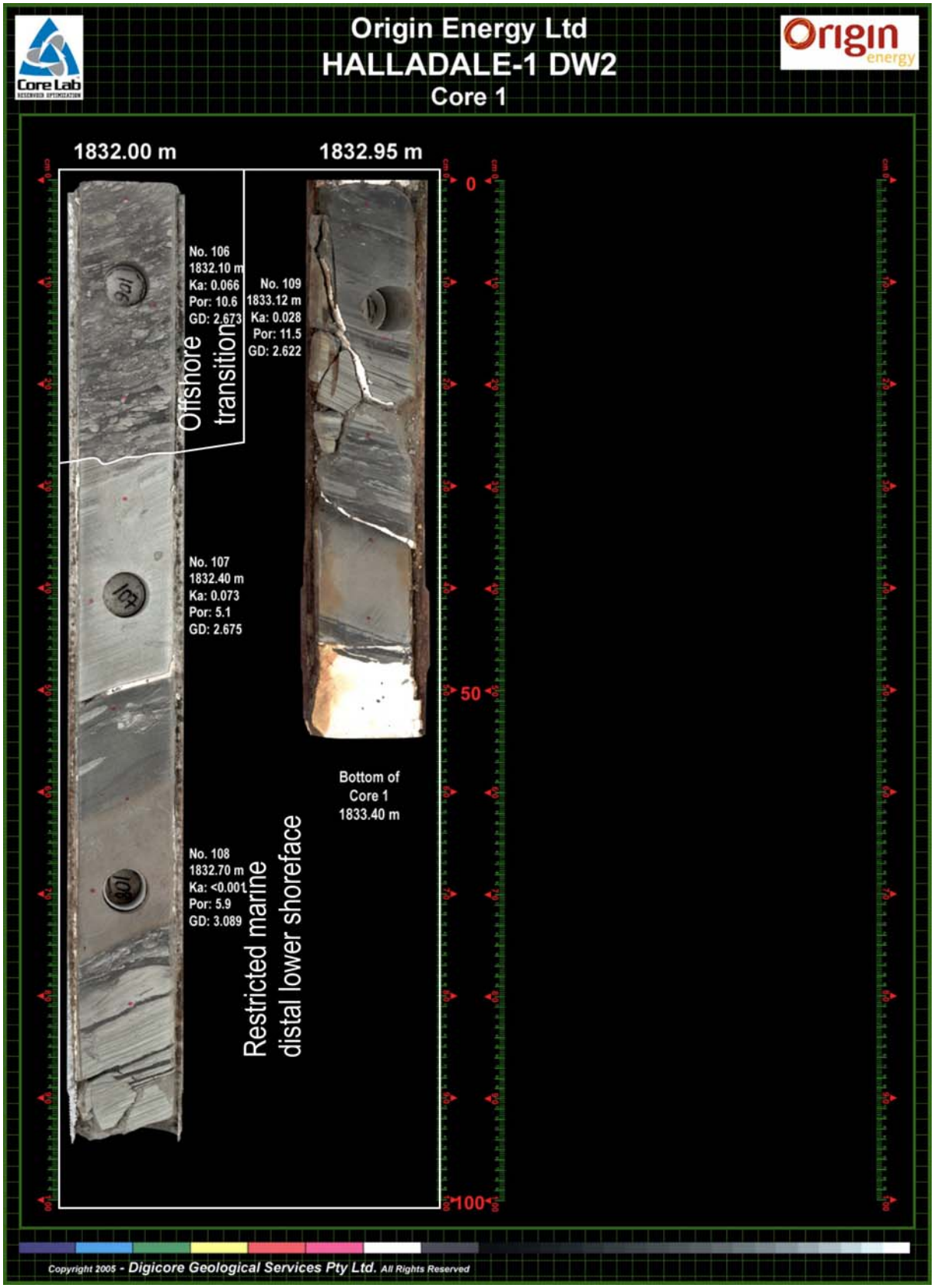
Origin Energy Ltd
HALLADALE-1 DW2
Core 1
1832.00 m
1832.95 m
No. 106
1832.10 m
Ka: 0.066
Por: 10.6
GD: 2.673
No. 109
1833.12 m
Ka: 0.028
Por: 11.5
GD: 2.622
Offshore transition
No. 107
1832.40 m
Ka: 0.073
Por: 5.1
GD: 2.675
Bottom of Core 1
1833.40 m
No. 108
1832.70 m
Ka: <0.001
Por: 5.9
GD: 3.089
Restricted marine distal lower shoreface
0
50
100
Copyright 2005 - Digicore Geological Services Pty Ltd. All Rights Reserved

HALLADALE-1 DW2

CORE 1

CORE GR

0 150

POROSITY (%)

0 5 10 15 20 25 30 35

PERMEABILITY (mD)

0.001 0.01 0.1 1 10 100 1000 10000

PLUG DATA

- Porosity
- Permeability

Palynology | Depth (M) | BI | Mud Silt Sand Gravel | Trace Fossils | Description | Facies | Sequence Stratigraphy: High Order | Low Order

1810

Poorly sorted, weakly laminated sandstone with common plant debris
Rare *Planolites* in interlaminated mudstone and massive sandstone

Crevasse splays; infilling abandoned channel

Abandonment

Plant debris along bedding surfaces and foreset laminations

Small channel fill; dunes and plane bedded bedforms

Plant debris concentrated along laminations

Pyrite associated with organic debris within sandstone laminations

Ponded water developed in abandoned channels, infilled by crevasse splays

Very poorly sorted, common plant debris and quartz granules
Grainsize variations defining foreset laminations

Very poorly cemented, plant debris concentrated on foreset laminations

Channel fill/ barform

Channel fills: complexes of dunes & plane bedded bedforms

Grainsize variation on foresets

Faint lamination defined by plant debris
Very poorly cemented

1815

Matrix supported, granule to small pebble quartz clasts
Rare mudstone rip up clasts

Common plant debris along lamination

Poor to moderately sorted, poorly cemented sandstone

Channel fill/ barform

Sub-angular to sub-rounded quartz granules

Massive to weakly laminated

Poor to moderately sorted, very poorly cemented sandstone with common quartz granules present on foreset laminations
Carbonate cemented zone. Foreset laminations continuous across cemented zone boundary
Common quartz granules as lags, rare mudstone clasts

Channel fill/ barform

Fluvial

1820

Zone homogenised by bioturbation

Rare bioturbation

Regularly spaced, thin mud drapes present on bed boundaries

Increasing marine influence

Common plant and wood debris along laminations

Tidally influenced fluvial channel fill

PSB SB

TRANSGRESSIVE SYSTEMS TRACT

TS

Massive mudstone containing linsen laminated massive sandstone with common plant debris

Ponded water developed in abandoned channels, infilled by crevasse splays

Massive sandstone containing common plant debris

Massive mudstone with thin bedded laminated sandstone
Abundant plant debris along laminations

Abandonment

Sub-angular to sub-rounded quartz granules present as a lag
Sorting increases from poor to moderate as grainsize decreases

1825

Poor to moderately sorted sandstone

Channel fill: complex of dunes & plane bedded bedforms

Poor to moderately sorted sandstone with rare matrix and cement

Common plant debris with very coarse-grained to granule quartz clasts
Sub-angular to sub-rounded, elongate to spherical quartz and mudstone clasts. Rare sideritised mudstone clasts
Sharp-based, fining upward sandstone beds interbedded with mudstone

Offshore transition

LATE LOWSTAND/EARLY TRANSGRESSIVE SYSTEMS TRACT

PSB SB SB

HIGHSTAND SYSTEMS TRACT

Upper offshore

Homogenised silty sandstone

Low diversity of ichnogenera in bioturbated zones

MFS

Offshore transition

Sharp-based, fining upward sandstone containing hummocky cross stratification. Biotubation increases toward the top of beds

TRANSGRESSIVE SYSTEMS TRACT

1830

Transgressive shoreface deposits

TSE

Restricted Marine

PSB

Well bioturbated greywacke containing coarse-grained to granule clasts
Low diversity assemblage dominated by *Teichichnus*. Dispersed sub-angular coarse-grained to granule grains
Lag comprising sub-rounded, elongate to spherical, pebble sized sideritised mudstone clasts.
Coarser grained sediment infilling vertical burrows, cross-cutting background of dominantly horizontal burrows

HIGHSTAND SYSTEMS TRACT

Offshore transition

Sample taken (1831.33 - 1831.5 m)

MFS

TRANSGRESSIVE SYSTEMS TRACT

HIGHSTAND SYSTEMS TRACT

Sharp-based sandstone containing HCS

Distal lower shoreface

Mudstone laminations present between sharp-based sandstone beds containing HCS.
Rare bioturbation present in sandstone beds - escape burrows

1835

Mud Silt Sand Gravel

Siliciclastic

- Siltstone - mudstone/anoxic mudstone
- Sandstone
- Conglomerate
- Tuff

Origin energy

delivering the goods

PHYSICAL SEDIMENTARY STRUCTURES

- Trough cross-bedding
- Planar cross-bedding
- Flat lamination
- Plane bedding
- Low-angle lamination
- Current Ripple Cross-lamination
- Wave Ripple Cross-lamination
- Flaser bedding
- Lenticular lamination
- Wavy lamination
- Hummocky cross-stratification
- Bioturbation
- Plant debris
- Wood
- Rip-up clasts
- Extraformational pebbles
- Soft sediment deformation
- Convoluted bedding
- Synaeresis cracks
- Stylolites
- Coaly trace
- Root trace
- Carbonaceous laminae
- Fault
- Erosional base
- Slumped sediment
- Fining upwards
- Coarsening upwards
- Herring bone cross stratification
- Calcite cementation
- Glauconite
- Pyrite
- Siderite/Fe-concretion
- Silica cementation
- Calcite-healed fracture
- Silica-healed fracture
- Fracture/fault with slickensides

ICHNOLOGY

- *Ophiomorpha*
- *Skolithos*
- *Diplocraterion*
- *Macaronichnus*
- *Thalassinoides*
- *Planolites*
- *Palaeophycus*
- *Rhizocorallium*
- *Teichichnus*
- *Phycosiphon*
- *Taedium*
- *Cylindrichnus*
- *Zoophycus*
- *Rosselia*
- *Conichnus*
- *Chondrites*
- *Undifferentiated*
- *Asterosoma*
- *Helminthopsis*
- *Schaubcylindrichnus*
- *Terebellina*
- *Glossifungites surface*
- *Escape burrow*
- *Cryptobioturbation*
- *Bergaueria*

Bioturbation Index

0 1 2 3 4 5 6

MACROFOSSILS

- *Brachiopods*
- *Molluscs*
- *Bryozoans*
- *Crinoids*
- *Forams*
- *Algae*
- *Stromatolites/stromatoporoids*
- *Unidentified shell fragments*
- *Ammonite*
- *Gastropods*

APPENDIX 6:
STAR INTERPRETATION REPORT

Origin energy

delivering the goods

Halladale-1 DW2

Simultaneous Acoustic and Resistivity (STAR) Interpretation Report

VIC/P37(v)
OTWAY BASIN

September 2005

SUMMARY

This report presents processed and interpreted STAR images from the interval 1680 – 1900 m within Halladale-1 DW2. The studied succession within the well is of Cretaceous age, and is characterised by variable structural dips, typically in the range 15-20º, as is listed below.

Structural Zone	Depth Interval	Tectonic Tilt	Comments
1680 – 1900 m			
Zone I	1680 – 1763	15.8°/124°	Bounded by fractures base
Zone II	1763 – 1827	19.2°/066°	Bounded by unconformity
Zone III	1827 – 1900	16.2°/071°	

Lithofacies identified from STAR images have been calibrated with core and cuttings descriptions. Core and cuttings descriptions match well with lithofacies interpretations derived using wireline log response and STAR image fabrics, and indicate a succession comprising sandstone and mudstone. Five lithofacies associations have been identified within the studied section. These are interpreted as having been deposited in fluvial, shoreface/tidal flat and offshore settings. The lithofacies associations identified are summarised as follows:

I. Mudstones that occur in fining upward or aggradational facies successions and are interpreted as shelf or offshore deposits.
II. Successions of thick bedded sandstones with dominant internal bedding fabrics inclined at angles between 10 and 30°. These deposits represent low sinuosity fluvial channels.
III. Stratified mudstones that are associated with fluvial channels and represent abandoned channel fills.
IV. Successions of stratified sandstones with rare intervals of heterolithic and mudstone lithofacies. The sandstones are characterised by interbedded low angle sedimentary dips (typically <10°) with intervals of higher sedimentary dips (typically <30°). These deposits represent a shoreface/tidal flat setting.
V. Heterolithic intercalations of sandstone and mudstone occurring with the shoreface/tidal flat sediments may reflect upper tidal flat or lower shoreface deposits.

Palaeotransport analyses of sandstones from Lithofacies Association II reveals them to be characterised by internal stratification fabrics with low azimuthal variation. The relationship between intra-set lamination (cross bedding) and coset boundaries suggest that sediment transport occurred normal to, i.e. bedforms migrated downcurrent, to the depositional dip. The cross bedding show a low azimuthal spread with a predominant east to southeast direction. The flat lying intraset surfaces (ISSf) show a 270° azimuthal spread, indicative of deposition within channel and crevasse splay environments.

Sedimentary dips within sandstones of Lithofacies Association IV display 180º azimuthal spread. There is an overall westerly orientation that reflects the predominant current direction. These sediments are mainly interpreted to have been deposited in a tidal flat/shoreface environment.

TABLE OF CONTENTS

SUMMARY **1**

TABLE OF CONTENTS **2**

LIST OF TABLES **4**

LIST OF FIGURES **5**

LIST OF ENCLOSURES **6**

INTRODUCTION **7**

Objectives **7**

Depth and directional references **7**

Processing and quality control **8**

Borehole conditions **8**

Data processing **9**

Speed correction *9*

Image processing *9*

Block depth shifts *9*

Dip processing *9*

Sedimentological analysis **11**

Tectonic tilt determination **11**

Classification of sedimentary features **11**

Borehole stress analysis **12**

Lithofacies characterisation **14**

Lithofacies identified from STAR logs. *14*

Calibration of image log fabrics using cuttings descriptions *15*

Image log calibration using cuttings *15*

STAR derived lithological fabric index *15*

Lithofacies associations **16**

Lithofacies Association I *16*

Lithofacies Association II *17*

Lithofacies Association III *17*

Lithofacies Association IV *17*

Lithofacies Association V *17*

Summary *18*

Summary of environmental interpretations **18**

Interval 1850 – 1900 m *18*

Interval 1800 –1830 m *19*

Bedform orientation and sediment dispersal **20**

Lithofacies Associations I **20**

Lithofacies Association II & III **20**

Lithofacies Association IV & V **21**

Conclusions **23**

REFERENCES **24**

LIST OF TABLES

Table 1 Summary of well details, study objectives and the data set used for this analysis.

Table 2 Summary of hole conditions through the study interval in Halladale-1 DW2

Table 3 Tectonic tilt summary of Halladale-1 DW2

Table 4 Classification of surfaces identified from STAR images

Table 5 Lithofacies identified from STAR images within the study interval

Table 6 Simple fabric index (applied to sandstone lithofacies) based upon mnemonics scheme used for STAR interpretation of lithofacies. Note the fabric index may approximate to a bioturbation index within sandstone lithologies free of granular-pebbly detritus

Table 7 Summary of deposits in the interval 1850 – 1890 m

Table 8 Summary of deposits in the interval 1800 – 1830 m

Table 9 Bedding orientations of Lithofacies Association II within the interval 1800 – 1830 m

Table 10 Bedding orientations of Lithofacies Association IV within the interval 1850 – 1900 m

LIST OF FIGURES

Figure 1. Cumulative automatic (A), muds and hets (B), and manual (C) dip azimuth plots for the studied section (1680 – 1900 m).

Figure 2 Dip categories used in this study

Figure 3. Orientation of borehole breakout (black) within Halladale-1 DW2. The fractures (light colour) are present in one interval only (1760 – 1770) and possibly associated with faulting.

Figure 4 STAR Image through laminated to massive mudstone (lithofacies Ml & Mm) and laminated heterolithic lithofacies (Hl).

Figure 5 STAR image through sandstone lithofacies with Sl(Sm) (1816.5 – 1817.25 m), Sm (1817.25 – 1818.25 m) and Sl (1818.25 – 1820.25 m). Laminated mudstone (Ml) is present at the base.

Figure 6 Cumulative dip azimuth plot for the interval 1800 – 1850 m. Surfaces are shown with structural dip removed.

Figure 7 Cumulative dip azimuth plot for the interval 1850 – 1900 m. Surfaces are shown with structural dip removed.

LIST OF ENCLOSURES

		Scale
Enclosure 1	Quality control plot of STAR log, 1680 - 1900 m	1:500
Enclosure 2	Overview structural summary log, 1680 – 1900 m	1:500
Enclosure 3	Data overview plot, 1800 – 1900 m	1:200
Enclosure 4	Sedimentological summary plot, 1800 – 1830 m	1:100
Enclosure 5	Sedimentological summary plot, 1850 – 1900 m	1:100
Enclosure 6	Core composite plot, 1805 – 1835 m	1:20

INTRODUCTION

The processing and interpretation of the Simultaneous Acoustic and Resistivity (STAR) images from Halladale-1 DW2 are documented in this report. The detailed sedimentological report is based on STAR images for the interval 1680 – 1900 m.

Objectives

The well details and project objectives for Halladale-1 DW2 are summarised in Table 1 with the data that was incorporated into this study.

Table 1. Summary of well details, study objectives and the data set used for this analysis.

Well Details	
Well: Surface Latitude: Surface Longitude: Intervals of interest:	Halladale-1 DW2 38° 34' 45.54" S 142° 43' 50.95" E Cretaceous succession interpreted as shelf, marginal marine and fluvial environments.
Summary of study objectives	
Log Depth Intervals	Objectives
1680 – 1900 m	Processing of STAR images to provide speed corrected false colour images. QC of images to determine the quantity of information that is interpretable.
1680 – 1900 m	Summary structural overview using automatic dip calculations, and manual dip-picking. Summary borehole stress using borehole breakout.
1680 – 1900 m	Overview sedimentological interpretation of features evident within STAR images with the aim of focusing upon variations in palaeocurrent transport directions. This required the manual characterisation of dip features and their interpretation over these intervals.
1800 – 1830 m 1850 – 1900 m	Detailed sedimentological interpretation and lithofacies characterisation.
Data incorporated in study	
1680 – 1900 m	Open hole logs from XMAC suite. Processed STAR data in DLIS format.
1680 – 1900 m	Cuttings description
1808 – 1834 m	Core 1 (1808.0 – 1833.4 m Driller's depth)

Depth and directional references

Unless otherwise mentioned, all depths in this report reference log depths. Orientation data is referenced using the standard convention of dip/dip azimuth. For example, 3°/313° indicates a dip of 3° (measured from the horizontal) towards 313° (referenced clockwise from north). Borehole orientation data follows a convention of deviation/azimuth of deviation. For example, 2°/300° indicates a 2° deviation from the vertical towards 300° (SW).

PROCESSING AND QUALITY CONTROL

The Simultaneous Acoustic and Resistivity (STAR) tool was run by Baker Atlas on 18th April 2005 in the 8½ inch section of Halladale-1 DW2 over the interval 1668 – 1927 m.

The Baker Atlas Simultaneous Acoustic and Resistivity tool is a pad based micro-resistivity imaging device, with an array of 24 measuring electrodes (buttons) on each of pad, with 144 buttons in total. The data is sampled at 0.1 inch vertically and horizontally with a bedding resolution of approximately 1 cm. The data is processed to provide 56% coverage of the borehole wall in an 8.5 inch hole.

Processing was carried out over the logged interval using Terrasciences TerraStation Formation Viewer module.

The mud system was Aqua Drill with a resistivity of 0.078 Ωm, a viscosity of 87 S and a density of 1.26 g/c3. The fluid losses encountered during drilling were minimal (3.7 cm^3). The borehole reached a maximum temperature of 79.5°C.

A STAR log quality control plot is shown in Enclosure 1. These plots provide detailed information concerning hole orientation, tool orientation, hole condition and STAR operating parameters.

Borehole conditions

STAR image quality is related to borehole condition, which is good throughout the section in Halladale-1 DW2 with clear geological detail visible and only very minor image artefacts. Borehole deviation is 21.72°/343.3° at 1654.3 m and 21.67°/344.05° at 1742.32 m, 21.51°/343.38° at 1795.6 m, and 19.03°/343.2° at 1941 m.

A summary of hole conditions is included in Table 2.

Within the study interval (1680 – 1900 m) the callipers show that the hole is consistently in gauge. There is little difference in the C1 and C2 callipers (typically only 0.25 inch) below 1785 m and the callipers usually overlie in this interval. Intervals of ovalisation (up to 3.5 inches) above 1785 m are not limited to one direction, but present in both calliper directions. Filter-cake is present over permeably zones.

Table 2. Summary of hole conditions through the study interval in Halladale-1 DW2.

Normal Hole Size	Interval Depth	Comments
1680 – 1900 m		
8.5	1680 - 1785	Up to 3.5” overgauge in the C2 calliper, up to 2.5” overgauge in the C1 calliper
	1785 – 1900*	In gauge

* interval contains up to 0.25” filter-cake build-up on permeable sections

Data processing

Speed correction

The accelerometer speed correction utility corrects STAR micro-resistivity data for minor variations in recording velocity induced by tool or cable friction. Extremes in velocity variation may occur when the tool is either stationary or rapidly accelerating as a result of being stuck or the logging being stopped for pipe removal. The most important parameter for the speed correction procedure is the zero-sum window, which prevents cumulative build-up of erroneous shifts within a window. Thus all shifts applied by the speed correction should add up to zero within a certain window length. The length of this window is decided by experimenting and the general roughness of the logging run. In the case of Halladale-1 DW2, a window of 4 ft was chosen. The speed correction shift curve is calculated by double integration of the Z-accelerometer curve with the cable speed representing the window constant. The resulting shift curve is then applied synchronously to all curves in the log.

Image processing

Before generating the false-colour images from the speed corrected data, the individual curves are transferred back to their physical depth referenced positions. The images are produced with two types of resistivity scaling:

- *Static normalised* images have the same relative resistivity scaling over larger intervals and therefore illustrate large-scale resistivity variations related to lithology and phase changes. Dependent on Emex current variability.

- *Dynamic normalised* images were scaled within a 0.5 m sliding window, thereby maximising the expression of more detailed rock fabrics (and noise).

In this study, the dynamic normalised images were used primarily for bedding, lithofacies and structure identification. Image polarity was correctly matched to openhole resistivity logs.

Block depth shifts

No block depth shifts were applied to the Halladale-1 DW2 data.

Dip processing

Two types of dip computation were conducted on the Halladale-1 DW2 dataset.

Computed dip correlations were carried out on the STAR data from the loaded interval (Enclosure 1). These correlations use refined least-squares algorithms with regression coefficients cut-offs for each correlation pair. The interval computation parameters were aimed at correlating bedding features using pad-to-pad (PTP) algorithms with the following parameters:

- 120 cm correlation interval, 60 cm step distance and a 70° search angle (referenced to borehole axis) and the cut-off set at 0.6 for individual curve pairs.

These parameters are referenced as “4X2X70” in Enclosure 1. This computation was repeated using a stacking of three consecutive correlation surfaces. The stacking of dips in this way tends to smooth dip patterns and trends and is a viable method of “quick-look”

identification of structural dip. These parameters are referenced as “4X2X70ST3” in Enclosure 1. Detailed interpretation of dip patterns should not be carried out on results from this processing.

Manual dips were computed directly from the images using the TerraStation Formation Viewer (e.g. Enclosure 2). The major advantage of the manual dip technique is that each feature may then be classified into a geological category and that only the results in which the interpreter has confidence are used for further interpretation. A further advantage of manual dip picking is the ability to measure and orientate discordant surfaces such as fractures and faults, which are unlikely to be correlated by standard interval correlation techniques

SEDIMENTOLOGICAL ANALYSIS

Tectonic tilt determination

Prior to detailed sedimentary analyses, it is first required to evaluate structural dip, so that the sedimentary surfaces identified in STAR images can be restored to their original orientation or "sedimentary dip". Structural dip (or tectonic tilt) is the attitude of formations resulting solely from tectonic movements. Structural dip is best determined from beds that were originally deposited as horizontally stratified deposits. These beds can include mudstones, or parallel stratified laminations within heterolithic successions comprising interbedded sandstone-mudstone laminae. The structural dip interpretation within well Trefoil 1 was an iterative process involving:

- Initial evaluation of automatic computed dips to identify general data trends.
- Manual picking of mudstone bed dips to confirm tectonic tilt throughout the studied succession.

Tectonic tilt evaluated on the basis of dip data through mudstone intervals is summarised in Table 3. Before undertaking a sedimentological interpretation structural dip was removed from the “manual” data set. The structural dip was removed following identification of intervals of strata (structural zones) of consistent structural dip. The structural dips are summarised in Enclosure 2.

Table 3. Tectonic tilt summary of Halladale-1 DW2.

Structural Zone	Depth Interval	Tectonic Tilt	Comments
1680 – 1900 m			
Zone I	1680 – 1763	15.9°/123°	Bounded by fractures at base
Zone II	1763 – 1827	19.2°/066°	Bounded by unconformity
Zone III	1827 – 1900	16.2°/071°	

Cumulative dip azimuth plots for mudstone bedding surfaces within the studied interval (1680 – 1900 m) from Halladale-1 DW2 are presented in Figure 1. These plots clearly illustrate the structural subdivisions proposed for this well.

Classification of sedimentary features

Classification of sedimentary surfaces recognised from borehole image logs is a three stage iterative process involving:

- First pass dip picking. This phase of feature identification is carried out in conjunction with examination of wireline logs, and results in a simple 2-fold sub-division of dip features into mudstone and "others".
- Structural dip is removed from the data set using a workstation based stereographic technique to provide sedimentary dips.
- Sedimentary dips are re-classified in the workstation environment. Wireline logs are used to drive lithofacies interpretation. Sedimentary dips within sandstone lithologies are characterised using a hierarchical scheme depending upon their dip and orientation.

The hierarchical scheme applied to Halladale-1 DW2 is illustrated in Figure 2 and Table 4 below, and sedimentary dips for the studied intervals 1800 - 1830 m and 1850 - 1900 m are indicated in Enclosures 4 - 5.

Borehole stress analysis

During drilling, stress is redistributed around the borehole producing compressional failure (borehole breakout) and tensile fracture (hydraulic fracturing). Borehole stress features are limited to borehole breakout that is present in fine grained lithologies only. Figure 3 shows the orientation of the breakout.

Table 4. Classification of surfaces identified from STAR images.

Dip type	Interpreted dip category	Colour	Description
LB	Lithological boundary	Blue green	Low true dip angle surfaces which define a marked resistivity between overlying and underlying beds. Wireline logs indicate a lithological contrast.
LBe	Erosional lithological boundary	Dark green	Erosive surfaces which define a marked resistivity between overlying and underlying beds. Truncation of bedding fabrics beneath the surface may be evident. Wireline logs indicate a lithological contrast.
LBc	Cemented lithological boundary	Pale blue green	Sharply defined highly resistive or conductive bed. Bounding surfaces may define planar or "nodular" features. Normally associated with change in wireline log response.
ISS	Intra set surface	Yellow	Inclined surfaces typically dipping at a true dip angle greater than 5°. Surfaces may be inclined at angles up to 25°-30° (i.e. close to angle of repose), and occur within distinct groups of similar orientation. Surfaces typically show cm-dm scale spacing in borehole image logs. They are discordant to set (or bed) and coset boundaries.
SB	Set (bed) boundary	Brown	Surfaces within sandstone lithologies which are typically (though not exclusively) inclined at sedimentary dip of < 15°. Set boundaries define a group or "set" of intraset surfaces of similar orientation. The set boundary is distinguished from the intraset surfaces by its different orientation. Set boundaries typically occur at dm - m scale spacing in borehole image logs.
CSB	Coset boundary	Cyan	A surface separating a group of sets of similar orientation. Note: Coset boundaries may also define a single bed or set displaying a significantly different internal fabric to those sets surrounding it. Set boundaries are typically identified at m scale spacing in borehole image logs. Note: Coset boundaries may also define a single bed or set at dm scale which displays a significantly different internal fabric to those sets surrounding it.
ISSf	Flat/horizontal	Purple	Near horizontal intraset surfaces with true dip angle (<5°), characterised by resistivity contrast several cm thick. Sedimentary dip azimuth may be variable due to flat lying nature of these beds, and errors associated with fitting dips to such surfaces. Surfaces typically show cm scale spacing in borehole image logs.
PDf	Poorly defined feature	Dark purple	These surfaces may be any of the above but are very poorly defined in terms of continuity around the borehole.
XB	Cross beds	Red	Cm-dm scale cross stratification fabric, too small to be characterised in detail.
MUDS	Shale bedding	Green	Confident bedding features with consistent magnitudes.
HETS	Heterolithic bedding	Orange	Confident bedding features with approximately consistent magnitudes.

Lithofacies characterisation

Lithofacies identification was first carried out using STAR images in conjunction with openhole log suites. The STAR interpretations were then calibrated against cuttings.

Lithofacies identified from STAR logs.

The sedimentological interpretation of STAR images was carried out with the aid of gamma ray, density, neutron porosity and sonic logs. Lithofacies were interpreted on the basis of variations in wireline log response in conjunction with fabrics observed in STAR images (Table 5). During interpretation, cuttings descriptions were also used to help provide a guide to lithology, but were found to have only moderate depth resolution (i.e. matching of cuttings description to log response) due to dispersion of cuttings during circulation of drilling muds. Three broad lithofacies were interpreted as being present, i.e. sandstones, mudstones and rare, finely inter-bedded heterolithic successions. Heterolithic successions comprise centimetre-decimetre scale interbedded sandstone and mudstone beds.

Lithofacies types were classified according to a simple scheme using mnemonics based upon interpreted lithology and contained fabric, the latter being determined from borehole image log and associated dip data. Examples of identified lithofacies are summarised below in Table 5.

Table 5. Lithofacies identified from STAR images within the study interval.

Inferred Lithology/Grain Size	Typical Log Response	Image Log Fabrics	Lithofacies Mnemonic
Sandstone	GR <70 API RHOB 2.0 – 2.5 g/cc HTNP 0.05 – 0.20	Laminated	Sl
		Fine scale mottled or "speckled" texture with poorly defined or disrupted lamination fabric	Sm
Heterolithics	GR 70 – 110 API RHOB 2.5 – 2.65 g/cc HTNP 0.20 – 0.25	Laminated	Hl
		Mottled with disrupted lamination fabric	Hm
Mudstone	GR 110 – 180 API RHOB >2.65 g/cc HTNP 0.25 – 0.35	Laminated	Ml
		Mottled with disrupted lamination fabric	Mm

The hierarchical combinations of different lithofacies mnemonics were used to provide detailed descriptions of lithofacies types. In these descriptions, the enclosure of lithofacies mnemonics in parenthesis was used to denote the minor presence of a lithofacies type, or poor development or preservation of a sedimentary structure, e.g.

- Mm (Ml) mottled mudstones with relict lamination or minor laminated intervals.
- Sm (Sl) mottled sandstone with poorly defined relict lamination.
- Sl (Sm) laminated sandstone with minor fabric loss due to mottling/ disruption of lamination etc.

Figures 4 - 5 illustrate examples of different lithofacies types for the lithologies identified, together with their fabric index.

Calibration of image log fabrics using cuttings descriptions

Calibration of image log fabrics was carried out using:

- Cuttings descriptions through the logged intervals. Cuttings descriptions are summarised on Enclosure 3.

Image log calibration using cuttings

Generally, cuttings descriptions match well with lithofacies interpretations derived using wireline log response and STAR image fabrics. Cuttings descriptions reveal a succession comprising sandstone and mudstone.

Characterisation of heterolithic successions comprising individual beds beneath the resolution of wireline logs is difficult. However, image logs revealing extreme resistivity variation within strata containing cm-dm scale bedding fabrics provide some insight as to the presence of these heterogeneous lithologies. Cuttings descriptions through successions interpreted from wireline log and STAR as comprising heterolithic deposits, invariably yield documentation of cuttings of mudstone and sandstone in varying proportions.

STAR derived lithological fabric index

The hierarchical lithofacies nomenclature scheme applied to description of lithofacies from borehole image logs was also used to provide a simple four-fold fabric index as illustrated for sandstones in Table 6 below. This type of fabric index may be useful for comparison of reservoir properties with image log derived lithological properties. Note, if mottled fabrics present within sandstones are due to bioturbation, this fabric index may also approximate to a four-fold bioturbation index, which may be useful in construction of sedimentary models using data derived from image logs.

Table 6. Simple fabric index (applied to sandstone lithofacies) based upon mnemonics scheme used for STAR interpretation of lithofacies. Note the fabric index may approximate to a bioturbation index within sandstone lithologies free of granular-pebbly detritus.

Lithofacies	Approximate degree of fabric development within sediments.	Fabric Index
Sl	Minimal <10%	1
Sl (Sm)	approximately 25 %	2
Sm (Sl)	approximately 75 %	3
Sm	near total 100 %	4

The implication of the fabric index is that low indices will result in strongly anisotropic reservoir properties (e.g. Kv > Kh). If due to phenomenon, such as bioturbation, creating mottled image fabric and loss of stratification, higher fabric indices may reflect more homogeneous reservoir properties (e.g. decrease in Kv:Kh ratio due to loss of stratification).

Lithofacies associations

The sedimentary deposits in the interval 1800 – 1900 m within Halladale-1 DW2 comprise a heterolithic succession of sandstones and mudstones. The successions can be sub-divided into a number of discrete sub-units based upon log trends and stacking patterns of interpreted lithofacies.

Some sub-units are characterised by blocky low and high gamma ray intervals and NPHI and RHOB log response that similarly alternate between sandstone and mudstone. Sedimentary dips within these successions vary from low to high within sandstones.

Other sub-units are characterised by serrated gamma ray log trends, and NPHI and RHOB log response that trends between sandstone and heterolithics. Sedimentary dips within these successions are variable. These deposits possibly represent deposition within tidal channels or shoreface settings.

The intervals with blocky between sandstone and mudstone are consistent with a model of deposition in a low sinuosity fluvial setting with periodic channel abandonment. The intervals with the serrated log signature may reflect deposition in a tidally influenced marginal marine setting.

The lithofacies identified are described in detail in the following sections. In the absence of core calibration the following discussions are should be considered speculative.

Observed vertical transitions in lithofacies types identified in borehole images have enabled lithofacies to be grouped into genetically related successions of strata or *lithofacies associations*, which have some environmental significance (Walker 1992a). Five lithofacies associations were identified within the studied data set, and their distribution within the studied intervals is illustrated in Enclosures 4 - 5. The lithofacies associations identified are summarised below.

Lithofacies Association I

Lithofacies Association I is argillaceous, mainly comprising mudstone lithologies (Ml and Mm), with minor interbedded heterolithic lithologies. The mudstones occur as thick deposits associated with the serrated gamma ray log trend (e.g. Enclosure 5) and commonly display a massive to slightly mottled and laminated fabric.

Generally, Lithofacies Association I forms relatively thick deposits up to several tens of metres thick, and is characterised by blocky to serrate, overall high gamma-ray log response (>110 API), reflecting the presence of a predominantly argillaceous succession of lithofacies types. Lithofacies Association I typically pass upward into sandy lithofacies of Lithofacies Association III or VI.

The mudstones of Lithofacies Association I display low sedimentary dip (typically <10°), with wide ranging dip azimuths (covering 360° spread) indicative of their original deposition as parallel stratified sediments upon a flat lying substrate.

Sedimentation within Lithofacies Association I was probably dominated by suspension fallout of argillaceous material, resulting in the accumulation of massive to laminated mudstone lithofacies (Ml, etc.).

Lithofacies Association II

This STAR derived lithofacies is sand dominated, mainly comprising, Sl, Sm, Sm(Sl) and Sl(Sm). Lithofacies Association II occurs in successions up to 10 m thick within the studied intervals. Few conclusions can be drawn concerning the spatial distribution of different lithologies within these deposits.

The coset boundaries occur at dm to m scale and dip data sets, in places, for Lithofacies Association IV indicate an azimuthal spread of up to 120°, with a low azimuthal dispersion within cosets. The coset boundaries within this lithofacies association have similar orientations to the XB indicating downcurrent progradation. Intervals comprising ISSf have orientations implying deposition as bedforms with a consistent current direction.

The cross stratified sediments of Lithofacies Association II represent the deposits of low sinuosity fluvial channels, whereas intervals dominated by Sl and the thin cross stratified sets indicates unconfined flows, possibly crevasse splays. Evidence of primary stratification within these deposits testifies to the development and migration of bedforms, with the cross-bedding indicating dunes and sand waves.

Palaeotransport implications for this lithofacies association are discussed in detail in the following sections.

Lithofacies Association III

Lithofacies Association III is very similar to Lithofacies Association I, except that it occurs as deposits, up to a few metres thick, within Lithofacies Association II. The mudstones in this lithofacies comprise Mm and Ml and show a preferred dip orientation indicating deposition on an inclined surface within an abandoned channel.

Lithofacies Association IV

Lithofacies Association IV comprises Sl, Sl(Sm), minor Sm(Sl) and rare intervals of heterolithic and mudstone lithofacies. Lithofacies Association IV is characterised by interbedded low angle sedimentary dips (typically <10°) with intervals of higher sedimentary dips (typically <30°). The succession is up to 10 m in thickness and the base of the Lithofacies Association is typically sharp.

The low angle stratification and cross bedding within these sediments is indicative of deposition by traction processes. The occurrence of these sediments associated with Lithofacies Association I and V, and the often variable orientations of cosets may be consistent with deposition from tidal currents within a shoreface/tidal flat setting. Successions where low angle surfaces display a preferred unimodal distribution of azimuths may indicate the presence of a more significant palaeoslope or sediment transport and deposition.

Lithofacies Association V

Lithofacies Association V comprises heterolithic lithologies. Heterolithic sediments consist of centimetre to decimetre scale interbedded sandstones and mudstones, and often display a mottled image fabric. Within the studied intervals, heterolithic deposits may form successions several metres thick. Heterolithic deposits overlie Lithofacies Associations IV, and display overall upward fining gamma ray log trend.

Sedimentary dips within heterolithic deposits are typically characterised by low angle fabrics (inclined typically <10° sedimentary dip). Removal of structural dip reveals these

bedding fabrics to be characterised wide ranging (up to 360° spread) dip azimuths, indicative of their original deposition as approximately horizontally stratified sediments. There are rare, thin intervals containing cross bedding that are interbedded with mudstone.

The heterolithic nature of these deposits suggests deposition via both tractional and suspension processes. In shoreface/tidal setting, this style of deposition may have occurred in a tidal flat environment.

Summary

The integrated analyses of wireline log signature and STAR fabric allows identification of a variety of different lithofacies types. Calibration with core has permitted detailed lithofacies interpretation from STAR logs whereas, in other intervals, the cuttings descriptions only permit limited lithofacies interpretation. Therefore, in absence of core calibration the environmental interpretations outlined in the following section should be treated with caution as it is only speculative.

Summary of environmental interpretations

A brief summary of the sedimentary successions analysed in detail and their environmental interpretation is provided in the following sections. Detailed discussions of palaeotransport observations are included in the Bedform Orientation and Sediment Dispersal section of this report.

Interval 1850 – 1900 m

Wireline logs and STAR interpretations through this interval indicate that it can be subdivided into two intervals; both comprising overall fining upward successions. The succession is sandstone at the base that passes upwards into mudstone. Details are summarised below in Table 7.

Table 7. Summary of deposits in the interval 1850 – 1900 m

Interval 1850 – 1900 m			
Depth (m)	**Lithofacies Association**	**Brief Description**	**Interpretation**
1850 - 1855	I	Laminated and massive mudstone	Shelf mudstone/offshore
1855 – 1863	IV	Sharp based sandstone with Sm, Sl, Sl(Sm) and Sm(Sl)	Lower tidal flat
1863 – 1866	V	Laminated heterolithics	Upper tidal flat
1866 – 1869	IV	Sharp based laminated sandstone	Tidal channel
1869 – 1874	I	Laminated mudstone	Shelf mudstone/offshore
1874 – 1880	V	Laminated heterolithics and mudstone	Lower shoreface?
1880 – 1898	IV	Sharp based sandstone with Sl(Sm), Sm(Sl), Sl and Sm	Tidal channel/tidal flat
1898 – 1900	I	Laminated mudstone	Shelf mudstone/offshore

Interval 1800 –1830 m

This interval comprises interbedded sandstones, with sharp bases and tops, and mudstones. Details are summarised in Table 8.

Table 8. Summary of deposits in the interval 1800 – 1830 m

Interval 1800 – 1830 m			
Depth (m)	**Lithofacies Association**	**Brief Description**	**Interpretation**
1800 - 1804	I	Laminated mudstone	Shelf mudstone/offshore?
1804 – 1808	II	Sandstone comprising Sm, Sl(Sm) and Sl	Low sinuosity fluvial channels
1808 – 1809.5	II	Laminated sandstone	Crevasse splay
1809.5 – 1811	III	Laminated mudstone	Abandoned channel
1811 – 1818.5	II	Sandstone comprising Sl, Sm, Sm(Sl)	Low sinuosity fluvial channels
1818.5 – 1820	II	Laminated sandstone	Tidal-fluvial channel
1820 – 1822	III	Laminated mudstone	Abandoned channel
1822 – 1827	II	Laminated sandstone	Low sinuosity fluvial channels
1827 – 1830	I	Laminated mudstone	Offshore

BEDFORM ORIENTATION AND SEDIMENT DISPERSAL

Following sub-division of the succession into the five lithofacies associations described above, detailed analysis of the orientation of different bedforms within these successions was undertaken in order to evaluate sediment dispersal, and orientation of the depositional system. Sedimentary dips for the different bedding categories identified are summarised in Enclosures 4 - 5. Cumulative dip azimuth plots for the interval 1800 – 1900 m are shown in Figures 6 – 7.

Lithofacies Association I

Sedimentary dips within mudstones from Lithofacies Association I typically display 360º azimuthal spread, indicative of the original deposition of this lithology as "flat lying" effectively parallel stratified sediments. These sediments are interpreted to have been deposited in shelf/offshore settings.

Lithofacies Association II & III

The low gamma ray log response typical of Lithofacies Association II indicates that these successions contain a significant proportion of clean, potentially high reservoir quality sandstones. This lithofacies association is interpreted as low sinuosity fluvial channels, crevasse splay and abandoned channel deposits on the basis of the dominance of cross bedding, low angle lamination and the low azimuthal spread of palaeocurrent data (120°).

The presence of low angle laminations and sets of cross bedding less than a metre in thickness indicates that the channels were shallow, as the thickness of the bedforms is proportional to the channel depth (Bridge and Tye, 2000). Intraset surfaces (XB) show a low azimuthal spread with a predominant east to southeast direction whereas the flat lying intraset surfaces (ISSf) show a 270° azimuthal spread, indicative of deposition within channel and crevasse splay environments.

The orientation of bedding surfaces within these intervals are summarised in Table 9 below.

Table 9. Bedding orientations of Lithofacies Association II within the interval 1800 – 1830 m

Interval 1800 – 1830 m (Log depth)				
Depth (m)	Orientation of ISSf's	Orientation of XB's	Orientation of CSB's, SB's	Comments
1804 - 1808	SW - SE	W - SW	CSB: SW SB: E – S	CSB oriented at low angle to XB, SB oriented at low angle to ISSf.
1808 – 1809.5	W			Shallow dipping ISSf within a crevasse splay
1809.5 - 1811				Mudstone
1811 – 1815	NE –SE	E – SE	NE – SE	CSB & SB oriented at low angle to XB indicating downstream accretion.
1815 – 1820	Sw – S	SW, SE	SE	CSB oriented at low angle to XB indicating downstream accretion
1820 – 1821.5				Mudstone
1821.5 - 1827	E – SE	E –SE	E – SE	CSB & SB oriented at low angle to XB indicating downstream accretion

Lithofacies Association IV & V

Sedimentary dips within sandstones of Lithofacies Association IV display 180º azimuthal spread. There is an overall westerly orientation that reflects the predominant current direction. These sediments are mainly interpreted to have been deposited in a tidal flat/shoreface environment.

The orientation of bedding surfaces within these intervals are summarised in Table 10 below.

Table 10. Bedding orientation of Lithofacies Association IV within the interval 1850 – 1900 m

Interval 1850 – 1900 m (Log depth)				
Depth (m)	Orientation of ISSf's	Orientation of XB's	Orientation of CSB's, SB's	Comments
1855.5 - 1858	SW, S	SE		Variable orientation may reflect original flat lying deposition in tidal flat environment.
1858 - 1863	Variable			Variable orientation may reflect original flat lying deposition in tidal flat environment.
1863 – 1869	Variable	SW, SE	S, SE	CSB and SB oriented at low angle to XB indicating down-current progradation
1869 - 1880				Mudstone and Lithofacies Association VI
1880 – 1890	NW – SW	NW – SW, SE	NW - S	Variable orientation of XB may reflect tidal currents. CSB & SB at high and low angles to XB indicates lateral and down-current bedform migration
1890 – 1898	NE – SW		SSE	Variable orientation of ISSf may reflect deposition as "flat lying" sediments

CONCLUSIONS

1. The studied successions dip at low angles in variable orientations. A number of structural zones have been defined, these are summarised as follows:

Interval 1680 – 1900 m

Zone I	1680 – 1763	15.9°/124°	Bounded by fractures at base
Zone II	1763 – 1827	19.2°/66°	Bounded by unconformity
Zone III	1827 – 1900	16.2°/71°	

2. The sedimentary succession is heterolithic, comprising sandstones, mudstones and heterolithic intervals, composed of dm scissile intercalations of sandstone and mudstone.

3. Five lithofacies associations have been identified, these comprise:

   I. Mudstones that occur in fining upward or aggradational facies successions and are interpreted as shelf or offshore deposits.
   II. Successions of thick bedded sandstones with dominant internal bedding fabrics inclined at angles between 10 and 30°. These deposits represent low sinuosity fluvial channels.
   III. Stratified mudstones that are associated with fluvial channels and represent abandoned channel fills.
   IV. Successions of stratified sandstones with rare intervals of heterolithic and mudstone lithofacies. The sandstones are characterised by interbedded low angle sedimentary dips (typically <10°) with intervals of higher sedimentary dips (typically <30°). These deposits represent a shoreface/tidal flat setting.
   V. Heterolithic intercalations of sandstone and mudstone occurring with the shoreface/tidal flat sediments may reflect upper tidal flat or lower shoreface deposits.

4. Palaeotransport analyses of sandstones from Lithofacies Association II reveals them to be characterised by internal stratification fabrics with low azimuthal variation. The relationship between intra-set lamination (cross bedding) and coset boundaries suggest that sediment transport occurred normal to, i.e. bedforms migrated downcurrent, to the depositional dip. The cross bedding show a low azimuthal spread with a predominant east to southeast direction. The flat lying intraset surfaces (ISSf) show a 270° azimuthal spread, indicative of deposition within channel and crevasse splay environments.

5. Sedimentary dips within sandstones of Lithofacies Association IV display 180° azimuthal spread. There is an overall westerly orientation that reflects the predominant current direction. These sediments are mainly interpreted to have been deposited in a tidal flat/shoreface environment.

6. In the absence of a detailed core calibration in Lithofacies Association IV and V, environmental interpretations are highly subjective. However, observed lithofacies stacking patterns do appear to be consistent with an interpretation of deposition of strata within shoreface/tidal setting.

REFERENCES

Bridge, J.S., and Tye, R.S., 2000. Interpreting the dimensions of ancient fluvial bars, channels and channel belts from wireline logs and cores. *American Association of Petroleum Geologists Bulletin*, 84, 1205-1228.

Walker, R.G. 1992a. Facies models. *In:* Walker, R.G. and James, N.P. eds. *Facies Models: Response to Sea Level Change*, Geological Association of Canada, Newfoundland, 1-14.

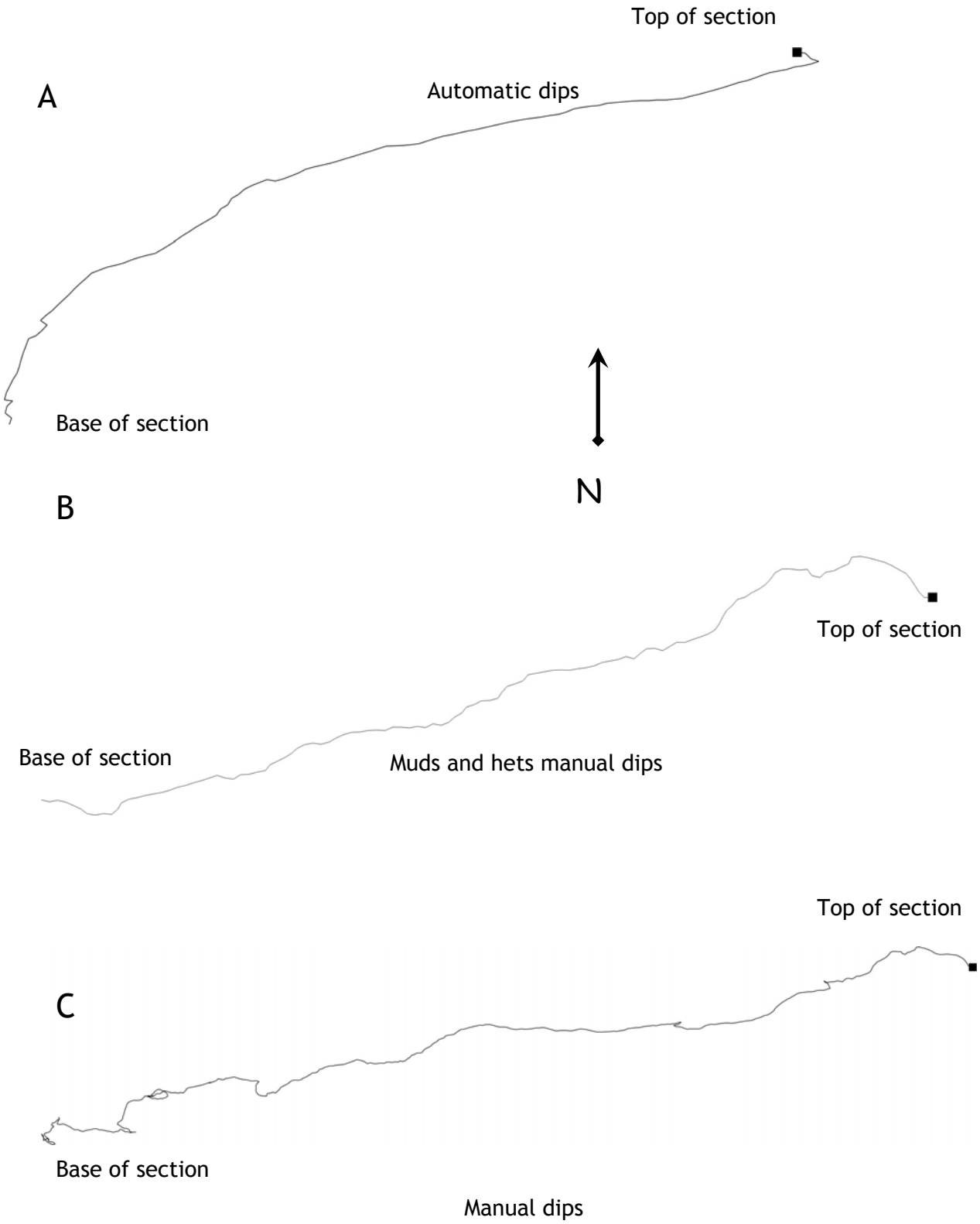

Figure 1. Cumulative automatic (A), muds and hets (B), and manual (C) dip azimuth plots for the studied section (1680 – 1900 m).

Code	Description	Interpreted category
MUD	Confident bedding features, with consistent magnitudes.	Shale Bedding
HETS	Confident bedding surfaces characterised by high resistivity contrasts.	Inter-bedded dm-scale sand and mud. (Heterolithics)
LB	Low true dip angle (typically less than 5°), marked resistivity contrast with overlying/underlying beds	Lithological boundary
LBe	Low true dip angle (typically less than 5°), marked resistivity contrast with overlying/underlying beds and truncation of underlying beds.	Erosional lithological boundary
LBc	Separates a highly resistive zone from overlying and underlying beds. May be a planar layer or non-planar nodular feature.	Cemented lithological boundary
SB	Surface (typically less than 15°) enclosing a bed that may have internal stratification with consistent dip and azimuth.	Set (bed) boundary
CSB	Surface separating groups of beds or a single bed displaying a significantly different character.	Coset boundary
ISS	Steeply dipping true dip angle (15-40°), highly discordant to set (bed) boundaries, and are characterised by resistivity contrast of cm scale with constant dip azimuth trends.	Intra set, cross-bedding surface
ISSF	Near horizontal surfaces with true dip angle (<5°), characterised by resistivity contrast several cm thick. Azimuth trends may be variable due to the low precision associated with determining the azimuth of flat lying beds.	Flat/horizontal intra set surface
FRAC	Generally discordant plane with moderate to steep dip (resistive or conductive).	Fracture
FAULTR	Generally discordant plane with moderate to steep dip, with identifiable displacement (resistive or conductive).	Fault

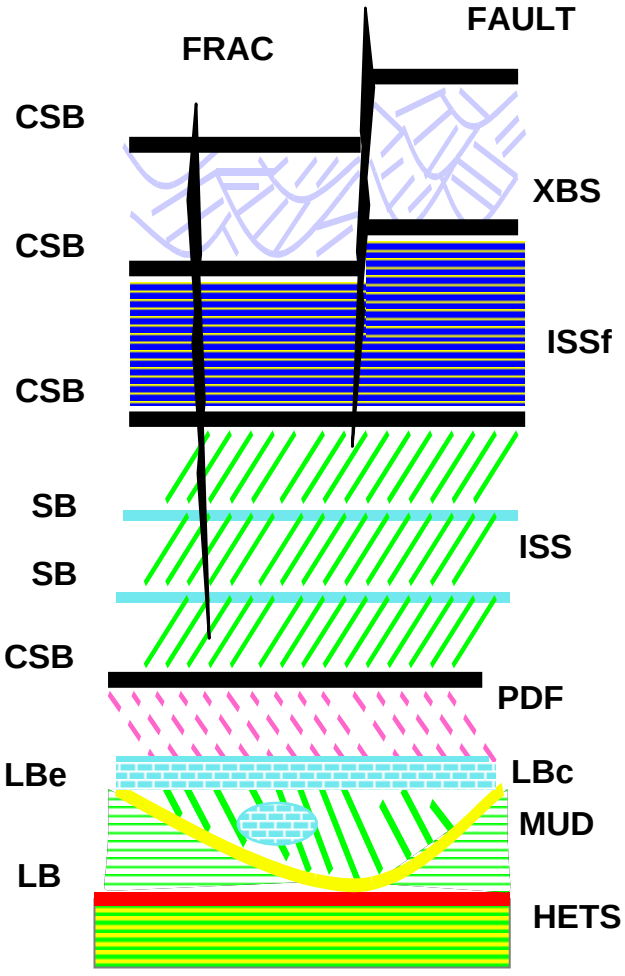

Figure 2. Dip categories used in this study.

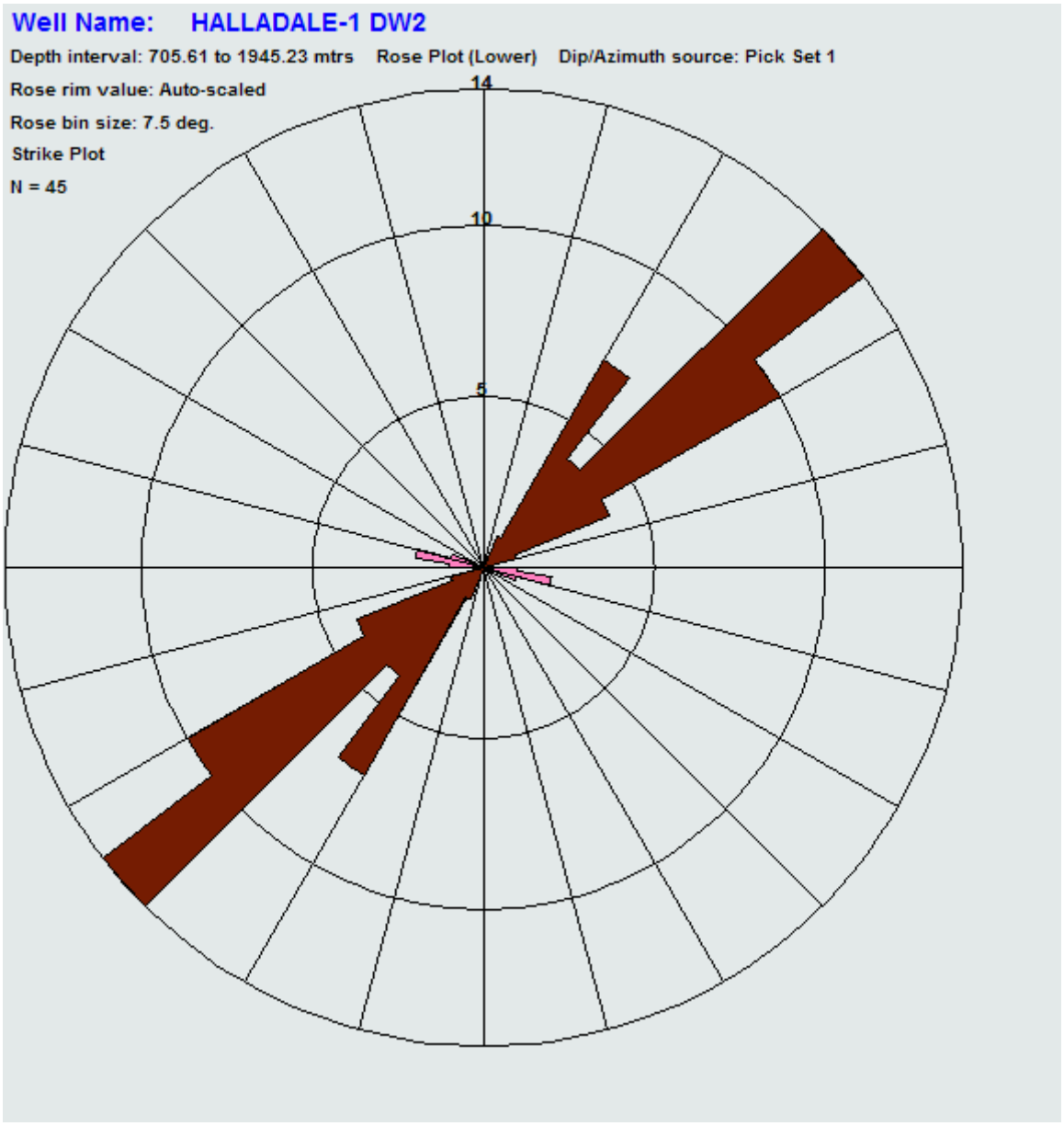

Figure 3. Orientation of borehole breakout (black) within Halladale-1 DW2. The fractures (light colour) are present in one interval only (1760 – 1770) and possibly associated with faulting.

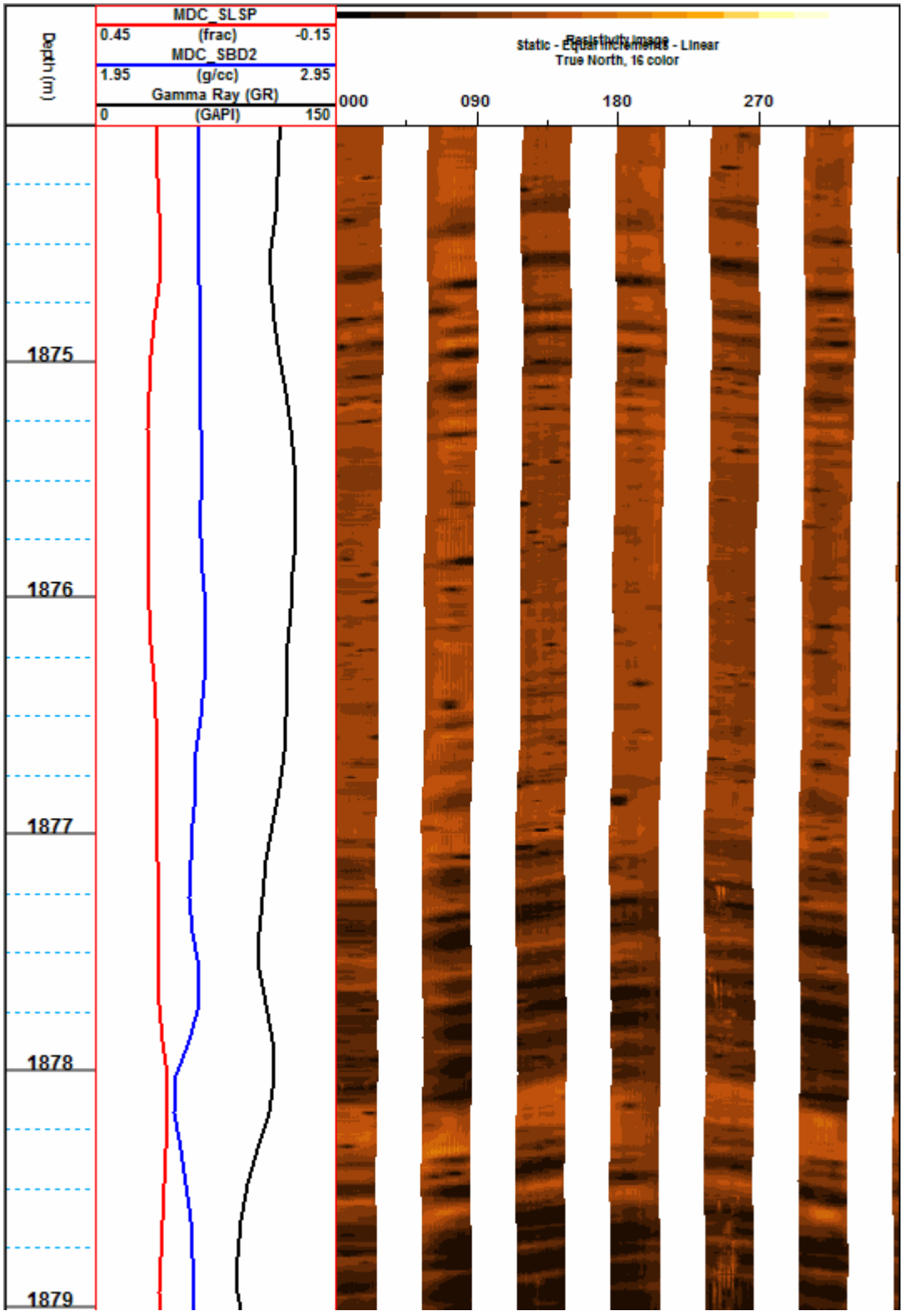

Figure 4. STAR Image through laminated to massive mudstone (lithofacies Ml & Mm) and laminated heterolithic lithofacies (Hl)

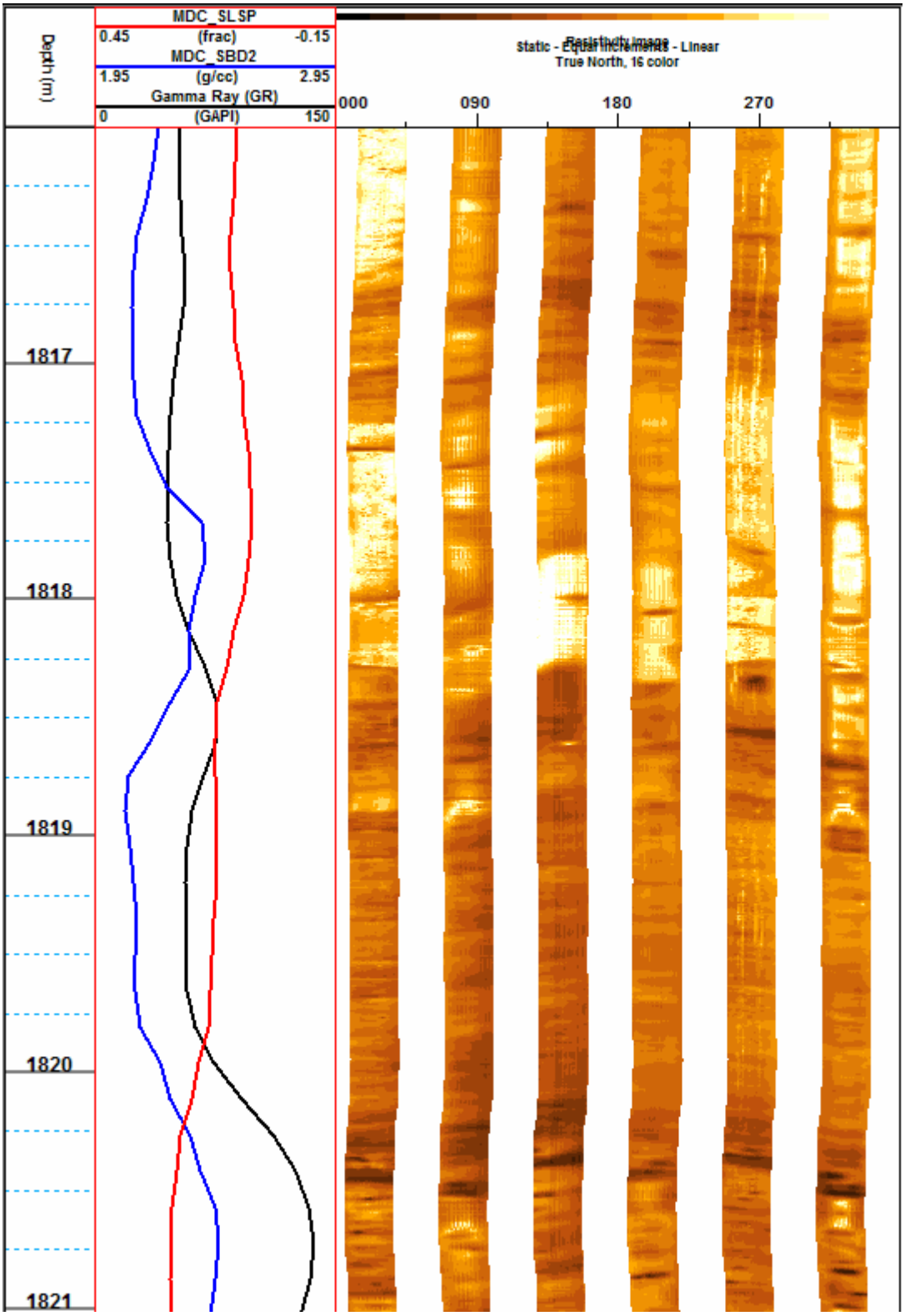

Figure 5. STAR image through sandstone lithofacies with Sl(Sm) (1816.5 – 1817.25 m), Sm (1817.25 – 1818.25 m) and Sl (1818.25 – 1820.25 m). Laminated mudstone (Ml) is present at the base.

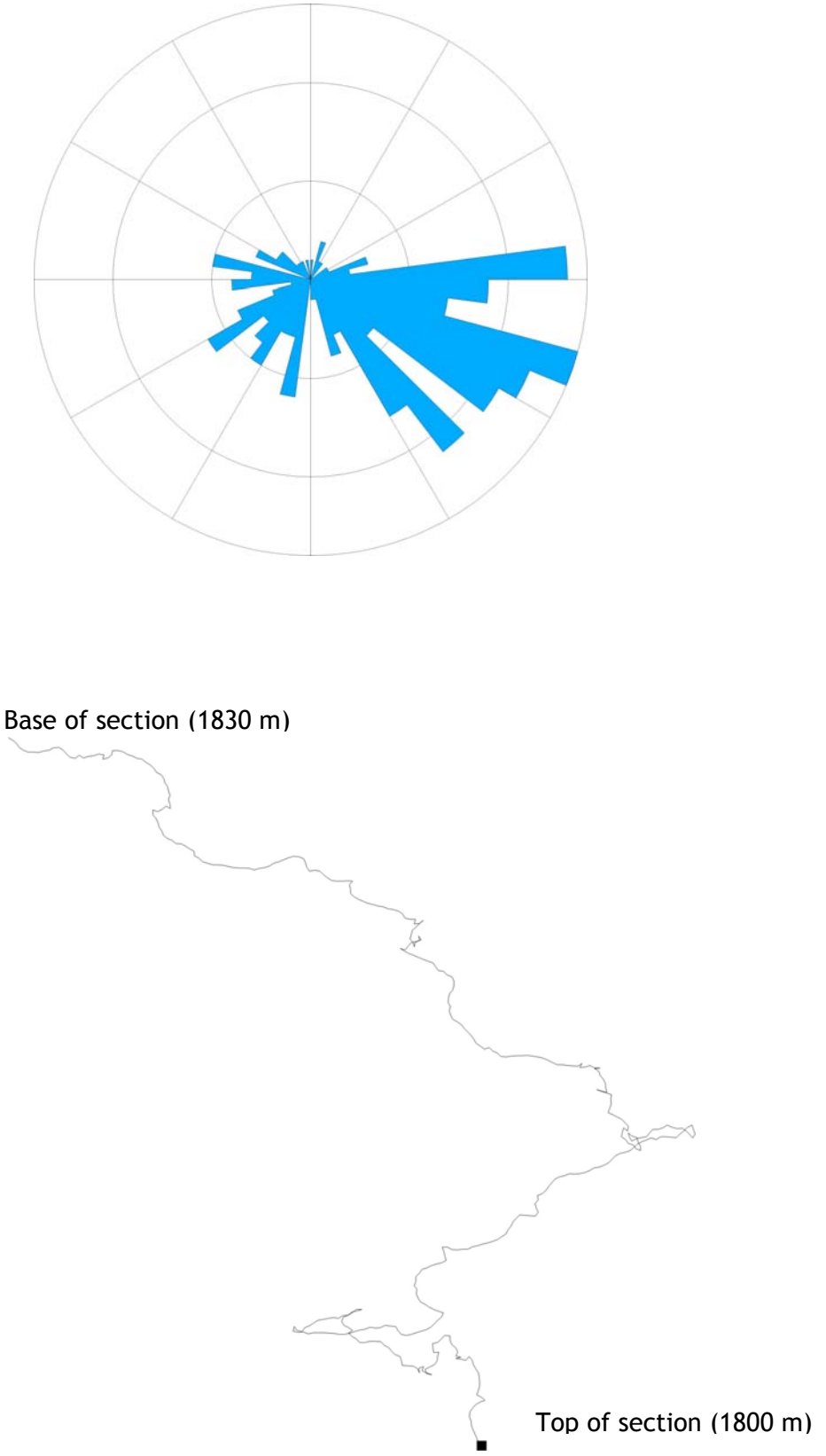

Figure 6. Cumulative dip azimuth plot for the interval 1800 – 1850 m. Surfaces are shown with structural dip removed.

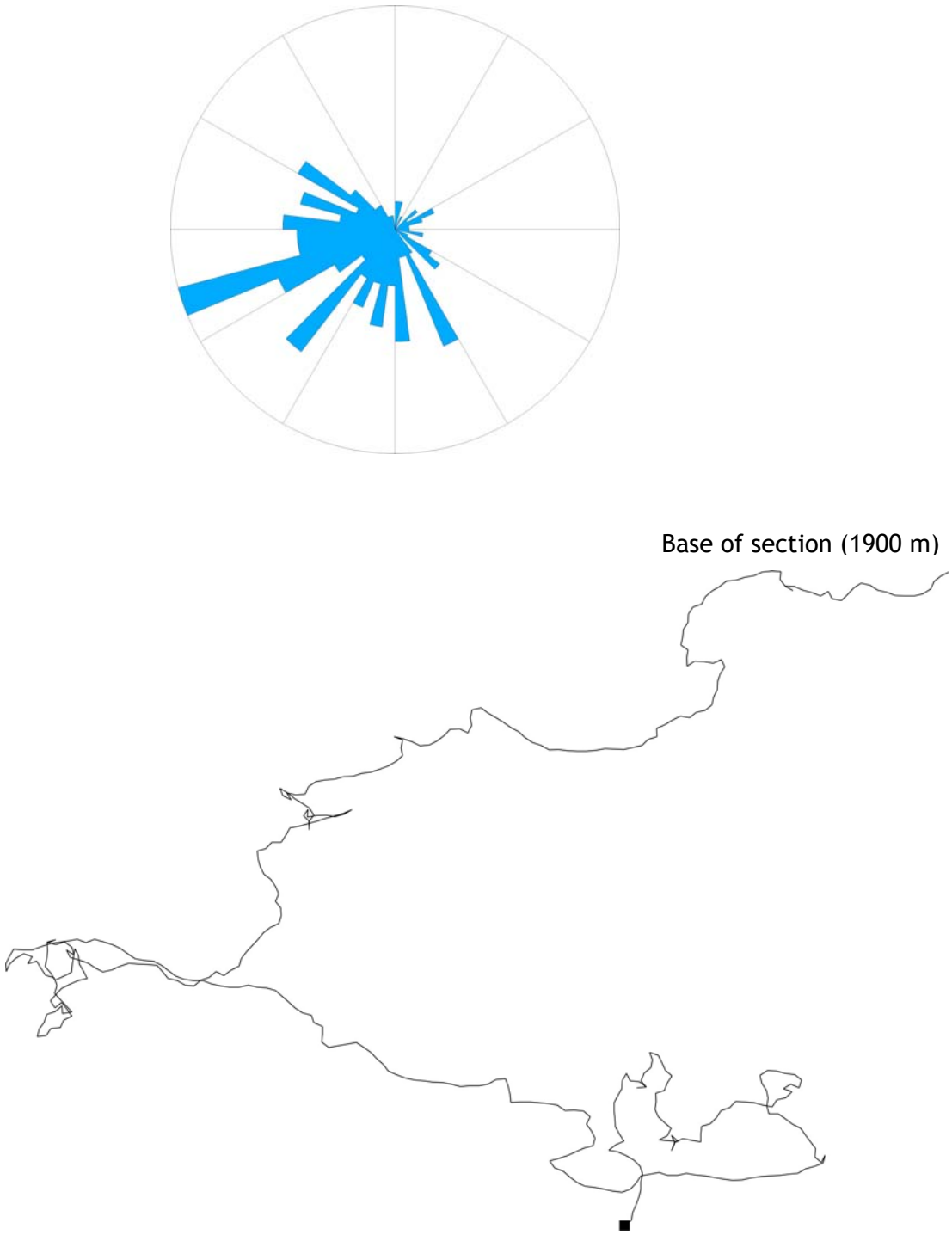

Figure 7. Cumulative dip azimuth plot for the interval 1850 – 1900 m. Surfaces are shown with structural dip removed.

ENCLOSURE 1: HALLADALE DW-2 1:500 1680 -1900 M QUALITY CONTROL PLOT

BIT SIZE: 8.5 IN
BH TEMP: 79.45 DegC
MUD CHLORIDES: 44000 mg/l
FLUID LOSS: 3.7 cm3
MUD DENSITY: 1.26 g/c3
MUD pH: 9
MUD TYPE: Aqua Drill
MUD VISCOSITY: 87 S
SURFACE LATITUDE: 38 34' 45.54" S
SURFACE LONGITUDE: 142 43' 50.95" E
RUN DATE:18-April-2005
1668.06 - 1926.82 METRES

Origin energy
delivering the goods

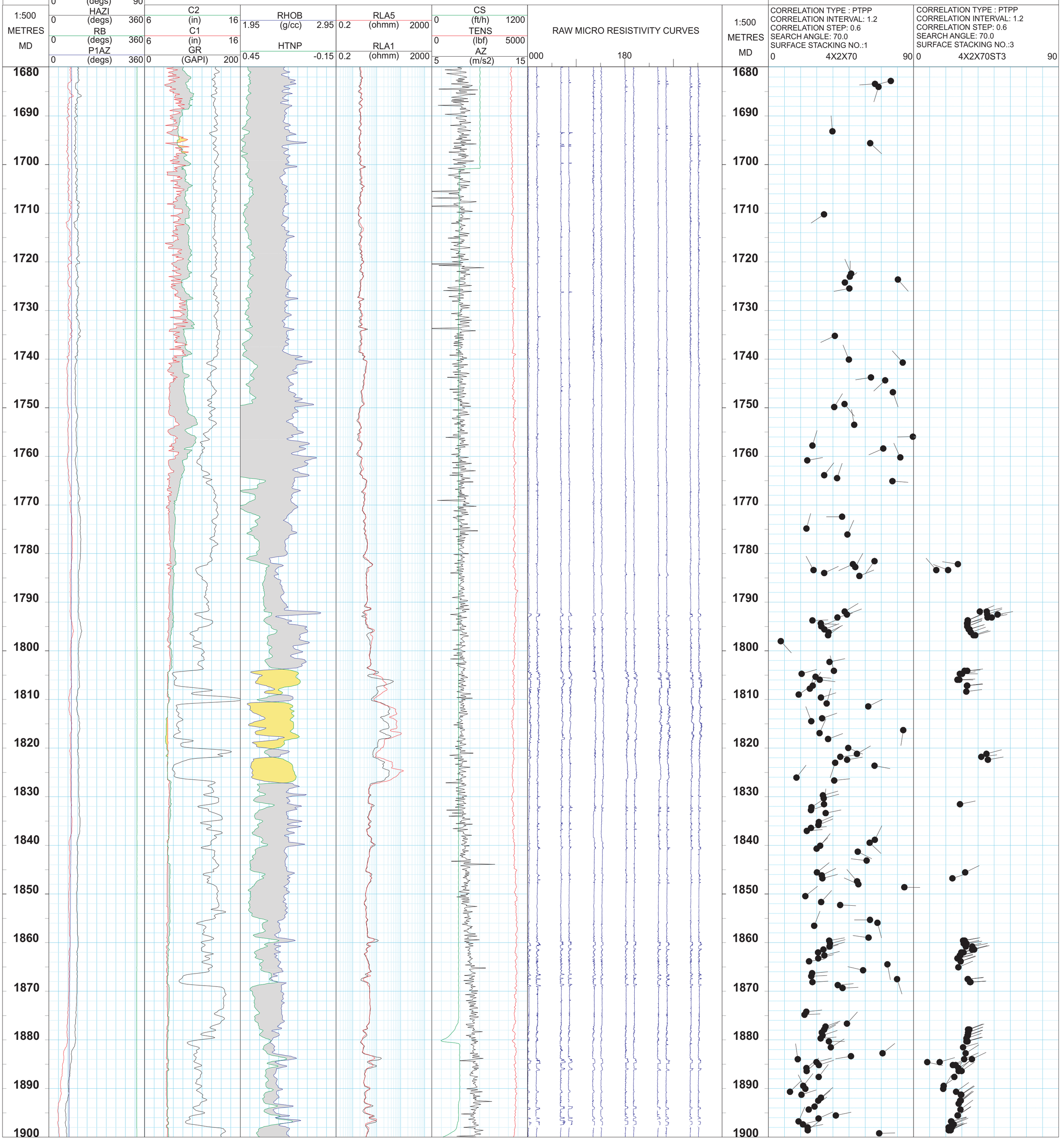

ENCLOSURE 2: HALLADALE DW-2 1:500 1680 - 1900 M STRUCTURAL SUMMARY PLOT

FRACTURE / FAULT STRIKE

ST FRAC
ST FAULT

MANUAL DIPS

LB
LBc
LBe
SB
CSB
ISS
ISSf
XSB
PDf
HETS
MUD
FAULT
FRAC

Origin energy

delivering the goods

1:500 METRES MD

C2 6 (in) 16
C1 6 (in) 16
GR 0 (GAPI) 150
RHOB 1.95 (g/cc) 2.95
HTNP 0.45 -0.15
RLA5 0.2 (ohmm) 2000
RLA1 0.2 (ohmm) 2000

0 Bass_FMI_0007.pck 90

STRUCTURAL ZONES
MUDS
HETS
Bass_FMI_0007.pck

AUTOMATIC COMPUTED DIPS
0 4X2X70ST3 90

ZONE I 15.9/124 DEG

ZONE II 19.2/066 DEG

ZONE III 16.2/071 DEG

1680 1690 1700 1710 1720 1730 1740 1750 1760 1770 1780 1790 1800 1810 1820 1830 1840 1850 1860 1870 1880 1890 1900

ENCLOSURE 3:

HALLADALE-1 DW2 1:200 1800 - 1900 M DATA OVERVIEW PLOT

Origin energy

delivering the goods

1:200 METRES MD	C2 (in) 6–16 / C1 (in) 6–16	GR (GAPI) 0–150	RHOB (g/cc) 1.95–2.95 / HTNP 0.45–-0.15	RLA5 (ohmm) 0.2–2000 / RLA1 (ohmm) 0.2–2000	CUTTINGS: CLAY, SILT, SAND, COAL; 0 % 100	STATIC FMI Equal bins - Linear Window: 4.00 ft, Step: 0.50 ft True North, 64 colour 0 360	MANUAL DIPS NOT CORRECTED FOR TECTONIC TILT LB, LBc, LBe, SB, CSB, ISS, ISSf, XSB, PDf, HETS, MUD, FAULT, FRAC 0 Bass_FMI_0007.pck 90	MUDS, HETS Bass_FMI_0007.pck	ISS, ISSf, XSB, SB, CSB Bass_FMI_0007.pck	MANUAL DIPS CORRECTED FOR TECTONIC TILT LB, LBc, LBe, SB, CSB, ISS, ISSf, XSB, PDf, HETS, MUD, FAULT, FRAC 0 Bass_FMI_0007.pck 90	MUDS, HETS Bass_FMI_0007.pck	ISS, ISSf, XSB, SB, CSB Bass_FMI_0007.pck	COMMENTS
1800–1802													Possible pro-delta/shelf
1802–1804													
1804–1806													Low sinuosity fluvial
1806–1808													
1808–1810													
1810–1812													Channel abandoment
1812–1814													Low sinuosity fluvial
1814–1816													
1816–1818													
1818–1820													
1820–1822													
1822–1824													Channel abandoment
1824–1826													Low sinuosity fluvial
1826–1828													
1828–1830													Possible pro-delta/shelf
1830–1832													
1832–1834													
1834–1836													
1836–1838													
1838–1840													
1840–1842													
1842–1844													
1844–1846													
1846–1848													
1848–1850													
1850–1852													
1852–1854													
1854–1856													
1856–1858													Possible shoreface/ tidal flat
1858–1860													
1860–1862													
1862–1864													
1864–1866													
1866–1868													
1868–1870													
1870–1872													Possible pro-delta/shelf
1872–1874													
1874–1876													
1876–1878													
1878–1880													
1880–1882													Possible shoreface/ tidal flat
1882–1884													
1884–1886													
1886–1888													
1888–1890													
1890–1892													
1892–1894													
1894–1896													
1896–1898													
1898–1900													Possible pro-delta/shelf

ENCLOSURE 4:

HALLADALE-1 DW2 1:100 1800 - 1830 M SEDIMENTOLOGICAL COMPOSITE PLOT

delivering the goods

MANUAL DIPS
LB
LBc
LBe
SB
CSB
ISS
ISSf
XSB
PDf
HETS
MUD
FAULT
FRAC

ROTATED DIPS
LB
LBc
LBe
SB
CSB
ISS
ISSf
XSB
PDf
HETS
MUD

FAULT
FRAC

LITHOFACIES
Sc
Sm
Sl
Sm(Sl)
Sl(Sm)
Scm
Scm(Sl)
Ml
Mm
Hl
Hm
Coal

1:100
METRES
MD

C2 6 (in) 16
C1 6 (in) 16
GR 0 (GAPI) 150
RHOB 1.95 (g/cc) 2.95
HTNP 0.45 -0.15
RLA5 0.2 (ohmm) 2000
RLA1 0.2 (ohmm) 2000

0 Bass_FMI_0007.pck 90
0 Bass_FMI_0007.pck 90

Static FMI Equal bins - Linear
Window: 4.00 ft, Step: 0.50 ft
True North, 64 colour
0 360

MUDS
HETS
Bass_FMI_0007.pck

ISS
ISSf
XB
Bass_FMI_0007.pck

LB
LBe
LBc
PDF
Bass_FMI_0007.pck

SB
CSB
Bass_FMI_0007.pck

LITHOFACIES ASSOCIATIONS
1
2
3
4
5

1800
1801
1802
1803
1804
1805
1806
1807
1808
1809
1810
1811
1812
1813
1814
1815
1816
1817
1818
1819
1820
1821
1822
1823
1824
1825
1826
1827
1828
1829
1830

ENCLOSURE 5:

HALLADALE-1 DW2 1:100 1850 - 1900 M SEDIMENTOLOGICAL COMPOSITE PLOT

Origin energy

delivering the goods

MANUAL DIPS
- LB
- LBc
- LBe
- SB
- CSB
- ISS
- ISSf
- XSB
- PDf
- HETS
- MUD
- FAULT
- FRAC

ROTATED DIPS
- LB
- LBc
- LBe
- SB
- CSB
- ISS
- ISSf
- XSB
- PDf
- HETS
- MUD

FAULT
FRAC

LITHOFACIES
- Sc
- Sm
- Sl
- Sm(Sl)
- Sl(Sm)
- Scm
- Scm(Sl)
- Ml
- Mm
- Hl
- Hm
- Coal

1:100 METRES MD

C2 6 (in) 16
C1 6 (in) 16
GR 0 (GAPI) 150
RHOB 1.95 (g/cc) 2.95
HTNP 0.45 -0.15
RLA5 0.2 (ohm) 2000
RLA1 0.2 (ohm) 2000
0 Bass_FMI_0007.pck 90
0 Bass_FMI_0007.pck 90

Static FMI Equal bins - Linear
Window: 4.00 ft, Step: 0.50 ft
True North, 64 colour
0 360

MUDS
HETS
Bass_FMI_0007.pck

ISS
ISSf
XB
Bass_FMI_0007.pck

LB
LBe
LBc
PDF
Bass_FMI_0007.pck

SB
CSB
Bass_FMI_0007.pck

LITHOFACIES ASSOCIATIONS
1
2
3
4
5

1850 1851 1852 1853 1854 1855 1856 1857 1858 1859 1860 1861 1862 1863 1864 1865 1866 1867 1868 1869 1870 1871 1872 1873 1874 1875 1876 1877 1878 1879 1880 1881 1882 1883 1884 1885 1886 1887 1888 1889 1890 1891 1892 1893 1894 1895 1896 1897 1898 1899 1900

ENCLOSURE 6:

HALLADALE-1 DW2 1:20 1805 -1835 M CORE COMPOSITE PLOT

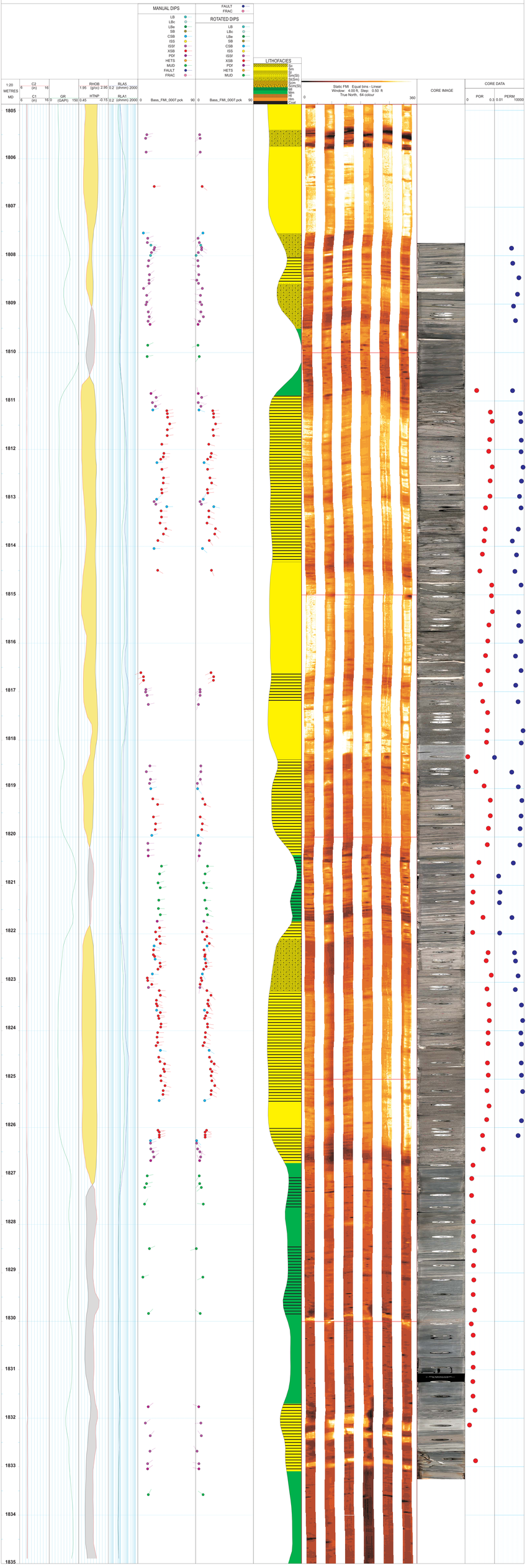

APPENDIX 7:
RCI INTERPRETATION REPORT

Halladale-1 DW1,DW2 & DW3

INTERPRETATION OF RESERVOIR CHARACTERIZATION INSTRUMENT (RCI)

OCTOBER 2005

DATE OF SURVEYS:
06/4/2005(DW1)
18/4/2005(DW2)
25/4/2005(DW3)

Origin Energy Resources Limited
Second Floor, South Tower, John Oxley Centre
339 Coronation Drive
MILTON QLD 4064

Joe Parver, April 2007

Baker Atlas RCI tool was used to obtain pressure data and collect reservoir fluid samples from Halladale-1 DW1, DW2 and DW3.

DW1 RCI Program (06/04/2005):

The DW1 first RCI program (logging run #2-pressure only) had pre-tests taken from 1519.5mMD to 1865.5mMD covering Nullawarre, Waarre C and Waarre A sands. During the first RCI program a total of 34 pre-tests were attempted of which 25 were successful and 9 were tight. A second RCI run (logging run#3-sample only) was carried out to collect fluid samples. The RCI tool got stuck after performing a fall off test at the first sample point (1772.6 mMD). Several attempts made to free the tool were unsuccessful. Finally two 840 cc fluid samples were collected at this point before a fishing operation being carried out. Eventually drill pipe was run to free the RCI tool. No more attempts were made to collect more samples.

DW2 RCI Program (18/04/2005):

The DW2 first RCI Program (logging run #2-pressure only) had pre-test taken from 1542.0mMD down to 1846.0mMD covering the Nullawarre and Waarre C sands. The RCI tool got stuck at 1852.0mMD after 23 pre-tests were taken. The tool eventually came free and was pulled out of the hole. A second RCI run (logging run#3-pressure and sample) was carried out using pipe convey logging (PCL) operation in order to perform additional pre-tests (8 pre-tests within Waarre A) and collect fluid samples (3 fluid samples from Waarre C). During the DW2 first and second RCI programs a total of 31 pre-tests were attempted of which 15 were successful and 16 were tight. Three RCI fluid samples (gas) were also taken at 1804.6mMD.

DW3 RCI Program (24/04/2005):

Halladale-1 DW-3 was drilled as an appraisal well targeting the water zone in Waarre C in order to define a water line. The DW3 RCI program (logging run #1-pressure only) had pre-tests taken from 1872.0mMD to 1904.4mMD covering Waarre C water zone. During the RCI program a total of 10 pre-tests were attempted which all were successful. No attempts were made to collect fluid samples.

A summary of the pre-test data for DW1, DW2 and DW3 are included in Appendix 8 of Halladale-1 WCR Basic Data.

During the DW1 and DW2 RCI programs a total of 5 samples were collected from Waarre C. The descriptions of these samples are shown below while the fluid composition and PVT analysis of the collected samples are included in Appendix 8 of the Halladale-1 WCR Basic Data.

Halladale-1 DW1

2x840 CC Gas sample from Waarre C at 1772.6 mMD
(CO2=0.5%, N2=2.0%, C1+C2=92.9%, C3+C4=2.7% & C5+=1.9%)

Halladale-1 DW2

3x 840 CC Gas sample from Waarre C at 1804.6 mMD
(CO2=0.4%, N2=1.4%, C1+C2=94.8%, C3+C4=1.9% & C5+=1.5%)

The interpretation of the RCI data is presented in Figures 3 to 5 while Figures 1 and 2 demonstrate data validation and quality check.

Figure 1 shows the initial mud hydrostatic pressure recorded by Baker Hughes RCI gauges for DW1, DW2 and DW3. The data indicates a gradient of 0.549 psi/ft equivalent to a mud density of 1.266 g/cc at the downhole conditions which is also consistent with the reported drilling data (1.26 g/cc).

Figure 2 illustrates the difference between the initial and final mud hydrostatic pressures recorded by Baker Hughes RCI gauges for DW1, DW2 and DW3. As shown in this plot the difference between these measurements is mainly close to zero (+/- 1.0 psi).

Figure3 shows all the RCI points from DW1, DW2 and DW3 recorded in the Waarre C and Waarre A. The DW1 Waarre C pre-test points lie on a gas trend with a gradient of 0.059 psi/ft equivalent to a gas density of 0.136 g/cc at the reservoir conditions and consistent with compositional analysis of the collected gas samples at this level (SG=0.66). Meanwhile, most of the DW1 Waarre A pre-test points are within the water zone except two points which seem to fit the aforementioned Waarre C gas line.

The DW2 Waarre C pre-test points also lie on a gas trend with similar gradient as DW1. Meanwhile, all of the DW2 Waarre A pre-test points appear to be within the water zone.

The DW-3 RCI data, which were measured to define a water line for the Waarre C sand, is also shown in this plot. The DW3 Waarre C pre-test points fit a water line with a gradient of 0.429 psi/ft equivalent to a water salinity of 18,000 ppm.

The intersects of the DW1 and DW2 Waarre C gas lines with DW3 Waarre C water line define gas water contacts for Black Watch (DW1) and Halladale (DW2) at 1770.0 and 1760.0 mss respectively. Meanwhile, a water line with a gradient of 0.429 psi/ft (similar to the DW3 Waarre C gradient) drawn through DW1 and DW2 Waarre A water points intersects the DW1 Waarre A gas line (which are superimposed by the Waarre C gas line) at 1766.0 mss as shown in this plot.

The trends of regional water line (based on the onshore RFT data) and Minerva water line are also shown in this plot.

Figure 4 shows the RFT pre-test points from some of the onshore and offshore wells and the position of Halladale-1 (DW1, DW2 and DW3) profile with respect to these data.

Figure 5 shows the DW1 and DW2 RCI data recorded in Nullawarre Formation. Most of the DW1 pre-tests appear to be supercharged. However a few limited valid RCI points together with the information from other hydrocarbon indicators (gas shows and density/neutron crossovers) indicate a potential for two separate gas columns which have been referred to Nullawarre upper and lower sands in this plot. On the basis of this assumption two gas lines with similar gradient as the Waarre C were drawn through the valid RCI points to represent these two gas columns. No water line can be interpreted from the DW1 pre-tests.

Almost all the DW2 Nullawarre RCI pre-tests are tight except one point which appears to be permeable. The mud log data does not indicate high gas reading for DW2 Nullawarre sand in this well. It was also assumed that the aforementioned single permeable RCI point in DW2 is a valid water point. Based on those assumptions a water line (with similar gradient as the Waarre C) was drawn through the DW2 only RCI point to represent Nullawarre water line.

On the basis of the above assumptions the estimated gas water contacts for the Nullawarre upper and lower sands are 1481.0 and 1515.0 mss.

The trend of a water line fitted through McIntee Nullawarre RFT points is also shown in this plot.

A summary of the results are shown in the following table.

Formation	RCI Profile	Fluid	Black Watch GWC (mss)	Halladale GWC (mss)
Waarre C	**Figure 4**	**Gas**	**1770.0**	**1760.0**
Waarre A	**Figure 4**	**Gas**	**1766.0**	**-**
Upper Nullawarre	**Figure 6**	**Gas**	**1481.0 (Est.)**	**-**

Lower Nullawarre	**Figure 6**	**Gas**	**1515.0 (Est.)**	**-**

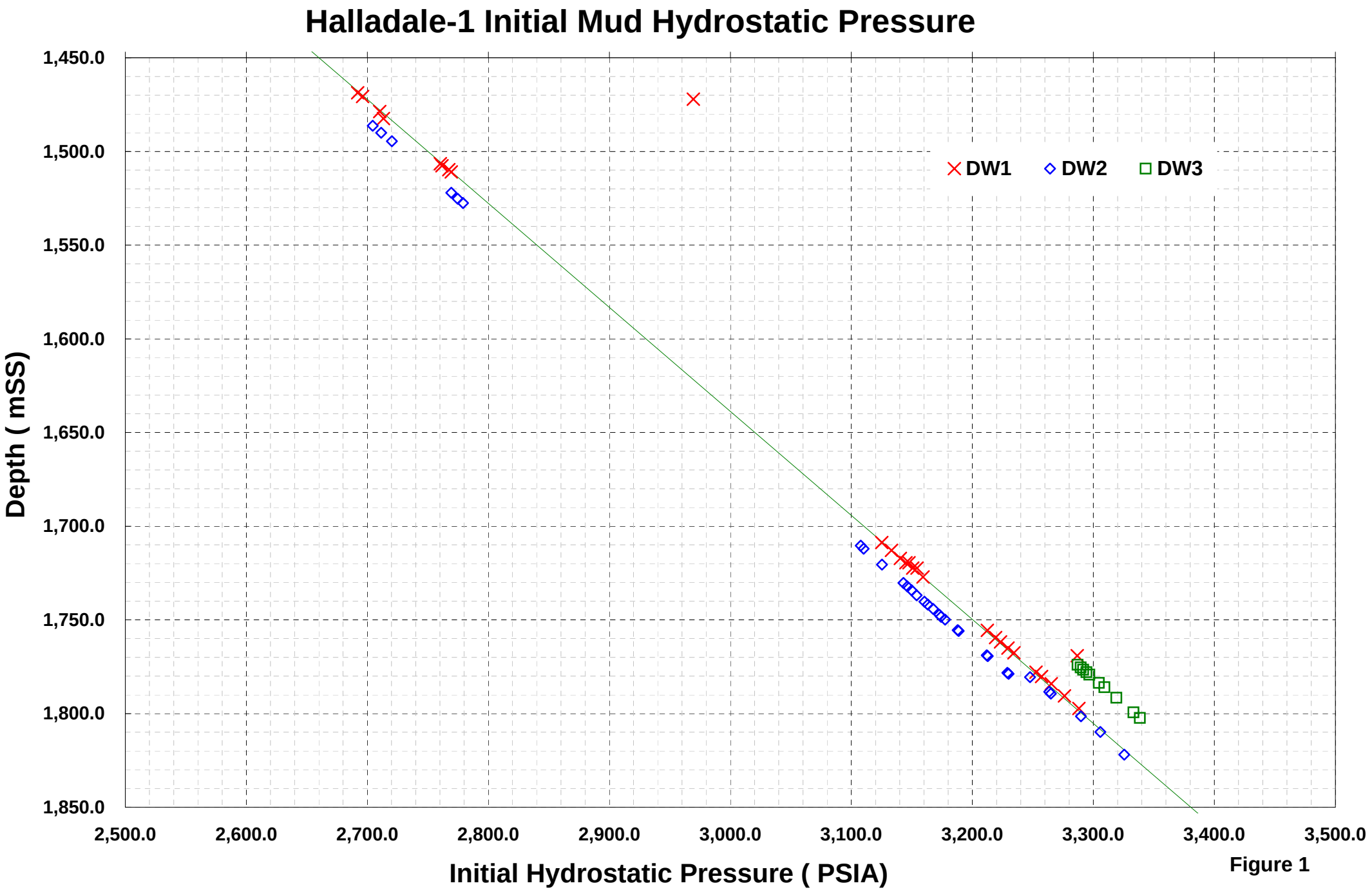
Halladale-1 Initial Mud Hydrostatic Pressure
1,450.0
1,500.0
1,550.0
1,600.0
1,650.0
1,700.0
1,750.0
1,800.0
1,850.0
Depth (mSS)
DW1
DW2
DW3
2,500.0
2,600.0
2,700.0
2,800.0
2,900.0
3,000.0
3,100.0
3,200.0
3,300.0
3,400.0
3,500.0
Initial Hydrostatic Pressure (PSIA)

Figure 1

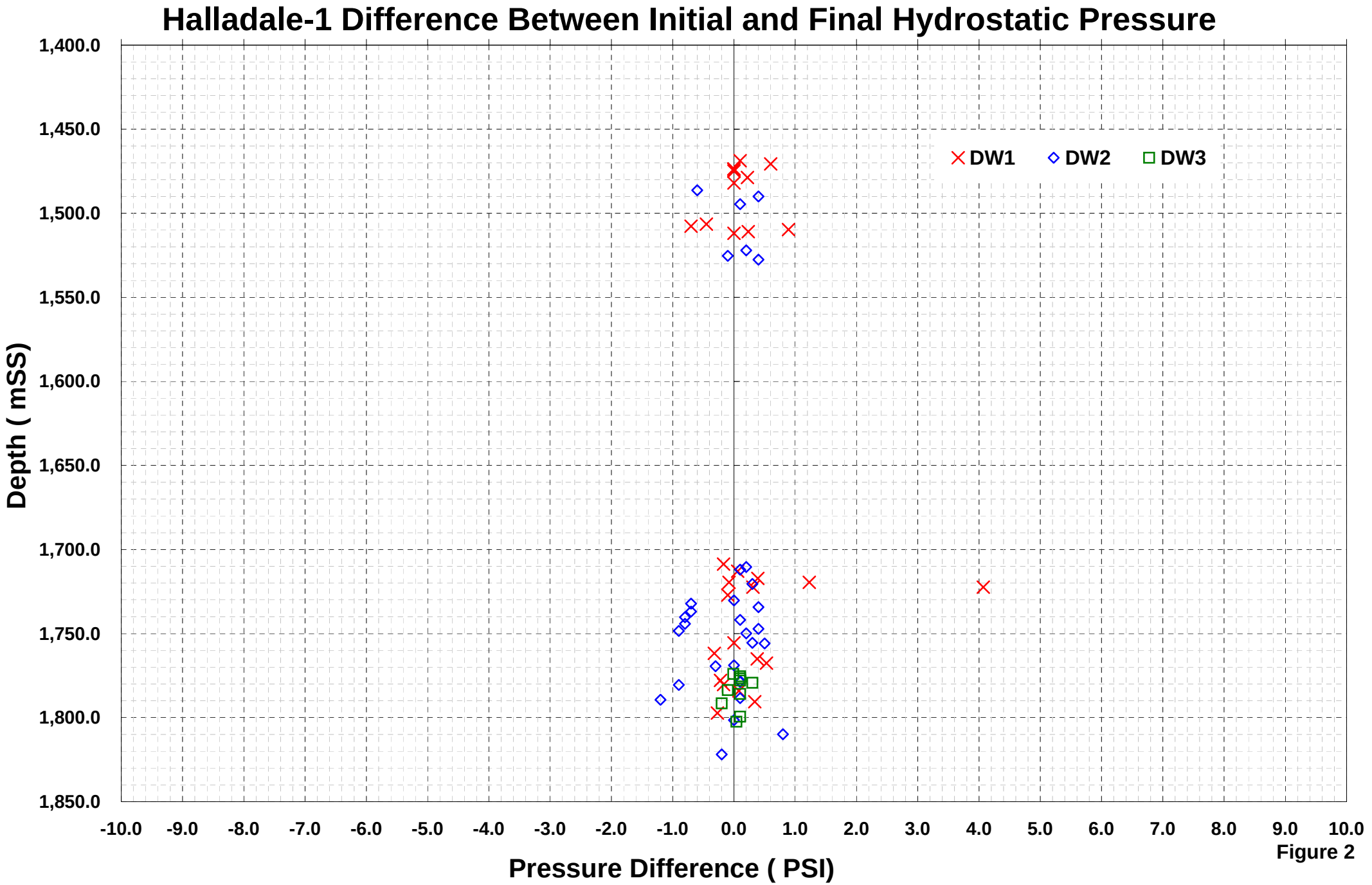
Halladale-1 Difference Between Initial and Final Hydrostatic Pressure
1,400.0
1,450.0
1,500.0
1,550.0
1,600.0
1,650.0
1,700.0
1,750.0
1,800.0
1,850.0
Depth (mSS)
DW1
DW2
DW3
-10.0
-9.0
-8.0
-7.0
-6.0
-5.0
-4.0
-3.0
-2.0
-1.0
0.0
1.0
2.0
3.0
4.0
5.0
6.0
7.0
8.0
9.0
10.0
Pressure Difference (PSI)

Figure 2

Halladale-1 DW1,DW2 &DW3 Waarre Pressure v.s. Depth Profile

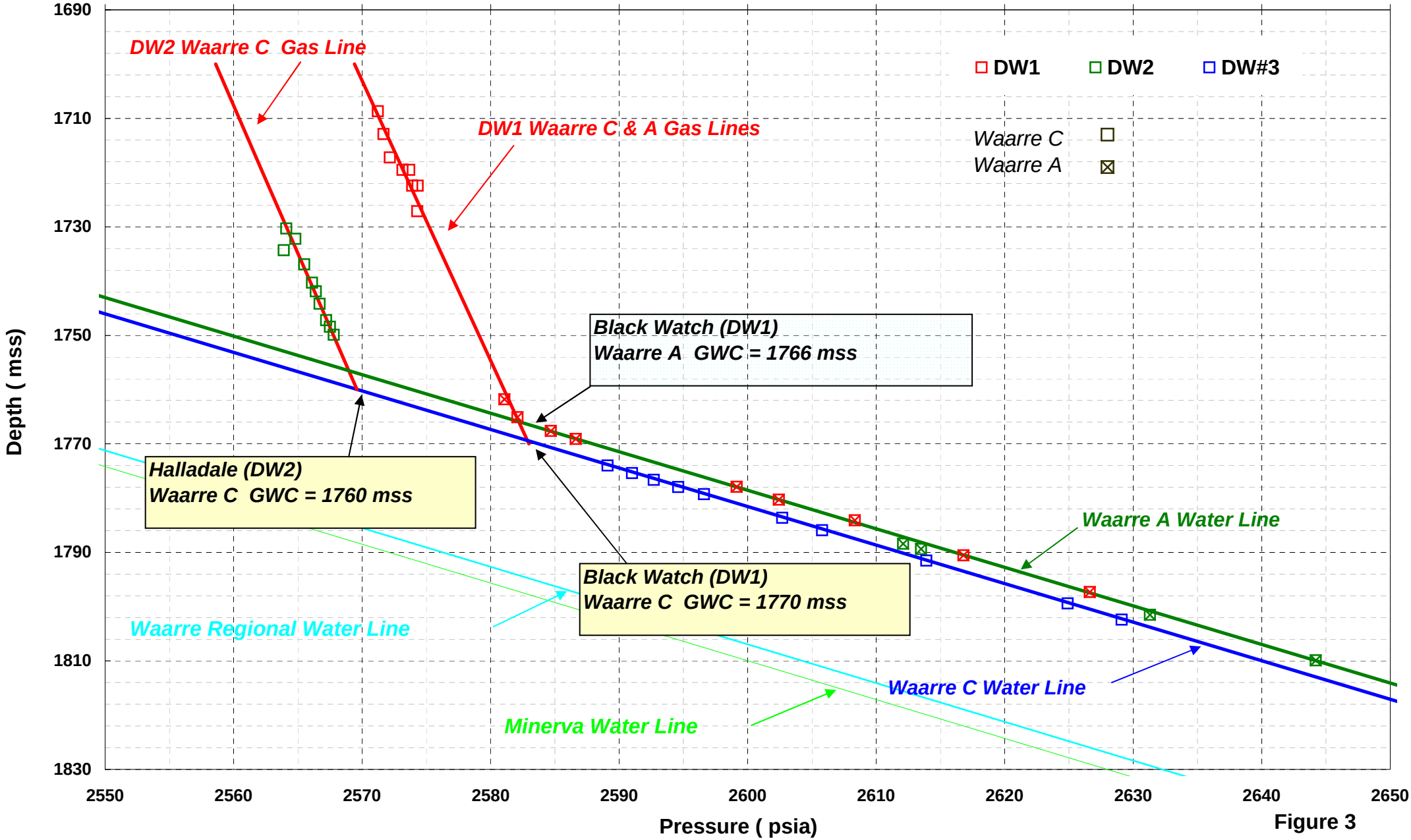

Figure 3

WAARRE FORMATION RFT PLOT

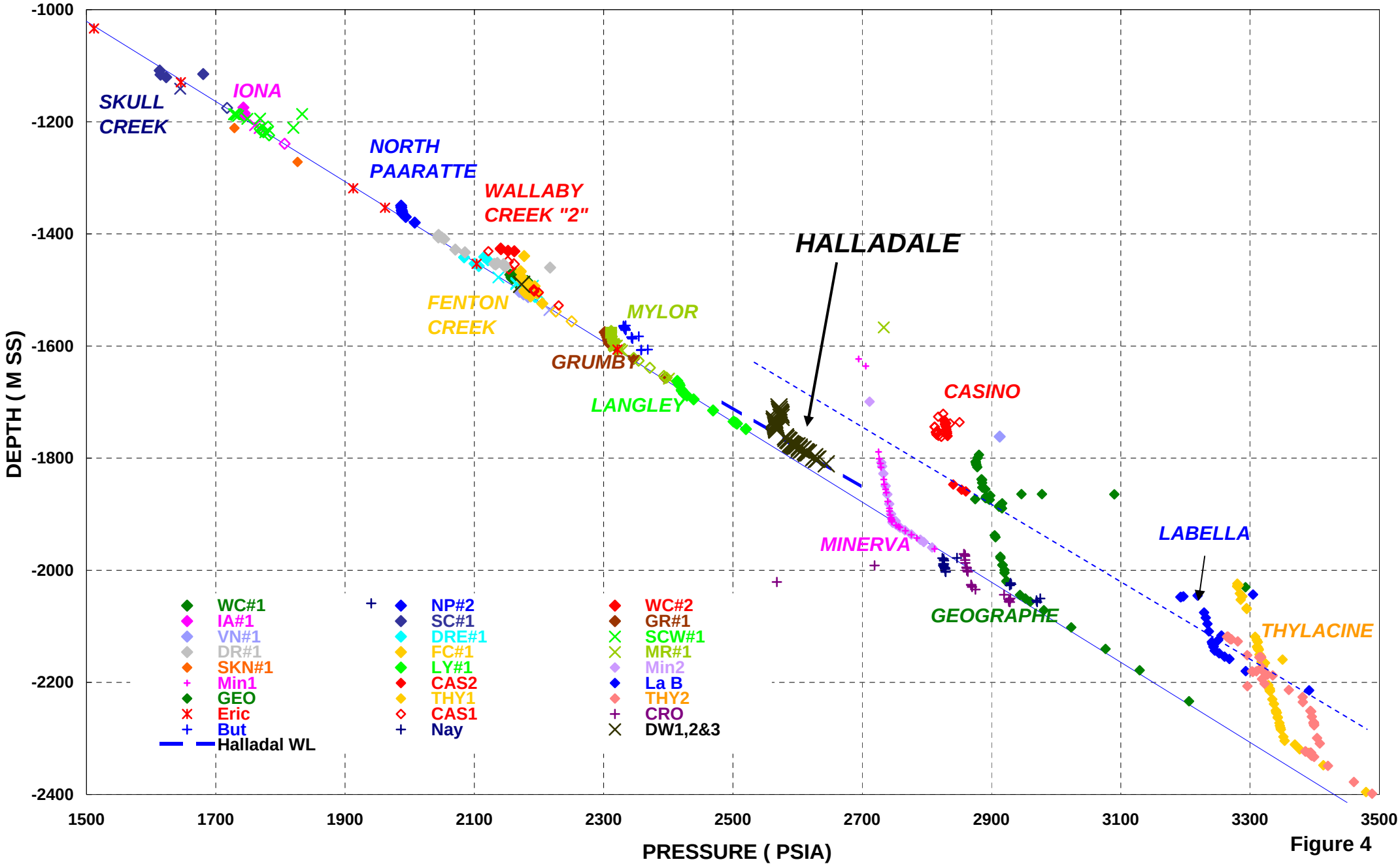

Figure 4

DW1&DW2 Nullawarre Pressure v.s. Depth Profile

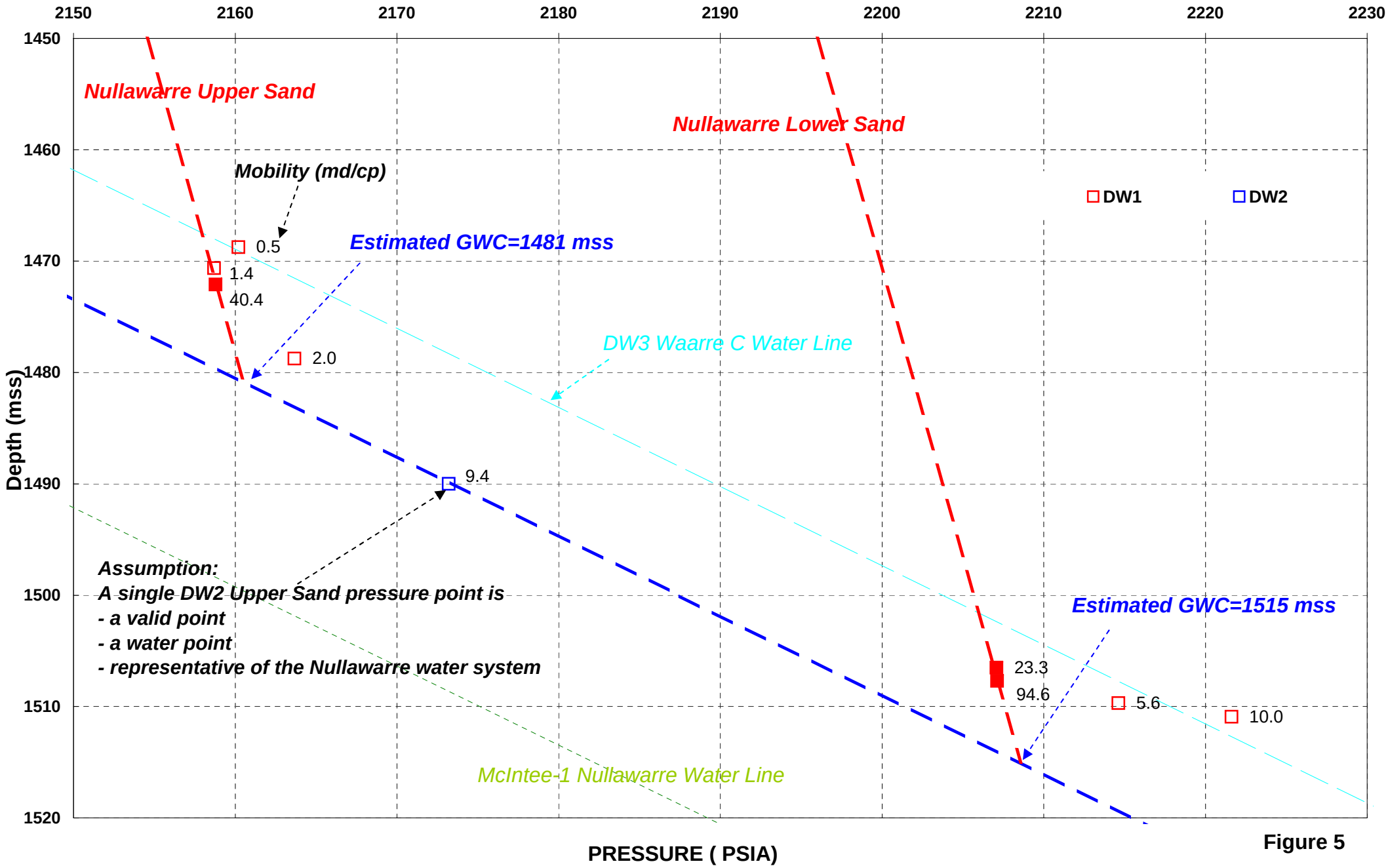

Figure 5

APPENDIX 8:
PVT REPORT

A. C. N. # 008 130 667
Adelaide, September 29, 2005
P. O. Box 410
Magill
S. A. 5072

Origin Energy Resources Limited
1 King William Street
PO Box 1199
Adelaide
S.A. 5000

Subject : Reservoir Fluid Study
Well: Halladale # 1
File: O – 25024

Attention: Mr. Joe Parvar

Dear Sirs,

In April this year, five RCI wireline bottom hole samples, collected by Baker Atlas, from two different deviations in subject well, were received in our Adelaide laboratory, where they were used in a reservoir fluid study. The results of the tests are presented in the following report.

After measuring the opening pressures, the contents of each tank were transferred, in single phase, into laboratory storage cylinders. A comparison of these opening pressures and of the compositions of all samples allowed us to select the most representative sample from each wireline run.

These compositions were determined by flashing the samples under atmospheric conditions into two phases. Through measurements of densities, molecular weights, quantities produced and compositions of the evolved stock tank gas and liquid from the flash experiments, we were able to mathematically recombine these products into the desired fluid compositions. The compositions were extended to C-12+ by means of Capillary Column Gas Chromatography on the flashed stock tank liquids.

Reservoir fluids from both DW 1 and DW 2 were charged to a visual P V T cell and thermally expanded to their respective reservoir temperatures of 167 and 174 °F. During constant composition expansions at these temperatures, dew point pressures of 2580 and 2610 psig were observed.

Other data obtained during these Pressure - Volume relations' experiments, include relative volume versus pressure, gas compressibility, specific volume and gas expansion above the dew point and the distribution of retrograde liquid versus pressure below it.

During flashes for geochemical sub-sampling, some additional tests including wax, asphaltenes

and BTX content, pour and cloud point on the liberated stock tank liquid and H2S, Mercaptans and COS on the liberated stock tank gas were performed and can be found on the summary page in the beginning of this report.

We thank Origin Energy Resources Limited for the opportunity to be of service. Please do not hesitate in contacting us should you require any further information or if we can assist you in any other way.

Yours Sincerely,

Jan G. Bon
Manager

PETROLAB

Company : Origin Energy Resources Limited
Well : Halladale # 1 DW1 & DW2 File : O - 25024

INDEX

Summary of Results	1
Field Characteristics and Transfer Details	2

DW 1 RCI Bottom Hole Samples

Compositional Analyses	3 - 8
Constant Mass Study	9 - 10
PLOTS :	
Relative Volume	11
Gas Formation Volume Factor	12
Gas Expansion Factor	13
Gas Deviation Factor	14
Reservoir Fluid Specific Volume	15
Viscosity of Reservoir Fluid	16
Retrograde Condensation	17

DW 2 RCI Bottom Hole Samples

Compositional Analyses	18 - 26
Constant Mass Study	27 - 28
PLOTS :	
Relative Volume	29
Gas Formation Volume Factor	30
Gas Expansion Factor	31
Gas Deviation Factor	32
Reservoir Fluid Specific Volume	33
Viscosity of Reservoir Fluid	34
Retrograde Condensation	35

PETROLAB

Company : Origin Energy Resources Limited	Page : 1 of 35
Well : Halladale # 1 DW1 & DW2	File : O - 25024

SUMMARY OF RESULTS

SATURATED VAPOUR:		DW 1	DW 2
Reservoir Temperature (°F)	:	167	174
Dew Point Pressure (psig)	:	2580	2610
Gas Formation Volume Factor (Bg)	:	0.00573	0.00598
Gas Expansion Factor (E)	:	174.58	167.30
Gas Deviation Factor (Z)	:	0.839	0.876
Specific Volume (CFT/LB)	:	0.11276	0.12195
Density (gm/cc)	:	0.1421	0.1314
Viscosity (centipoise)	:	0.0192	0.0187
Molecular Weight	:	19.29	18.61
Gas Gravity (Air = 1.000)	:	0.668	0.644
Gross Heating Value (BTU/ft3)	:	1143	1121

Total Plant Products in Dew Point Fluid (GPMM):		DW 1	DW 2
Ethane	:	1402	1140
Propane	:	598	438
Butanes	:	366	257
Pentanes Plus	:	563	487

Physical Properties

		DW 1	DW 2
Cloud Point (°C)	:	-5	-22
Pour Point (°C)	:	-21	< -22
Asphaltene Content (% wt)	:	< 0.1	< 0.1
Wax Content (% wt)	:	0.6	0.7

GAS CONTAMINANTS RESULTS

				DW 1	DW 2
H2S *	PPM Vol	(1)		**< 0.2**	**< 0.2**
H2S *	PPM Vol	(2)		**< 0.2**	**< 0.2**
H2S *	PPM Vol	(2)		**< 0.2**	**< 0.2**
COS *	PPM Vol	(2)		**N/D**	**N/D**
Hg *	mg/m^3	(2)		**--**	**0.16**
Hg *	mg/m^3	(2)		**--**	**0.21**

(1) Draeger Tube
(2) Wet Chemistry

* Note: Analyses performed out of pressure vessel. Some component adsorbtion could have lowered values.

BTX RESULTS DW 1

	B	T	X
Wt% of BTX - ST Gas	0.02	0.10	0.18
Wt% of BTX - ST Liq	0.84	0.27	4.32
Wt% of BTX - Well Stream	**0.03**	**0.10**	**0.21**

BTX RESULTS DW 2

	B	T	X
Wt% of BTX - ST Gas	0.17	0.28	0.64
Wt% of BTX - ST Liq	0.32	1.13	6.28
Wt% of BTX - Well Stream	**0.17**	**0.28**	**0.65**

FIELD CHARACTERISTICS :

		DW1	DW2
Field Name	:	Black Watch	Halladale
Formation Name	:	Waarre	Waarre
Well Name	:	Halladale DW1	Halladale DW2
Date first well completed	:	--	--
Original reservoir pressure (psia)	:	2571	2564
Reservoir temperature (°F)	:	166.8	173.7
@ Sample depth (mMD)	:	1772.6	1804.6

WELL CHARACTERISTICS :

Depth datum	:	--	--
Elevation above MSL (m)	:	21.5	21.5
Total depth (mMD)	:	1847.6	1858.5
Perforated interval	:	--	--
Tubing size (inch)	:	--	--
Tubing shoe (mRT)	:	--	--
Casing size (inch)	:	--	--
Reservoir temperature (°F)	:	166.8	173.7
Last reservoir pressure (psia)	:	2571	2564
date	:	--	--
Status of well	:	P&A	P&A

DW 1 RCI Transfer Details @ 4500 psig & 25 °C Transferred on April 13, 2005

RCI Tank No.	Contents	Sample Depth (m)	Opening Press. (psi)	Transferred to Cylinder no.	CCs Water Recovered
369106	Gas	1772.6	4750	L-227 / L-007	0
369197	Gas	1772.6	4200	L-128 / L-104	trace

DW 2 RCI Transfer Details @ 4500 psig & 25 °C Transferred on April 26, 2005

RCI Tank No.	Contents	Sample Depth (mMD)	Opening Press. (psi)	Transferred to Cylinder no.	CCs Water Recovered
189727	Gas	1804.6	4150	L-332	20
189732	Gas	1804.6	4225	L-188	20
189768	Gas	1804.6	2125	L-076	0

PETROLAB

FINGERPRINT ANALYSIS
BY CAPILLARY GAS CHROMATOGRAPHY
On Stock Tank Oil from atmospheric flash of sample in cylinder # L - 007

Component		Mol %
Hexanes minus	C6-	0.75
Hexanes	C6	2.55
Heptanes	C7	14.47
Octanes	C8	16.11
Nonanes	C9	24.85
Decanes	C10	22.90
Undecanes	C11	10.60
Dodecanes	C12	3.80
Tridecanes	C13	1.70
Tetradecanes	C14	0.81
Pentadecanes	C15	0.54
Hexadecanes	C16	0.31
Heptadecanes	C17	0.22
Octadecanes	C18	0.14
Nonadecanes	C19	0.09
Eicosanes	C20	0.05
Heneicosanes	C21	0.05
Docosanes	C22	0.03
Tricosanes	C23	0.02
Tetracosanes	C24	0.01
Pentacosanes	C25	0.00
Hexacosanes	C26	0.00
Heptacosanes	C27	0.00
Octacosanes	C28	0.00
Nonacosanes	C29	0.00
Triacontanes	C30	0.00
Hentriacontanes	C31	0.00
Dotriacontanes	C32	0.00
Tritriacontanes	C33	0.00
Tetratriacontanes	C34	0.00
Pentatriacontanes Plus	C35+	0.00
TOTAL		100.00

Molecular Weight Calculated *	:	125.2
Density @ 60 °F Calculated *	:	0.7656
Molecular Weight Measured	:	--
Density @ 60 °F Measured	:	--

*Calculation based on generalized properties as published by Katz and Firoozabadi

FINGERPRINT ANALYSIS
BY CAPILLARY GAS CHROMATOGRAPHY
On Stock Tank Oil from atmospheric flash of sample in cylinder # L - 007

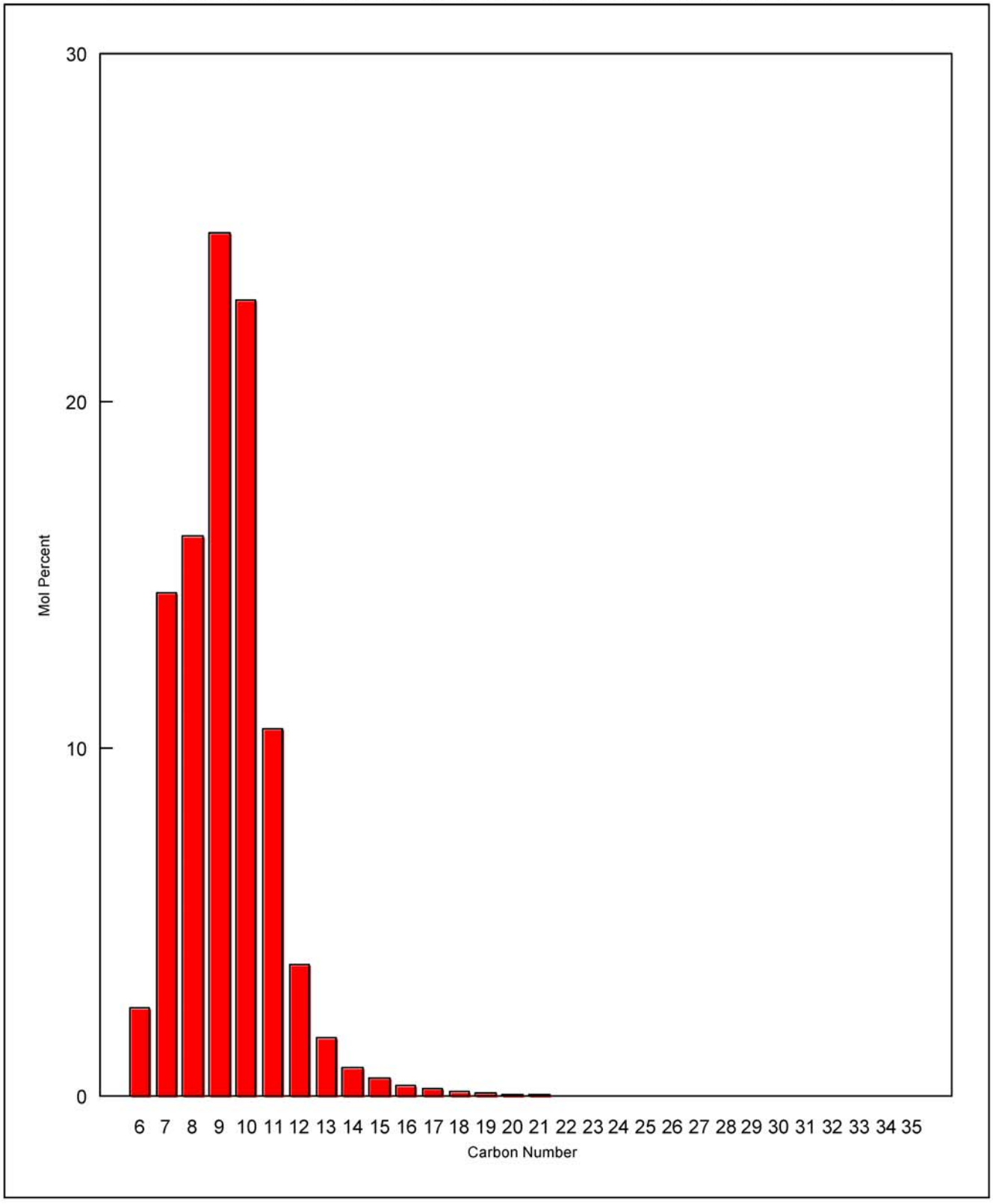

PETROLAB

Company : Origin Energy Resources Limited	Page : 5 of 35
Well : Halladale # 1 DW-1	File : O - 25024

COMPOSITIONAL ANALYSIS OF BOTTOM HOLE RESERVOIR FLUID

Cylinder # L - 007 ex RCI chamber # 369106 Position 5

Component		Stock Tank Liquid Mol %	Stock Tank Gas Mol %	Reservoir Fluid Mol %
Hydrogen Sulphide	H2S	0.00	0.00	0.00
Carbon Dioxide	CO2	0.01	0.49	0.49
Nitrogen	N2	0.00	2.11	2.11
Methane	C1	0.46	87.49	87.49
Ethane	C2	0.14	5.24	5.24
Propane	C3	0.20	2.17	2.17
Iso-Butane	iC4	0.11	0.52	0.52
N-Butane	nC4	0.19	0.62	0.62
Iso-Pentane	iC5	0.16	0.21	0.21
N-Pentane	nC5	0.17	0.17	0.17
Hexanes	C6	2.53	0.30	0.30
Heptanes	C7	14.37	0.38	0.38
Octanes	C8	16.00	0.14	0.14
Nonanes	C9	24.68	0.10	0.10
Decanes	C10	22.74	0.05	0.05
Undecanes	C11	10.53	0.01	0.01
Dodecanes Plus	C12+	7.72	0.00	0.00
TOTAL		100.00	100.00	100.00

Ratios				
Molar Ratio	:	0.0000	1.0000	1.0000
Mass Ratio	:	0.0003	0.9997	1.0000
Liquid Ratio (bbl/bbl)	:	1.0000 @ SC	--	-- @ PT*
Gas Liquid Ratio	:	1.0000 bbl @ SC	17000000 SCF	--
Stream Properties				
Molecular Weight	:	123.4	19.28	19.29
Density obs. (gm/cc)	:	0.7647 @ 60 °F	--	-- @ PT*
Gravity (AIR = 1.000)	:	53.4 °API @ 60 °F	0.668	--
GHV (BTU/scf)	:	--	1143	--
Hexanes Plus Properties				
Mol %	:	98.56	0.98	0.98
Molecular Weight	:	124.6	98.9	99.0
Density (gm/cc @ 60 °F)	:	0.7667	0.6877	0.6881
Gravity (°API @ 60 °F)	:	52.9	74.1	73.9
Heptanes Plus Properties				
Mol %	:	96.03	0.68	0.68
Molecular Weight	:	125.6	105.5	105.6
Density (gm/cc @ 60 °F)	:	0.7683	0.6962	0.6967
Gravity (°API @ 60 °F)	:	52.5	71.6	71.4
Decanes Plus Properties				
Mol %	:	40.99	0.06	0.06
Molecular Weight	:	146.1	136.1	134.4
Density (gm/cc @ 60 °F)	:	0.7892	0.7299	0.7298
Gravity (°API @ 60 °F)	:	47.6	62.2	62.2
Undecanes Plus Properties				
Mol %	:	18.25	0.01	0.01
Molecular Weight	:	161.1	146.9	148.1
Density (gm/cc @ 60 °F)	:	0.8012	0.7399	0.7451
Gravity (°API @ 60 °F)	:	45.0	59.6	58.2
Dodecanes Plus Properties				
Mol %	:	7.72	0.00	0.00
Molecular Weight	:	180.4	--	180.4
Density (gm/cc @ 60 °F)	:	0.8151	--	0.8151
Gravity (°API @ 60 °F)	:	41.9	--	41.9

* (P)ressure : 2556 psig * (T)emperature : 167 °F

PETROLAB

FINGERPRINT ANALYSIS
BY CAPILLARY GAS CHROMATOGRAPHY
On Stock Tank Oil from atmospheric flash of sample in cylinder # L - 128

Component		Mol %
Hexanes minus	C6-	0.04
Hexanes	C6	0.25
Heptanes	C7	5.40
Octanes	C8	12.61
Nonanes	C9	28.45
Decanes	C10	31.33
Undecanes	C11	15.51
Dodecanes	C12	4.42
Tridecanes	C13	1.22
Tetradecanes	C14	0.35
Pentadecanes	C15	0.17
Hexadecanes	C16	0.10
Heptadecanes	C17	0.08
Octadecanes	C18	0.04
Nonadecanes	C19	0.02
Eicosanes	C20	0.01
Heneicosanes	C21	0.00
Docosanes	C22	0.00
Tricosanes	C23	0.00
Tetracosanes	C24	0.00
Pentacosanes	C25	0.00
Hexacosanes	C26	0.00
Heptacosanes	C27	0.00
Octacosanes	C28	0.00
Nonacosanes	C29	0.00
Triacontanes	C30	0.00
Hentriacontanes	C31	0.00
Dotriacontanes	C32	0.00
Tritriacontanes	C33	0.00
Tetratriacontanes	C34	0.00
Pentatriacontanes Plus	C35+	0.00
TOTAL		100.00

Molecular Weight Calculated *	:	130.0
Density @ 60 °F Calculated *	:	0.7722
Molecular Weight Measured	:	--
Density @ 60 °F Measured	:	--

*Calculation based on generalized properties as published by Katz and Firoozabadi

FINGERPRINT ANALYSIS
BY CAPILLARY GAS CHROMATOGRAPHY
On Stock Tank Oil from atmospheric flash of sample in cylinder # L - 128

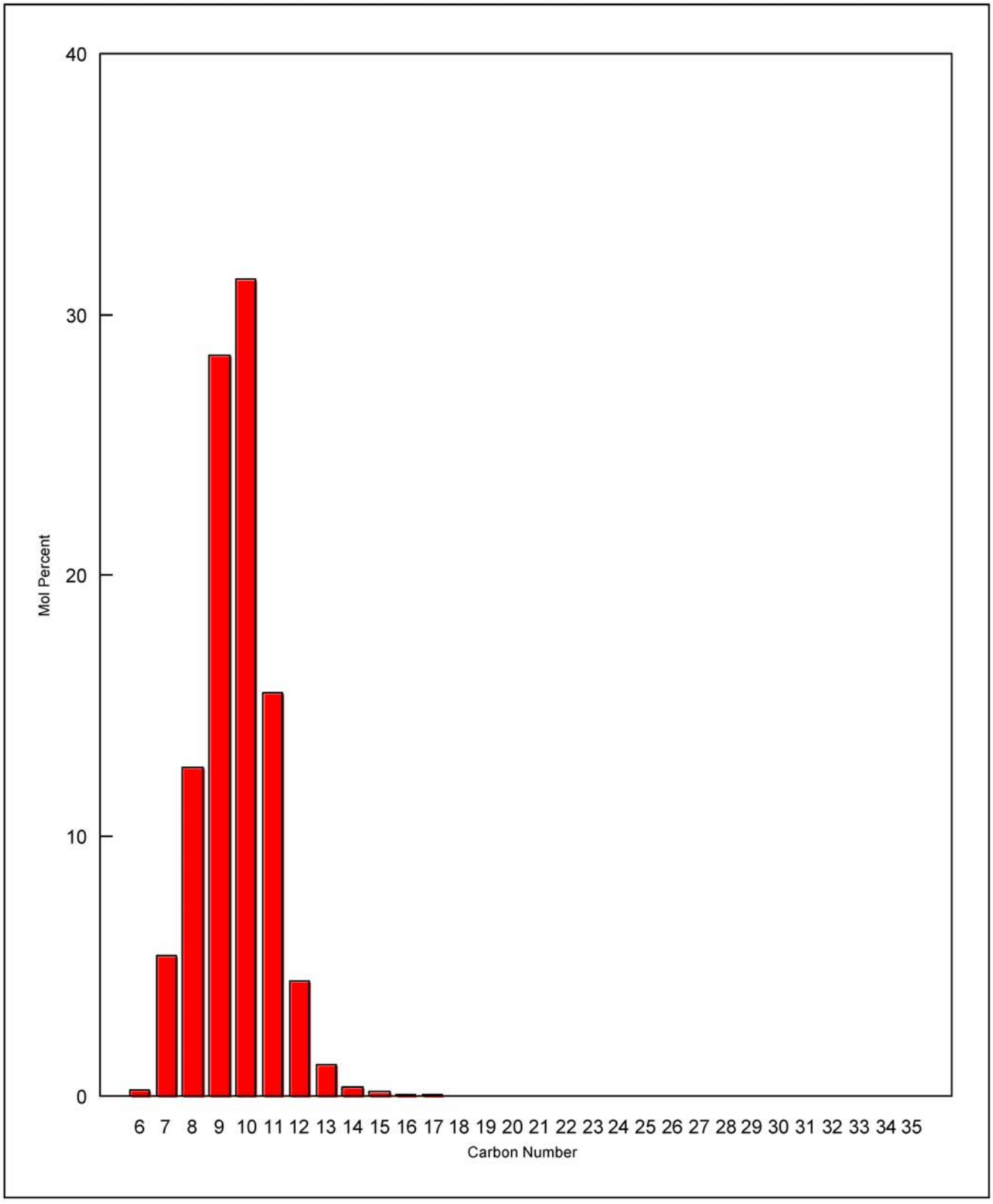

PETROLAB

COMPOSITIONAL ANALYSIS OF BOTTOM HOLE RESERVOIR FLUID

Cylinder # L - 128 ex RCI chamber # 369197 Position 6

Component		Stock Tank Liquid Mol %	Stock Tank Gas Mol %	Reservoir Fluid Mol %
Hydrogen Sulphide	H2S	0.00	0.00	0.00
Carbon Dioxide	CO2	0.01	0.46	0.46
Nitrogen	N2	0.00	1.88	1.88
Methane	C1	0.47	87.88	87.85
Ethane	C2	0.14	5.30	5.30
Propane	C3	0.20	2.19	2.19
Iso-Butane	iC4	0.12	0.56	0.56
N-Butane	nC4	0.17	0.56	0.56
Iso-Pentane	iC5	0.15	0.19	0.19
N-Pentane	nC5	0.15	0.15	0.15
Hexanes	C6	0.25	0.26	0.26
Heptanes	C7	5.33	0.34	0.34
Octanes	C8	12.44	0.12	0.12
Nonanes	C9	28.06	0.08	0.09
Decanes	C10	30.90	0.03	0.04
Undecanes	C11	15.30	0.00	0.01
Dodecanes Plus	C12+	6.32	0.00	0.00
TOTAL		100.00	100.00	100.00
Ratios				
Molar Ratio	:	0.0004	0.9996	1.0000
Mass Ratio	:	0.0024	0.9976	1.0000
Liquid Ratio (bbl/bbl)	:	1.0000 @ SC	--	-- @ PT*
Gas Liquid Ratio	:	1.0000 bbl @ SC	2200000 SCF	--
Stream Properties				
Molecular Weight	:	127.8	19.09	19.13
Density obs. (gm/cc)	:	0.7704 @ 60 °F	--	-- @ PT*
Gravity (AIR = 1.000)	:	52.0 °API @ 60 °F	0.661	--
GHV (BTU/scf)	:	--	1137	--
Hexanes Plus Properties				
Mol %	:	98.60	0.83	0.86
Molecular Weight	:	129.0	97.6	98.9
Density (gm/cc @ 60 °F)	:	0.7723	0.6859	0.6901
Gravity (°API @ 60 °F)	:	51.5	74.6	73.3
Heptanes Plus Properties				
Mol %	:	98.35	0.57	0.60
Molecular Weight	:	129.1	103.8	105.3
Density (gm/cc @ 60 °F)	:	0.7725	0.6941	0.6992
Gravity (°API @ 60 °F)	:	51.5	72.2	70.7
Decanes Plus Properties				
Mol %	:	52.52	0.03	0.05
Molecular Weight	:	142.0	134.0	137.1
Density (gm/cc @ 60 °F)	:	0.7853	0.7278	0.7500
Gravity (°API @ 60 °F)	:	48.5	62.7	57.0
Undecanes Plus Properties				
Mol %	:	21.62	0.00	0.01
Molecular Weight	:	153.5	--	153.5
Density (gm/cc @ 60 °F)	:	0.7947	--	0.7947
Gravity (°API @ 60 °F)	:	46.4	--	46.4
Dodecanes Plus Properties				
Mol %	:	6.32	0.00	0.00
Molecular Weight	:	169.4	--	169.4
Density (gm/cc @ 60 °F)	:	0.8069	--	0.8069
Gravity (°API @ 60 °F)	:	43.7	--	43.7

* (P)ressure : 2556 psig * (T)emperature : 167 °F

CONSTANT MASS STUDY
@ 167 °F
Using Bottom Hole Sample ex RCI chamber # 369106 Position 5 - transferred into Cylinder # L-007

Pressure (psig)		Relative Volume (V/Vsat) (1)	Formation Volume Factor (Bg) (2)	Gas Expansion Factor (E) (3)	Deviation Factor (Z)	Specific Volume (CFT/LB)	Gas Viscosity (Centipoise) (4)
5000		0.5890	0.00337	296.43	0.955	0.06641	0.0291
4500		0.6309	0.00361	276.72	0.921	0.07114	0.0271
4000		0.6848	0.00392	254.93	0.889	0.07722	0.0251
3500		0.7594	0.00435	229.91	0.863	0.08562	0.0231
3000		0.8679	0.00497	201.16	0.846	0.09786	0.0210
2900		0.8955	0.00513	194.95	0.844	0.10098	0.0205
2800		0.9251	0.00530	188.71	0.842	0.10432	0.0201
2700		0.9569	0.00548	182.44	0.840	0.10790	0.0197
2600		0.9924	0.00568	175.93	0.839	0.11190	0.0193
2580	*	1.0000	0.00573	174.58	0.839	0.11276	0.0192
2557	**	1.0089	0.00578	173.03	0.839	0.11377	0.0192
2400		1.0745	0.00615	162.47	0.839	0.12116	0.0185
2200		1.1744	0.00673	148.66	0.841	0.13242	0.0178
2000		1.2971	0.00743	134.59	0.845	0.14626	0.0171
1800		1.4486	0.00830	120.52	0.850	0.16334	0.0164
1600		1.6414	0.00940	106.36	0.857	0.18508	0.0158
1400		1.8931	0.01084	92.22	0.866	0.21347	0.0152
1200		2.2354	0.01280	78.10	0.878	0.25206	0.0146
1000		2.7156	0.01555	64.29	0.891	0.30621	0.0142
800		3.4468	0.01974	50.65	0.908	0.38866	0.0137
600		4.6588	0.02669	37.47	0.926	0.52532	0.0133

* Dew Point Pressure
** Reservoir Pressure

(1) Cubic feet of gas at indicated pressure and temperature per cubic foot at reservoir pressure
(2) Cubic feet of gas at indicated pressure and temperature per cubic foot at 14.696 psia and 60 °F
(3) Cubic feet of gas at 14.696 psia and 60 °F per cubic foot at indicated pressure and temperature
(4) Calculated from correlation of Lee, Gonzales and Eakin

CONSTANT MASS STUDY
@ 167 °F
Using Bottom Hole Sample ex RCI chamber # 369106 Position 5 - transferred into Cylinder # L-007

Pressure (psig)		Relative Volume (V/Vsat) (1)	Retrograde Liquid Deposit (Bbl/MMSCF) (2)	(Volume%) (3)
2580	*	1.0000	0.00	0.000
2557	**	1.0089	0.02	0.002
2400		1.0745	0.13	0.013
2200		1.1744	0.35	0.034
2000		1.2971	0.72	0.071
1800		1.4486	1.20	0.118
1600		1.6414	1.73	0.170
1400		1.8931	2.31	0.226
1200		2.2354	2.92	0.286
1000	***	2.7156	3.04	0.298
800	***	3.4468	3.12	0.306
600	***	4.6588	3.17	0.311

* Dew Point Pressure
** Reservoir Pressure

*** Retrograde Liquid Extrapolated

(1) Cubic feet of gas at indicated pressure and temperature per cubic foot at saturation pressure
(2) Barrels of liquid at indicated pressure and temperature per MMSCF of original reservoir fluid
(3) Percent of reservoir hydrocarbon pore space at dew point

RELATIVE VOLUME

Equation of best fit

V/VSat = +8.76E+00 -9.39E-03 * P +4.30E-06 * P^2 -8.78E-10 * P^3 +6.56E-14 * P^4

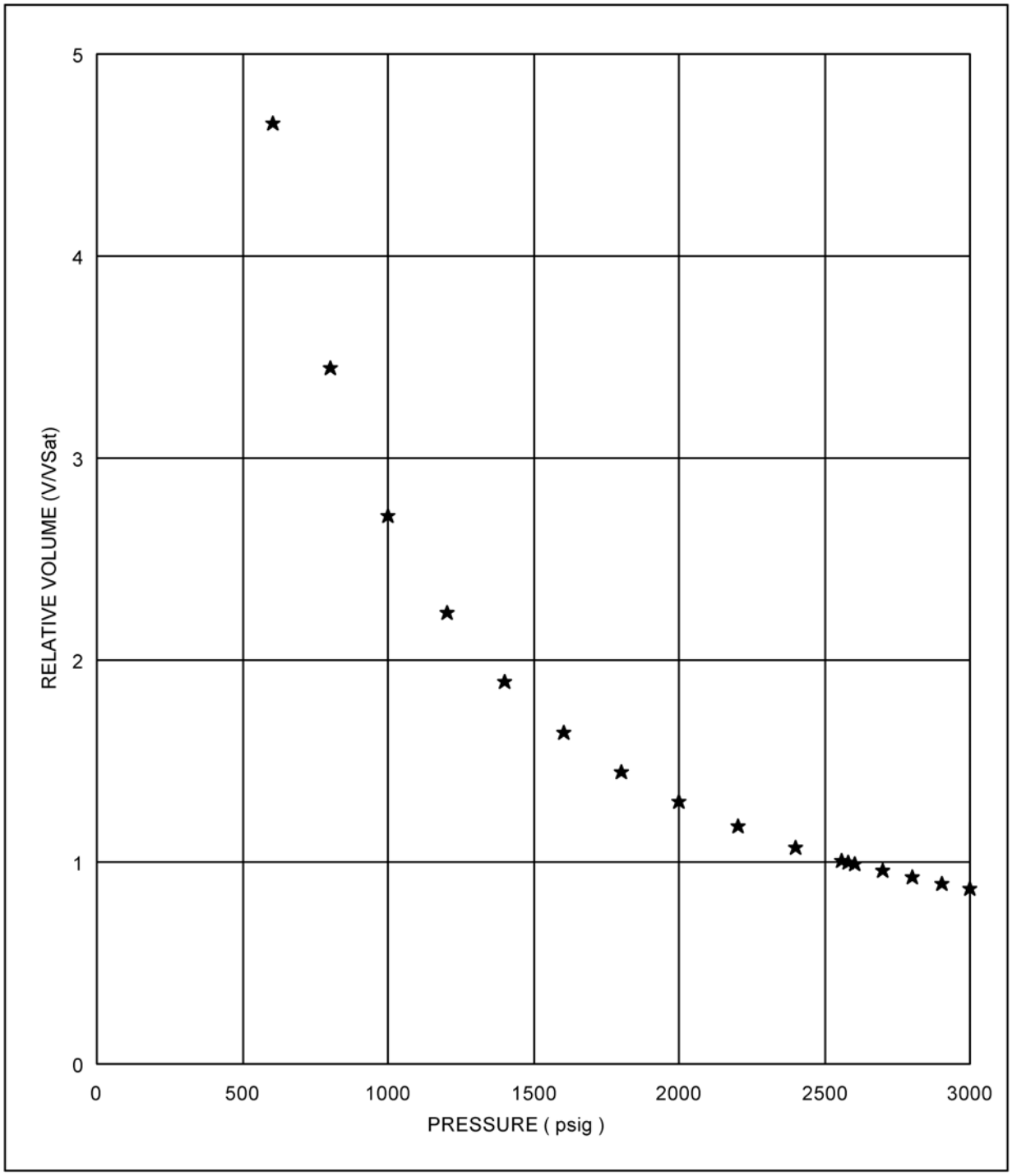

GAS FORMATION VOLUME FACTOR

Equation of best fit

Bg = +5.69E-02 -6.93E-05 * P +3.39E-08 * P^2 -5.79E-12 * P^3 +0.00E+00 * P^4

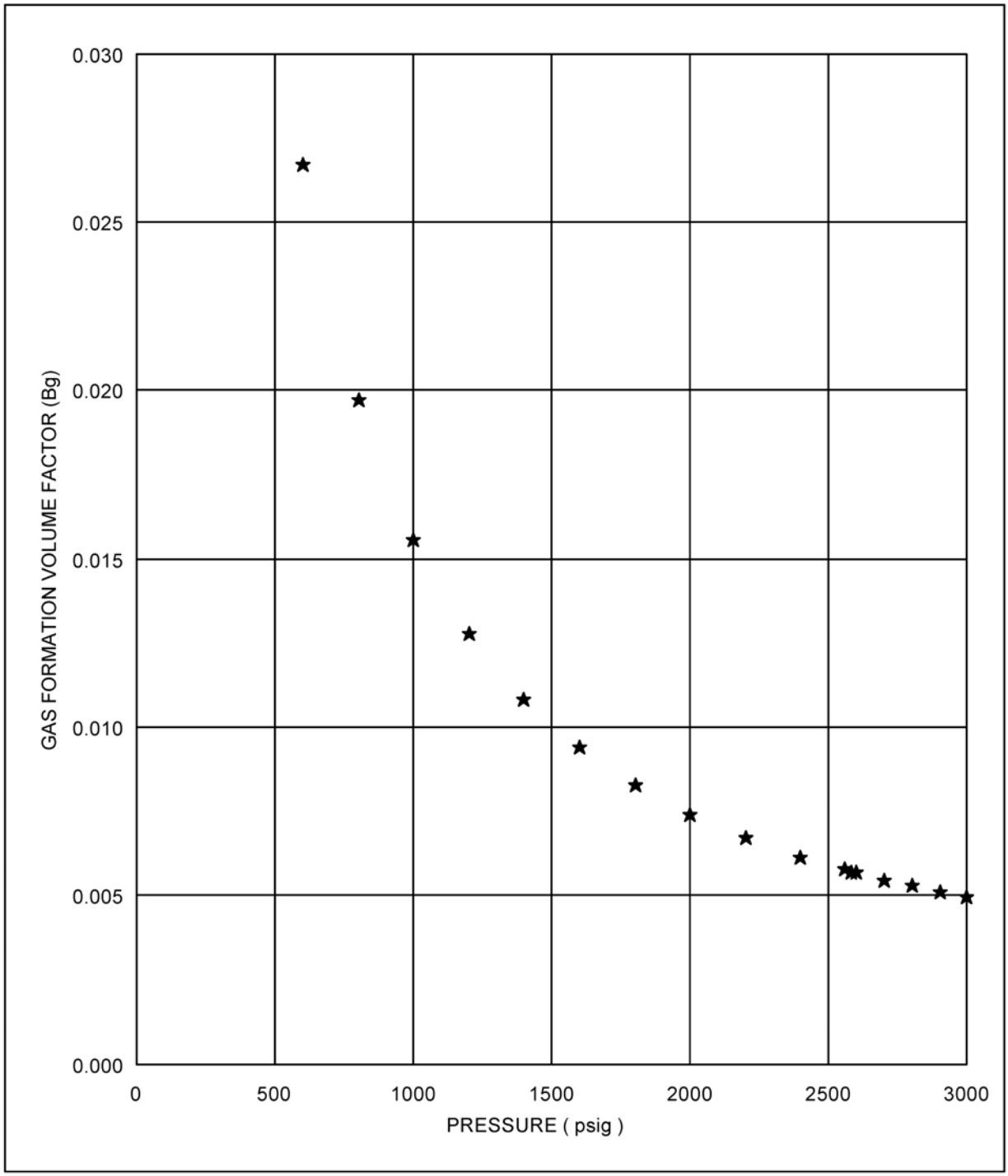

GAS EXPANSION FACTOR

Equation of best fit

E = +5.88E-01 +5.71E-02 * P +8.27E-06 * P^2 -1.64E-09 * P^3 +0.00E+00 * P^4

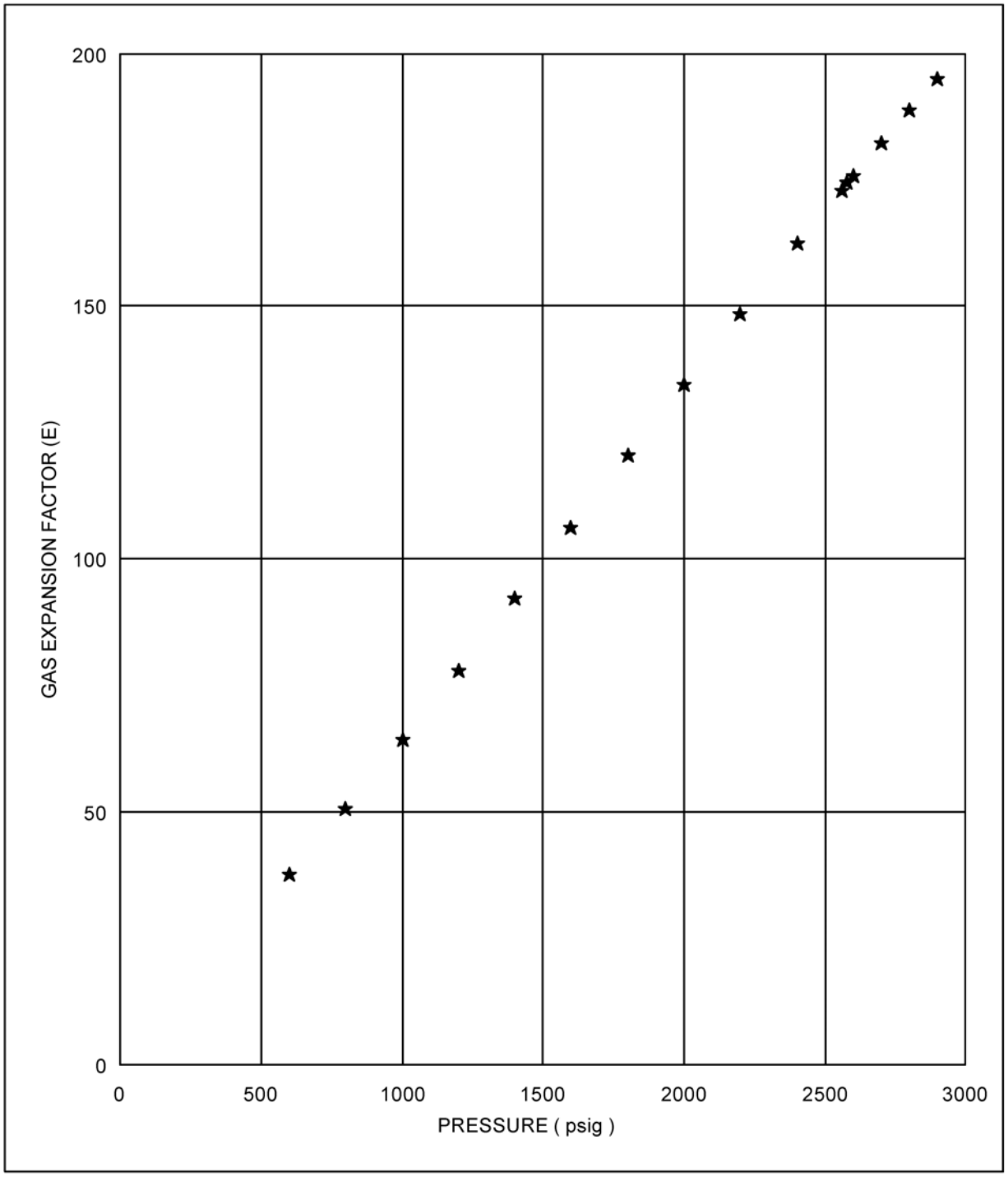

GAS DEVIATION FACTOR

Equation of best fit

Z

$$Z = +9.94E\text{-}01 \ -1.32E\text{-}04 * P \ +2.96E\text{-}08 * P^2 \ -5.55E\text{-}13 * P^3 \ +\text{-}6.72E\text{-}17 * P^4$$

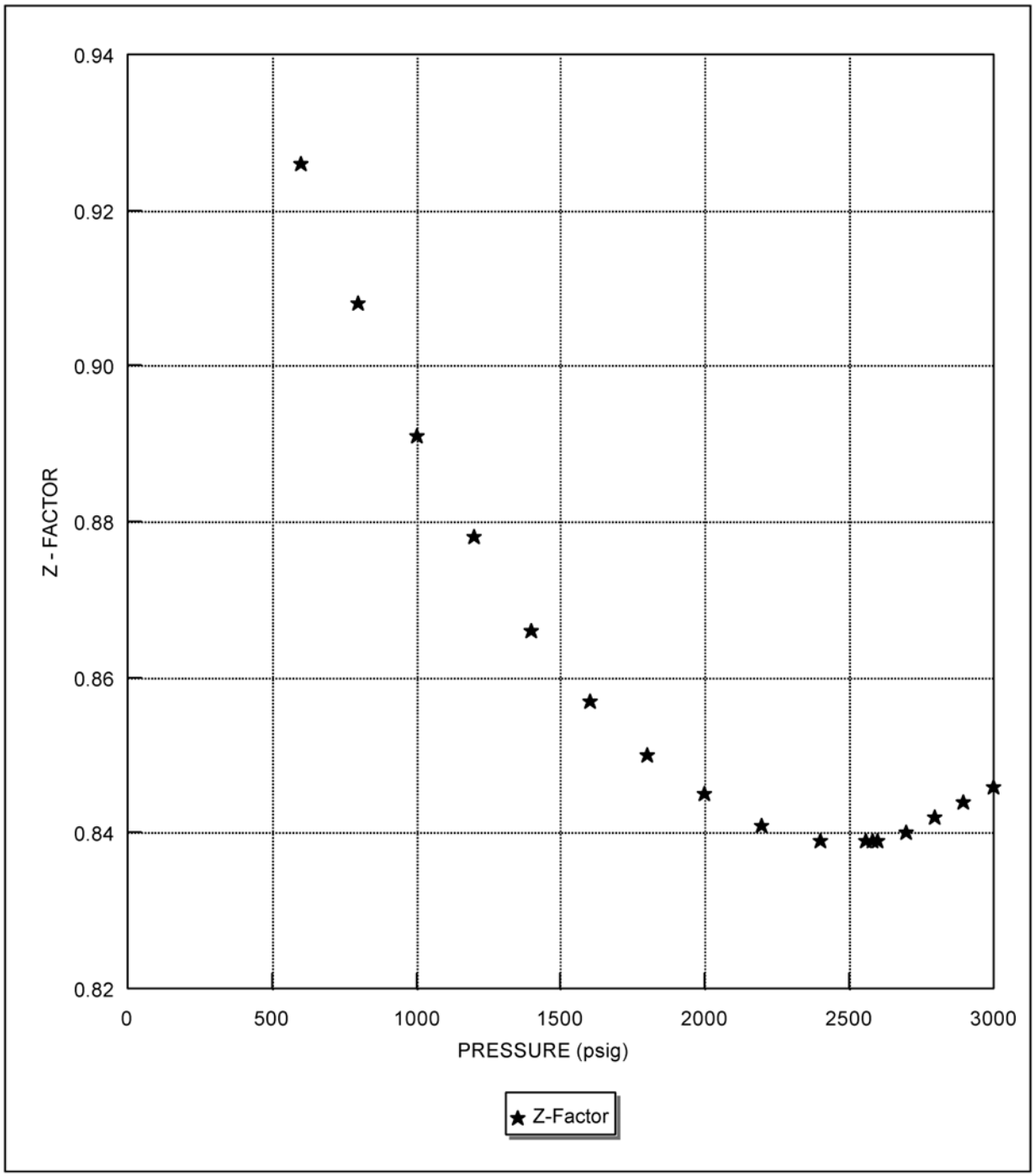

RESERVOIR FLUID SPECIFIC VOLUME

Equation of best fit

SV = +1.12E+00 -1.36E-03 * P +6.68E-07 * P^2 -1.14E-10 * P^3 +0.00E+00 * P^4

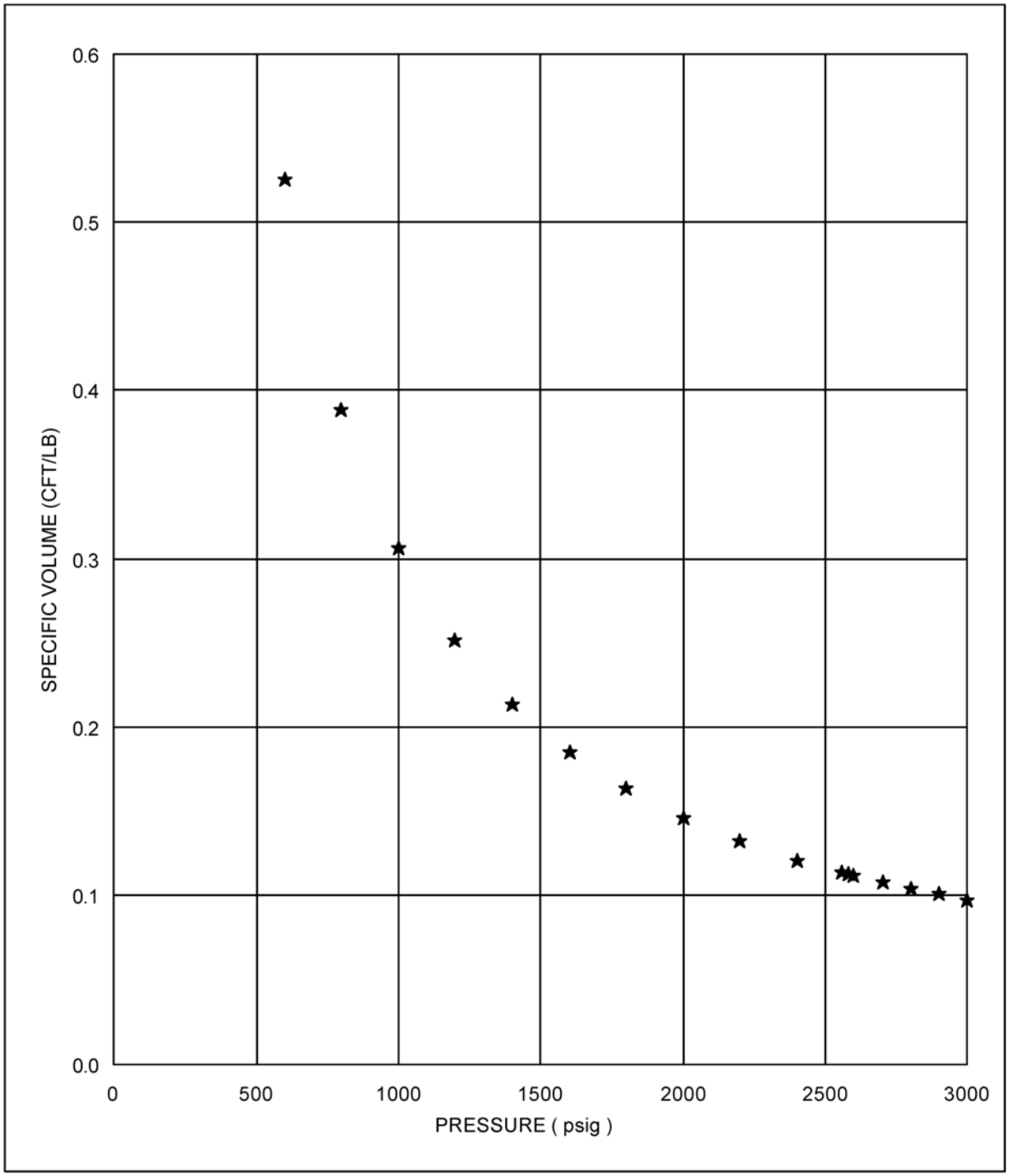

VISCOSITY OF RESERVOIR FLUID

Equation of best fit

μ = +1.28E-02 +3.96E-07 * P +1.09E-09 * P^2 -1.03E-13 * P^3 +0.00E+00 * P^4

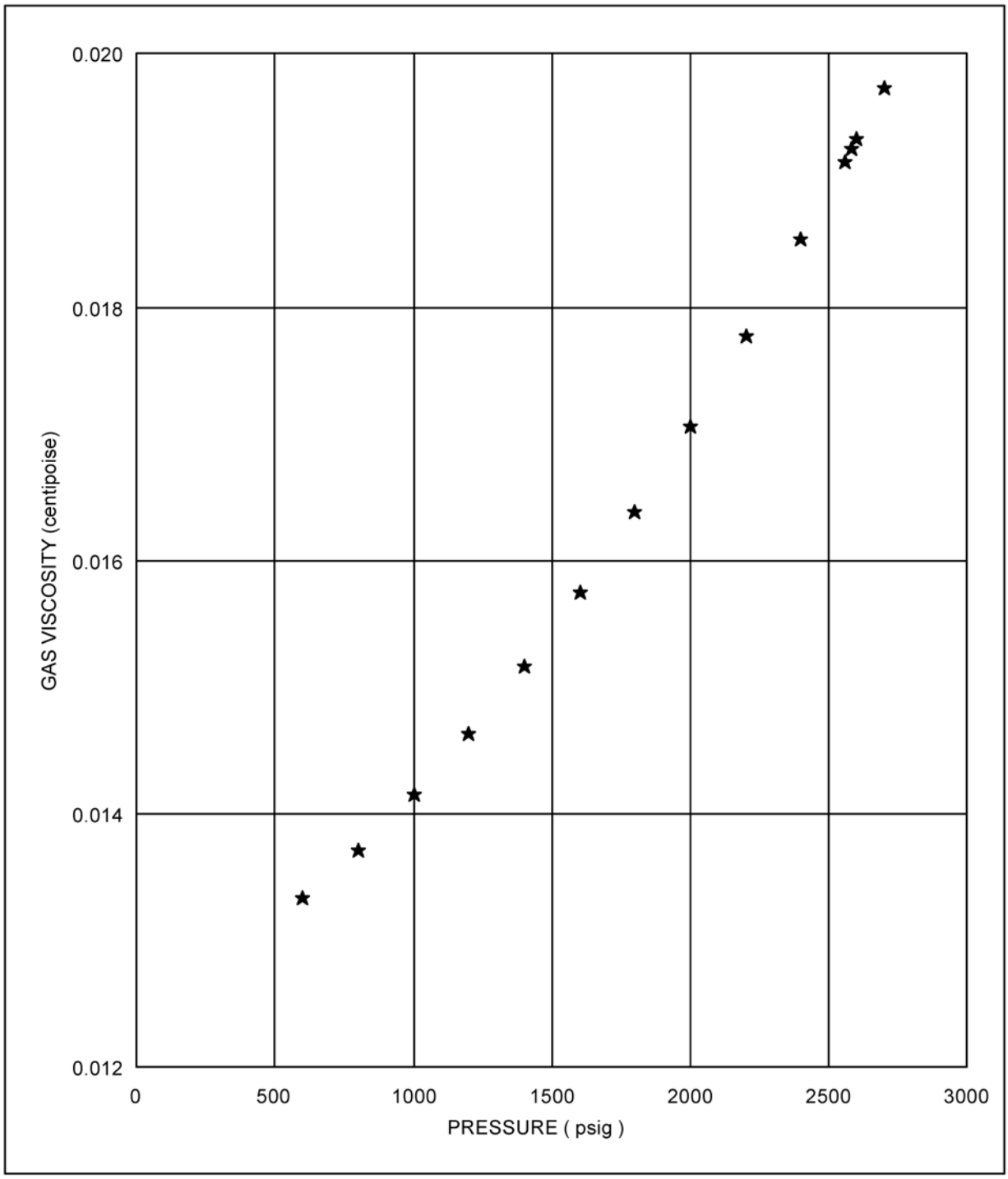

RETROGRADE CONDENSATION

Equation of best fit

Constant Mass

RLD = +8.58E-02 +6.58E-04 * P -5.49E-07 * P^2 +1.05E-10 * P^3 +1.46E-15 * P^4

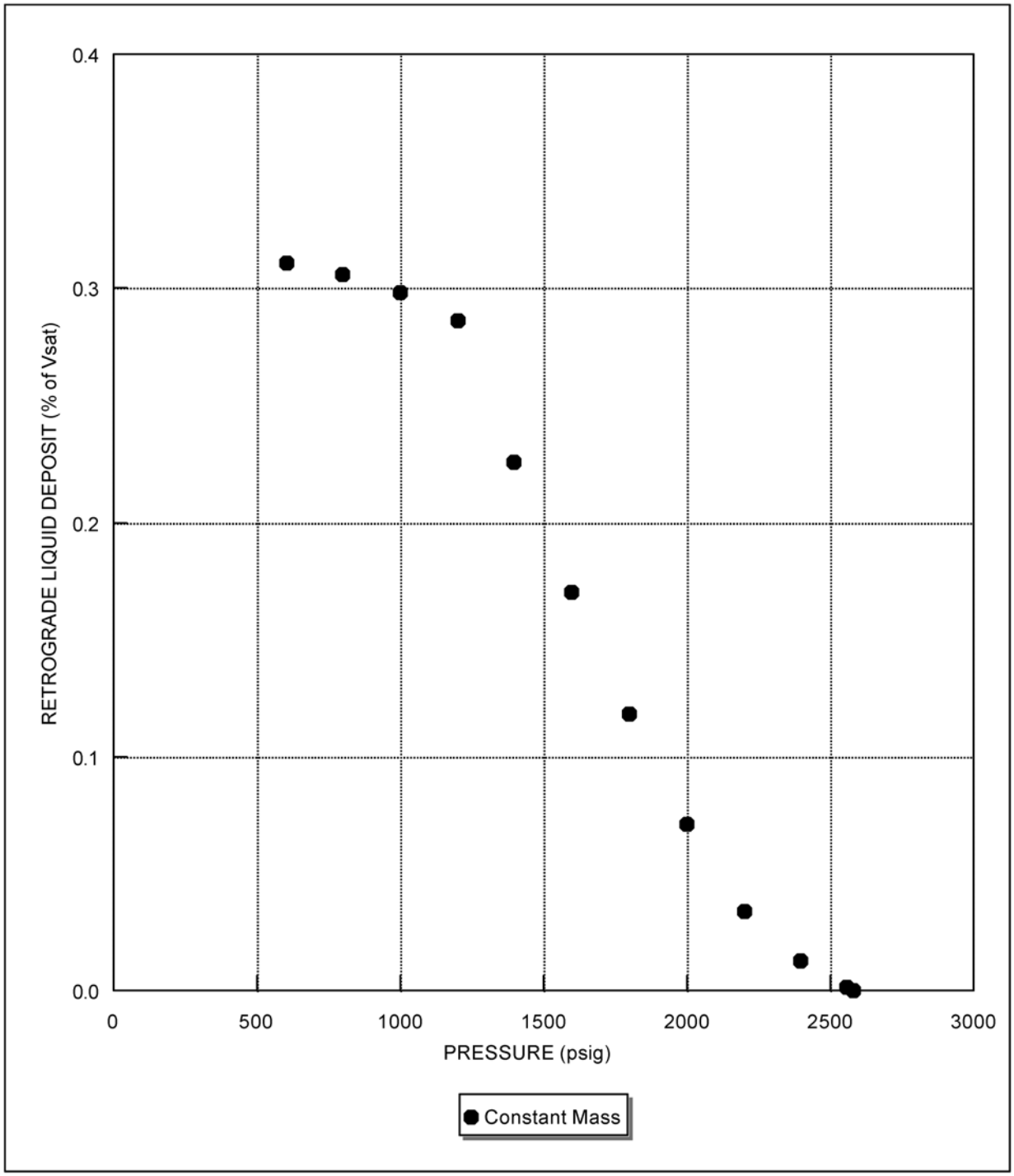

PETROLAB

FINGERPRINT ANALYSIS
BY CAPILLARY GAS CHROMATOGRAPHY
On Stock Tank Oil from atmospheric flash of sample in cylinder # L - 332

Component		Mol %
Hexanes minus	C6-	1.69
Hexanes	C6	2.33
Heptanes	C7	11.19
Octanes	C8	10.41
Nonanes	C9	16.25
Decanes	C10	18.26
Undecanes	C11	12.68
Dodecanes	C12	8.29
Tridecanes	C13	6.15
Tetradecanes	C14	4.20
Pentadecanes	C15	3.04
Hexadecanes	C16	1.82
Heptadecanes	C17	1.24
Octadecanes	C18	0.68
Nonadecanes	C19	0.30
Eicosanes	C20	0.17
Heneicosanes	C21	0.12
Docosanes	C22	0.03
Tricosanes	C23	0.02
Tetracosanes	C24	0.01
Pentacosanes	C25	0.00
Hexacosanes	C26	0.02
Heptacosanes	C27	0.06
Octacosanes	C28	1.03
Nonacosanes	C29	0.01
Triacontanes	C30	0.00
Hentriacontanes	C31	0.00
Dotriacontanes	C32	0.00
Tritriacontanes	C33	0.00
Tetratriacontanes	C34	0.00
Pentatriacontanes Plus	C35+	0.00
TOTAL		100.00

Molecular Weight Calculated *	:	141.5
Density @ 60 °F Calculated *	:	0.7833
Molecular Weight Measured	:	--
Density @ 60 °F Measured	:	--

*Calculation based on generalized properties as published by Katz and Firoozabadi

FINGERPRINT ANALYSIS
BY CAPILLARY GAS CHROMATOGRAPHY
On Stock Tank Oil from atmospheric flash of sample in cylinder # L - 332

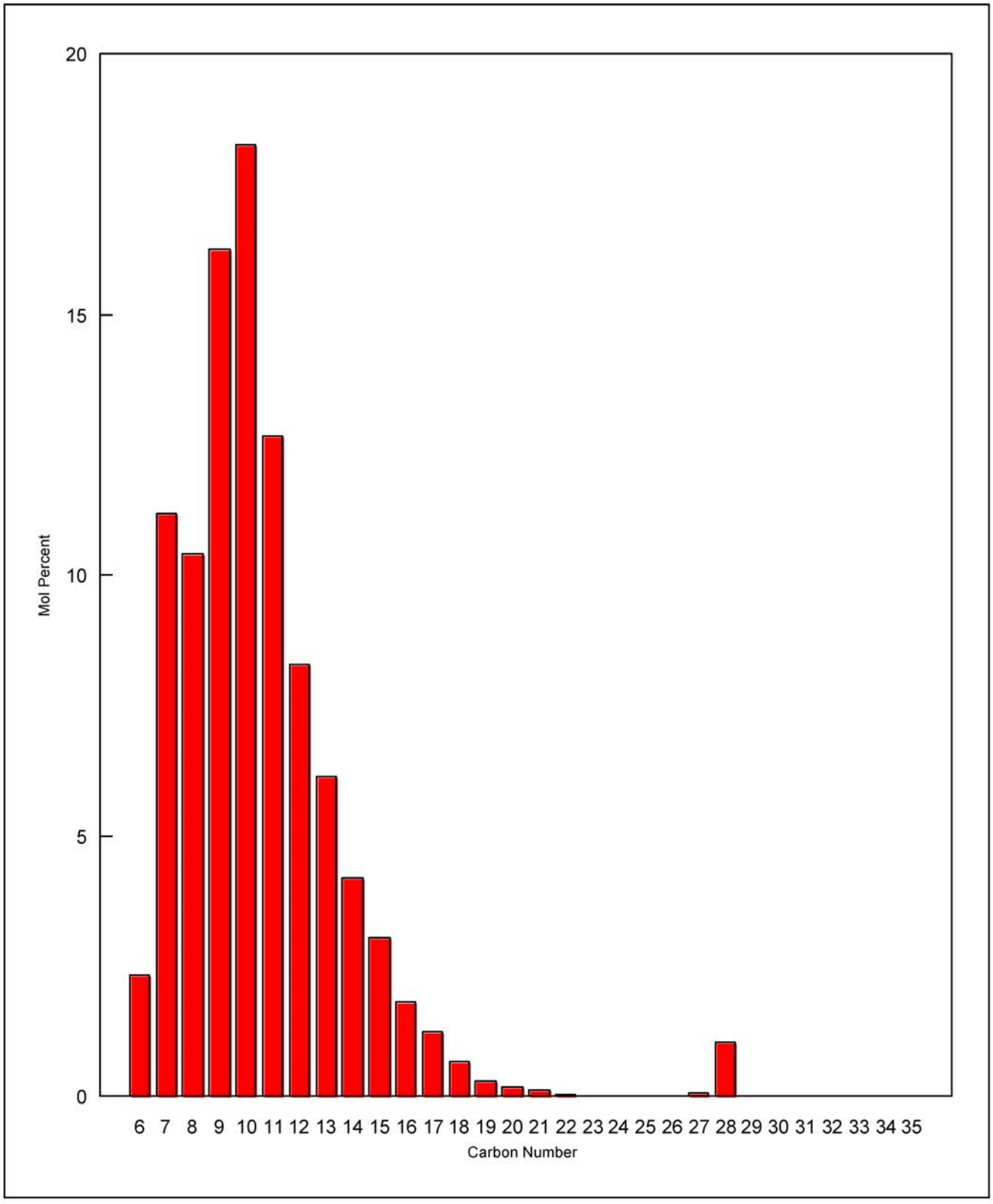

PETROLAB

Company : Origin Energy Resources Limited	Page : 20 of 35
Well : Halladale # 1 DW-2	File : O - 25024

COMPOSITIONAL ANALYSIS OF BOTTOM HOLE RESERVOIR FLUID

Cylinder # L - 332 ex RCI chamber # 189727 Position 1

Component		Stock Tank Liquid Mol %	Stock Tank Gas Mol %	Reservoir Fluid Mol %
Hydrogen Sulphide	H2S	0.00	0.00	0.00
Carbon Dioxide	CO2	0.01	0.47	0.47
Nitrogen	N2	0.00	1.36	1.36
Methane	C1	0.48	90.74	90.65
Ethane	C2	0.11	4.17	4.17
Propane	C3	0.15	1.62	1.62
Iso-Butane	iC4	0.07	0.30	0.30
N-Butane	nC4	0.12	0.38	0.38
Iso-Pentane	iC5	0.09	0.12	0.12
N-Pentane	nC5	0.10	0.10	0.10
Hexanes	C6	2.34	0.18	0.18
Heptanes	C7	11.25	0.27	0.28
Octanes	C8	10.47	0.10	0.11
Nonanes	C9	16.34	0.09	0.11
Decanes	C10	18.37	0.06	0.08
Undecanes	C11	12.75	0.03	0.04
Dodecanes Plus	C12+	27.35	0.01	0.03
TOTAL		100.00	100.00	100.00

Ratios				
Molar Ratio	:	0.0010	0.9990	1.0000
Mass Ratio	:	0.0078	0.9922	1.0000
Liquid Ratio (bbl/bbl)	:	1.0000 @ SC	--	-- @ PT*
Gas Liquid Ratio	:	1.0000 bbl @ SC	723848 SCF	--
Stream Properties				
Molecular Weight	:	141.0	18.43	18.56
Density obs. (gm/cc)	:	0.7842 @ 60 °F	--	-- @ PT*
Gravity (AIR = 1.000)	:	48.8 °API @ 60 °F	0.638	--
GHV (BTU/scf)	:	--	1110	--
Hexanes Plus Properties				
Mol %	:	98.88	0.74	0.83
Molecular Weight	:	142.2	103.8	108.4
Density (gm/cc @ 60 °F)	:	0.7857	0.6940	0.7070
Gravity (°API @ 60 °F)	:	48.4	72.2	68.5
Heptanes Plus Properties				
Mol %	:	96.54	0.56	0.65
Molecular Weight	:	143.6	110.1	115.1
Density (gm/cc @ 60 °F)	:	0.7874	0.7018	0.7164
Gravity (°API @ 60 °F)	:	48.0	69.9	65.8
Decanes Plus Properties				
Mol %	:	58.47	0.10	0.15
Molecular Weight	:	165.6	141.5	145.8
Density (gm/cc @ 60 °F)	:	0.8058	0.7350	0.7590
Gravity (°API @ 60 °F)	:	43.9	60.8	54.7
Undecanes Plus Properties				
Mol %	:	40.10	0.04	0.07
Molecular Weight	:	180.1	152.7	163.7
Density (gm/cc @ 60 °F)	:	0.8158	0.7451	0.7804
Gravity (°API @ 60 °F)	:	41.8	58.2	49.7
Dodecanes Plus Properties				
Mol %	:	27.35	0.01	0.03
Molecular Weight	:	195.5	169.8	186.4
Density (gm/cc @ 60 °F)	:	0.8256	0.7591	0.8076
Gravity (°API @ 60 °F)	:	39.7	54.7	43.5

* (P)ressure : 2549 psig * (T)emperature : 174 °F

PETROLAB

FINGERPRINT ANALYSIS
BY CAPILLARY GAS CHROMATOGRAPHY
On Stock Tank Oil from atmospheric flash of sample in cylinder # L - 188

Component		Mol %
Hexanes minus	C6-	0.20
Hexanes	C6	0.78
Heptanes	C7	7.06
Octanes	C8	10.68
Nonanes	C9	22.69
Decanes	C10	27.08
Undecanes	C11	15.45
Dodecanes	C12	6.76
Tridecanes	C13	3.50
Tetradecanes	C14	1.88
Pentadecanes	C15	1.33
Hexadecanes	C16	0.73
Heptadecanes	C17	0.58
Octadecanes	C18	0.32
Nonadecanes	C19	0.17
Eicosanes	C20	0.12
Heneicosanes	C21	0.09
Docosanes	C22	0.07
Tricosanes	C23	0.07
Tetracosanes	C24	0.04
Pentacosanes	C25	0.04
Hexacosanes	C26	0.04
Heptacosanes	C27	0.03
Octacosanes	C28	0.24
Nonacosanes	C29	0.05
Triacontanes	C30	0.00
Hentriacontanes	C31	0.00
Dotriacontanes	C32	0.00
Tritriacontanes	C33	0.00
Tetratriacontanes	C34	0.00
Pentatriacontanes Plus	C35+	0.00
TOTAL		100.00

Molecular Weight Calculated *	:	136.6
Density @ 60 °F Calculated *	:	0.7792
Molecular Weight Measured	:	--
Density @ 60 °F Measured	:	--

*Calculation based on generalized properties as published by Katz and Firoozabadi

FINGERPRINT ANALYSIS
BY CAPILLARY GAS CHROMATOGRAPHY
On Stock Tank Oil from atmospheric flash of sample in cylinder # L - 188

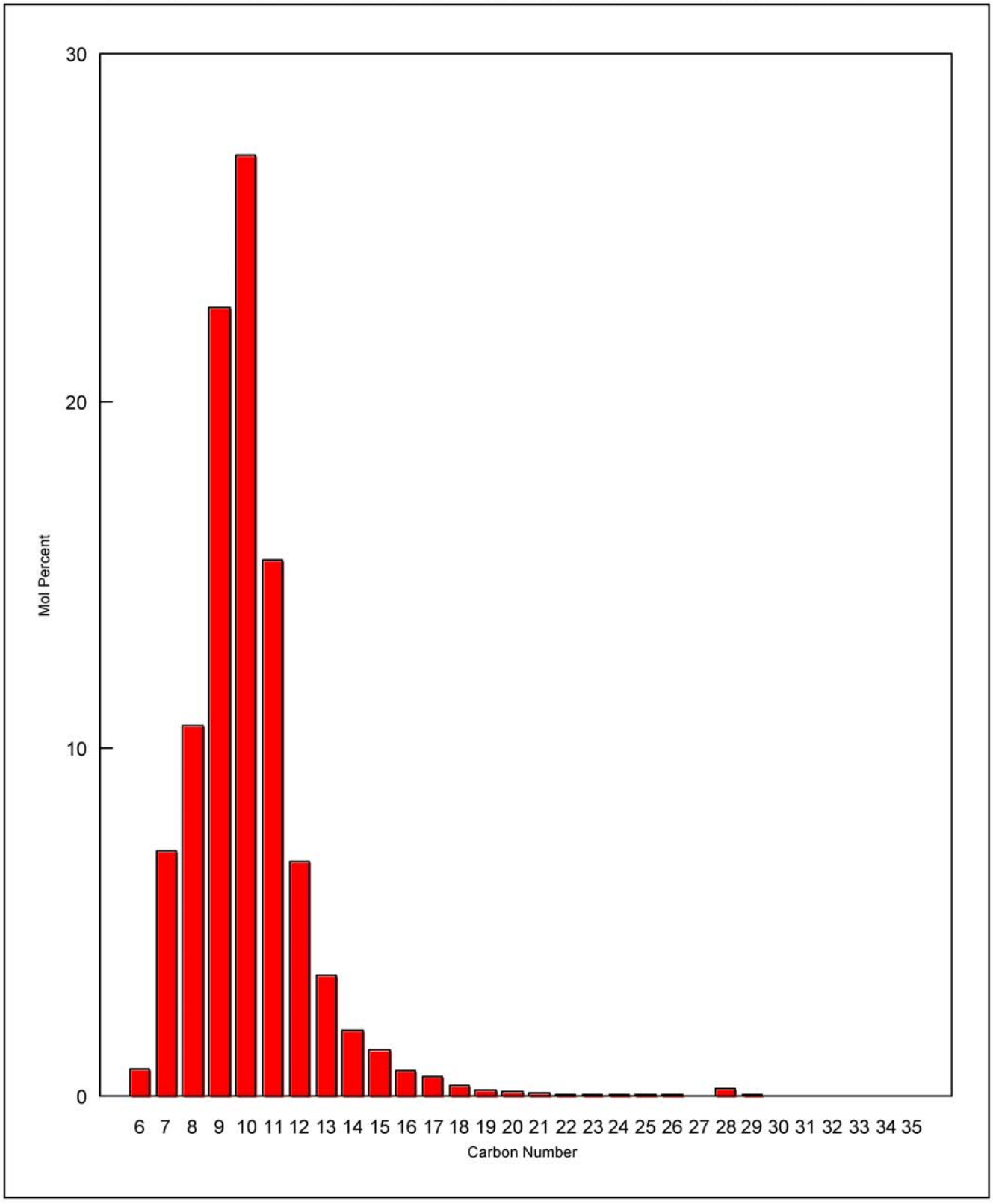

PETROLAB

Company : Origin Energy Resources Limited	Page : 23 of 35
Well : Halladale # 1 DW-2	File : O - 25024

COMPOSITIONAL ANALYSIS OF BOTTOM HOLE RESERVOIR FLUID

Cylinder # L - 188 ex RCI chamber # 189732 Position 2

Component		Stock Tank Liquid Mol %	Stock Tank Gas Mol %	Reservoir Fluid Mol %
Hydrogen Sulphide	H2S	0.00	0.00	0.00
Carbon Dioxide	CO2	0.00	0.39	0.39
Nitrogen	N2	0.00	1.36	1.36
Methane	C1	0.48	90.50	90.47
Ethane	C2	0.12	4.26	4.26
Propane	C3	0.14	1.59	1.59
Iso-Butane	iC4	0.08	0.38	0.38
N-Butane	nC4	0.13	0.42	0.42
Iso-Pentane	iC5	0.10	0.13	0.13
N-Pentane	nC5	0.11	0.11	0.11
Hexanes	C6	0.77	0.20	0.20
Heptanes	C7	6.99	0.30	0.30
Octanes	C8	10.58	0.16	0.16
Nonanes	C9	22.47	0.12	0.13
Decanes	C10	26.82	0.07	0.08
Undecanes	C11	15.30	0.01	0.01
Dodecanes Plus	C12+	15.90	0.00	0.01
TOTAL		100.00	100.00	100.00
Ratios				
Molar Ratio	:	0.0003	0.9997	1.0000
Mass Ratio	:	0.0023	0.9977	1.0000
Liquid Ratio (bbl/bbl)	:	1.0000 @ SC	--	-- @ PT*
Gas Liquid Ratio	:	1.0000 bbl @ SC	2447181 SCF	--
Stream Properties				
Molecular Weight	:	134.7	18.57	18.61
Density obs. (gm/cc)	:	0.7780 @ 60 °F	--	-- @ PT*
Gravity (AIR = 1.000)	:	50.2 °API @ 60 °F	0.643	--
GHV (BTU/scf)	:	--	1119	--
Hexanes Plus Properties				
Mol %	:	98.84	0.86	0.89
Molecular Weight	:	135.8	102.4	103.6
Density (gm/cc @ 60 °F)	:	0.7796	0.6923	0.6958
Gravity (°API @ 60 °F)	:	49.8	72.7	71.7
Heptanes Plus Properties				
Mol %	:	98.06	0.66	0.69
Molecular Weight	:	136.2	108.0	109.3
Density (gm/cc @ 60 °F)	:	0.7801	0.6993	0.7033
Gravity (°API @ 60 °F)	:	49.7	70.7	69.5
Decanes Plus Properties				
Mol %	:	58.02	0.08	0.10
Molecular Weight	:	152.3	135.6	137.4
Density (gm/cc @ 60 °F)	:	0.7949	0.7294	0.7406
Gravity (°API @ 60 °F)	:	46.3	62.3	59.4
Undecanes Plus Properties				
Mol %	:	31.20	0.01	0.02
Molecular Weight	:	168.1	146.9	157.4
Density (gm/cc @ 60 °F)	:	0.8069	0.7399	0.7739
Gravity (°API @ 60 °F)	:	43.7	59.6	51.2
Dodecanes Plus Properties				
Mol %	:	15.90	0.00	0.01
Molecular Weight	:	188.4	--	188.4
Density (gm/cc @ 60 °F)	:	0.8209	--	0.8209
Gravity (°API @ 60 °F)	:	40.7	--	40.7

* (P)ressure : 2549 psig * (T)emperature : 174 °F

PETROLAB

FINGERPRINT ANALYSIS
BY CAPILLARY GAS CHROMATOGRAPHY
On Stock Tank Oil from atmospheric flash of sample in cylinder # L - 076

Component		Mol %
Hexanes minus	C6-	0.54
Hexanes	C6	1.44
Heptanes	C7	8.99
Octanes	C8	10.82
Nonanes	C9	20.80
Decanes	C10	25.67
Undecanes	C11	17.21
Dodecanes	C12	7.89
Tridecanes	C13	3.68
Tetradecanes	C14	1.56
Pentadecanes	C15	0.79
Hexadecanes	C16	0.32
Heptadecanes	C17	0.16
Octadecanes	C18	0.06
Nonadecanes	C19	0.02
Eicosanes	C20	0.01
Heneicosanes	C21	0.01
Docosanes	C22	0.01
Tricosanes	C23	0.00
Tetracosanes	C24	0.00
Pentacosanes	C25	0.00
Hexacosanes	C26	0.00
Heptacosanes	C27	0.00
Octacosanes	C28	0.02
Nonacosanes	C29	0.00
Triacontanes	C30	0.00
Hentriacontanes	C31	0.00
Dotriacontanes	C32	0.00
Tritriacontanes	C33	0.00
Tetratriacontanes	C34	0.00
Pentatriacontanes Plus	C35+	0.00
TOTAL		100.00

Molecular Weight Calculated *	:	132.8
Density @ 60 °F Calculated *	:	0.7745
Molecular Weight Measured	:	--
Density @ 60 °F Measured	:	--

*Calculation based on generalized properties as published by Katz and Firoozabadi

FINGERPRINT ANALYSIS
BY CAPILLARY GAS CHROMATOGRAPHY
On Stock Tank Oil from atmospheric flash of sample in cylinder # L - 076

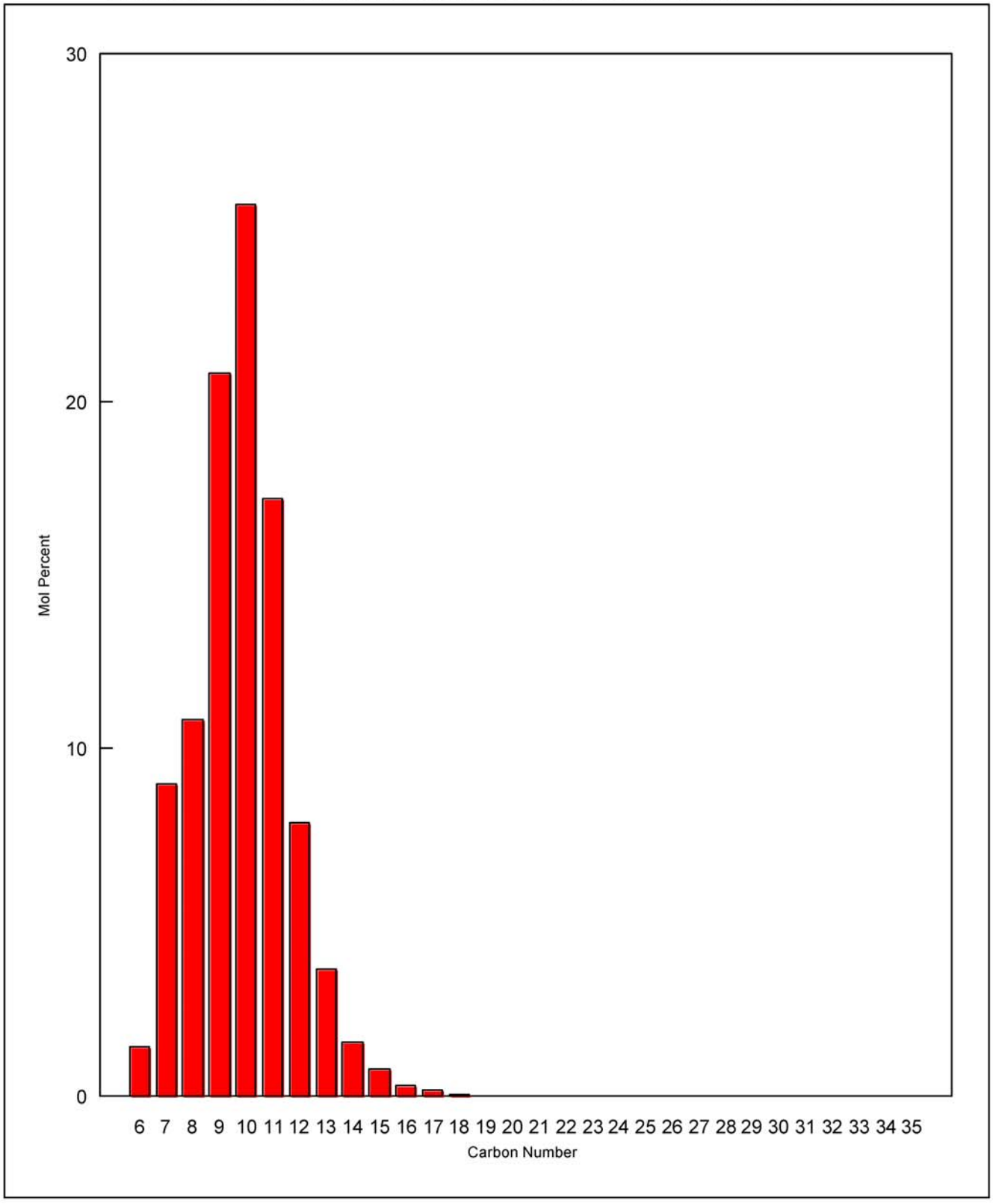

PETROLAB

Company : Origin Energy Resources Limited	Page : 26 of 35
Well : Halladale # 1 DW-2	File : O - 25024

COMPOSITIONAL ANALYSIS OF BOTTOM HOLE RESERVOIR FLUID

Cylinder # L - 076 ex RCI chamber # 189768 Position 3

Component		Stock Tank Liquid Mol %	Stock Tank Gas Mol %	Reservoir Fluid Mol %
Hydrogen Sulphide	H2S	0.00	0.00	0.00
Carbon Dioxide	CO2	0.01	0.50	0.50
Nitrogen	N2	0.00	1.38	1.38
Methane	C1	0.48	90.91	90.89
Ethane	C2	0.11	4.20	4.20
Propane	C3	0.15	1.61	1.61
Iso-Butane	iC4	0.07	0.32	0.32
N-Butane	nC4	0.11	0.35	0.35
Iso-Pentane	iC5	0.08	0.11	0.11
N-Pentane	nC5	0.09	0.09	0.09
Hexanes	C6	1.43	0.15	0.15
Heptanes	C7	8.94	0.21	0.21
Octanes	C8	10.76	0.07	0.07
Nonanes	C9	20.68	0.05	0.05
Decanes	C10	25.53	0.02	0.03
Undecanes	C11	17.11	0.03	0.03
Dodecanes Plus	C12+	14.45	0.00	0.01
TOTAL		100.00	100.00	100.00

Ratios				
Molar Ratio	:	0.0002	0.9998	1.0000
Mass Ratio	:	0.0016	0.9984	1.0000
Liquid Ratio (bbl/bbl)	:	1.0000 @ SC	--	-- @ PT*
Gas Liquid Ratio	:	1.0000 bbl @ SC	3447296 SCF	--
Stream Properties				
Molecular Weight	:	131.1	18.23	18.26
Density obs. (gm/cc)	:	0.7737 @ 60 °F	--	-- @ PT*
Gravity (AIR = 1.000)	:	51.2 °API @ 60 °F	0.631	--
GHV (BTU/scf)	:	--	1098	--
Hexanes Plus Properties				
Mol %	:	98.90	0.53	0.55
Molecular Weight	:	132.2	100.7	102.0
Density (gm/cc @ 60 °F)	:	0.7753	0.6901	0.6941
Gravity (°API @ 60 °F)	:	50.8	73.4	72.2
Heptanes Plus Properties				
Mol %	:	97.47	0.38	0.40
Molecular Weight	:	132.9	107.3	108.8
Density (gm/cc @ 60 °F)	:	0.7762	0.6985	0.7032
Gravity (°API @ 60 °F)	:	50.6	70.9	69.5
Decanes Plus Properties				
Mol %	:	57.09	0.05	0.07
Molecular Weight	:	147.9	141.8	136.9
Density (gm/cc @ 60 °F)	:	0.7906	0.7352	0.7409
Gravity (°API @ 60 °F)	:	47.3	60.8	59.3
Undecanes Plus Properties				
Mol %	:	31.56	0.03	0.04
Molecular Weight	:	159.1	147.0	149.3
Density (gm/cc @ 60 °F)	:	0.7993	0.7400	0.7515
Gravity (°API @ 60 °F)	:	45.4	59.5	56.6
Dodecanes Plus Properties				
Mol %	:	14.45	0.00	0.01
Molecular Weight	:	173.4	--	173.4
Density (gm/cc @ 60 °F)	:	0.8100	--	0.8100
Gravity (°API @ 60 °F)	:	43.0	--	43.0

* (P)ressure : 2549 psig * (T)emperature : 174 °F

CONSTANT MASS STUDY
@ 174 °F
Using Bottom Hole Sample ex RCI chamber # 189732 Position 2 - transferred into Cylinder # L-188

Pressure (psig)		Relative Volume (V/Vsat) (1)	Formation Volume Factor (Bg) (2)	Gas Expansion Factor (E) (3)	Deviation Factor (Z)	Specific Volume (CFT/LB)	Gas Viscosity (Centipoise) (4)
5000		0.5897	0.00352	283.69	0.987	0.07192	0.0272
4500		0.6325	0.00378	264.52	0.953	0.07713	0.0255
4000		0.6896	0.00412	242.61	0.924	0.08410	0.0237
3500		0.7664	0.00458	218.30	0.899	0.09346	0.0219
3000		0.8766	0.00524	190.85	0.882	0.10690	0.0201
2900		0.9046	0.00541	184.94	0.880	0.11032	0.0198
2800		0.9346	0.00559	179.00	0.878	0.11398	0.0194
2700		0.9680	0.00579	172.84	0.877	0.11804	0.0191
2650		0.9861	0.00589	169.66	0.877	0.12026	0.0189
2610	*	1.0000	0.00598	167.30	0.876	0.12195	0.0187
2549	**	1.0238	0.00612	163.41	0.876	0.12485	0.0185
2400		1.0857	0.00649	154.09	0.875	0.13240	0.0180
2200		1.1851	0.00708	141.17	0.876	0.14453	0.0174
2000		1.3087	0.00782	127.83	0.880	0.15960	0.0168
1800		1.4596	0.00872	114.62	0.884	0.17799	0.0162
1600		1.6515	0.00987	101.30	0.890	0.20140	0.0157
1400		1.9019	0.01137	87.96	0.898	0.23194	0.0151
1200		2.2397	0.01339	74.70	0.908	0.27313	0.0147
1000		2.7137	0.01622	61.65	0.919	0.33093	0.0143
800		3.4276	0.02049	48.81	0.932	0.41800	0.0139
600		4.6160	0.02759	36.24	0.947	0.56292	0.0135

* Dew Point Pressure
** Reservoir Pressure

(1) Cubic feet of gas at indicated pressure and temperature per cubic foot at reservoir pressure
(2) Cubic feet of gas at indicated pressure and temperature per cubic foot at 14.696 psia and 60 °F
(3) Cubic feet of gas at 14.696 psia and 60 °F per cubic foot at indicated pressure and temperature
(4) Calculated from correlation of Lee, Gonzales and Eakin

CONSTANT MASS STUDY
@ 174 °F
Using Bottom Hole Sample ex RCI chamber # 189732 Position 2 - transferred into Cylinder # L-188

Pressure (psig)		Relative Volume (V/Vsat) (1)	Retrograde Liquid Deposit (Bbl/MMSCF) (2)	(Volume%) (3)
2610	*	1.0000	0.00	0.000
2549	**	1.0238	0.01	0.001
2400		1.0857	0.04	0.004
2200		1.1851	0.11	0.010
2000		1.3087	0.22	0.021
1800		1.4596	0.50	0.047
1600		1.6515	0.90	0.085
1400		1.9019	1.05	0.099
1200		2.2397	0.98	0.092
1000	***	2.7137	0.92	0.086
800	***	3.4276	0.85	0.080
600	***	4.6160	0.79	0.074

* Dew Point Pressure
** Reservoir Pressure

*** Retrograde Liquid Extrapolated

(1) Cubic feet of gas at indicated pressure and temperature per cubic foot at saturation pressure
(2) Barrels of liquid at indicated pressure and temperature per MMSCF of original reservoir fluid
(3) Percent of reservoir hydrocarbon pore space at dew point

RELATIVE VOLUME

Equation of best fit

V/VSat = +8.62E+00 -9.18E-03 * P +4.19E-06 * P^2 -8.54E-10 * P^3 +6.37E-14 * P^4

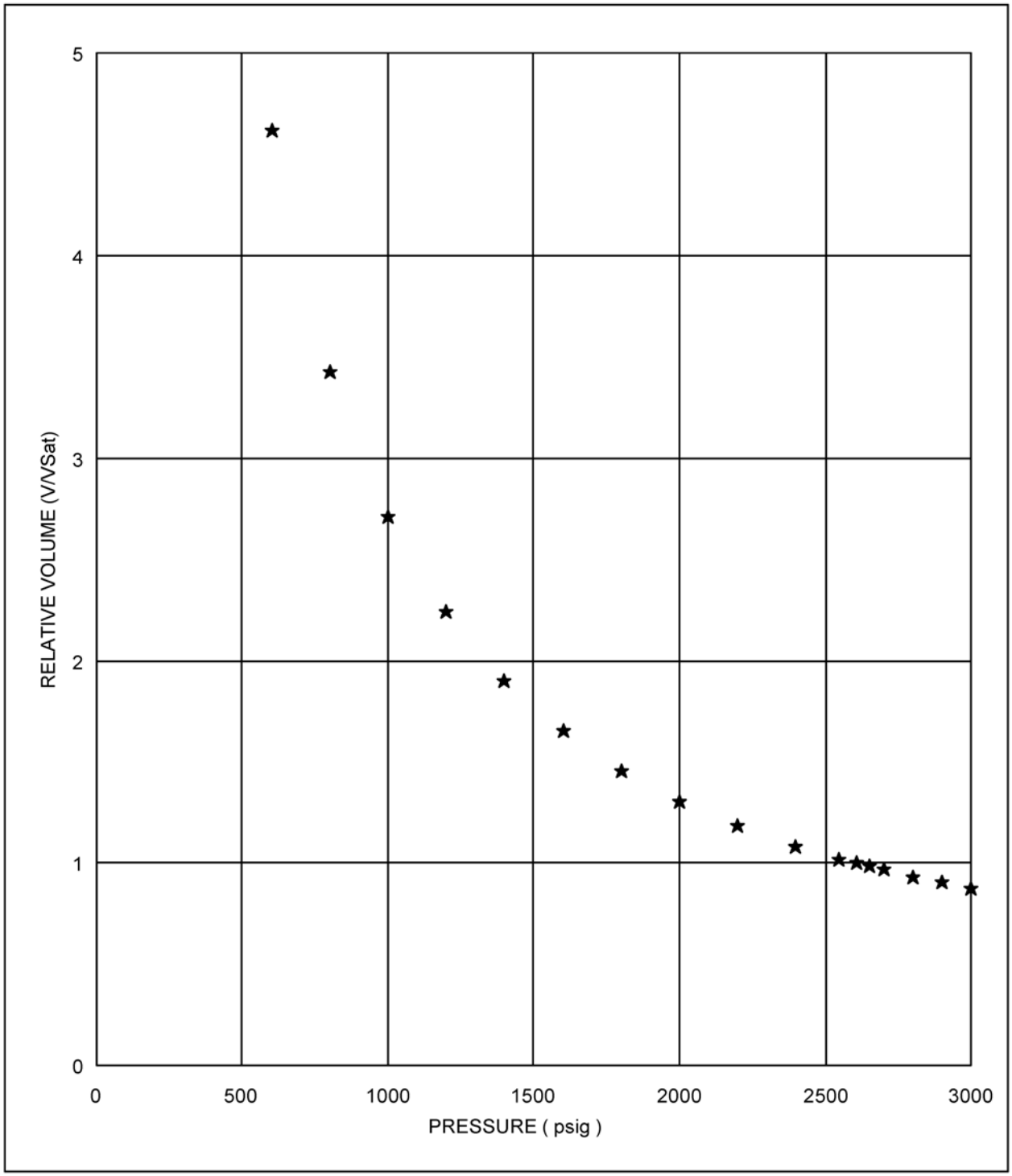

GAS FORMATION VOLUME FACTOR

Equation of best fit

Bg = +5.84E-02 -7.05E-05 * P +3.44E-08 * P^2 -5.88E-12 * P^3 +0.00E+00 * P^4

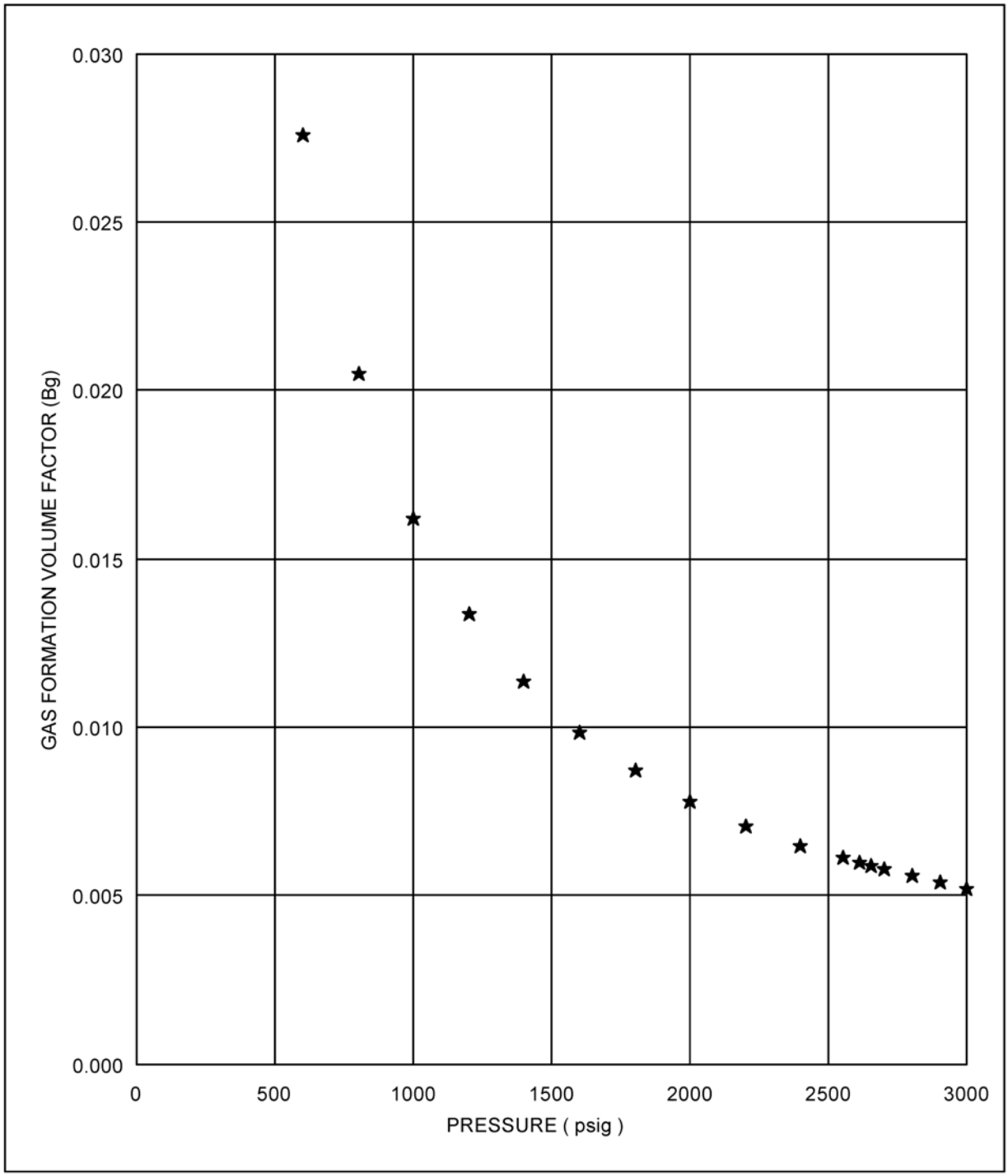

GAS EXPANSION FACTOR

Equation of best fit

E = +9.94E-01 +5.51E-02 * P +7.00E-06 * P^2 -1.40E-09 * P^3 +0.00E+00 * P^4

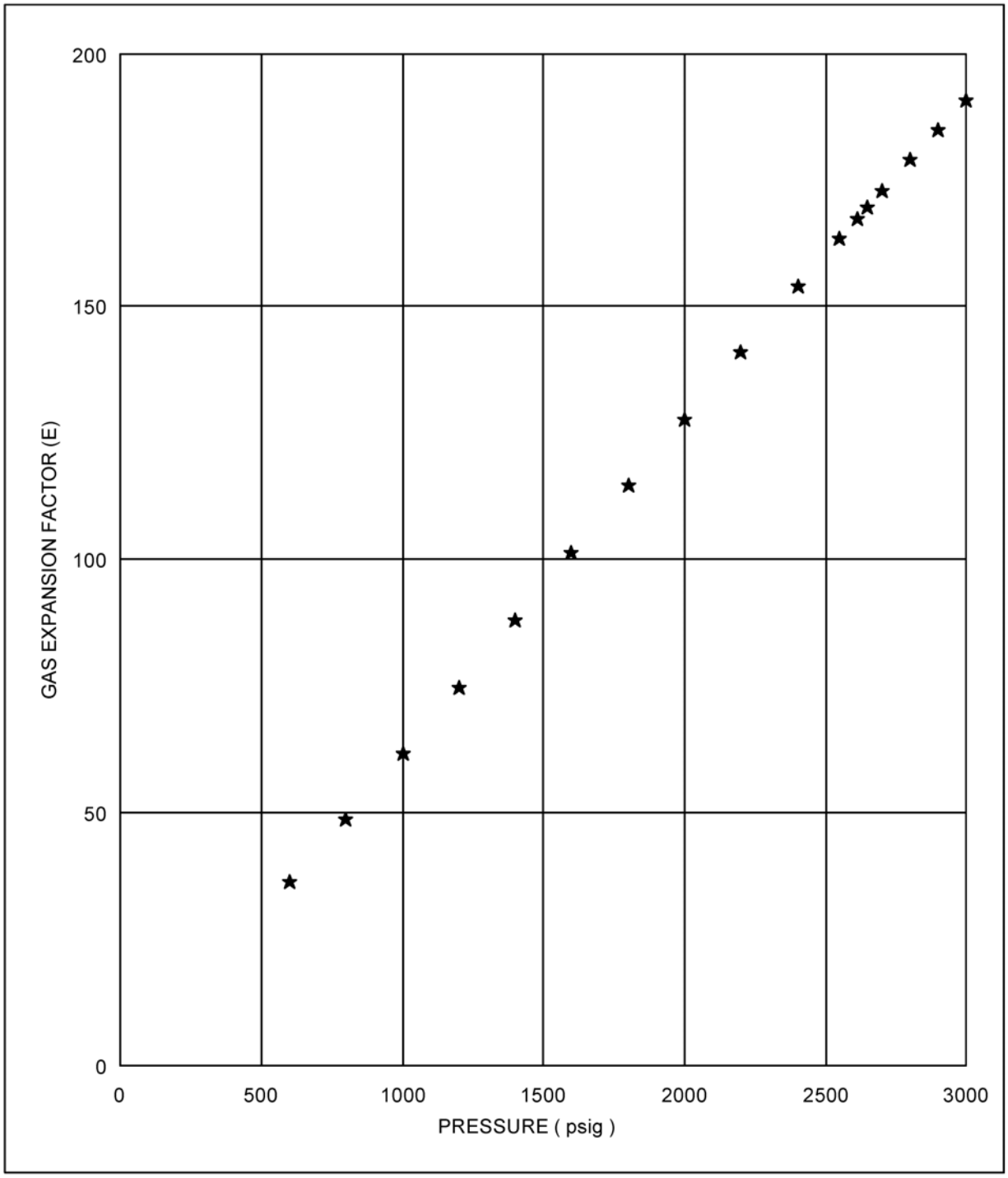

GAS DEVIATION FACTOR

Equation of best fit

Z

$$Z = +1.00E+00 -9.90E-05 * P +1.68E-08 * P^2 +1.74E-12 * P^3 +-2.36E-16 * P^4$$

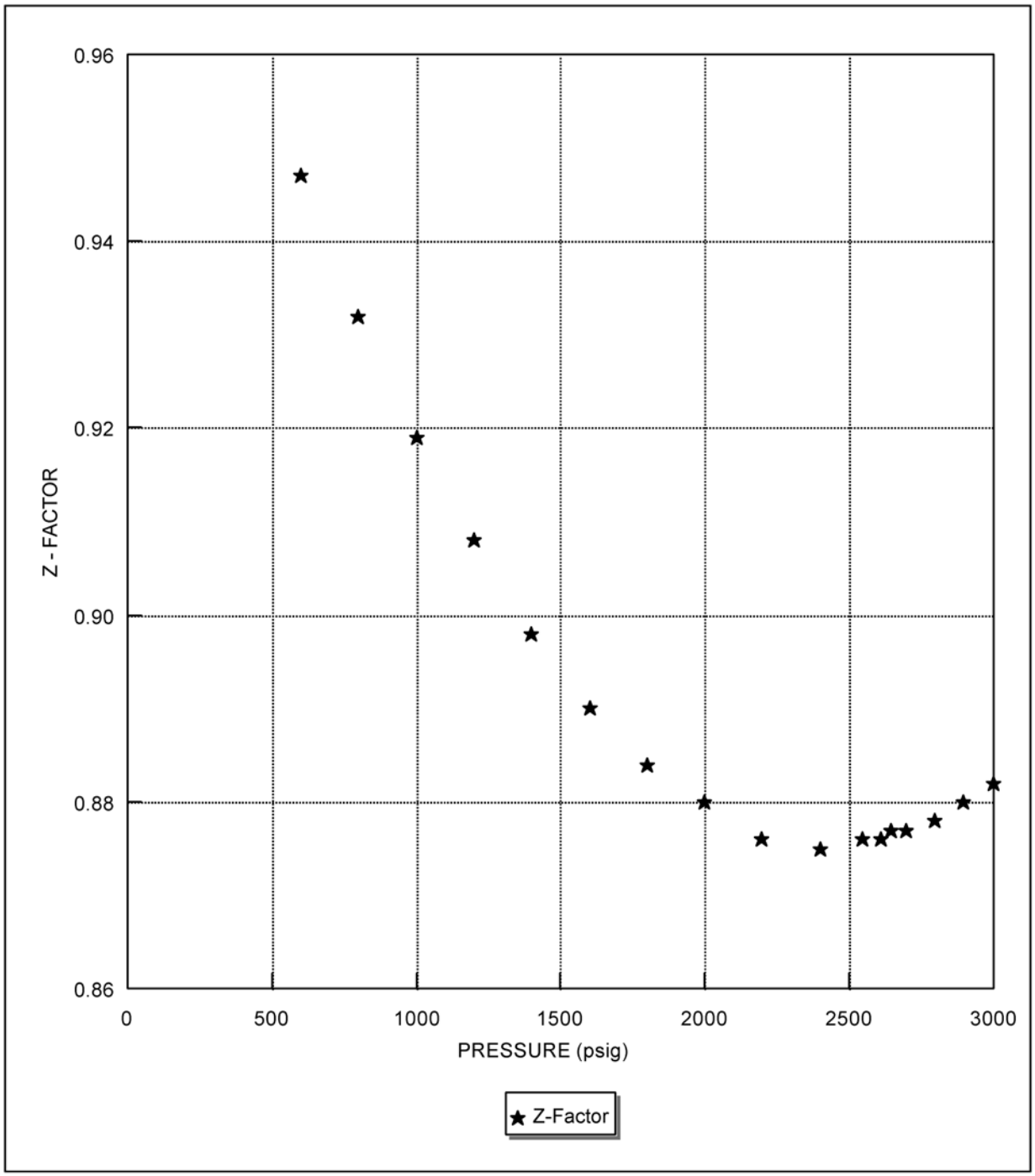

RESERVOIR FLUID SPECIFIC VOLUME

Equation of best fit

SV = +1.19E+00 -1.44E-03 * P +7.03E-07 * P^2 -1.20E-10 * P^3 +0.00E+00 * P^4

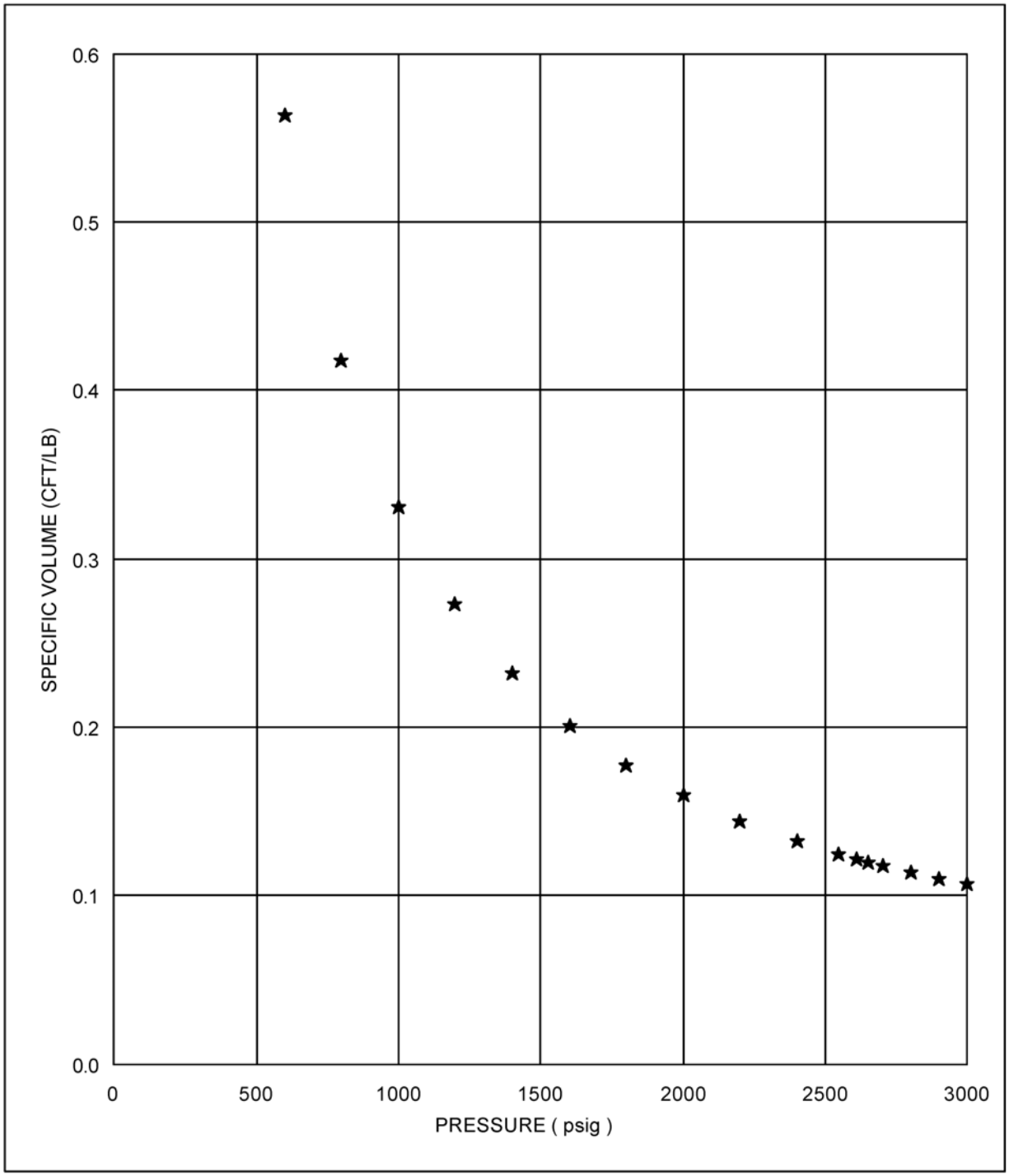

VISCOSITY OF RESERVOIR FLUID

Equation of best fit

$\mu = +1.30E-02 +4.93E-07 * P +8.78E-10 * P^2 -8.26E-14 * P^3 +0.00E+00 * P^4$

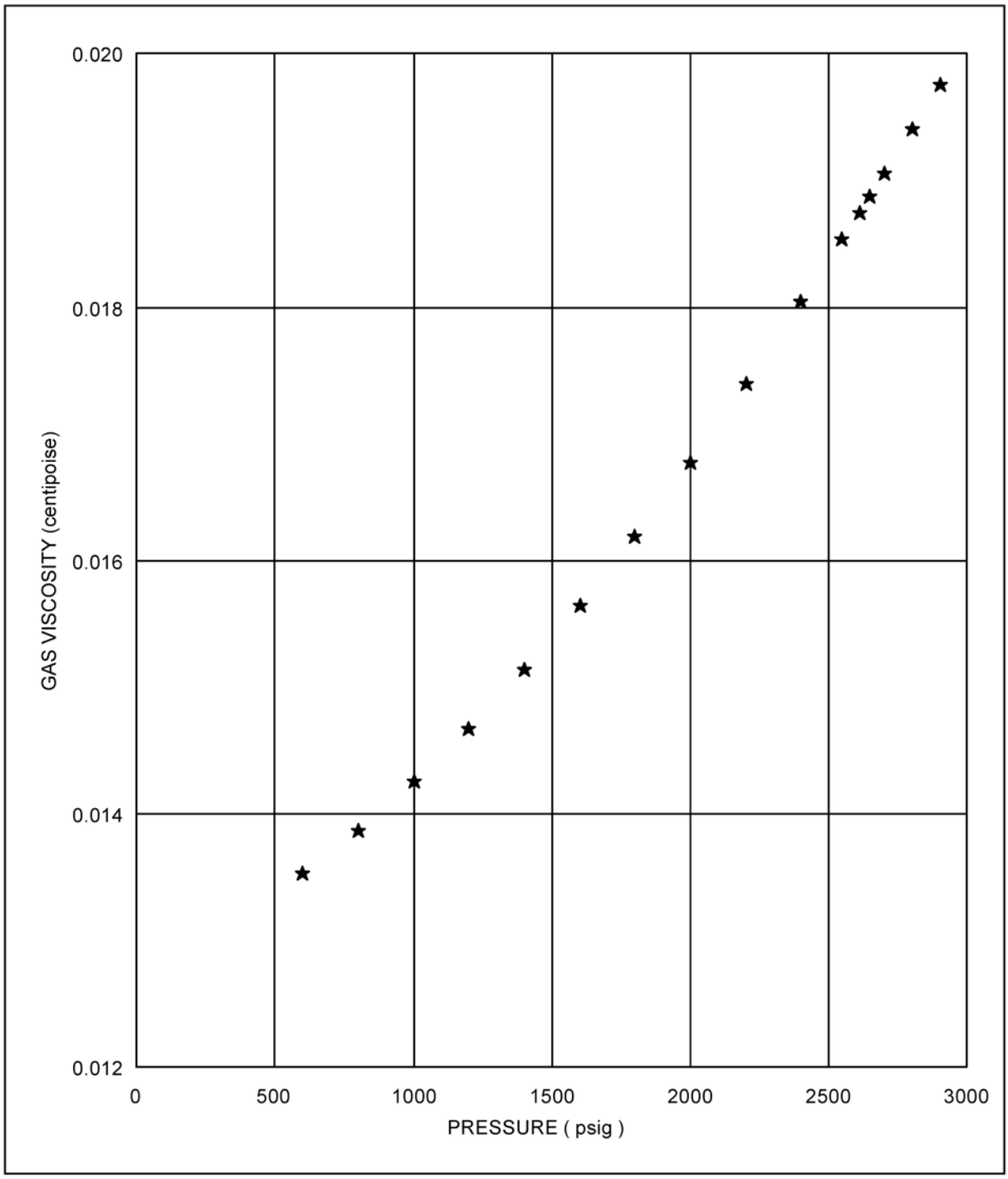

RETROGRADE CONDENSATION

Equation of best fit

Constant Mass

RLD = +1.39E-01 -3.47E-04 * P +5.72E-07 * P^2 -3.35E-10 * P^3 +6.08E-14 * P^4

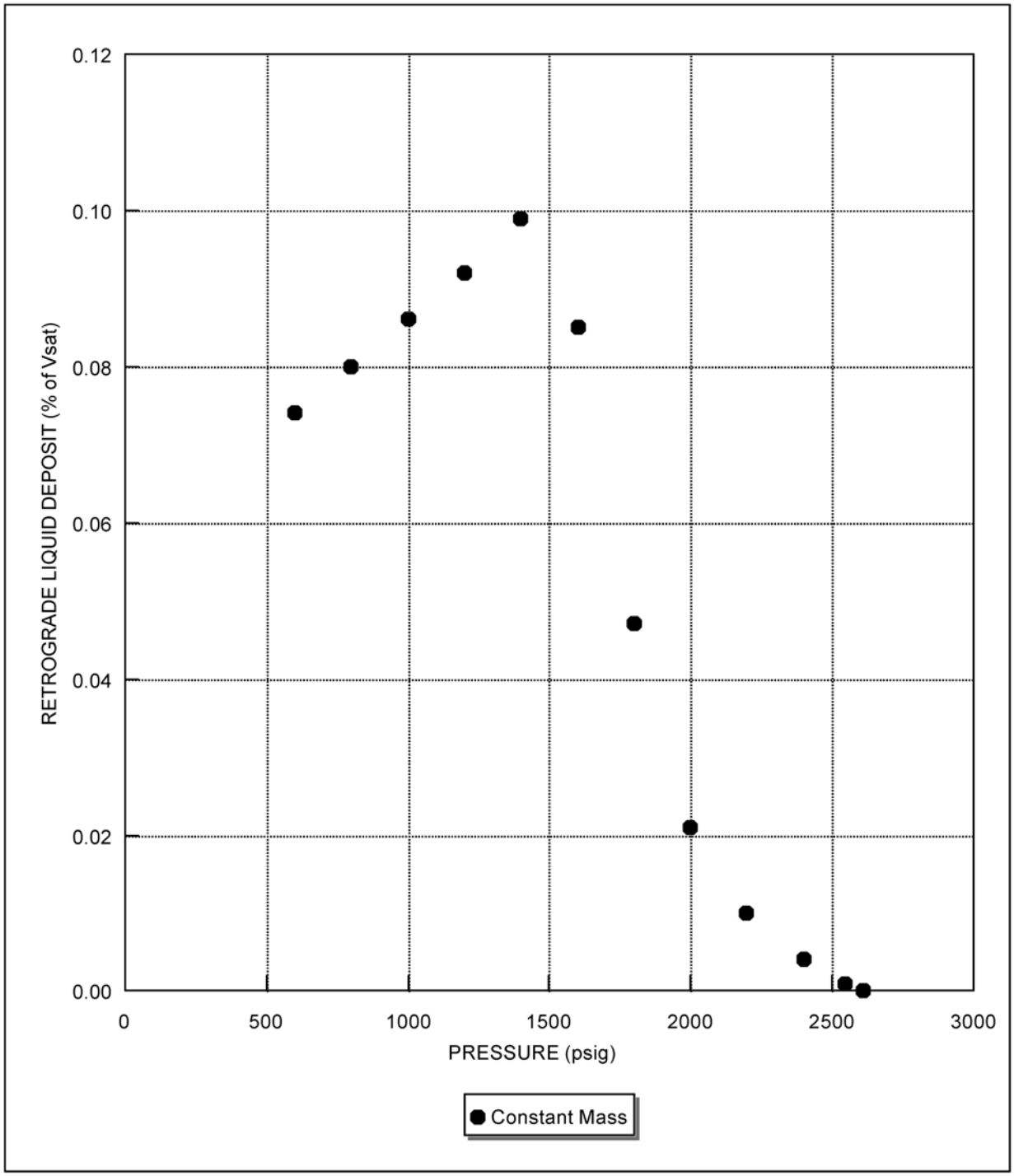

APPENDIX 9:
CONDENSATE GEOCHEMISTRY REPORT

HYDROCARBON CHARACTERISATION STUDY

HALLADALE-1

PROFESSIONAL OPINION

Prepared by:
Cindy Barber

Prepared for:
Origin Energy

February 2007

GEOTECH
GEOTECHNICAL SERVICES PTY LTD
41- 45 Furnace Road, Welshpool, Western Australia. 6106
Locked Bag 27, Cannington, Western Australia. 6987
Email: geotech@geotechnical-services.com.au
Telephone: (08) 9458 8877 (24 Hours)
Facsimile: (08) 9458 8857
ACN 050 543 194
Quality Endorsed Company
ABN 58 050 543 194

EXECUTIVE SUMMARY

Two condensates from Halladale-1 (DW1 exL-128 and DW2 exL-332) were submitted by Origin Energy for geochemical analysis.

A geochemical program was undertaken to evaluate the two Halladale-1 condensates with regards to source, thermal maturity and depositional environment. This report provides a compilation of data obtained from GC-MS analysis of the samples, together with an interpretation of these data

The two Halladale-1 condensates display n-alkane profiles indicative of high thermal maturity. Neither sample appears to have been altered through secondary processes, such as biodegradation and water washing. Pristane to phytane ratios in the Halladale-1 condensates are very high (7.44 and 7.78 for DW1 and DW2, respectively) and are considered indicative of oxic conditions having prevailed during deposition of the associated source rocks.

The two condensates contain high relative abundances of 1,2,5-trimethylnaphthalene, suggesting contamination from low maturity organic matter indigenous to sediments along the migration pathway or in the reservoir. The low Methyl Phenanthrene Indices (0.67 and 0.37 for DW1 and DW2, respectively) indicate low to moderate thermal maturity, which is inconsistent with saturate data, and further supports mixing of the organic matter within the condensates with low maturity organic matter from an additional source.

Biomarker data attest to derivation of organic matter in both samples largely from marine algal sources, although there is also a contribution of terrestrial higher plant derived material. Isosterane distributions classify the depositional environment of the associated source rocks as near shore marine, in an estuary or bay type setting. The abundance of marine derived organic matter with a concomitant contribution of terrigenous derived material is consistent with deposition in such a setting.

The overall composition of the two condensates is very comparable, indicating the samples to be genetically related and attesting to derivation from the same, or very similar, source facies.

HYDROCARBON CHARACTERISATION STUDY

HALLADALE-1

TABLE OF CONTENTS

		Page Number
1	INTRODUCTION	4
2	RESULTS AND INTERPRETATION	5
3	CONCLUSIONS	12
4	REFERENCES	13
APPENDIX A:	DATA AND TABLES	15
APPENDIX B:	ANALYTICAL PROCEDURES	51

1 INTRODUCTION

Two condensates from Halladale-1 (DW1 exL-128 and DW2 exL-332) were submitted by Origin Energy for geochemical analysis.

A geochemical program was undertaken to evaluate the two Halladale-1 condensates with regards to source, thermal maturity and depositional environment. This report provides a compilation of data obtained from GC-MS analysis of the samples, together with an interpretation of these data

One hardcopy and one electronic copy of this report have been sent to Andrew Constantine at Origin Energy. Any queries related to it may be directed to Cindy Barber or Dr Birgitta Hartung-Kagi at Geotechnical Services Pty Ltd.

All data and information are proprietary to Origin Energy and regarded as highly confidential by all Geotech personnel.

Geotechnical Services has endeavoured to use techniques and equipment to achieve results and information as accurately as it possibly can. However, such equipment and techniques are not necessarily perfect. Therefore, Geotechnical Services shall not be held responsible or liable for the results of any actions taken on the basis of the information contained in this document. Moreover, this report should not be the sole reference when considering issues that may have commercial implications.

2 RESULTS AND INTERPRETATION

2.1 WHOLE OIL GC-MS

The two Halladale-1 condensates (DW1 and DW2) were initially submitted for whole oil GC-MS analysis. Whole oil GC-MS allows for analysis of the gasoline range hydrocarbons as well as providing an overall profile of components up to approximately C_{30}. The physical processes of biodegradation, water washing and evaporative-fractionation readily alter the distribution and relative abundance of the gasoline range hydrocarbons.

Figure 1 shows the whole oil mass chromatograms obtained from analysis of the two samples. The distributions of n-alkanes in the condensates are very comparable, both showing a prominence of mid-molecular components (n-C_8 to n-C_{14}) and maxima at around n-C_{12}. Halladale-1 DW1 exL-128 does, however, contain a slightly higher relative abundance of high molecular n-alkanes (>n-C_{22}). Furthermore, Halladale-1 DW2 exL-332 shows some evidence of contamination, the high molecular weight ester, 2-ethylhexyldecanoate, being a prominent component in the whole oil chromatogram.

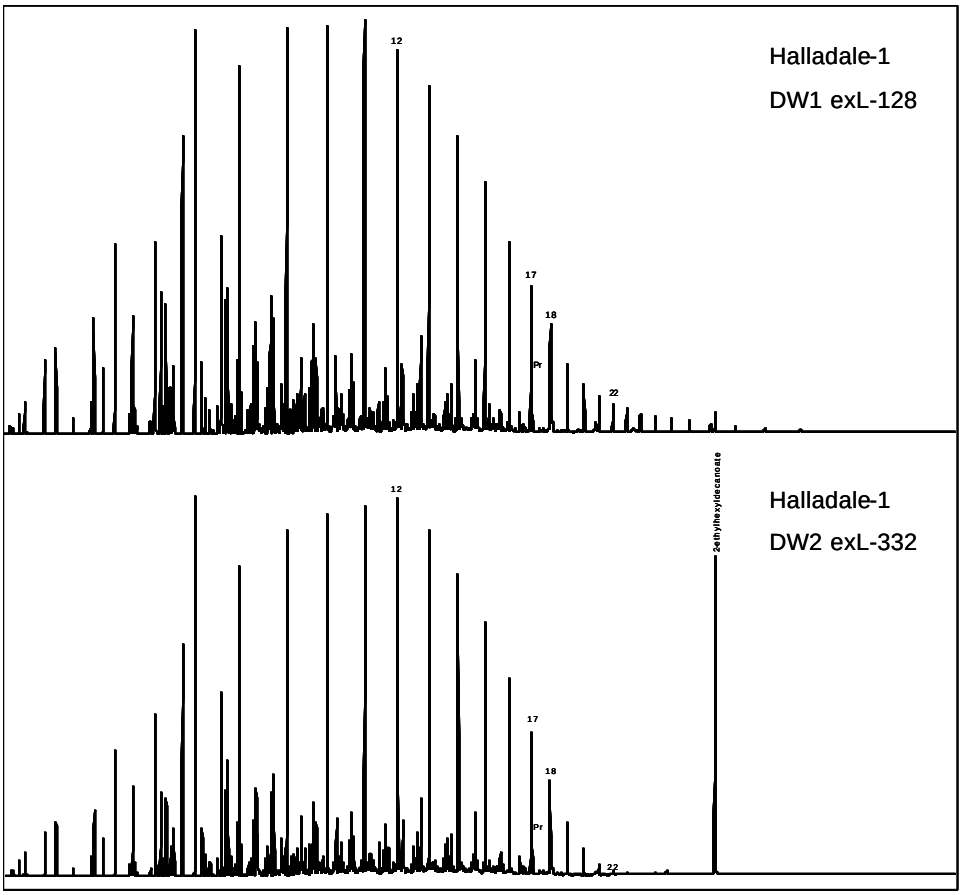

Figure 1. Whole oil GC-MS chromatograms of the Halladale-1 condensates

Gasoline range data obtained from the two Halladale-1 condensates have been used to construct the whole oil characterisation plot presented in Figure 2. Neither sample appears to have been altered by secondary processes, such as biodegradation and water washing, to any significant extent.

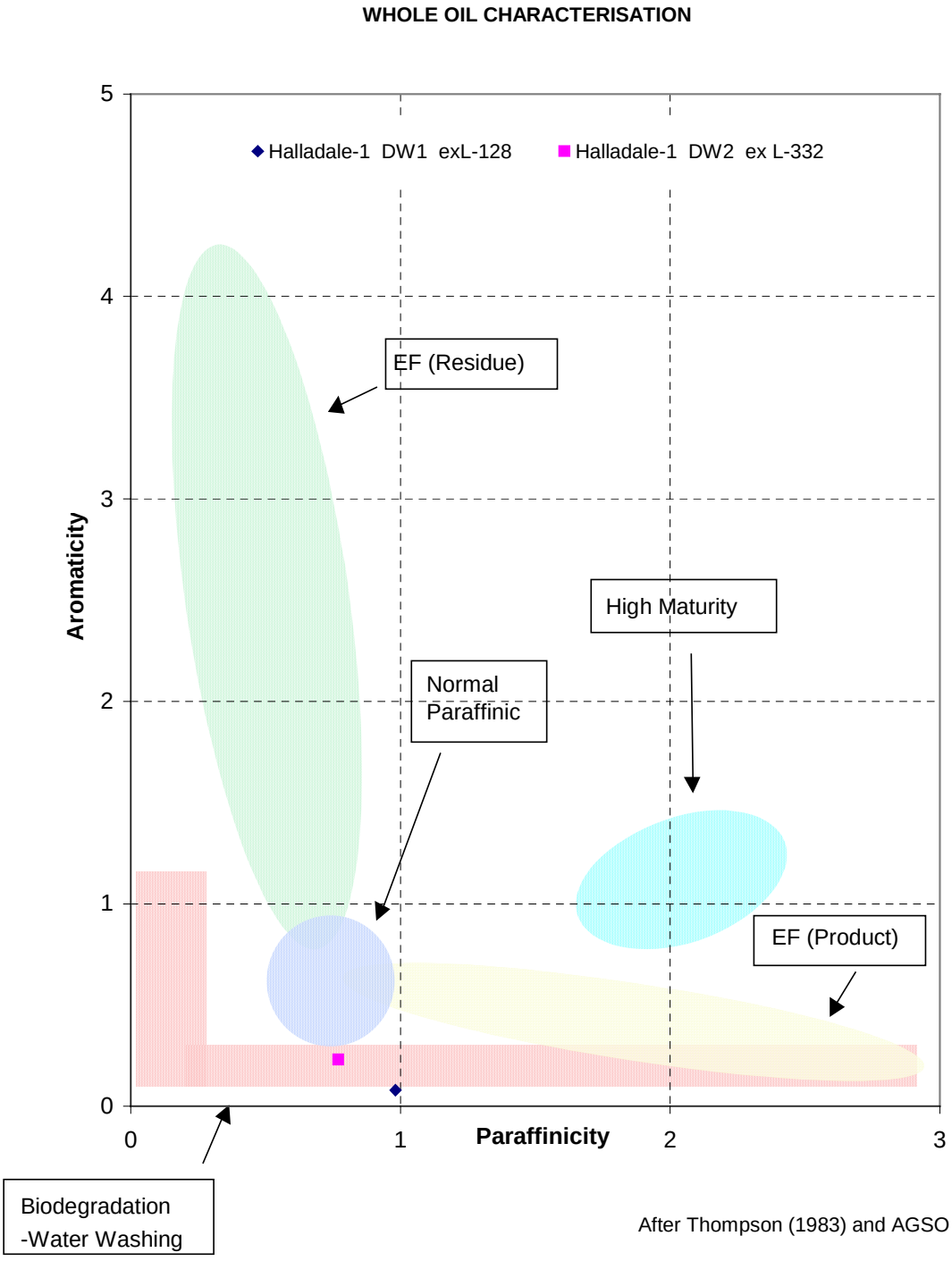

Key: Paraffinicity = n-heptane / methylcyclohexane
Aromaticity = toluene / n-heptane
EF = Evaporative Fractionation

Figure 2. Whole oil characterisation plot of the two Halladale-1 condensates

2.2 SATURATE GC-MS

The two Halladale-1 condensates were submitted for liquid chromatographic separation in order to isolate the saturate, aromatic and polar components as individual fractions. The saturate fractions were subsequently analysed by GC-MS and the resulting mass chromatograms are presented in Figure 3. The saturate fractions show a prominence of low molecular weight (n-C_9 – n-C_{14}) n-alkanes with components extending out to around n-C_{30} in the case of Halladale-1 DW-1. The Halldale-1 DW2 samples shows little to no components beyond n-C_{22}. Both condensates display n-alkane profiles indicative of high thermal maturity, the low pristane/n-C_{17} and phytane/n-C_{18} parameters values supporting this interpretation. The very low abundance of high molecular weight components also suggests the organic matter in both samples is derived primarily from marine sources.

Pristane to phytane ratios in the Halladale-1 condensates are very high (7.44 and 7.78 for DW1 and DW2, respectively) and are considered indicative of oxic conditions having prevailed during deposition of the associated source rocks. The overall composition of the two samples is very comparable, suggesting derivation from a common source facies.

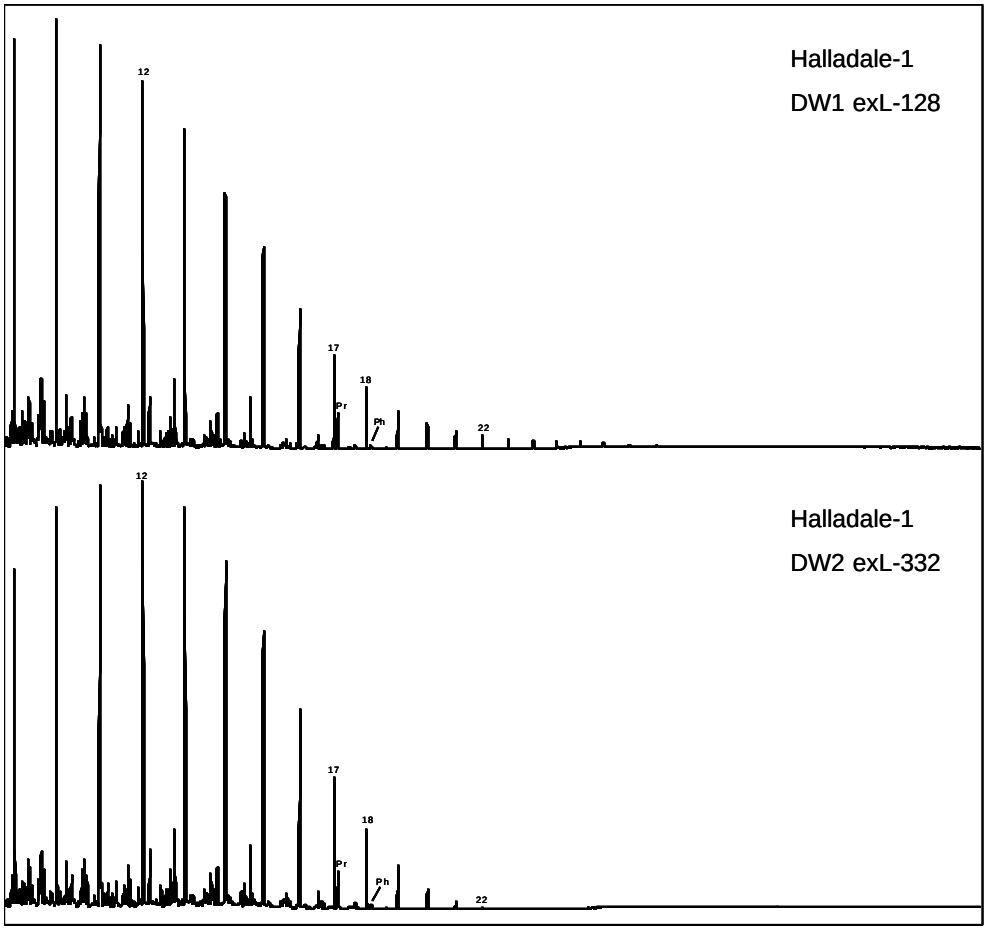

Figure 3. Saturate mass chromatograms from analysis of the Halladale-1 condensates

2.3 AROMATIC AND BRANCHED/CYCLIC GC-MS

The Halladale-1 condensates were subsequently submitted for detailed molecular characterisation in order to gain information not only regarding maturity, but also source and depositional environment.

Studies by van Aarssen et al. (2000) suggest that processes such as in-reservoir mixing of oils, significant biodegradation and mixing with organic matter indigenous to sediments along the migration pathway or to sediments within the reservoir, can be identified by plotting relative abundances of selected trimethylnaphthalenes, tetramethylnaphthalenes and pentamethylnaphthalenes. The relative abundances of these selected alkylnaphthalenes in the Halladale-1 condensates are shown in the ternary plot presented in Figure 4.

Crude oils from Moorari, Eaglehawk and Parrot Hill have also been plotted in the ternary diagram to illustrate how secondary processes can alter the distribution of naphthalenes in a sample. The Moorari crude oil is rich in 1,2,5-TMN which has decreased the value for the TMNr. The sample consequently plots away from the TMNr corner. It has been proposed that the Moorari oil has mixed with organic matter indigenous to sediments along the migration pathway or to sediments within the reservoir (van Aarssen et al., 1999). The Eaglehawk oil is an example of a biodegraded sample which has a low value for the TeMNr relative to PMNr. Such a distribution is typical of biodegraded oils since microbial alteration results in the selective degradation of 1,3,6,7-TeMN (van Aarssen et al., 1999). The distribution of naphthalenes in the Parrot Hill oil is believed to be indicative of in-reservoir mixing of two or more crude oils. The TMNr for this sample is consistent with a mature oil whilst values for both TeMNr and PMNr are consistent with low maturity, indicating the Parrot Hill oil to be a mixture of a condensate and a low maturity oil (van Aarssen et al., 1999).

The Halladale-1 condensates do not plot within the ‘maturity centre’ on the ternary plot in Figure 4, suggesting there has been some alteration of the samples’ compositions or mixing of organic matter from multiple sources. The two condensates contain high relative abundances of 1,2,5-trimethylnaphthalene which has resulted in low TMNr values. These data suggest the high maturity Halladale-1 condensates also contain a contribution of low maturity organic matter. Such mixing may have occurred along the migration pathway, whereby the Halladale-1 liquids have mixed with organic matter indigenous to sediments. A contribution of low maturity organic matter indigenous to sediments within the reservoir is also possible.

Further support for mixing of the Halladale-1 condensates with low maturity organic matter derives from evaluation of calculated aromatic maturity parameters. Figure 5 presents total ion chromatograms showing the distribution of aromatic components in the two samples. Both

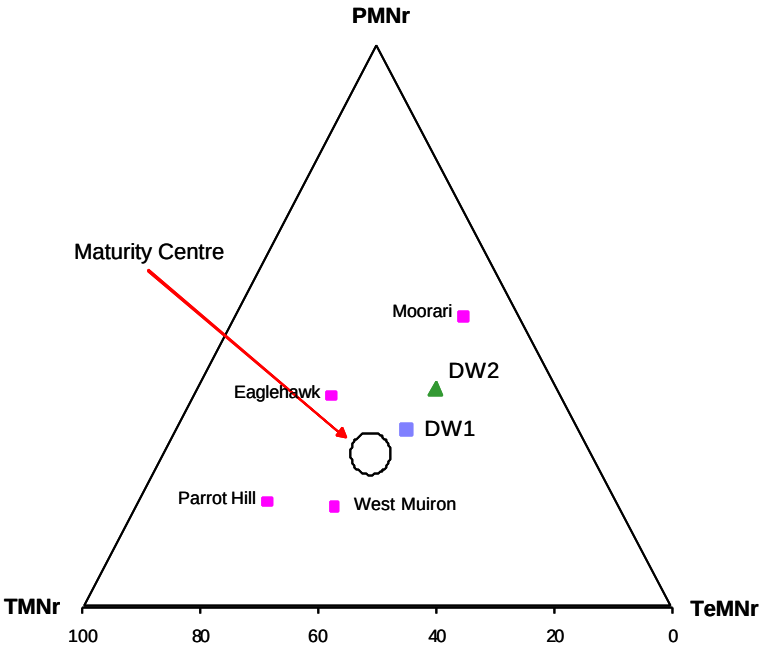

After van Aarssen et al., 2000

Figure 4. Ternary plot showing the distribution of naphthalenes in the Halladale-1 condensates

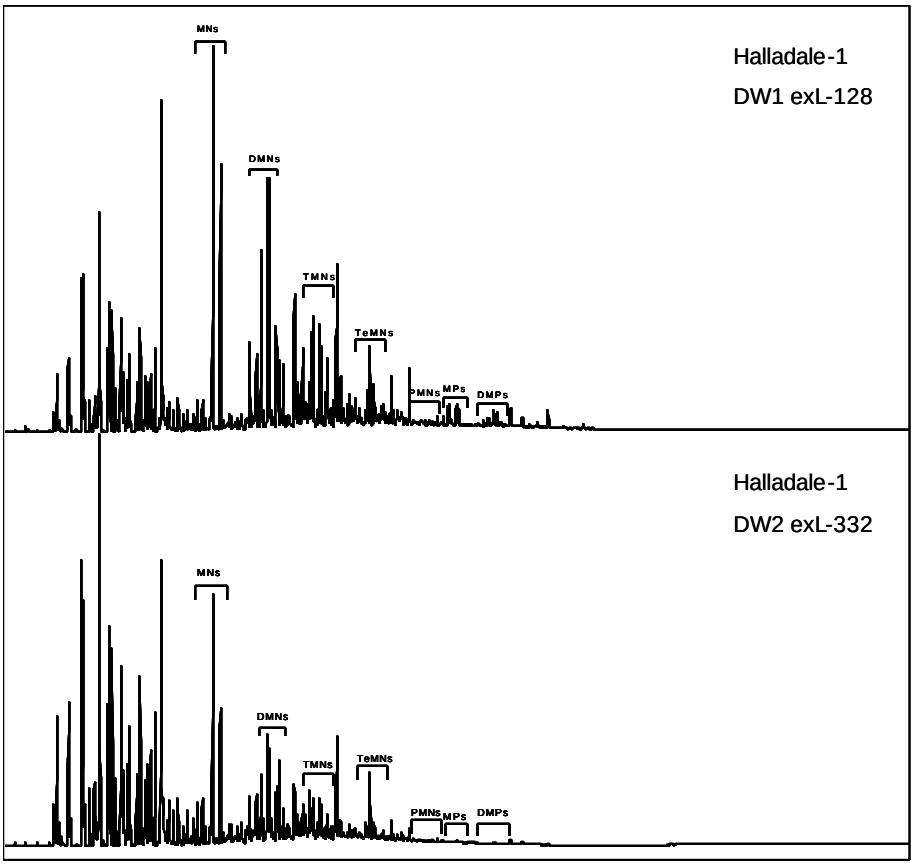

Figure 5. Total ion chromatograms showing the distribution of aromatic components in the Halladale-1 condensates

chromatograms are characterised by a high relative abundance of low molecular weight aromatic hydrocarbons, indicative of high thermal maturity. Methyl Phenanthrene Indices (MPI), however, are consistent with only low to moderate levels of thermal maturity. Values of 0.67 and 0.37 for Halladale-1 DW1 and DW2, respectively, are equivalent to vitrinite reflectance values of only 0.80% and 0.62%, respectively. The Halladale-1 DW2 condensate, which has produced the lower MPI value indicative of lower thermal maturity, also plots further away from the 'maturity centre' in the ternary plot in Figure 4. This suggests that migration contamination is more significant in the Halladale-1 DW2 sample.

Analysis of the m/z 217 mass chromatograms obtained from GC-MS analysis of the branched/cyclic fraction of the two Halladale-1 condensates (Figure 6) attests to derivation of organic matter largely from marine algal sources, although there is a contribution of terrestrial higher plant derived material. Although biomarker components are present in both samples in relatively low abundance, the samples show a high relative abundance of algal derived C27 steranes and diasteranes, resulting in C27/C29 sterane and diasterane ratios of

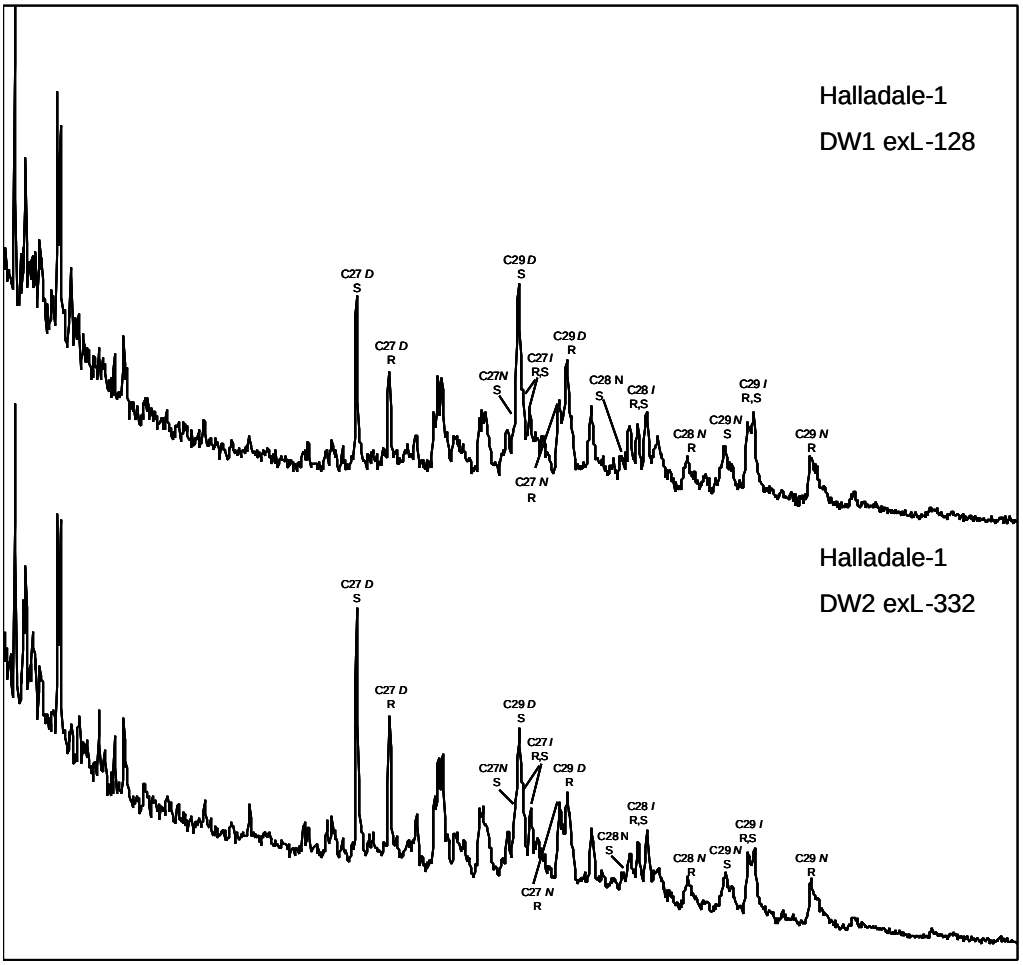

Figure 6. Partial m/z 217 mass chromatograms showing the distribution of steranes in the Halladale-1 condensates

1.40 and 0.63, respectively, for DW1 and 1.49 and 1.15, respectively, for DW2. Figure 7 shows a triplot of isosterane components which classifies the depositional environment of the associated source rocks as near shore marine, in an estuary or bay type setting. The abundance of marine derived organic matter with a concomitant contribution of terrigenous derived material is consistent with deposition in such a setting.

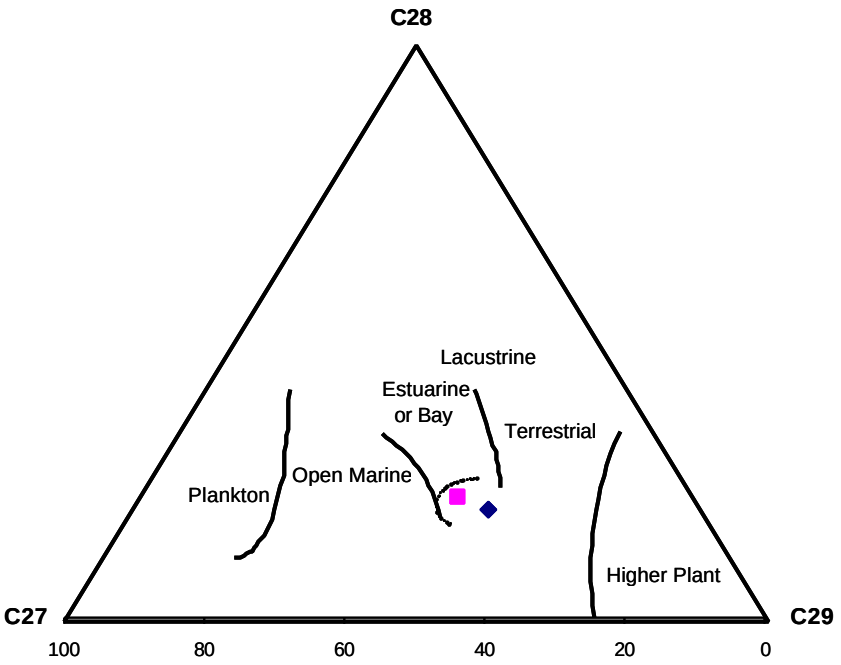

(After Huang and Meinschein, 1979)

Figure 7. Ternary plot showing the distribution of isosteranes in the Halladale-1 condensates

The higher plant biomarkers retene, cadalene and i-HMN-IV are all present in the aromatic fraction of the Halladale-1 condensates, together producing Higher Plant Indices (HPI) of 2.36 and 4.65 for DW1 and DW2, respectively. Since these components enter the geosphere through incorporation of plant detrital matter into sediments, the presence of these biomarkers is believed to be indicative of a contribution to the organic matter from terrigenous sources. The presence of diterpane components such as isopimaranes and beyerane, which are reported to derive from higher plant resin material, further supports a contribution of organic matter from land plant debris to both samples.

The good comparability between aromatic and biomarker profiles in the two Halladale-1 condensates attests to the samples being genetically related and indicates derivation of associated source rocks for both samples from the same, or very similar, source facies.

3 CONCLUSIONS

The two Halladale-1 condensates display n-alkane profiles indicative of high thermal maturity. Neither sample appears to have been altered through secondary processes, such as biodegradation and water washing. Pristane to phytane ratios in the Halladale-1 condensates are very high (7.44 and 7.78 for DW1 and DW2, respectively) and are considered indicative of oxic conditions during deposition of the associated source rocks.

The two condensates contain high relative abundances of 1,2,5-trimethylnaphthalene suggesting contamination from low maturity organic matter indigenous to sediments along the migration pathway or in the reservoir. The low Methyl Phenanthrene Indices (0.67 and 0.37 for DW1 and DW2, respectively) indicate low to moderate thermal maturity, which is inconsistent with saturate data, and further supports mixing of the organic matter within the condensates with low maturity organic matter from an additional source.

Biomarker data attest to derivation of organic matter in both samples largely from marine algal sources, although there is also a contribution of terrestrial higher plant derived material. Isosterane distributions classify the depositional environment of the associated source rocks as near shore marine, in an estuary or bay type setting. The abundance of marine derived organic matter with a concomitant contribution of terrigenous derived material is consistent with deposition in such a setting.

The overall composition of the two condensates is very comparable, indicating the samples to be genetically related and attesting to derivation from the same, or very similar, source facies.

4 REFERENCES

van Aarssen, B.G.K., Alexander, R. and Kagi, R.I. (2000) Reconstructing the geological history of Australian crude oils using aromatic hydrocarbons. *The APPEA Journal*, 283-292.

van Aarssen, B.G.K., Bastow, T.P., Alexander, R and Kagi, R.I., 1999 – Distributions of methylated naphthalenes in crude oils: indicators of maturity, biodegradation and mixing. Org. Geochem. **30**, 1213-1227.

Alexander, R., Kagi, R.I., Rowland, S.J., Sheppard, P.N. and Chirila, T.V. (1985) The effects of thermal maturity on distributions of dimethylnaphthalenes and trimethylnaphthalenes in some Ancient sediments and petroleums. *Geochimica et Cosmochimica Acta* **49**, 385-395.

Huang, W.-Y. and Meinschein, W.G. (1979) Sterols as ecological indicators. *Geochimica et Cosmochimica Acta* **43**, 739-745.

Peters, K.E. and Moldowan, J.M., 1993 –The Biomarker Guide - Interpreting molecular fossils in petroleum and ancient sediments. Prentice Hall, Englewood Cliffs, New Jersey 07632.

Radke, M. and Welte, D.H., 1983 – The methylphenanthrene index (MPI). A maturity parameter based on aromatic hydrocarbons. Advances in Org. Geochem., 1981. J. Wiley and Sons, New York, 504-512.

Thompson, K.F.M., 1983 – Classification and thermal history of petroleum based on light hydrocarbons. Geochim. Cosmochim. Acta. **47**, 303-316.

APPENDIX A

DATA AND TABLES

DATA AND TABLES

HALLADALE-1

TABLE OF CONTENTS

Analysis	Table	Figure
Whole Oil GC-MS	1	1
Liquid Chromatography/Saturate GC-MS	2,3	2
Aromatic GC-MS	4	3
Branched/Cyclic GC-MS	5	4

TABLE 1-1

ANALYSIS OF CRUDE OIL BY GC-MS

HALLADALE-1, DW1 exL-128, Condensate

Composition of C4 to C8 Fraction

Compound	*Rel.Wt%*	*Compound*	*Rel.Wt%*
isobutane (A)	0.5	1,1-dimethylcyclopentane (O)	0.9
n-butane (B)	0.9	2-methylhexane/2,3-dimethylpentane (P)	6.9
isopentane (C)	2.2	3-methylhexane (Q)	5.1
n-pentane (D)	2.5	1 cis-3-dimethylcyclopentane (R)	1.4
2,2-dimethylbutane (E)	0.4	1 trans-3-dimethylcyclopentane (S)	1.4
(cyclopentane		1 trans-2-dimethylcyclopentane (T)	2.1
2,3-dimethylbutane (F+G))	1.2	n-heptane (U)	15.2
2-methylpentane (H)	3.9	methylcyclohexane (V)	15.4
3-methylpentane (I)	1.8	1 cis-2-dimethylcyclopentane (W) +	-
n-hexane (J)	5.3	toluene (X)	1.2
methylcyclopentane (K)	3.4	n-octane (Y)	20.3
2,4-dimethylpentane (L)	1.0	ethylbenzene (Z)	0.3
benzene (M)	0.2	M+P-xylene (AA)	1.7
cyclohexane (N)	4.7	O-xylene (BB)	0.4

Calculated Data from the C4 to C8 Fraction

Paraffin Index I	2.4	I/M (Water washing)	7.2
Paraffin Index II	28.6	V/X (Water washing)	12.8
J/K (Maturity)	1.6	I/J (Biodegradation)	0.3
		V/U (Biodegradation)	1.0

- = Below detection limit or not determined
26/02/2007

Paraffin Index I = (P+Q)/(R+S+T)
Paraffin Index II = %U in N to V

FIGURE 1A-1

Sample : **HALLADALE-1, DW1, exL-128, Condensate**
File ID : 351701W

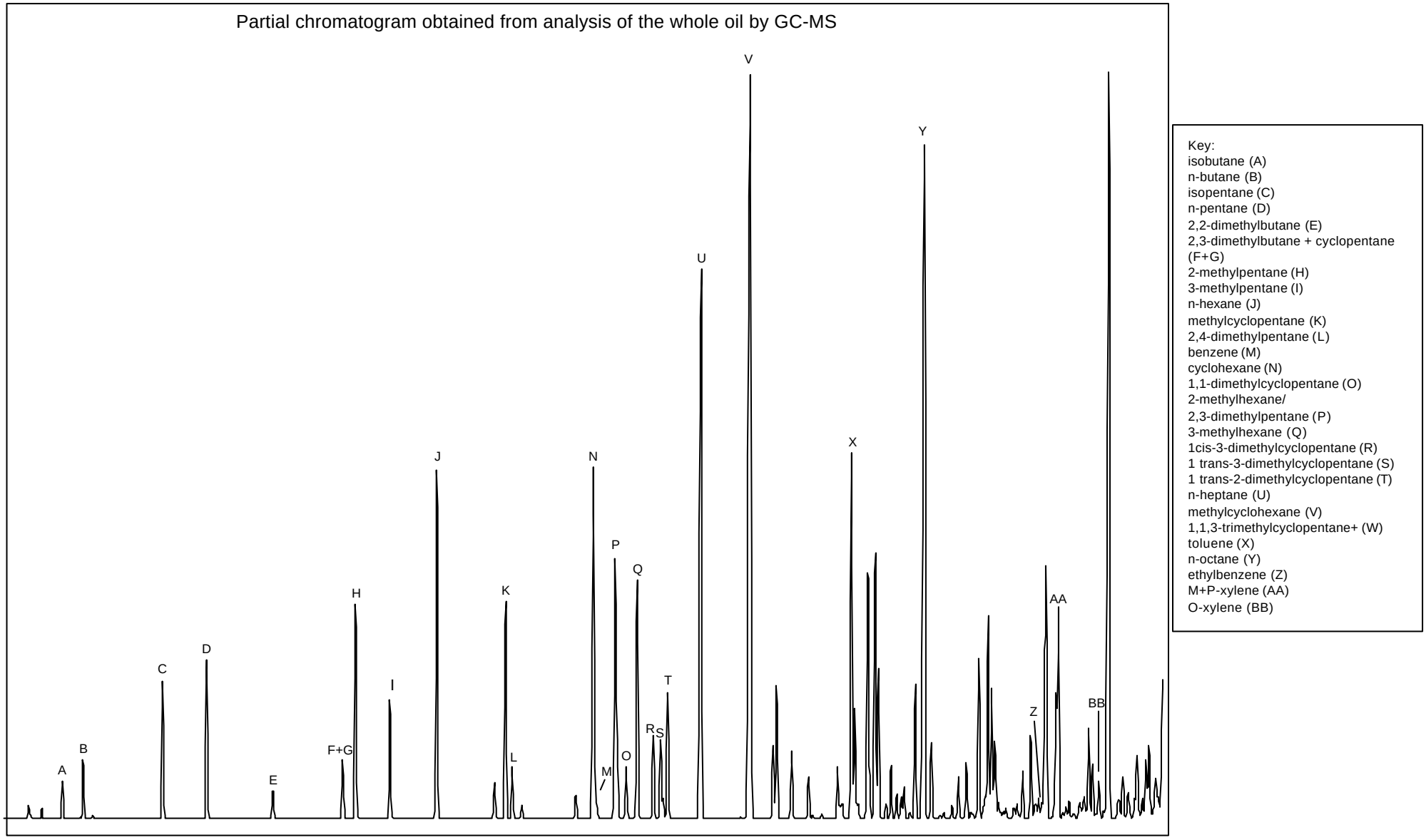

GEOTECHNICAL SERVICES PTY LTD

FIGURE 1B-1

Sample : **HALLADALE-1, DW1, exL-128, Condensate**
File ID : 351701W

GEOTECH

Chromatogram obtained from analysis of the whole oil by GC-MS

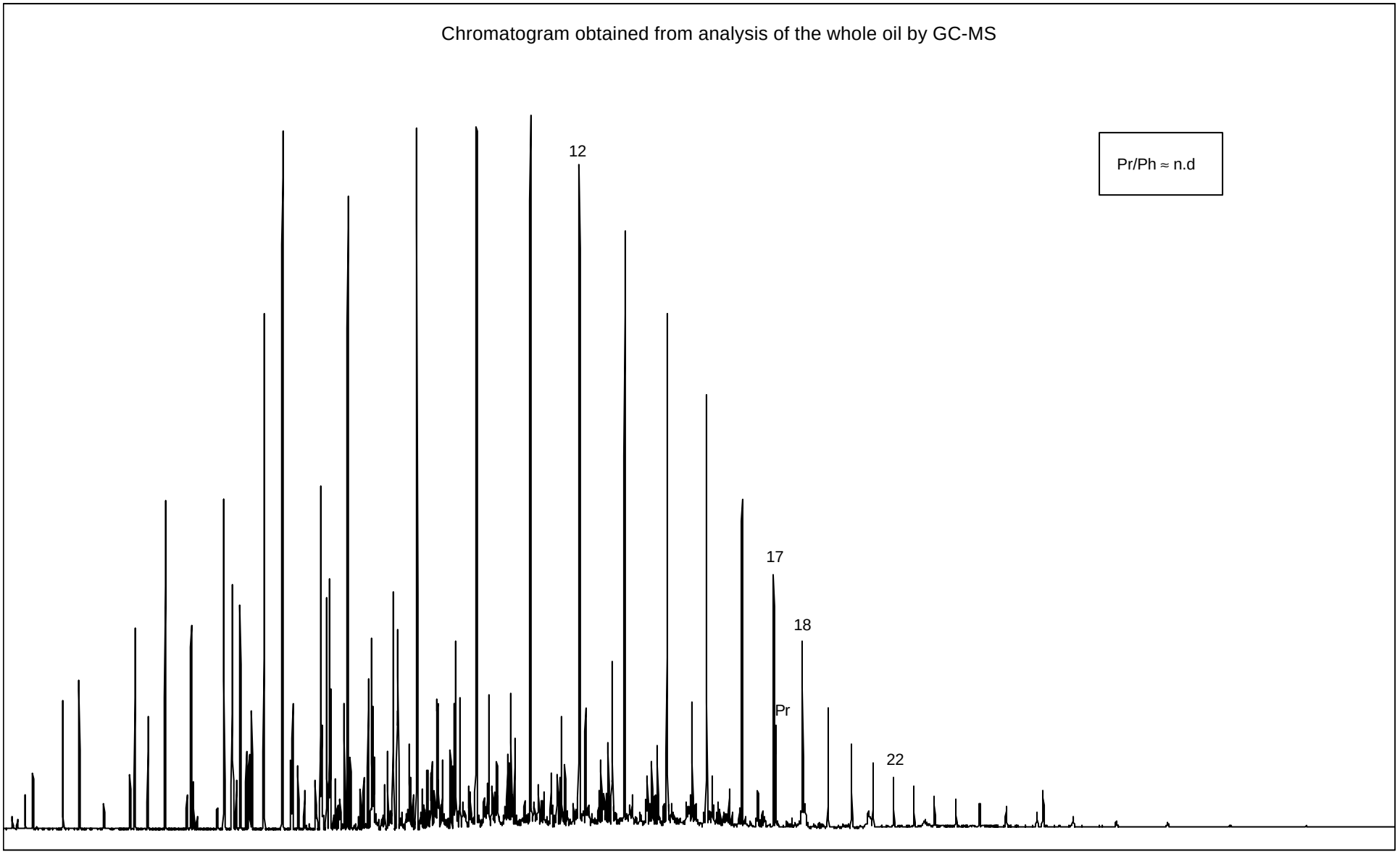

TABLE 1-2

ANALYSIS OF CRUDE OIL BY GC-MS

HALLADALE-1, DW2 exL-332, Condensate

Composition of C4 to C8 Fraction

Compound	*Rel.Wt%*	*Compound*	*Rel.Wt%*
isobutane (A)	0.5	1,1-dimethylcyclopentane (O)	0.8
n-butane (B)	0.8	2-methylhexane/2,3-dimethylpentane (P)	5.3
isopentane (C)	1.6	3-methylhexane (Q)	4.1
n-pentane (D)	2.1	1 cis-3-dimethylcyclopentane (R)	1.3
2,2-dimethylbutane (E)	0.3	1 trans-3-dimethylcyclopentane (S)	1.3
(cyclopentane		1 trans-2-dimethylcyclopentane (T)	2.0
2,3-dimethylbutane (F+G))	1.0	n-heptane (U)	13.8
2-methylpentane (H)	3.0	methylcyclohexane (V)	17.9
3-methylpentane (I)	1.4	1 cis-2-dimethylcyclopentane (W) +	-
n-hexane (J)	4.4	toluene (X)	3.2
methylcyclopentane (K)	3.5	n-octane (Y)	19.1
2,4-dimethylpentane (L)	0.7	ethylbenzene (Z)	0.7
benzene (M)	0.6	M+P-xylene (AA)	4.4
cyclohexane (N)	5.4	O-xylene (BB)	0.8

Calculated Data from the C4 to C8 Fraction

Paraffin Index I	2.0	I/M (Water washing)	2.5
Paraffin Index II	26.6	V/X (Water washing)	5.6
J/K (Maturity)	1.3	I/J (Biodegradation)	0.3
		V/U (Biodegradation)	1.3

- = Below detection limit or not determined
26/02/2007

Paraffin Index I = (P+Q)/(R+S+T)
Paraffin Index II = %U in N to V

FIGURE 1A-2

Sample : **HALLADALE-1, DW2, exL-332, Condensate**
File ID : 351702W

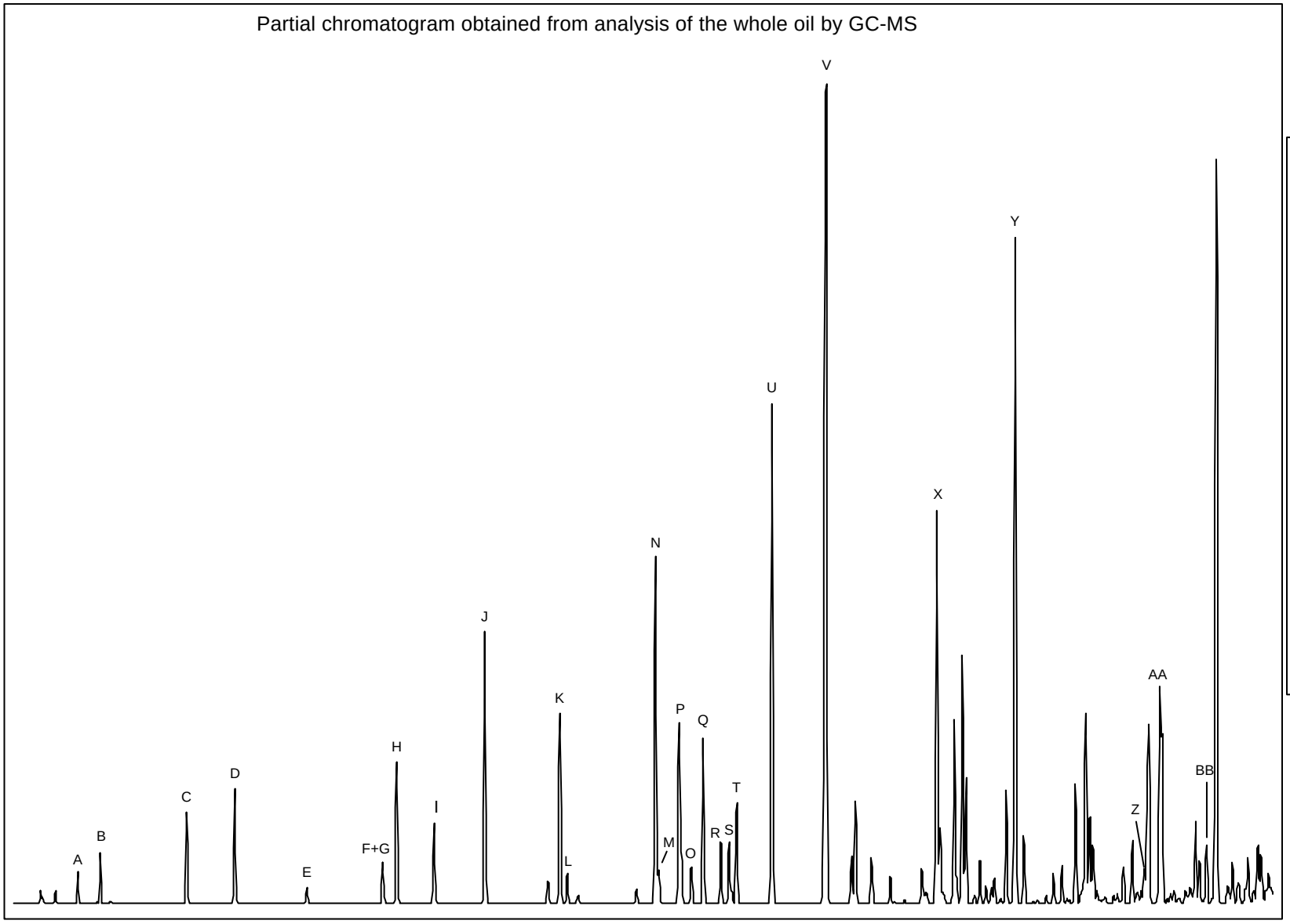

Key:
isobutane (A)
n-butane (B)
isopentane (C)
n-pentane (D)
2,2-dimethylbutane (E)
2,3-dimethylbutane + cyclopentane (F+G)
2-methylpentane (H)
3-methylpentane (I)
n-hexane (J)
methylcyclopentane (K)
2,4-dimethylpentane (L)
benzene (M)
cyclohexane (N)
1,1-dimethylcyclopentane (O)
2-methylhexane/
2,3-dimethylpentane (P)
3-methylhexane (Q)
1cis-3-dimethylcyclopentane (R)
1 trans-3-dimethylcyclopentane (S)
1 trans-2-dimethylcyclopentane (T)
n-heptane (U)
methylcyclohexane (V)
1,1,3-trimethylcyclopentane+ (W)
toluene (X)
n-octane (Y)
ethylbenzene (Z)
M+P-xylene (AA)
O-xylene (BB)

FIGURE 1B-2

Sample : **HALLADALE-1, DW2, exL-332, Condensate**
File ID : 351702W

GEOTECH

Chromatogram obtained from analysis of the whole oil by GC-MS

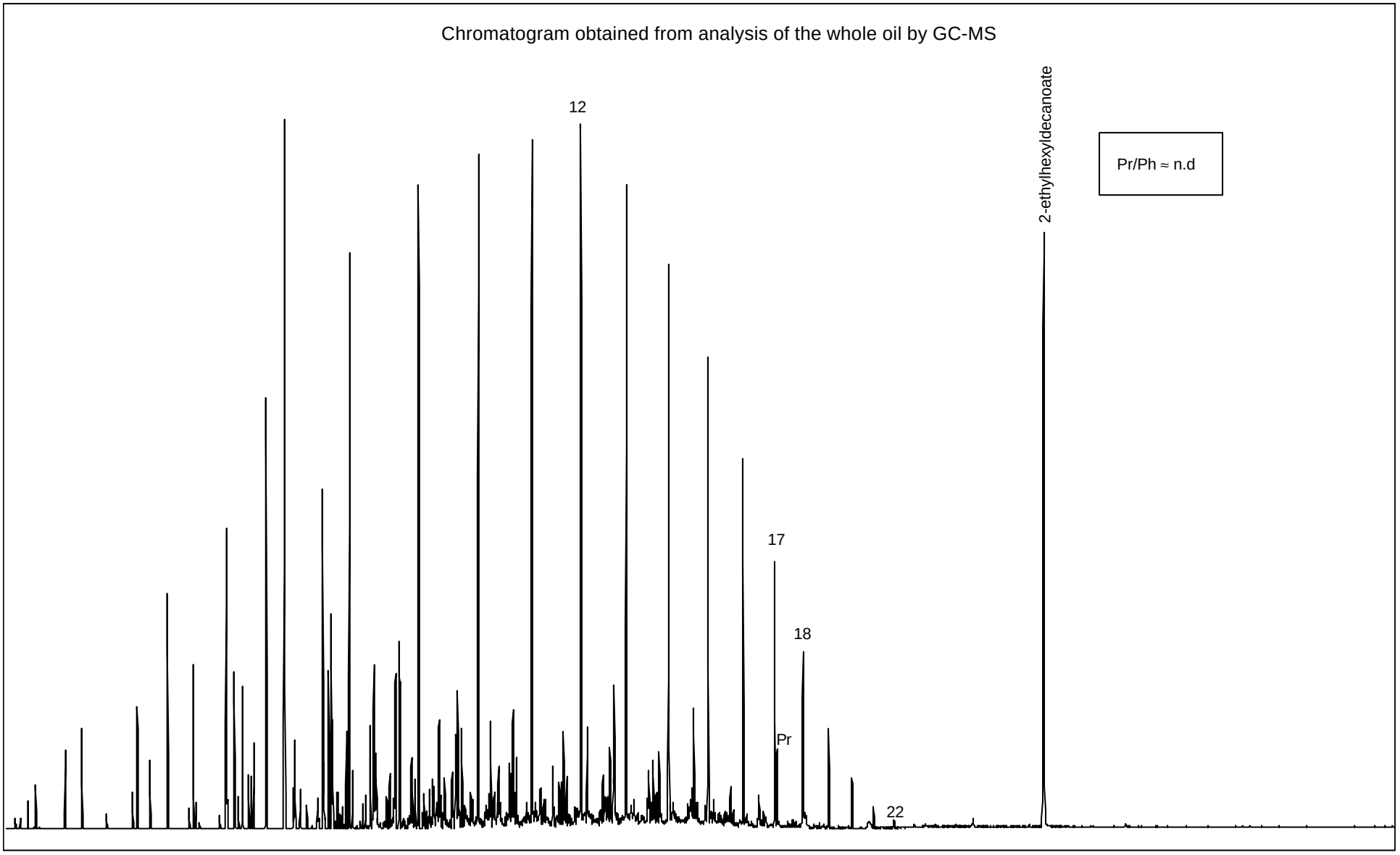

TABLE 2

LIQUID CHROMATOGRAPHY DATA

OIL

HALLADALE-1

Yields (%) and Selected Ratios

		------Hydrocarbons------			------Non-hydrocarbons------			Sats / Aros	Asph. / NSO	HC / Non HC
SAMPLE	Sample Type	Sats	Aros	HC's	NSOs	Asph.	Non HC's			
DW-1, exL-128	Condensate	93.2	3.1	96.3	3.7	nd	3.7	29.9	nd	25.8
DW-2, exL-332	Condensate	90.1	3.8	93.8	6.2	nd	6.2	23.8	nd	15.2

26/02/2007

nd = no data

TABLE 3

ANALYSIS OF SATURATED HYDROCARBONS BY GC-MS

OIL

HALLADALE-1

A. Selected Ratios

SAMPLE	Sample Type	Prist./Phyt.	Prist./n-C17	Phyt./n-C18	CPI(1)	CPI(2)	(C21+C22)/(C28+C29)
DW-1, exL-128	Condensate	7.44	0.45	0.09	nd	1.02	4.31
DW-2, exL-332	Condensate	7.78	0.33	0.07	nd	nd	nd

HALLADALE-1

B. n-Alkane Distributions

SAMPLE	nC12	nC13	nC14	nC15	nC16	nC17	Pr	nC18	Ph	nC19	nC20	nC21	nC22	nC23	nC24	nC25	nC26	nC27	nC28	nC29	nC30	nC31
DW-1, exL-128	23.9	19.7	15.5	11.6	8.3	5.6	2.5	3.6	0.3	2.4	1.5	1.1	0.9	0.7	0.6	0.5	0.4	0.4	0.3	0.2	nd	nd
DW-2, exL-332	23.2	20.4	17.1	13.3	9.5	6.3	2.1	3.9	0.3	2.2	1.0	0.4	0.1	0.1	nd	nd	nd	nd	nd	nd	nd	nd

CPI(1)= $\frac{(C23+C25+C27+C29)+(C25+C27+C29+C31)}{2x(C24+C26+C28+C30)}$

CPI(2)=$\frac{(C23+C25+C27)+(C25+C27+C29)}{2x(C24+C26+C28)}$

26/02/2007

nd = no data

FIGURE 2-1

Sample : **HALLADALE-1, DW-1, exL-128, Condensate**
File ID : 351701SB

Chromatogram obtained from the analysis of saturated hydrocarbons by GC-MS

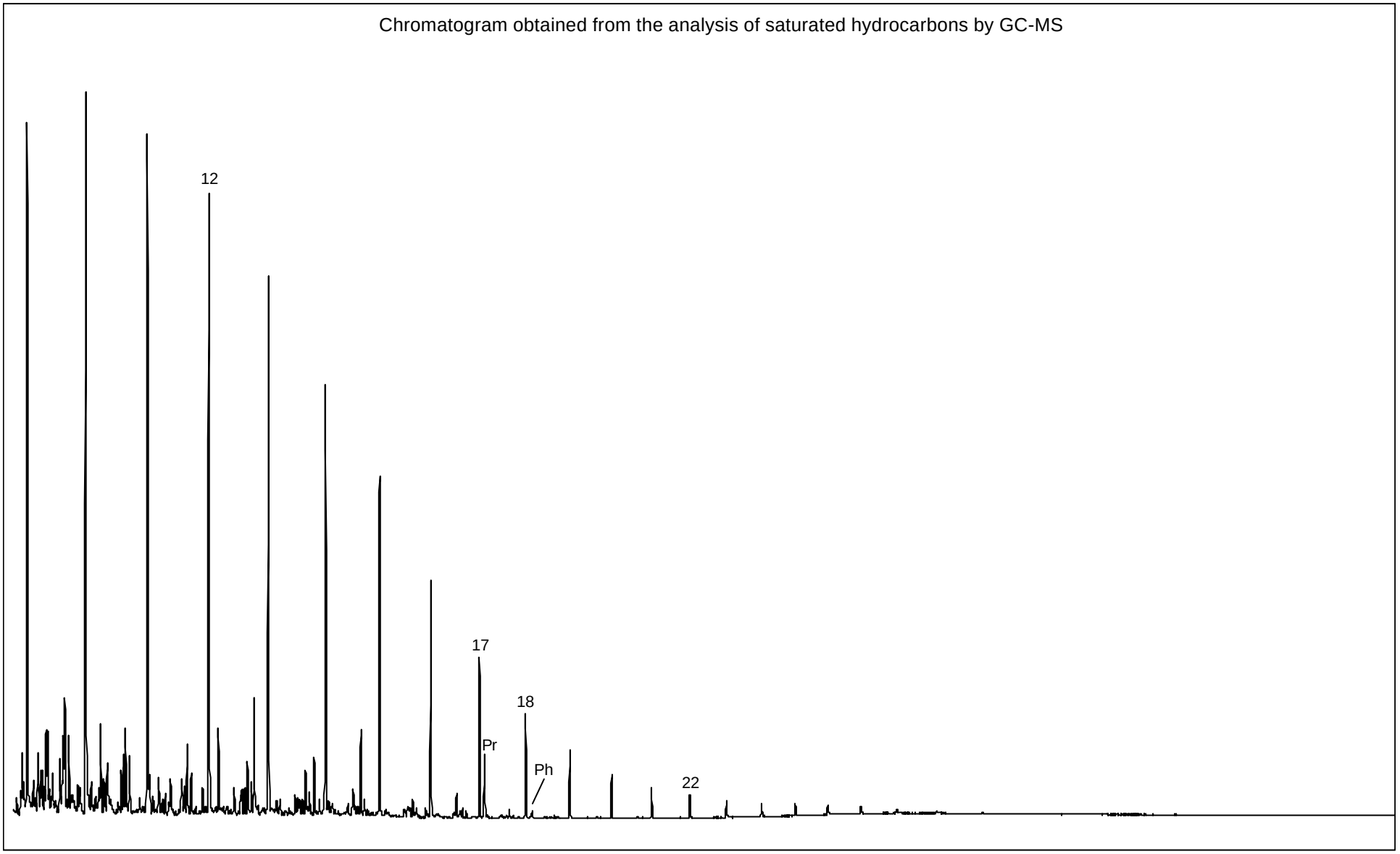

FIGURE 2-2

Sample : **HALLADALE-1, DW-2, exL-332, Condensate**
File ID : 351702SB

GEOTECH

Chromatogram obtained from the analysis of saturated hydrocarbons by GC-MS

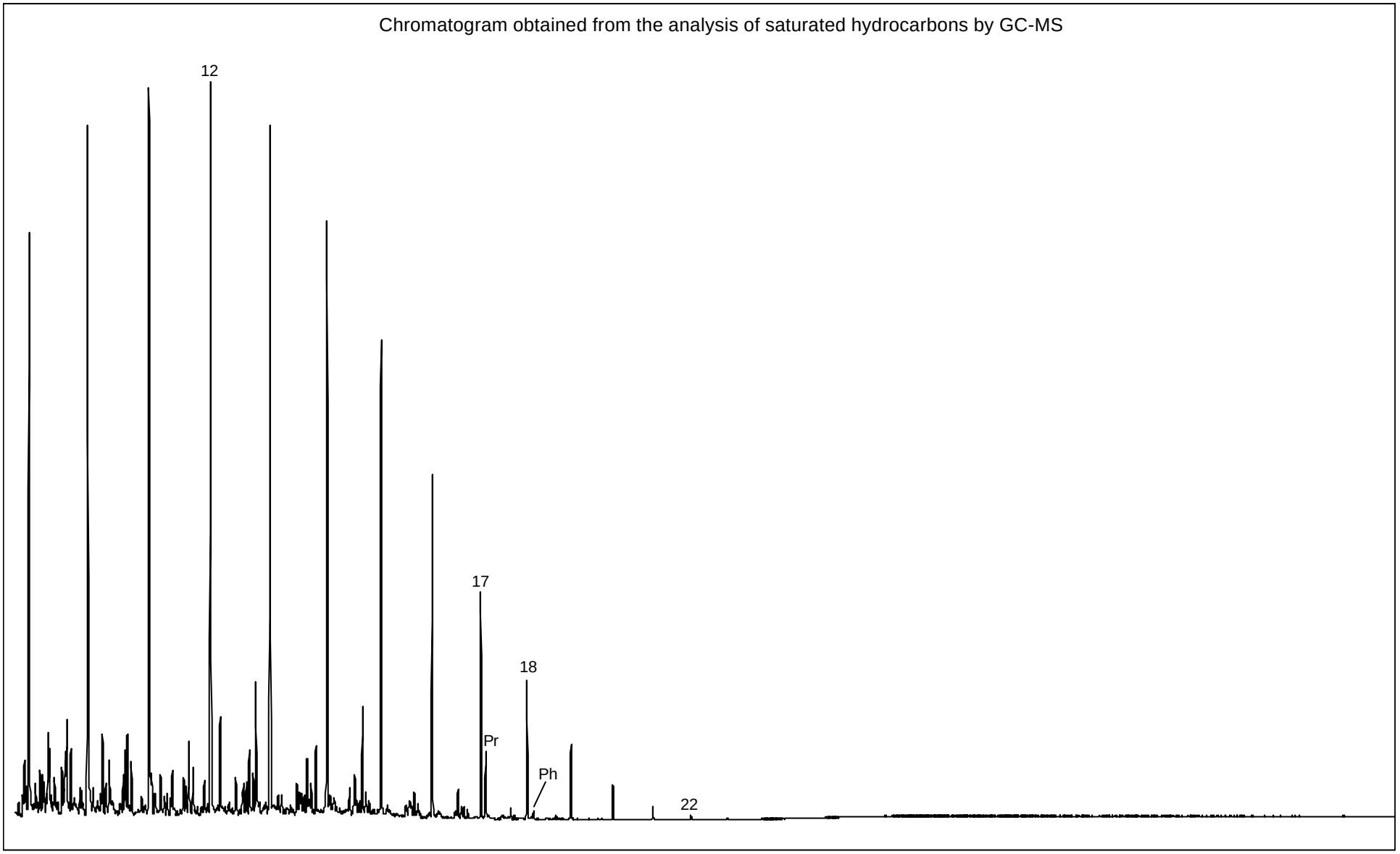

TABLE 4

ANALYSIS OF AROMATIC HYDROCARBONS BY GC-MS

HALLADALE-1

SAMPLE	TYPE	DNR-1	DNR-5	DNR-6	TNR-1	TNR-5	TNR-6	MPR-1	MPI-1	MPI-2	Rc(a)	Rc(b)
DW1-ex L-128	Condensate	5.41	nd	2.52	0.72	1.41	0.39	2.25	0.67	0.72	0.80	1.90
DW2-ex L-332	Condensate	4.20	nd	1.97	0.49	2.76	0.31	2.21	0.37	0.38	0.62	2.08

response factors have not been applied to these ratios

HALLADALE-1

SAMPLE	TYPE	1,7-DMP/X (m/z 206)	RETENE/9-MP (m/z 219,192)	1MP/9MP	HPI
DW1-ex L-128	Condensate	0.58	0.41	0.84	2.36
DW2-ex L-332	Condensate	0.57	0.27	0.73	4.65

HPI = Higher Plant Index (i.e (retene + cadalene + iHMN-IV)/1,3,6,7-TeMN))

FIGURE 3A-1

Sample: **HALLADALE-1, DW1, ex L-128, Condensate**

File ID: 351701A

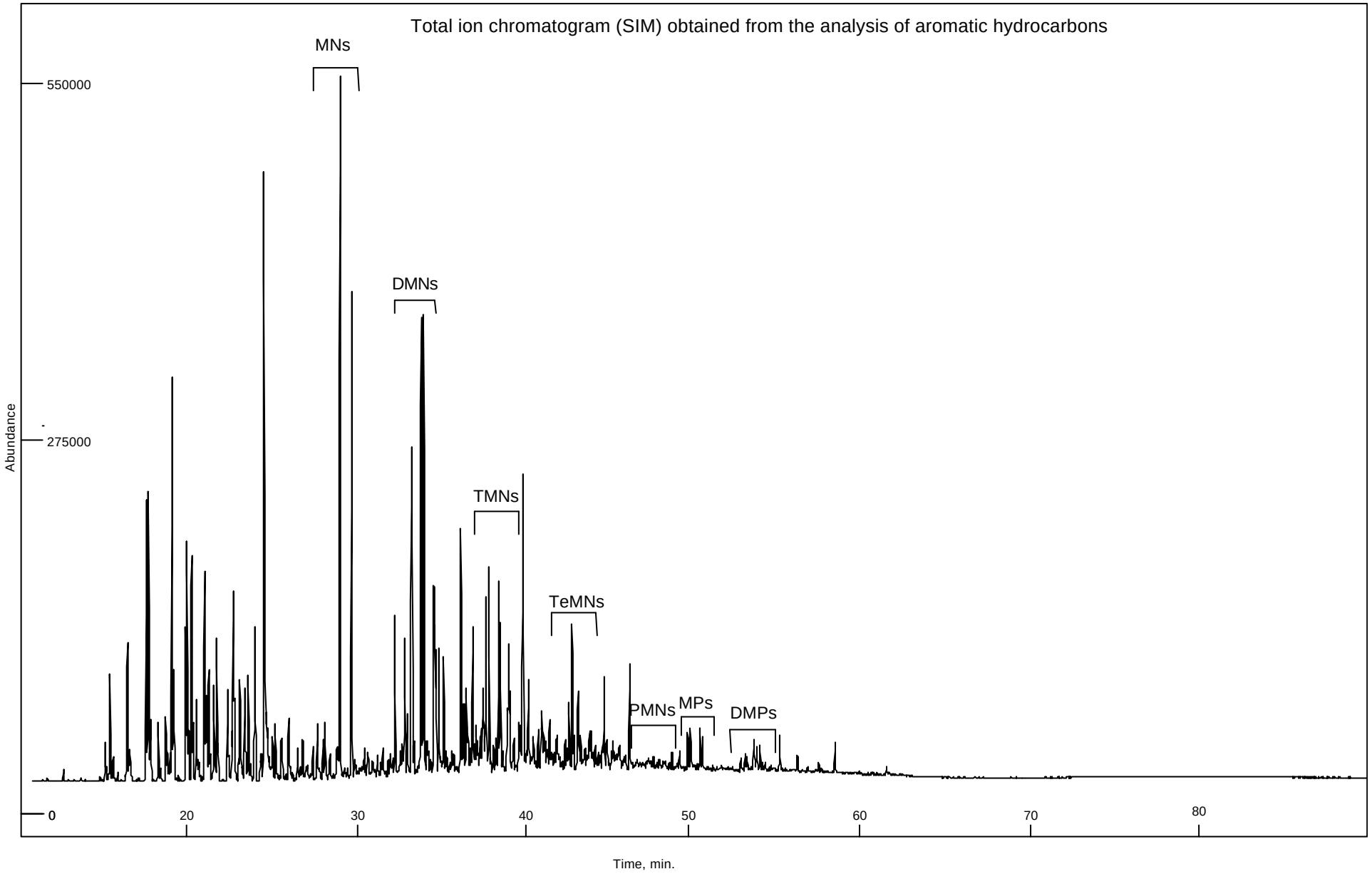

FIGURE 3B-1

Sample: **HALLADALE-1, DW1, ex L-128, Condensate**

File ID: 351701A

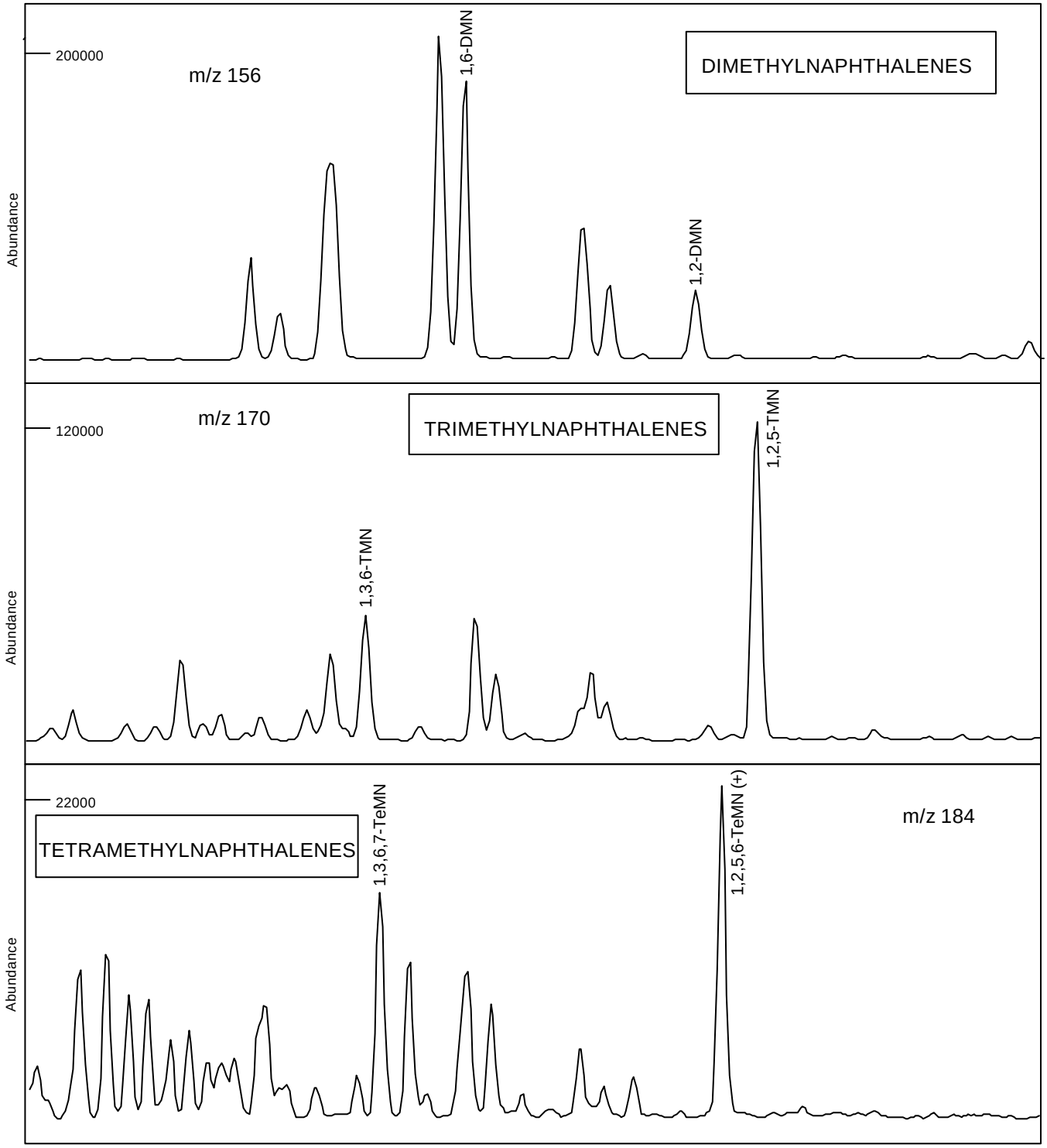

FIGURE 3C-1

Sample: **HALLADALE-1, DW1, ex L-128, Condensate**

File ID: 351701A

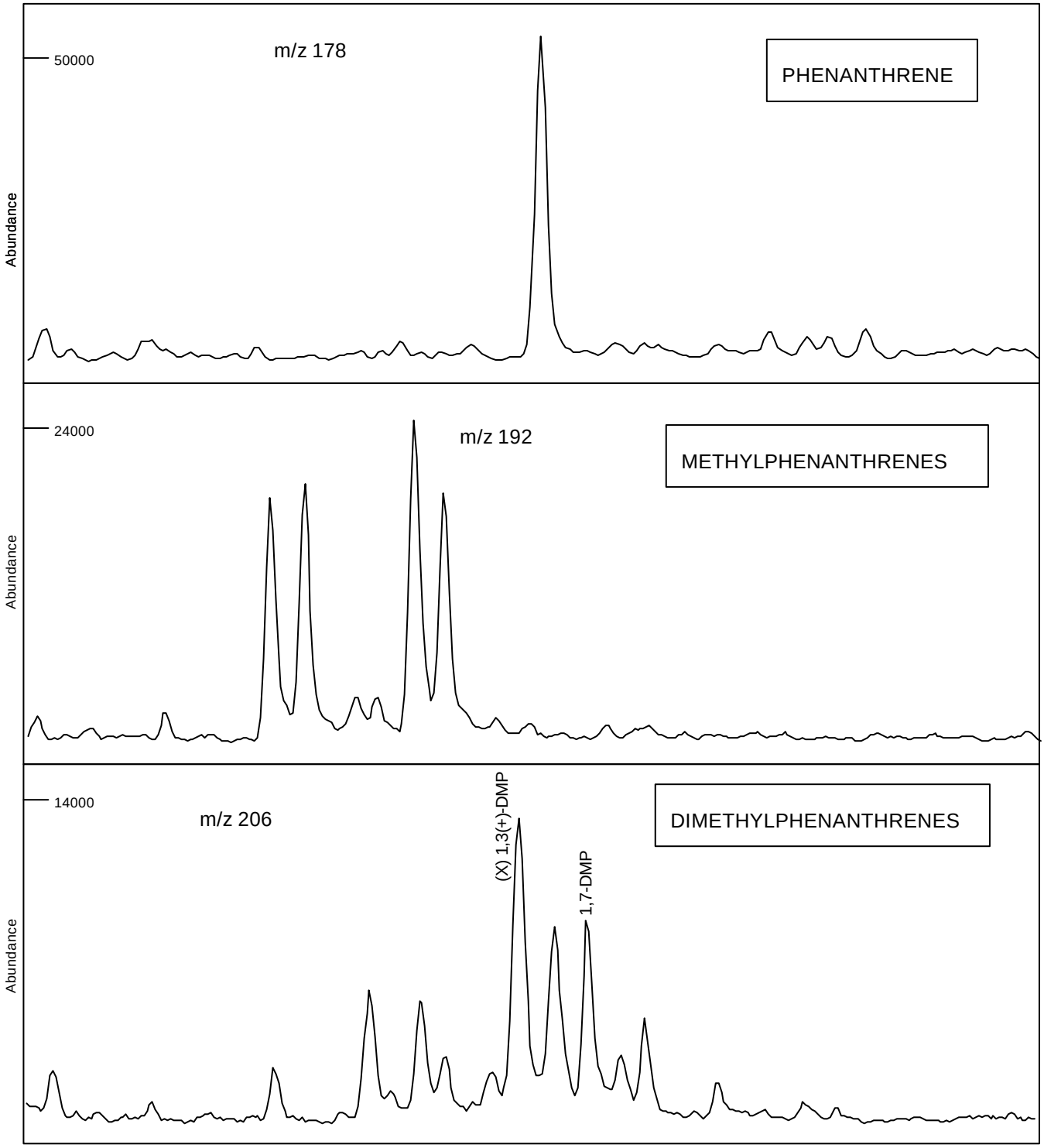

FIGURE 3D-1

Sample: **HALLADALE-1, DW1, ex L-128, Condensate**

File ID: 351701A

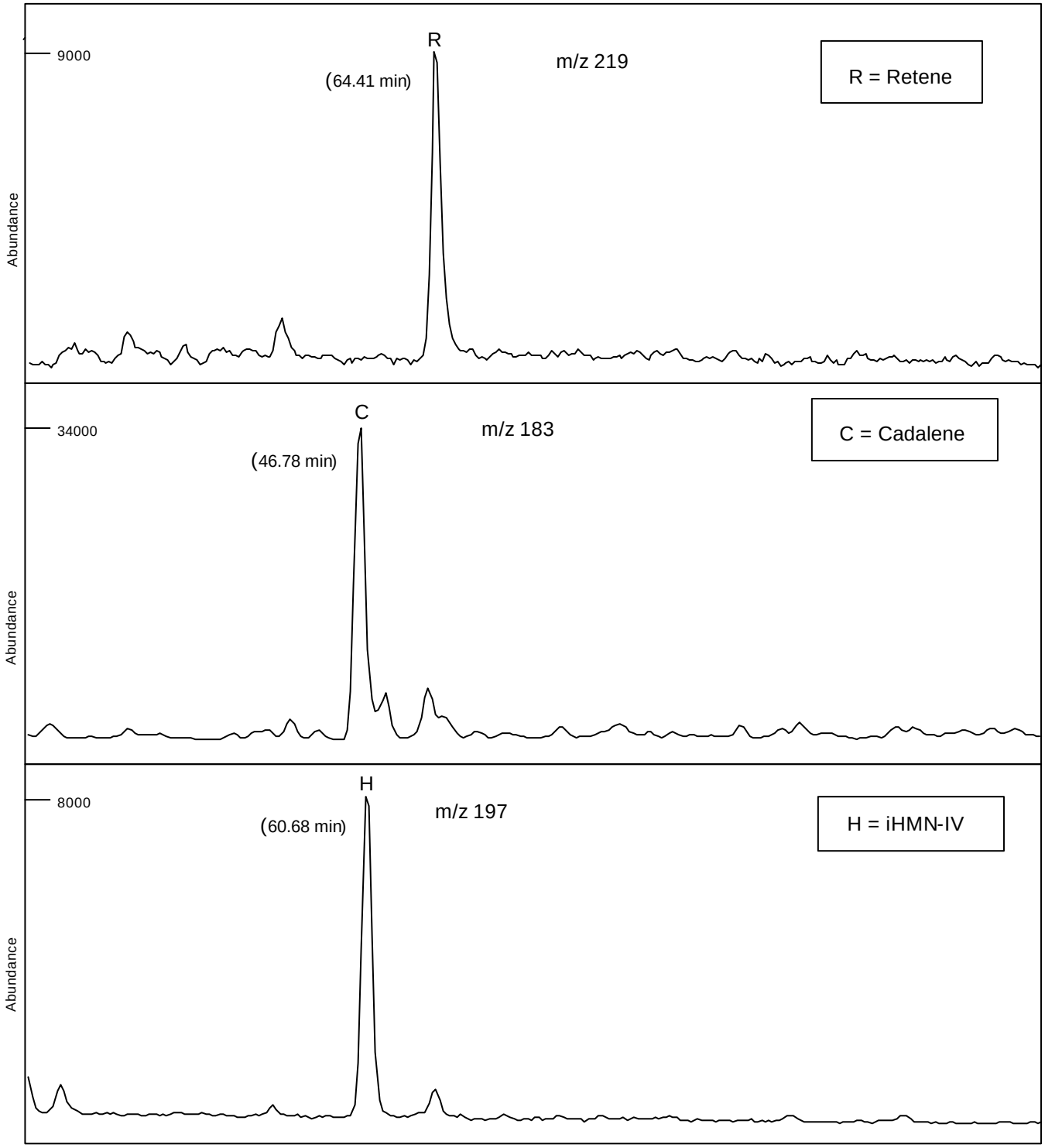

FIGURE 3E-1

Sample: **HALLADALE-1, DW1, ex L-128, Condensate**

File ID: 351701A

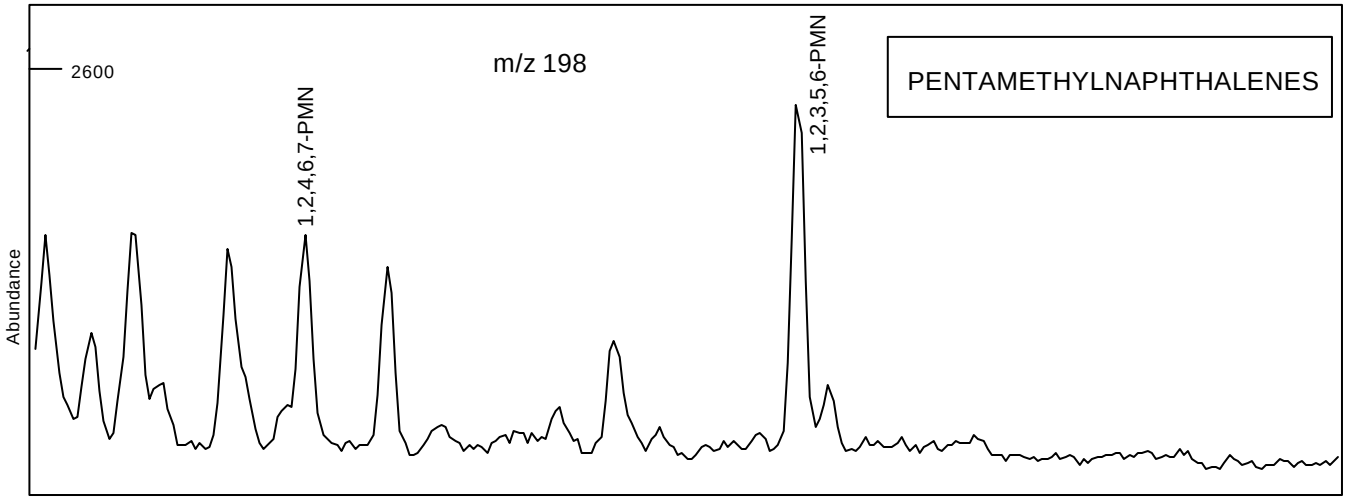

FIGURE 3A-2

Sample: **HALLADALE-1, DW2, ex L-332, Condensate**

File ID: 351702A

GEOTECH

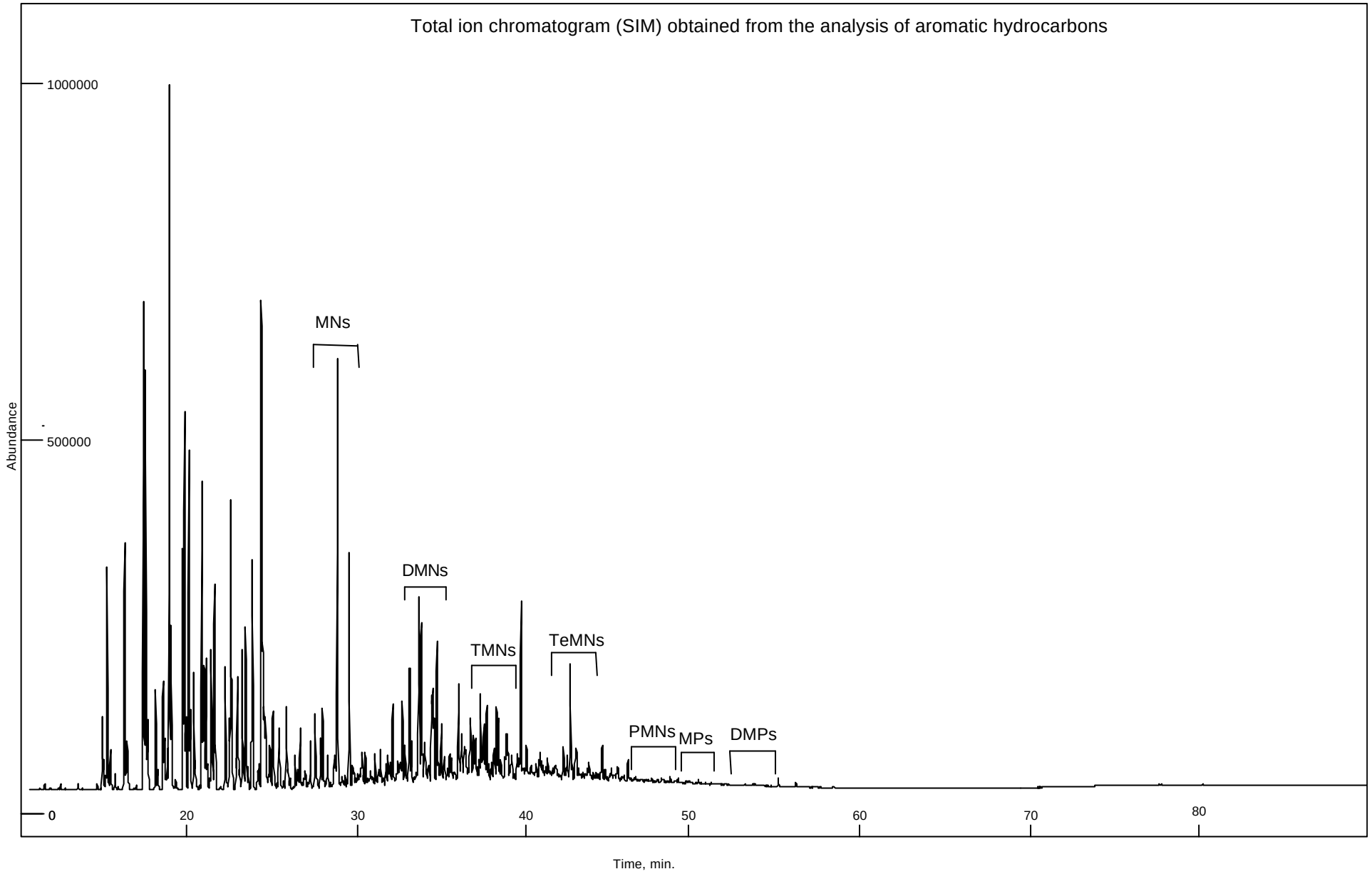

FIGURE 3B-2

Sample: **HALLADALE-1, DW2, ex L-332, Condensate**

File ID: 351702A

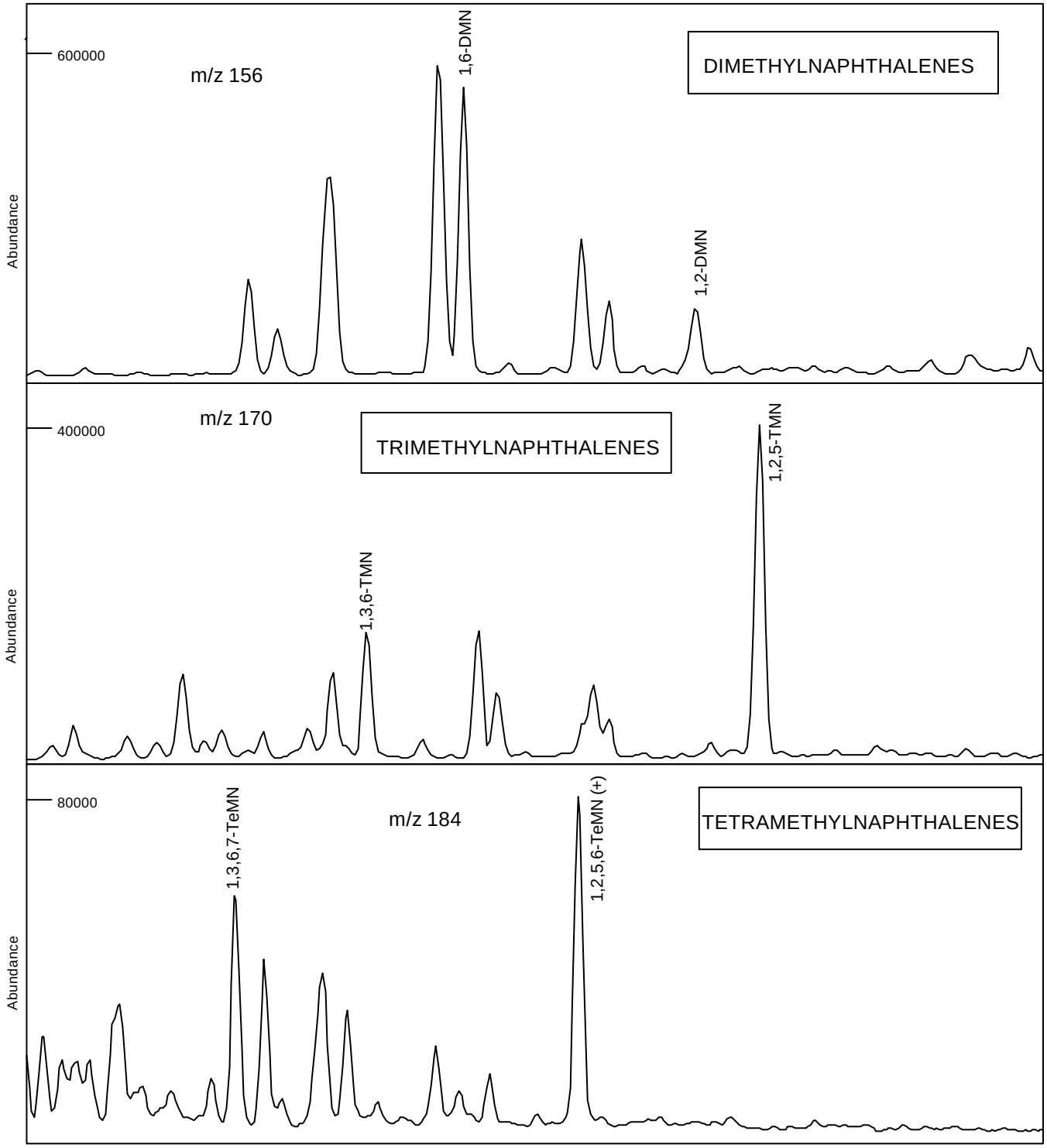

FIGURE 3C-2

Sample: **HALLADALE-1, DW2, ex L-332, Condensate**

File ID: 351702A

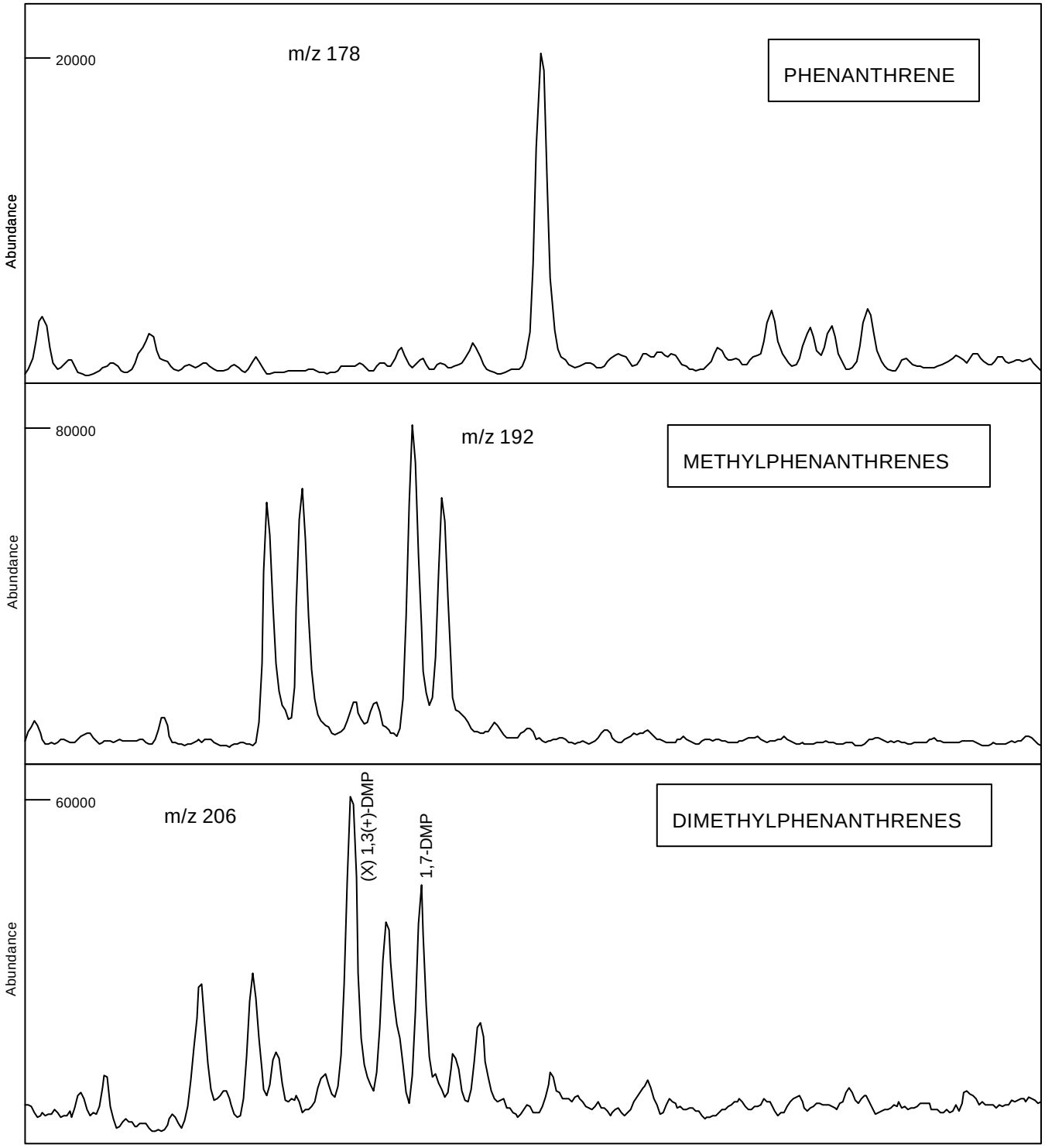

FIGURE 3D-2

Sample: **HALLADALE-1, DW2, ex L-332, Condensate**

File ID: 351702A

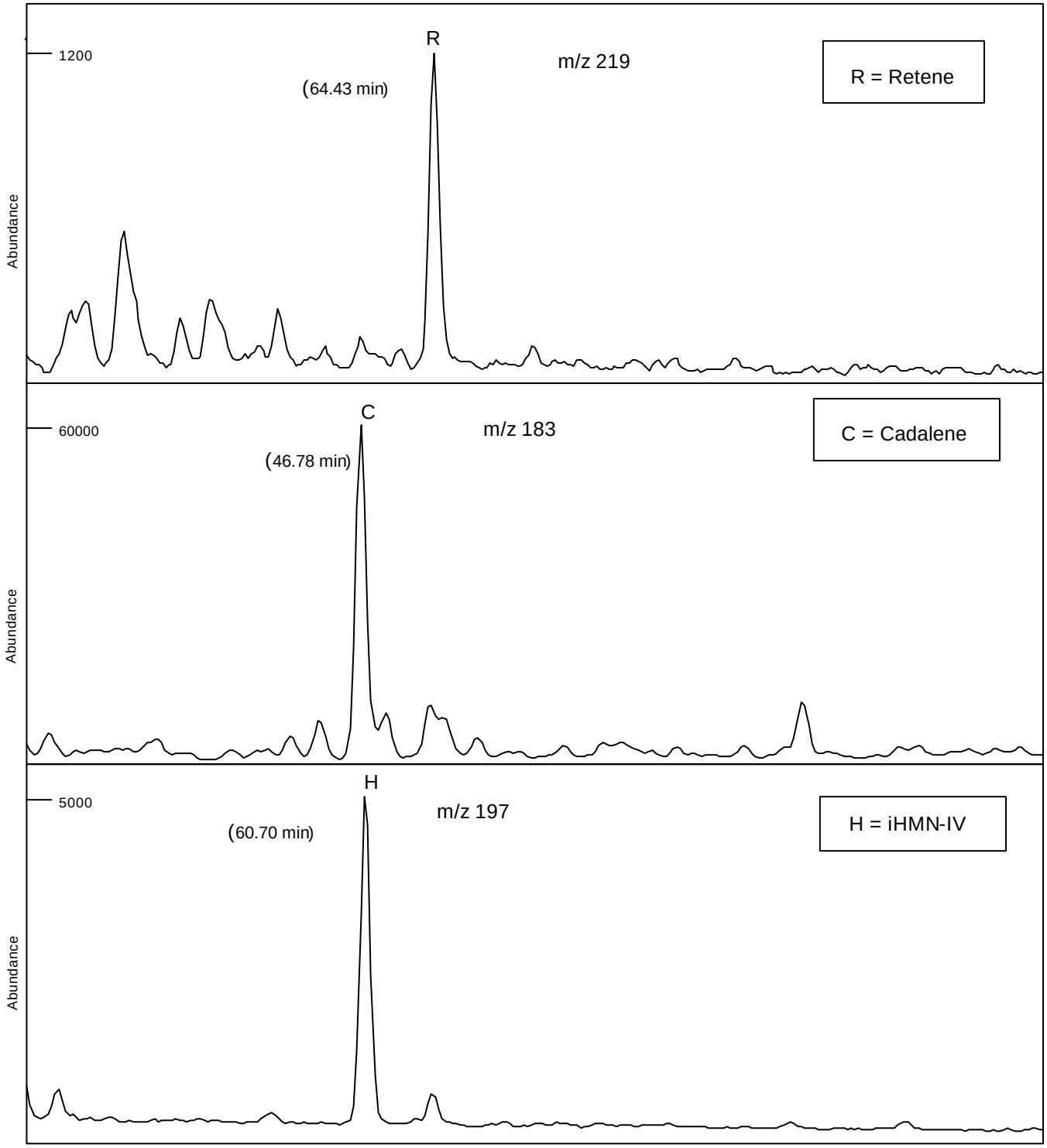

FIGURE 3E-2

Sample: **HALLADALE-1, DW2, ex L-332, Condensate**

File ID: 351702A

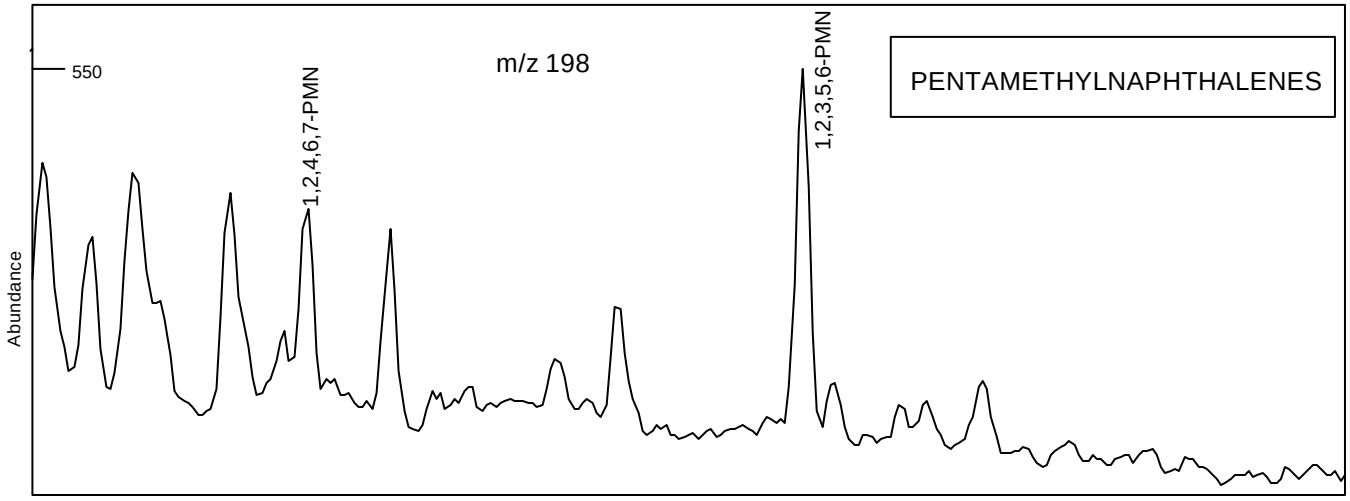

TABLE 5-1

ANALYSIS OF BRANCHED AND CYCLIC SATURATED HYDROCARBONS BY GC-MS

HALLADALE-1, DW-1, exL-128, Condensate (Topped)

GEOTECH

	Selected Parameters	*Ion(s)*	*Value*
1.	18α(H)-hopane/17α(H)-hopane (Ts/Tm)	191	0.82
2.	C30 hopane/C30 moretane	191	5.84
3.	C31 22S hopane/C31 22R hopane	191	1.29
4.	C32 22S hopane/C32 22R hopane	191	1.12
5.	C29 20S ααα sterane/C29 20R ααα sterane	217	1.22
6.	C29 ααα steranes (20S / 20S+20R)	217	0.55
7.	$\frac{\text{C29 αββ steranes}}{\text{C29 ααα steranes + C29 αββ steranes}}$	217	0.55
8.	C27/C29 diasteranes	259	0.63
9.	C27/C29 steranes	217	1.40
10.	18α(H)-oleanane/C30 hopane	191	nd
11.	$\frac{\text{C29 diasteranes}}{\text{C29 ααα steranes + C29 αββ steranes}}$	217	1.16
12.	$\frac{\text{C30 (hopane + moretane)}}{\text{C29 (steranes + diasteranes)}}$	191/217	1.47
13.	C15 drimane/C16 homodrimane*	123	0.97
14.	Rearranged drimanes/normal drimanes*	123	1.91

*Parameters generated from untopped sample

nd = no data

FIGURE 4A-1

Sample : **HALLADALE-1, DW-1, exL-128, Condensate**

File ID : 351701K

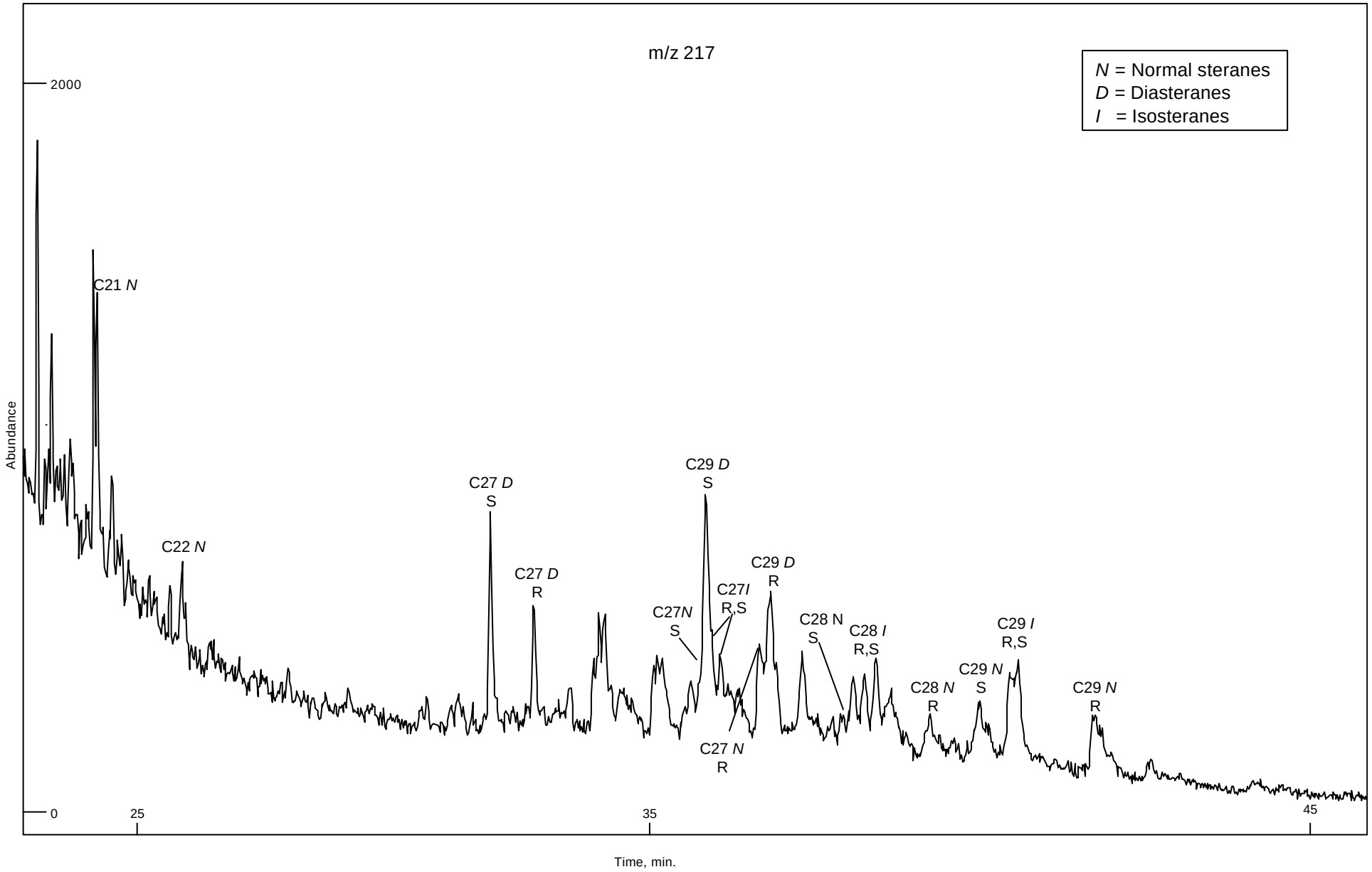

FIGURE 4B-1

Sample : **HALLADALE-1, DW-1, exL-128, Condensate**

File ID : 351701K

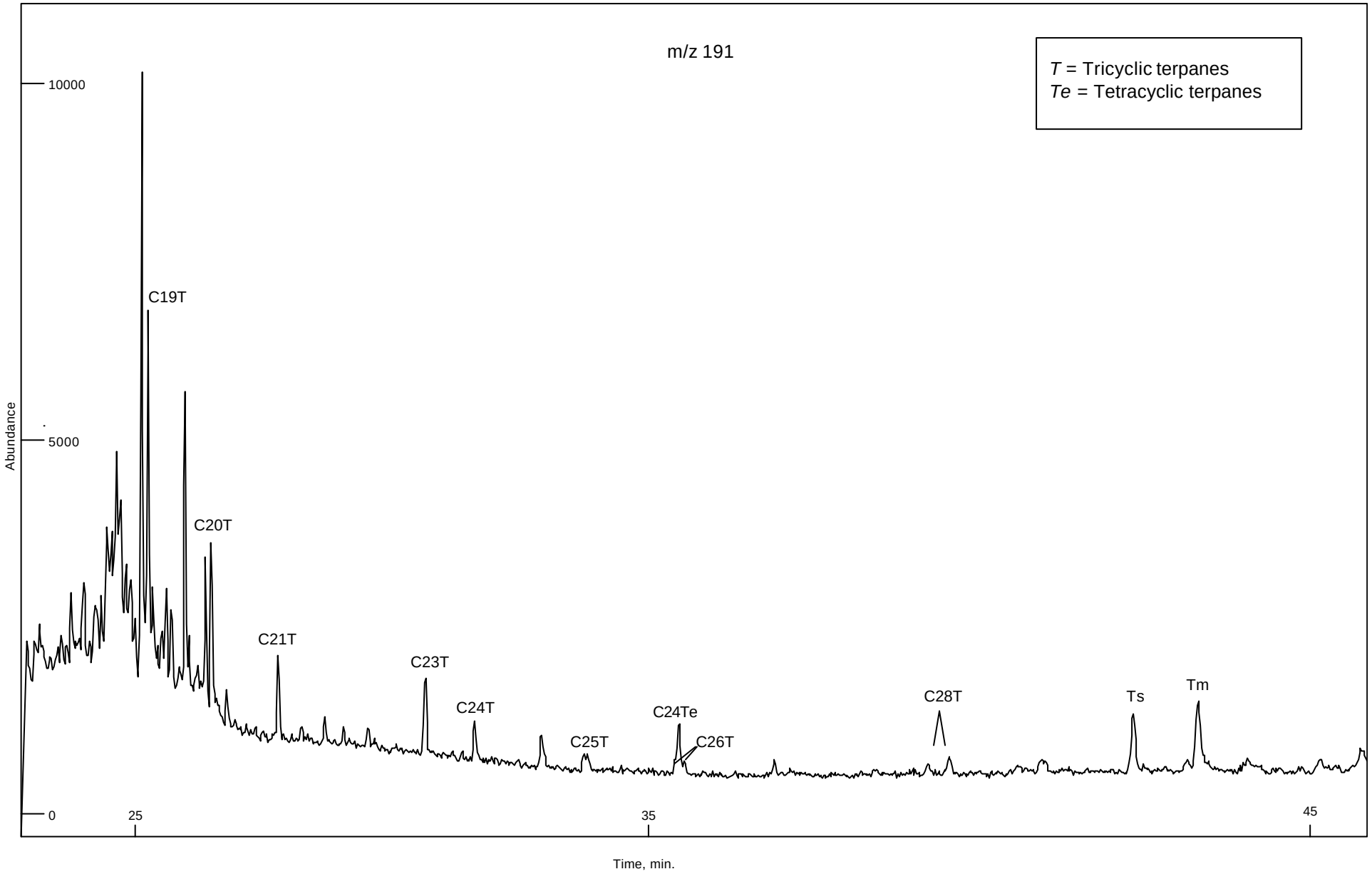

FIGURE 4C-1

Sample : **HALLADALE-1, DW-1, exL-128, Condensate**

File ID : 351701K

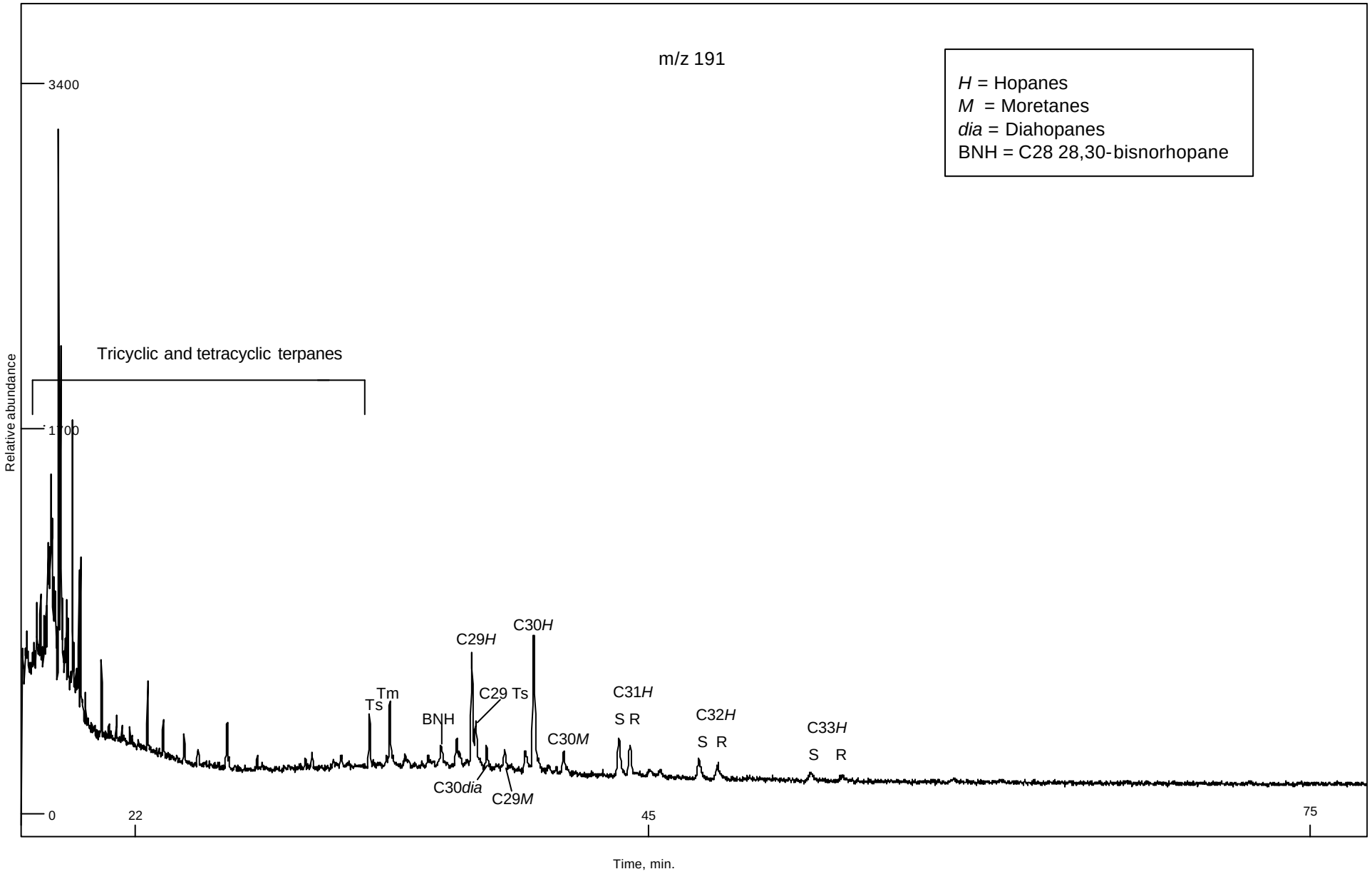

FIGURE 4D-1

Sample : **HALLADALE-1, DW-1, exL-128, Condensate**

File ID : 351701K

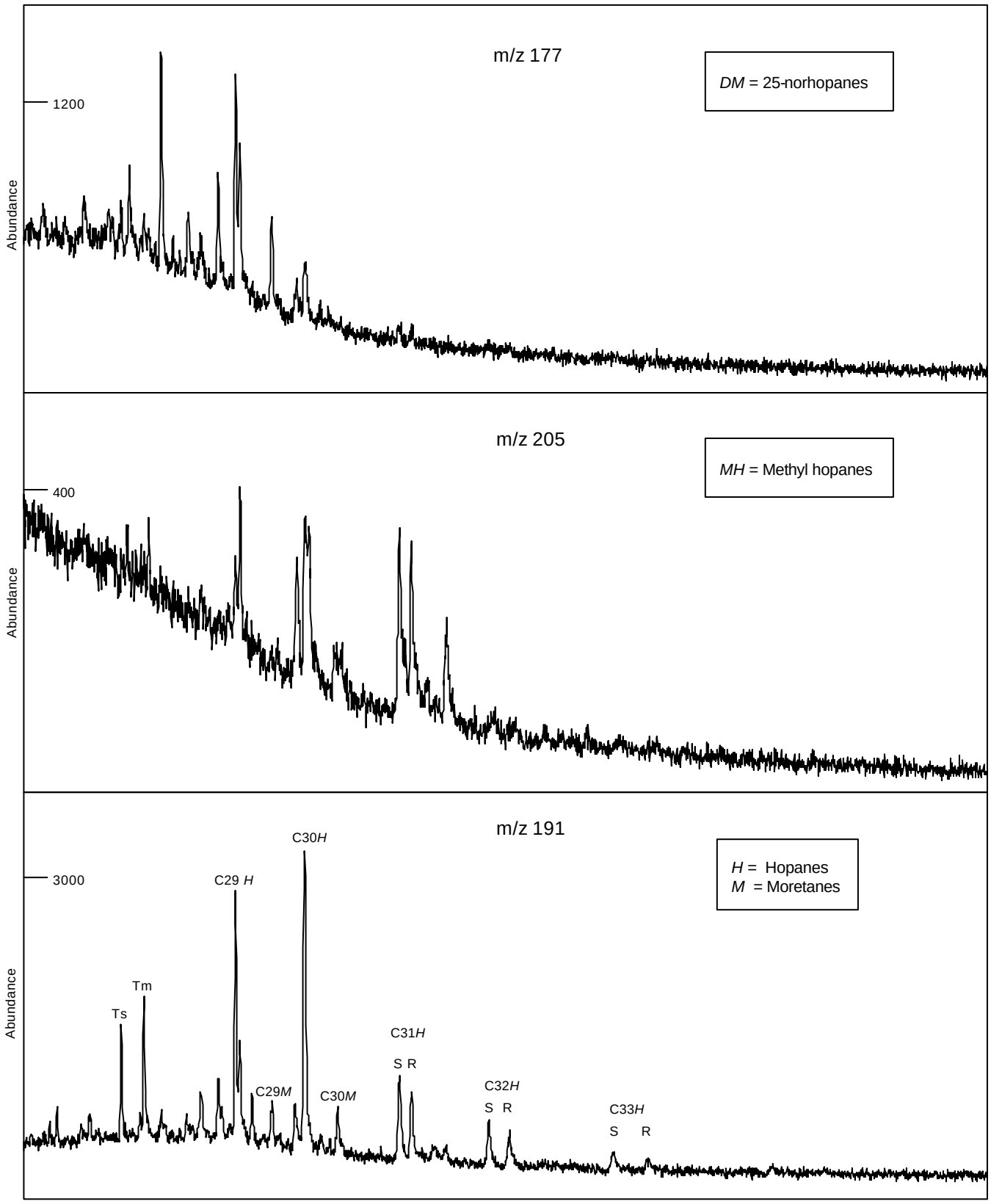

FIGURE 4E-1

Sample : **HALLADALE-1, DW-1, exL-128, Condensate**

File ID : 351701K

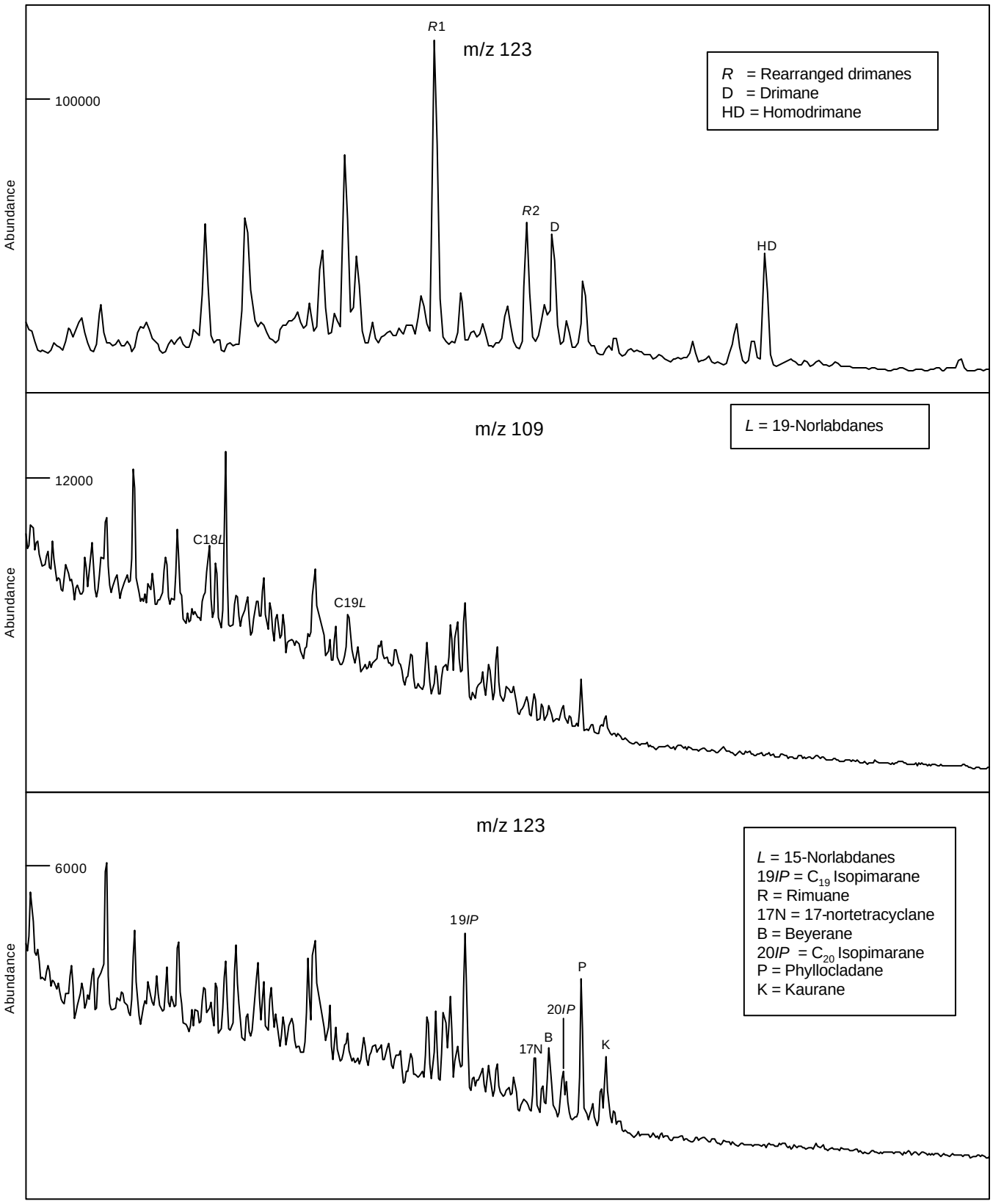

FIGURE 4F-1

Sample : **HALLADALE-1, DW-1, exL-128, Condensate**

File ID : 351701K

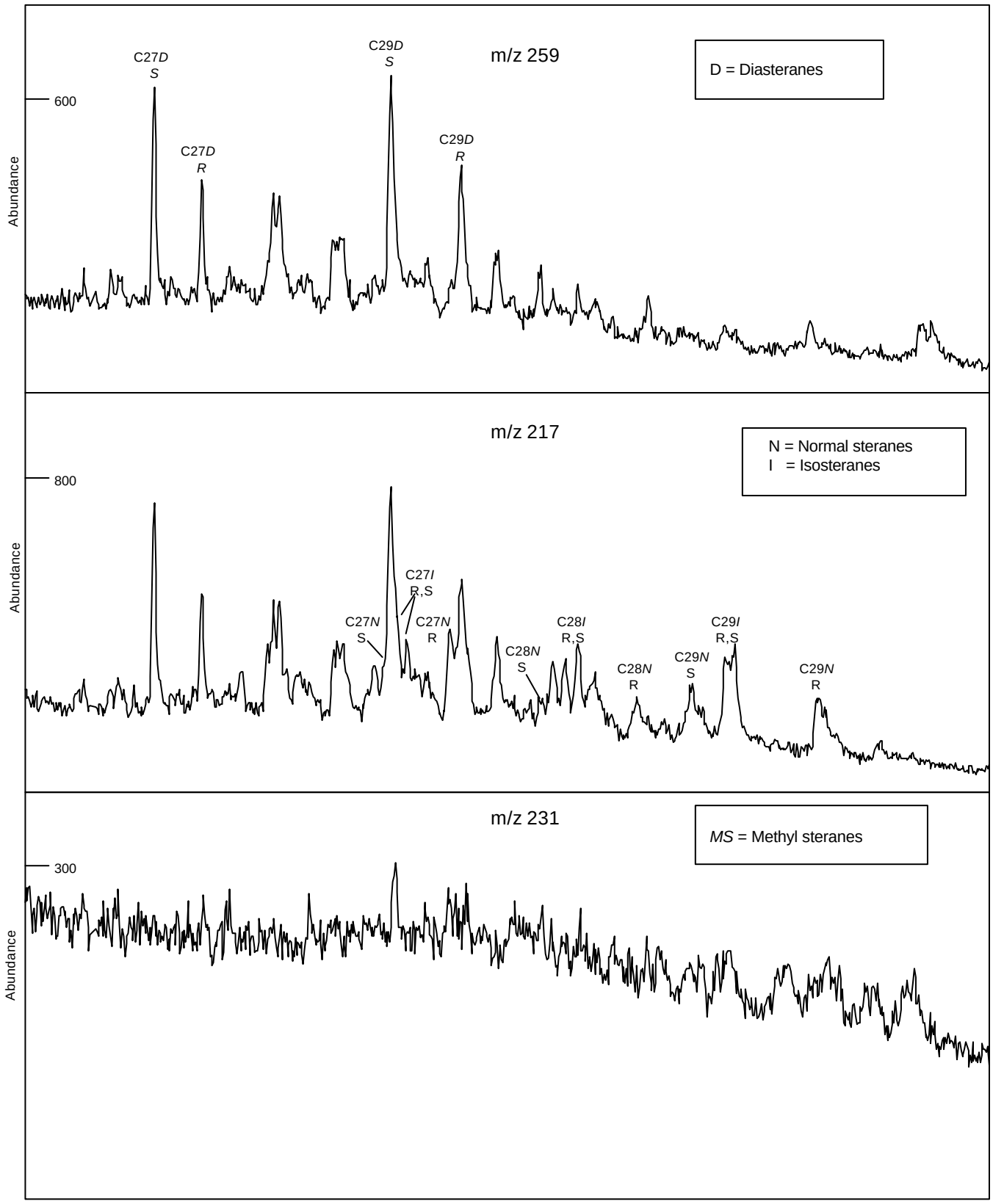

TABLE 5-2

ANALYSIS OF BRANCHED AND CYCLIC SATURATED HYDROCARBONS BY GC-MS

HALLADALE-1, DW-2, exL-332, Condensate (Topped)

GEOTECH

	Selected Parameters	*Ion(s)*	*Value*
1.	18α(H)-hopane/17α(H)-hopane (Ts/Tm)	191	1.04
2.	C30 hopane/C30 moretane	191	5.11
3.	C31 22S hopane/C31 22R hopane	191	1.35
4.	C32 22S hopane/C32 22R hopane	191	1.55
5.	C29 20S ααα sterane/C29 20R ααα sterane	217	0.82
6.	C29 ααα steranes (20S / 20S+20R)	217	0.45
7.	$\frac{\text{C29 αββ steranes}}{\text{C29 ααα steranes + C29 αββ steranes}}$	217	0.54
8.	C27/C29 diasteranes	259	1.15
9.	C27/C29 steranes	217	1.49
10.	18α(H)-oleanane/C30 hopane	191	nd
11.	$\frac{\text{C29 diasteranes}}{\text{C29 ααα steranes + C29 αββ steranes}}$	217	1.01
12.	$\frac{\text{C30 (hopane + moretane)}}{\text{C29 (steranes + diasteranes)}}$	191/217	1.56
13.	C15 drimane/C16 homodrimane*	123	0.94
14.	Rearranged drimanes/normal drimanes*	123	1.99

*Parameters generated from untopped sample

nd = no data

FIGURE 4A-2

Sample : **HALLADALE-1, DW-2, exL-332, Condensate**

File ID : 351702K

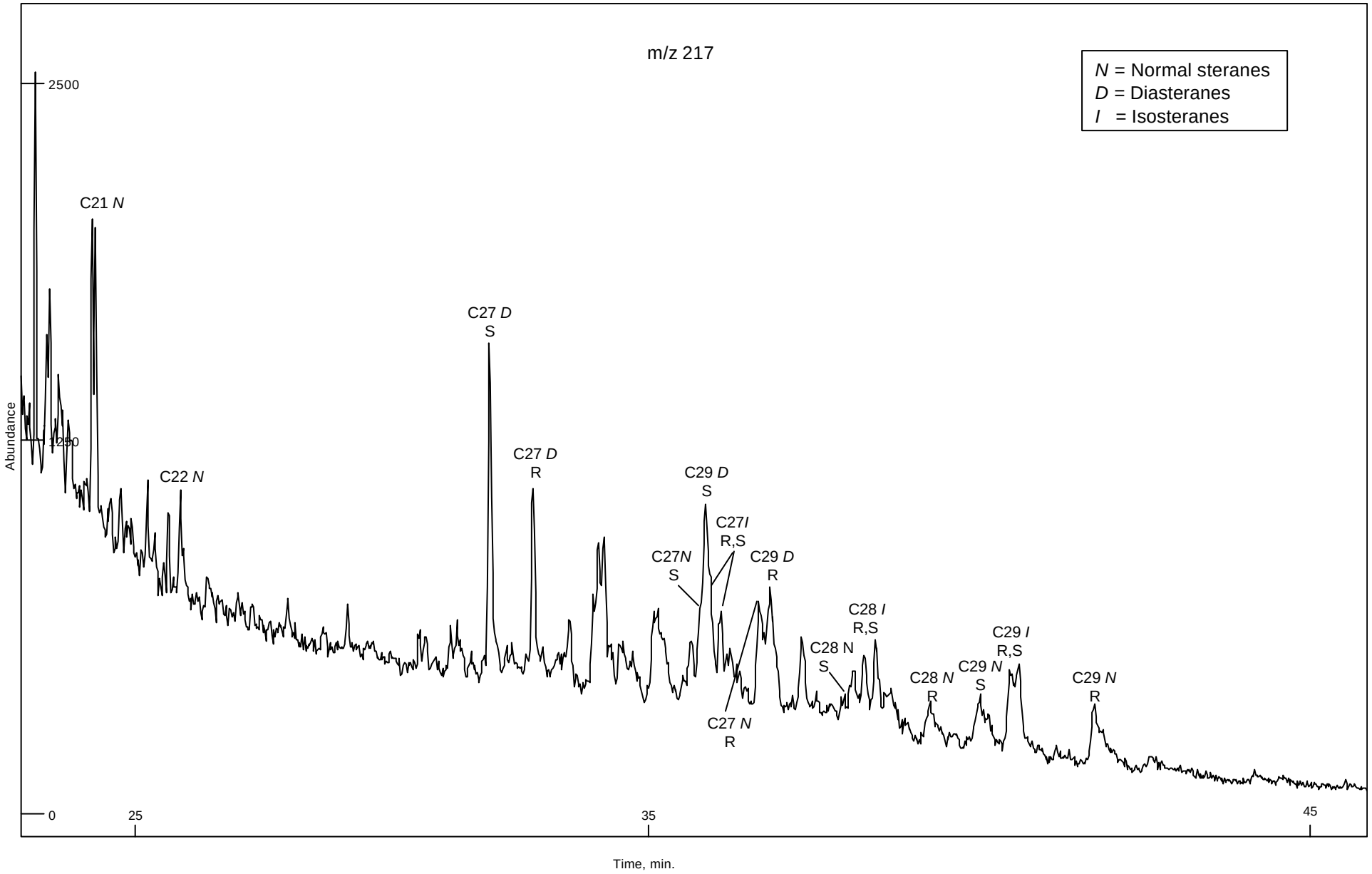

FIGURE 4B-2

Sample : **HALLADALE-1, DW-2, exL-332, Condensate**

File ID : 351702K

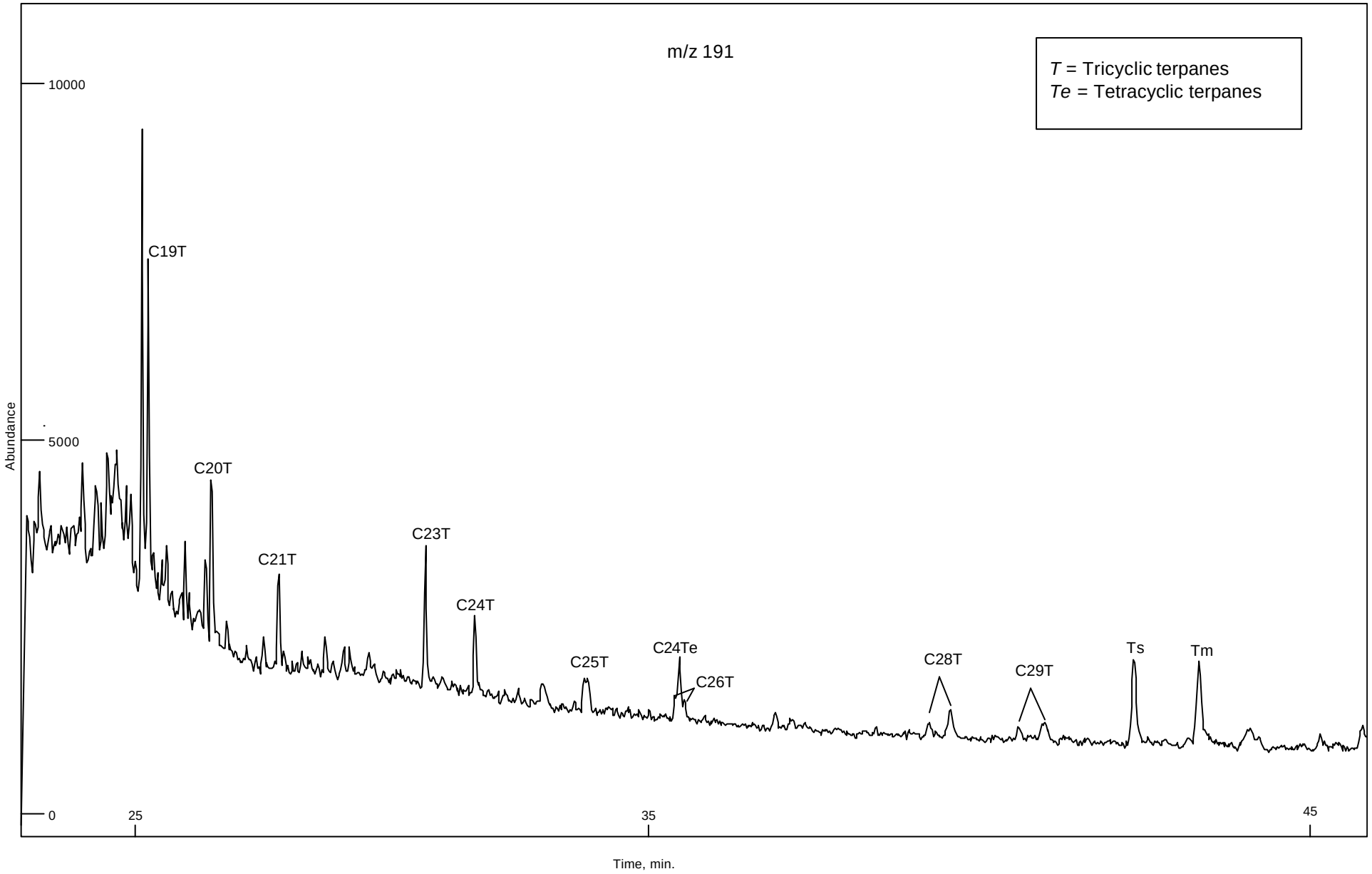

FIGURE 4C-2

Sample : **HALLADALE-1, DW-2, exL-332, Condensate**

File ID : 351702K

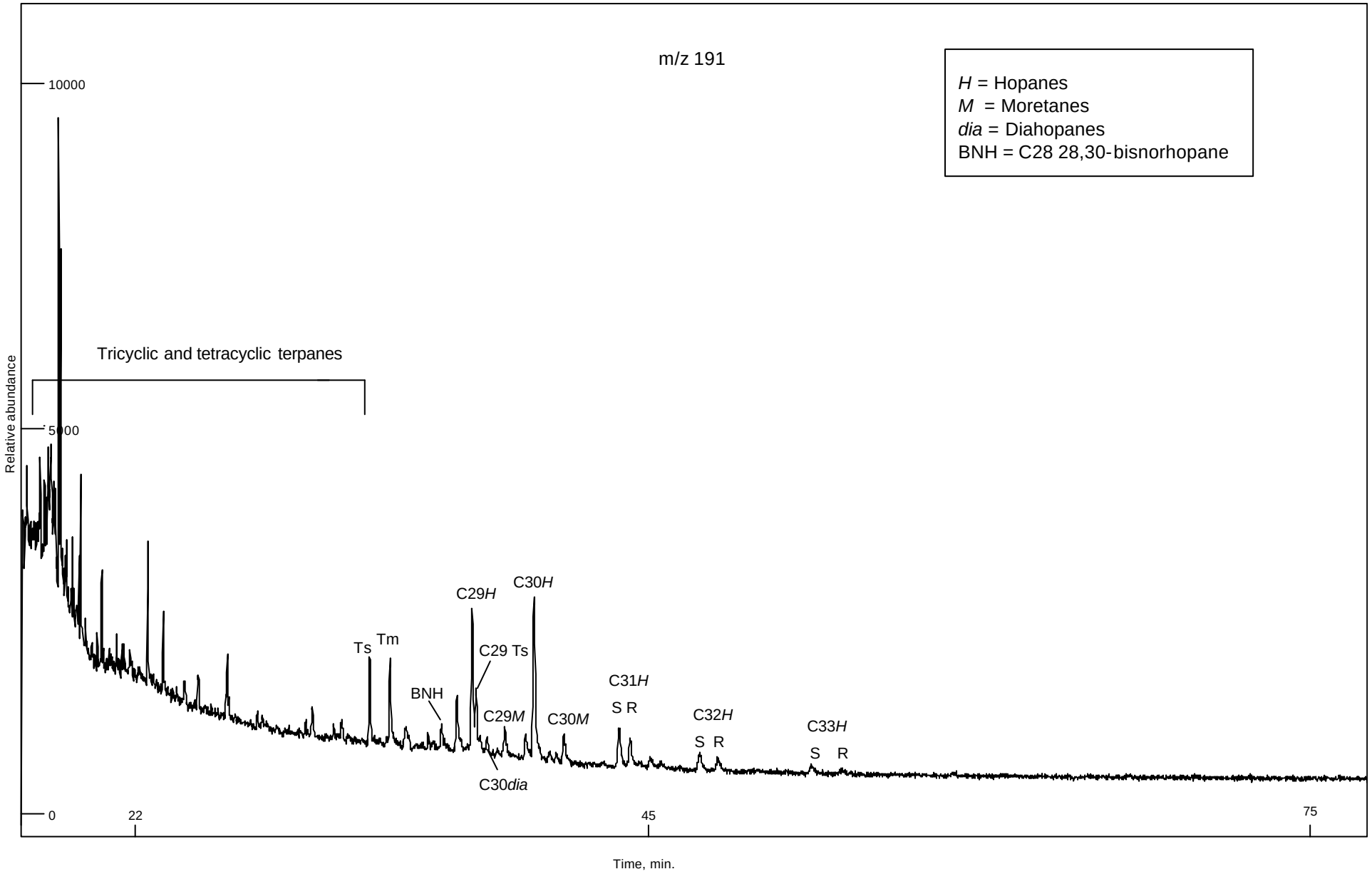

GEOTECHNICAL SERVICES PTY LTD

FIGURE 4D-2

Sample : **HALLADALE-1, DW-2, exL-332, Condensate**

File ID : 351702K

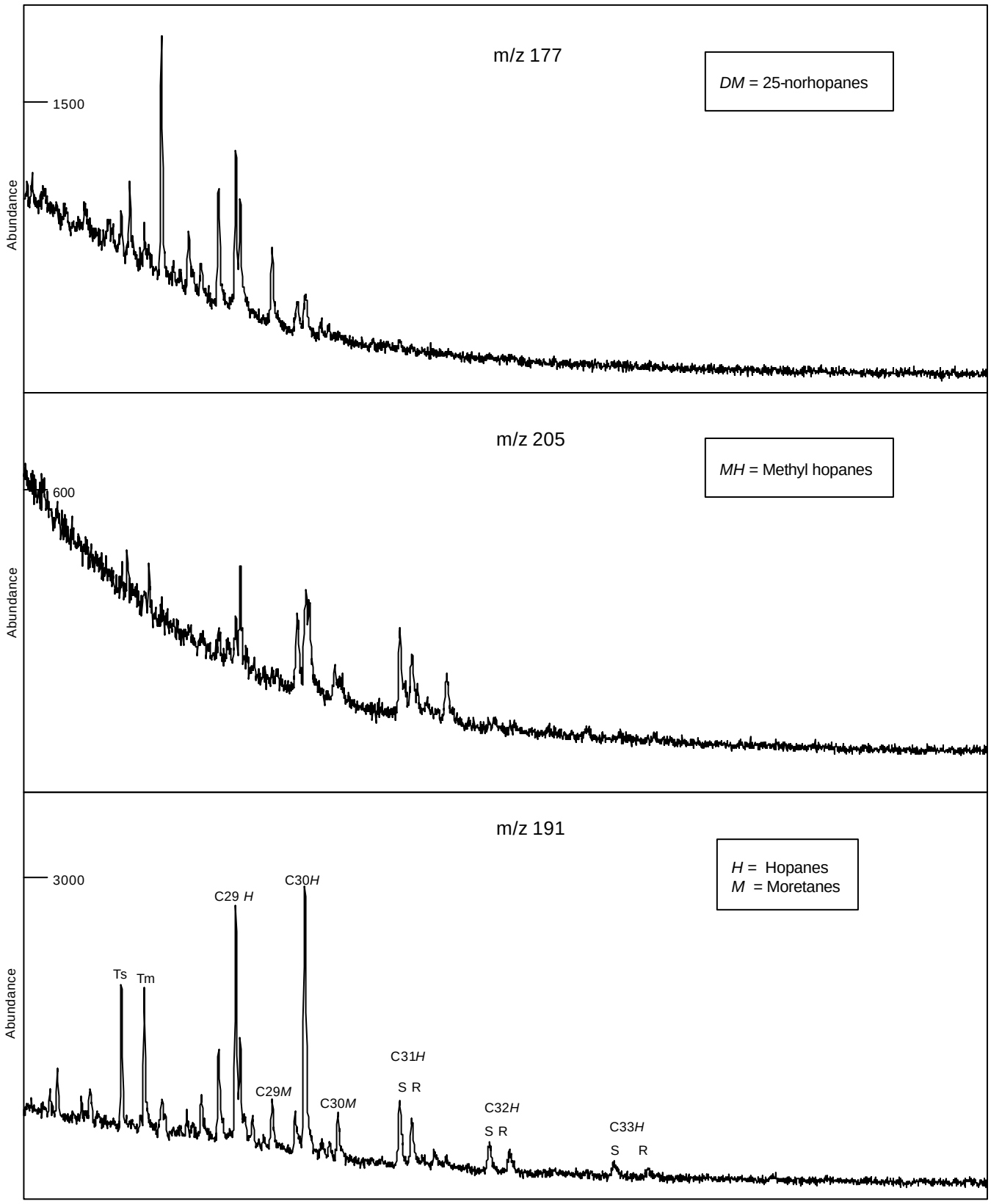

FIGURE 4E-2

Sample : **HALLADALE-1, DW-2, exL-332, Condensate**

File ID : 351702K

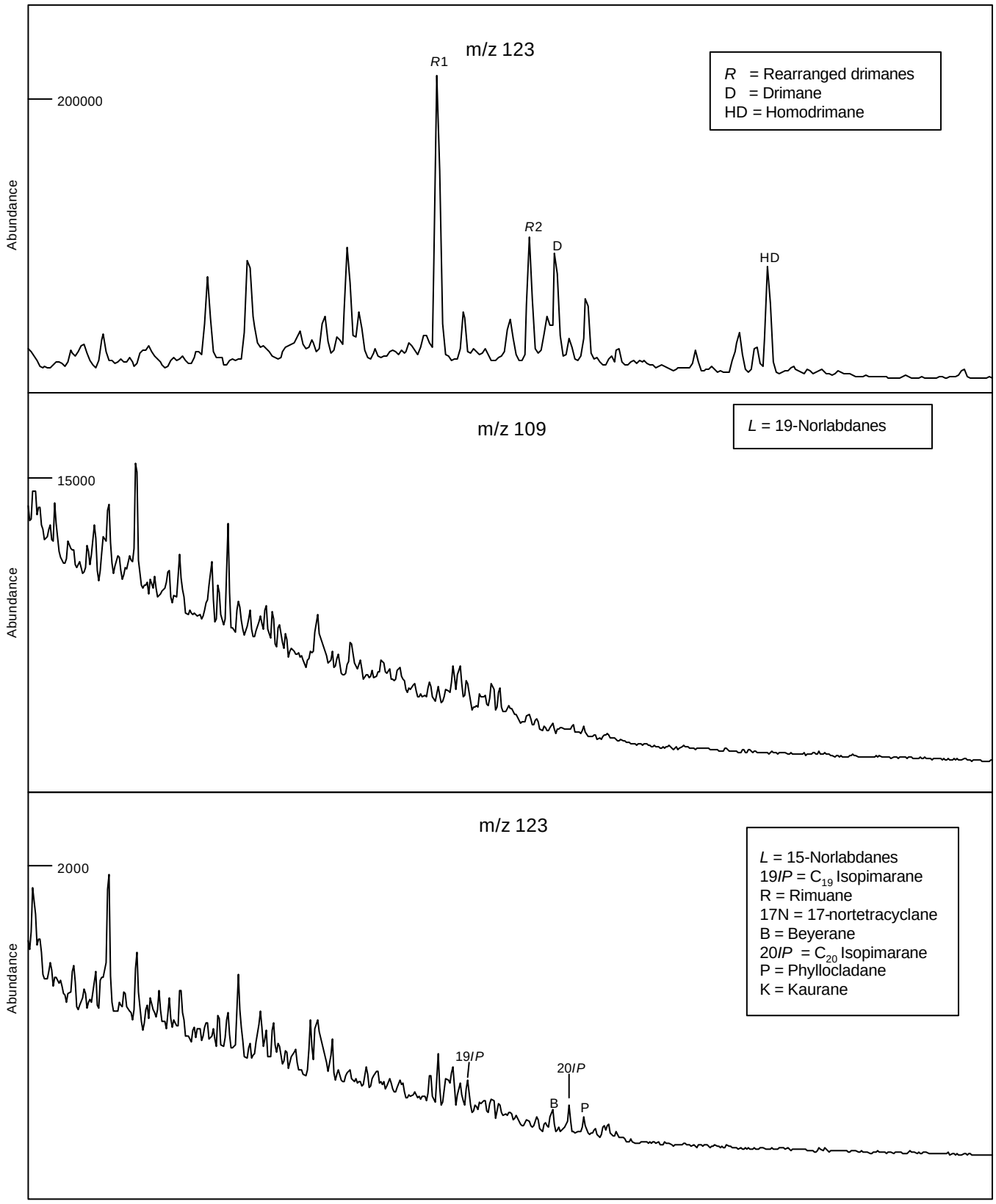

FIGURE 4F-2

Sample : **HALLADALE-1, DW-2, exL-332, Condensate**

File ID : 351702K

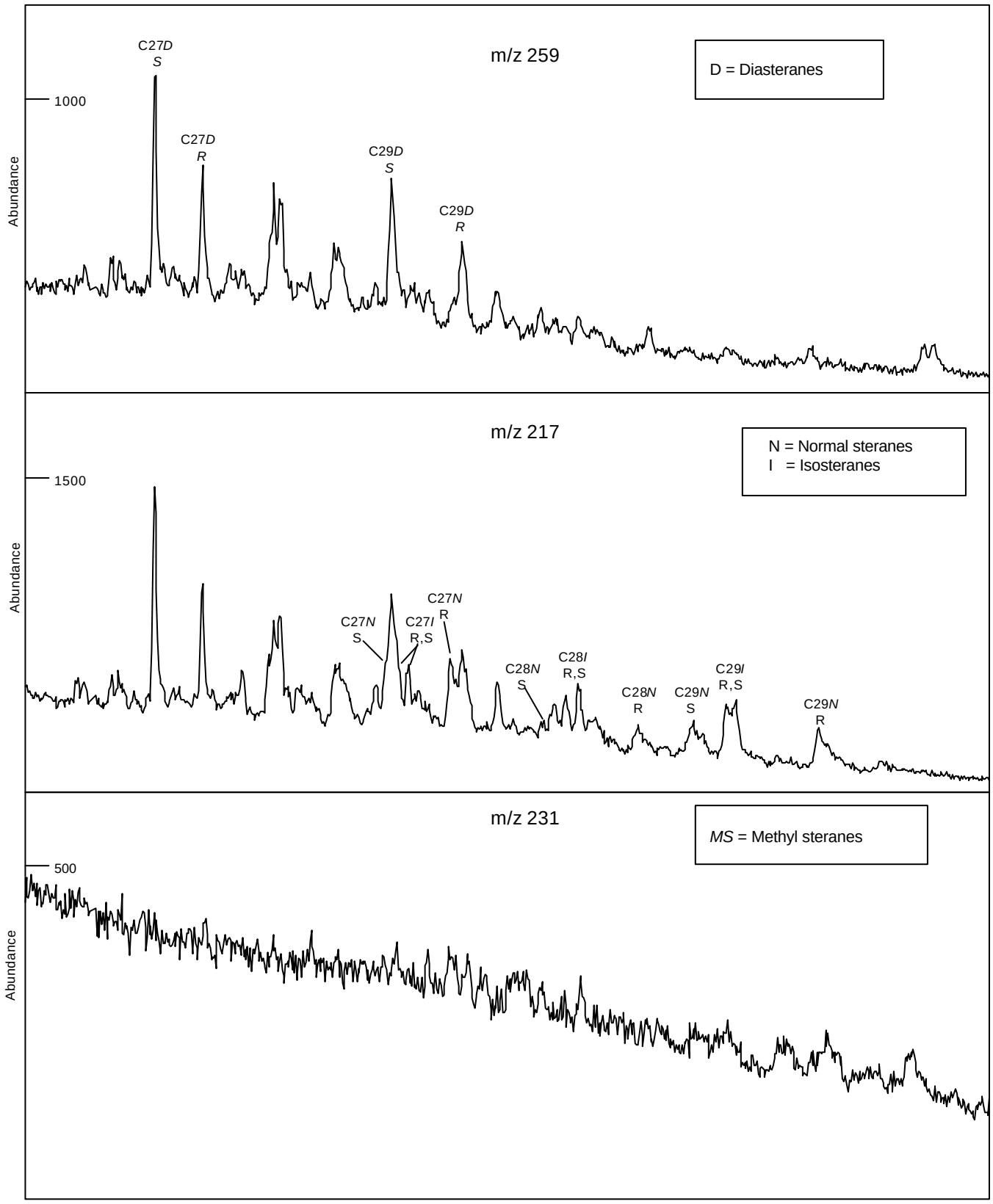

APPENDIX B

ANALYTICAL PROCEDURES

ANALYTICAL PROCEDURES

HYDROCARBON CHARACTERISATION ANALYSES

B.1 Whole Oil or 'Hexane' Solubles GC-MS

Fluid samples and extracts (from solid products) were analysed by GC-MS in scan mode producing a chromatogram of the compounds present from C_9 to C_{36}.

B.2 Liquid Chromatographic Separation

Fluid products and extracts (from solid products) were separated into saturate, aromatic and NSO (polars) fractions.

This separation was achieved by liquid column chromatography using activated silica gel adsorbent and eluting solvents of varying polarity. The saturate, aromatic and NSO fractions were recovered by evaporation of the solvent by fractional distillation.

B.3 Saturate GC-MS

The saturate fraction obtained from liquid chromatographic separation was analysed by GC-MS in scan mode producing a chromatogram of the compounds present from C_9 to C_{34}.

B.4 Aromatic GC-MS

The aromatic fraction obtained from liquid chromatographic separation was analysed by GC-MS in selected ion monitoring (SIM) mode.

B.5 Branched/cyclic GC-MS

The saturate fractions were treated with ZSM-5 in order to isolate the branched/cyclic compounds, which were then analysed by GC-MS. In those cases where insufficient saturate material was obtained to perform the separation, the entire saturate fraction was analysed by the branched/cyclic GC-MS method.

APPENDIX 10:
MUD GAS ISOTOPE AND CONDENSATE SPECIFIC ISOTOPE ANALYSIS REPORT

Geochemical Interpretation of Halladale Gas, VIC/P37(V), Otway Basin

Bob Davis

Petroleum Systems Analysis Team
GeoSolutions, Exploration and New Ventures

February 2006

ABN 63 005 482 986

CONFIDENTIAL

This document is the property of Woodside Energy Ltd., and the copyright therein is vested in Woodside Energy Ltd. All rights reserved. Neither the whole nor any part of this document may be disclosed to others or reproduced, stored in a retrieval system, or transmitted in any form by any means (electronic, mechanical, reprographic recording or otherwise) without prior written consent of the copyright owner.

Approval Signatures

Prepared by:

_____ _____
Bob Davis, EGL1-01 20/02/2006
Senior Geochemist

Reviewed by:

_____ _____
Andrew Murray, EGL-1 20/02/2006
Coordinator, Petroleum Systems Analysis

Approved by:

_____ _____
Steve Rigby, EW 20/02/2006
Team Leader, E&NV SE Australia

EXECUTIVE SUMMARY

A suite of isotubes and MDT gases from Halladale-1 DW-1 (Black Watch), DW-2 (Halladale) and DW-3 were subjected to compositional and isotopic analysis. Halladale gas is fairly dry, and was probably expelled from isotopically heavy humic or mixed humic/lacustrine organic matter within the early to peak gas window. The low concentration of carbon dioxide in these gases most likely derives from low maturity Type III organic matter. Gases from Waarre C sands in DW-1 and DW-2 are isotopically distinctive, suggesting they are in separate compartments. This is supported by pressure profiles, which display an offset of c. 10 psi. There is no convincing evidence of flow barriers between the Waarre A and C sands in Halladale-1 DW-1, and Waarre C sands in DW-2 and DW-3 although significant variability within isotope values hints at poor communication.

At least three families of gases are present in the Shipwreck Trough. Family 1 includes Halladale, Boggy Creek, Casino, Fenton Creek, Lavers and Mylor. Family 2 consists of Geographe, Thylacine and La Bella, whereas Family 3 contains Minerva and (the unrelated accumulation) Port Fairy. There is evidence of multiple source rocks or multiple charge events contributing to the Halladale accumulation.

TABLE OF CONTENTS

1 BUSINESS CASE 5

2 INTRODUCTION 7

2.1 BACKGROUND 7
2.2 MUD GAS ISOTOPES 7
2.3 RCI GAS INVENTORY 12
2.4 GAS COMPOSITION 12
2.5 ISOTOPE ANALYSES 17
2.6 CONDENSATE CSIA 20
2.7 NON-HYDROCARBON GASES 21

3 CONCLUSIONS 23

4 REFERENCES ..... ERROR! BOOKMARK NOT DEFINED.

FIGURES

Figure 1: Location map 6
Figure 2: Halladale mud gas isotope profiles (TVDSS) 9
Figure 3: Methane vs ethane isotopes (all isotubes) 10
Figure 4: Propane vs ethane isotopes (all isotubes) 10
Figure 5: Methane vs ethane isotopes (Waarre isotubes and RCI) 11
Figure 6: Propane vs ethane isotopes (Waarre isotubes and RCI) 12
Figure 7: Comparison of Halladale-1 DW1 and DW2 RCI pressure gradients 14
Figure 8: Gas compositions, DW1 and DW2 (Petrolab vs Isolab) 15
Figure 9: Pixler plot of Otway Basin gases 16
Figure 10: Schoell's genetic classification of natural gases 18
Figure 11: Whiticar plot of methane vs. ethane and propane isotopes 19
Figure 12: Whiticar plot of propane vs. ethane isotopes 19
Figure 13: Shipwreck Trough Gas CSIA Profiles 20
Figure 14: Halladale DW-1 whole fluid CSIA Profile 21
Figure 15: Genetic origin of CO_2 in natural gases 22

TABLES

Table 1: Isotube data, Halladale-1 8
Table 2: RCI fluid inventory Halladale-1 12
Table 3: Gas compositions from PVT analysis (Petrolab) 13
Table 4: Isotopic composition of Halladale gas 17

1 Business Case

With the discovery of gas at Halladale in April 2005, a need to characterise the gas for integration with existing data, and further calibration of the charge model was identified. This report summarises the state of our knowledge of the chemistry of Otway gases to date.

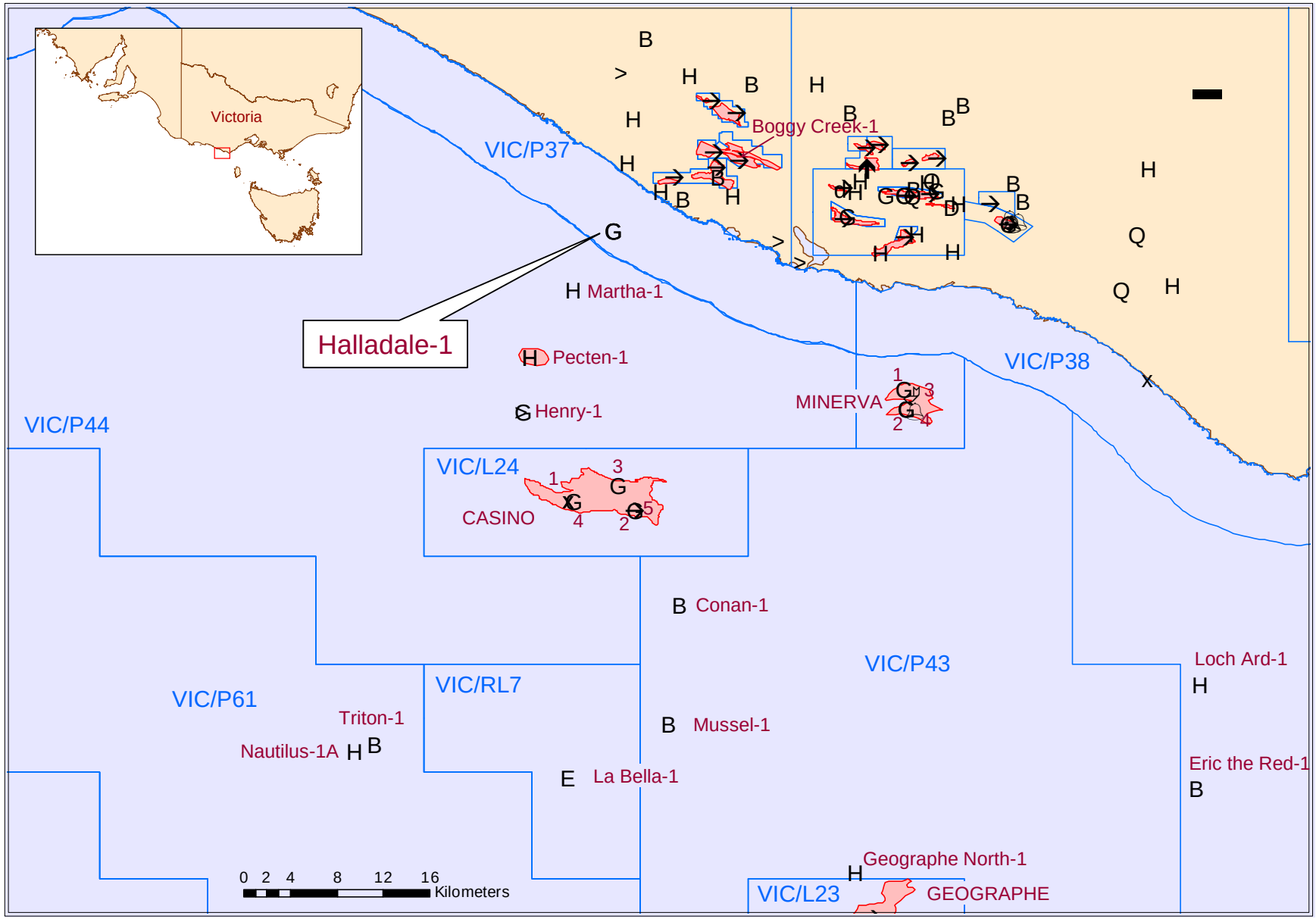

Figure 1: Location map

2 Introduction

2.1 Background

Halladale-1 (38°34'45.54"S, 142°43'50.95"E) was spudded on 22nd April 2005 in 45 m (LAT) of water, on the western flank of the Shipwreck Trough, VIC/P37(V), some 4 km from the coast of Victoria (Figure 1). Drilling operations were managed by Woodside Energy Ltd (62.5% equity) under an agreement with the operator, Origin Energy (37.5% equity). Three wells were drilled in succession from the Halladale-1 location. Halladale-1 DW-1 (Black Watch prospect) deviated to the south and intersected a gross gas-bearing interval of 59m TVT in the Waarre Formation. Halladale-1 DW-2 (Halladale prospect) deviated to the north and intersected a gross gas-bearing interval of 21m TVT in the Waarre Formation. Halladale-1 DW-3 was deviated down-flank from the Halladale gas to the northeast, to obtain aquifer pressures in the Waarre Formation.

2.2 Mud Gas Isotopes

A total of 78 isotubes were collected from the three Halladale wells, comprising 33 from DW-1, 27 from DW-2 and 18 from DW-3. Compositional analyses were performed on all samples, followed by isotope analysis of selected mud gases. The results of mud gas analysis are presented in Table 1 and plotted in Figure 2.

The majority of the well section, from c. 1210m to c. 1860m TVDSS, yields isotopically heavy methane, with $\delta^{13}C$ values ranging from -35‰ to -32‰. This is characteristic of very mature gas - much more so than attained by the sediments penetrated by the well, suggesting pervasive migration of high maturity gas throughout the sedimentary column. Almost all samples cluster tightly on methane vs. ethane and ethane vs. propane plots in Figure 3 and Figure 4, suggesting gas of similar provenance pervades the entire section. An exception is thin sands within the Paaratte Formation, which in DW-2 yield isotopically lighter methane ($\delta^{13}C$ of -40‰). This is confirmed by a similar result in DW-3, though no isotope results were obtained for this interval in DW-1 (Figure 2). Isotopically lighter methane suggests these sands have been charged with gas of lower average maturity, however substantially heavier ethane ($\delta^{13}C$ of -18‰) suggests higher maturity. Both of these observations may be accounted for by another mechanism – biodegradation and methanogenesis – suggesting the Paaratte gas may be in contact with artesian water.

Well	Isotech Lab No.	Sample Date	Sample Time	MDKB Meters	TVDSS Meters	Gas Units %	GC Date	O_2 + Ar ppm	CO_2 ppm	N_2 ppm	CO ppm	C_1 ppm	C_2 ppm	C_2H_4 ppm	C_3 ppm	C_3H_6 ppm	iC_4 ppm	nC_4 ppm	iC_5 ppm	nC_5 ppm	C_6+ ppm	$\delta^{13}C_1$ per mil	$\delta^{13}C_2$ per mil	$\delta^{13}C_3$ per mil	Comments
DW-1	89606	3/30/2005	12:45	850	827	0.0203	9/29/2005	219600	660	779700	0	4	0	0	0	0	0	0	0	0	1				
DW-1	89607	3/31/2005	3:01	908.8	886.6	0.011	9/29/2005	219700	430	779900	0	4	0	0	0	0	0	0	0	0	2				
DW-1	89608	3/31/2005	4:03	951.7	929.1	0.052	9/29/2005	209900	4300	785700	0	68	3	0	1	1	1	0	3	1	57				
DW-1	89609	3/31/2005	5:21	1003	979.4	0.052	9/29/2005	207200	5300	787400	0	58	3	1	1	1	1	0	2	1	67				
DW-1	89610	3/31/2005	6:07	1050.7	1025.3	0.119	9/29/2005	204600	4800	790100	0	428	6	3	1	1	1	0	2	1	65				
DW-1	89611	3/31/2005	7:22	1101	1072.9	0.152	9/29/2005	200300	6100	793100	0	404	11	7	1	1	1	0	2	1	69				
DW-1	89612	3/31/2005	8:34	1150	1118.9	0.092	9/29/2005	207000	6900	785800	0	213	9	6	1	1	1	0	1	0	33				
DW-1	89613	3/31/2005	10:04	1200	1166.6	0.104	9/29/2005	203300	4800	791500	0	292	10	3	10	1	12	10	5	3	62				
DW-1	89614	3/31/2005	11:58	1248.6	1211.9	1.376	9/29/2005	201600	6300	787700	140	3950	174	40	21	6	19	11	6	4	71	-34.9	-19.2		
DW-1	89615	3/31/2005	12:01	1250.3	1213.6	0.508	9/29/2005	201300	6800	787900	30	3610	175	10	22	2	22	12	7	4	67				
DW-1	89616	3/31/2005	14:08	1300	1260.6	0.04	9/29/2005	219800	690	779500	0	28	1	0	0	0	0	0	0	0	4				
DW-1	89617	3/31/2005	16:01	1350.3	1308.3	0.1	9/29/2005	214800	4800	779600	0	720	24	1	3	0	6	2	2	1	19				
DW-1	89618	3/31/2005	18:02	1400	1355.5	0.59	9/29/2005	210700	6200	777100	0	5450	336	1	102	1	20	20	5	3	16	-34.5			
DW-1	89619	3/31/2005	20:58	1436.4	1390	2	9/29/2005	199700	6200	749100	0	42600	1630	0	489	1	72	83	19	14	45				
DW-1	89620	3/31/2005	21:00	1436.6	1390.2	4.1	9/29/2005	193300	6400	731500	0	65200	2500	0	737	1	107	121	28	21	67	-32.6	-23.5	-22.8	
DW-1	89621	3/31/2005	21:37	1450.2	1403.1	1.17	9/29/2005	207600	6900	774300	0	10300	586	0	219	0	35	45	10	8	34	-33.1			
DW-1	89622	4/01/2005	12:22	1500	1450.3	1.07	9/29/2005	204200	9000	775600	0	10200	601	0	255	1	45	58	14	11	47	-33.0			
DW-1	89623	4/01/2005	1:27	1521.4	1470.6	5.881	9/29/2005	195800	8600	745700	0	47600	1570	0	467	1	70	85	19	15	50	-32.9	-23.6	-22.9	
DW-1	89624	4/01/2005	1:33	1522.2	1471.3	5.838	9/29/2005	199400	7900	747600	0	43000	1420	0	423	1	63	77	17	14	41				
DW-1	89625	4/01/2005	1:48	1535.3	1483.7	23.015	9/29/2005	159600	9100	629100	0	193000	6700	0	1810	1	234	265	56	43	99	-33.0	-23.3	-23.1	
DW-1	89626	4/01/2005	2:27	1550	1497.7	1.181	9/29/2005	212500	5200	775100	0	6620	349	0	129	0	20	27	6	5	22	-32.4			
DW-1	89627	4/01/2005	3:04	1566.1	1512.9	11.56	9/29/2005	187000	7100	699400	0	101700	3420	1	958	1	130	149	32	25	58				
DW-1	89628	4/01/2005	3:06	1567.5	1514.3	22.495	9/29/2005	167400	8000	636600	0	179500	6190	0	1690	1	220	248	53	40	93	-33.1	-23.4	-22.3	
DW-1	89629	4/01/2005	4:19	1600	1545	1.307	9/29/2005	209500	8100	773300	0	8420	419	0	130	0	22	31	8	7	33	-33.0	-23.5	-23.4	
DW-1	89630	4/01/2005	6:31	1650	1592.4	1.202	9/29/2005	208100	8600	774200	0	8640	338	0	61	1	14	19	7	6	32	-33.6			
DW-1	89631	4/01/2005	8:25	1700	1639.9	1.038	9/29/2005	197100	6400	788400	0	7470	449	2	134	1	19	23	8	7	37	-32.9	-24.0	-23.5	
DW-1	89632	4/01/2005	10:35	1750	1687.3	0.437	9/29/2005	216600	3400	777900	0	1910	104	0	36	0	5	7	2	2	10	-32.7			
DW-1	89633	4/01/2005	11:52	1778.9	1714.6	31.91	9/29/2005	142200	9900	548200	0	282200	12400	0	3750	3	493	495	102	75	149	-33.9	-23.8	-23.4	
DW-1	89634	4/01/2005	12:27	1785.5	1721	41.02	9/30/2005	127300	10500	516500	0	325000	14500	0	4560	3	620	624	130	96	173	-33.3	-22.9	-22.3	
DW-1	89635	4/04/2005	6:18	1800.4	1735.1	0.1	9/30/2005	218100	760	780300	0	749	50	0	16	0	2	3	1	1	6				
DW-1	89636	4/04/2005	8:14	1852.5	1784.8	0.31	9/30/2005	217000	1100	777800	0	3800	189	0	56	0	7	9	2	2	7	-33.3	-23.7	-22.6	cryo-enrichment
DW-1	89637	4/04/2005	14:05	1900	1830.4	0.05	9/30/2005	216600	2000	780700	0	596	26	0	13	0	3	5	1	1	8				
DW-1	89638	4/04/2005	16:44	1918	1847.7	0.09	9/30/2005	215700	2600	781100	0	566	21	0	9	0	3	4	2	1	9				
DW-2	89639	4/11/2005	12:50	901.5	879.4	0.021	9/30/2005	216000	110	783800	0	23	2	0	2	0	1	1	2	1	23				
DW-2	89640	4/11/2005	2:41	950.2	928.1	0.028	9/30/2005	212400	100	787300	0	143	5	0	2	0	2	1	3	2	50				
DW-2	89641	4/11/2005	4:22	1001.9	979.5	0.028	9/30/2005	209200	80	790600	0	92	3	0	1	0	1	1	3	1	49				
DW-2	89642	4/11/2005	6:06	1056.3	1033.2	0.047	9/30/2005	215000	110	784700	0	186	4	0	2	0	1	1	1	1	35				
DW-2	89643	4/11/2005	8:01	1107.1	1082.3	0.03	9/30/2005	212800	130	786800	0	187	4	0	1	0	1	1	1	1	26				
DW-2	89644	4/11/2005	10:02	1150.1	1123.6	0.041	9/30/2005	212900	110	786900	0	64	2	0	1	0	1	1	1	0	18				
DW-2	89645	4/11/2005	13:45	1200	1170.3	0.06	9/30/2005	212200	150	787400	0	195	4	1	2	0	3	2	2	1	25				
DW-2	89646	4/11/2005	16:30	1250	1216.7	0.71	9/30/2005	211500	130	782300	0	5710	256	1	56	0	12	10	4	3	36	-35.0			
DW-2	89647	4/11/2005	19:00	1300	1262.9	0.34	9/30/2005	210700	110	786300	0	2590	131	2	43	1	16	12	7	4	48	-39.3			
DW-2	89648	4/11/2005	21:24	1350	1309	0.21	9/30/2005	211200	110	787400	0	1100	56	3	20	1	12	7	5	3	35	-38.9			
DW-2	89649	4/12/2005	2:35	1400	1354.9	0.202	9/30/2005	211700	110	786900	0	1160	80	0	25	0	9	8	5	3	37	-33.6			
DW-2	89650	4/12/2005	9:20	1450	1400.9	0.51	9/30/2005	213400	130	781700	0	4280	289	1	116	0	19	26	7	6	41	-32.4	-23.5	-22.9	
DW-2	89651	4/12/2005	16:30	1500	1447.3	0.35	9/30/2005	215100	170	781900	0	2560	112	1	51	0	12	17	6	5	36	-32.4			
DW-2	89652	4/13/2005	19:00	1550	1493.8	0.79	9/30/2005	211200	320	779800	0	8320	258	0	59	1	7	9	3	3	22	-32.7	-23.7	-22.8	
DW-2	89653	4/13/2005	20:30	1600	1540.2	0.78	9/30/2005	210800	330	780800	0	7640	322	0	71	1	8	10	3	3	21	-33.1	-24.2	-23.5	
DW-2	89654	4/14/2005	0:32	1650	1586.6	0.53	9/30/2005	213500	560	782100	0	3590	149	6	25	1	5	5	2	2	19	-33.0			
DW-2	89655	4/14/2005	5:38	1700	1633	0.59	9/30/2005	210700	810	783800	0	4480	183	1	37	1	5	4	2	1	10	-33.0			
DW-2	89656	4/14/2005	17:30	1750	1679.5	0.26	9/30/2005	210400	220	787300	0	1900	86	1	28	0	4	6	2	2	8	-32.3			
DW-2	89657	4/14/2005	21:10	1783	1710.2	3.52	9/30/2005	199600	290	748700	0	49500	1450	0	346	1	40	44	9	7	21	-32.3	-23.1	-22.8	
DW-2	89658	4/15/2005	0:37	1800	1726.1	0.99	9/30/2005	210900	290	780600	0	7770	273	2	87	1	13	16	4	4	16	-32.2			
DW-2	89659	4/15/2005	1:50	1805.8	1731.4	4.32	9/30/2005	198200	270	744200	0	54900	1750	1	473	1	62	68	15	12	35				
DW-2	89660	4/15/2005	3:17	1807.9	1733.4	12.623	9/30/2005	154400	280	600300	0	234700	7630	2	2000	2	242	258	51	39	81	-32.2	-23.1	-22.5	
DW-2	89661	4/16/2005	2:25	1809.7	1735.1	7.13	9/30/2005	200200	270	738400	0	58600	1830	1	473	1	59	66	14	12	37				
DW-2	89662	4/16/2005	2:50	1812.5	1737.7	28.3	9/30/2005	162200	270	599700	0	226700	8120	3	2210	3	264	286	59	45	100	-32.1	-23.1	-22.4	
DW-2	89663	4/17/2005	17:15	1850	1772.6	0.52	9/30/2005	216100	310	779200	0	4170	161	1	42	0	5	7	2	1	8	-32.2			
DW-2	89664	4/17/2005	15:30	1900	1819.7	0.6	9/30/2005	215800	370	778800	0	4820	147	0	41	0	5	7	2	2	10	-32.1			
DW-2	89665	4/17/2005	18:30	1941.7	1859.1	0.27	9/30/2005	216900	330	781100	0	1590	51	0	19	0	3	4	1	1	7	-31.9			
DW-3	89666	4/22/2005	5:40	1250.2	1217.4	0.57	9/30/2005	216000	240	780400	0	3160	142	0	30	0	7	5	2	1	9	-35.4			
DW-3	89667	4/22/2005	7:21	1300	1264.4	0.142	9/30/2005	216700	310	781700	0	1210	53	1	13	0	4	3	2	1	6	-39.6			
DW-3	89668	4/22/2005	9:22	1350	1311.3	0.06	9/30/2005	208300	330	790700	0	582	27	1	9	0	6	3	3	1	8				
DW-3	89669	4/22/2005	11:17	1400	1358.2	0.32	9/30/2005	216100	1700	780000	0	2060	106	0	24	0	4	4	2	1	5	-33.9			
DW-3	89670	4/22/2005	13:50	1450	1404.3	0.65	9/30/2005	216100	2400	778600	0	2600	162	0	56	0	9	13	4	3	13	-32.8			
DW-3	89671	4/22/2005	16:20	1500	1449.7	0.35	9/30/2005	215700	3000	779000	0	2060	142	0	66	0	12	16	4	4	15	-32.5			
DW-3	89672	4/22/2005	20:23	1550	1494.3	0.16	9/30/2005	216800	1700	780400	0	988	60	0	22	0	4	5	2	1	7				
DW-3	89673	4/23/2005	4:45	1600	1537.7	0.17	9/30/2005	217400	830	780800	0	877	35	0	5	0	1	1	0	0	2				
DW-3	89674	4/23/2005	9:38	1650	1581	0.19	9/30/2005	217300	1200	780400	0	1090	36	0	4	0	1	1	0	0	2	-34.2			
DW-3	89675	4/23/2005	15:25	1700	1624.3	0.19	9/30/2005	216800	1500	780500	0	1100	45	0	6	0	1	1	1	0	2	-33.6			
DW-3	89676	4/23/2005	21:30	1750	1667.6	0.21	9/30/2005	217000	1900	779800	0	1270	62	0	12	0	1	1	0	0	2	-33.3			
DW-3	89677	4/24/2005	4:09	1800	1710.9	0.06	9/30/2005	217200	1900	780300	0	567	24	0	8	0	1	2	0	0	1				
DW-3	89678	4/24/2005	8:03	1836.6	1742.9	0.21	9/30/2005	216900	2000	779600	0	1390	59	0	15	0	2	3	1	1	2	-32.9			
DW-3	89679	4/24/2005	9:21	1855.9	1759.9	0.2	9/30/2005	217100	1900	779300	0	1650	67	0	19	0	2	4	1	1	4	-32.5			
DW-3	89680	4/24/2005	10:49	1883.8	1784.5	0.37	9/30/2005	216900	2000	778800	0	2190	96	0	27	0	3	5	1	1	8	-32.7	-23.7	-22.9	cryo-enrichment
DW-3	89681	4/24/2005	14:30	1900	1798.6	0.32	9/30/2005	217000	1900	778800	0	2180	91	0	29	0	4	6	2	2	10	-32.6	-23.6	-22.7	cryo-enrichment
DW-3	89682	4/24/2005	14:30	1950	1842.9	0.31	9/30/2005	216200	2500	778500	0	2660	111	1	35	0	5	6	2	2	10	-32.7			
DW-3	89683	4/24/2005	16:20	1969	1859.9	0.25	9/30/2005	217100	2100	778600	0	2030	100	1	29	0	3	4	1	1	4	-33.2			

Table 1: Isotube data, Halladale-1

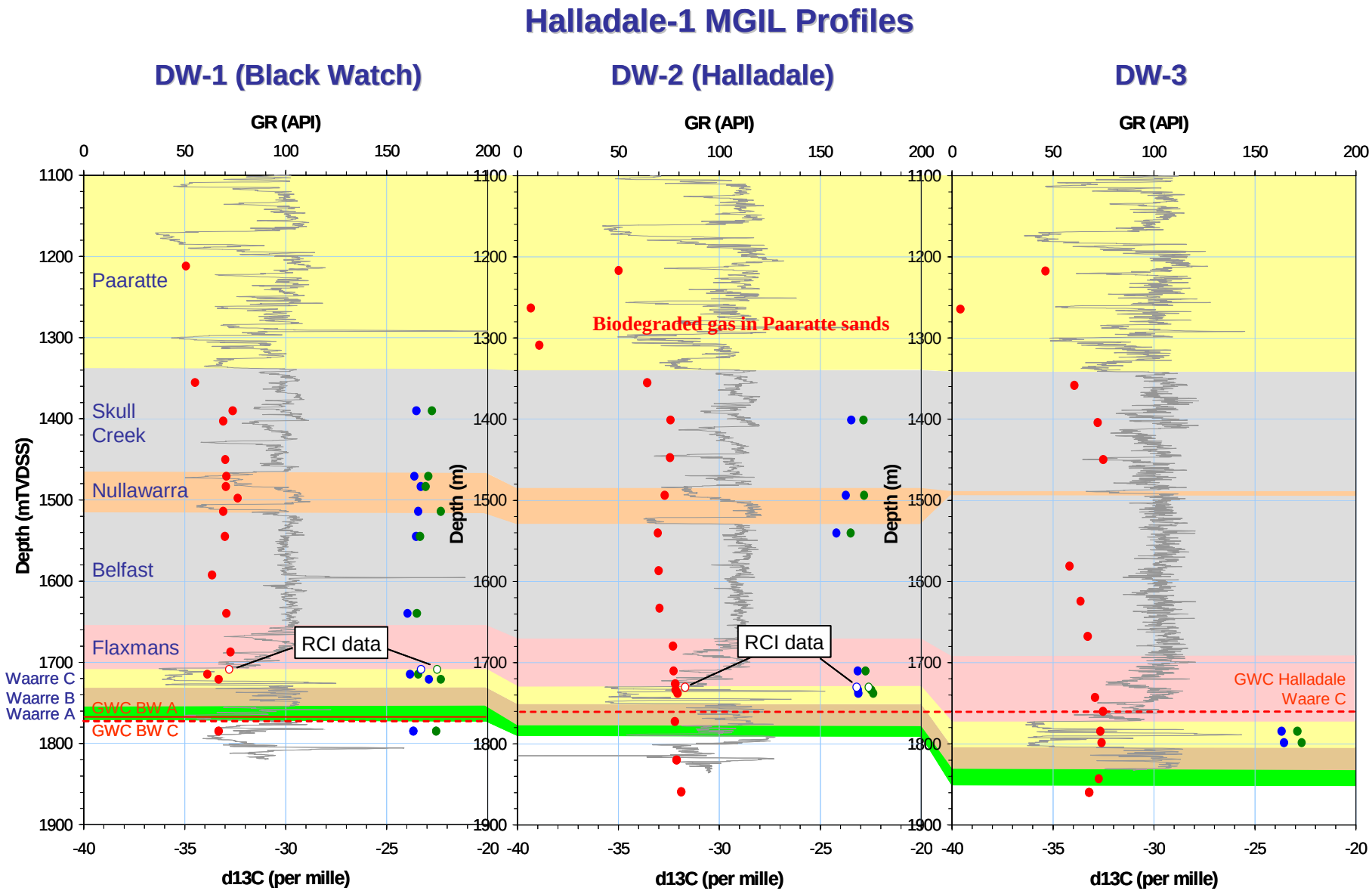

Figure 2: Halladale mud gas isotope profiles (TVDSS)

If available, propane values would have helped to clarify whether biodegradation was indeed the cause of the anomalous isotopic composition of Paarratte gas, as propane is highly sensitive to biodegradation and would be even heavier (less negative) than ethane. Unfortunately, none were obtained within the Paaratte Formation in any of the wells.

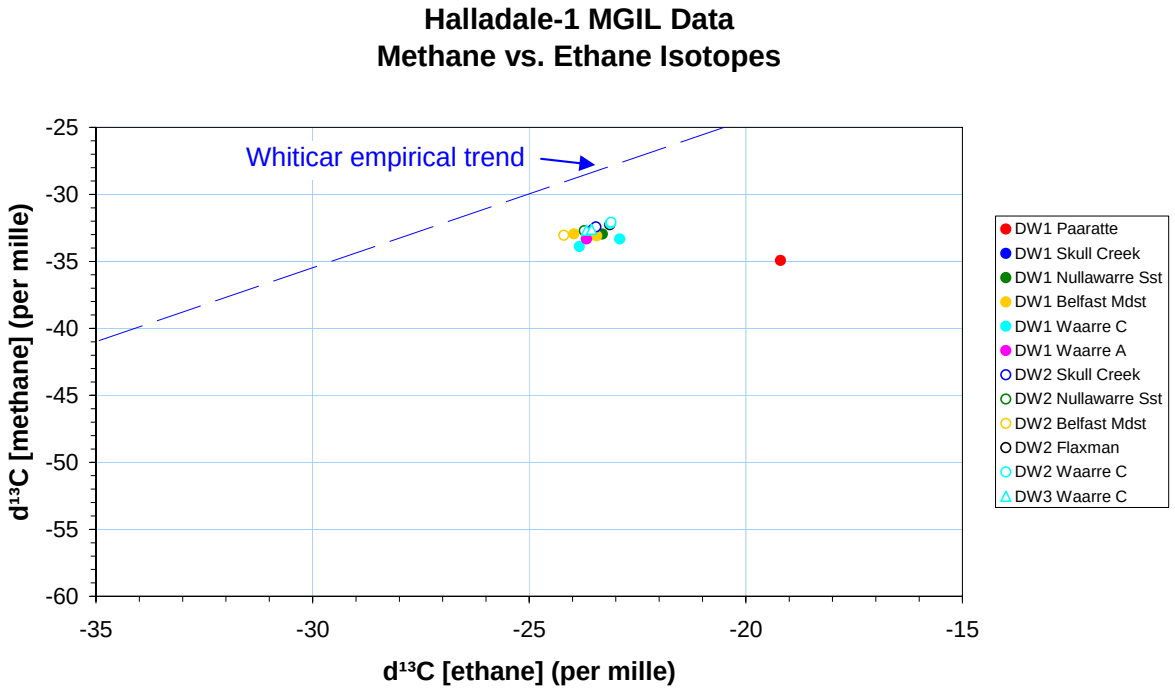

Figure 3: Methane vs ethane isotopes (all isotubes)

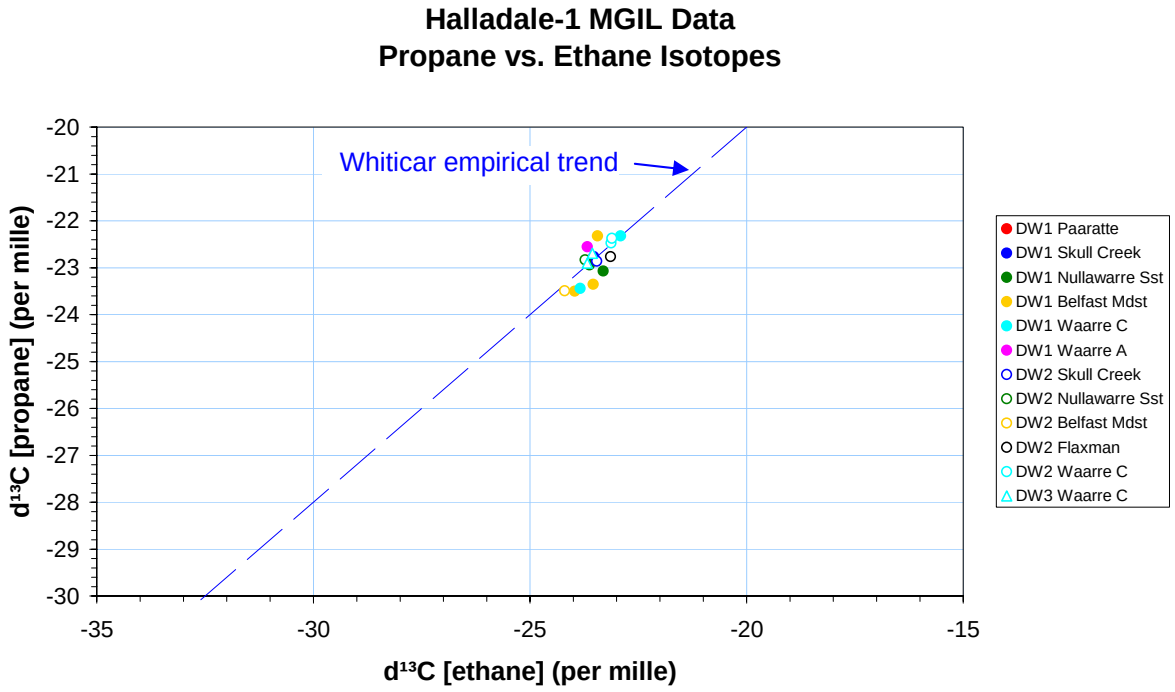

Figure 4: Propane vs ethane isotopes (all isotubes)

As gases are the most mobile of fluids in the subsurface, they are anticipated to reach thermodynamic equilibrium more readily than heavier components of petroleum. Gas isotope data can be measured to a precision of ± 0.1‰ on recovered fluids, and to about ± 0.5‰ in isotube samples. Differences larger than combined sampling and analytical error can therefore be used in a reservoir geochemical context to indicate flow barriers.

The spread in isotope data of c. 2‰ methane and c. 1‰ ethane and propane between the Waarre A and C sands in Halladale-1 DW-1, and Waarre C sands in DW-2 and DW-3 (Figure 5 and Figure 6) hints at compartmentalisation, but given the modest precision of mud gas isotope analysis, it is insufficient to definitively indicate flow barriers between the wells.

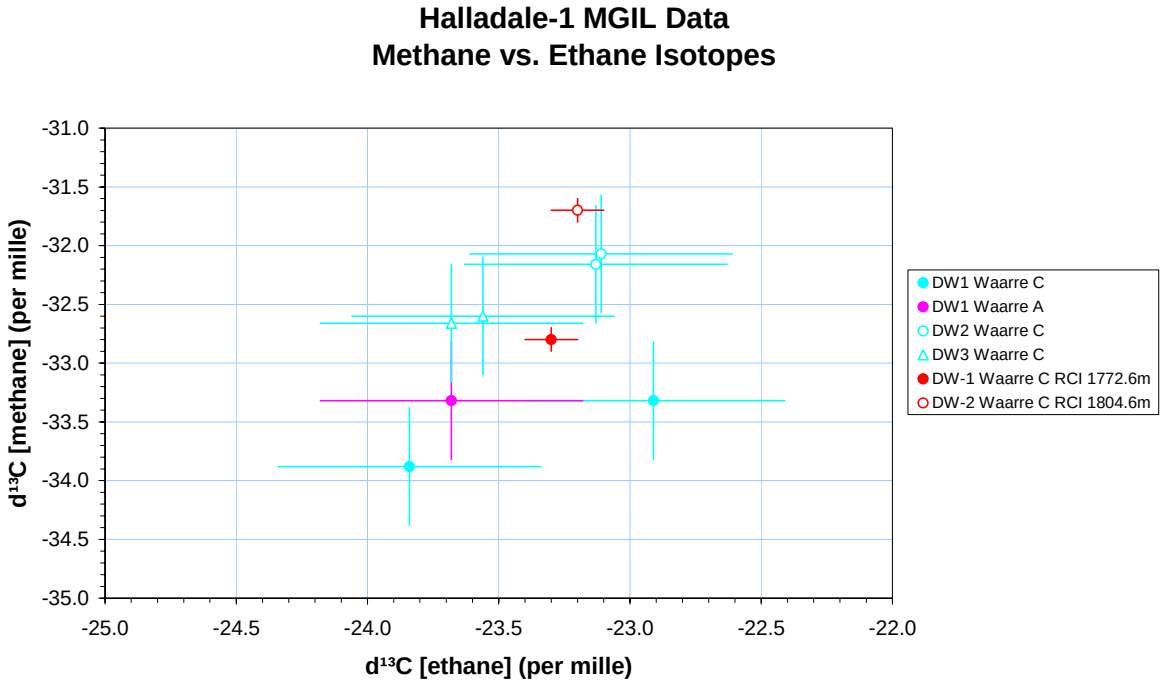

Figure 5: Methane vs ethane isotopes (Waarre isotubes and RCI)

RCI samples collected in Waarre C sands in DW-1 and DW-2 display very similar wet gas isotopes, but differ in methane isotopes by 1.1‰. This is five times the analytical precision, suggesting that Waarre C gas in DW-1 is not in thermodynamic equilibrium with Waarre C gas in DW-2, implying they are in separate compartments. This is supported by pressure profiles, which display an offset of c. 10 psi between gas legs in DW-1 and DW-2 (Figure 7).

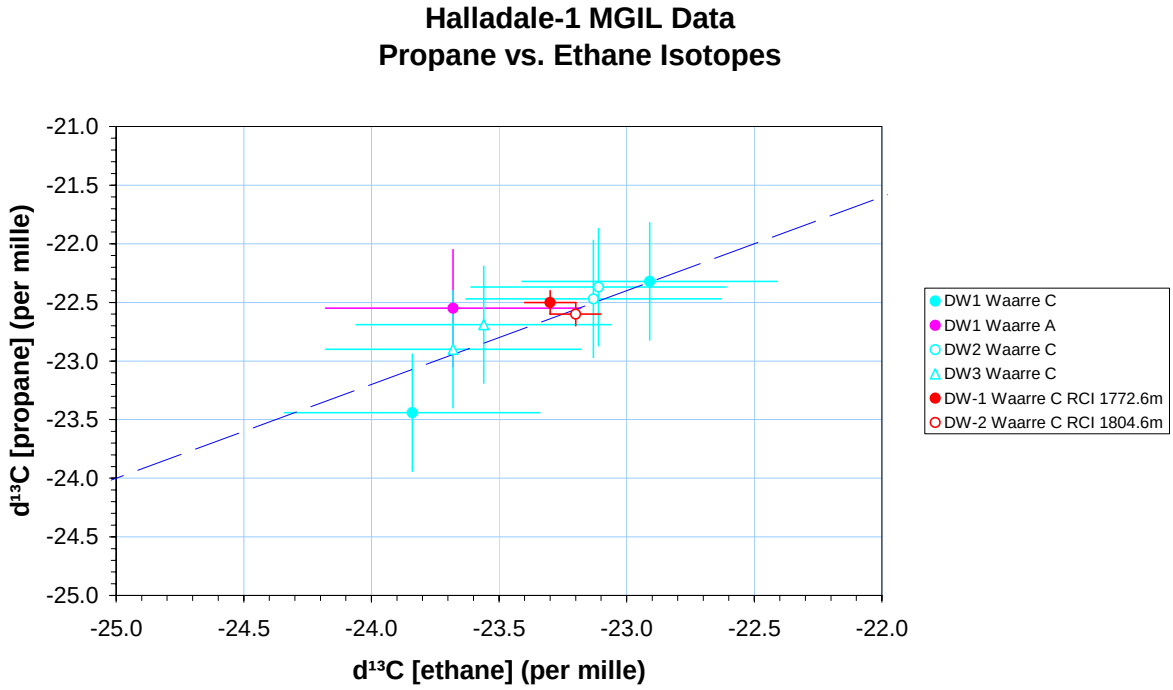

Figure 6: Propane vs ethane isotopes (Waarre isotubes and RCI)

2.3 RCI Gas Inventory

Five 840 cc wireline RCI samples were acquired from the gas columns in Halladale DW-1 (Blackwatch) and Halladale DW-2 (Halladale) (Table 2).

Well	*Date*	*Suite/Run*	*Depth (mKB)*	*Depth (TVDSS)*	*Serial #*	*Transferred into*	*Phase*
DW-1	06/04/05	1/3	1772.6	1708.7	369197		Gas
DW-1	06/04/05	1/3	1772.6	1708.7	369106	L-128	Gas
DW-2	19/04/05	1/3	1804.6	1730.3	189727	L-332	Gas
DW-2	19/04/05	1/3	1804.6	1730.3	189732	L-188	Gas
DW-2	19/04/05	1/3	1804.6	1730.3	189768	L-076	Gas

Table 2: RCI fluid inventory Halladale-1

2.4 Gas Composition

PVT analysis of the Halladale gases was performed at Petrolab (Australia) Pty Ltd., Magill, South Australia. The gases proved to be methane-rich (88-91%) with small amounts of nitrogen (1.4-1.9%) and carbon dioxide (0.4-0.5%) (Table 3). CGR is negligible at < 2

bbl/mmscf gas. PVT analyses suggest that Halladale-1 DW1 is wetter than gases from DW2, raising the possibility of a separate compartment. Compartmentalisation is supported by RCI data, which indicate a pressure offset of c. 10 psi between DW1 and DW2 gas legs. Differences in composition between DW1 and DW2 are not, however, supported by the pressure data. If anything, DW2 displays a slightly higher gradient than DW1, implying a denser (more liquids-rich) gas, although the difference between 0.19 psi/m and 0.206 psi/m is likely to be within measurement error.

Well	***DW-1***	***DW-2***	***DW-2***	***DW-2***
Depth (TVDSS)	1708.7	1730.3	1730.3	1730.3
Cylinder #	L-128	L-332	L-188	L-076
CO2	0.46	0.47	0.39	0.50
N2	1.88	1.36	1.36	1.38
C1	87.88	90.74	90.50	90.91
C2	5.30	4.17	4.26	4.20
C3	2.19	1.62	1.59	1.61
iC4	0.56	0.30	0.38	0.32
nC4	0.59	0.38	0.42	0.35
iC5	0.19	0.12	0.13	0.11
nC5	0.15	0.10	0.11	0.09
C6	0.26	0.18	0.20	0.15
C7	0.34	0.27	0.30	0.21
C8	0.12	0.10	0.16	0.07
C9	0.08	0.09	0.12	0.05
C10	0.03	0.06	0.07	0.02
C11	0.00	0.03	0.01	0.03
C12	0.00	0.01	0.00	0.00
Calculated CGR (bbl/MMSCF @ STP)	-	1.4	0.4	0.3
Wetness (C2-C4/C1-C4)	9.0%	6.7%	6.8%	6.7%

Table 3: Gas compositions from PVT analysis (Petrolab)

Gases from DW1 and DW2 were subjected to compositional and isotope analysis by Isolab in the Netherlands. Gas compositions were found to be extremely similar between the PVT and geochemistry labs (Figure 8).

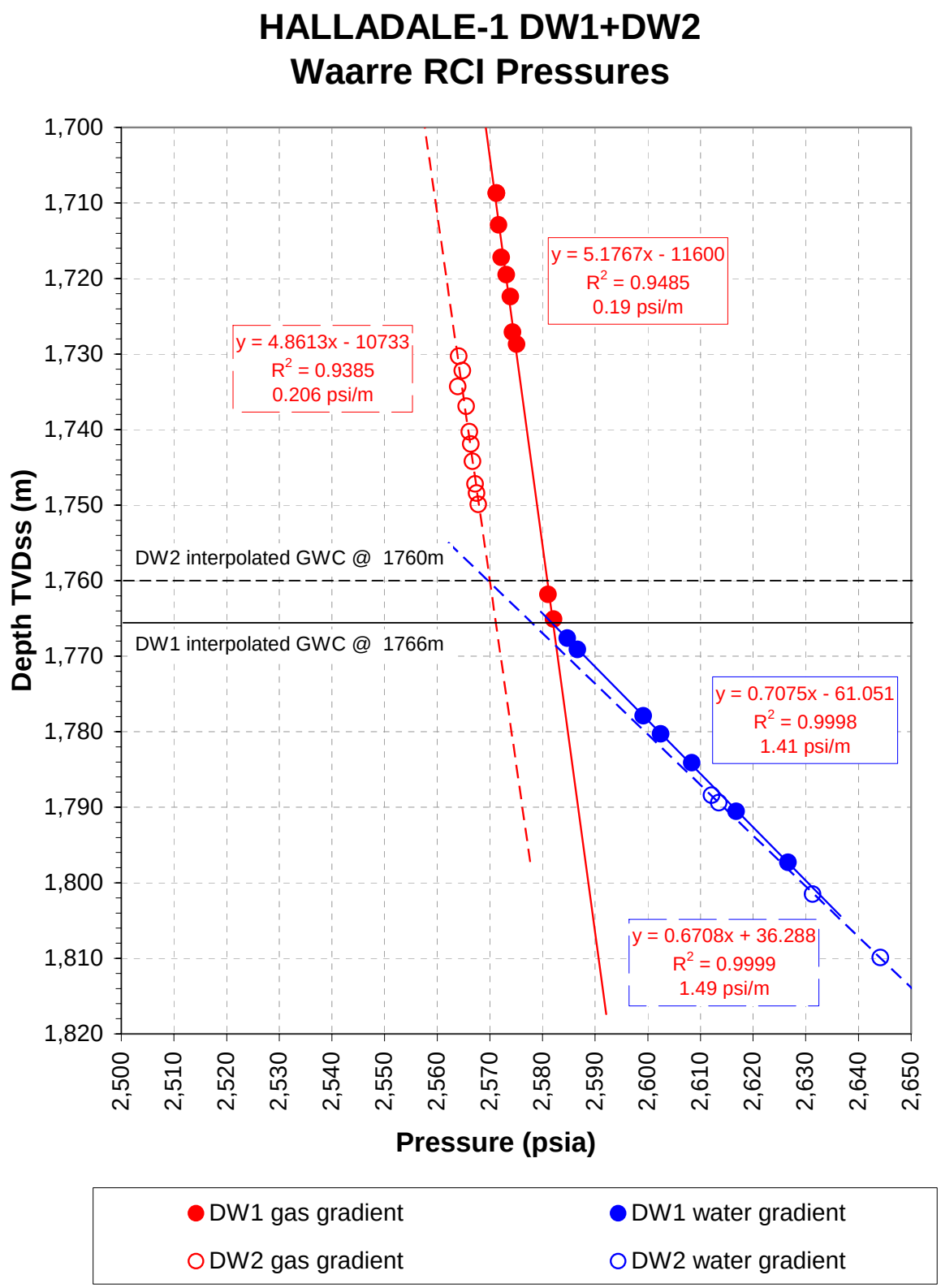

Figure 7: Comparison of Halladale-1 DW1 and DW2 RCI pressure gradients

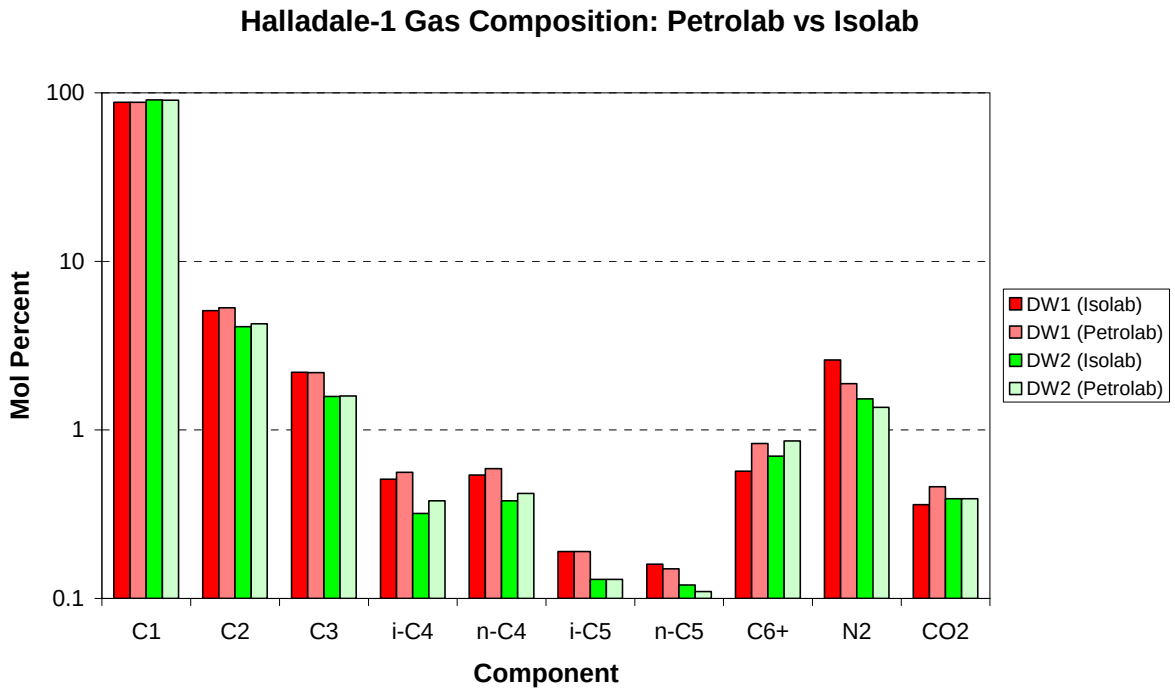

Figure 8: Gas compositions, DW1 and DW2 (Petrolab vs Isolab)

Pixler ratios show that the distribution of gaseous hydrocarbons in Halladale is comparable to Thylacine and La Bella, but somewhat drier (more mature) than Geographe and wetter (less mature) than Minerva. Pine Lodge and Boggy Creek gases are very dry, suggesting they are either highly mature, primarily biogenic of severely biodegraded. The anomalously high C1/C3 ratio of the former suggests it has been biodegraded, as propane is the earliest wet gas component to be removed by bacterial action, whereas the latter does not display anomalous C1/C3 ratio, so is likely to be either highly mature, or mixed with a large proportion of biogenic methane. Boggy Creek methane is in fact isotopically heavy (-35.5‰) suggesting it is dry due to expulsion from a high maturity source.

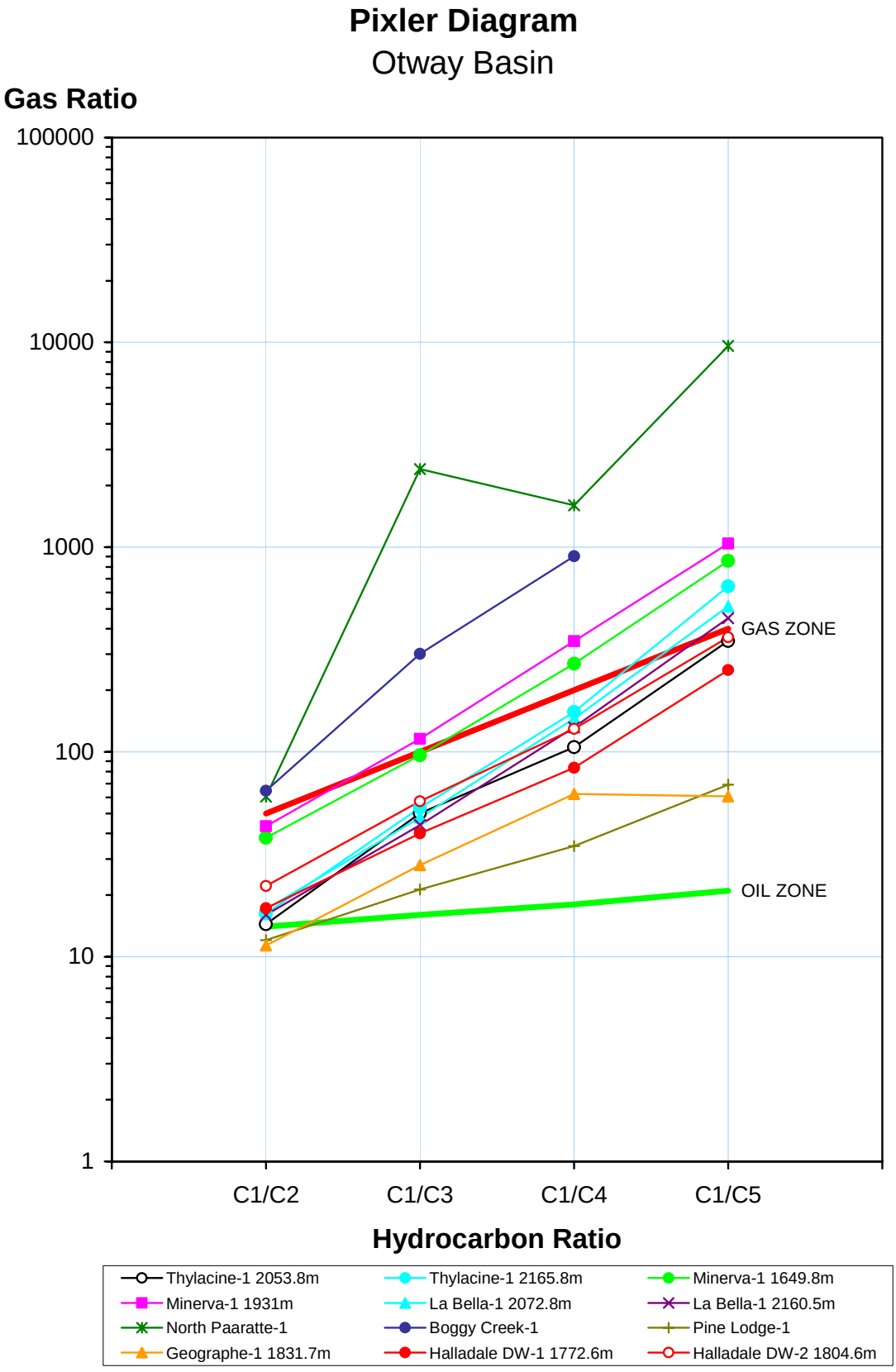

Figure 9: Pixler plot of Otway Basin gases

2.5 Isotope Analyses

The objectives of isotopic analysis of petroleum gases are threefold - firstly to establish the maturity and provenance of the gas; secondly to corroborate the modelled maturity of the proposed source rock in the basin model, and thirdly to provide an indication of communication between reservoirs. Gases, particularly methane, are highly mobile and may be expected to reach thermodynamic equilibrium rapidly in the subsurface. Differences in composition, particularly isotopic composition, may be interpreted in conjunction with the fill-spill history, to infer connectivity or compartmentalisation between adjacent wells.

The isotopic composition of the Halladale gases was determined by Isolab in Neerijnen, Holland and results are presented in Table 4. As previously observed, methane differs by about 1‰ between the two gases, which is significantly greater than experimental error (± 0.1‰), supporting the contention that DW1 and DW2 are in separate compartments.

Sample ID	$\delta^{13}C$ C_1	$\delta^{13}C$ C_2	$\delta^{13}C$ C_3	$\delta^{13}C$ i-C_4	$\delta^{13}C$ n-C_4	$\delta^{13}C$ i-C_5	$\delta^{13}C$ n-C_5	δD C_1	$\delta^{13}C$ CO_2	$\delta^{15}N$ N_2
DW1 1772.6 mKB	-32.8	-23.3	-22.5	-22.0	-21.6	-22.5	-22.2	-166.0	-12.9	-4.3
DW2 1804.6 mKB	-31.7	-23.2	-22.6	-22.1	-21.9	-22.9	-22.8	-163.0	-12.2	+4.1

Table 4: Isotopic composition of Halladale gas

Halladale-1 gas contains almost the most isotopically heavy (least negative) methane values encountered in the Otway basin to date. Conventional interpretation using a Schoell diagram suggests they were expelled toward the base of the conventional gas window for marine (labile) source rocks (Figure 10).

A Whiticar plot of methane versus ethane and propane isotope data reveals that methane is highly discordant with wet gases and therefore is probably not co-genetic. Halladale methane-ethane and methane-propane pairs lie far from the empirical trends observed by Whiticar, suggesting mixing with a proportion of bacterial methane (Figure 11). Whiticar's ethane-propane plot, however, suggests that the wet gases are concordant, and on account of their extremely heavy (less negative) isotopic composition, could have been generated at very high maturity (c. 2.5% Ro. vit.).

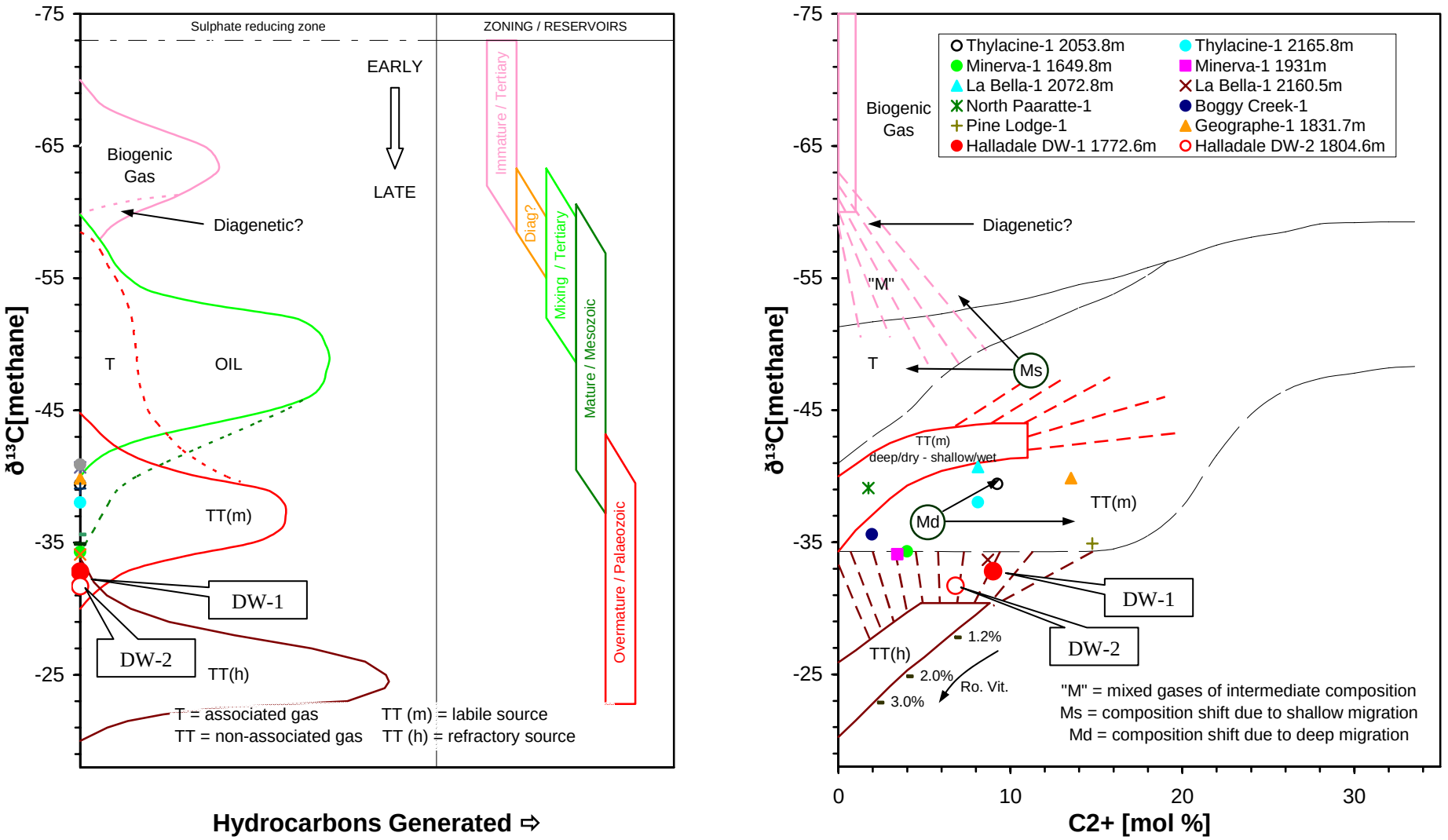

Figure 10: Schoell's genetic classification of natural gases

The proportion of wet gas components makes it unlikely that Halladale gas is highly mature, and is it more probable that the source kerogen is either humic (terrestrial), and/or isotopically heavy (e.g. lacustrine).

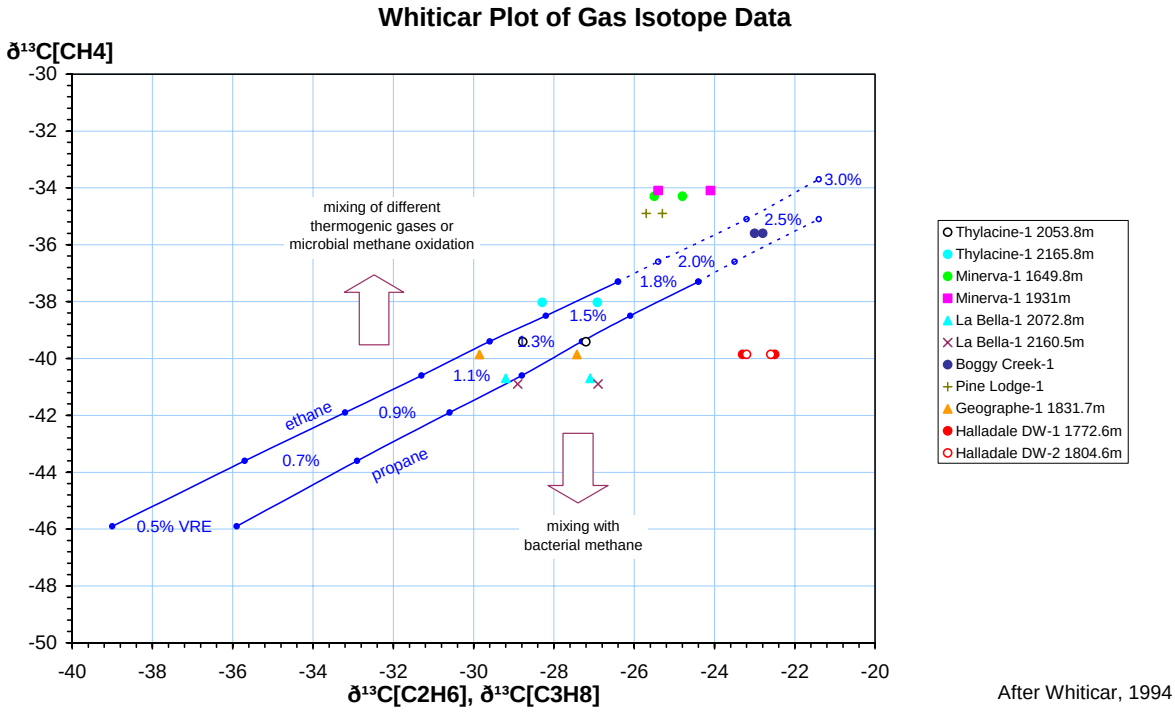

After Whiticar, 1994

Figure 11: Whiticar plot of methane vs. ethane and propane isotopes

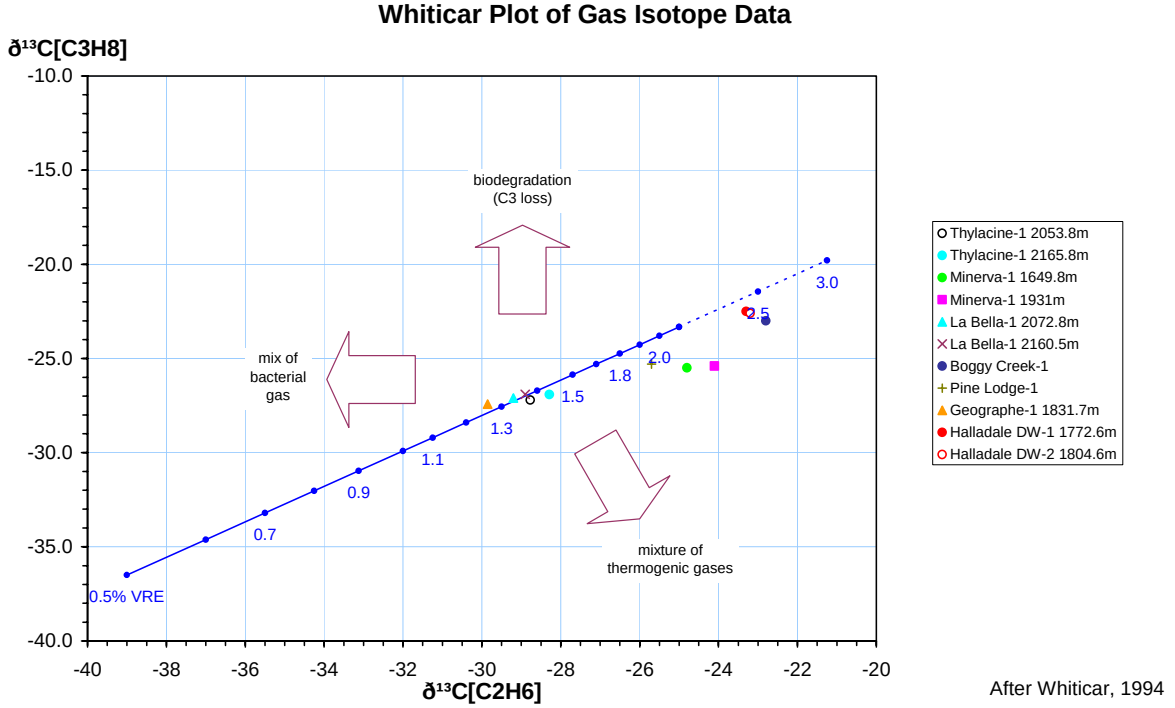

After Whiticar, 1994

Figure 12: Whiticar plot of propane vs. ethane isotopes

Halladale wet gas is isotopically very similar to Boggy Creek, suggesting it may be genetically related (Figure 12). This is reinforced by the proximity of the two fields (Figure 1). Open file isotope data from the Shipwreck Trough suggest there are three families of fluids. Halladale gas has an affinity with the Casino Field to the south, and onshore Fenton Creek, Lavers and Mylor discoveries to the north, but not with Minerva to the southeast (Figure 13).

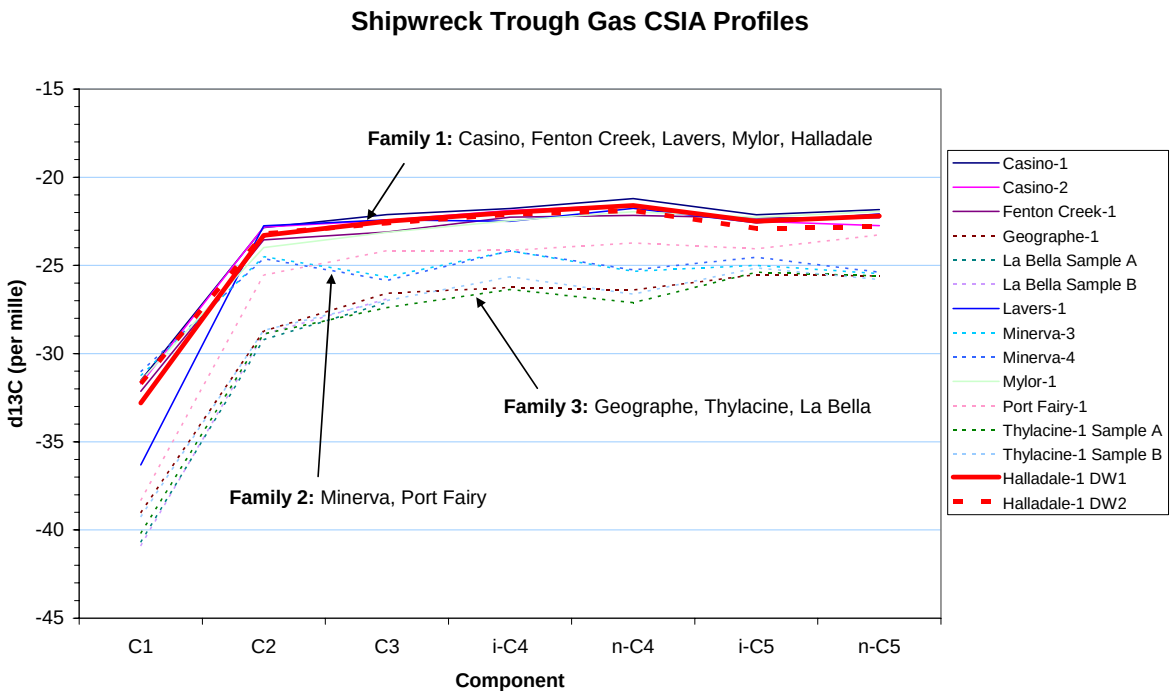

Figure 13: Shipwreck Trough Gas CSIA Profiles

2.6 Condensate CSIA

Combining the isotopic composition of the gas with the delta-^{13}C isotopic composition of the condensate yields a whole fluid CSIA profile. This is plotted together with paraffin concentration in normalised mole percent in Figure 14. Oil range paraffins become increasingly isotopically light (i.e. more negative) with increasing carbon number. This is characteristic of a high maturity (isotopically heavy) gas mixing with a less mature (isotopically light) liquids fraction, and suggests either multiple source rocks or multiple charge events have resulted in a mixed fluid in the Halladale structure.

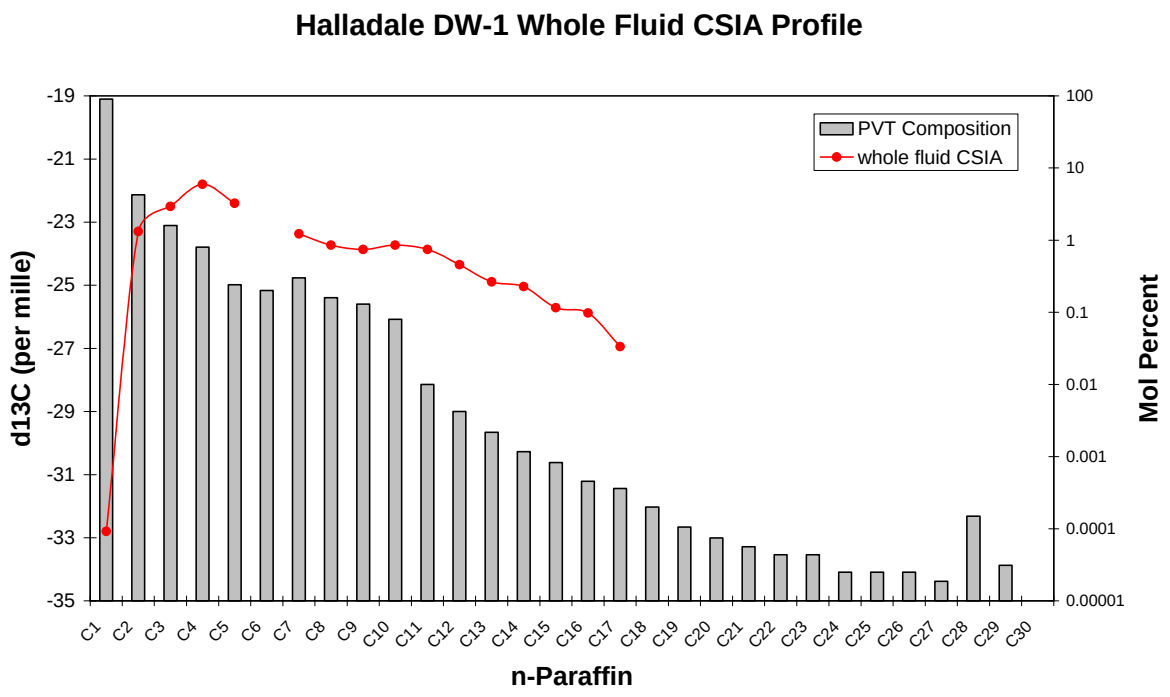

Figure 14: Halladale DW-1 whole fluid CSIA Profile

2.7 Non-Hydrocarbon Gases

Halladale gas contains 0.4-0.5% CO_2 and 1.4-1.9% nitrogen (Table 3). Stable carbon isotope analysis of the carbon dioxide yielded $\delta^{13}C$ values of -12.2 to -12.9‰. This is typical of CO_2 generated as a by product of marine or freshwater methanogenesis (Figure 15). It is also close to the range of isotope values observed in CO_2 expelled from Type III organic matter during diagenesis, and is therefore unlikely to be related to the high levels of CO_2 seen in onshore fields such as Caroline, which are of a magmatic or juvenile origin.

Nitrogen unexpectedly yielded quite different isotopic composition between DW-1 and DW-2 gas. The former displays $\delta^{15}N$ of -4.3‰ (relative to air, with $\delta^{15}N$ of 0‰) whereas the latter contained $\delta^{15}N$ of +4.1‰. This was queried with Isolab and the values confirmed. The gases were measured consecutively, followed by a standard, and there is no obvious reason why they should differ by more than 8‰.

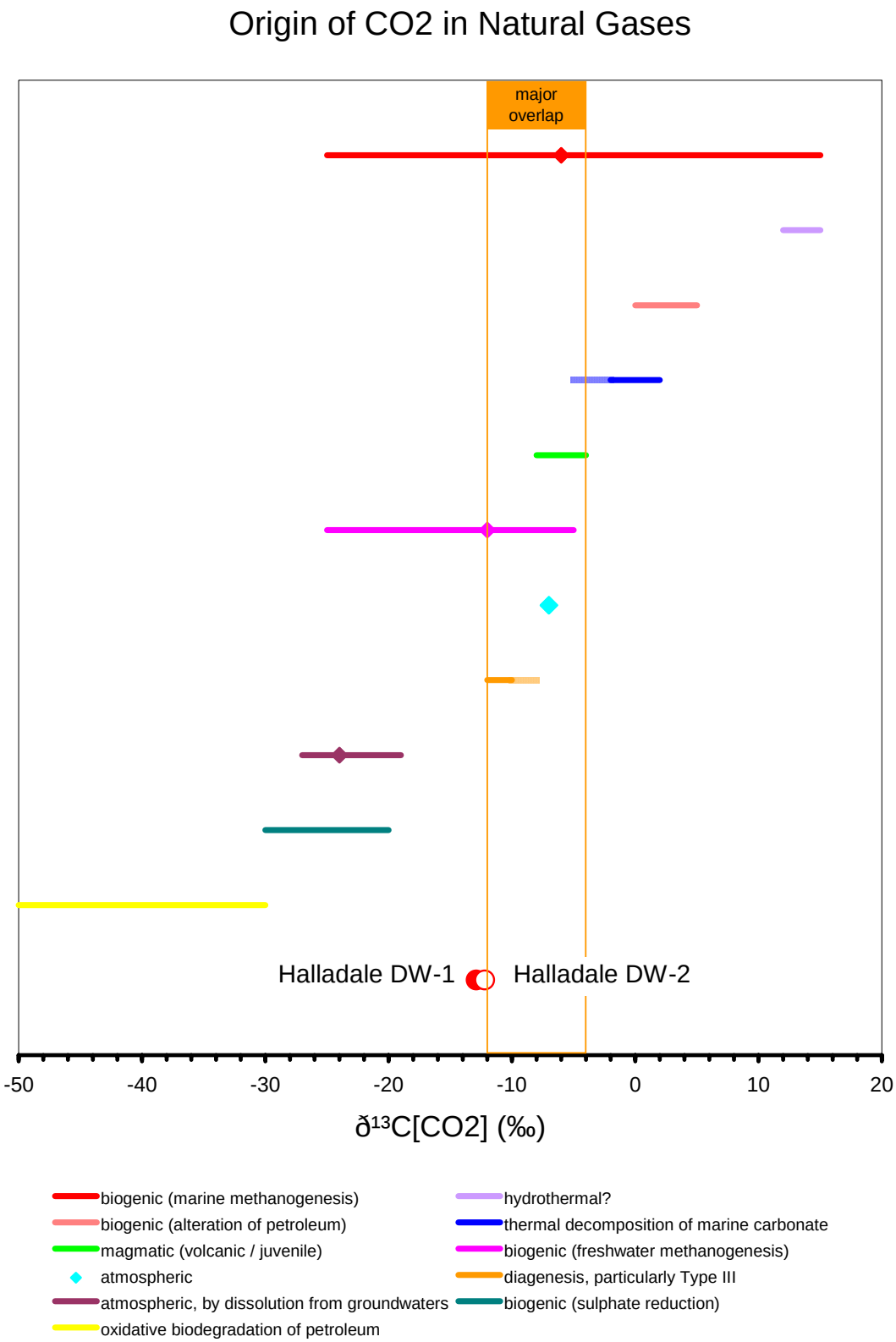

Figure 15: Genetic origin of CO_2 in natural gases

3 Conclusions

- Halladale gases are fairly dry, consisting of 88-91% methane and 7-9% wet gas, with 0.4-0.5% CO_2 and 1.4-1.9% nitrogen. Pixler ratios are consistent with a gas expelled within the early to peak gas window.

- Stable carbon isotope ratios are suggestive of a highly mature gas, expelled towards the base of the conventional gas window, but it is more probable that the origin of these isotope ratios is an isotopically heavy humic or lacustrine source kerogen at a much lower level of thermal maturity.

- Isotope data from isotubes are insufficiently distinctive to definitively indicate flow barriers between the Waarre A and C sands in Halladale-1 DW-1, and Waarre C sands in DW-2 and DW-3. RCI samples from Waarre C sands in DW-1 and DW-2 are isotopically distinctive, suggesting they are in separate compartments. This is supported by pressure profiles, which display an offset of c. 10 psi.

- On the basis of isotope profiles, three families of gases are identified in the Shipwreck Trough. Halladale has an affinity with other Family 1 gases, Boggy Creek, Casino, Fenton Creek, Lavers and Mylor. It is unrelated to Family 2 (Geographe, Thylacine, La Bella) or Family 3 (Minerva, Port Fairy).

- A strongly inclined paraffin CSIA (compound specific isotope) profile suggests mixing of a high maturity isotopically heavy gas, with a less mature isotopically light gas. This may be the result of either multiple source rocks or multiple charge events contributing to the Halladale accumulation.

- Carbon dioxide is isotopically light and was most likely expelled from Type III organic matter during diagenesis.

Isotech Mudgas Data (Isotubes)

Halladale-1

Well Name	Isotech Lab No.	Sample Date	Sample Time	Depth 1 Meters	TVDSS Meters	Gas Units %	GC Date	O_2 + Ar ppm	CO_2 ppm	N_2 ppm	CO ppm	C_1 ppm	C_2 ppm	C_2H_4 ppm	C_3 ppm	C_3H_6 ppm	iC_4 ppm	nC_4 ppm	iC_5 ppm	nC_5 ppm	C_6+ ppm	$\delta^{13}C_1$ per mil	$\delta^{13}C_2$ per mil	$\delta^{13}C_3$ per mil	Comments	Formation
DW-1	89606	3/30/2005	12:45	850	827	0.0203	9/29/2005	219600	660	779700	0	4	0	0	0	0	0	0	0	0	1					Pember Mdst
DW-1	89607	3/31/2005	3:01	908.8	886.6	0.011	9/29/2005	219700	430	779900	0	4	0	0	0	0	0	0	0	0	2					Pebble Point
DW-1	89608	3/31/2005	4:03	951.7	929.1	0.052	9/29/2005	209900	4300	785700	0	68	3	0	1	1	1	0	3	1	57					Paaratte
DW-1	89609	3/31/2005	5:21	1003	979.4	0.052	9/29/2005	207200	5300	787400	0	58	3	1	1	1	1	0	2	1	67					Paaratte
DW-1	89610	3/31/2005	6:07	1050.7	1025.3	0.119	9/29/2005	204600	4800	790100	0	428	6	3	1	1	1	0	2	1	65					Paaratte
DW-1	89611	3/31/2005	7:22	1101	1072.9	0.152	9/29/2005	200300	6100	793100	0	404	11	7	1	1	1	0	2	1	69					Paaratte
DW-1	89612	3/31/2005	8:34	1150	1118.9	0.092	9/29/2005	207000	6900	785800	0	213	9	6	1	1	1	0	1	0	33					Paaratte
DW-1	89613	3/31/2005	10:04	1200	1166.6	0.104	9/29/2005	203300	4800	791500	0	292	10	3	10	1	12	10	5	3	62					Paaratte
DW-1	89614	3/31/2005	11:58	1248.6	1211.9	1.376	9/29/2005	201600	6300	787700	140	3950	174	40	21	6	19	11	6	4	71	-34.9	-19.2			Paaratte
DW-1	89615	3/31/2005	12:01	1250.3	1213.6	0.508	9/29/2005	201300	6800	787900	30	3610	175	10	22	2	22	12	7	4	67					Paaratte
DW-1	89616	3/31/2005	14:08	1300	1260.6	0.04	9/29/2005	219800	690	779500	0	28	1	0	0	0	0	0	0	0	4					Paaratte
DW-1	89617	3/31/2005	16:01	1350.3	1308.3	0.1	9/29/2005	214800	4800	779600	0	720	24	1	3	0	6	2	2	1	19					Paaratte
DW-1	89618	3/31/2005	18:02	1400	1355.5	0.59	9/29/2005	210700	6200	777100	0	5450	336	1	102	1	20	20	5	3	16	-34.5				Skull Creek
DW-1	89619	3/31/2005	20:58	1436.4	1390	2	9/29/2005	199700	6200	749100	0	42600	1630	0	489	1	72	83	19	14	45					Skull Creek
DW-1	89620	3/31/2005	21:00	1436.6	1390.2	4.1	9/29/2005	193300	6400	731500	0	65200	2500	0	737	1	107	121	28	21	67	-32.6	-23.5	-22.8		Skull Creek
DW-1	89621	3/31/2005	21:37	1450.2	1403.1	1.17	9/29/2005	207600	6900	774300	0	10300	586	0	219	0	35	45	10	8	34	-33.1				Skull Creek
DW-1	89622	4/01/2005	12:22	1500	1450.3	1.07	9/29/2005	204200	9000	775600	0	10200	601	0	255	1	45	58	14	11	47	-33.0				Skull Creek
DW-1	89623	4/01/2005	1:27	1521.4	1470.6	5.881	9/29/2005	195800	8600	745700	0	47600	1570	0	467	1	70	85	19	15	50	-32.9	-23.6	-22.9		Nullawarre Sst
DW-1	89624	4/01/2005	1:33	1522.2	1471.3	5.838	9/29/2005	199400	7900	747600	0	43000	1420	0	423	1	63	77	17	14	41					Nullawarre Sst
DW-1	89625	4/01/2005	1:48	1535.3	1483.7	23.015	9/29/2005	159600	9100	629100	0	193000	6700	0	1810	1	234	265	56	43	99	-33.0	-23.3	-23.1		Nullawarre Sst
DW-1	89626	4/01/2005	2:27	1550	1497.7	1.181	9/29/2005	212500	5200	775100	0	6620	349	0	129	0	20	27	6	5	22	-32.4				Nullawarre Sst
DW-1	89627	4/01/2005	3:04	1566.1	1512.9	11.56	9/29/2005	187000	7100	699400	0	101700	3420	1	958	1	130	149	32	25	58					Belfast Mdst
DW-1	89628	4/01/2005	3:06	1567.5	1514.3	22.495	9/29/2005	167400	8000	636600	0	179500	6190	0	1690	1	220	248	53	40	93	-33.1	-23.4	-22.3		Belfast Mdst
DW-1	89629	4/01/2005	4:19	1600	1545	1.307	9/29/2005	209500	8100	773300	0	8420	419	0	130	0	22	31	8	7	33	-33.0	-23.5	-23.4		Belfast Mdst
DW-1	89630	4/01/2005	6:31	1650	1592.4	1.202	9/29/2005	208100	8600	774200	0	8640	338	0	61	1	14	19	7	6	32	-33.6				Belfast Mdst
DW-1	89631	4/01/2005	8:25	1700	1639.9	1.038	9/29/2005	197100	6400	788400	0	7470	449	2	134	1	19	23	8	7	37	-32.9	-24.0	-23.5		Belfast Mdst
DW-1	89632	4/01/2005	10:35	1750	1687.3	0.437	9/29/2005	216600	3400	777900	0	1910	104	0	36	0	5	7	2	2	10	-32.7				Flaxman
DW-1	89633	4/01/2005	11:52	1778.9	1714.6	31.91	9/29/2005	142200	9900	548200	0	282200	12400	0	3750	3	493	495	102	75	149	-33.9	-23.8	-23.4		Waarre C
DW-1	89634	4/01/2005	12:27	1785.5	1721	41.02	9/30/2005	127300	10500	516500	0	325000	14500	0	4560	3	620	624	130	96	173	-33.3	-22.9	-22.3		Waarre C
DW-1	89635	4/04/2005	6:18	1800.4	1735.1	0.1	9/30/2005	218100	760	780300	0	749	50	0	16	0	2	3	1	1	6					Waarre B
DW-1	89636	4/04/2005	8:14	1852.5	1784.8	0.31	9/30/2005	217000	1100	777800	0	3800	189	0	56	0	7	9	2	2	7	-33.3	-23.7	-22.6	**	Waarre A
DW-1	89637	4/04/2005	14:05	1900	1830.4	0.05	9/30/2005	216600	2000	780700	0	596	26	0	13	0	3	5	1	1	8					Eumarella
DW-1	89638	4/04/2005	16:44	1918	1847.7	0.09	9/30/2005	215700	2600	781100	0	566	21	0	9	0	3	4	2	1	9					Eumarella

Isotech Mudgas Data (Isotubes)

Halladale-1

Well Name	Isotech Lab No.	Sample Date	Sample Time	Depth 1 Meters	TVDSS Meters	Gas Units %	GC Date	O_2 + Ar ppm	CO_2 ppm	N_2 ppm	CO ppm	C_1 ppm	C_2 ppm	C_2H_4 ppm	C_3 ppm	C_3H_6 ppm	iC_4 ppm	nC_4 ppm	iC_5 ppm	nC_5 ppm	C_6+ ppm	$\delta^{13}C_1$ per mil	$\delta^{13}C_2$ per mil	$\delta^{13}C_3$ per mil	Comments	Formation
DW-2	89639	4/11/2005	12:50	901.5	879.4	0.021	9/30/2005	216000	110	783800	0	23	2	0	2	0	1	1	2	1	23					Pebble Point
DW-2	89640	4/11/2005	2:41	950.2	928.1	0.028	9/30/2005	212400	100	787300	0	143	5	0	2	0	2	1	3	2	50					Paaratte
DW-2	89641	4/11/2005	4:22	1001.9	979.5	0.028	9/30/2005	209200	80	790600	0	92	3	0	1	0	1	1	3	1	49					Paaratte
DW-2	89642	4/11/2005	6:06	1056.3	1033.2	0.047	9/30/2005	215000	110	784700	0	186	4	0	2	0	1	1	1	1	35					Paaratte
DW-2	89643	4/11/2005	8:01	1107.1	1082.3	0.03	9/30/2005	212800	130	786800	0	187	4	0	1	0	1	1	1	1	26					Paaratte
DW-2	89644	4/11/2005	10:02	1150.1	1123.6	0.041	9/30/2005	212900	110	786900	0	64	2	0	1	0	1	1	1	0	18					Paaratte
DW-2	89645	4/11/2005	13:45	1200	1170.3	0.06	9/30/2005	212200	150	787400	0	195	4	1	2	0	3	2	2	1	25					Paaratte
DW-2	89646	4/11/2005	16:30	1250	1216.7	0.71	9/30/2005	211500	130	782300	0	5710	256	1	56	0	12	10	4	3	36	-35.0				Paaratte
DW-2	89647	4/11/2005	19:00	1300	1262.9	0.34	9/30/2005	210700	110	786300	0	2590	131	2	43	1	16	12	7	4	48	-39.3				Paaratte
DW-2	89648	4/11/2005	21:24	1350	1309	0.21	9/30/2005	211200	110	787400	0	1100	56	3	20	1	12	7	5	3	35	-38.9				Paaratte
DW-2	89649	4/12/2005	2:35	1400	1354.9	0.202	9/30/2005	211700	110	786900	0	1160	80	0	25	0	9	8	5	3	37	-33.6				Skull Creek
DW-2	89650	4/12/2005	9:20	1450	1400.9	0.51	9/30/2005	213400	130	781700	0	4280	289	1	116	0	19	26	7	6	41	-32.4	-23.5	-22.9		Skull Creek
DW-2	89651	4/12/2005	16:30	1500	1447.3	0.35	9/30/2005	215100	170	781900	0	2560	112	1	51	0	12	17	6	5	36	-32.4				Skull Creek
DW-2	89652	4/13/2005	19:00	1550	1493.8	0.79	9/30/2005	211200	320	779800	0	8320	258	0	59	1	7	9	3	3	22	-32.7	-23.7	-22.8		Nullawarre Sst
DW-2	89653	4/13/2005	20:30	1600	1540.2	0.78	9/30/2005	210800	330	780800	0	7640	322	0	71	1	8	10	3	3	21	-33.1	-24.2	-23.5		Belfast Mdst
DW-2	89654	4/14/2005	0:32	1650	1586.6	0.53	9/30/2005	213500	560	782100	0	3590	149	6	25	1	5	5	2	2	19	-33.0				Belfast Mdst
DW-2	89655	4/14/2005	5:38	1700	1633	0.59	9/30/2005	210700	810	783800	0	4480	183	1	37	1	5	4	2	1	10	-33.0				Belfast Mdst
DW-2	89656	4/14/2005	17:30	1750	1679.5	0.26	9/30/2005	210400	220	787300	0	1900	86	1	28	0	4	6	2	2	8	-32.3				Flaxman
DW-2	89657	4/14/2005	21:10	1783	1710.2	3.52	9/30/2005	199600	290	748700	0	49500	1450	0	346	1	40	44	9	7	21	-32.3	-23.1	-22.8		Flaxman
DW-2	89658	4/15/2005	0:37	1800	1726.1	0.99	9/30/2005	210900	290	780600	0	7770	273	2	87	1	13	16	4	4	16	-32.2				Flaxman
DW-2	89659	4/15/2005	1:50	1805.8	1731.4	4.32	9/30/2005	198200	270	744200	0	54900	1750	1	473	1	62	68	15	12	35					Waarre C
DW-2	89660	4/15/2005	3:17	1807.9	1733.4	12.623	9/30/2005	154400	280	600300	0	234700	7630	2	2000	2	242	258	51	39	81	-32.2	-23.1	-22.5		Waarre C
DW-2	89661	4/16/2005	2:25	1809.7	1735.1	7.13	9/30/2005	200200	270	738400	0	58600	1830	1	473	1	59	66	14	12	37					Waarre C
DW-2	89662	4/16/2005	2:50	1812.5	1737.7	28.3	9/30/2005	162200	270	599700	0	226700	8120	3	2210	3	264	286	59	45	100	-32.1	-23.1	-22.4		Waarre C
DW-2	89663	4/17/2005	17:15	1850	1772.6	0.52	9/30/2005	216100	310	779200	0	4170	161	1	42	0	5	7	2	1	8	-32.2				Waarre B
DW-2	89664	4/17/2005	15:30	1900	1819.7	0.6	9/30/2005	215800	370	778800	0	4820	147	0	41	0	5	7	2	2	10	-32.1				Eumarella
DW-2	89665	4/17/2005	18:30	1941.7	1859.1	0.27	9/30/2005	216900	330	781100	0	1590	51	0	19	0	3	4	1	1	7	-31.9				Eumarella

Isotech Mudgas Data (Isotubes)

Halladale-1

Well Name	Isotech Lab No.	Sample Date	Sample Time	Depth 1 Meters	TVDSS Meters	Gas Units %	GC Date	O_2 + Ar ppm	CO_2 ppm	N_2 ppm	CO ppm	C_1 ppm	C_2 ppm	C_2H_4 ppm	C_3 ppm	C_3H_6 ppm	iC_4 ppm	nC_4 ppm	iC_5 ppm	nC_5 ppm	C_6+ ppm	$\delta^{13}C_1$ per mil	$\delta^{13}C_2$ per mil	$\delta^{13}C_3$ per mil	Comments	Formation
DW-3	89666	4/22/2005	5:40	1250.2	1217.4	0.57	9/30/2005	216000	240	780400	0	3160	142	0	30	0	7	5	2	1	9	-35.4				Paaratte
DW-3	89667	4/22/2005	7:21	1300	1264.4	0.142	9/30/2005	216700	310	781700	0	1210	53	1	13	0	4	3	2	1	6	-39.6				Paaratte
DW-3	89668	4/22/2005	9:22	1350	1311.3	0.06	9/30/2005	208300	330	790700	0	582	27	1	9	0	6	3	3	1	8					Paaratte
DW-3	89669	4/22/2005	11:17	1400	1358.2	0.32	9/30/2005	216100	1700	780000	0	2060	106	0	24	0	4	4	2	1	5	-33.9				Skull Creek
DW-3	89670	4/22/2005	13:50	1450	1404.3	0.65	9/30/2005	216100	2400	778600	0	2600	162	0	56	0	9	13	4	3	13	-32.8				Skull Creek
DW-3	89671	4/22/2005	16:20	1500	1449.7	0.35	9/30/2005	215700	3000	779000	0	2060	142	0	66	0	12	16	4	4	15	-32.5				Skull Creek
DW-3	89672	4/22/2005	20:23	1550	1494.3	0.16	9/30/2005	216800	1700	780400	0	988	60	0	22	0	4	5	2	1	7					Belfast Mdst
DW-3	89673	4/23/2005	4:45	1600	1537.7	0.17	9/30/2005	217400	830	780800	0	877	35	0	5	0	1	1	0	0	2					Belfast Mdst
DW-3	89674	4/23/2005	9:38	1650	1581	0.19	9/30/2005	217300	1200	780400	0	1090	36	0	4	0	1	1	0	0	2	-34.2				Belfast Mdst
DW-3	89675	4/23/2005	15:25	1700	1624.3	0.19	9/30/2005	216800	1500	780500	0	1100	45	0	6	0	1	1	1	0	2	-33.6				Belfast Mdst
DW-3	89676	4/23/2005	21:30	1750	1667.6	0.21	9/30/2005	217000	1900	779800	0	1270	62	0	12	0	1	1	0	0	2	-33.3				Belfast Mdst
DW-3	89677	4/24/2005	4:09	1800	1710.9	0.06	9/30/2005	217200	1900	780300	0	567	24	0	8	0	1	2	0	0	1					Flaxman
DW-3	89678	4/24/2005	8:03	1836.6	1742.9	0.21	9/30/2005	216900	2000	779600	0	1390	59	0	15	0	2	3	1	1	2	-32.9				Flaxman
DW-3	89679	4/24/2005	9:21	1855.9	1759.9	0.2	9/30/2005	217100	1900	779300	0	1650	67	0	19	0	2	4	1	1	4	-32.5				Flaxman
DW-3	89680	4/24/2005	10:49	1883.8	1784.5	0.37	9/30/2005	216900	2000	778800	0	2190	96	0	27	0	3	5	1	1	8	-32.7	-23.7	-22.9	**	Waarre C
DW-3	89681	4/24/2005	14:30	1900.04	1798.6	0.32	9/30/2005	217000	1900	778800	0	2180	91	0	29	0	4	6	2	2	10	-32.6	-23.6	-22.7	**	Waarre C
DW-3	89682	4/24/2005	14:30	1950	1842.9	0.31	9/30/2005	216200	2500	778500	0	2660	111	1	35	0	5	6	2	2	10	-32.7				Waarre A
DW-3	89683	4/24/2005	16:20	1969	1859.9	0.25	9/30/2005	217100	2100	778600	0	2030	100	1	29	0	3	4	1	1	4	-33.2				Waarre A

Chemical analysis based on standards accurate to within 2%

**Ethane and propane isotope data obtained via cryo-enrichment

APPENDIX 11:
FLUID INCLUSION SCREENING REPORT

UWI# 999999999999
FIS# FI050074a

Fluid Inclusion Technologies, Inc.
Innovations in Petroleum Risk Management

A Stratigraphic Reconstruction of Bulk Volatile Chemistry from Fluid Inclusions in:

HALLADALE 1

Prepared October 18, 2005 for

Origin

Fluid Inclusion Technologies, Inc.
2217 North Yellowood Avenue
Broken Arrow, OK 74012 U.S.A.

Phone (918) 461-8984
Fax (918) 461-2085
FIT@fittulsa.com

Data Reduction: FITsolve-5 http://www.fittulsa.com

Limited Distribution Notice: This document is proprietary - for the exclusive use of Origin and other wholly owned subsidiaries of Origin and by Fluid Inclusion Technologies Inc. in confidence solely for use in performance of work under contracts with Origin . This document is not to be published or referenced in another publication, nor its contents otherwise disseminated without the expressed written consent of Origin .

A Stratigraphic Reconstruction of Bulk Volatile Chemistry from Fluid Inclusions in:

HALLADALE 1

Prepared October 18, 2005
by
Fluid Inclusion Technologies, Inc.

Executive Summary for well: HALLADALE 1

Petroleum Indications, Type and Quality: The section above approximately 1390 m contains dry gas species and sulfur compounds suggestive of an FIS microseep. These features are considered encouraging for deeper liquid petroleum exploration in the area. Thin sections from 920 m, 1010 m and 1260 m consist largely of sandstone and contain no visible liquid petroleum inclusions. Benzene anomalies at 1030 m, 1210 m and 1290 m may be sensing nearby charge, although the interpretation is complicated somewhat by the co-occurrence of sulfur compounds.

The section below 1785 m contains gas and intermittent liquid-range petroleum indications. The latter are recorded at 1795 m, 1840 m, 1870 m, 1885 m and 1905 m. Thin sections reveal rare, yellow-fluorescent, moderate gravity oil inclusions at 1840 m and rare, yellow-fluorescent moderate and white-fluorescent upper-moderate gravity petroleum inclusions at 1905 m. Lithologies are dominated by sandstone and shale. Shale contains appreciable gas-prone and minor mature(?) oil-prone kerogen. Mature source rock can contribute to FIS responses, and may do so here.

Proximal Pay Indications: Benzene anomalies (possibly with associated acetic acid but unclear due to co-elution effects from sulfur compounds) are documented at 1030 m, 1210 m and 1290 m. These species (benzene and organic acid) generally indicate the nearby presence of reservoired hydrocarbons; however, in this case the interpretation is not nearly as definitive due to possible interference from bacterial species (see below).

Potential Seals: Possible seals are identified at 900 m, 1200 m, 1770 m, 1840 m and 1940 m.

Evidence for Bacterial or Thermal Alteration: Evidence for a bacterial microseep is documented above 1390 m. FIS microseeps often occur above or near deeper charge. The features are generated by microseepage of light thermogenic hydrocarbons from depth followed by bacterial sulfate reduction at temperatures below about 65 C. The presence of these shallow features is considered encouraging for finding deeper oil or condensate bearing reservoirs in the area.

Other: Nothing of note.

Summary of Results for well: HALLADALE 1

This report contains Fluid Inclusion Stratigraphy and Fluid Inclusion Petrography results for HALLADALE 1 and was prepared for Origin by *Fluid Inclusion Technologies, 2217 N. Yellowood Ave., Broken Arrow, OK 74133; ph: (918) 461-8984; fax: (918) 461-2085; www.fittulsa.com.*

Table I: Logistical Information

Client:	**Origin**	Analyzed Depth:	**805 - 1969 Meters**
Well:	**HALLADALE 1**	Sample Spacing:	**See Individual Spectra**
		Sample Total:	**174**

Table II: Fluid Inclusion Petrography from HALLADALE 1

Well Name: Halladale 1

Sample Depth	Rock Type	Petroleum Fluid Inclusion Populations												Kerogen (possible source rk)					Bitumen	
		Population 1				Population 2				Population 3										
Units: (Meters)	*Dominant / Subordinate*	*Fluorescence Color*	*API Gravity (estimated)*	*Host Mineral & occurrence*	*Abundance*	*Fluorescence Color*	*API Gravity (estimated)*	*Host Mineral & occurrence*	*Abundance*	*Fluorescence Color*	*API Gravity (estimated)*	*Host Mineral & occurrence*	*Abundance*	*Host Rock*	*Type*	*OP Fluor Color*	*GP Abundance*	*OP Abundance*	*Type*	*Abundance*
920	ss																			
1010	ss																			
1260	ss,sh													sh	go	yl	c	r		
1795	ss,sh													sh	go	or	c	r		
1840	shly ss	yl	m	dq	r									sh	gp		c			
1905	sh,ss	yl	m	dq	r	wt	um	dq	r					sh	go	or	a	sv		

ss: sandstone	mt: metamorphic rock	m: moderate	r: rare	ds: dead petroleum stain
si: siltstone	no: none	um: upper-moderate	sv: several	po: pore-occluding bitmn
sh: shale	br: brown	h: high	c: common	pb: pyrobitumen
cb: carbonate	or: orange	dq: frac in detrital quartz	a: abundant	
sa: salt	yl: yellow	dr: quartz dust rim	xa: very abundant	Notes:
an: anhydrite	wt: white	qc: quartz cement	go: oil and gas prone	
ch: chert	bl: blue	df: frac detrital feldspar	op: oil prone	
co: coal	l: low	cm: matrix carbonate	gp: gas prone	
ig: igneous rock	ul: upper-low	cc: carbonate cement	ls: live petroleum stain	

Table III: FIS Terminology: Abbreviations and Acronyms

HC Type & Quality		Anomalous HC Zones		Fluid Contacts	
NHC	non-hydrocarbon	**MP**	migration pathway	**OWC**	oil-water contact
DG	dry gas	**PC**	present day ptrlm column	**GWC**	gas-water contact
WG	wet gas	**PPC**	paleo-ptrlm column	**GOC**	gas-oil contact
GC	gas condensate	**RI**	recycled ptrlm inclusions	**POWC**	paleo-oil-water contact
VO	volatile oil	**SR**	source rock	**PGWC**	paleo-gas-water contact
O	oil	**GP**	gas prone kerogen	**PGOC**	paleo-gas-oil contact
BD	biodegraded	**OP**	oil prone kerogen		
TA	thermally altered	**OGP**	oil and gas prone kerogen		
		CNT	contamination		

Water-Soluble Anomalies		Miscellaneous	
WS	undifferentiated water-soluble anomaly	**SL**	seal
WSSR	source rock related water-soluble anomaly	**MS**	microseep
WSTA	water-soluble anomaly sourced from thermal alteration		
PTPL	proximity to oil or gas-condensate		
PTPG	proximity to gas		

Petrographic Observations					
A	abundant	**IG**	igneous rock	**SA**	salt
AN	anhydite	**L**	low	**SH**	shale
BL	blue	**LG**	large	**SI**	siltstone
BR	brown	**M**	moderate	**SM**	small
C	common	**MD**	medium	**SS**	sandstone
CB	carbonate	**MT**	metamorphic rock	**ST**	petroleum stain
CC	carbonate cement	**NO**	none	**SV**	several
CH	chert	**OR**	orange	**UL**	upper-low
CM	matrix carbonate	**PB**	pyrobitumen	**UM**	upper-moderate
CO	coal	**PF**	pore filling bitumen	**V**	variable
DF	detrital feldspar	**PR**	pore rimming bitumen	**W**	weak
DQ	detrital quartz	**QC**	quartz cement	**WT**	white
DR	quartz dust rim	**R**	rare	**XA**	extremely abundant
H	high	**S**	strong	**YL**	yellow

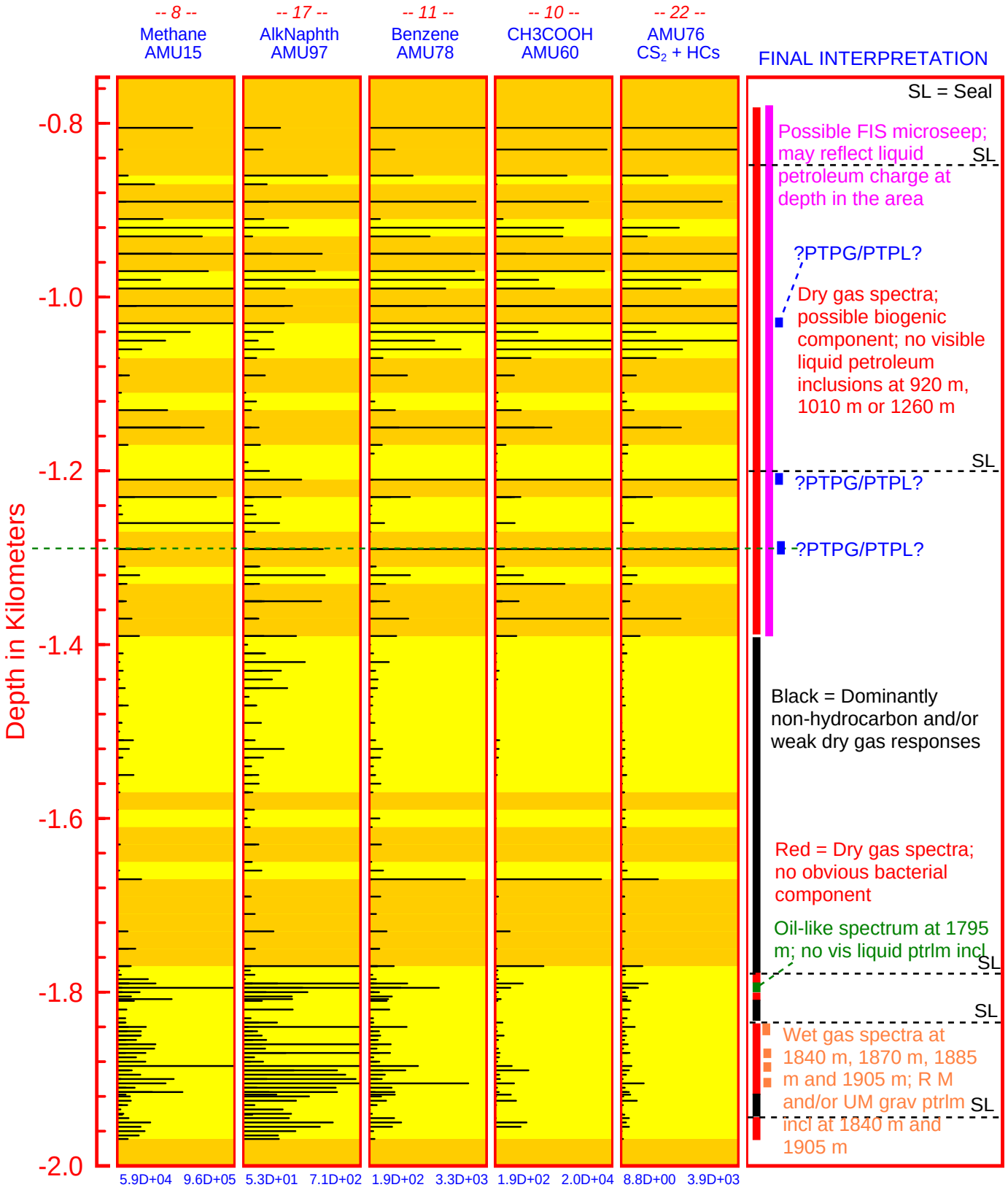

Figure 1: FIS Summary Tracks (see Sect. A for further explanation)

HALLADALE 1 : All FIS Data

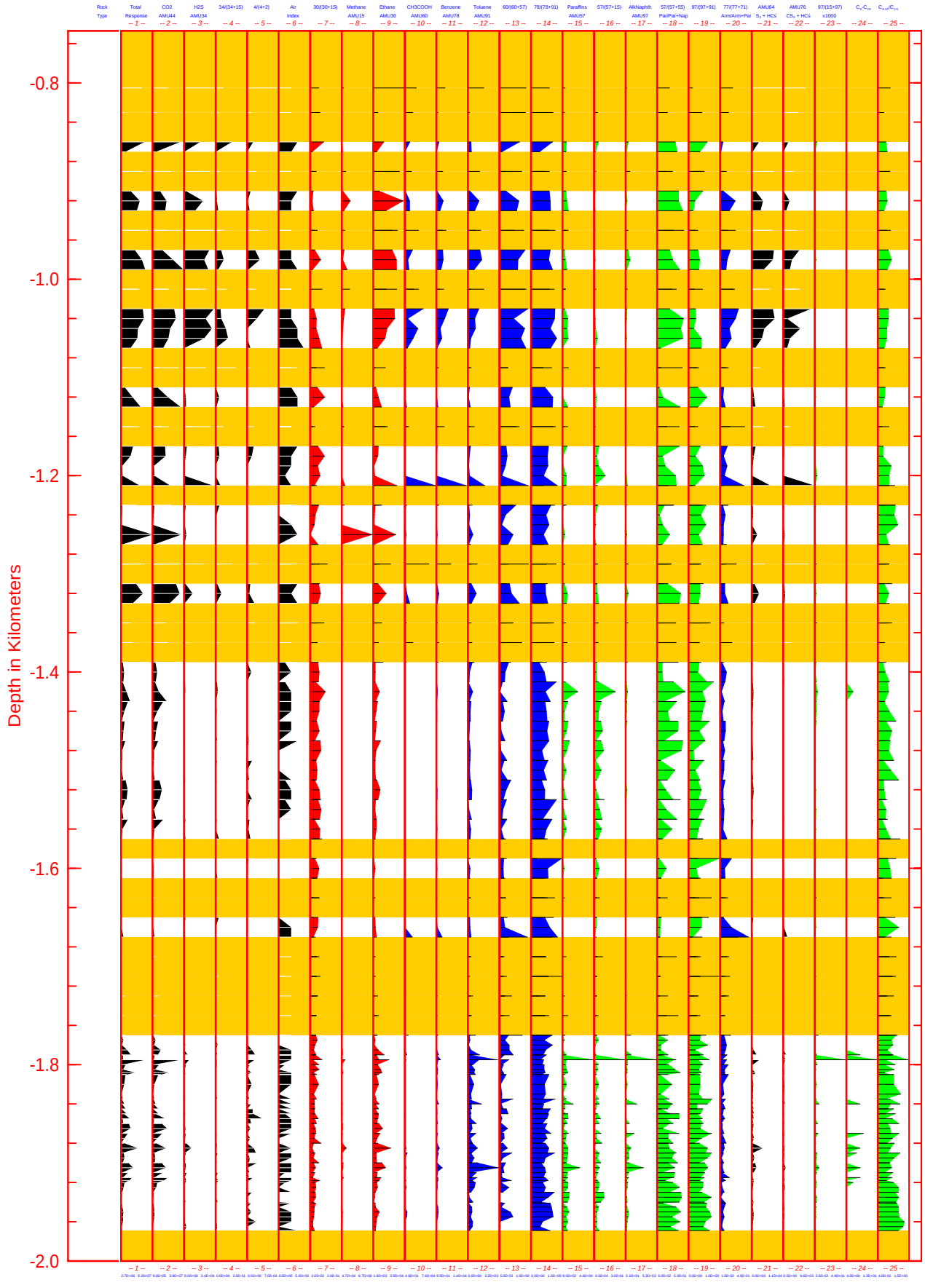

Fluid Inclusion Technologies, Inc.
http://www.fittulsa.com

FIT

UWI# 999999999999
FIS# *FI*050074*a*

HALLADALE 1: 90% of all FIS Data

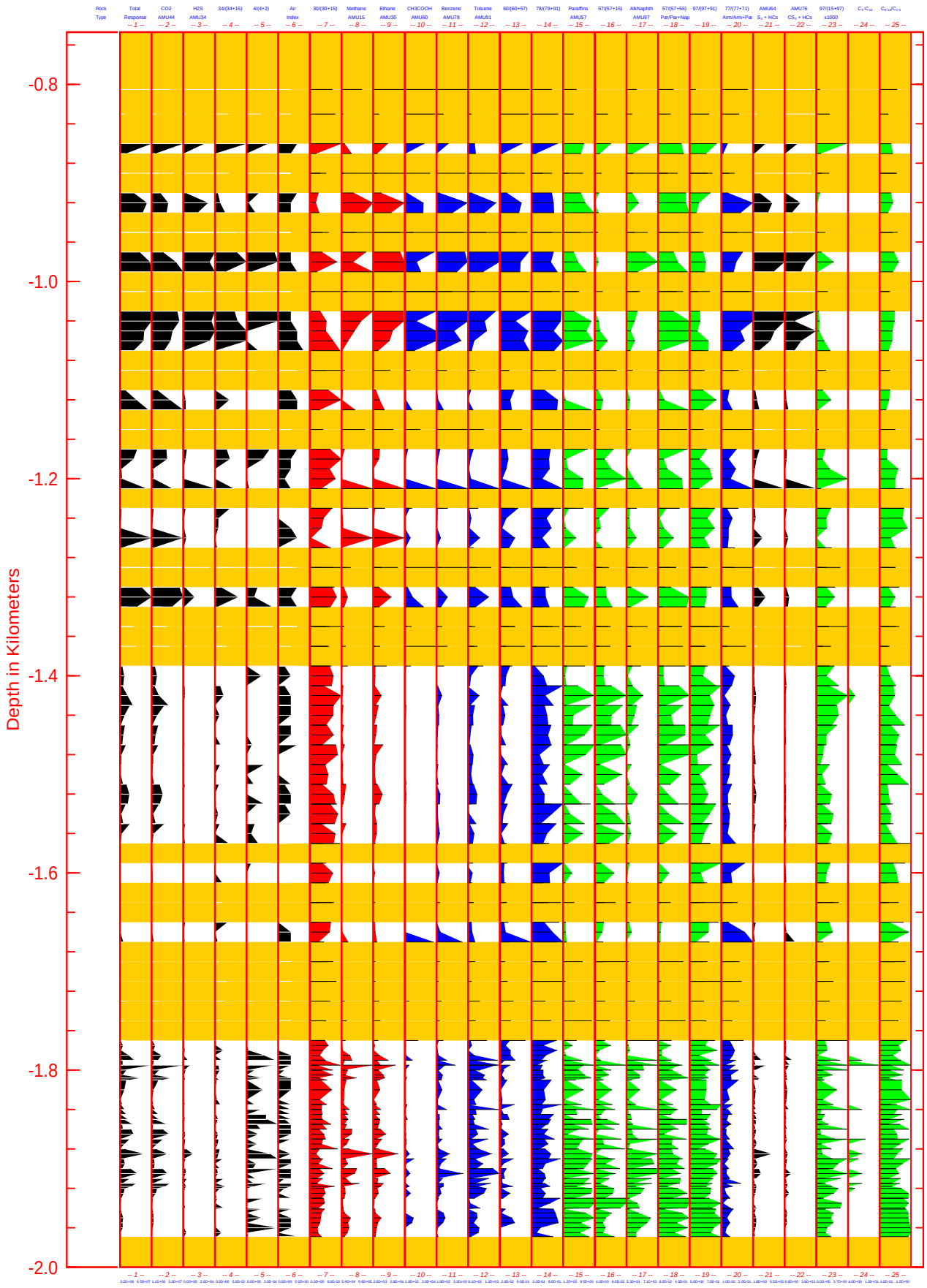

Fluid Inclusion Technologies, Inc.
http://www.fittulsa.com

UWI#999999999999
FIS#FI050074a

Contents

Executive Summary for well: HALLADALE 1 **v**

Summary of Results for well: HALLADALE 1 **vii**

Plate 1: All FIS Data **xii**

Plate 2: 90% of All FIS Data **xiv**

1 Overview of FIT, Inc. and Fluid Inclusion Stratigraphy **1**
1.1 General Logistics of Initiating an FIS Analysis 1
1.2 Organization of this Report 2
1.3 Output Formats 2

2 Analytical Results **3**
2.1 FIS Depth Profiles Showing all Data 3
2.2 FIS Depth Profiles Showing 90% of all Data 9

3 Photomicroscopy **15**

Appendices

A Interpretation of Fluid Inclusion Stratigraphy (FIS) Data **25**
A.1 FIS Analysis 25
A.1.1 Introduction to FIS Analysis 25
A.1.2 Introduction to FIS Data Interpretation 25
A.1.3 FIS Data Consists of Two Parts 26
A.2 FIS Mass Spectra 26
A.2.1 Understanding FIS Mass Spectra 26
A.2.2 Five Types of FIS Mass Spectra 28
A.2.3 Summary of the Five Spectral Types 33
A.2.4 Combinations of Spectral Types 33
A.3 Interpreting FIS Track Plots and Petrographic Data in a Geologic Context . . 34
A.3.1 Significance of FIS petroleum indications 34
A.3.2 Petroleum Type and Quality 36
A.3.3 Water-soluble Anomalies and Proximal Pay Indications 38
A.3.4 Seals 39
A.3.5 Microseepage 39
A.3.6 Fluid Contacts 39
A.4 Individual Track Plots 40
A.4.1 Explanation and Significance of Individual Track Plots 40
A.4.2 Ratios vs. Absolute Abundance 40
A.4.3 Mass Assignments 44

B Reference Spectra **47**
B.1 Oil Inclusion Reference Standards 47
B.2 Frac Sand Hydrocarbon Background Standards 47
B.3 Cooked Frac Sand Hydrocarbon Background Standards 47
B.4 Kindblade Trackplots 47

C Individual Spectra **53**

List of Tables

I Logistical Information vii
II Fluid Inclusion Petrography from HALLADALE 1 vii
III FIS Terminology: Abbreviations and Acronyms viii
IV Identification of Organic and Inorganic Species Represented in Track Plots . . 3
V Partial Fragmentation Pattern for Carbon Dioxide 27
VI Partial Fragmentation Pattern for Gas-Range Hydrocarbons 29
VII Partial Fragmentation Pattern for Liquid-Range Hydrocarbons 30
VIII Partial Fragmentation Pattern for Water-Soluble Species 31
IX Partial Fragmentation Pattern for Sulfur Compounds 32

List of Figures

1 FIS Summary Tracks ix
2 All FIS Data: Tracks $1-5$ 4
3 All FIS Data: Tracks $6-10$ 5
4 All FIS Data: Tracks $11-15$ 6
5 All FIS Data: Tracks $16-20$ 7
6 All FIS Data: Tracks $21-25$ 8
7 90% of all FIS Data: Tracks $1-5$ 10
8 90% of all FIS Data: Tracks $6-10$ 11
9 90% of all FIS Data: Tracks $11-15$ 12
10 90% of all FIS Data: Tracks $16-20$ 13
11 90% of all FIS Data: Tracks $21-25$ 14
12 Photomicroscopy from HALLADALE 1 16
13 Photomicroscopy from HALLADALE 1 17
14 Photomicroscopy from HALLADALE 1 18
15 Photomicroscopy from HALLADALE 1 19
16 Photomicroscopy from HALLADALE 1 20
17 Photomicroscopy from HALLADALE 1 21
18 Oil Spectra 48
19 Frac Sand Spectra a 49
20 Frac Sand Spectra b 50
21 Cooked Frac Sand Spectra a 51
22 Kindblade Oil Standards 52

1 Overview of FIT, Inc. and Fluid Inclusion Stratigraphy

Fluid Inclusion Technologies (FIT), Inc., is a laboratory-based petroleum service organization established in 1997 and offering a variety of analytical services including some previously proprietary technologies. **Fluid Inclusion Stratigraphy (FIS)**, the most widely applicable of these technologies is a rapid analytical technique that involves the automated analysis of volatile compounds trapped within micron-sized cavities in rock material taken from well cuttings, core or outcrop samples. These "fluid inclusions" are representative samples of subsurface fluids, and are not subject to fractionation during sampling or evaporative loss during sample storage for any length of time. The procedure has major impact in the areas of **both Petroleum Production and Exploration Applications** providing information unattainable via more traditional methods and, has been instrumental in the discovery of significant petroleum reserves, influenced exploration and acreage acquisition decisions and provided innovative options for resource estimation, petroleum production and enhanced oil recovery operations. **Fluid Inclusion Stratigraphic Analysis**, often in combination with other patented techniques, emerging geochemical methodologies and standard microscopic methods, all available through Fluid Inclusion Technologies, Inc., provides a unique and unequaled industry product boasting an impressive list of proven applications including determination of **Product Type**, **Hydrocarbon Migration**, **Seals and Seal Integrity**, **Fluid Contacts**, **Proximity to Reservoired Petroleum**, **Pay Zone/By Passed Pay Delimitation**, **Reservoir-Scale Compartmentallization** and **Fluid Pressure Compartments**. Further information regarding the application of **FIS Analysis** and the other technical services we provide to problems in petroleum exploration and production is available elsewhere in this report and on our website:"www.fittulsa.com".

1.1 General Logistics of Initiating an FIS Analysis

To Initiate an FIS Analysis: contact FIT[1] directly to discuss goals of the study, sample requirements, turnaround time, pricing, and other related aspects. New clients are particularly encouraged to consult with our staff during the early stages of project development to optimize sample selection, preparation and shipment. Rock materials for FIS Analysis are shipped directly to C&M Storage[2], our sample handling facility, for sample preparation including any necessary crushing/sieving, subsampling and washing. The turnaround time for a typical FIS Analysis is preliminary data in 1-2 weeks time following receipt of samples by C&M and final report 1-2 weeks following preliminary analysis. These times are approximate and depend on the amount of sample preparation required, job size and analytical backlog. At the time of issue of this report, the cost for obtaining an FIS Analysis was $5,500 U.S. for a full-well analysis (up to 575 samples) and $3,000 U.S. for a short-well analysis (up to 180 samples). The cost includes the automated mass spectrometric analysis, preparation of and fluid inclusion petrography on selected thin-sections sampled throughout the well, and interpretation in the form of annotated depth plots (see Figure 1).

When sampling for FIS Analysis: the technique is equally applicable to cuttings, core and outcrop samples, but all samples will ultimately be reduced to cuttings-sized rock material. Wells drilled with any mud system can be analyzed (including oil-based systems),

[1]Fluid Inclusion Technologies, 2217 N. Yellowood Ave., Broken Arrow, 74012, USA., phone (918) 461-8984
[2]Attn: FIS Analysis, C&M Storage, 3311 Hwy, 77 South, Schulenburg, TX 78956, USA

as can samples of any age (i.e., fresh cuttings or those warehoused for many years). Our suggested sampling interval for general well studies is 30 ft (10 m). Pay-delineation studies, reservoir-scale studies or other applications involving rapidly changing fluid chemistries should be sampled at the tightest possible spacing, depending on sample availability (e.g., 1-3 ft). A maximum of 575 samples can be analyzed for a given well. Approximately 1 gm of clean rock material is needed for each sample. In most cases, some amount of additional washing is required - even for "washed samples", thus, it is best to send enough to ensure ample material after a final wash. It is further recommended that "clean lith cuts" be provided to minimize costs associated with additional sample preparation as all sample washing and preparation costs will be charged back to the client. The quoted price for an FIS Analysis is exclusive of sample preparation, handling and shipping; estimates for these project-specific services are available upon request.

1.2 Organization of this Report

Analytical results of the FIS analysis of HALLADALE 1 are presented graphically in Sections 2.1 and 2.2 as a series of profiles each illustrating the variation of a particular atomic mass (m/z) or ratio of two masses with measured depth. A general discussion of the interpretation of FIS data including the significance of particular features and trends (or their absence) is provided in Appendix A. The remaining information provided in subsequent sections includes: 1) reference spectra, collected on internal standards and used to monitor inter- and intra-analytical consistency of the quadrupole analyses which are presented and discussed in Appendix B; and 2) mass spectra from all samples which are listed individually by depth in Appendix C.

1.3 Output Formats

Analytical results of the present study are available in electronic format as described below. The first five items are included on the 3.5" floppy diskette provided with each color hard-copy of the final report. The remaining file, FI050074a-1.pdf, is available upon request for a nominal fee.

1. FI050074a-1.las – LAS-format, 26-column file containing recorded depth and Tracks 1-25 from the *FIT Analysis* of HALLADALE 1
2. FI050074a-1.txt – TXT-format, 26-column file containing recorded depth and Tracks 1-25 from the *FIT Analysis* of HALLADALE 1
3. FI050074a-2.las.Z – LAS-format (compressed), 181-column file containing recorded depth and background corrected, normalized, standardized individual mass spectra (m/z 2-180) from the *FIT Analysis* of HALLADALE 1
4. FI050074a-s.pdf – PDF format, electronic file of the summary tracks and annotations from the *FIT Analysis* of HALLADALE 1
5. FI050074a-c.pdf – PDF format, electronic file of the poster containing *90% of all FIS Data* from the *FIT Analysis* of HALLADALE 1
6. FI050074a-1.pdf – PDF format, electronic file of the final report (entire document) of the *FIT Analysis* of HALLADALE 1

2 Analytical Results

2.1 FIS Depth Profiles Showing all Data

Millivolt responses for selected ionic species or species ratios resulting from FIS mass spectrometric analysis are displayed in Figures 2-6 (trackplots one through twenty-five). The identity of the individual ions involved in construction of the trackplots are listed in Table IV below. The tracks are organized into groups of related compounds; tracks 1-6 representing inorganic gases, tracks 7-9 representing dry organic gases, tracks 8-14 representing water soluble organic species or ratios of "more soluble" to "less soluble" species, and tracks 15-20 and 21-25 representing petroleum components of higher molecular weight and two sulfur compounds. The general interpretation of *FIS* data shown in the trackplots is discussed in Appendix A.

Table IV: Identification of Organic and Inorganic Species Represented in Track Plots

Mass #	Description
2	hydrogen (H_2^+)
4	helium ($^4He^+$)
15	C_1 fragment (CH_3^+); largely methane
30	C_2 fragment ($C_2H_6^+$); largely ethane
34	hydrogen sulfide (H_2S^+)
44	dominantly carbon dioxide (CO_2^+); possible C_3 fragment overlap
55	contribution from C_4 and greater naphthenes
57	contribution from C_4 and greater paraffins
60	dominantly acetic acid (CH_3COOH^+); possible dominance by carbonyl sulfide (COS^+) in some cases
64	S_2 or SO_2 plus hydrocarbons
71	contribution from C_5 and greater paraffins
76	CS_2 plus hydrocarbons
77	contribution from aromatic species
78	benzene ($C_6H_6^+$) with possible contribution by carbon disulfide (CS_2^+)
91	toluene ($C_7H_7^+$)
97	C_7 alkylated naphthene fragment

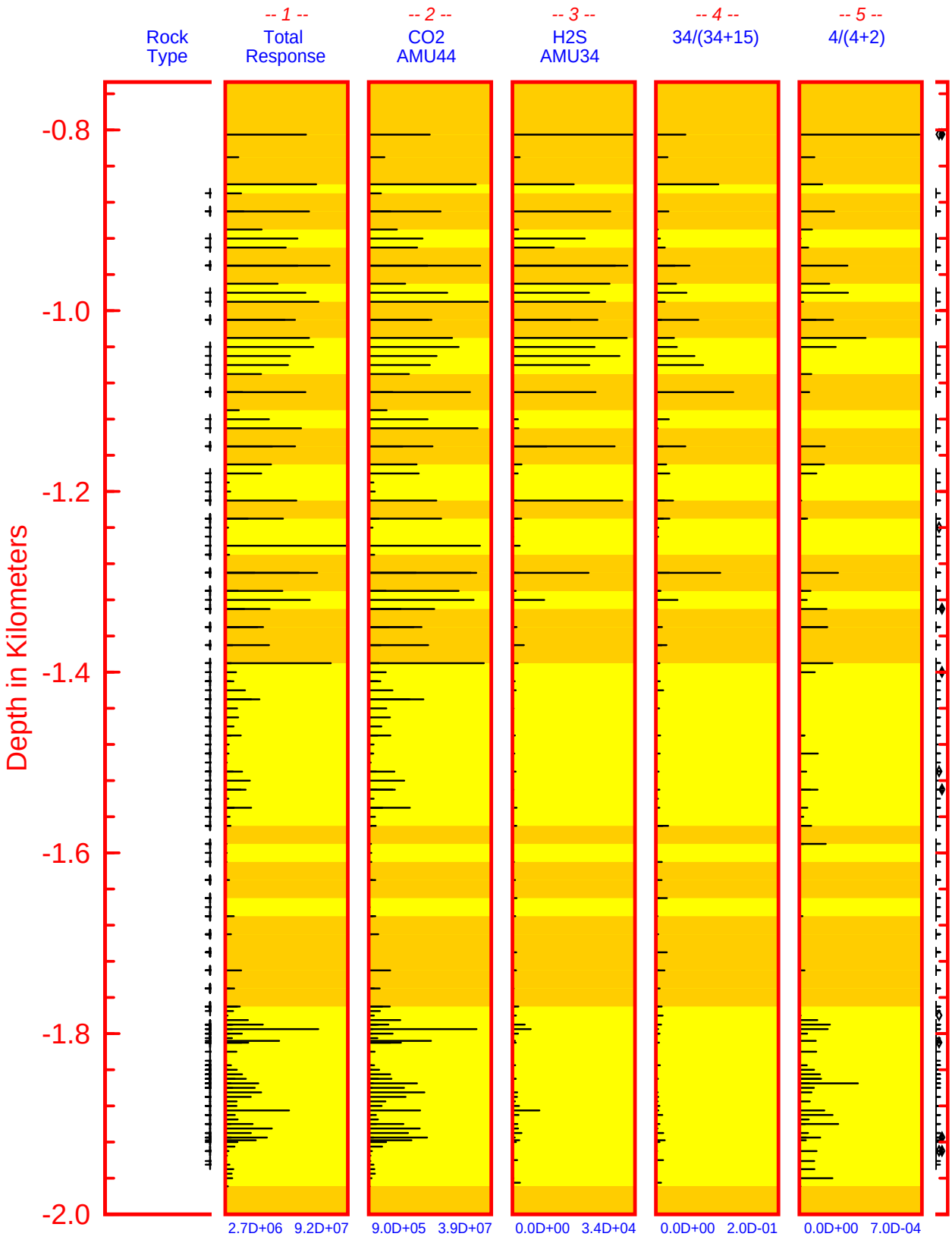

Figure 2: All FIS Data: Tracks 1 – 5 (see Sect. A.3 for explanation)

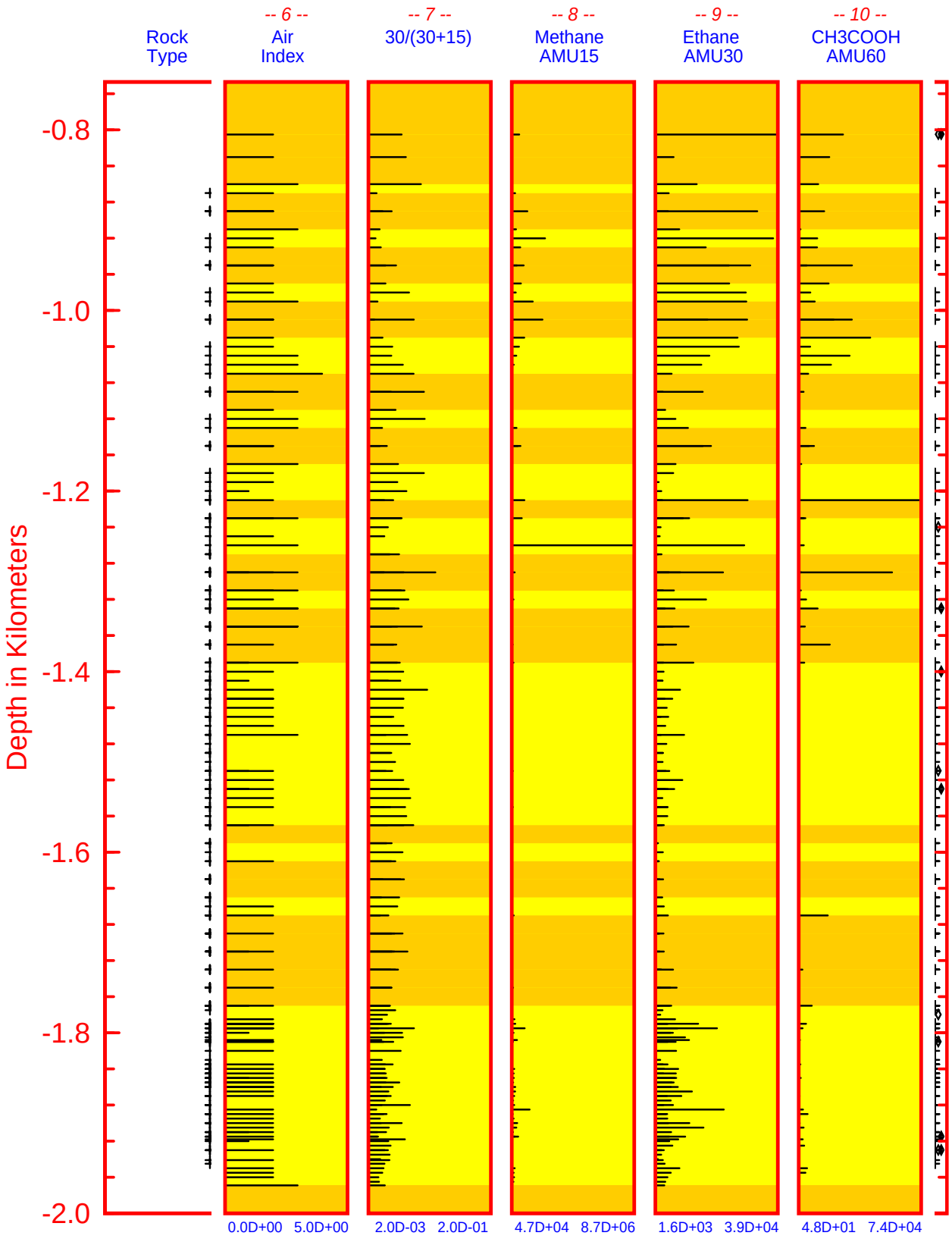

Figure 3: All FIS Data: Tracks 6 – 10 (see Sect. A.3 for explanation)

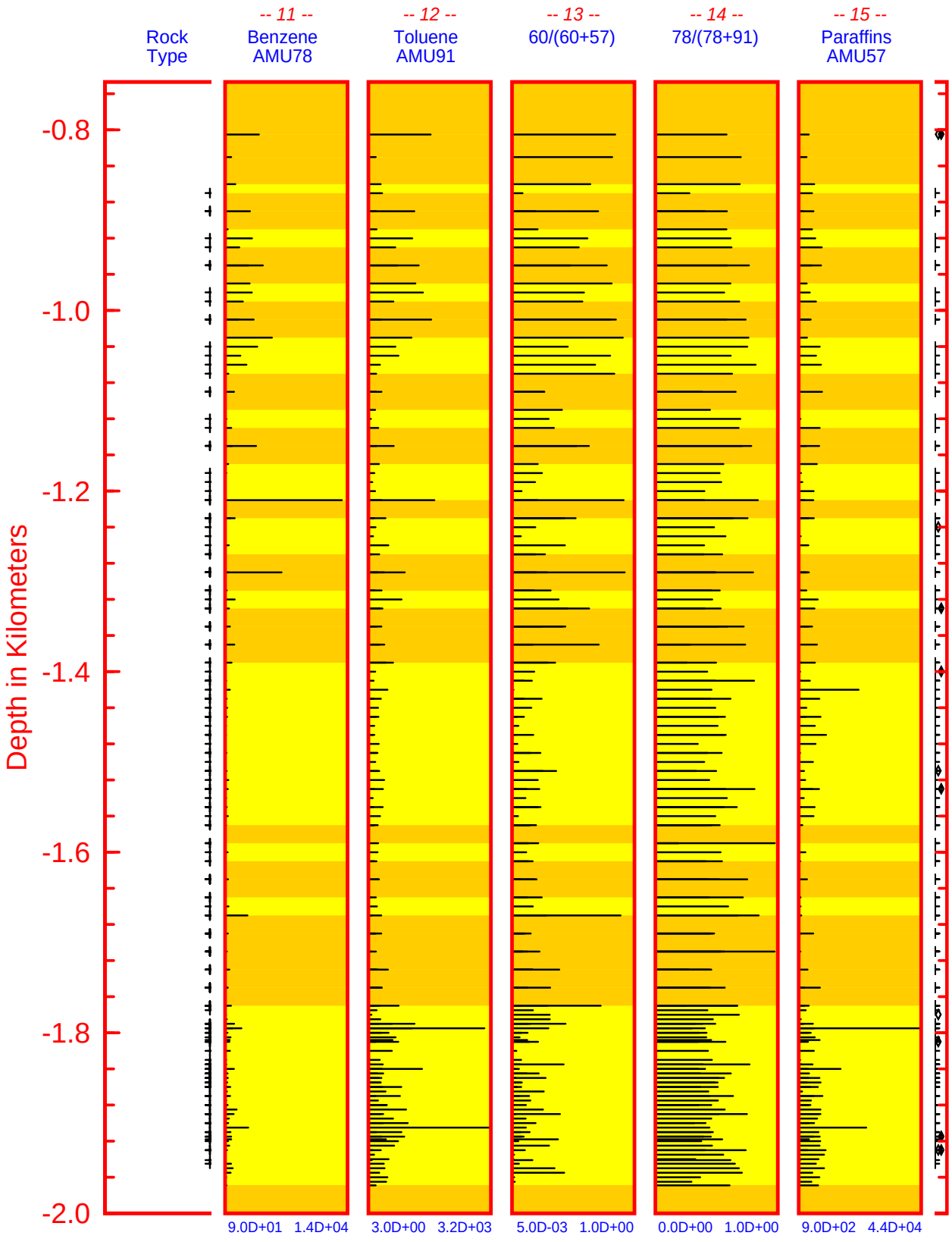

Figure 4: All FIS Data: Tracks 11 – 15 (see Sect. A.3 for explanation)

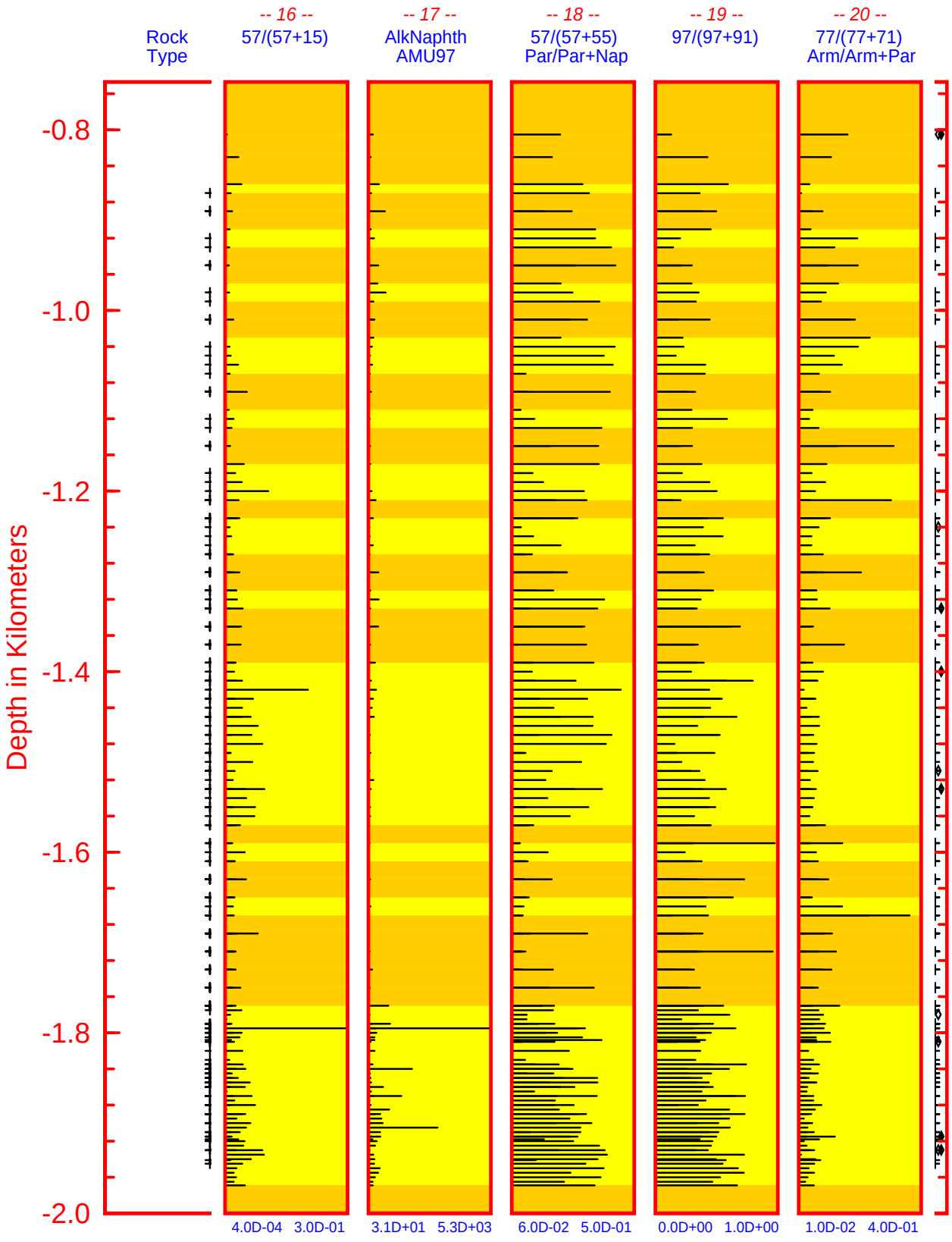

Figure 5: All FIS Data: Tracks 16 – 20 (see Sect. A.3 for explanation)

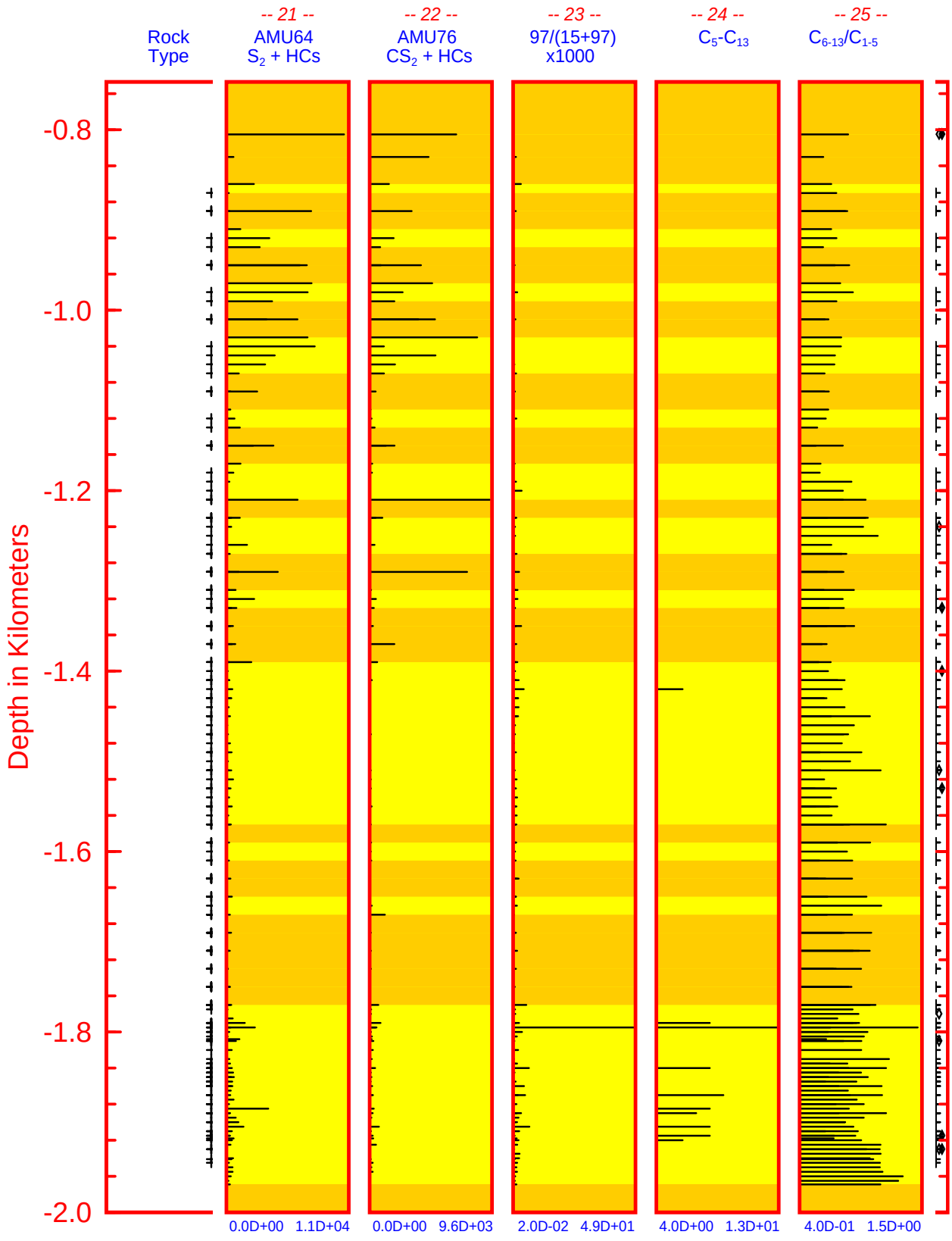

Figure 6: All FIS Data: Tracks 21 – 25 (see Sect. A.3 for explanation)

2.2 FIS Depth Profiles Showing 90% of all Data

Figures 7-11 show the same data as that given in Figures 2-6 of Section 2.1 *except* the upper and lower 5% of the data have been removed in each track and the scale along the abscissa adjusted accordingly in order to accentuate small deviations from background and reduce attenuation effects associated with scale-dominating responses. The identity of the individual ions involved in construction of the trackplots are listed in Table IV. The tracks are organized into groups of related compounds; tracks 1-6 representing inorganic gases, tracks 7-9 representing dry organic gases, tracks 8-14 representing water soluble organic species or ratios of "more soluble" to "less soluble" species, and tracks 15-20 and 21-25 representing petroleum components of higher molecular weight and two sulfur compounds. The general interpretation of *FIS* data shown in the trackplots is discussed in Appendix A.

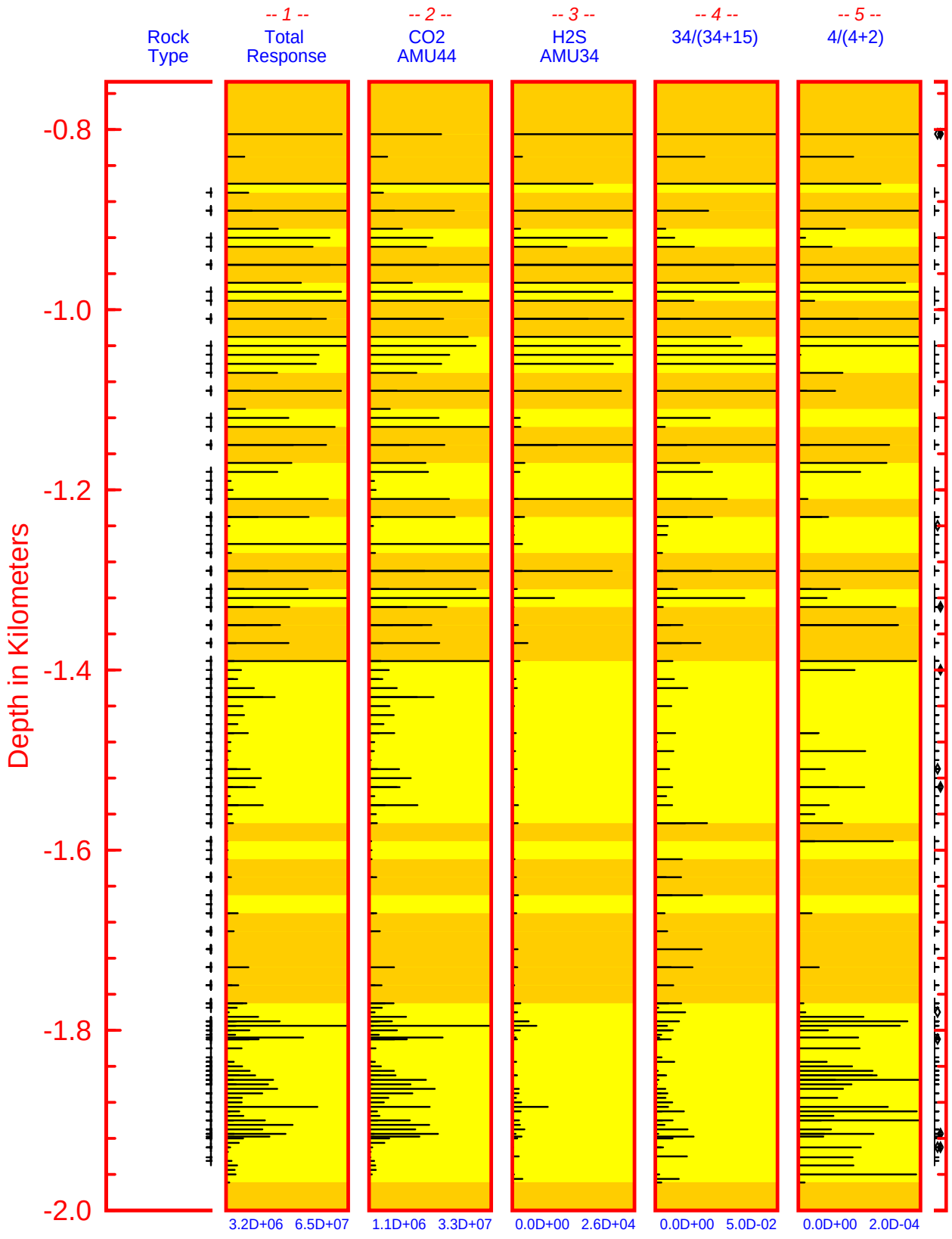

Figure 7: 90% of all FIS Data: Tracks 1 – 5 (see Sect. A.3 for explanation)

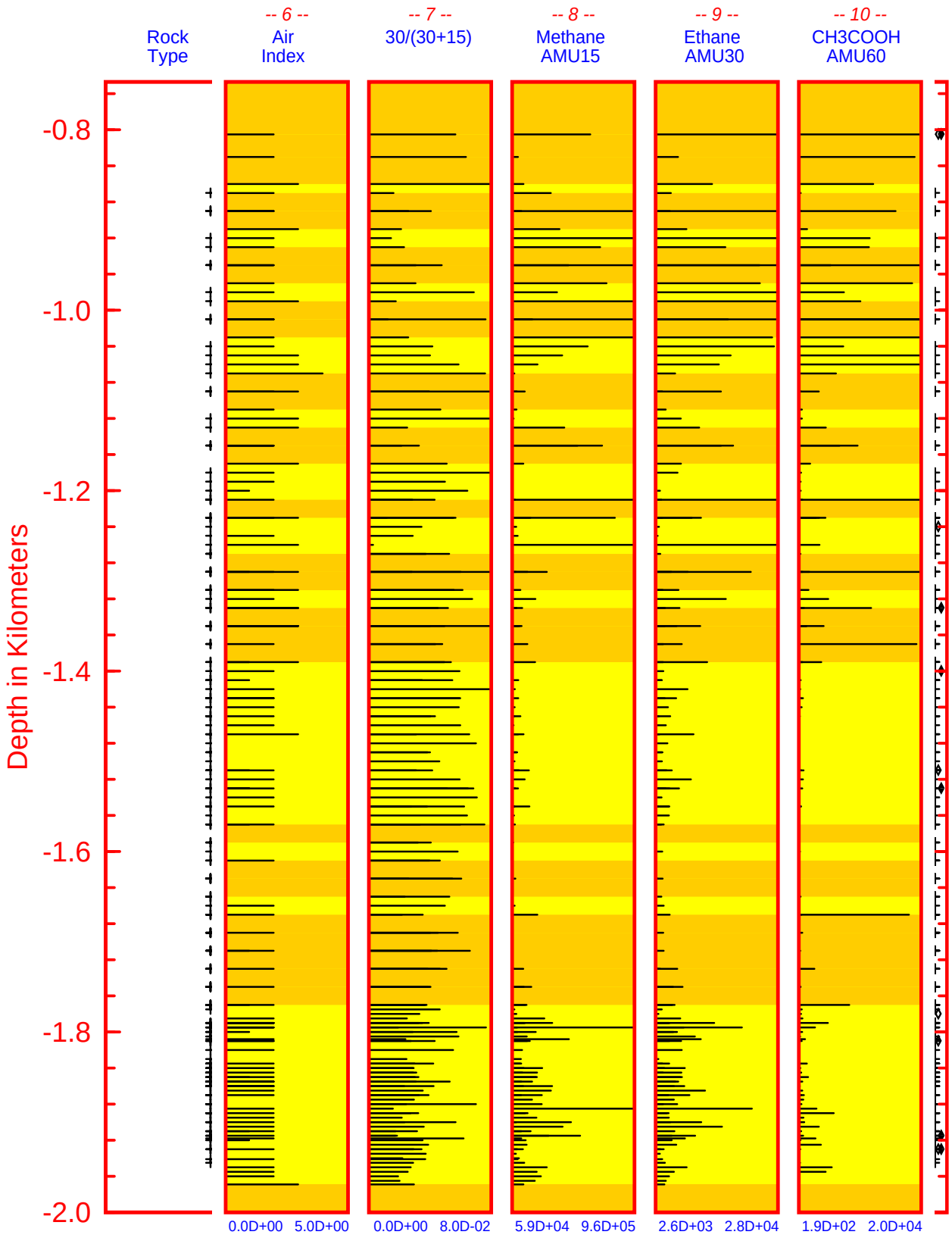

Figure 8: 90% of all FIS Data: Tracks 6 – 10 (see Sect. A.3 for explanation)

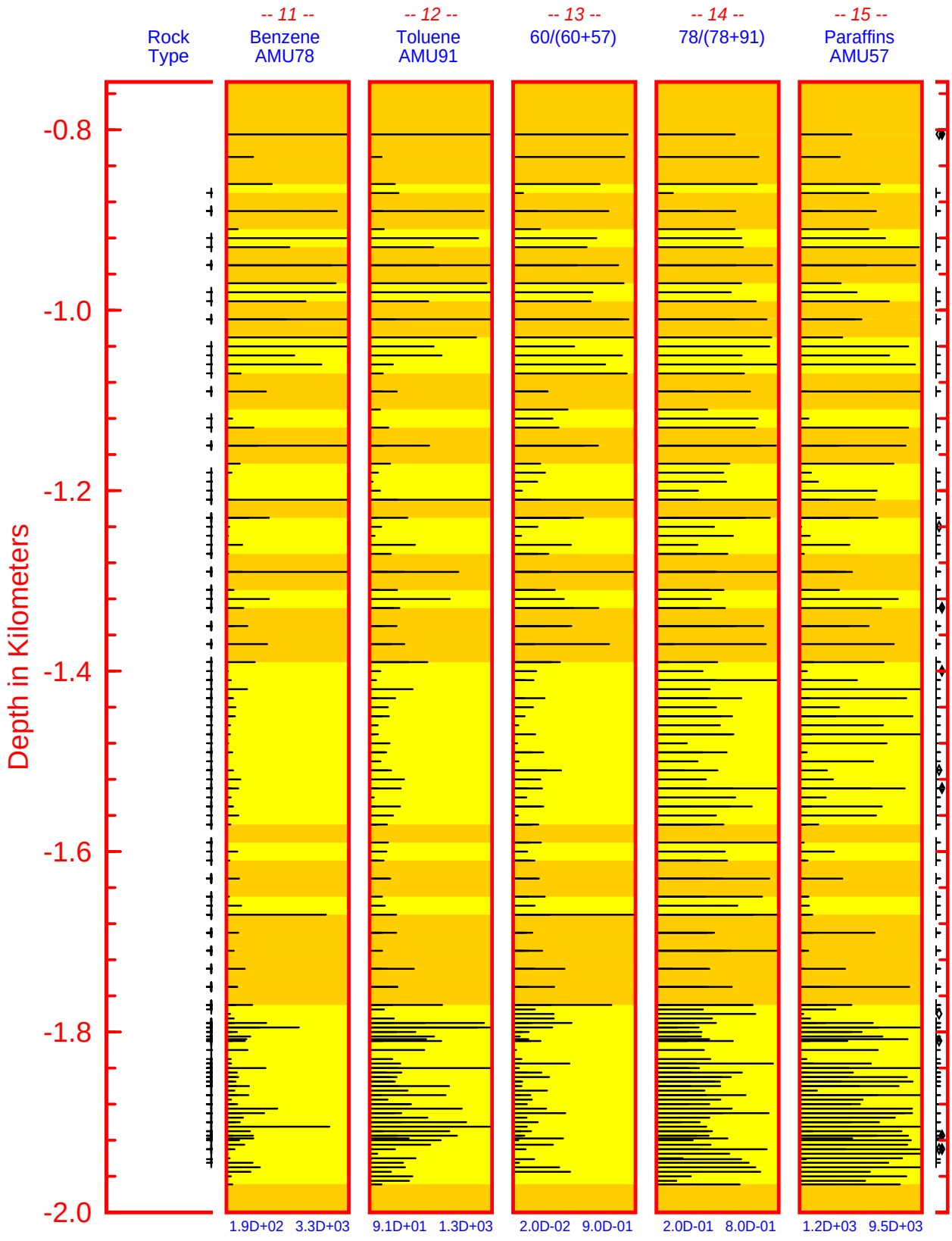

Figure 9: 90% of all FIS Data: Tracks 11 – 15 (see Sect. A.3 for explanation)

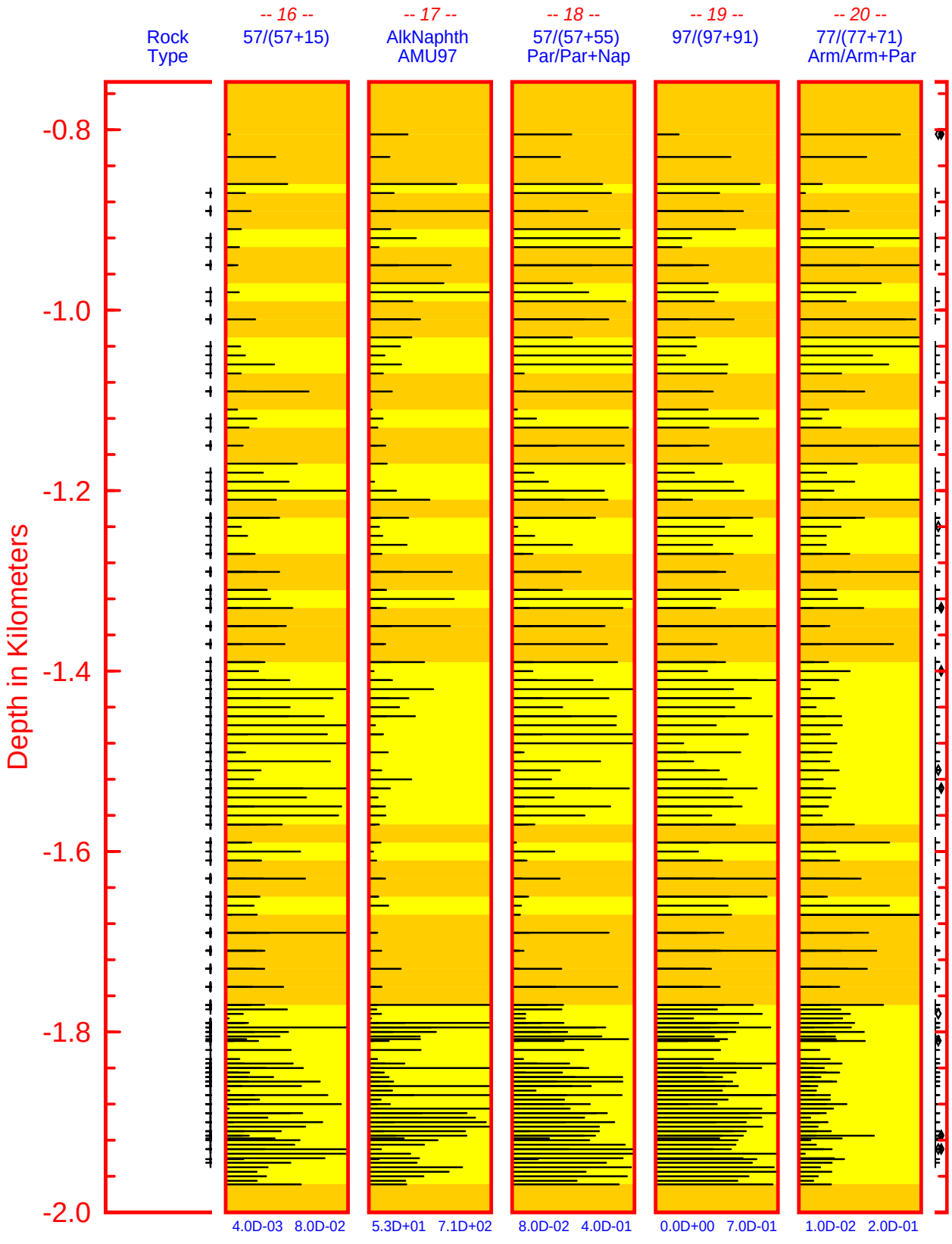

Figure 10: 90% of all FIS Data: Tracks 16 – 20 (see Sect. A.3 for explanation)

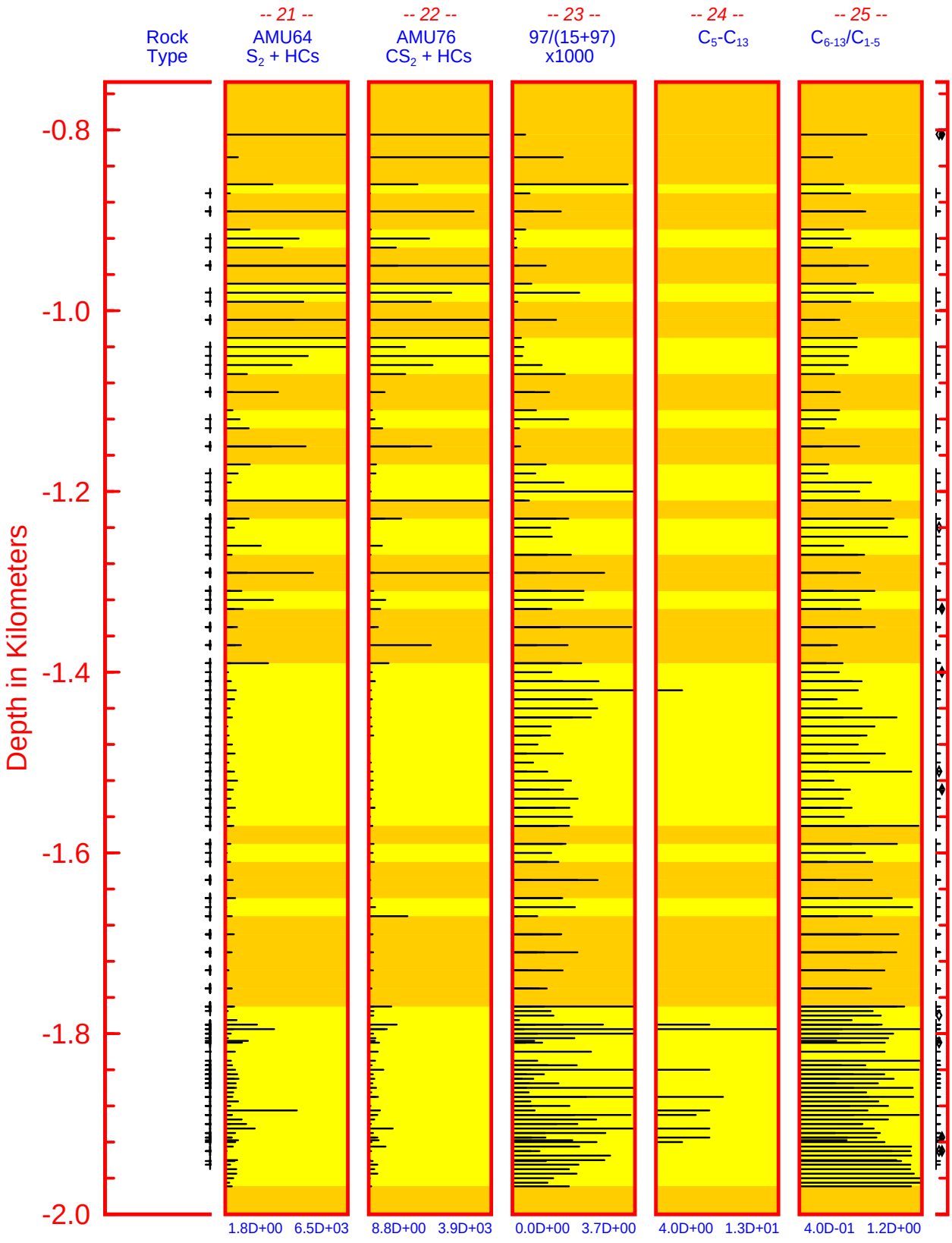

Figure 11: 90% of all FIS Data: Tracks 21 – 25 (see Sect. A.3 for explanation)

3 Photomicroscopy

Thin sections were prepared from HALLADALE 1 samples at depths warranting further examination following preliminary assessment of the *FIS* analytical results. The sections were then examined under a petrographic microscope using a variety of fluid inclusion techniques (e.g., UV-fluorescence, microthermometry, etc.) in order to verify the presence of petroleum-bearing inclusions in the rock samples and to explore textural relationships that may yield additional information on the timing of hydrocarbon migration or generation. Petrographic examination is also necessary to verify that petroleum-bearing fluid inclusions present in the samples and responsible for the observed mass spectra are not relict features (i.e., that they were not already present in the mineral grains prior to deposition). The following figures contain photomicrographs representative of samples from HALLADALE 1 at the depths indicated.

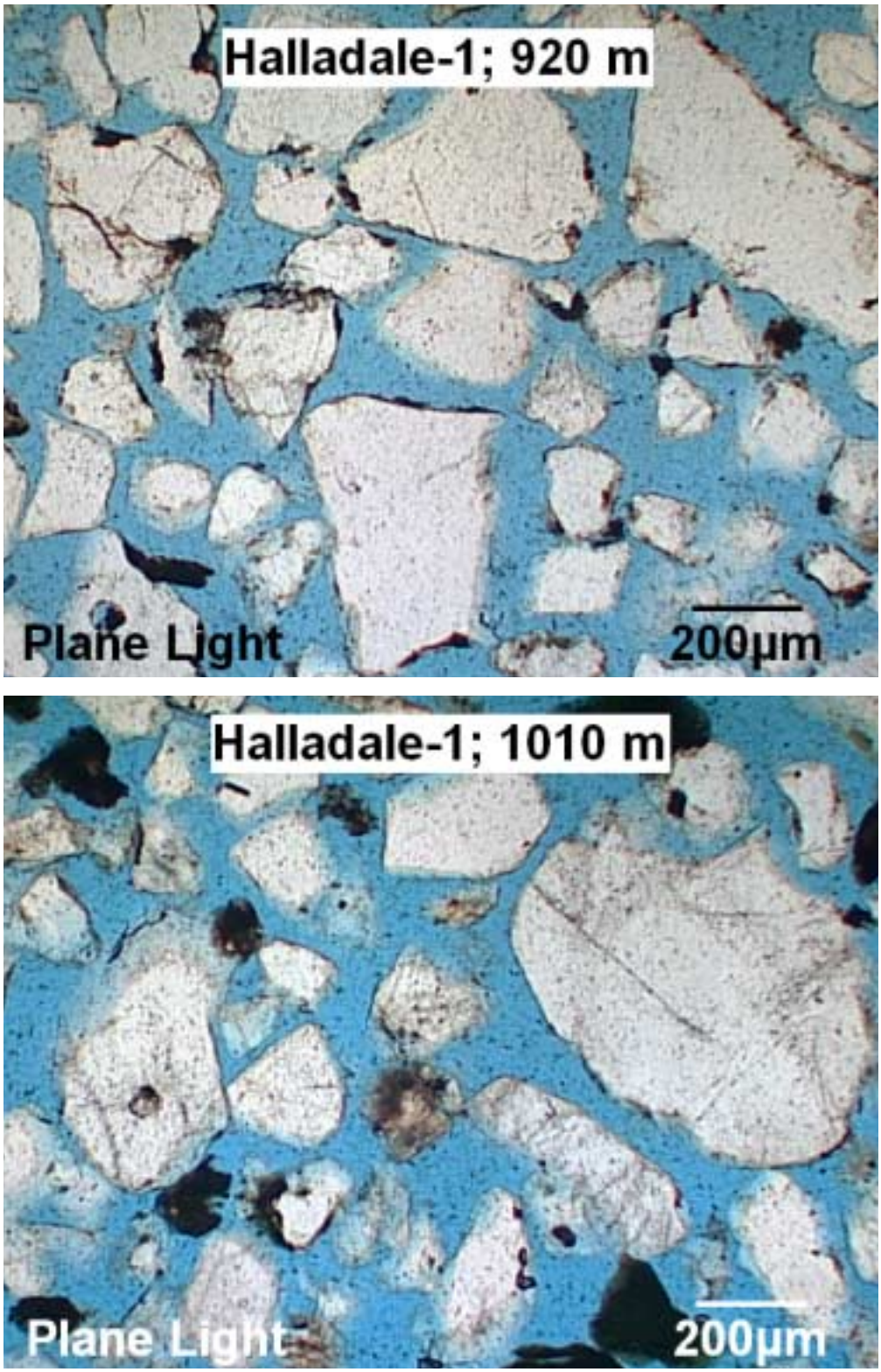

Figure 12: Photomicroscopy from HALLADALE 1

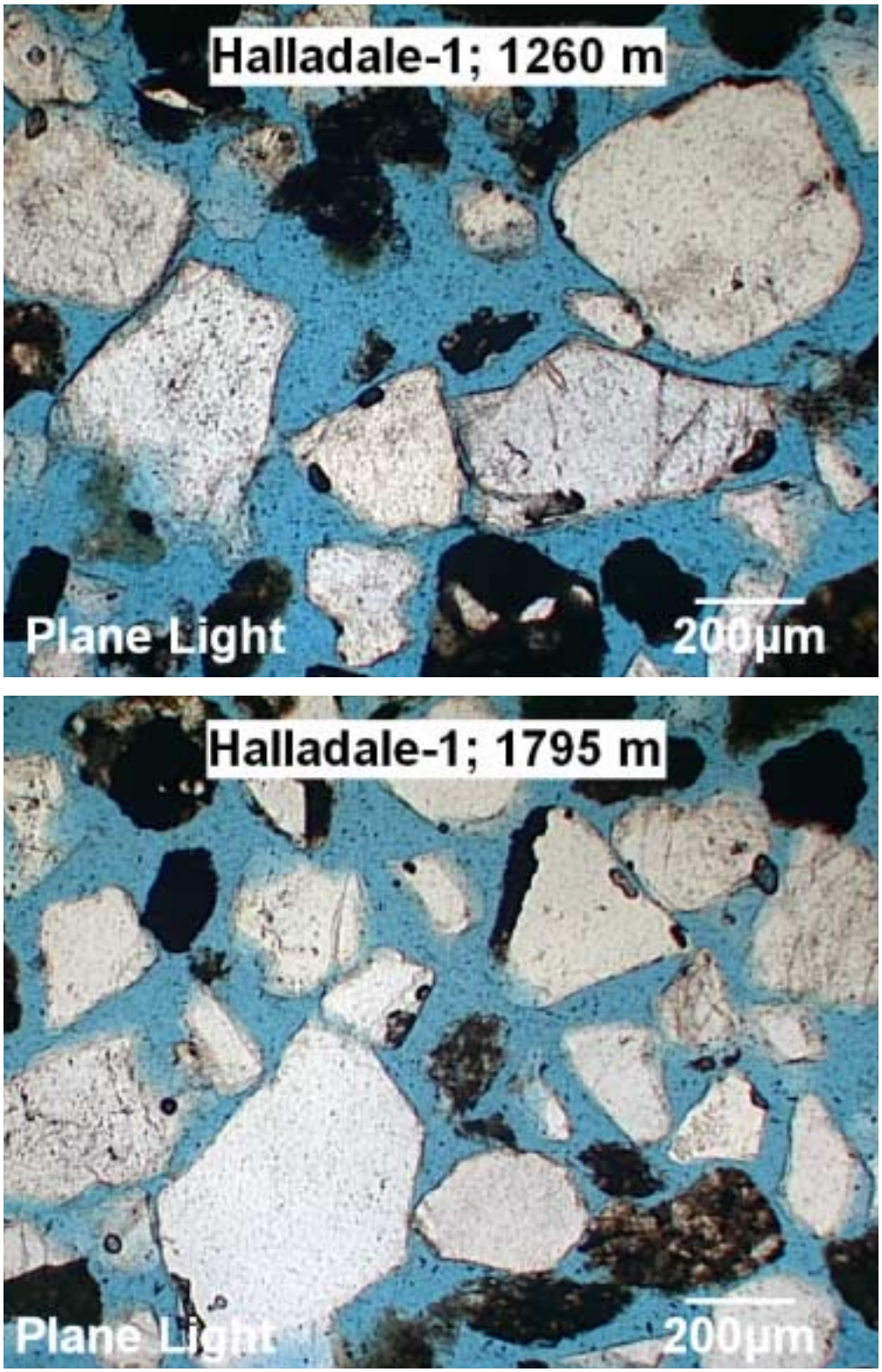

Figure 13: Photomicroscopy from HALLADALE 1

Figure 14: Photomicroscopy from HALLADALE 1

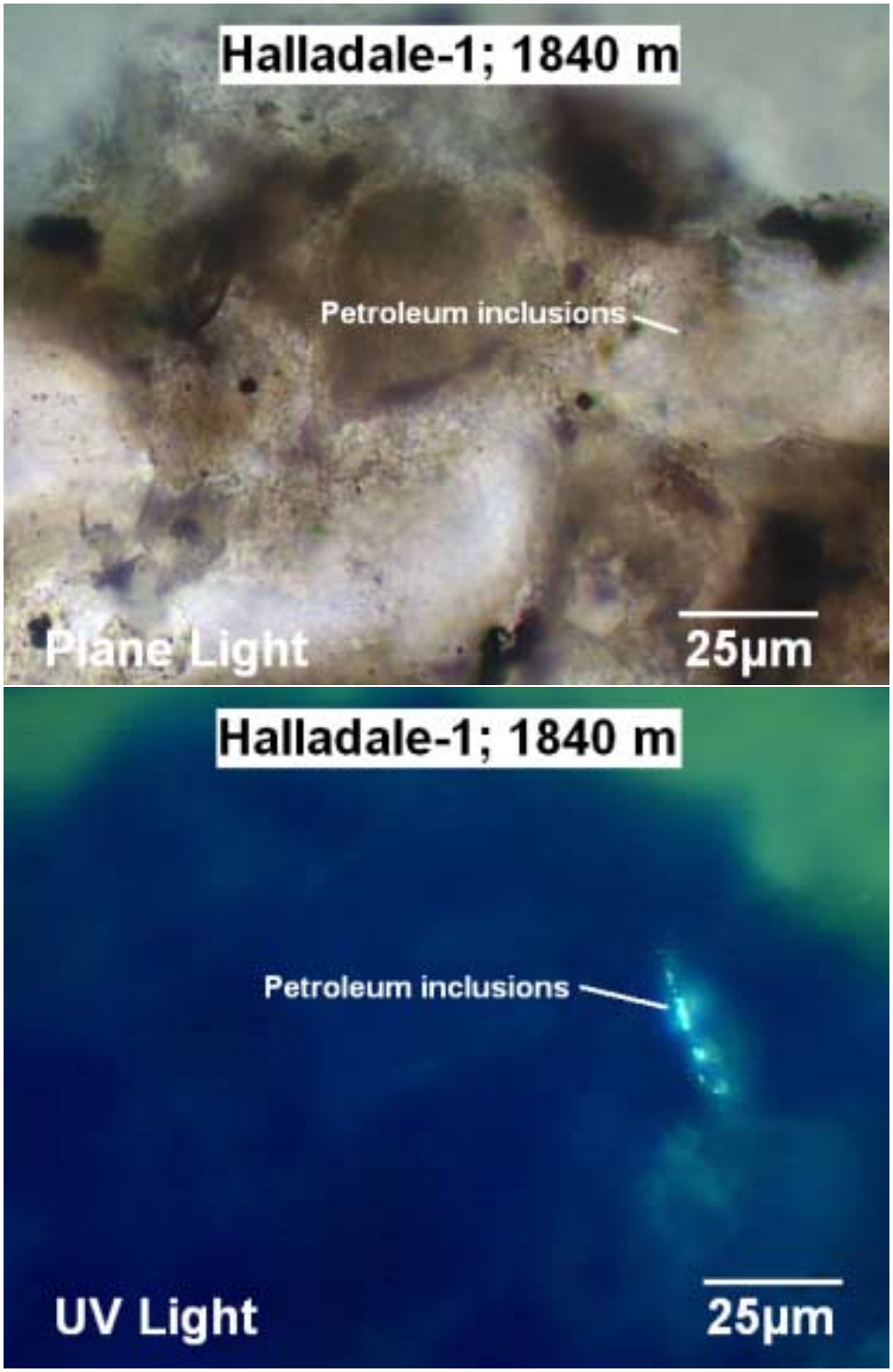

Figure 15: Photomicroscopy from HALLADALE 1

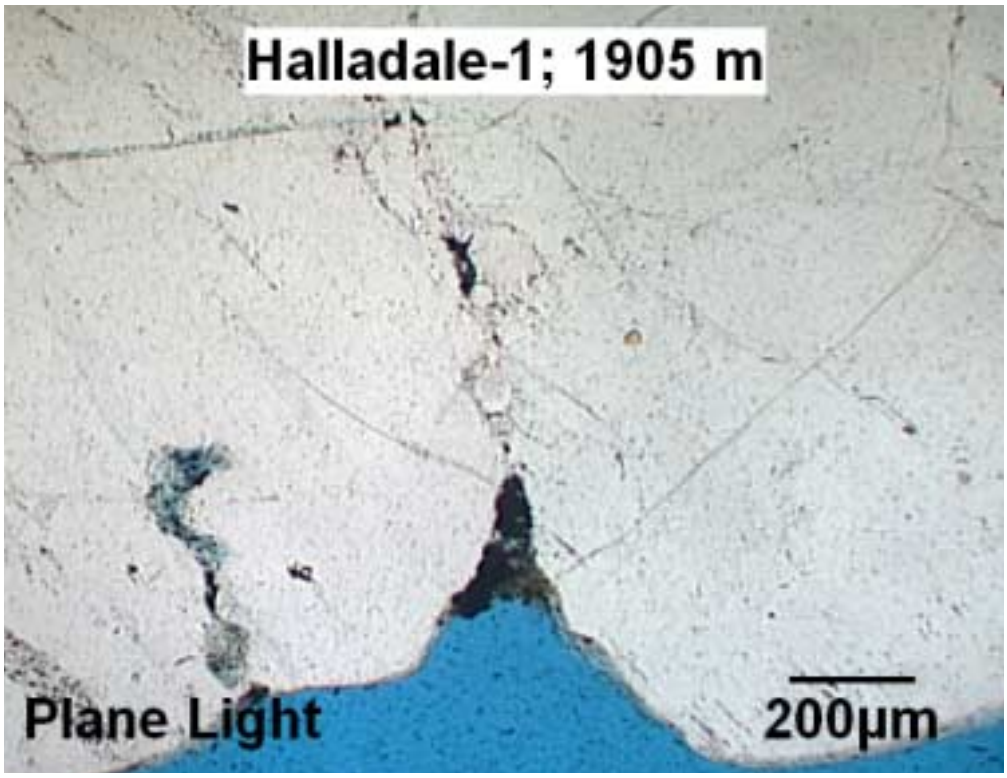

Figure 16: Photomicroscopy from HALLADALE 1

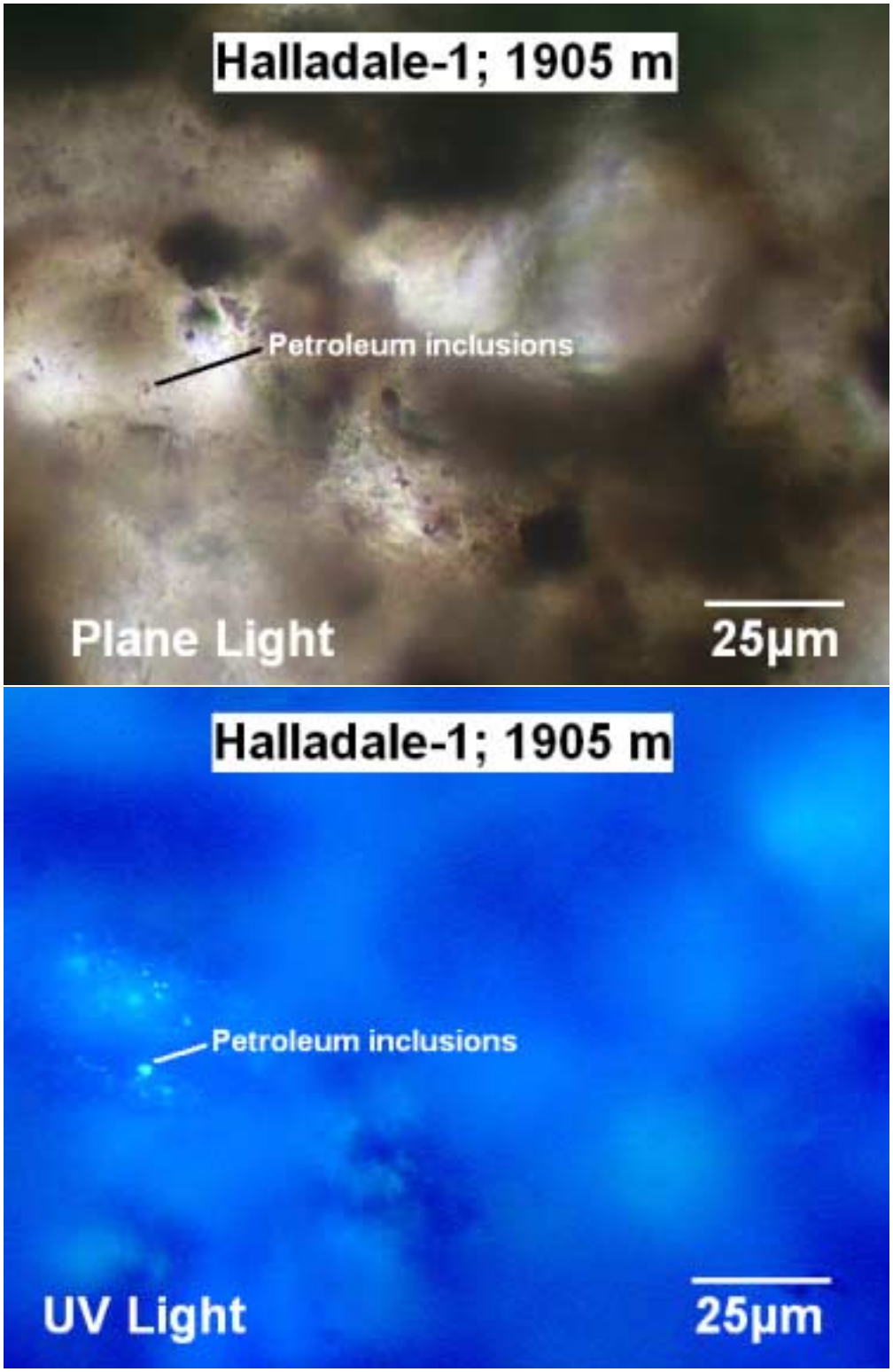

Figure 17: Photomicroscopy from HALLADALE 1

Appendices

A Interpretation of Fluid Inclusion Stratigraphy (FIS) Data

A.1 FIS Analysis

A.1.1 Introduction to FIS Analysis

Fluid Inclusion Stratigraphy involves the rapid, complete analysis of volatiles trapped as fluid inclusions in rock samples using quadrupole mass analyzers attached to an automated, high-vacuum sample introduction system. The technique documents the presence and relative bulk abundance of ionized volatile fragments with mass/charge ratio of $1 \leq m/z \leq 180$ that have been released from fluid inclusions by crushing of natural samples. This includes most geologically important inorganic species as well as organic species with less than or equal to 13 carbon atoms. The resulting analysis of the petroleum fraction is comparable to the low molecular weight fraction of a whole-oil gas chromatographic - mass spectrometric (GCMS) analysis (without devolatilization of the gas fraction); hence, the major classes of hydrocarbons (e.g., aromatics, naphthenes and paraffins) are represented. Unlike GCMS, where the quadrupole is front-ended with a GC, boiling point separation is not achieved and all species are analyzed simultaneously. Hence, significant interference can occur among species with the same mass to charge ratio. However, what FIS lacks in compound specificity, it makes up for in sensitivity and speed, allowing detection of petroleum in samples that are well beyond the reach of standard GCMS methodologies.

Prior to analysis, samples of rock material are freed of significant interfering contamination by washing, picking and magnetic separation as necessary to remove drilling fluids, lost circulation materials, other solid mud additives such as gilsonite, and metallic particles from the drillstring. Cleaned samples are loaded with appropriate standards into specially designed autosamplers and are heated in a vacuum oven for a minimum of 24 hours. This is done to remove adsorbed organic and inorganic volatile material that could interfere with the analysis. The autosampling device is placed in the vacuum system and evacuated to appropriate high vacuum. Bulk fluid inclusion volatiles are afterwards instantaneously released from each sample in a sequential manner by automated mechanical crushing. Volatile organic and inorganic species are dynamically pumped through quadrupole mass analyzers where they are ionized, separated according to their mass/charge and recorded.

Fluid Inclusion Stratigraphy is unique in several ways: 1) the methodology and theoretical framework are the result of a long-standing research and development effort, 2) the cumulative experience and database of documented case histories are the most extensive in the world and 3) the technology represents the most rapid analytical capability of its kind available. The resulting dataset can provide a nearly continuous log of present and past pore fluid chemistry through the stratigraphic section penetrated by a well, and, given adequate sample coverage, the data can be mapped in two or three dimensions.

A.1.2 Introduction to FIS Data Interpretation

The following sections provide guidelines for interpreting Fluid Inclusion Stratigraphy (FIS) data that were developed during evaluation of a large number of wells from many geologic and structural environments over the years. This methodology was followed in preparing the annotated depth plots found at the front of this report and is adequate for most circumstances. There are two levels of interpretation to be considered:

1. Interpretation of FIS data by itself (basically describing what volatiles are present and in what relative proportion).

2. Interpretation of the significance of FIS data in a geologic context to answer a specific petroleum system question.

These guidelines concentrate on addressing the first level of interpretation, both because potential geologic scenarios are too variable to be thoroughly considered here, and because the end user is in the best position to judge the ultimate significance of these data after integrating the FIS data set with other information. When interpreting FIS data, the following statements apply:

1. FIS interpretations are generally qualitative.

2. Chemical relationships displayed in FIS data are either obvious or they are unreliable as exploration tools.

3. FIS interpretations are usually simple, but may be equivocal without supporting information.

A.1.3 FIS Data Consists of Two Parts

There are two parts to a conventional FIS data set, and each must be evaluated in detail.

1. Stratigraphic profiles of critical species and species ratios with depth (Sections 2.1 & 2.2).

2. Individual mass spectra for each sample (Appendix C).

A mass spectrum is a graphical display of the log of the ion current (measured on the mass spectrometers' detectors) as a function of the mass-to-charge ratio (m/z) of the detected ions (this will become clearer after reading the sections below). The amplitude of the ion current is proportional to the quantity of each type of ion, which, in turn, is proportional to the abundance of the species in the original gas mixture. Discrete peaks occur because the charged substances have discrete masses and discrete charges (usually single and positive).

There is a tendency for end users to concentrate on interpreting the first part of the data set (depth plots) and ignore the second (individual mass spectra). However, as will be shown, evaluation of individual FIS mass spectra is as important to the overall FIS interpretation as pattern-recognition of whole-oil chromatograms is to evaluating oil families. Imagine taking a single species present in a chromatogram and plotting it as a function of depth in the reservoir without ever considering its relationship to other species that are present. Certainly useful information results, but not nearly as much as could be offered by looking at the overall species distribution in the chromatogram in addition to the absolute abundance of a species or the ratio of two species as a function of depth. Similarly, both FIS depth plots and individual mass spectra are important to the final interpretation.

A.2 FIS Mass Spectra

A.2.1 Understanding FIS Mass Spectra

FIS data are collected on quadrupole mass spectrometers. These instruments distinguish among positively charged species using an electrodynamic field produced by application of combined RF and DC voltages to two pairs of metal rods in the filter section. A species

with a specific ratio of mass to charge (m/z) will have a dynamically stable trajectory within the field formed by the voltages on the rods, while all other species are filtered out. By continuously varying the applied voltages, a range of charged substances can be sequentially stabilized and allowed to traverse the length of the filter assembly to the detector. FIS data currently provided consists of measured responses on m/z 1-180. This mass range allows detection of all volatile inorganic species as well as organic compounds with up to 13 carbon atoms (C_{13}). Detection is accomplished either with a Faraday cup, which reads ion currents directly from the filter without amplification, or by an electron multiplier, which amplifies the single charge of a given ion into a current.

In order for species to be detected they must be charged (ionized). This is accomplished by bombarding volatiles released from fluid inclusions with electrons that are thermionically emitted from a hot filament. Energy transference from electrons to neutral particles generally results in positively charged parent ions, while excess energy obtained by a molecule in the initial ionizing collision results in fragmentation of the parent molecule into several species. For a single parent molecule, the resulting mass spectrum is known as a fragmentation pattern. The distribution of ions from a given species can generally be predicted by considering all combinations of molecules and isotopic variants. The following example illustrates this concept.

Molecular carbon dioxide has a formula CO_2 and most common molecular mass of 44. In detail, the mass of a given molecule of CO_2 can be 44, 45, 46, 47, 48 or 49 because both carbon and oxygen have two significant, naturally occurring isotopes (^{12}C, ^{13}C, ^{16}O, and ^{18}O). Hence, the fragmentation pattern of CO_2 would be expected to contain the singly charged species CO_2^+, CO^+, C^+ and O^+ with all possible isotopic permutations (14 possible masses). Additionally, doubly charged species can be produced. These species, although much rarer, have m/z of exactly half of their singly charged counterparts (e.g., $^{12}C^{16}O^{16}O^{++}$ has m/z of 44/2 = 22). Some peaks associated with doubly charged ions appear midway between two integer m/z locations (e.g., $^{13}C^{16}O^{16}O^{++}$ has m/z of 45/2 = 22.5). In general, instrument parameters favor the production of singly charged species. The relative frequency at which a given species will be produced and detected reflects natural isotopic abundance, ion production statistics and instrument parameters. In the above example of CO_2, the representative fragmentation pattern shown in Table V has been reported.

Table V: Partial Fragmentation Pattern for Carbon Dioxide

Mass	Species	Abundance	Mass	Species	Abundance
6	$^{12}C^{++}$	0.0005	28	$^{12}C^{16}O^{+}$	15
8	$^{16}O^{++}$	0.00046	29	$^{13}C^{16}O^{+}$	0.15
12	$^{12}C^{+}$	6.3	30	$^{12}C^{18}O^{+}$	0.029
13	$^{13}C^{+}$	0.063	31	$^{13}C^{18}O^{+}$	0.0029
16	$^{16}O^{+}$	13	44	$^{12}C^{16}O^{16}O^{+}$	100
18	$^{18}O^{+}$	0.0088	45	$^{13}C^{16}O^{16}O^{+}$	1.2
22	$^{12}C^{16}O^{16}O^{++}$	0.52	46	$^{12}C^{18}O^{16}O^{+}$	0.38
22.5	$^{13}C^{16}O^{16}O^{++}$	0.0047	47	$^{13}C^{18}O^{16}O^{+}$	0.0034
23	$^{12}C^{18}O^{16}O^{++}$	0.0012	48	$^{12}C^{18}O^{18}O^{+}$	0.00054
			49	$^{13}C^{18}O^{18}O^{+}$	0.000043

In spite of the usage in the previous paragraph, the term "parent peak" is generally given to the most intense peak of the mass spectrum of a single compound, while the term "molecular peak" is given to the singly charged ion with the same atomic mass as that of the pure compound. In the example above, both the parent and molecular peaks of CO_2 occur at m/z = 44. It is frequently the case, however, that the most intense peak is not the molecular peak. For instance, many normal paraffins with three or more carbon atoms (n-propane and greater) have parent peaks at m/z = 43, 57 or 71.

Complex volatile mixtures have mass spectra characterized by multiple, interfering ions on a given m/z, making it difficult or impossible to find a "clean" peak indicative of a specific species. Generally, higher m/z positions display more interference, but even low m/z have these overlaps (e.g. HD^+ and $^3He^+$ both appear at m/z = 3). This brings us back to one of the original points mentioned in the Introduction: mass spectra of multicomponent gas mixtures are qualitative in the sense that the absolute abundance of most species cannot be calculated. Nevertheless, similar compounds give similar fragmentation patterns that tend to be distinct from other classes of compounds. Because of this, the major classes of organic species (paraffins, naphthenes and aromatics) can be distinguished and their relative abundance estimated. Similarly, it is useful to consider the assemblage of anomalous peaks in a given mass spectrum, as these will often indicate the presence of compounds that are concentrated by similar subsurface processes (e.g., the water-soluble species benzene, toluene and acetic acid as the primary indicators of "proximal pay"). It is these assemblages that are most useful for distinguishing among major types of FIS mass spectra, as well as inferring the presence of a specific compound even where interfering ions are possible.

A.2.2 Five Types of FIS Mass Spectra

FIS mass spectra can be classified into five end member types:

1. *Non-hydrocarbon* FIS Mass Spectra
2. *Gas-range Enriched* FIS Mass Spectra
3. *Liquid-range Enriched* FIS Mass Spectra
4. *Water-soluble Enriched* FIS Mass Spectra
5. *Sulfur-compound Enriched* FIS Mass Spectra

Mixtures and gradations among these ideal end members are common. In considering the fragmentation patterns of organic species, it is useful to keep in mind the general formulas for the three dominant hydrocarbon classes:

1. *Paraffins:* C_nH_{2n+2}
2. *Naphthenes:* C_nH_{2n}
3. *Aromatics:* C_nH_{2n-6}

Non-Hydrocarbon FIS Mass Spectra

Non-hydrocarbon spectra generally show four major clusters or "humps" centered at approximately m/z 15, 28, 42 and 55. The tallest three peaks in these spectra occur within the

first three clusters at m/z 18, 28 and 44, and are attributable largely to water and carbon dioxide (with possible contributions from nitrogen on m/z 28). Most of the other peaks in the m/z 2-46 range of non-hydrocarbon spectra can be attributed to inorganic species or very minor organic contributions. Water and carbon dioxide are the two most abundant volatile species in subsurface pore fluids, hence their predominance here. FIS analysis is a bulk extraction technique, hence, many generations of fluid inclusions are potentially analyzed simultaneously. Because hydrocarbon inclusions are always present in much lower abundance than aqueous inclusions in a given rock volume, water and CO_2 peaks will generally dominate all FIS mass spectra, even those displaying hydrocarbon enrichment.

The fourth cluster of peaks, centered on m/z 55, represents minor amounts of hydrocarbons that are present in nearly all samples, as most hydrocarbons have a significant contribution in the m/z 55-57 area. Note, however, that even the largest of these peaks is generally three orders of magnitude below the major non-hydrocarbon peaks. Also, note that m/z 55 is commonly more abundant than m/z 57. The m/z 55 peak represents a major contribution from naphthenes, while the m/z 57 peak is generally a primary paraffin peak. The relative enrichment of naphthenes over paraffins in aqueous-dominated (non-hydrocarbon) FIS spectra may reflect the relative solubility of these species in water, as the progression from least soluble to most soluble follows the general rule: paraffins<naphthenes<aromatics. It is probable that these minor species are dissolved within aqueous fluid inclusions. The solubility of even relatively insoluble C_4 paraffin in water can be several hundred parts per million, well within the detection limit of the FIS system.

Gas-Range Enriched FIS Mass Spectra

Gas-enriched spectra are characterized by strong responses on C_1-C_5 hydrocarbons with dwindling responses in the C_6-C_8 range, and essentially no response in the C_9+ range. Drier gases may exhibit responses only in the C_1-C_3 range. Naturally occurring hydrocarbon gases tend to be dominated by short-chain paraffins; hence, these are the primary peaks to look for in identifying gas FIS spectra. Predominant peaks (parent and some significant subordinates with intensity of at least 10% of the parent) for low-molecular weight normal paraffins and naphthenes (cycloparaffins) are shown in Table VI.

Table VI: Partial Fragmentation Pattern for Gas-Range Hydrocarbons

Methane	**Ethane**	**Propane**	**n-Butane**	**n-Pent**	**n-Hex**	**Cyclopent**	**Cyclohex**
16(100%)	28	29	43	43	57	42	56
15	27	28	29	42	43	70(30%)	84(75%)
14	30(25%)	27	28	41	41	41	41
13	29	44(27%)	27	27	56	55	55
	26	43	41	28	29	39	42
		39	39	29	27	27	69
		41	42	57	42	40	27
			58(9%)	72(9%)	39	29	39
					86(15%)		

Here, molecular peaks are shown with their intensities relative to the parent peak. Note that the molecular peaks for C_4-C_6 normal paraffins are not among the top five most intense peaks (a feature of fragmentation patterns that was mentioned previously). Considering the location of the above peaks, a gas-enriched mass spectrum should contain peak clusters at m/z 13-16, 26-30, 39-44 and 55-57. Note that this is precisely where the four peak clusters are located in the previously described non-hydrocarbon mass spectrum (where they were attributed largely to CO_2 and water, nitrogen and minor hydrocarbon contributions). The distinction lies in the relative proportion of these species. Gases can typically contain 90% C_1 and 95% C_1-C_3. Hence, FIS gas spectra typically have prominent C_1-C_3 clusters. The water triad at m/z 16-18, which commonly shows a pattern of monotonic increase from 16 to 18 in non-hydrocarbon spectra can become disturbed at high gas concentrations so that masses 15 and 16 become dominant, even to the point of being more intense than mass 18. Similarly, the 26, 27, 39, 41 and 43 peaks generally display significantly higher intensities than in non-hydrocarbon spectra. The ratio of mass 57 to mass 55 (C_4+ paraffins / C_4+ naphthenes) may become quite high, reflecting the paraffinic nature of many gases.

Liquid-Range Enriched FIS Mass Spectra

FIS spectra that contain significant quantities of liquid-range petroleum species display repetitive peak clusters corresponding to fragments with successive carbon numbers in the C_7-C_{13} range as shown in Table VII.

Table VII: Partial Fragmentation Pattern for Liquid-Range Hydrocarbons

Carbon #	m/z Cluster	Parent (nC)	Molecular (nC)
C7	95-101	43, 57, 41	100(14%)
C8	109-115	43, 57, 41	114(7%)
C9	123-129	43, 57, 41	128(8%)
C10	137-143	43, 57, 41	142(7%)
C11	151-157	43, 57, 41	156(4%)
C12	165-171	57, 43, 71	170(8%)
C13	179-185	43, 57, 41	184(5%)

Note, again, that molecular peaks for high-molecular weight hydrocarbon species are generally only 5-15% of the parent peak. Also note that the three most intense peaks for the C_7-C_{13} paraffins are usually the same, and represent some of the most intense peaks previously identified for the C_4-C_6 gas-range paraffins.

Only normal (straight-chain) paraffins have been considered in the above table. Typical C_6-C_{10} (gasoline) fractions contain 40% paraffins, 50% naphthenes and 10% aromatics by volume. Typical C_{11}-C_{13} (kerosene) fractions contain 30% paraffins, 50% naphthenes and 20% aromatics by volume. As the general formula for naphthenes suggests, molecular peaks are shifted downward by 2 m/z units (e.g., the C_7 naphthene molecular peak is at 98). Hence the major contribution at 43 for normal paraffins becomes 41 for naphthenes, 57 becomes 55, and so on. This is why the ratio of 57 to 55 is plotted in basic FIS data packages: to track the relative distribution of paraffinic and naphthenic compounds as well as the processes that fractionate them (e.g., dissolution in an aqueous phase; recall the solubility law for hydrocarbon species). Aromatic fragmentation patterns will be considered under the explanation of

water-soluble FIS mass spectra.

Natural liquid petroleum is a complex mixture containing hundreds of specific compounds within these classes. Thus, the qualitative nature of FIS mass spectra is reiterated. Major classes of organic compounds can be identified, distinguished and tracked semi-quantitatively, but specific compounds cannot be quantified except under special circumstances. From the foregoing discussion it becomes apparent that even though the FIS analytical procedure does not scan past the molecular peak of nC_{12}, contributions on low molecular weight species can include species well above C_{13}. The maximum carbon number contributing to the FIS mass spectrum is limited only by the volatility of the given compounds within the high vacuum system and their abundance. However, it is unlikely that $C_{20}+$ compounds contribute significantly to FIS responses, given their volumetrically low abundance and vapor pressures.

Water-Soluble Enriched FIS Mass Spectra

FIS mass spectra containing anomalous concentrations of water-soluble volatile species are perhaps the most interesting of the main spectral types. Key indicator species are acetic acid, benzene and toluene (see Table VIII). Other common compounds include methane, ethane and carbon dioxide (fragmentation patterns previously outlined).

Table VIII: Partial Fragmentation Pattern for Water-Soluble Species

Formic A.	**Acetic A.**	**Propionic A.**	**Butyric A.**	**Benzene**	**Toluene**	**Xylenes**
29	43	28	60	78(100%)	91	91
46(61%)	45	29	73	77	92(75%)	106(65%)
45	60(60%)	74(79%)	27	52	39	105
28	15	45	41	51	65	39
17	42	73	42	50	51	51
44	29	57	43	39	63	77
			88(3%)			

Aromatics tend to have strong molecular peaks, unlike many paraffinic and naphthenic compounds. The species above are easily identified in mass spectra because major peaks occur within the valleys formed between the peak clusters of predominant paraffinic and naphthenic ions. These species (particularly aromatics) are present at some level in most FIS spectra that contain liquid-range hydrocarbons, because, as outlined above, aromatic species comprise 10-30% of most oils by volume. However, typically, aromatic peaks are 0.5-1 order of magnitude less intense than the adjacent paraffin/naphthene m/z cluster. Although there are no quantitative rules, aromatics are considered anomalous when visual aromatic peak heights becomes sub-equal to, or greater than, adjacent paraffin/naphthene peak clusters. Aromatic peak heights 1-2 orders of magnitude higher than the adjacent peak clusters are not uncommon in FIS spectra that indicate strong enrichment of water-soluble species.

Organic acids represent the most common organic species reported from formation water analyses, and of these, the mono-functional acids dominate. Acetic acid and propionic acid generally have the highest reported concentrations and abundance generally decreases with increased carbon number. As can be seen from the table above, some major peaks have potential interferences with CO_2. The most promising peaks for recognition of organic acids

are m/z 60 and, perhaps, 73-74. Organic acids are considered to be present in anomalous concentration when a distinct peak occurs at m/z 60. In the absence of organic acids this location generally lies in a "peak-height valley", even on hydrocarbon-enriched FIS mass spectra. In extremely enriched samples the intensity of the 60 peak is greater than all masses in the 60-180 m/z range.

Where anomalous, the assemblage of species outlined above are present in proportions much different (and greater) than their concentrations in typical petroleum. The commonality that they hold is their relatively high solubility in water compared to paraffinic and naphthenic compounds of similar molecular weight. For instance, benzene is about 100-300 times more soluble in water than n-hexane, and about 3 times more soluble than toluene. Acetic acid is completely miscible in water. Benzene concentrations of several 10's of ppm are typical of oilfield brines, while organic acid concentrations of several thousand ppm have been recognized. Hence, these species in FIS spectra are generally interpreted to be held in solution within aqueous inclusions, rather than present within a free hydrocarbon phase. The origins of these compounds are outlined in a later section, but the most interesting from an exploration standpoint involves stripping from present-day petroleum accumulations and transport via diffusion into the surrounding water-dominated pore network. Considering relative solubility rules, one would predict that the ratio of paraffins to naphthenes (e.g., inferred by a m/z ratio such as 57/55) would be low. In fact, this is generally the case; further evidence that it is relative solubility in water that is driving the distribution of these species in water-soluble enriched FIS mass spectra.

Sulfur-Compound Enriched FIS Mass Spectra

The final type of end-member FIS mass spectrum contains anomalous concentrations of sulfur compounds. The species H_2S, COS, CS_2 and SO_2 and/or native sulfur gas are key indicators, although not all may be present in a given sample (see Table IX).

Table IX: Partial Fragmentation Pattern for Sulfur Compounds

H_2S	COS	S_2(?)	SO_2	CS_2	S_8
34(100%)	60(100%)	64	64(100%)	76(100%)	64
32	32	32	48	32	256(60%)
33	28		32	44	160
				78	128
					192
					258
					96
					32

As can be seen, sulfur compounds tend to have strong molecular peaks, and enrichment is indicated if some combination of the m/z peaks 34, 60, 64 and 76 display anomalous intensities. Because these m/z positions generally occur in abundance valleys, the same qualitative rules apply as for acetic acid; namely, if a discrete peak is observed at one of these primary ion locations, the species is considered anomalous. The peak intensity need not rise to the level of the adjacent paraffin peak, although in extreme cases, it may. The 60 peak has a major interference with organic acids as outlined in the previous section. Hence the presence of COS

is inferred (but not demonstrated) only in the presence of other sulfur species. The m/z 32 would appear to be a good one for indicating sulfur presence; however, this ion location suffers major potential interference from atmospheric oxygen (O_2^+).

Care must be taken when interpreting sulfur-enriched FIS spectra, because at first glance they resemble the water-soluble enriched spectra. Ideally, the distinction lies in the location of CS_2 at m/z 76 (as opposed to benzene at 78), H_2S at m/z 34 and S_2^+ and/or SO_2 at m/z 64. SO_2 presence can be verified by the presence of a paired anomaly at 64 and 48. In practice, it is sometimes difficult to distinguish between sulfur-enrichment and water-soluble species enrichment when these species are not strongly anomalous, and combinations of the two spectra occur as well.

A.2.3 Summary of the Five Spectral Types

The above is a relatively detailed account of the characteristics of the five major classes of FIS mass spectra. In the end, however, the best way to recognize and distinguish among spectral types is to compare them to the end-member examples presented herein and categorize them by eye. After examining a few examples of each, pattern recognition will become easy. Understanding the complexities outlined in the previous sections is important, but usually unnecessary for first-order interpretation of FIS mass spectra. To summarize:

Non-hydrocarbon Spectra: Characterized by four peak clusters centered on m/z 15, 28, 42 and 55; the first three being dominant. Most peaks are attributable to water and carbon dioxide.

Gas-range enriched: Characterized by strong responses on C_1-C_5 (m/z 12-72) and lesser intensities on higher molecular weight ion locations. Peak clusters may be more broad at m/z 12-30 and 37-46. Predominance of masses 15 and 16, and high 57/55 ratios is possible.

Liquid-range enriched: Characterized by the presence of C_7-C_{13}+ species as regularly-spaced peak clusters in the m/z 95-180 range, which are dominated by ions from paraffinic and naphthenic compounds. Aromatic species contribute subordinate peak clusters between the paraffin-naphthene peaks (although, typically only benzene, toluene and xylenes are resolved).

Water-soluble enriched: Characterized by methane, ethane, organic acids, benzene and toluene. Acetic Acid (m/z 60) and aromatic peak clusters (m/z 78, 91, 105) attain intensities near or greater than those of adjacent paraffin-naphthene peak clusters.

Sulfur-compound enriched: Characterized by the presence of H_2S, COS, CS_2 and SO_2 and/or native sulfur gas as indicated by anomalies on some combination of the m/z peaks 34, 48, 60, 64 and 76.

A.2.4 Combinations of Spectral Types

Combined FIS spectra are common, and appear as superimposed end member types. Although combinations of all end member spectra have been noted, the most common are gas + liquids and liquids + water-solubles. Recall that FIS is a bulk technique and samples the entire fluid history of the pore system. Hence, mixed FIS spectra might be expected if the sample has experienced temporally distinct charges of petroleum (or brine) types or contained a heterogeneous (immiscible) fluid in the pore system at some time.

A.3 Interpreting FIS Track Plots and Petrographic Data in a Geologic Context

Fluid inclusions are the only direct records of paleofluids existing in the subsurface, and as such, have the potential to record conditions accompanying geologic processes, including petroleum migration. By studying the subsurface distribution of paleofluid chemistries with FIS, one can obtain valuable and unique information on three major exploration topics:

1. Petroleum migration or paleocharge
2. Seals
3. Proximity to undrilled pay

and two major production topics:

1. Pay zone and bypassed pay delimitation
2. Reservoir compartmentalization.

The previous discussions have concentrated on identifying spectral types in FIS data. This is a necessary first interpretive step. The next task is to evaluate the significance of FIS depth trends in their own right (now knowing their spectral origins), and eventually, in light of other available information to answer specific questions, such as were enumerated above. Petrographic data from anomalous fluid inclusion zones are often critical elements of these higher order interpretations, as will be seen, which why petrographic follow-up work is conducted as a routine part of every FIS analysis (see Table of Petrographic Observations).

A.3.1 Significance of FIS petroleum indications

The most basic question that FIS can address is "Is there any evidence for present or past petroleum in this borehole?" Documentation of an FIS hydrocarbon anomaly generally provides a positive answer to this question, but could indicate other processes as well. Possible explanations for an FIS hydrocarbon anomaly are discussed in the following paragraphs.

Migration without trapping

A migration pathway may be indicated when FIS responses are low or moderate, when contamination and recycled inclusions can be discounted, when quoted visual petroleum inclusion abundances are "rare" or "several" (see Table of Petrographic Observations), and when no other petrographic or log evidence of current petroleum charge is identified in the zone. There are a number of factors that influence inclusion abundance and, consequently, raw FIS response strength, including geologic setting, extent of diagenesis, rock type and permeability. However, it has been demonstrated that both visual petroleum inclusion abundance and FIS strength within many porous reservoir rocks is proportional to hydrocarbon saturation or paleosaturation in a relative sense. Because migration occurs at average bulk-volume petroleum saturations below those encountered in charged reservoirs, FIS signal strength and visual inclusion abundance are generally lower along migration pathways than in charged reservoirs from the same area.

Current Charge

A zone that displays strong FIS hydrocarbon indications and high visual petroleum inclusion abundance (i.e., common, abundant or extremely abundant) may reflect penetrated pay, but could also indicate paleo-charge or, in some cases, a migration pathway (e.g., where inclusion abundance is enhanced by extensive microfracturing). A provisional interpretation of current charge is strengthened if residual petroleum (especially live oil stain) is identified in thin section, and particularly if water-soluble petroleum species (so-called "proximal pay indicators"; see below) are recorded in FIS data (e.g., in the seal overlying the anomaly, in the water leg underlying the anomaly, or in low permeability zones within the reservoir section itself). Any independent indications (e.g., from electric logs or mudlog gas shows) provide further encouragement.

Paleo-charge

Intervals of strong FIS response, high visual inclusion abundance (i.e., common, abundant or extremely abundant) and significant bitumen (e.g., dead oil stain or asphaltic residue) without accompanying water-soluble anomalies or independent evidence of current charge, may represent a paleo-column, but could also represent current charge or in rare cases a migration pathway. The interpretation of paleo-charge is favored if a valid DST has shown the interval to be currently wet.

Recycled inclusions

Very rarely, detritus that is generated from previous sedimentary rock may contain inherited petroleum inclusions. These inclusions must be recognized, as they clearly do not provide any useful information about the current petroleum system(s). Petrographic or microthermometric criteria can often be used to argue the origin of these inclusions, for instance, the presence of petroleum inclusions along recycled quartz overgrowths, or measured homogenization temperatures that are too high to have been produced during the current burial history. Associated FIS depth trends are usually erratic and poorly compartmentalized, and inclusion abundance is typically low. Inherited inclusions may be restricted to specific geologic units that derived detritus from a particular provenance, and are not found in intercalated chemical precipitates (e.g. bedded carbonates or diagenetic cements).

Heavy bitumen stain

In some instances, pore-occluding bitumen may contribute to FIS signals. Here, solid petroleum behaves as any other cement, and is capable of trapping residual hydrocarbons as bitumen-hosted fluid inclusions. These may be invisible due to the opacity of the solid petroleum host. Petroleum species may also desorb from pore-occluding bitumen during crushing, much as they do from mature kerogen (see below). Bitumen-sourced FIS responses may be inferred when strongly anomalous zones contain low visible petroleum inclusion abundance but have significant amounts of bitumen (e.g., common, abundant or extremely abundant). Abundant pore-filling bitumen in porous rock implies significant petroleum saturation at some time, so low visual petroleum inclusion abundance is unexpected (and not commonly encountered). In such cases it is possible either that the size of the inclusions are below the resolution of the light microscope (< 1 micron), that grain surface conditions (e.g., wettability) did not favor trapping of inclusions, or that the section was diagenetically quiescent during and after charging (i.e., little or no cementation or microfracturing).

Mature Source Rock

Mature source rock can contribute to FIS responses. Here, the signal is the combined effect of species desorbed from freshly crushed kerogen surfaces and conventional fluid inclusions that represent trapped in-situ generated petroleum. The chemistry and strength of FIS responses in source rocks tend to reflect kerogen type and maturity, at least in a general sense. Hence, mature gas-prone kerogen with limited liquids potential typically gives dry gas responses, while mature source rocks with liquid-prone or mixed kerogen types (including some coals) tend to have significant responses on both gas and liquid-range petroleum species. Furthermore, as maturation proceeds, FIS hydrocarbon responses progress from low (immature) to high (mature) to low again or dry gas (overmature). These trends are very qualitative, and FIS response in source intervals should not be used as a substitute for classical source rock analysis techniques. An in situ origin (local generation) is suggested for FIS responses if petrographic data from the anomalous zone reveals low permeability rock containing significant quantities of mature kerogen (common, abundant or extremely abundant). Liquid-prone kerogen is likely to be mature if it exhibits moderate to strong orange fluorescence. Coal-related FIS responses are often quite waxy, may be enriched in aromatics, and typically have large relative contributions from higher molecular weight species (i.e., flat spectral profiles).

Contamination

Except in rare cases, contamination is not a significant issue in FIS data. Pre-analytical washing and vacuum heating procedures are sufficient to remove most surface-adsorbed organic compounds that are volatile under FIS analytical conditions, including natural fluids such as residual oils, as well as elements of the mud system, including oil based mud. Insoluble organic additives (particularly natural materials like gilsonite) pose a greater threat, as they may not be removed by standard treatment, and can give responses similar to indigenous kerogen or bitumen. Infrequently, an organic-based mud system will contribute to FIS response, and in rare instances may be dominant. This tends to occur in recently drilled, unconsolidated mud-rich sections, which are difficult to wash without complete loss of sample. Contamination has also been suspected in some diapiric or bedded salt sections, where drilling encapsulation of these species is facilitated by the easily dissolved and precipitated halite. Processed contaminants often have a distinctive (and unnatural looking) chemistry, which might include extreme light end depletion, very low aromatics (particularly benzene, which may be removed for environmental reasons) or extremely high toluene (possibly residue from soxhlet extraction). Petrographic criteria can generally be used to assess the likelihood of contamination in a given anomalous FIS zone.

A.3.2 Petroleum Type and Quality

Interpreted petroleum type and quality is based predominantly on the characteristics of individual mass spectra from each depth as already discussed (sample spectra are located in Appendix C). Three factors are considered: the maximum carbon number detected, the qualitative abundance of low molecular weight alkanes relative to high molecular weight alkanes (including the general slope of the imaginary line connecting the C_1-C_{13} alkanes), and the presence or absence of species or ratios indicative of bacterial or thermal alteration (including souring processes). It is important to note that the interpreted petroleum type assumes a single, uniform petroleum inclusion population. The actual migration or charging history, on the other hand, may have involved multiple pulses with different composition (e.g., oil and

gas) and the relative abundance of these inclusions will influence the bulk spectra. Additionally, total inclusion abundance will affect the spectra insofar as higher molecular weight species represent a smaller volumetric proportion of petroleum and are also less volatile, hence decrease below instrumentation detection limits before low molecular weight species. Consequently, some samples with low oil inclusion abundance generate wet gas mass spectra, for instance. Optical inclusion abundance and characteristics should be consulted, where provided, to verify the interpreted petroleum type (see Table of Petrographic Observations). With the above limitations in mind, the following petroleum types are identified on the basis of spectral characteristics:

Dry gas: mostly C_1 with lesser C_2-C_3 and no higher hydrocarbons.

Wet gas: C_1-C_9 may be present, but C_6+ species are in minimal abundance. The alkane slope is extreme.

Gas-condensate: C_1-C_{11} may be present. The alkane slope is quite steep, reflecting a very gas-enriched phase.

Volatile oil: C_1-C_{13} present. Slight gas-range enrichment is observed and the alkane slope is moderate to steep.

Oil: C_1-C_{13} is present. The alkane slope may be flat to moderate.

Biodegradation is suggested if sulfur compounds such as H_2S, COS, CS_2, S_2 (+/- SO_2) and/or thiols are present in addition to petroleum species. Ratios of paraffins to naphthenes may be low as well, as bacteria typically prefer to metabolize alkanes compared to other classes of petroleum compounds. Petrographic data may provide further evidence for biodegradation in the form of low-gravity petroleum inclusions. Bacterial activity is generally restricted to maximum burial temperatures below 65-70°C; hence FIS evidence of biodegradation is most commonly observed in rocks that are currently below this temperature.

Thermal alteration of liquid petroleum species can produce spectra very similar to those generated from biodegraded hydrocarbons, because the products of two common processes, bacterial sulfate reduction (BSR) and thermochemical sulfate reduction (TSR), are essentially identical. The best distinction is made from current bottom-hole temperature data, which, if above 140°C or so may be indicative of TSR, and if below 70°C or so is more consistent with BSR. Potential interpretive problems arise in the intervening temperature range, when deeply buried sediments are unroofed or when petroleum altered at shallow depths becomes buried to greater depth. Petrographic data may help, as pyrobitumen frequently accompanies TSR, while low-gravity liquid petroleum inclusions often occur in association with bacterially altered oils. Additional temperature or thermal maturity data (including fluid inclusion homogenization temperatures) may also be useful.

The presence of significant amounts of sulfur species can indicate a sour petroleum phase, where the souring process may in some cases be a reflection of the source rock, but could also reflect BSR or TSR. A study of TSR sour gas pools in Canada suggests that evaluating the relative proportion of products and reactants can provide a measure of sour gas potential. As TSR progresses, long-chain alkanes decrease while low molecular weight petroleum species increase along with CO_2, aromatics organic acids and the various sulfur compounds enumerated above. Ironically, H_2S alone may not be as accurate an indicator of H_2S content, as it is scavenged naturally (e.g., to form pyrite in iron-rich rocks) and by the metallic internal surfaces of the analytical system.

A.3.3 Water-soluble Anomalies and Proximal Pay Indications

Water-soluble species, particularly benzene and toluene, have been used for decades to search for geochemical halos surrounding petroleum accumulations. The limitation of conventional techniques is that fluid samples are rarely intentionally collected from wet reservoirs. However, similar water-soluble species anomalies have been found in FIS data. Compounds generally include some subset of the following: methane, ethane, CO_2, acetic acid, benzene, toluene and xylenes, as well as low paraffin-to-naphthene and high aromatic-to-paraffin ratios. There are three dominant sources of this FIS volatile suite: maturation of kerogen-rich rock, thermal alteration of liquid petroleum, and diffusive stripping from a present-day charged petroleum reservoir proximal to the borehole. The latter of these three possibilities is the most important from an exploration standpoint, and is the FIS analog of the classic technique of analyzing formation fluids for benzene.

Criteria to distinguish among the three potential sources of water-soluble anomalies are often found during petrographic examination. A kerogen source may be inferred if the interval contains a substantial amount of mature kerogen, and where FIS responses include appreciable contributions from other hydrocarbon species (e.g., where water-soluble species are superimposed on an otherwise normal hydrocarbon response). Thermal alteration may be expected if pyrobitumen is present, and, particularly, if sulfur compounds are also detected in FIS data (see discussion above). These species may have resulted from thermochemical sulfate reduction at temperatures above 140°C. Extreme examples of this process are found in deep Devonian sour gas pools of the Western Canada Sedimentary Basin.

True "proximity to pay" (a.k.a., PTP) anomalies tend to occur in cuttings from shale rich lithologies, that are geometrically connected to penetrated or lateral pay. Examples include top or lateral lithologic or structural seals to a charged reservoir, and transition zones or water legs underlying petroleum. The signal is always a present-day feature and is thought to result from drilling encapsulation of penetrated pore fluids within easily sheared or thermally reconstituted lithologies. A significant amount of unpublished analytical data as well as a large body of empirical observation support this interpretation, although details of the process are still debated. Petrographic criteria are generally sufficient to interpret PTP signals, and these include absence of evidence for the other two possible origins, as well as presence of distinctively sheared, shale-rich cuttings.

PTP signals can be found along with direct FIS hydrocarbon indications in flushed reservoirs. Here, the water-soluble anomalies may be sourced from irreducible petroleum saturation with the paleo-reservoir, or may indicate an updip charge (possibly the leaked or structurally disturbed petroleum column that once resided at the well location).

PTP anomalies can be classified into two chemical subtypes: acetic acid + benzene dominant, and benzene dominant. Acetic acid is though to be sourced from high molecular weight compounds within the petroleum phase; hence, its presence suggests the nearby accumulation is oil or gas-condensate. Benzene without accompanying acetic acid suggests a drier petroleum phase, most likely wet gas. Dry gas generally does not give a PTP response because the key indicator species are not present in the petroleum phase, hence cannot be fractionated into nearby aqueous fluid.

When PTP anomalies are identified, a possible link to a nearby reservoir should be investigated. Many scenarios are possible, including an overlying penetrated charge, lateral production in a shallower section that is not under closure at the well location, or charge in remaining updip closure in a reservoir that tested wet at the well location.

A.3.4 Seals

FIS seals are inferred at boundaries marking abrupt changes in FIS species strength or chemistry. The underlying assumption is that detected fluids are more or less synchronous on either side of the boundary and that some process has prevented free mixing of species across this barrier. In detail the boundary may represent a change in lithology, poroperm or a structural element. In the case of in-situ generated petroleum the boundary might represent a transition from poor to better source rock, or immature to mature source intervals. In the case of migrated petroleum the boundary might represent the extent of petroleum migration through porous rock, or the top seal to a present or past petroleum column. Basal compartment limits may represent seals or, in some cases, fluid contacts or paleocontacts (see below). In general, only the tops of FIS compartments are identified on interpreted FIS depth plots. If fluids were not synchronous on either side of the compartment boundary (e.g. a post-migration unconformity) then the seal interpretation would be in error. Seals may be selective or chromatographic, in which case low molecular weight species may migrate across the boundary, while higher molecular weight species do not.

A.3.5 Microseepage

FIS microseeps are analogous to gas chimneys seen in seismic data, and surface manifestations of deeper charge identified in surface geochemical surveys. They are interpreted to result from near-vertical migration of light hydrocarbons followed by bacterial alteration in the shallow subsurface at temperature-depth conditions permissible for bacterial activity. Most bacteria are restricted to temperatures below 65-70°C; hence, anomalies may be observed in the upper 1-3 km of rock column, depending on the prevailing geothermal gradient. Key indictor species include light hydrocarbons, CO_2, possibly organic acids and aromatic compounds, and sulfurous volatiles, including H_2S, COS, CS_2, S_2 (+/- SO_2) and in some cases thiols. H_2S is often sequestered within pyrite in iron-rich siliciclastics, hence is less common in shale-bearing lithologies. Inclusion formation in such low temperature environments may be aided by precipitation of bacterial carbonate. FIS microseeps are geometrically distinct, often beginning at the surface and abruptly disappearing at the appropriate temperature-controlled depth.

The presence of an FIS microseep appears to be a good indicator of deeper charge in the immediate vicinity, although weak seeps may represent regional signals within shallow aquifers. Data suggest that these anomalies overlie 75-80% of productive reservoirs, while only 10% of non-productive areas display similar signals. Hence, the presence of a strong seep within a dry hole might indicate deeper or nearby lateral charge in the area.

A.3.6 Fluid Contacts

The basal boundary (abrupt or transitional) of any strong FIS compartment is a candidate for a present or past fluid contact, although the interpretation is often equivocal. The most compelling evidence for a present day contact occurs where hydrocarbon-dominant FIS signals (the petroleum leg) give way to water-soluble dominant signals (PTP in the water leg) and where visual petroleum inclusion abundance displays a parallel decrease. When inclusion abundance is high in the petroleum zone but PTP signals are not present in the water leg, it is possible that a paleo-charge is recorded. If the base of the anomaly corresponds to the base of the reservoir, or an abrupt decrease in reservoir quality, then the actual fluid contact (or

paleo-contact) may reside further downdip.

A.4 Individual Track Plots

A.4.1 Explanation and Significance of Individual Track Plots

The following is a synopsis of the significance of the different patterns of mass abundances and abundance ratios shown in Tracks 1-25. Note that not all species are quantified using their parent or molecular peaks (e.g., methane at $m/z = 15$) in order to minimize interfering contributions from other species.

A.4.2 Ratios vs. Absolute Abundance

Both ratios of key ionized compounds as well as absolute abundances of key compounds (relative to a natural oil inclusion standard) are used in interpretation. Absolute abundances of species can be influenced by the efficiency of inclusion formation, the size distribution of the inclusions, the saturation and residence time of the fluid within the pore system and the relative proportion of fluid of a given composition that moved through that stratigraphic compartment. Chemical ratios, on the other hand, are not as susceptible to lithologic/diagenetic controls on inclusion formation/distribution, hence, may be better suited for displaying chemical compartments in some cases. They are also useful for enhancing some of the subtle trends within the data, and for characterizing chemical variability among petroleum inclusion compartments, which could be related to source, timing, or migration process. Ratio plots are not completely independent of inclusion abundance, as the intensity of mass spectrometer responses is somewhat non-linear with respect to ion concentration. Both types of plots should be considered during interpretation.

Track 1: Total Response - This represents the sum of the positive responses on all measured masses from $1 \leq m/z \leq 180$. These data are potentially useful for some data normalization schemes, or for estimating the relative percentage of a given compound in the analyzed sample. Note that responses are generally dominated by water and carbon dioxide, and that absolute quantification is not possible because water cannot be quantitatively analyzed with this system. The polar nature of water causes it to adhere to metallic surfaces inside the instrument resulting in false readings by the detector. However, two characteristics of the total response are noteworthy. First, total responses are often orders of magnitude greater for samples yielding proximity spectra than for other samples originating outside the hydrocarbon zone, even though the lithologies are usually clay rich, hence low in natural inclusion abundance. This is one line of evidence that leads us to hypothesize that proximity samples are dominated by drilling induced inclusions which trap some of the present day formation fluid. Secondly, inferred petroleum migration compartments are often characterized by high total responses. This suggests that both organic and inorganic inclusions are anomalously represented within these compartments. The significance of this correlation is not fully understood, but may document a fracture forming process occurring during focused movement of basinal fluids, including petroleum. If so, it may eventually provide additional information about the nature and mechanisms of secondary petroleum migration.

Track 2: $m/z = 44$ Dominant peak for carbon dioxide (CO_2^+), with possible minor contribution from C_3^+ hydrocarbon fragments and acetic acid. Anomalous values have been noted associated with pan-evaporative dolomitization of limestones in China and Oman. CO_2 response is often

high in proximity samples which show elevated levels of acetic acid. CO_2 is generally present in anomalous concentrations in FIS microseeps, where it is a product of bacterial alteration of seeping light hydrocarbons.

Track 3: $m/z = 34$ - Dominant peak for hydrogen sulfide (H_2S^+). Anomalous values associated with petroleum may indicate sour oil or gas. H_2S is also noted at times in association with shallow dry gas of probable biogenic origin (including FIS microseeps) and with some proximity zones. H_2S is probably not quantitatively analyzed due to rapid scavenging by metallic surfaces of the analytical system.

Track 4: 34/(34+15) - H_2S/(H_2S+methane). Not frequently used, but ratio tends to be elevated in sour gas zones.

Track 5: 4/(4+2) - Helium fraction $^4He^+/(^4He^+ + H_2^+)$; ratioed to mass $m/z = 2$ to indicate the presence of anomalous He. Helium anomalies have been found in association with unconformities, thrust faults which sole in crystalline rocks, arkosic detritus sourced from such crystalline rocks (e.g., granite wash), gas sourced from old, radioactive shales and mafic hypabyssal volcanic rocks. An abrupt change in helium abundance has been documented within Precambrian rocks worldwide. It is possible that this reflects a fundamental evolutionary step in the Precambrian atmosphere.

Track 6: Air Confidence - This represents the results of an algorithm which performs five tests for the presence of the air components nitrogen, oxygen, and argon. The plot is scaled in integer values from zero to five, corresponding to zero to five positive tests. Values in the 4-5 range indicate a high confidence for air. Some anomalies may represent small leaks in the vacuum system. Natural air inclusions have been recognized in vadose cements below paleoexposure surfaces, as well as in some aeolian sands and evaporites.

Track 7: 30/(30+15) - ethane/(ethane+methane). Except for very dry gas, petroleum migration zones generally show elevated ratios of ethane to methane, provided that the petroleum is transported as a separate phase. Petroleum transported as a dissolved solute species in aqueous solution (e.g., in the case of proximity) may have low ratios of ethane to methane, due to the relatively higher solubility of methane in solution.

Track 8: $m/z = 15$ - CH_3^+; mostly derived from methane, with minor contributions from all other paraffins and NH_2^+, if present. Used as a relatively clean peak for methane; response is nearly as great as for the methane molecular peak. Anomalies are associated with oil and gas migration as well as water zones carrying significant dissolved gas. Distinction between dry gas and oil is accomplished by comparing responses on higher molecular weight fragments (e.g., $m/z = 97$). Transport in aqueous solution is suggested by co-occurrence of other water-soluble hydrocarbons as well as high ratios of water soluble to water insoluble species (e.g., 60/57, 55/57, 77/71). Methane dominated dry gas of possible biogenic origin is often documented in offshore wells at depths above 1200 m. These zones also often indicate anomalous sulfur species, which might document the activity of sulfate-reducing bacteria. In rapidly buried, relatively young sections, (e.g., offshore Trinidad and Gulf Coast) biogenic gas inclusions may be detected to much greater depths. These are FIS microseeps and are thought to sourced from leakage of light petroleum from depth.

Track 9: $m/z = 30$ - Ethane molecular peak ($C_2H_6^+$). Use similar to that of methane ($m/z = 15$).

Track 10: $m/z = 60$ - Acetic aid (CH_3COOH), with possible contribution from COS in some environments. Acetic acid anomalies may be sourced from source rock maturation, thermal alteration of liquid petroleum or diffusive stripping from oil or gas-condensate accumulations (the latter are known as proximity-to-pay indications or PTP). It is thought that PTP represent samples of present day formation fluids, which are entrapped during drilling, probably through thermal and mechanical processes acting on clay-bearing lithologies in the neighborhood of the drill bit. Our understanding of the sources and sinks of organic acids and water-soluble aromatics, particularly benzene, suggest that the signal must be actively fed; hence, it is unlikely that we would see these signals preserved for geologic time in paleo-reservoirs, or along migration paths, although this has not been fully demonstrated. The strength of the signal is dependent on so many variables, including drilling conditions, lithology, formation fluid and oil chemistry, temperature, hydrodynamics, etc., that it is doubtful that quantitative assessment of distance from accumulation is possible. As with most FIS interpretations, documenting proximity is deemed significant, while its absence is not necessarily so, unless a particular area is well calibrated. Thermal processes within the reservoir in which liquid-range petroleum is broken down to lower molecular weight petroleum with one byproduct being organic acid probably source acetic acid, in the context described above. As such, the presence of organic acid anomalies with benzene and or toluene anomalies suggests that the accumulation has some liquid-range component, although a few barrels of condensate per MMCF of gas appears to be enough to provide a signal, at least in relatively low salinity formation fluids which are very close to pay zones. As mentioned above, other sources of organic acids are possible, including maturation of source rocks (particularly coals), severe thermal degradation of oil (particularly during thermochemical sulfate reduction) and stripping from residual oil in high Sw zones or recently flushed reservoirs; hence, the nearby reservoired hydrocarbons may very well be subeconomic. COS and acetic acid can be expected in some of the same environments, so the distinction between the two is not always possible. However, COS tends to be less water soluble, and has a higher affinity for the petroleum phase than acetic acid.

Track 11: $m/z = 78$ - Benzene ($C_6H_6^+$). High values are associated with samples containing inclusions with liquid-range petroleum, as well as samples displaying "proximity" signals. A distinction can be made between these two by looking at individual spectra, or by comparing the response on the relatively insoluble paraffins (e.g., $m/z = 57$ or 71). Note however, that some samples may indicate both oil inclusions and proximity to pay; and it is here that individual mass spectra must be studied. Such mixed spectra are indicative of some pay zones (particularly those with significant Sw, as well as zones through which petroleum has migrated, and are now water wet, but are presently in communication with the previously migrated petroleum. Benzene rich proximity signals without associated acetic acid may indicate a nearby wet gas accumulation.

Track 12: $m/z = 91$ - Toluene ($C_7H_7^+$). This ion is interpreted in much the same way as benzene ($m/z = 78$). However, toluene has lower water solubility, so tends to be less anomalous or even absent from some proximity zones.

Track 13: 60/(60+57) - Acetic acid/(acetic acid + paraffins). This ratio tends to deflect to higher values in water bearing zones and shallow microseeps and to lower values in petroleum inclusion zones. Very high values are associated with proximity zones. Acetic acid has tremendous water solubility, while paraffins are relatively insoluble in water.

Track 14: 78/(78+91) - benzene/(benzene+toluene). This ratio is of limited utility in many cases, as these species are often not abundant enough to provide a coherent depth plot. In some cases, oil inclusion zones tend to deflect toward lower values, while proximity zones tend to deflect toward higher values. This is because oils typically have benzene to toluene ratios of about 0.5, while benzene has about 3 times higher solubility than toluene in water. Water washed oils will have lower ratios as will oils that have lost lighter ends through a semi-permeable seal.

Track 15: $m/z = 57$ - Paraffin fragment ($C_4H_9^+$). Anomalous values are associated with zones of oil and wet gas inclusions. Paraffins have lower solubility than other hydrocarbon classes, hence ratioing to these can define migration and reservoir processes (see next entries).

Track 16: 57/(57+15) - Paraffins/(paraffins+methane). This ratio plot displays the proportion of C_4 and greater paraffins relative to methane. The ratio will generally deflect to higher values in oil inclusion zones and toward lower values in dry gas zones. The ratio will also generally decrease within proximity zones due to the high solubility of methane relative to C_4^+ paraffins in aqueous solution.

Track 17: $m/z = 97$ - Alkylated naphthenes fragment ($C_7H_{13}^+$); basically naphthenes with methyl chains. This species tends to be anomalously high in petroleum inclusion zones which contain an appreciable liquid component (e.g., oils and condensates).

Track 18: 57/(57+55) - Paraffins/(paraffins+naphthenes). This ratio can be used for several purposes. Very low values are indicative of biodegraded oil, because bacteria prefer the paraffinic fraction. Low values are also documented in some proximity zones, due to the limited solubility of paraffins relative to naphthenes in aqueous solutions. Very high values are typical of dry gas zones as gases tend to be enriched in paraffins, although this trend must be used with caution. It is better to observe the relative change in this ratio with depth: If it decreases from baseline through a petroleum inclusion zone, liquid petroleum is more likely; if it increases, a lighter fraction might be expected. Again, these are generalizations which must be used cautiously. It is always best to follow up FIS work with thin section petrography to further investigate the characteristics of the entrapped petroleum phase. This ratio may also be used to identify transition zones from low to high Sw, and low-contrast pay zones. In general, we find that residual oil within water-rich zones under pay intervals tends to have higher ratios, probably due to the washing of more soluble naphthenes from the petroleum prior to entrapment. However, the water leg itself may have low ratios due to preferential concentration of naphthenes in the water phase.

Track 19: 97/(97+91) - Alkylated naphthenes/(alkylated naphthenes + toluene). This ratio tends to deflect toward higher values in zones containing liquid petroleum inclusions and toward lower values in proximity zones. Alkylated naphthenes are relatively water insoluble as compared to toluene.

Track 20: 77/(77+71) - C_6^+ aromatics/(C_5^+ paraffins+C_6^+ aromatics). This ratio tends to deflect toward higher values in zones of proximity and toward lower values in zones containing liquid petroleum inclusions. Both trends reflect the relative solubility of aromatics (high) and paraffins (low).

Track 21: $m/z = 64$ - C_5^+, S_2 and SO_2. Volatilized native sulfur has been noted in conjunction with sour gas pools in Canada, and, along with other chemical indicators may indicate sour gas risk. In some cases, mass 64 appears to be concentrated in water legs to these pools, or

wet reservoir sections that are plumbed to a deeper source of these species. It has also been found in conjunction with FIS microseeps.

Track 22: $m/z = 76$ - CS_2 and C_6^+ hydrocarbons. CS_2 has been found in conjunction with biodegraded hydrocarbons, in association with FIS microseeps and as a byproduct of thermochemical sulfate reduction.

Track 23: 97/(15+97)*1000 - Alkylated naphthene/(alkylated naphthene + methane) - This track can be used to illustrate the relative proportions of low and high molecular weight species. The track deflects to higher values in oily or light end depleted zones and to lower values in gassy zones.

Track 24: $C_5 - C_{13}$ Presence - This algorithm records the highest molecular weight range hydrocarbon group present in each individual spectra, and provides a quick visual record of zones containing the corresponding petroleum compounds. For example, if the C_5 group is the highest molecular weight range hydrocarbon group present in a given sample, a ranking of 5 is assigned; if C_6 is the highest carbon number represented, then a ranking of 6 is assigned, and so on until a ranking of 13 is assigned if the presence of species in the C_{13} range is detected. Mathematically, the algorithm tests for the presence of a group (i.e., carbon number) by scanning the spectra for a coherent signal comprised of at least two out of three of the major peaks associated with the particular molecular weight range.

Track 25: C_{6-13}/C_{1-5} - A semi-quantitative parameter relating the abundance of liquid-range hydrocarbons to gas-range hydrocarbons. The ratio can be used in a qualitative sense to construct "psuedo GOR's".

A.4.3 Mass Assignments

In addition to the Tracks 1-25 described above, mass spectra over the range $1 \leq m/z \leq 180$ are presented for each individual sample in Appendix C. The following descriptions contain additional information about species assignments for individual masses:

- $m/z = 2$ - Hydrogen (H_2^+); largely from H_2O, which makes up most of the evolved fluid in almost all samples.
- $m/z = 3$ - Deuterated hydrogen and helium-3 (HD and $^3He^+$).
- $m/z = 12$ - Carbon (C^+).
- $m/z = 14$ - Nitrogen (N^+) and CH_2^+; Nitrogen in conjunction with argon and oxygen anomalies suggests air. If not an analytical artifact (episodic burps of atmosphere leak into the analytical chamber), the presence of air may indicate a vadose zone below a subaerial exposure, or the presence of aeolean sand. If response on mass $m/z = 14$ exceeds that on masses $m/z = 13$ and $m/z = 15$ then nitrogen is likely present. CH_2^+ will generally be accompanied by relatively larger responses on $m/z = 15$ (CH_3^+), and $m/z = 16$ (CH_4^+) (due to it's fragmentation origin from CH_4, for instance). The most convincing distinction between analytical artifact and paleo-air occurs when several closely spaced samples have air anomalies, or when several replicate analyses of the same sample give the same result.
- $m/z = 16$ - Molecular peak for methane (CH_4^+), but major interference by O^+ fragment of water.

- $m/z = 17$ - Dominated by OH^+ fragment from water
- $m/z = 18$ - Dominated by water parent peak (H_2O^+)
- $m/z = 22$ - Doubly charged carbon dioxide ($CO2^{2+}$); minor contribution from neon ($^{22}Ne^+$)
- $m/z = 28$ - Dominated by diatomic nitrogen (N_2^+) and CO^+ fragment from carbon dioxide. Minor C_2^+ hydrocarbon contribution
- $m/z = 32$ - Oxygen (O^+) and sulfur (S^+). If $m/z = 32$ is larger than $m/z = 31$ and $m/z = 33$, oxygen is likely. If sulfur is present other likely peaks, such as $m/z = 34$ (H_2S), $m/z = 48$ (SO^+) and $m/z = 64$ (S_2^+, SO_2^+) should be checked. Oxygen can be a possible paleoexposure indicator when used in conjunction with other peaks (see discussion on Air Confidence, and Nitrogen).
- $m/z = 40$ - Argon (Ar^+) with possible significant interference by C_3^+ hydrocarbon fragments. High value of $m/z = 40$ relative to adjacent $m/z = 39$ and $m/z = 41$ peaks suggests argon.
- $m/z = 48$ - Sulfate fragment (SO^+); also, C_4^+
- $m/z = 55$ - Naphthene fragment ($C_4H_7^+$). High values are found in petroleum inclusion bearing intervals. Naphthenes have intermediate solubility between aromatics and paraffins. This m/z is usually ratioed to $m/z = 57$ (see below).
- $m/z = 71$ - Paraffin fragment ($C_5H_{11}^+$). Same use as $m/z = 57$.
- $m/z = 77$ - Aromatic fragment ($C_6H_5^+$). Same general use as for benzene and toluene.
- $m/z = 85$ - Paraffin fragment ($C_6H_{13}^+$). Same use as $m/z = 57$.
- $95 \leq m/z \leq 103$ - peaks centered within this range are mostly $C_7 - C_8$ fragments
- $110 \leq m/z \leq 115$ - peaks centered within this range are mostly $C_8 - C_9$ fragments
- $122 \leq m/z \leq 126$ - peaks centered within this range are mostly $C_9 - C_{10}$ fragments
- $134 \leq m/z \leq 138$ - peaks centered within this range are mostly $C_{10} - C_{11}$ fragments
- $148 \leq m/z \leq 152$ - peaks centered within this range are mostly $C_{11} - C_{12}$ fragments
- $160 \leq m/z \leq 164$ - peaks centered within this range are mostly $C_{12} - C_{13}$ fragments
- $175 \leq m/z \leq 180$ - peaks centered within this range are mostly $C_{13} - C_{14}$ fragments

B Reference Spectra

In order to insure consistent and high-quality results during routine Fluid Inclusion Stratigraphic Analysis and the intercomparability of wells analyzed weeks, months or even years apart, a number of machine-dependent parameters are monitored on a daily basis through the analysis of internal analytical standards. Information recorded during these analyses are used to evaluate the performance of individual components of the stratigraphic analyzers. Additionally, this information permits characterization of any systematic fluxuations that may have affected species sensitivity during the course of an FIS Analysis and are, in fact, used quantify these effects during post-analytical data reduction. The natural materials used as internal standards are described briefly below.

B.1 Oil Inclusion Reference Standards

Oil inclusion reference materials (petroleum inclusion-bearing siliceous carbonate rock fragments from the Kindblade Fm., Lawton, Oklahoma), are analyzed 11 times during each analytical run. The results are given in Figure 18. Ideally, spectra should show a whole-oil like signature with good representation of ionized fragments out to at least $m/z \approx 150$. Daily variation occurs due to inhomogenieties in inclusion abundance and distribution within individual samples of this natural rock, as well as from minor instrumental fluctuations.

B.2 Frac Sand Hydrocarbon Background Standards

Clean quartz sand, devoid of hydrocarbons, is analyzed 22 times during each analytical run. The results are given in Figures 19 and 20. Ideally, spectra should show no structured responses on $m/z > 60$.

B.3 Cooked Frac Sand Hydrocarbon Background Standards

Clean quartz sand which has been heated to 1000°C to remove a large percentage of the fluid inclusion population is analyzed 11 times during each analytical run. The results are given in Figure 21. Ideally, these spectra should show approximately an order of magnitude less total response than those from the preceeding "Frac Sand Standard", as well as an increase in air components (e.g., nitrogen at $m/z = 28$; oxygen at $m/z = 32$; argon at $m/z = 40$) resulting from entrapment of air into evacuated cavities during the heating treatment. These spectra should also show little to no structured response for $m/z > 60$.

B.4 Kindblade Trackplots

Selected peaks from oil inclusion inclusion reference standards used to monitor internal standardization and normalization procedures.

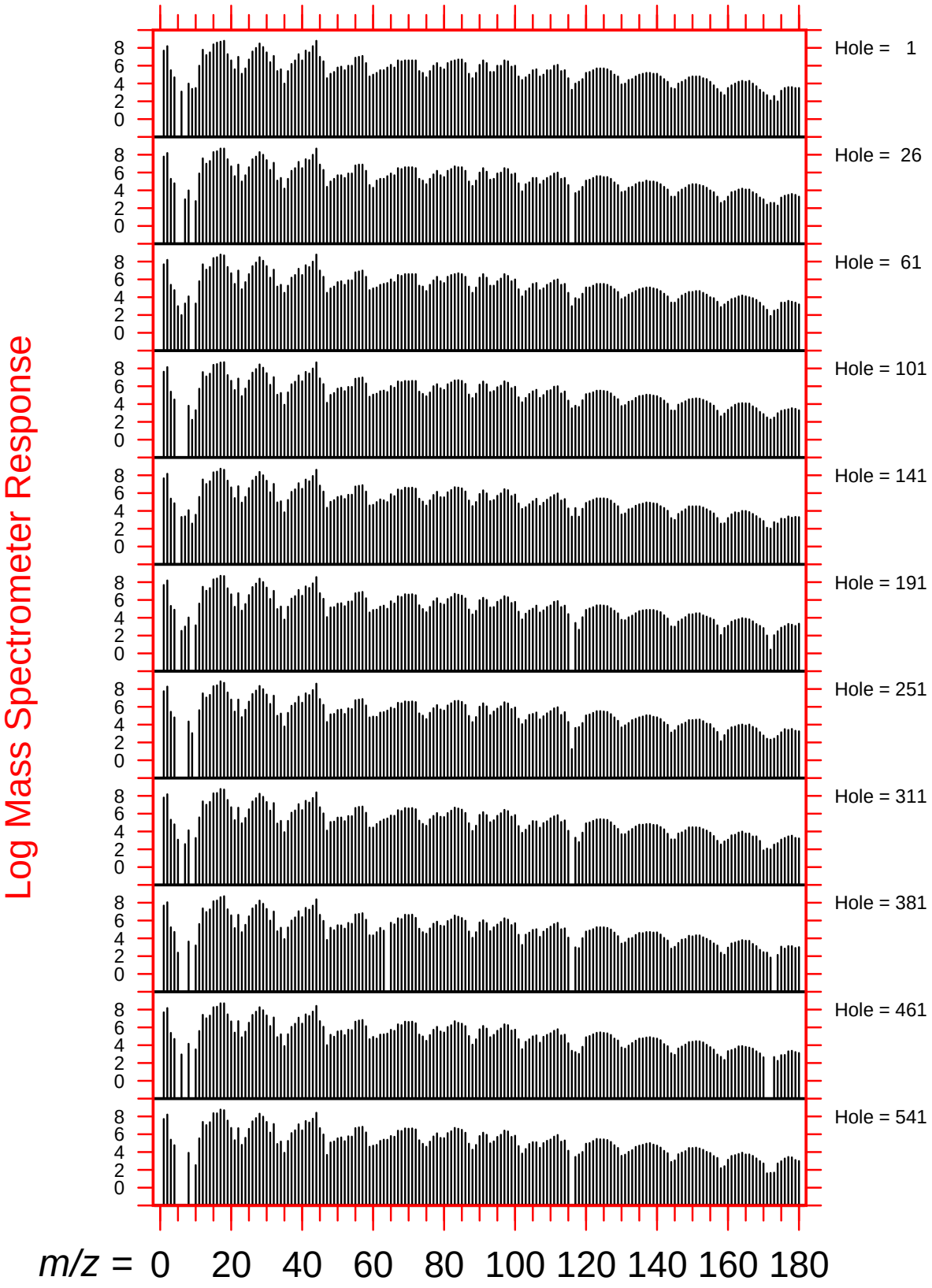

Figure 18: Oil Spectra

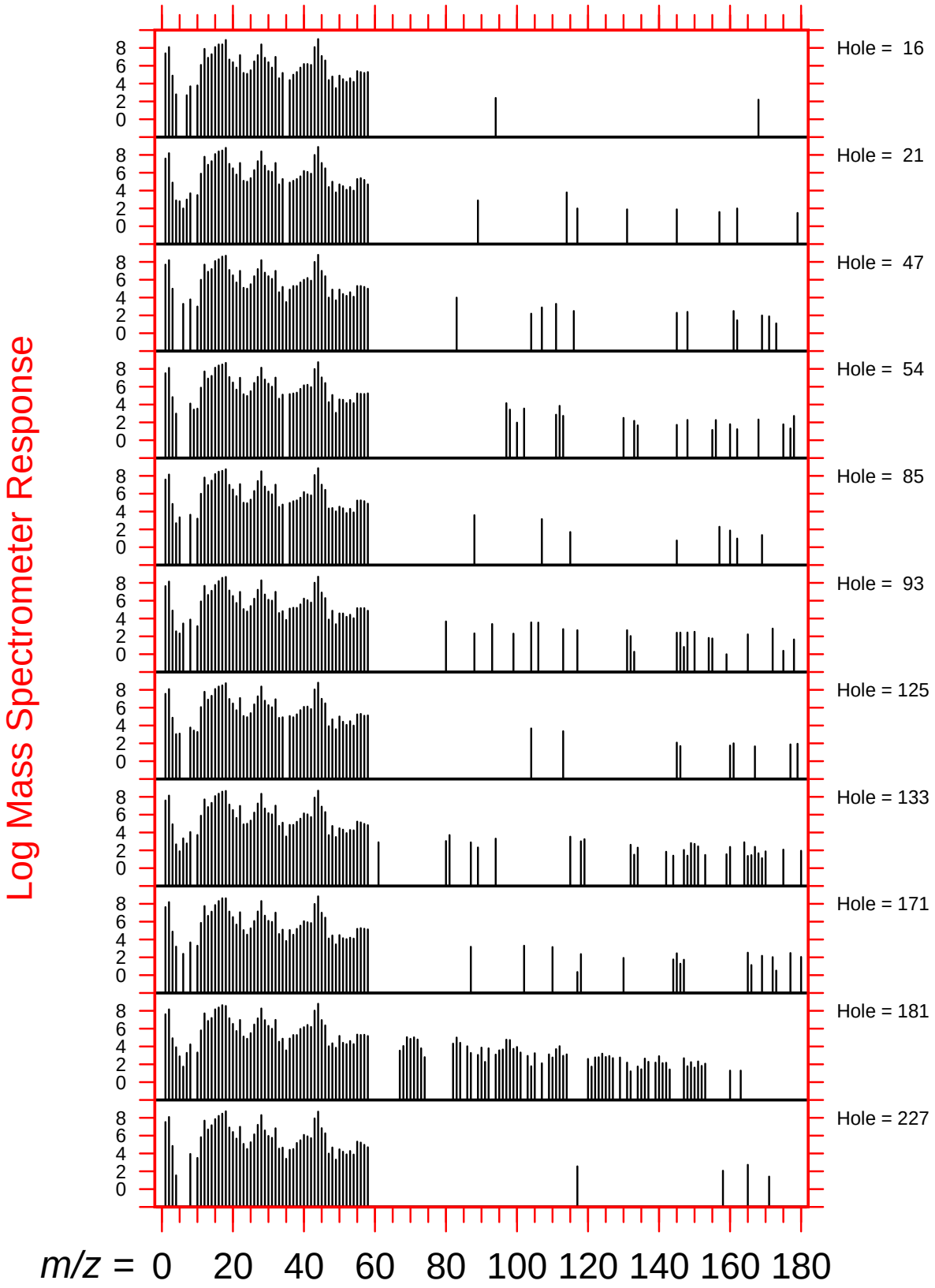

Figure 19: Frac Sand Spectra

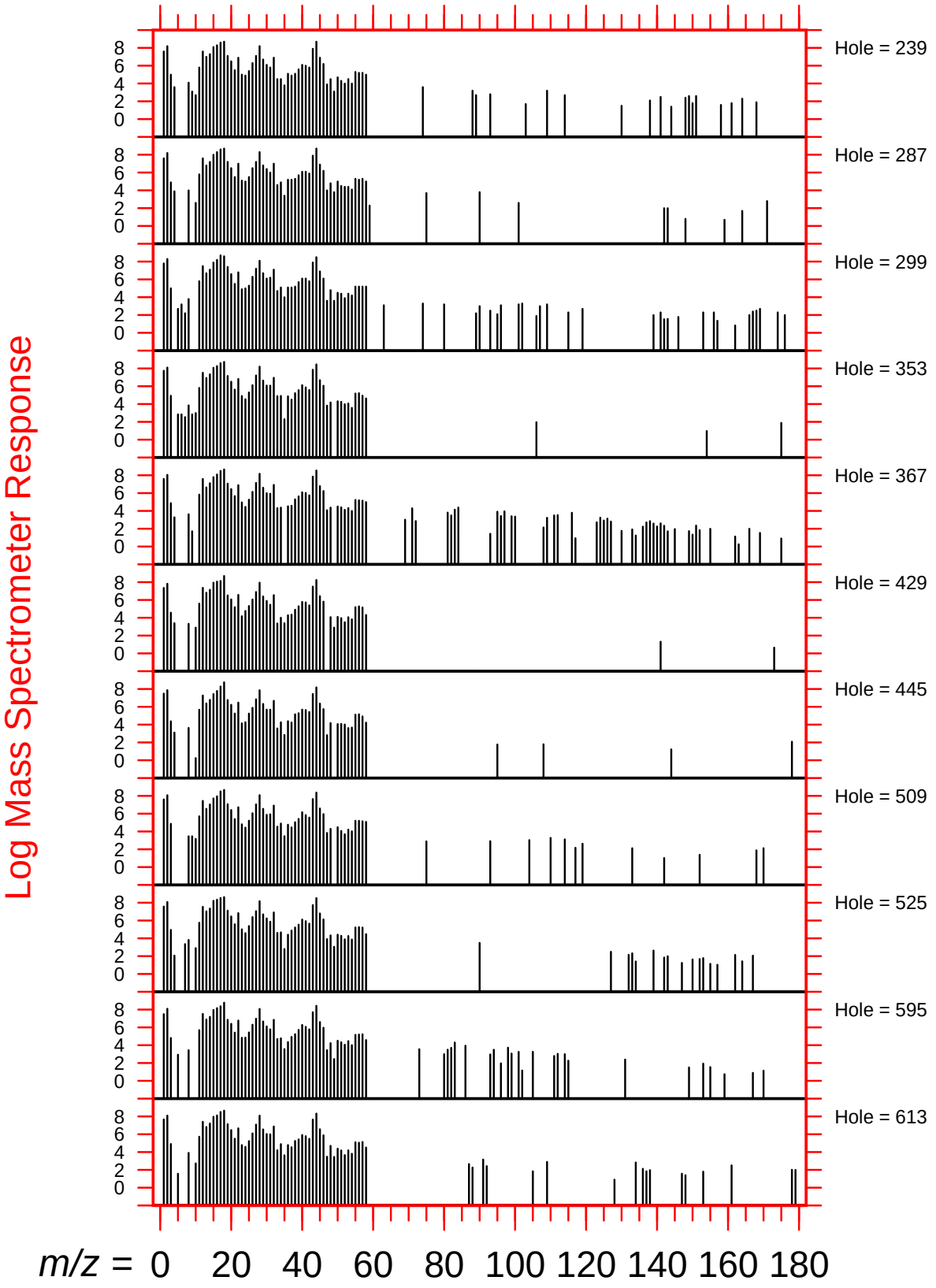

Figure 20: Frac Sand Spectra

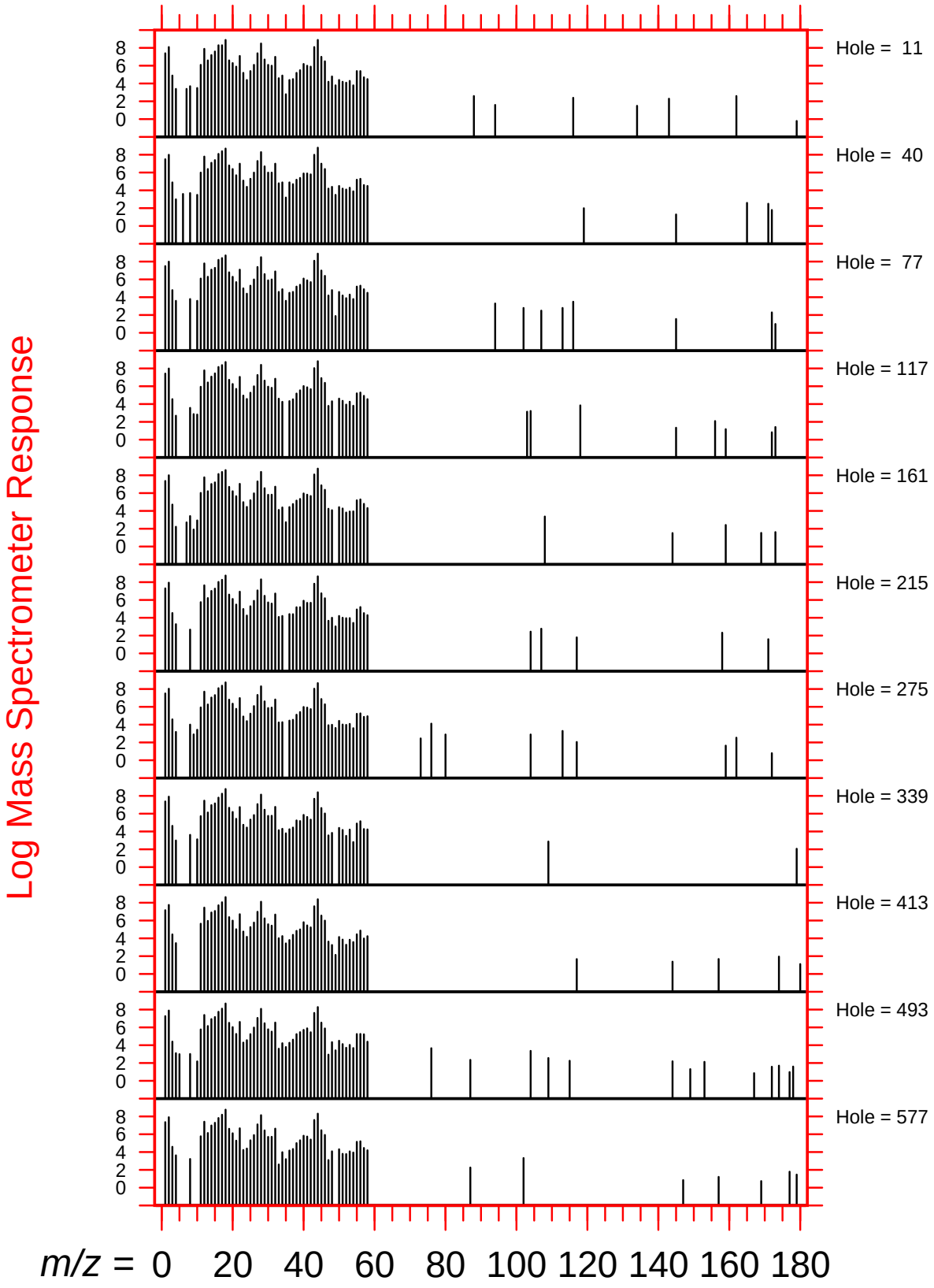

Figure 21: Cooked Frac Sand Spectra

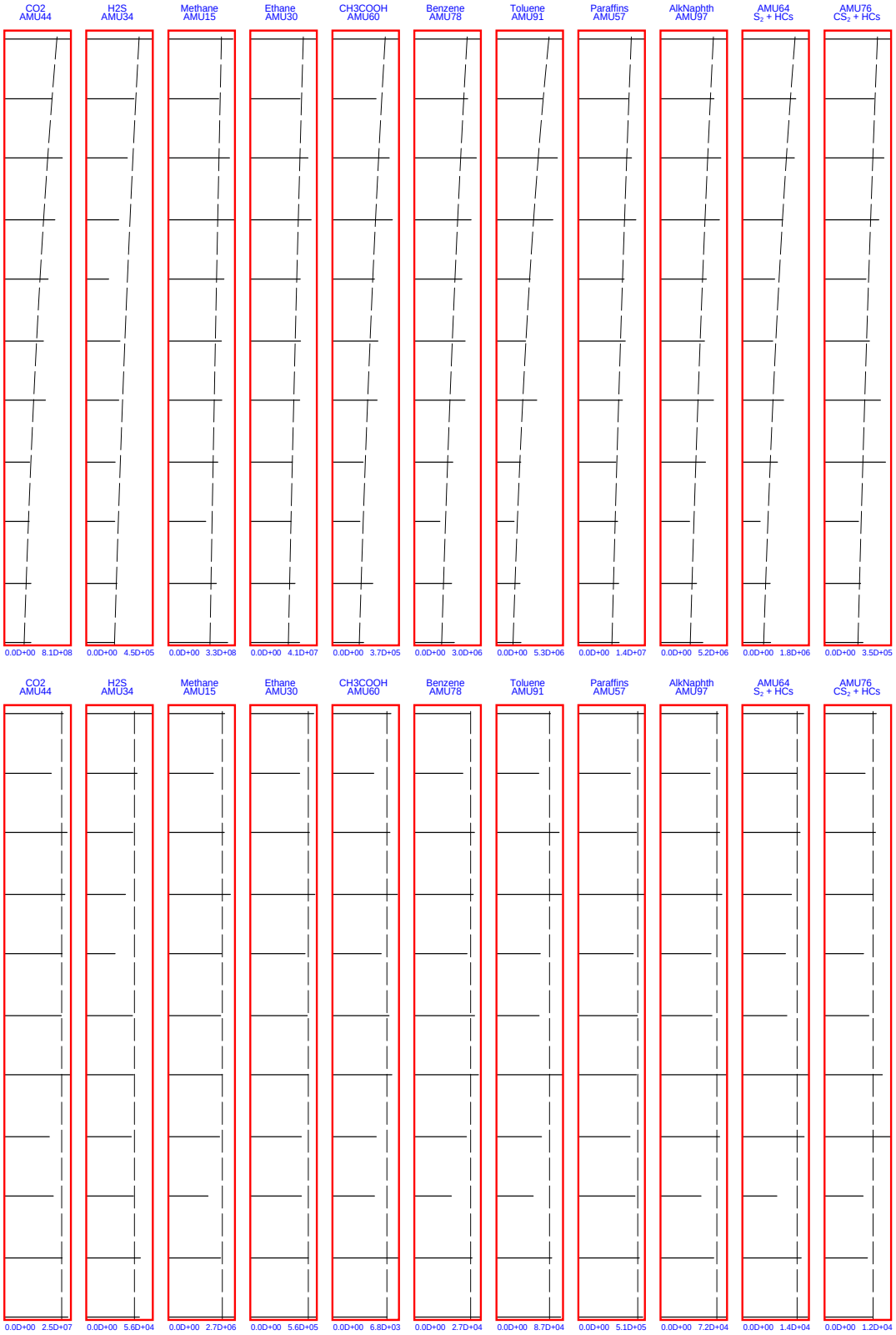

Figure 22: Kindblade Oil Standards Before (top) and After (bottom) Correction

C Individual Spectra

Individual spectra for each sample from HALLADALE 1 are shown on the following pages. Each spectrum is indexed according to depth and indicates the log of the millivolt response for atomic mass units (AMU, m/z) from $2 \leq m/z \leq 180$.

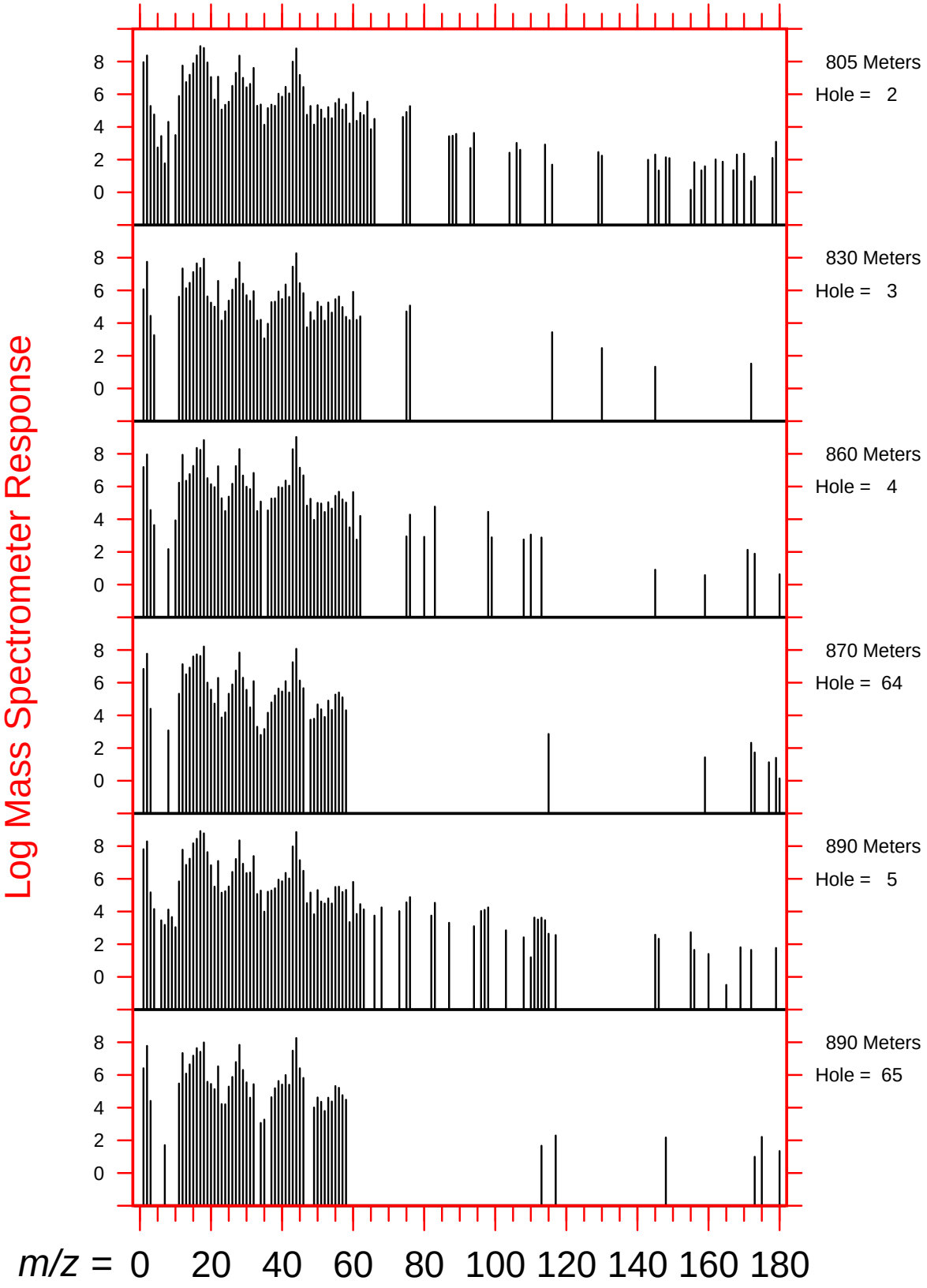
Log Mass Spectrometer Response
805 Meters
Hole = 2
830 Meters
Hole = 3
860 Meters
Hole = 4
870 Meters
Hole = 64
890 Meters
Hole = 5
890 Meters
Hole = 65
m/z = 0 20 40 60 80 100 120 140 160 180

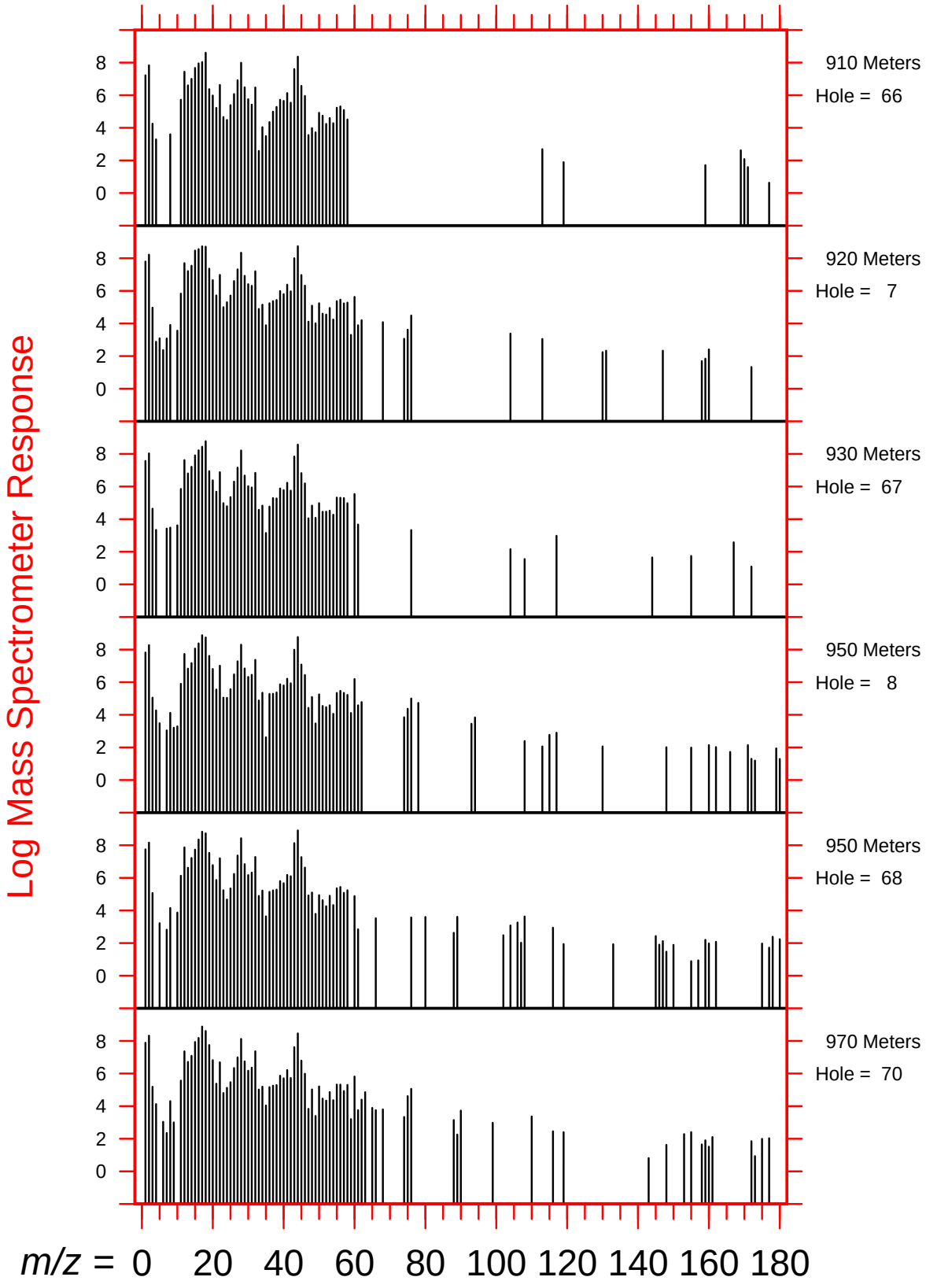
Log Mass Spectrometer Response
910 Meters
Hole = 66
920 Meters
Hole = 7
930 Meters
Hole = 67
950 Meters
Hole = 8
950 Meters
Hole = 68
970 Meters
Hole = 70
0
2
4
6
8
m/z = 0 20 40 60 80 100 120 140 160 180

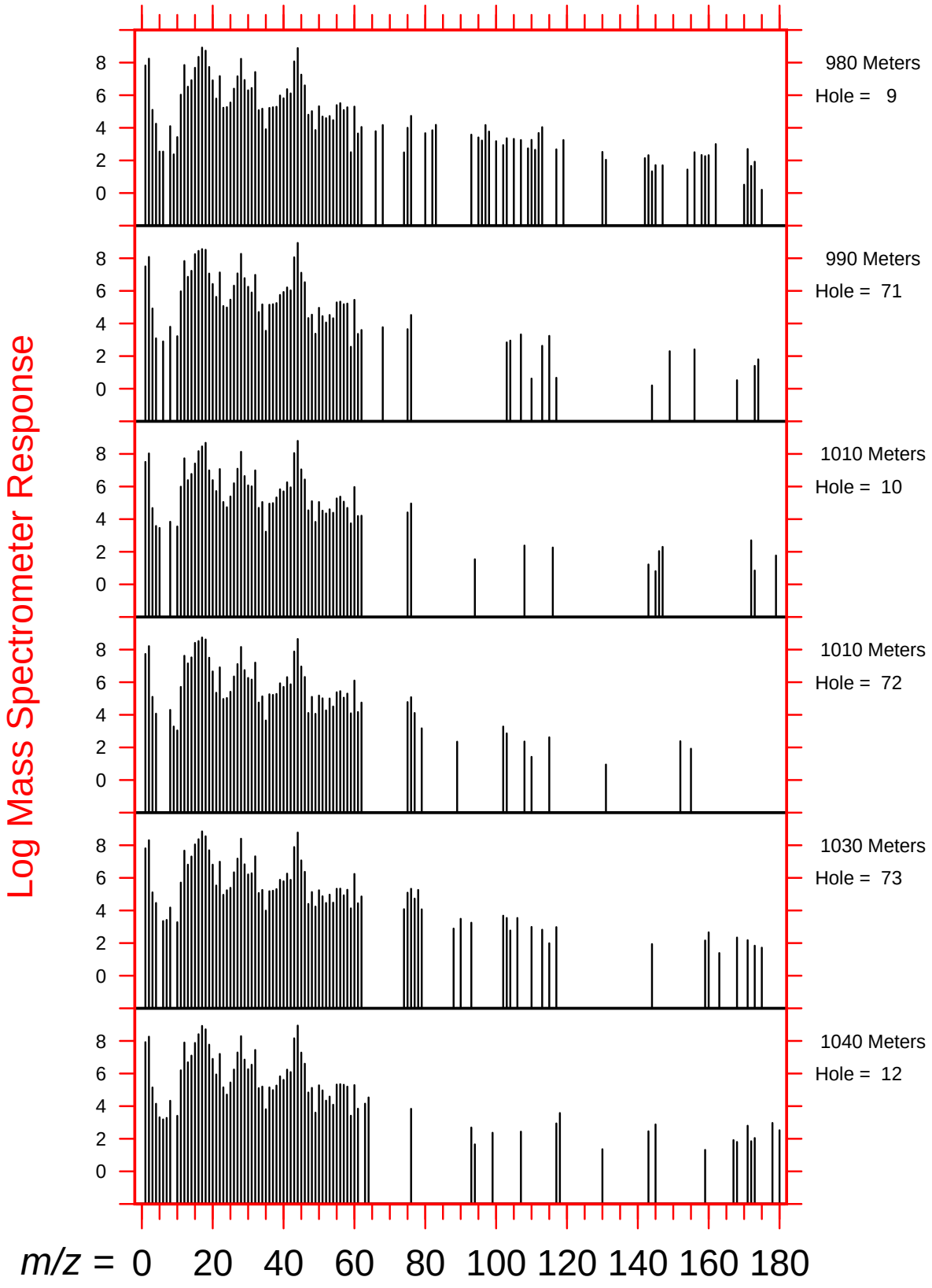
Log Mass Spectrometer Response
980 Meters
Hole = 9
990 Meters
Hole = 71
1010 Meters
Hole = 10
1010 Meters
Hole = 72
1030 Meters
Hole = 73
1040 Meters
Hole = 12
0
2
4
6
8
m/z = 0 20 40 60 80 100 120 140 160 180

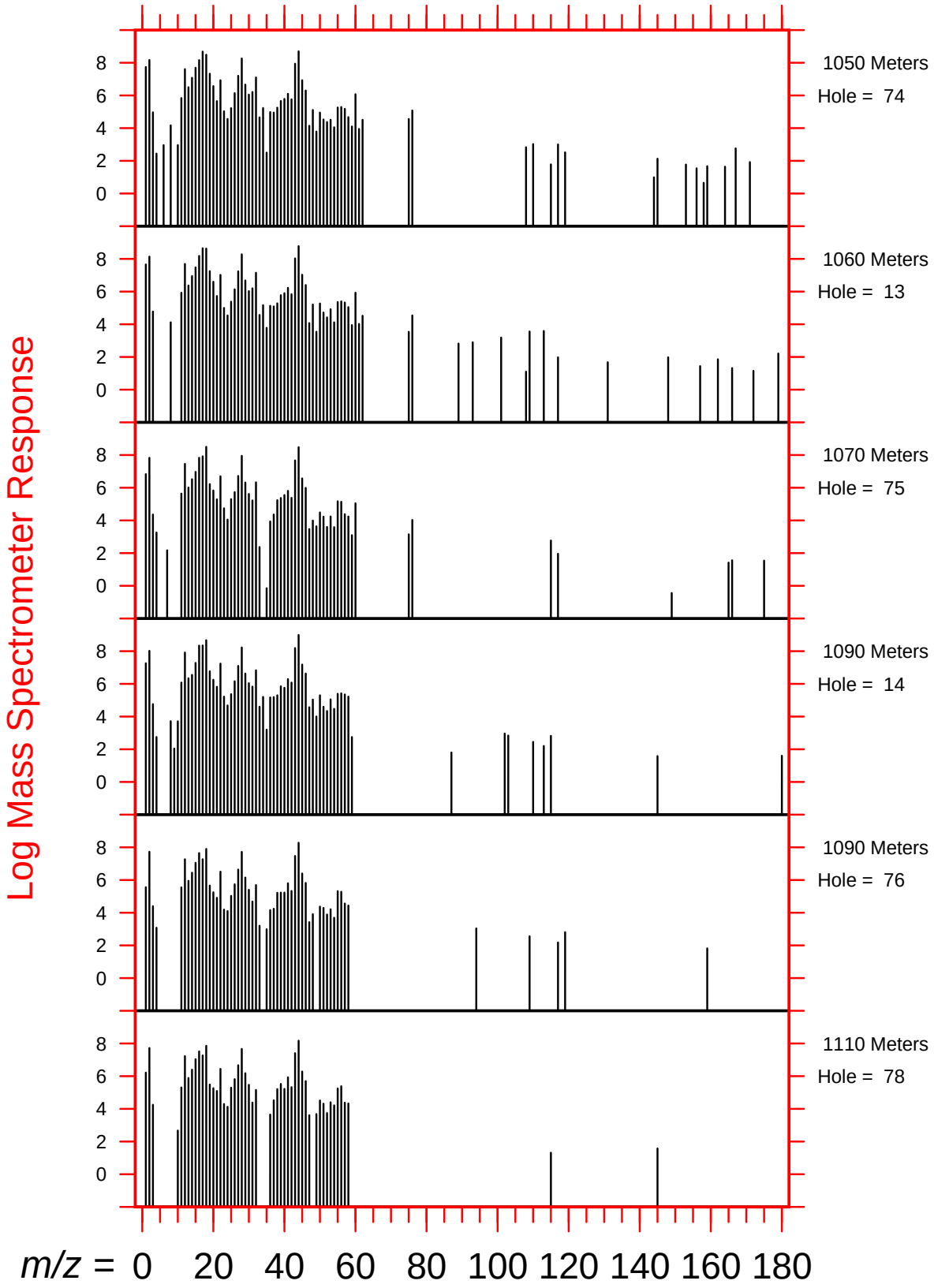
Log Mass Spectrometer Response
1050 Meters
Hole = 74
1060 Meters
Hole = 13
1070 Meters
Hole = 75
1090 Meters
Hole = 14
1090 Meters
Hole = 76
1110 Meters
Hole = 78
0
2
4
6
8
m/z = 0 20 40 60 80 100 120 140 160 180

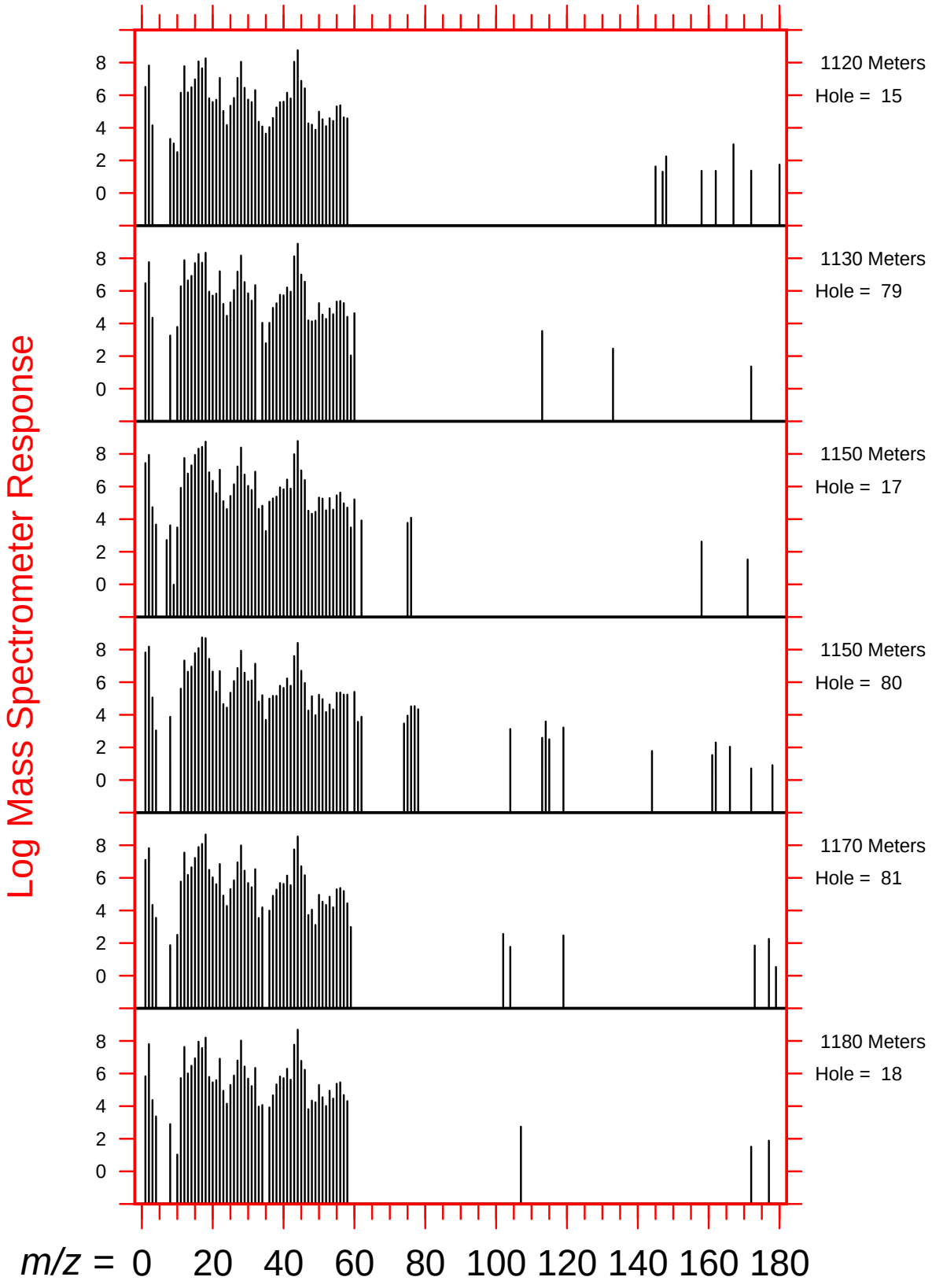
Log Mass Spectrometer Response
1120 Meters
Hole = 15
1130 Meters
Hole = 79
1150 Meters
Hole = 17
1150 Meters
Hole = 80
1170 Meters
Hole = 81
1180 Meters
Hole = 18
0
2
4
6
8
m/z = 0 20 40 60 80 100 120 140 160 180

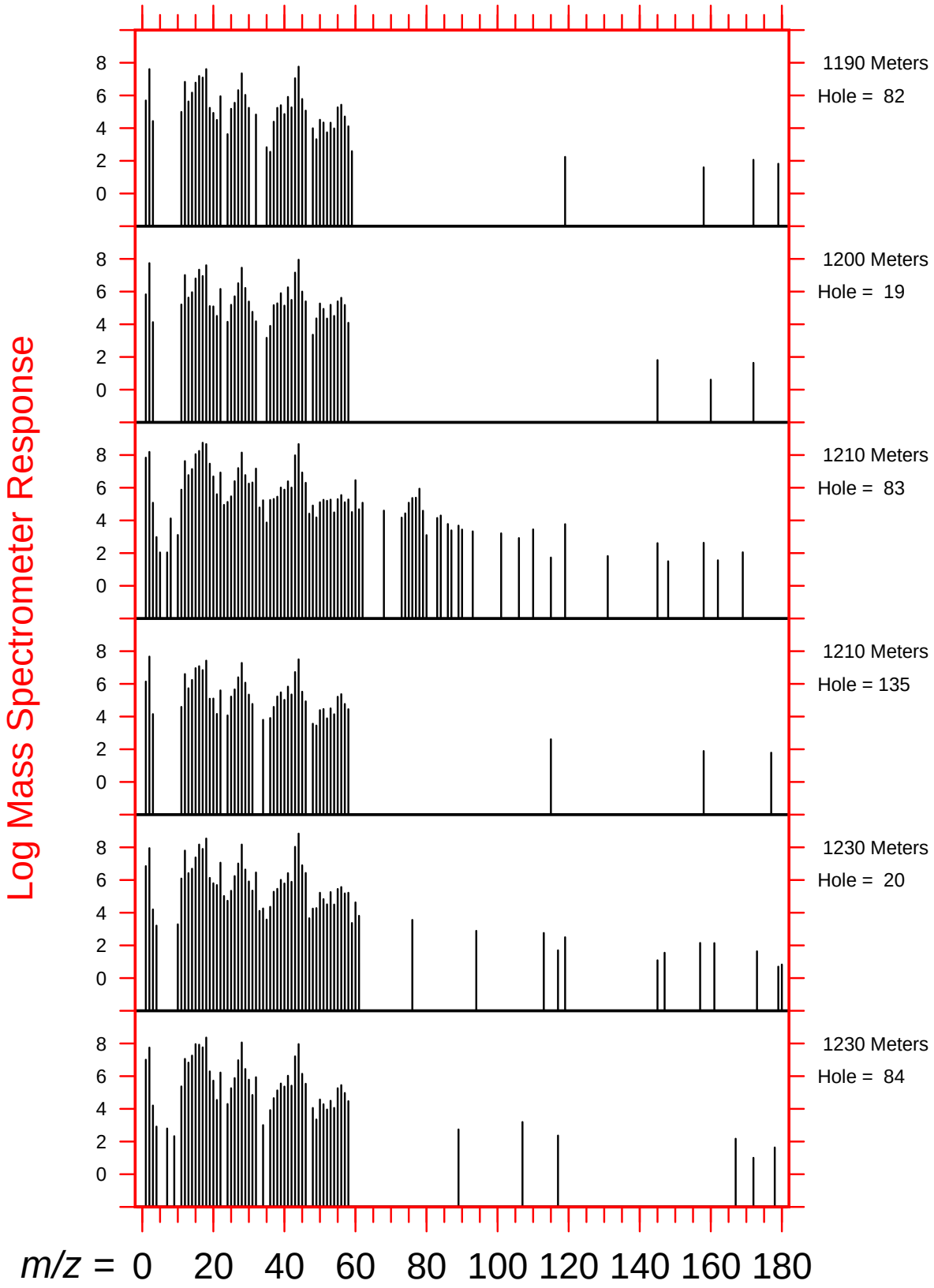
Log Mass Spectrometer Response
1190 Meters
Hole = 82
1200 Meters
Hole = 19
1210 Meters
Hole = 83
1210 Meters
Hole = 135
1230 Meters
Hole = 20
1230 Meters
Hole = 84
0
2
4
6
8
m/z = 0 20 40 60 80 100 120 140 160 180

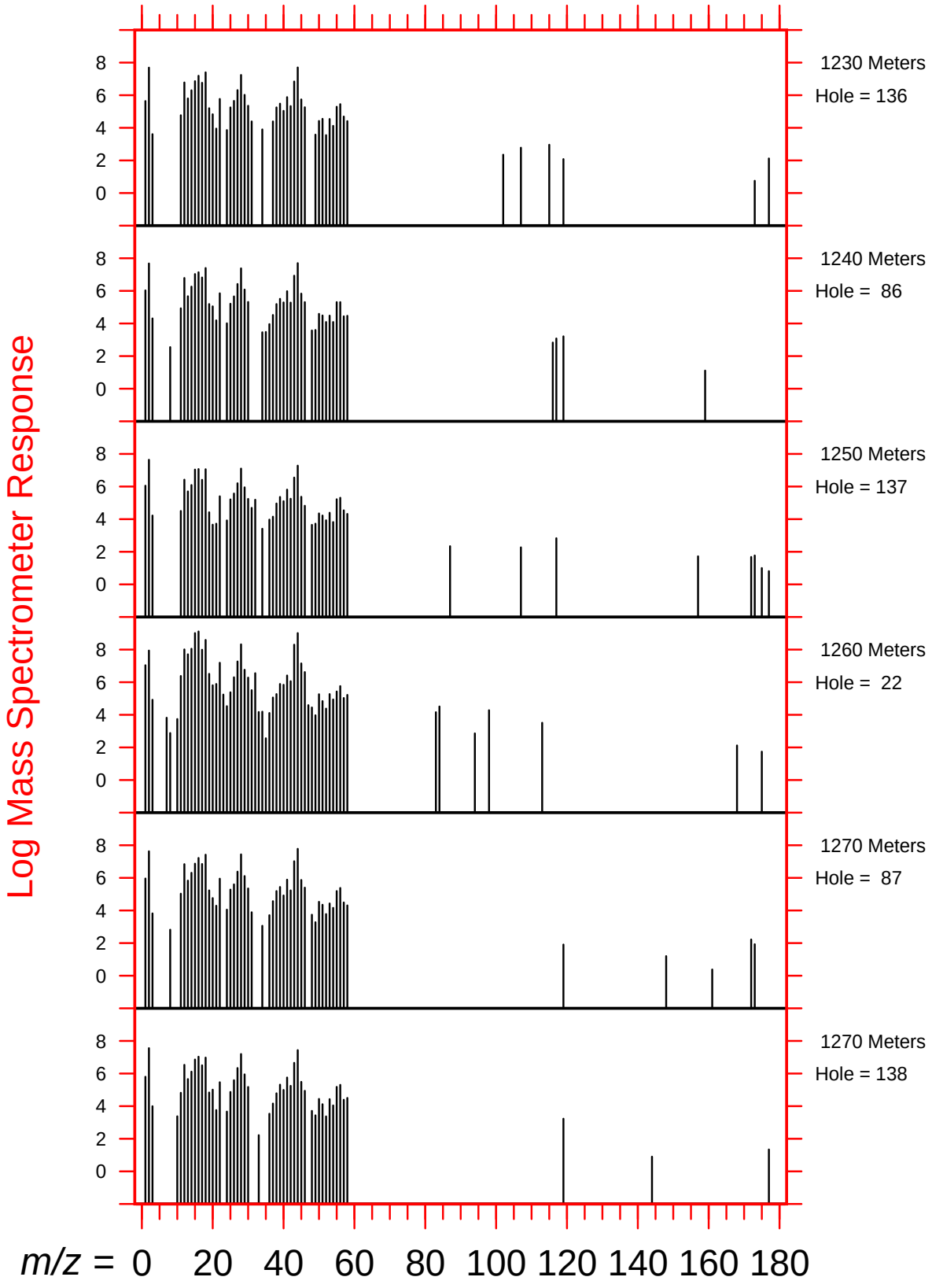
Log Mass Spectrometer Response
1230 Meters
Hole = 136
1240 Meters
Hole = 86
1250 Meters
Hole = 137
1260 Meters
Hole = 22
1270 Meters
Hole = 87
1270 Meters
Hole = 138
m/z = 0 20 40 60 80 100 120 140 160 180

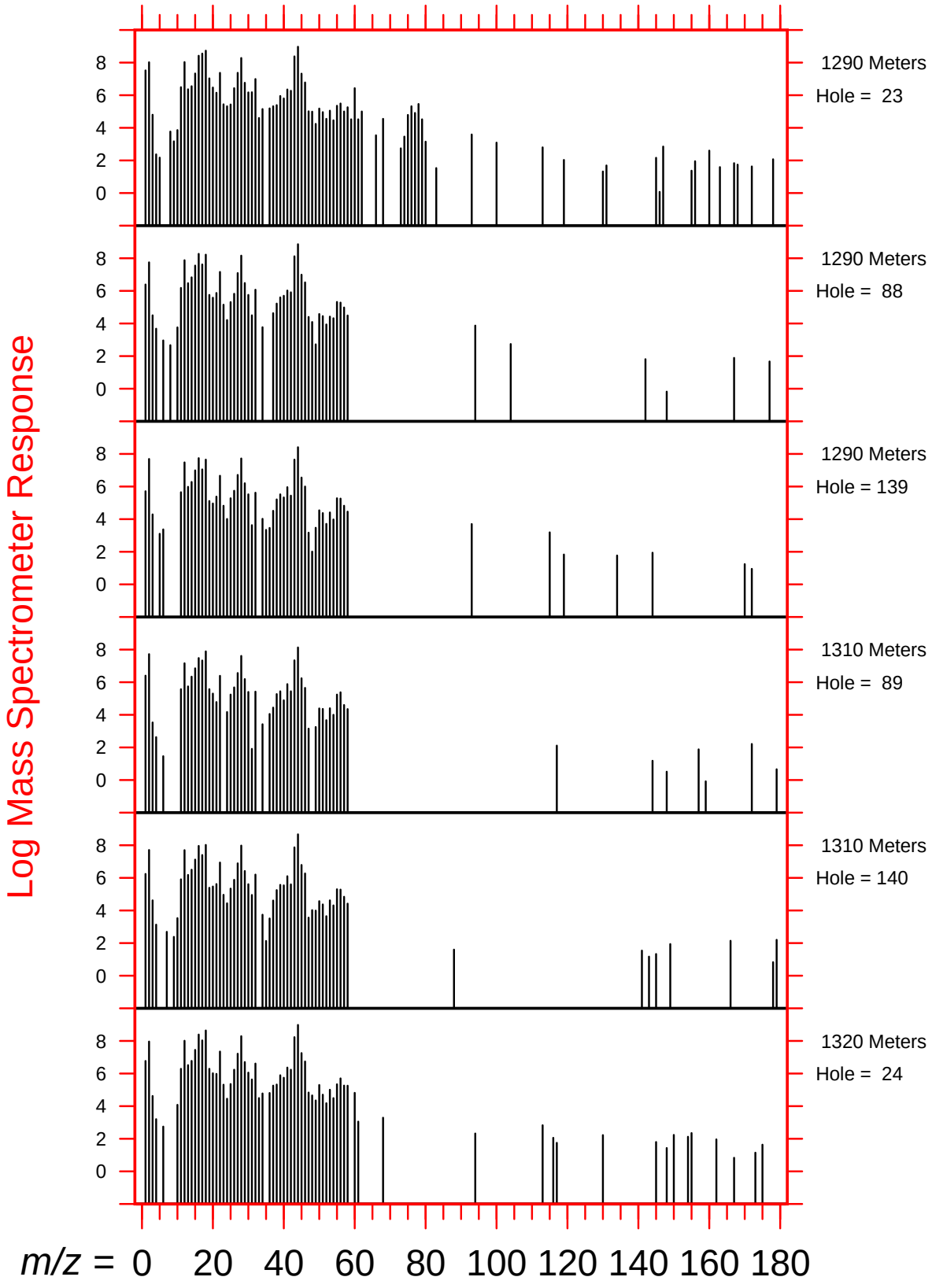
Log Mass Spectrometer Response
1290 Meters
Hole = 23
1290 Meters
Hole = 88
1290 Meters
Hole = 139
1310 Meters
Hole = 89
1310 Meters
Hole = 140
1320 Meters
Hole = 24
0
2
4
6
8
m/z = 0 20 40 60 80 100 120 140 160 180

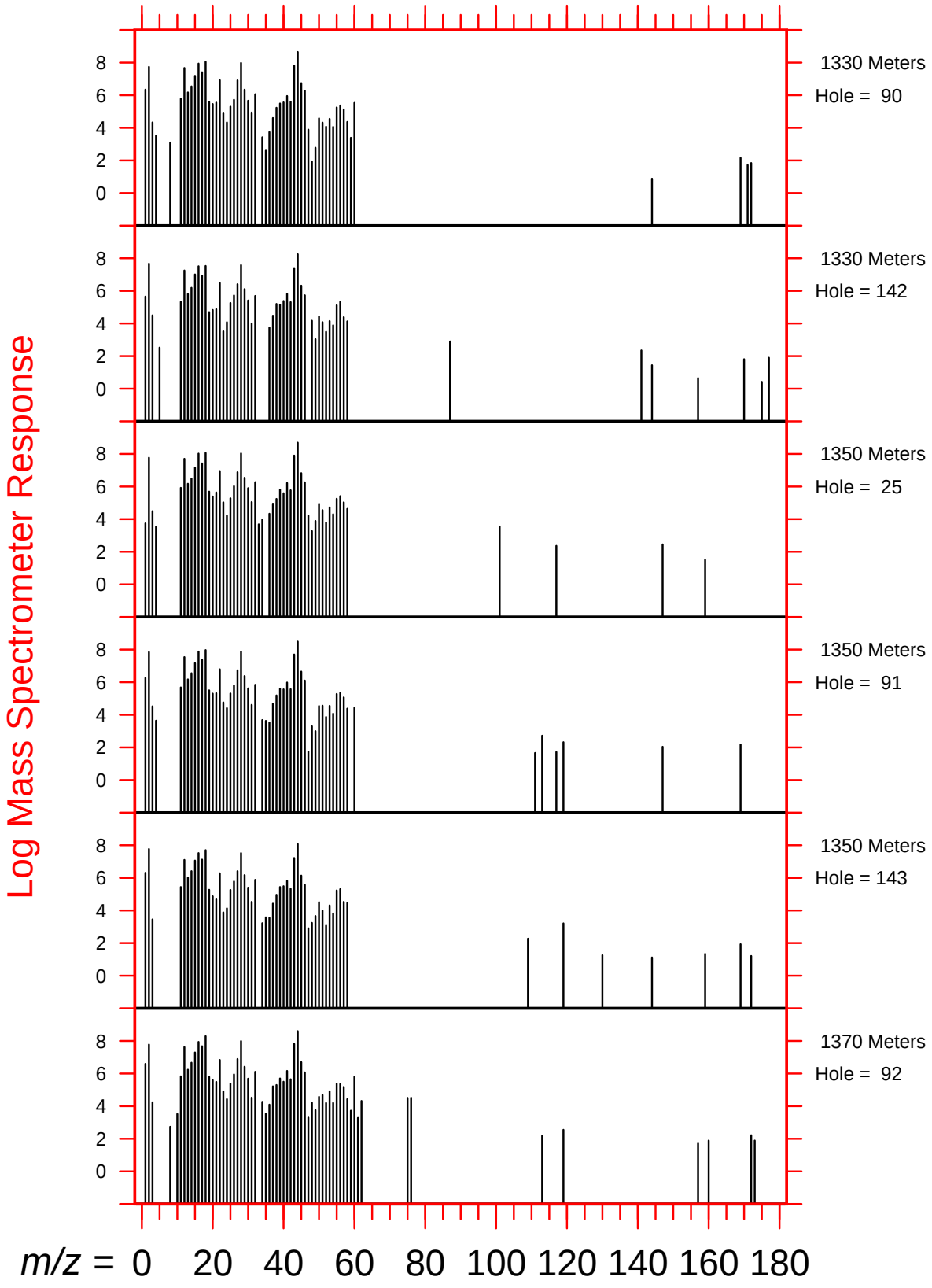
Log Mass Spectrometer Response
1330 Meters
Hole = 90
1330 Meters
Hole = 142
1350 Meters
Hole = 25
1350 Meters
Hole = 91
1350 Meters
Hole = 143
1370 Meters
Hole = 92
0
2
4
6
8
m/z = 0 20 40 60 80 100 120 140 160 180

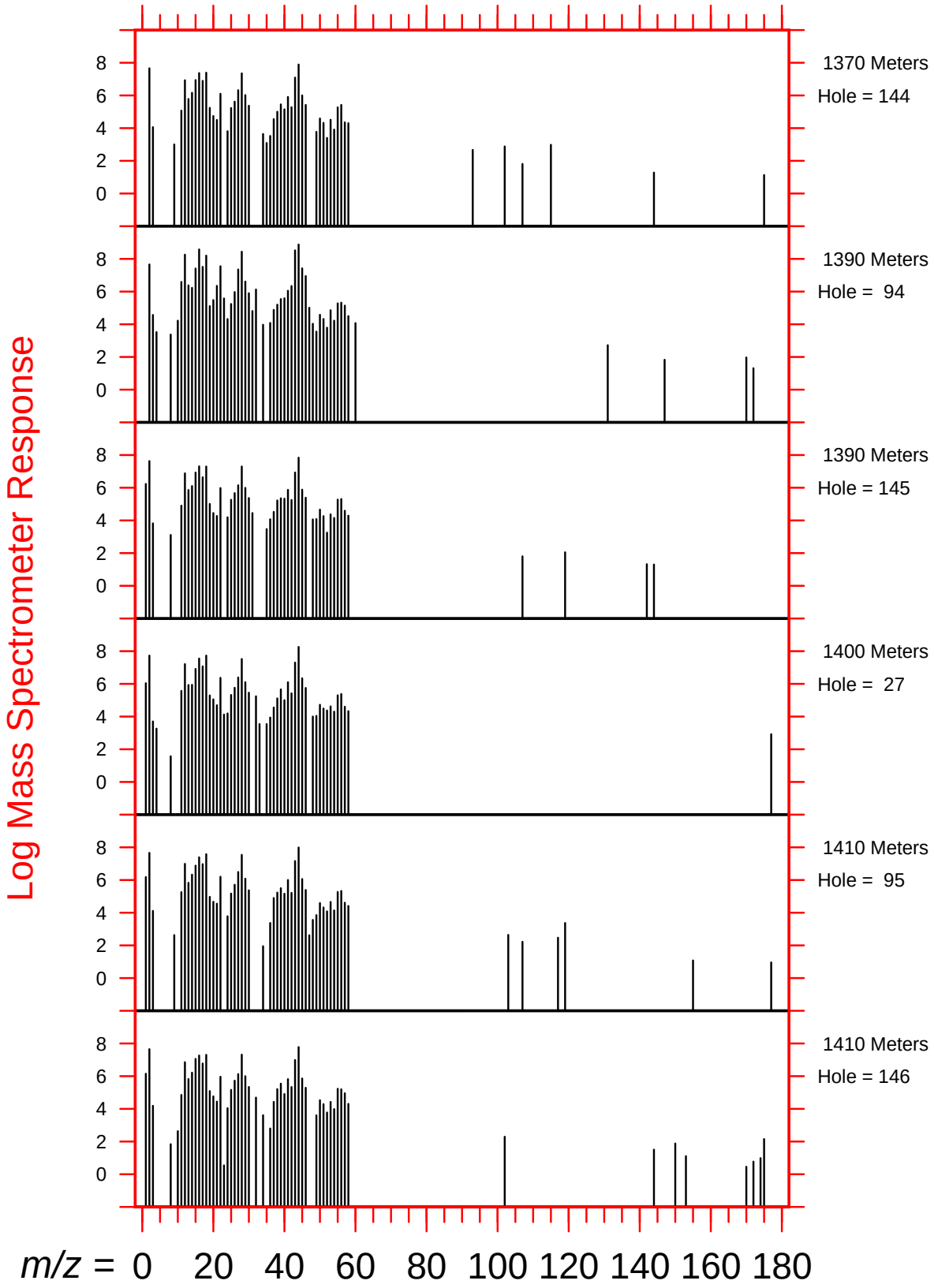
Log Mass Spectrometer Response
1370 Meters
Hole = 144
1390 Meters
Hole = 94
1390 Meters
Hole = 145
1400 Meters
Hole = 27
1410 Meters
Hole = 95
1410 Meters
Hole = 146
0
2
4
6
8
m/z = 0 20 40 60 80 100 120 140 160 180

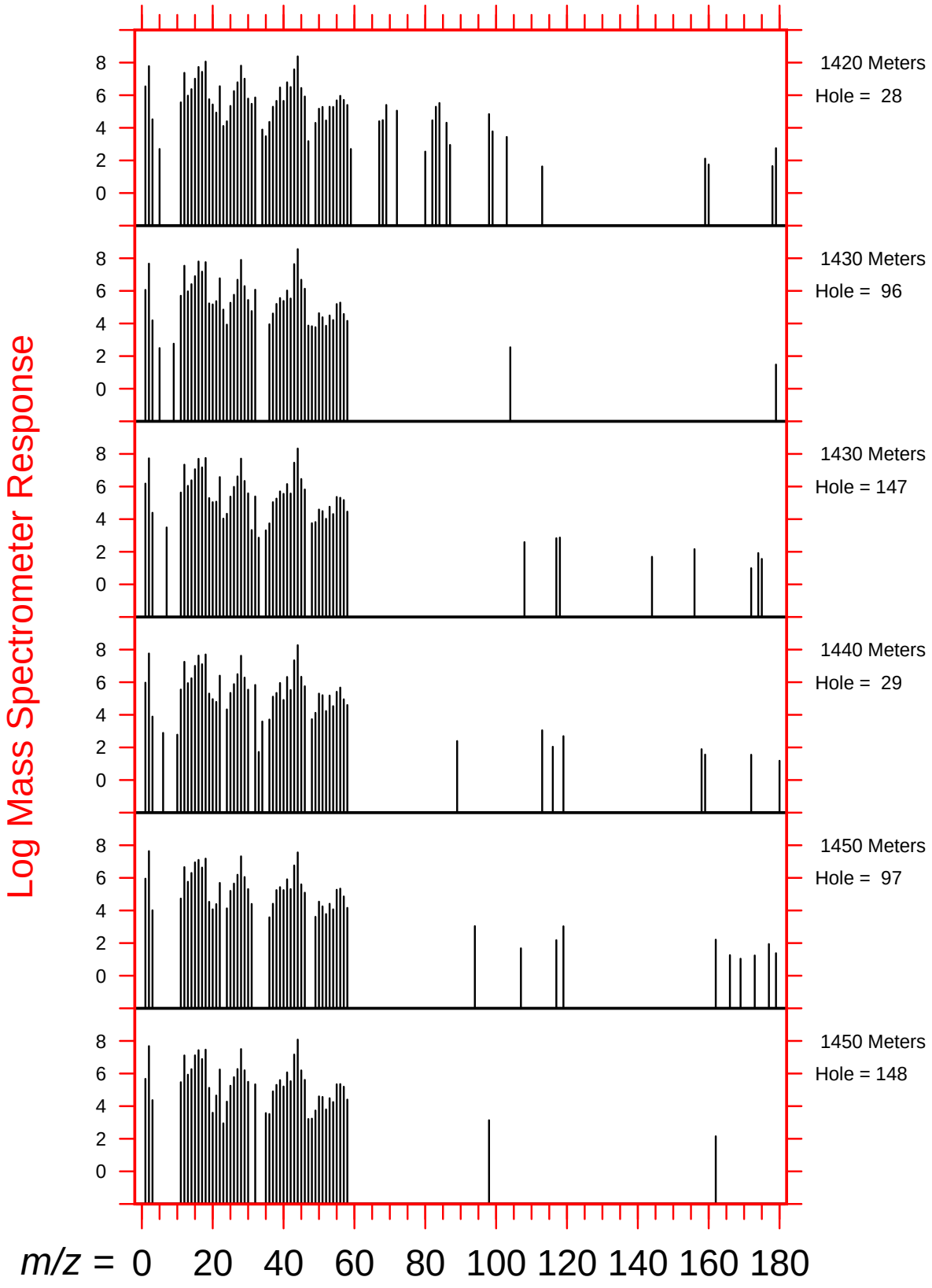
Log Mass Spectrometer Response
1420 Meters
Hole = 28
1430 Meters
Hole = 96
1430 Meters
Hole = 147
1440 Meters
Hole = 29
1450 Meters
Hole = 97
1450 Meters
Hole = 148
m/z = 0 20 40 60 80 100 120 140 160 180

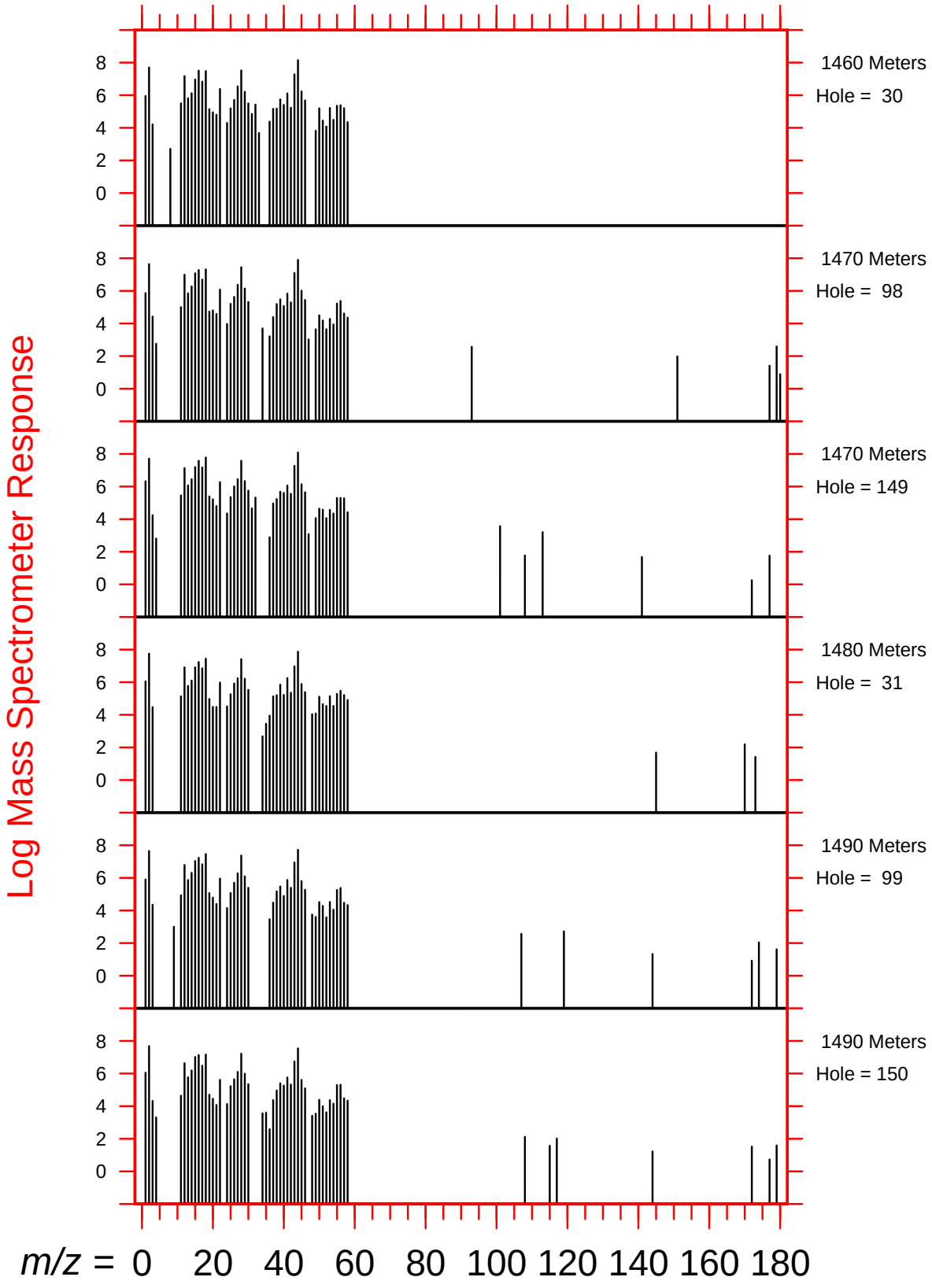
Log Mass Spectrometer Response
1460 Meters
Hole = 30
1470 Meters
Hole = 98
1470 Meters
Hole = 149
1480 Meters
Hole = 31
1490 Meters
Hole = 99
1490 Meters
Hole = 150
m/z = 0 20 40 60 80 100 120 140 160 180

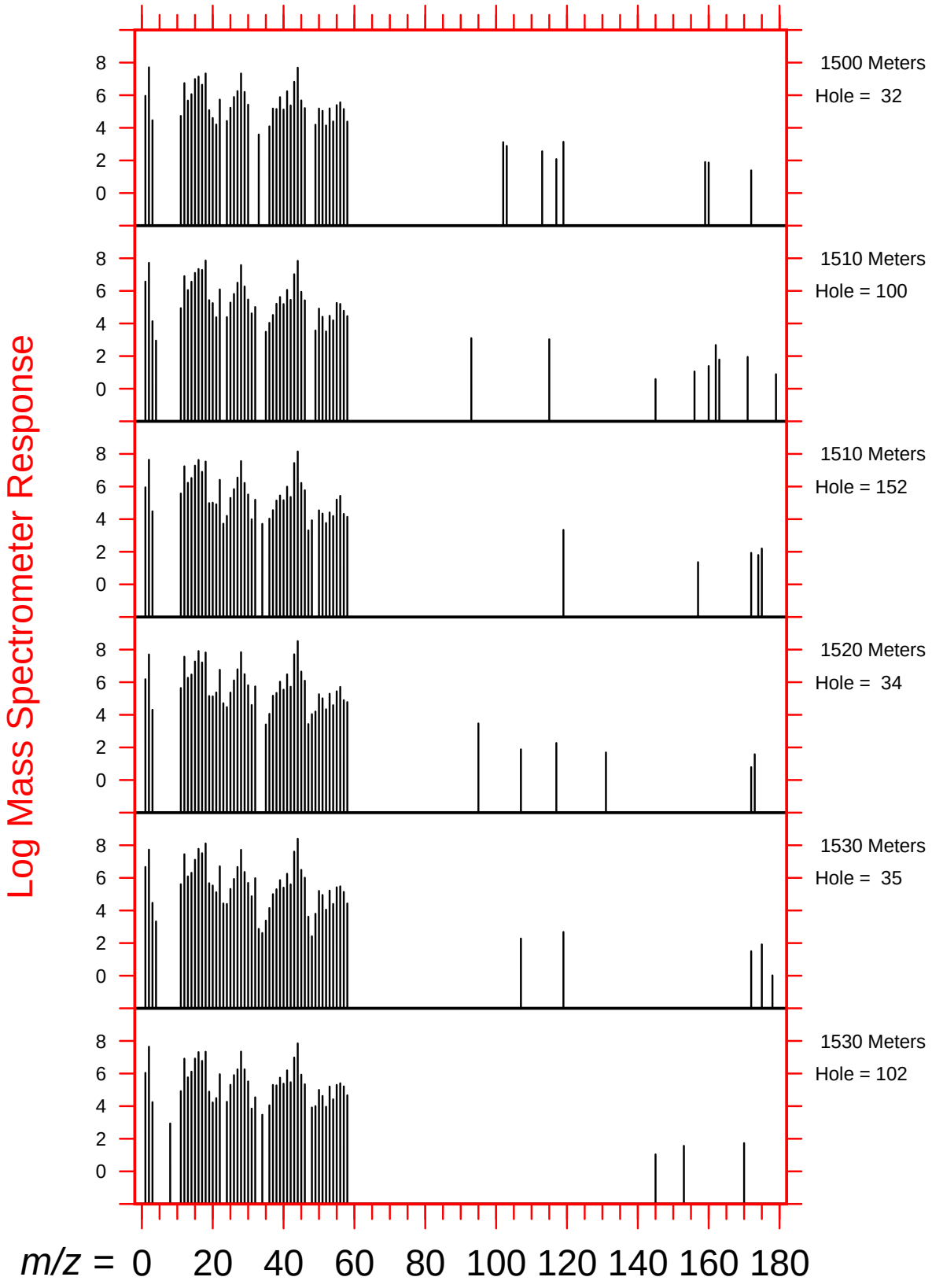
Log Mass Spectrometer Response
1500 Meters
Hole = 32
1510 Meters
Hole = 100
1510 Meters
Hole = 152
1520 Meters
Hole = 34
1530 Meters
Hole = 35
1530 Meters
Hole = 102
0
2
4
6
8
m/z = 0 20 40 60 80 100 120 140 160 180

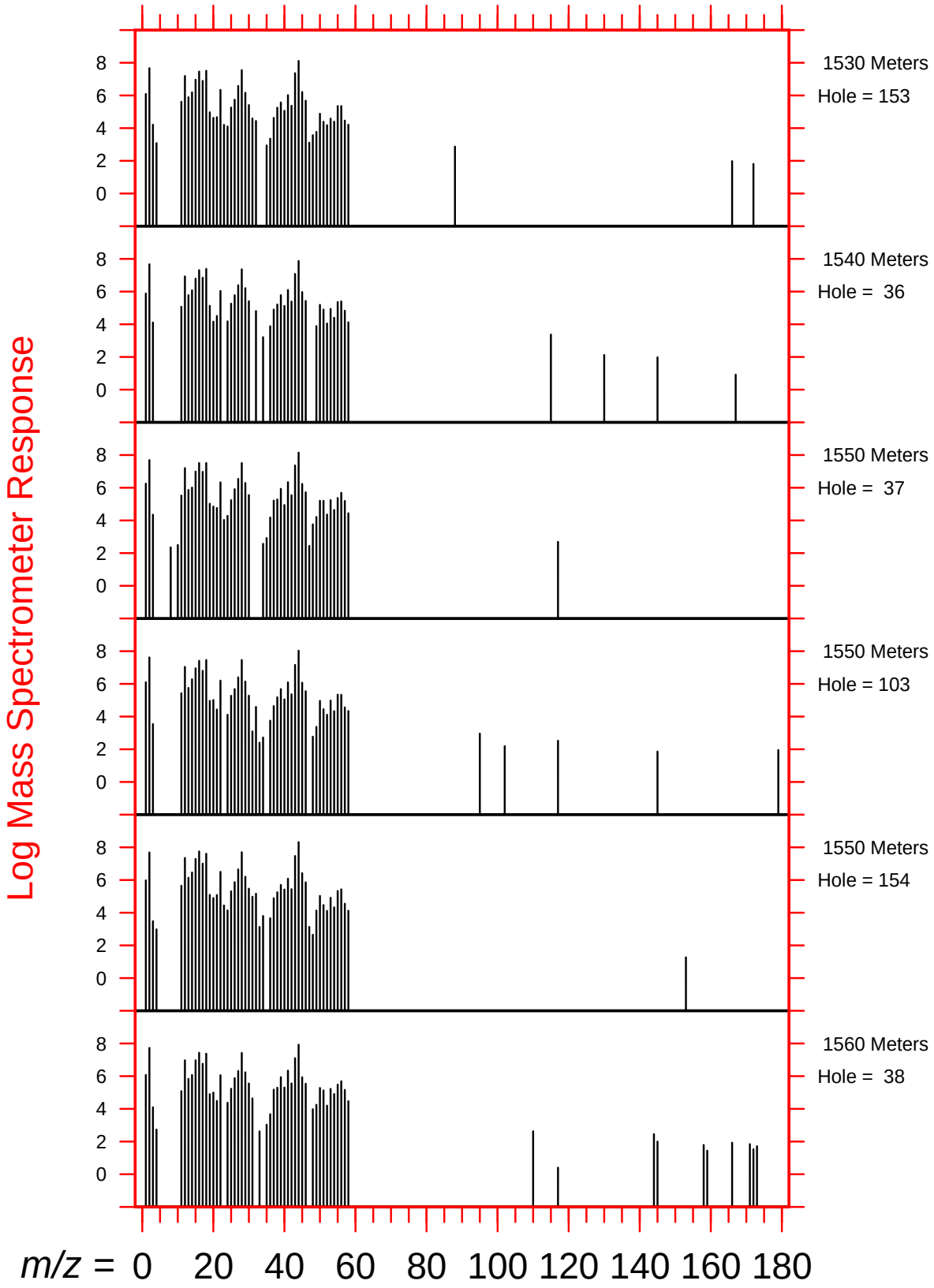
Log Mass Spectrometer Response
1530 Meters
Hole = 153
1540 Meters
Hole = 36
1550 Meters
Hole = 37
1550 Meters
Hole = 103
1550 Meters
Hole = 154
1560 Meters
Hole = 38
0
2
4
6
8
m/z = 0 20 40 60 80 100 120 140 160 180

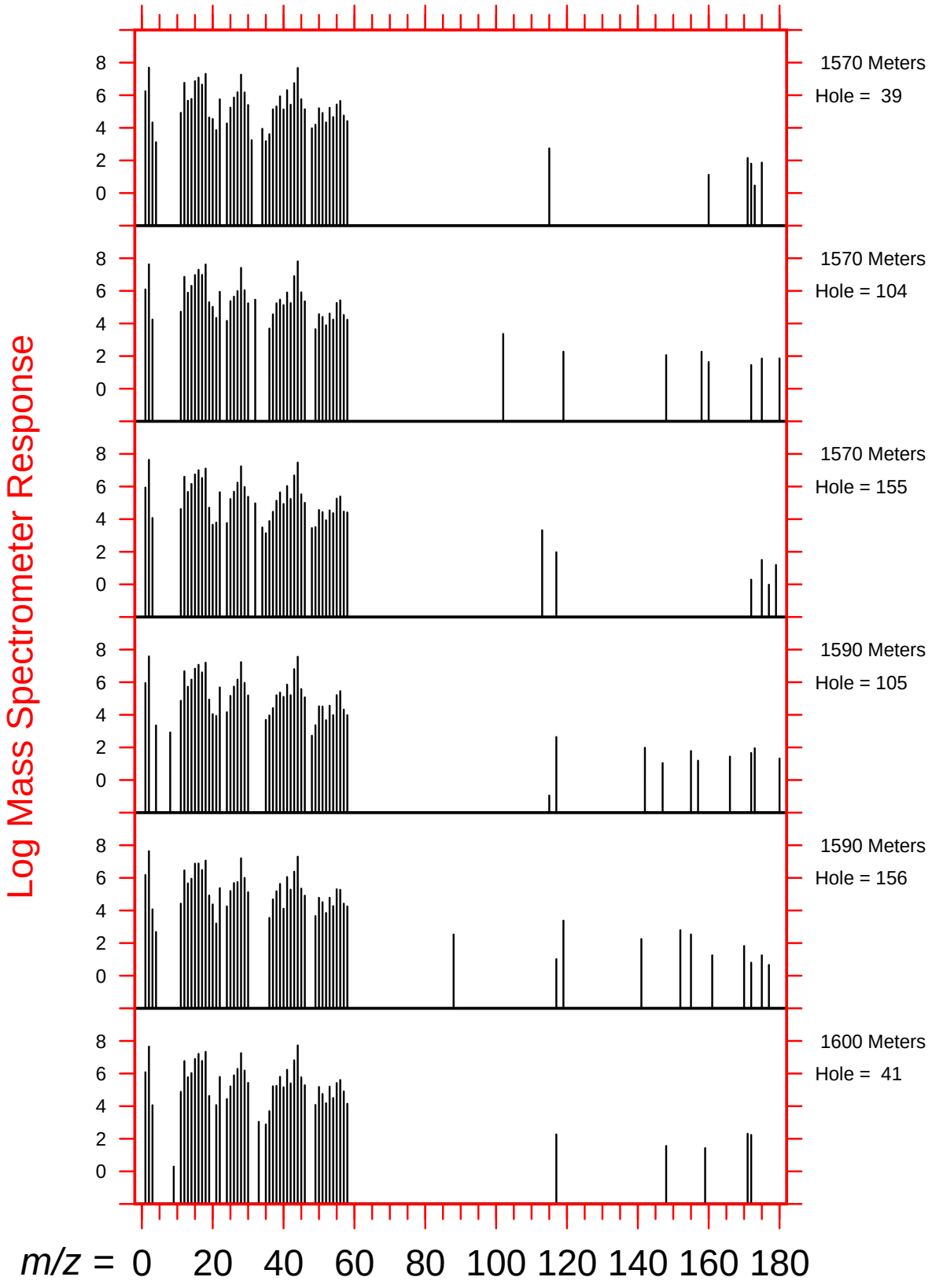
Log Mass Spectrometer Response
1570 Meters
Hole = 39
1570 Meters
Hole = 104
1570 Meters
Hole = 155
1590 Meters
Hole = 105
1590 Meters
Hole = 156
1600 Meters
Hole = 41
0
2
4
6
8
m/z = 0 20 40 60 80 100 120 140 160 180

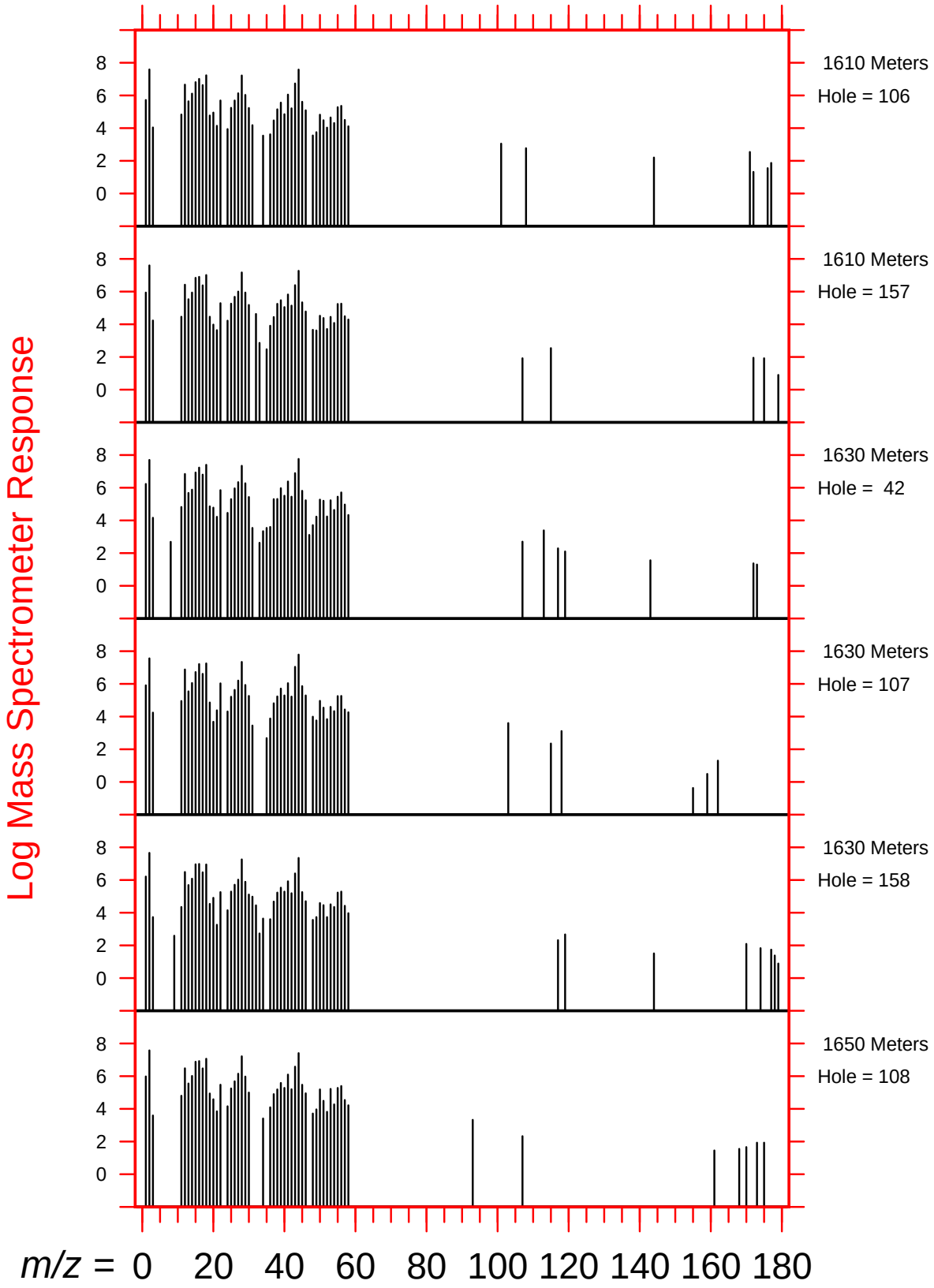
Log Mass Spectrometer Response
1610 Meters
Hole = 106
1610 Meters
Hole = 157
1630 Meters
Hole = 42
1630 Meters
Hole = 107
1630 Meters
Hole = 158
1650 Meters
Hole = 108
0
2
4
6
8
m/z = 0 20 40 60 80 100 120 140 160 180

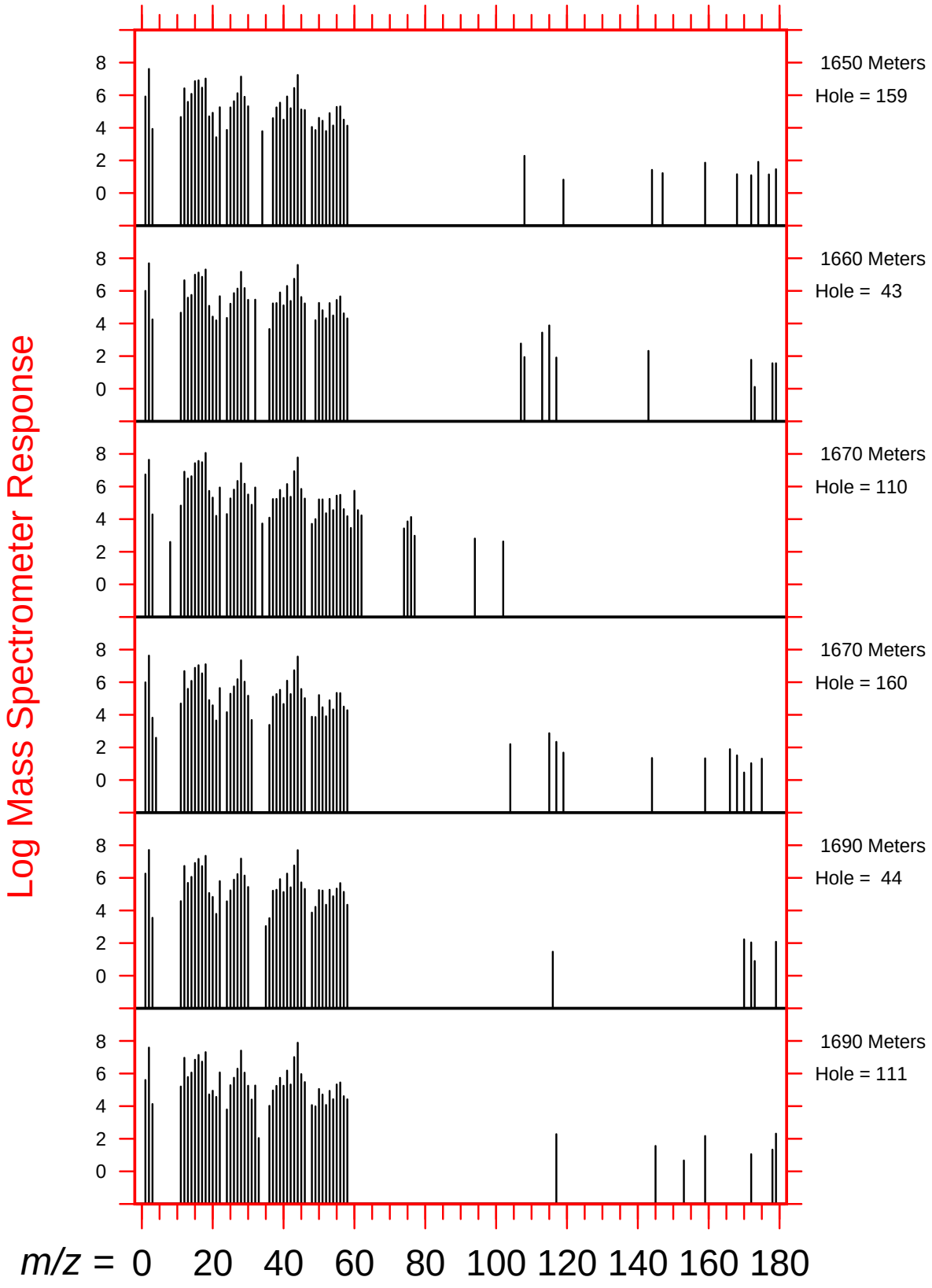
Log Mass Spectrometer Response
1650 Meters
Hole = 159
1660 Meters
Hole = 43
1670 Meters
Hole = 110
1670 Meters
Hole = 160
1690 Meters
Hole = 44
1690 Meters
Hole = 111
0
2
4
6
8
m/z = 0 20 40 60 80 100 120 140 160 180

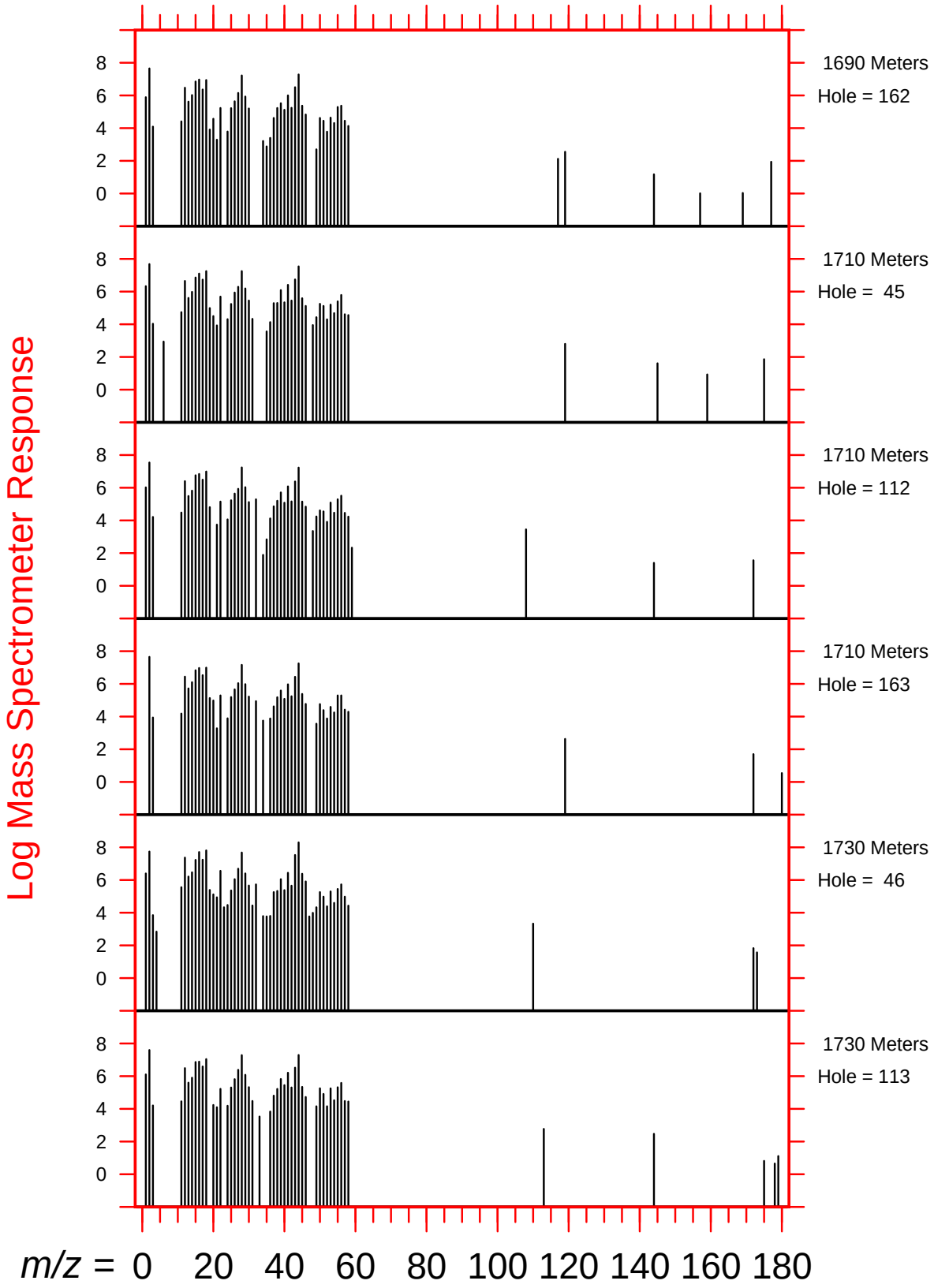
Log Mass Spectrometer Response
1690 Meters
Hole = 162
1710 Meters
Hole = 45
1710 Meters
Hole = 112
1710 Meters
Hole = 163
1730 Meters
Hole = 46
1730 Meters
Hole = 113
m/z = 0 20 40 60 80 100 120 140 160 180

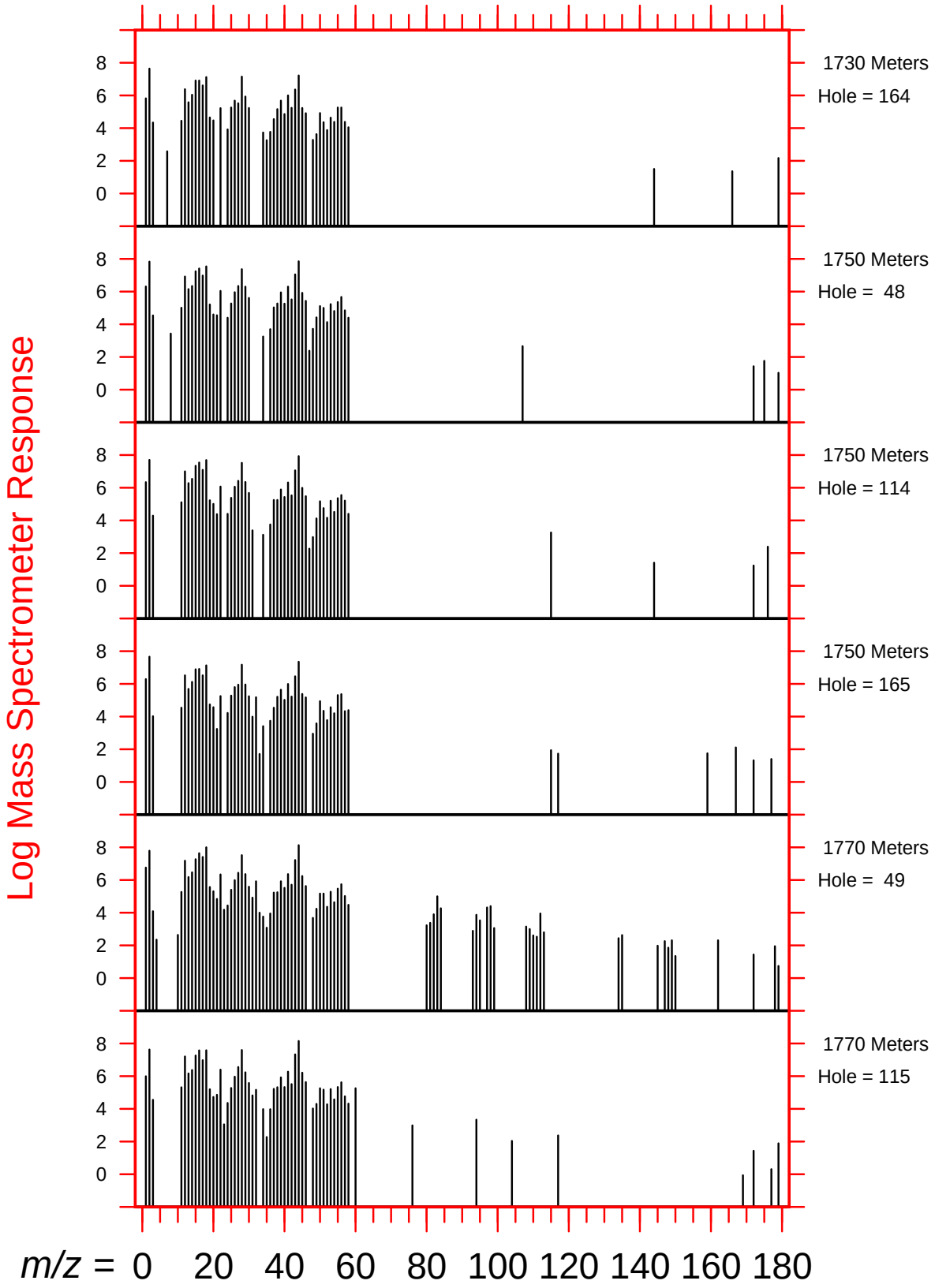
Log Mass Spectrometer Response
1730 Meters
Hole = 164
1750 Meters
Hole = 48
1750 Meters
Hole = 114
1750 Meters
Hole = 165
1770 Meters
Hole = 49
1770 Meters
Hole = 115
m/z = 0 20 40 60 80 100 120 140 160 180

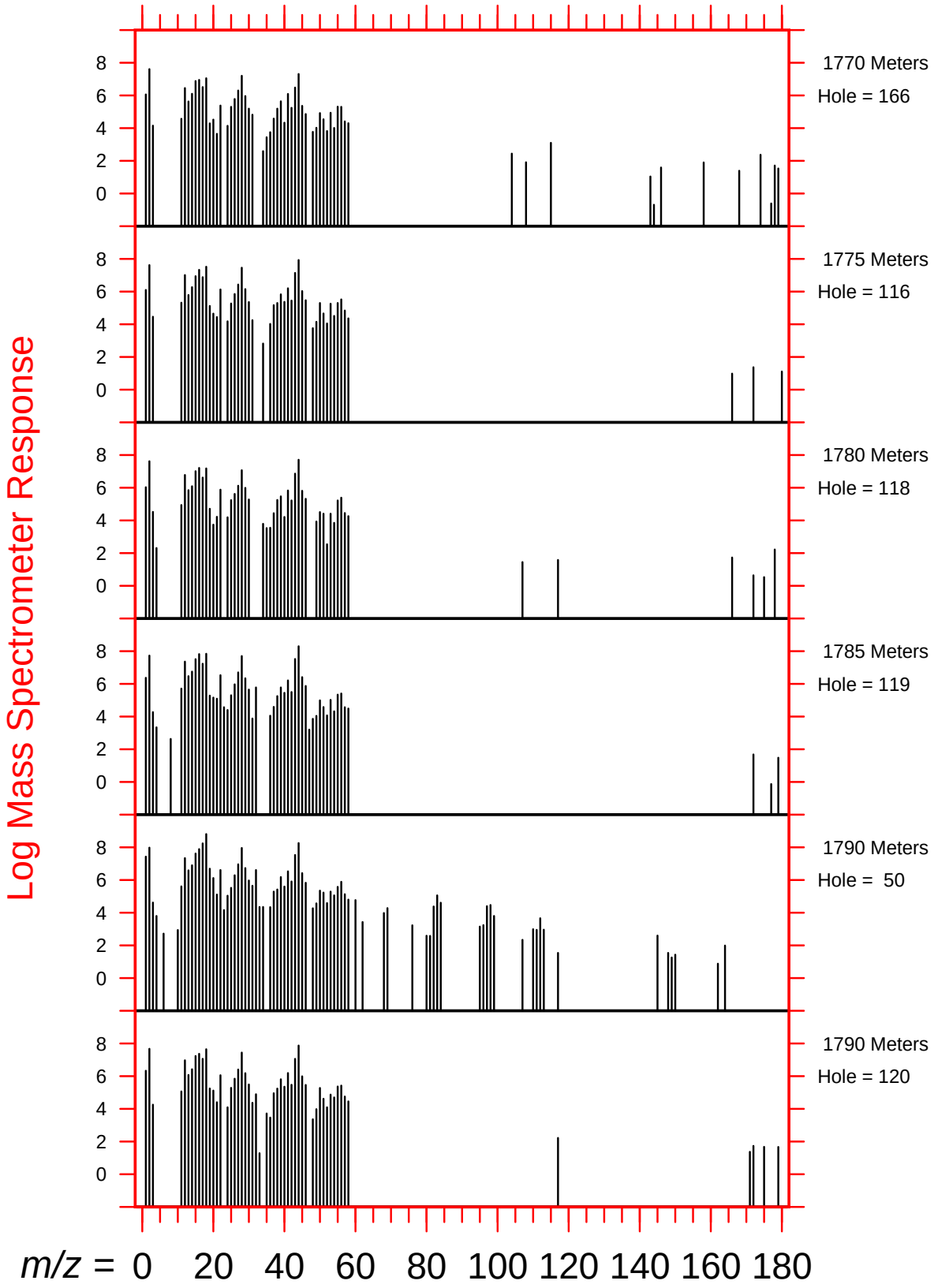
Log Mass Spectrometer Response
1770 Meters
Hole = 166
1775 Meters
Hole = 116
1780 Meters
Hole = 118
1785 Meters
Hole = 119
1790 Meters
Hole = 50
1790 Meters
Hole = 120
m/z = 0 20 40 60 80 100 120 140 160 180

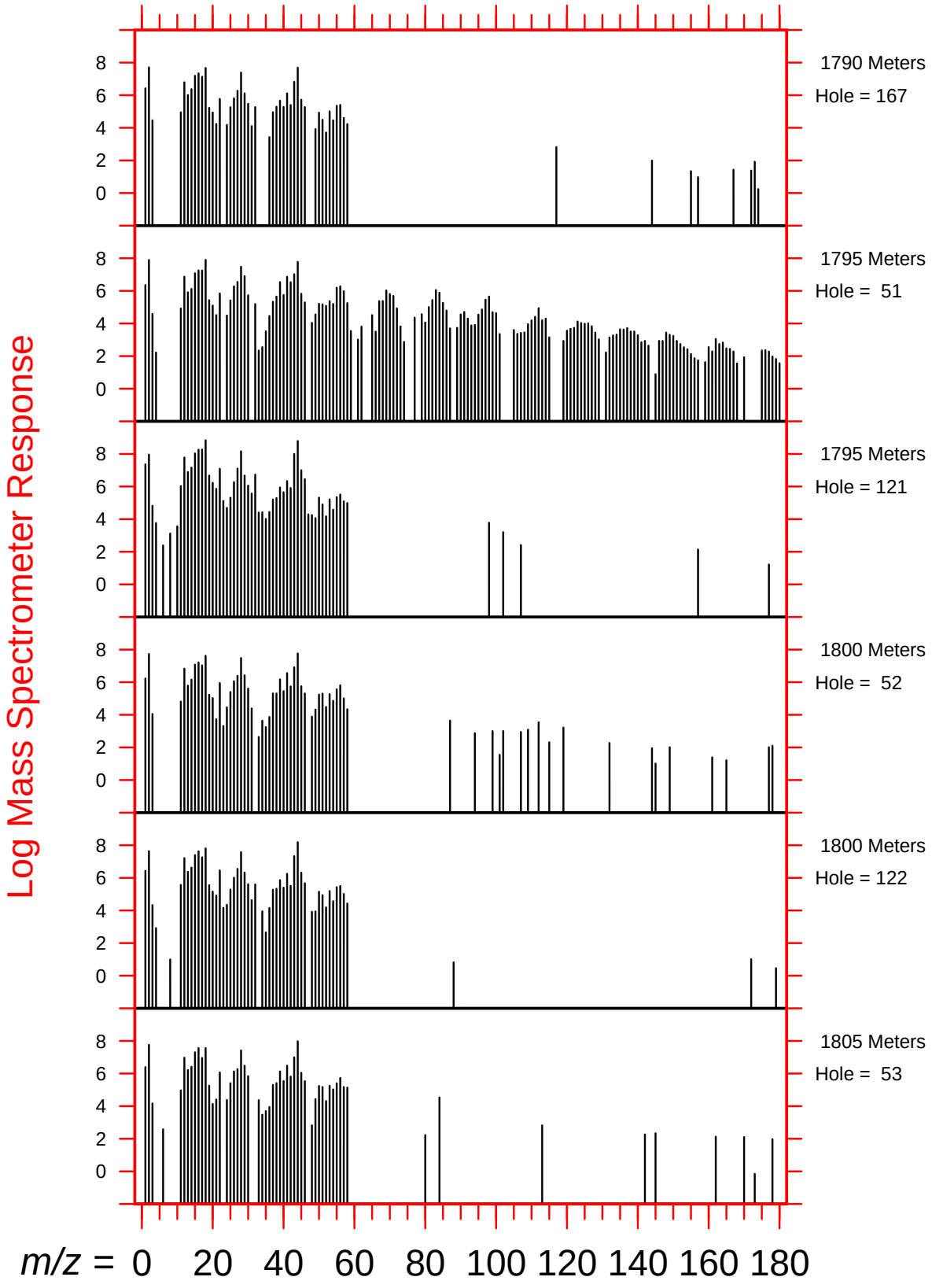
Log Mass Spectrometer Response
1790 Meters
Hole = 167
1795 Meters
Hole = 51
1795 Meters
Hole = 121
1800 Meters
Hole = 52
1800 Meters
Hole = 122
1805 Meters
Hole = 53
0
2
4
6
8
m/z = 0 20 40 60 80 100 120 140 160 180

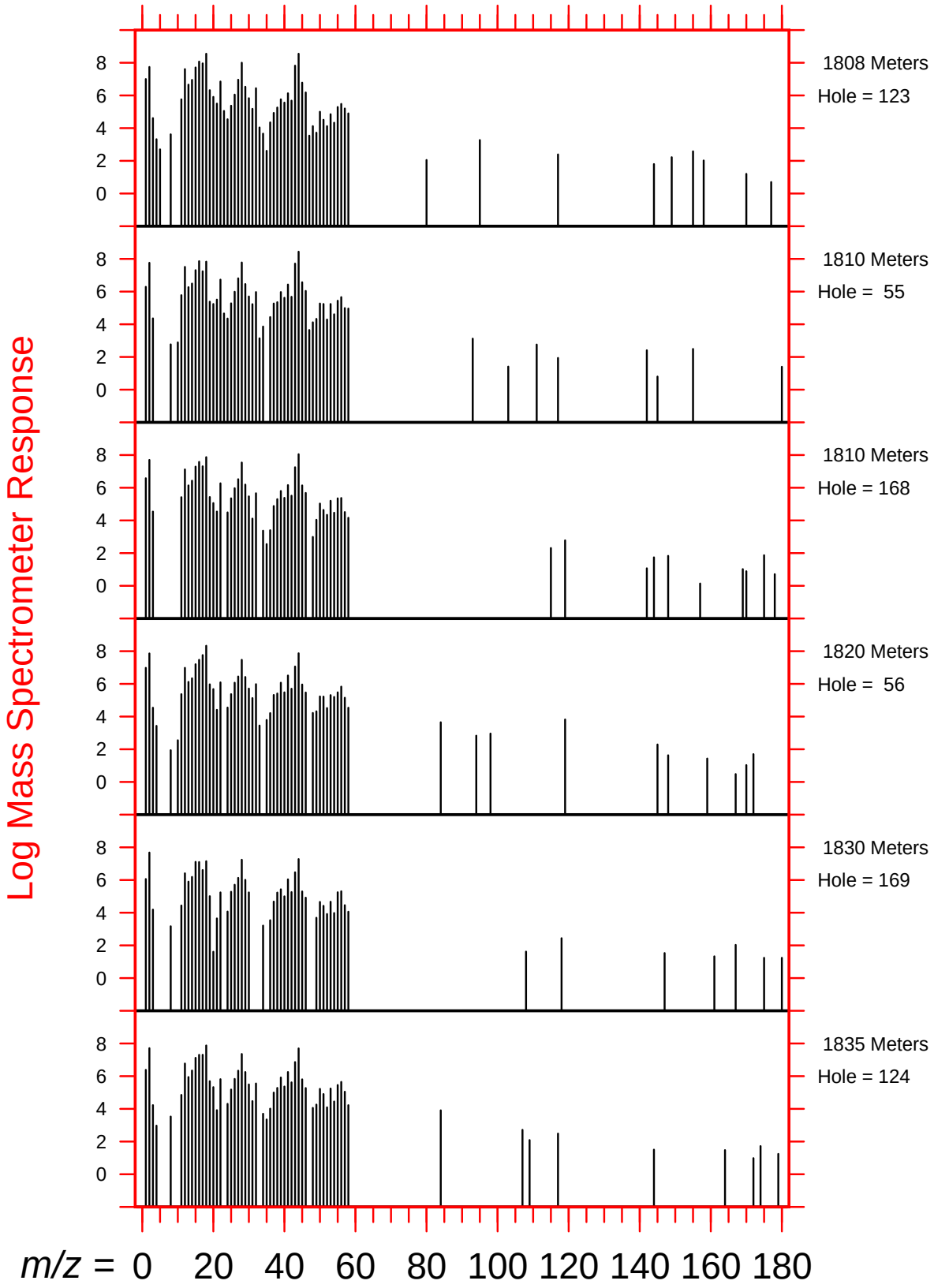
Log Mass Spectrometer Response
1808 Meters
Hole = 123
1810 Meters
Hole = 55
1810 Meters
Hole = 168
1820 Meters
Hole = 56
1830 Meters
Hole = 169
1835 Meters
Hole = 124
0
2
4
6
8
m/z = 0 20 40 60 80 100 120 140 160 180

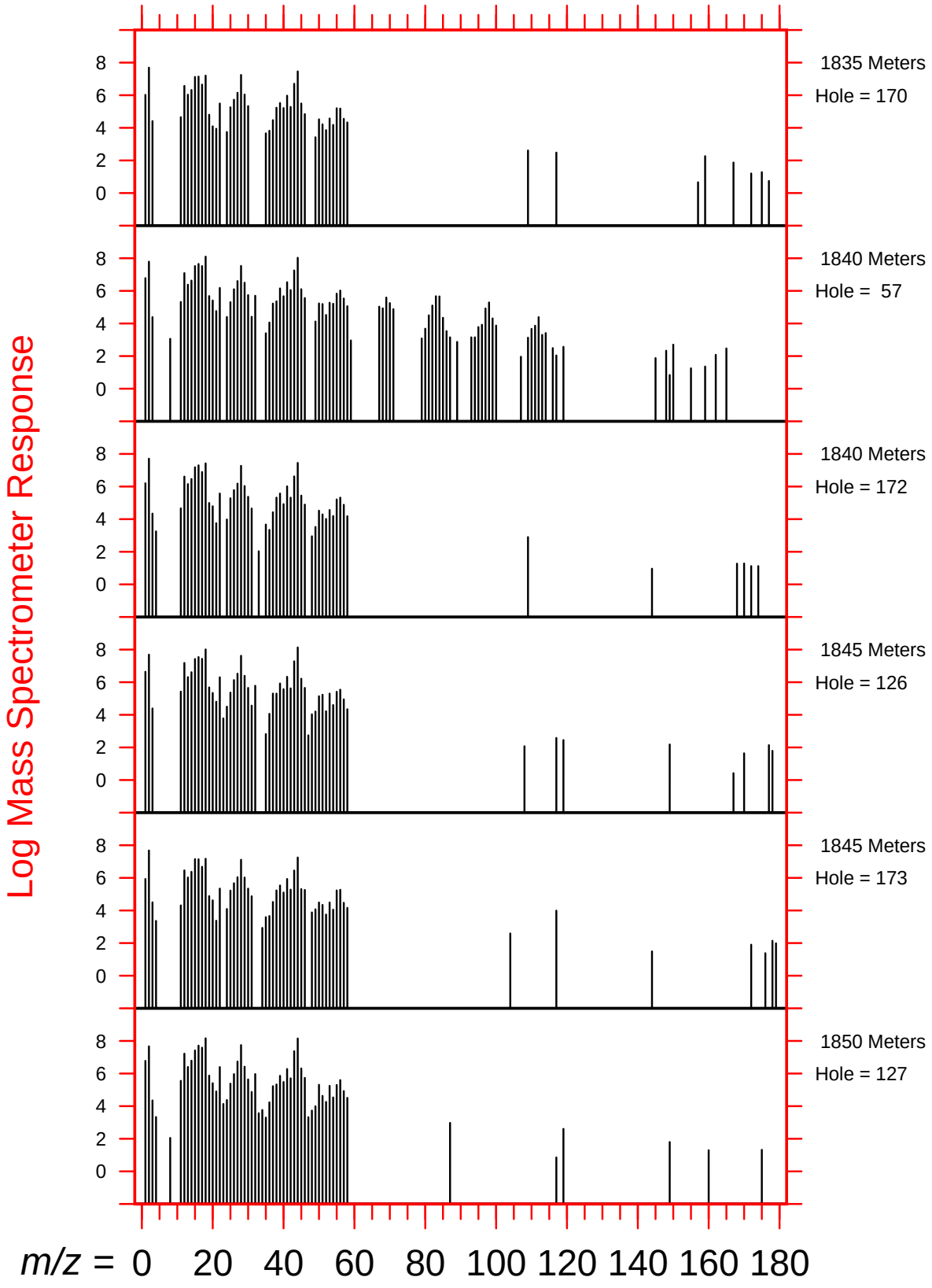
Log Mass Spectrometer Response
1835 Meters
Hole = 170
1840 Meters
Hole = 57
1840 Meters
Hole = 172
1845 Meters
Hole = 126
1845 Meters
Hole = 173
1850 Meters
Hole = 127
0
2
4
6
8
m/z = 0 20 40 60 80 100 120 140 160 180

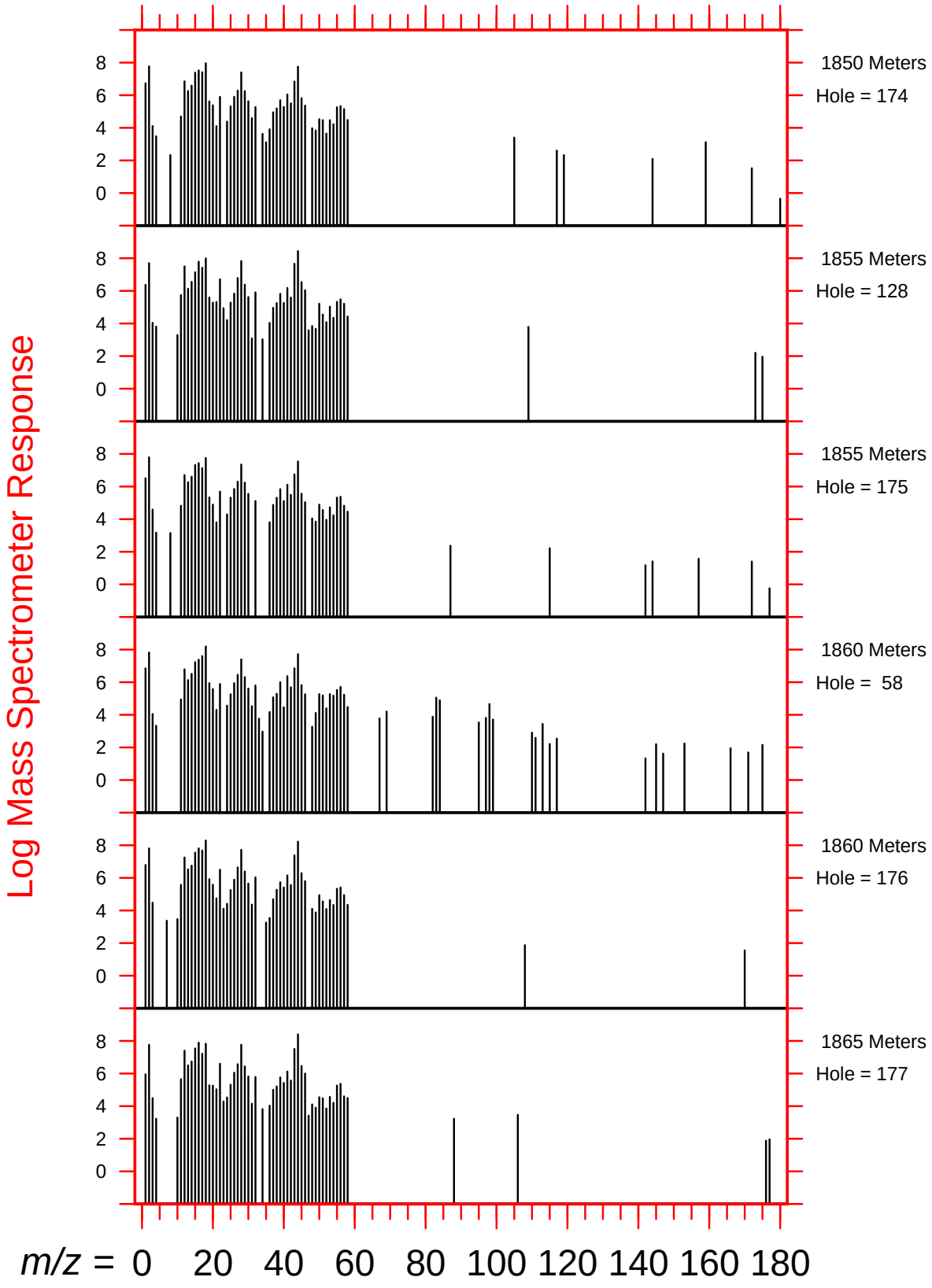
Log Mass Spectrometer Response
1850 Meters
Hole = 174
1855 Meters
Hole = 128
1855 Meters
Hole = 175
1860 Meters
Hole = 58
1860 Meters
Hole = 176
1865 Meters
Hole = 177
0
2
4
6
8
m/z = 0 20 40 60 80 100 120 140 160 180

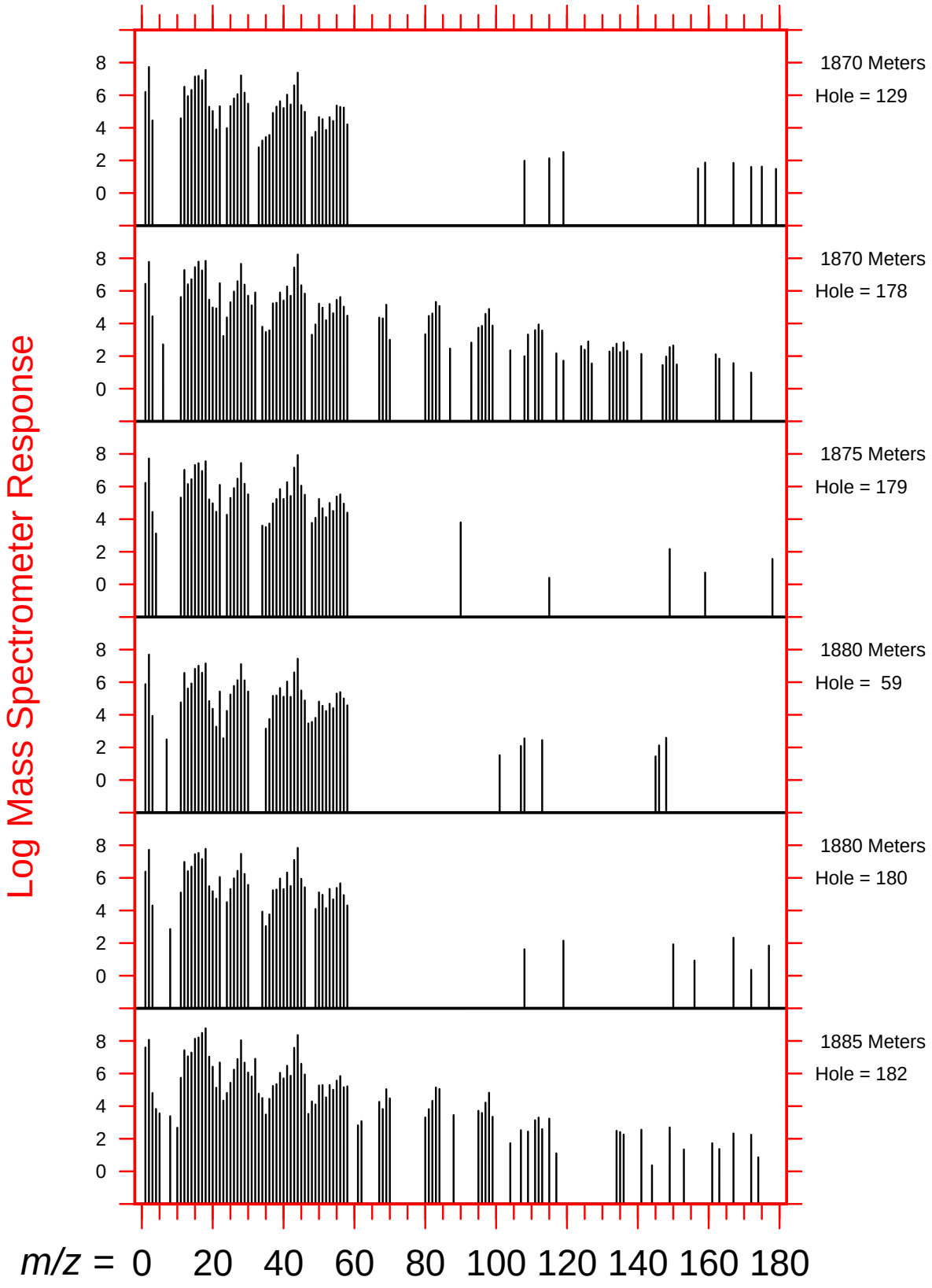
Log Mass Spectrometer Response
1870 Meters
Hole = 129
1870 Meters
Hole = 178
1875 Meters
Hole = 179
1880 Meters
Hole = 59
1880 Meters
Hole = 180
1885 Meters
Hole = 182
0
2
4
6
8
m/z = 0 20 40 60 80 100 120 140 160 180

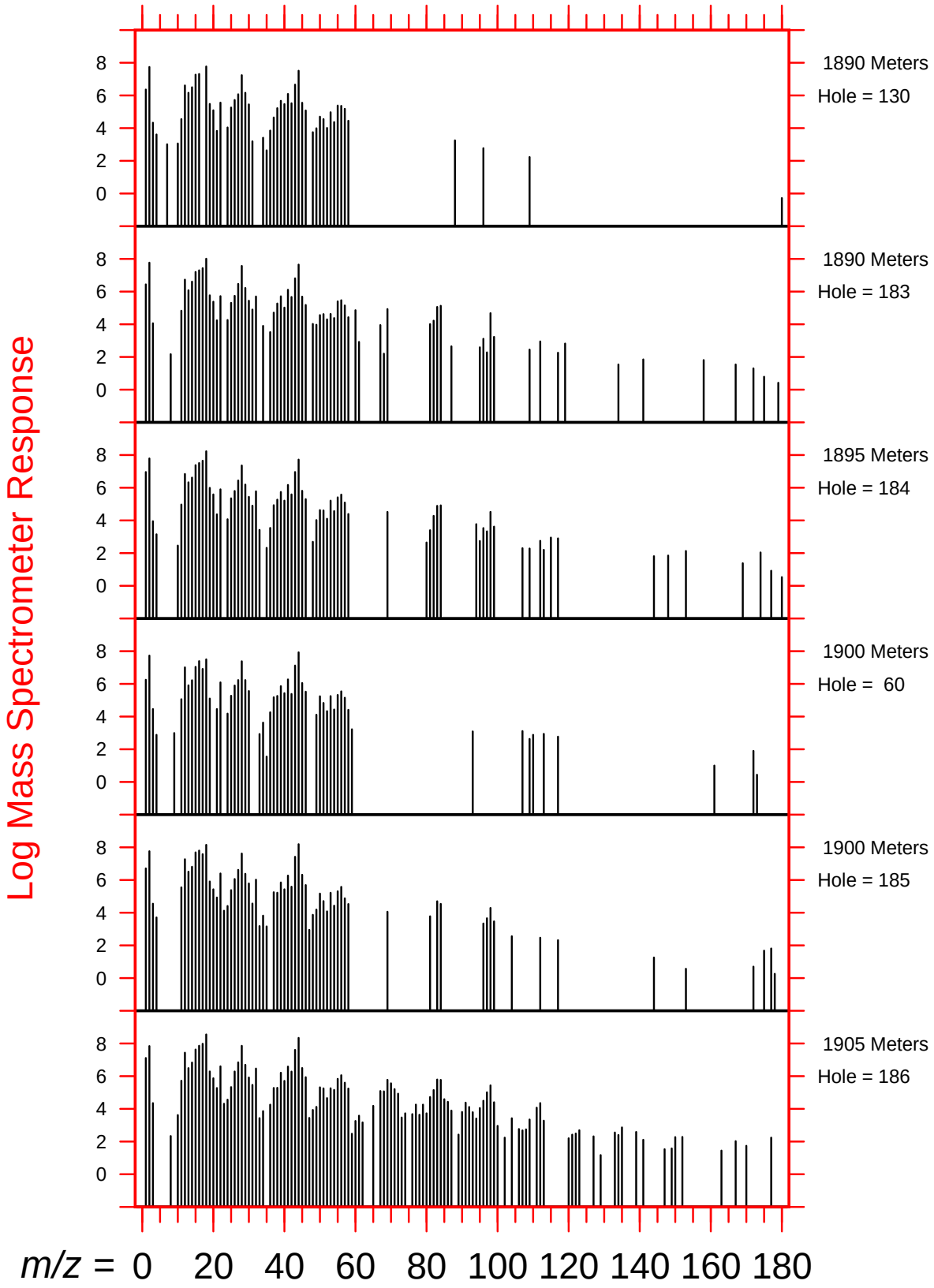
Log Mass Spectrometer Response
1890 Meters
Hole = 130
1890 Meters
Hole = 183
1895 Meters
Hole = 184
1900 Meters
Hole = 60
1900 Meters
Hole = 185
1905 Meters
Hole = 186
0
2
4
6
8
m/z = 0 20 40 60 80 100 120 140 160 180

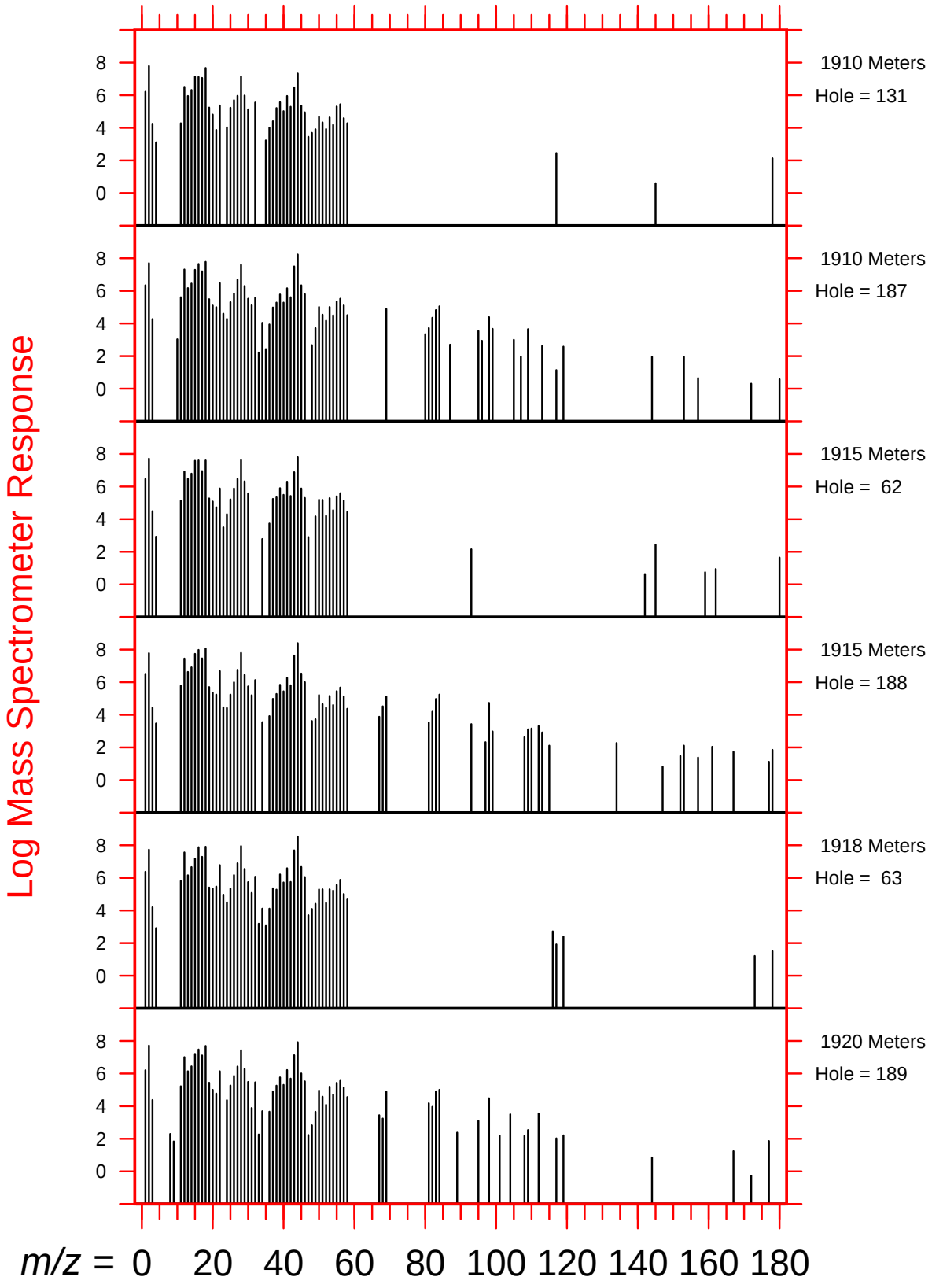
Log Mass Spectrometer Response
1910 Meters
Hole = 131
1910 Meters
Hole = 187
1915 Meters
Hole = 62
1915 Meters
Hole = 188
1918 Meters
Hole = 63
1920 Meters
Hole = 189
m/z = 0 20 40 60 80 100 120 140 160 180

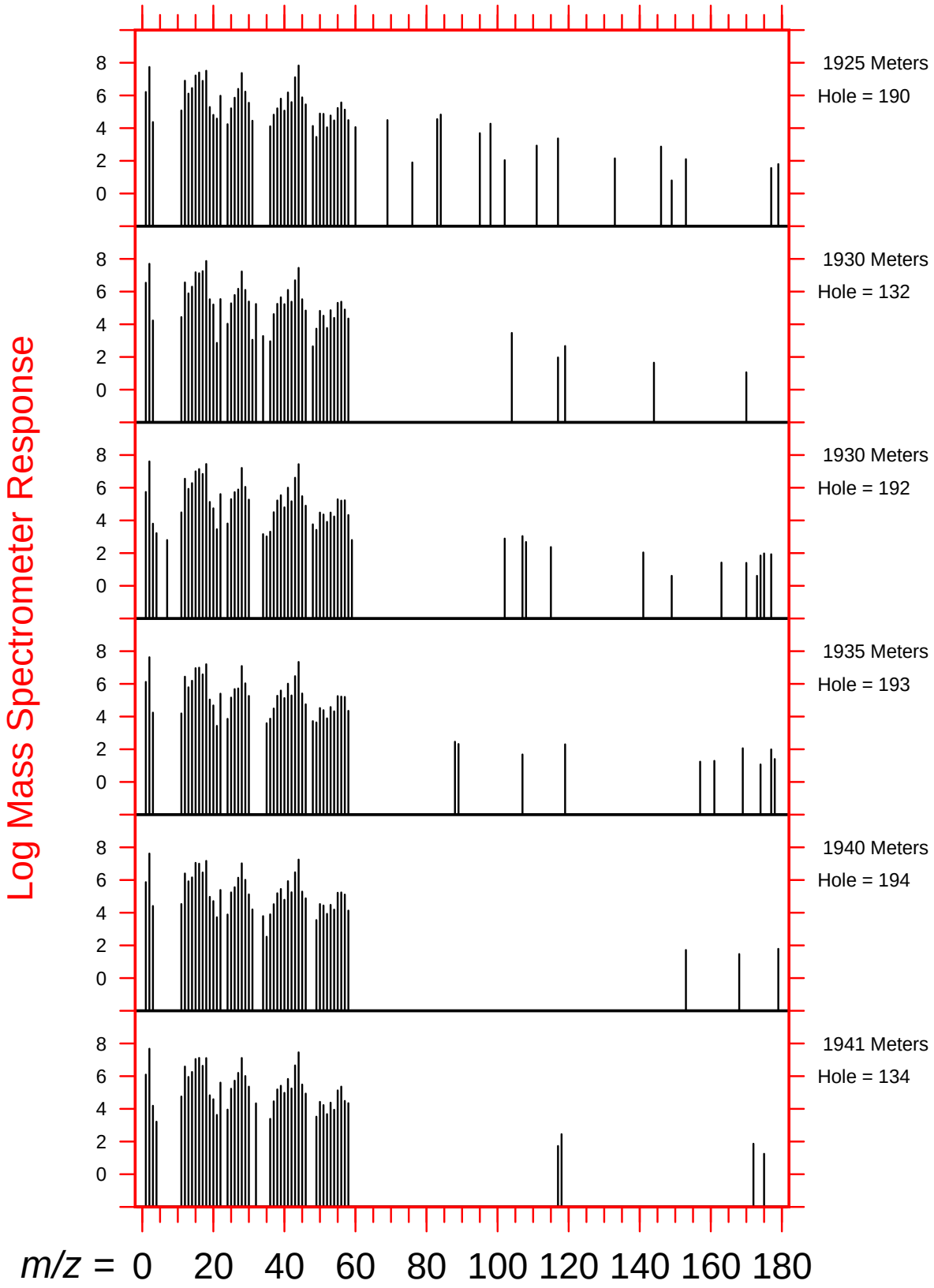
Log Mass Spectrometer Response
1925 Meters
Hole = 190
1930 Meters
Hole = 132
1930 Meters
Hole = 192
1935 Meters
Hole = 193
1940 Meters
Hole = 194
1941 Meters
Hole = 134
0
2
4
6
8
m/z = 0 20 40 60 80 100 120 140 160 180

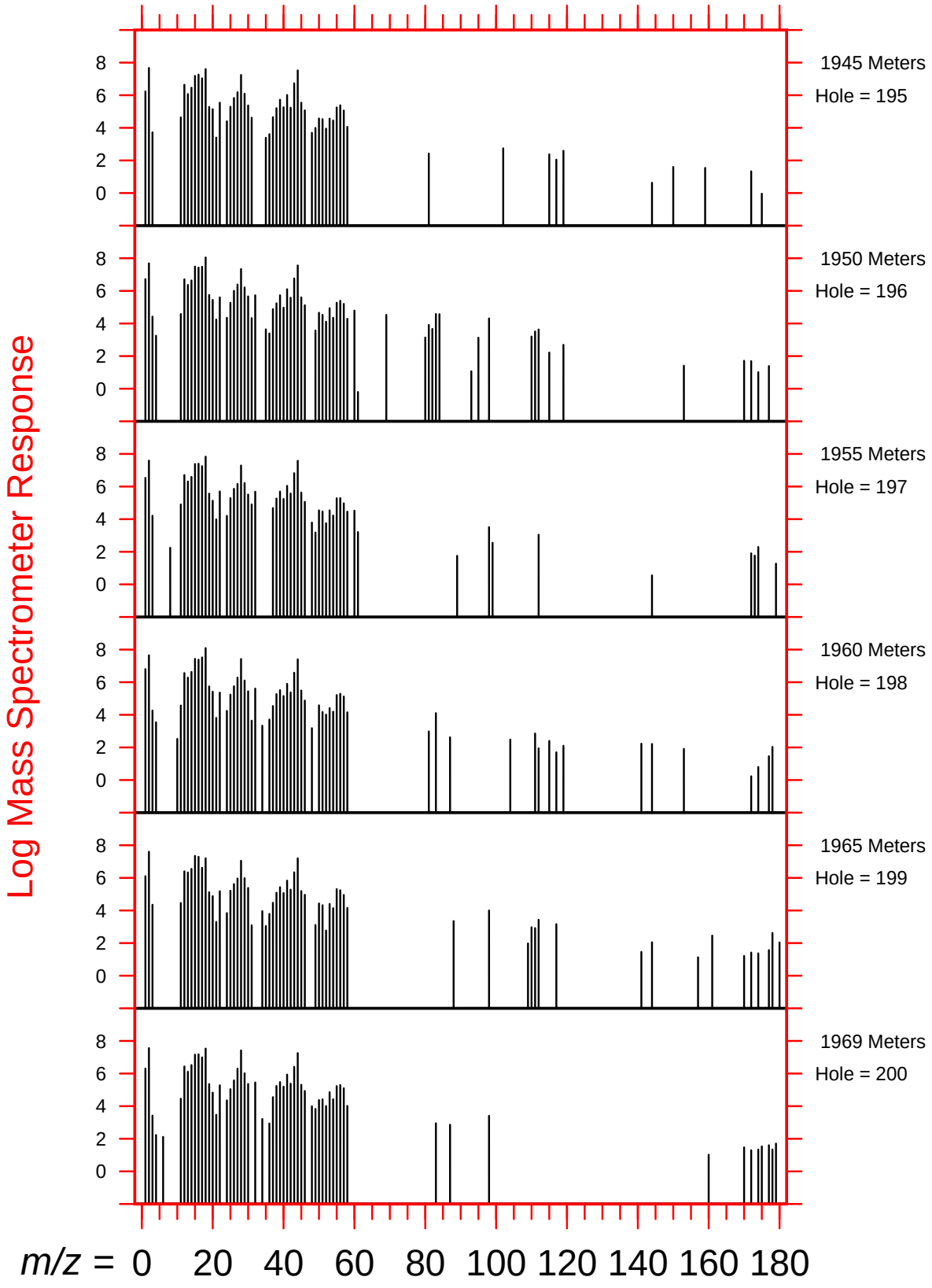
Log Mass Spectrometer Response
1945 Meters
Hole = 195
1950 Meters
Hole = 196
1955 Meters
Hole = 197
1960 Meters
Hole = 198
1965 Meters
Hole = 199
1969 Meters
Hole = 200
0
2
4
6
8
m/z = 0 20 40 60 80 100 120 140 160 180

Halladale-1 Fluid Inclusion Stratigraphy (FIS)

Halladale-1 DW2

Fluid Inclusion Stratigraphy

Hydrocarbon Indicators

Lab: FIT

Depth Unit: metres

C1Threshold	C1 Threshold
2.00E+06	2.00E+06

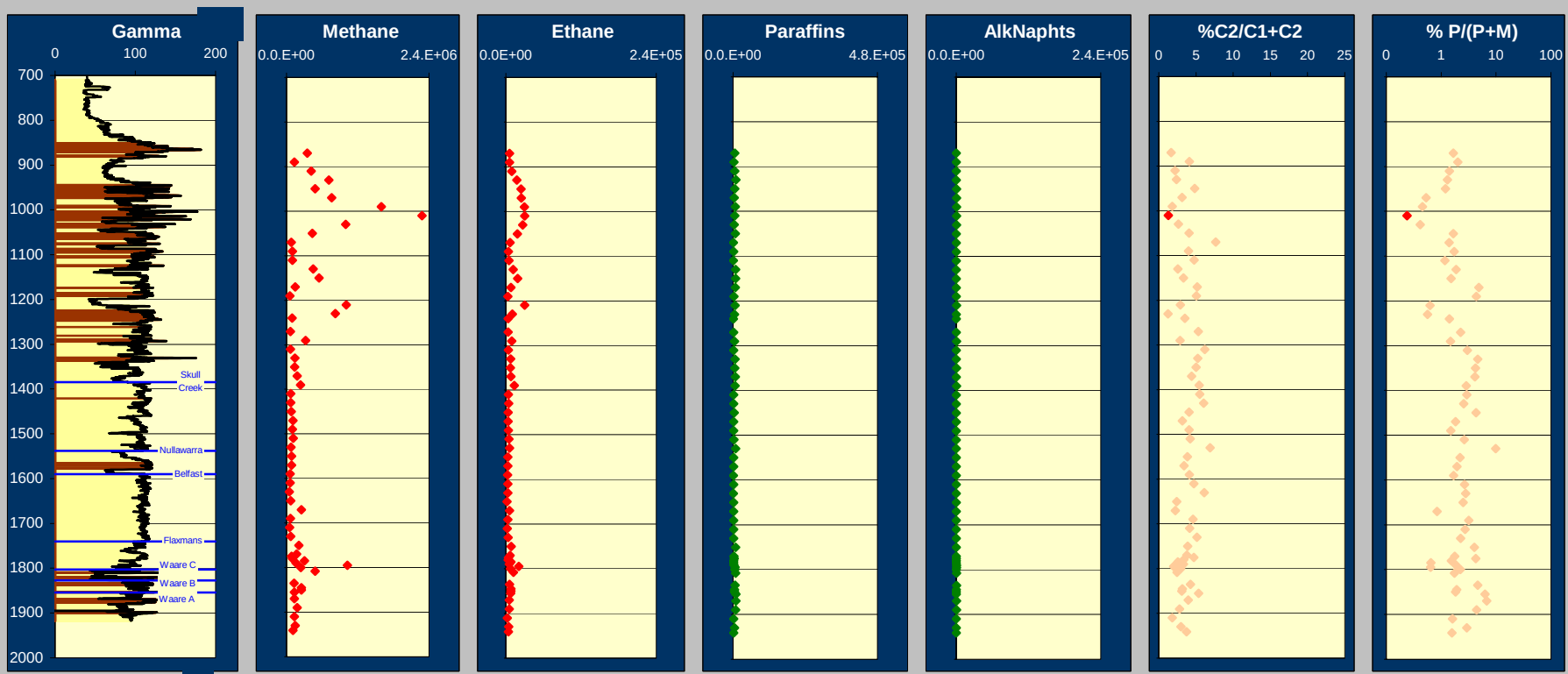

Comments:

No significant anomalies are present with the exception of a dry gas signal at 1795m (Flaxmans)

	Min	Max	Depth Grid
Depth Range Analysed	870	1941	
Depth Range to View	700	2000	100
Over-ride defaults	700	2000	100

Halladale-1 DW2

Fluid Inclusion Stratigraphy

Proximity-to-Pay Indicators

Lab: FIT

Depth Unit: metres

B Threshold 1.00E+04

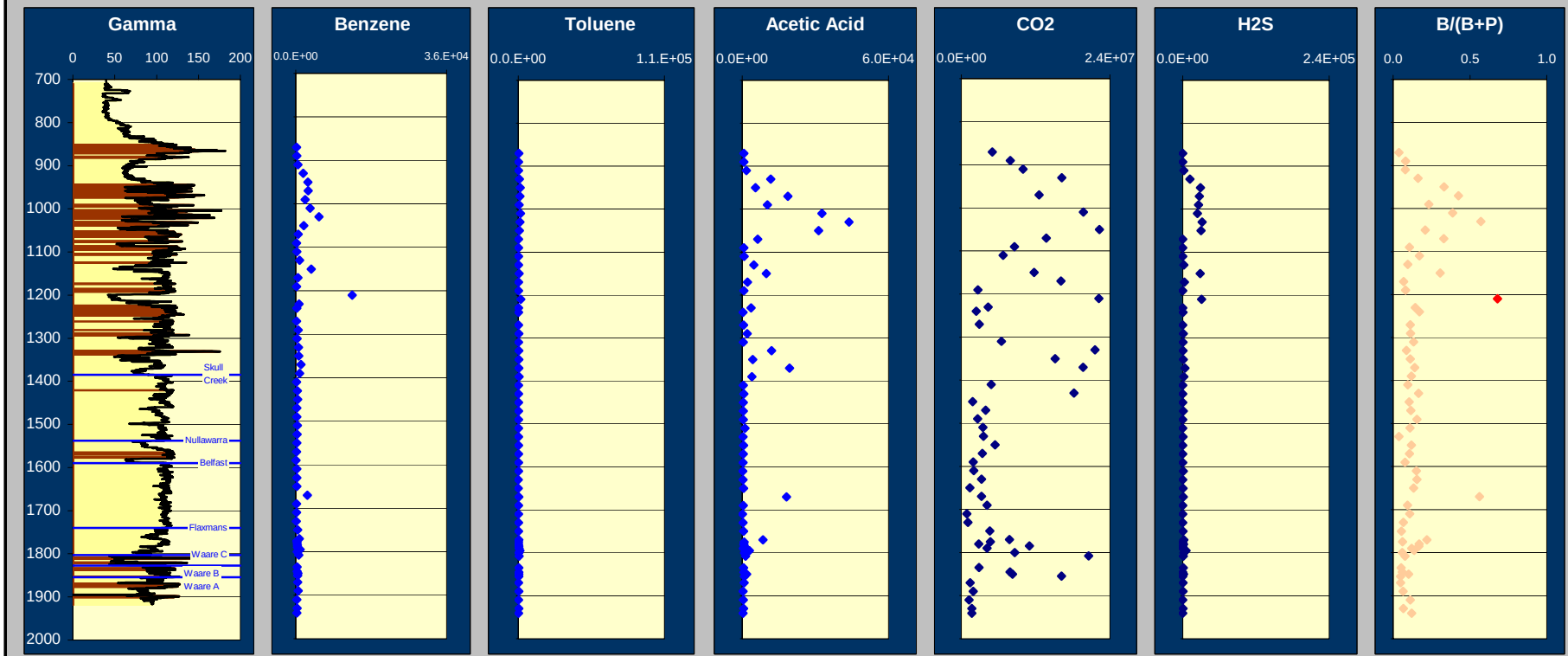

Comments:

No significant and consistent PTP anomalies present. Minor Bz anomalies in the Paraatte Formation but not a complete PTP signal.

Large CO2 anomalies persist throughout the section, consistent with Type III o.m.

(Adjust Depth Range on the Hydrocarbon Sheet)

Halladale 1 DWZ

Composite Well Log

Scale 1:500

Origin

Well Location